VOLUME 111 NUMBER 2

THE ASTROPHYSICAL JOURNAL

AN INTERNATIONAL REVIEW OF SPECTROSCOPY AND ASTRONOMICAL PHYSICS

MARCH 1950

A NEW STABLE STATE OF THE NEGATIVE HYDROGEN ION . . . *Egil Hylleraas* 209
EQUATION OF STATE OF HYDROGEN, HELIUM, AND RUSSELL MIXTURE AT HIGH TEMPERATURES AND PRESSURES . *R. E. Marshak, P. M. Mars, and H. York* 214
RADIAL VELOCITIES OF 2111 STARS . . . . . *Ralph E. Wilson and Alfred H. Joy* 221
AN ATLAS OF SPECTRA OF SIX STARS OF CLASSES R AND N . . *Rosco F. Sanford* 262
VARIATIONS IN VELOCITY AND SPECTRUM OF EIGHT N-TYPE LONG-PERIOD VARIABLE STARS . . . . . *Rosco F. Sanford* 270
A SURVEY OF INTERNAL MOTIONS IN THE PLANETARY NEBULAE . *O. C. Wilson* 279
THE BAND SPECTRUM OF CO^+. II. COMET-TAIL SYSTEM ($A^2\Pi - X^2\Sigma$) *K. Narahari Rao* 306
SINGLET ELECTRONIC STATES OF THE *TiO* MOLECULE . . . . *John G. Phillips* 314
THE INTERSTELLAR λ 4430 BAND . . . . *Jesse L. Greenstein and Lawrence H. Aller* 328
THE PECULIAR STAR HD 30353 . . . . . *William P. Bidelman* 333
ON THE TURBULENT VELOCITIES OF SOLAR GRANULES *R. S. Richardson and M. Schwarzschild* 351
THE USE OF SAVART FRINGES IN THE OBSERVATION OF ZEEMAN EFFECTS IN SUNSPOTS . . . . . *Yngve Öhman* 362
THE ROTATIONAL VELOCITIES OF GROUPS OF STARS, AS DETERMINED FROM THE APPARENT ROTATIONAL VELOCITIES . . . . . *Archibald Brown* 366
A COMET MODEL. I. THE ACCELERATION OF COMET ENCKE . *Fred L. Whipple* 375
RADIAL OSCILLATIONS OF THE GENERALIZED ROCHE MODEL . . *Zdeněk Kopal* 395
ETA CARINAE. I. THE NEBULOSITY . . . . . *E. Gaviola* 408
PHOTOELECTRIC STUDIES. III. COLOR-LUMINOSITY ARRAYS FOR THE COMA BERENICES AND URSA MAJOR CLUSTERS . . . . . *Olin J. Eggen* 414
THE MOVING CLUSTER IN PERSEUS . . . . *Nancy G. Roman and W. W. Morgan* 426

NOTES

NOTE ON THE SPECTRUM OF THE AIRGLOW IN THE RED REGION . . . . . *C. T. Elvey* 432
IDENTIFICATION OF THE 6560 A. EMISSION IN THE SPECTRUM OF THE NIGHT SKY *A. B. Meinel* 433
SPECTROSCOPIC DISTANCE MODULI FOR 224 O AND B STARS . . . . . *Jane Ramsey* 434
RADIAL VELOCITIES OF FIFTEEN STARS OF THE RR LYRAE TYPE . . . . . *A. Colacevich* 437
ON THE SPECTROSCOPIC BINARY τ^6 ERIDANI . . . . . *Jorge Sahade* 438
SPECTROGRAPHIC OBSERVATIONS OF THE STAR η_1 HYDRI . . *Jorge Sahade and Julio Albarracín* 442
A NOTE ON THE SPECTRUM OF SIGMA ORIONIS . . . . . *G. R. Miczaika* 443
ON A GENERALIZATION OF THE VARIATIONAL METHOD FOR PROBLEMS OF RADIATIVE TRANSFER *V. Kourganoff* 443
NOTE ON THE CHEMICAL COMPOSITION OF THE SUN . . . . . *Marjorie Hall Harrison* 446
NOTE ON THE EFFECT OF UNEQUAL MOLECULAR WEIGHTS ON THE INTERNAL TEMPERATURE-DENSITY DISTRIBUTION OF A STAR . . . . . *R. E. Marshak and G. M. Wing* 447

THE UNIVERSITY OF CHICAGO PRESS
CHICAGO, ILLINOIS, U.S.A.

March 1950 Vol. 111, No. 2

THE ASTROPHYSICAL JOURNAL

AN INTERNATIONAL REVIEW OF SPECTROSCOPY AND ASTRONOMICAL PHYSICS

Edited by

W. W. MORGAN
Managing Editor

S. CHANDRASEKHAR

Yerkes Observatory of the University of Chicago

PAUL W. MERRILL
Mount Wilson Observatory of the Carnegie Institution of Washington

HARLOW SHAPLEY
Harvard College Observatory
Cambridge, Massachusetts

N. U. MAYALL
Lick Observatory
University of California

With the Collaboration of the American Astronomical Society

Collaborating Editors:

1948-50	1949-51	1950-52
CECILIA H. PAYNE-GAPOSCHKIN Harvard College Observatory	W. BAADE Mount Wilson Observatory	LYMAN SPITZER, JR. Princeton University Observatory
H. N. RUSSELL Princeton University	LEO GOLDBERG Observatory of the University of Michigan	A. N. VYSSOTSKY Leander McCormick Observatory
ANDREW McKELLAR Dominion Astrophysical Observatory, Victoria	G. HERZBERG National Research Council, Ottawa	ALBERT E. WHITFORD Washburn Observatory

The Astrophysical Journal is published bimonthly by the University of Chicago at the University of Chicago Press, 5750 Ellis Avenue, Chicago, Illinois, during July, September, November, January, March, and May. ¶The subscription price is $12.00 a year; the price of single copies is $3.00. Orders for service of less than a full year will be charged at the single-copy rate. ¶Postage is prepaid by the publishers on all orders from the United States and its possessions. No extra charge for countries in the Pan American Postal Union. ¶Postage is charged extra as follows: for Canada and Newfoundland, 42 cents on annual subscriptions (total $12.42); on single copies, 7 cents (total $3.07); for all other countries in the Postal Union, 96 cents on annual subscriptions (total $12.96), on single copies 16 cents (total $3.16). ¶Patrons are requested to make all remittances payable to The University of Chicago Press, in United States currency or its equivalent by postal or express money orders or bank drafts.

The following is an authorized agent:

For the British Empire, except North America and Australasia: The Cambridge University Press, Bentley House, 200 Euston Road, London, N.W. 1, England. Prices of yearly subscriptions and of single copies may be had on application.

Claims for missing numbers should be made within the month following the regular month of publication. The publishers expect to supply missing numbers free only when losses have been sustained in transit, and when the reserve stock will permit.

Business correspondence should be addressed to The University of Chicago Press, Chicago 37, Illinois.

Communications for the editors and manuscripts should be addressed to: W. W. Morgan, Editor of The Astrophysical Journal, Yerkes Observatory, Williams Bay, Wisconsin.

Line drawings and photographs should be made by the author, and all marginal notes such as co-ordinates, wave lengths, etc., should be included in the cuts. It will not be possible to set up such material in type.

One copy of the corrected galley proof should be returned as soon as possible to the editor, Yerkes Observatory, Williams Bay, Wisconsin. Authors should take notice that the manuscript will not be sent to them with the proof.

The cable address is "Observatory, Williamsbay, Wisconsin."

The articles in this journal are indexed in the *International Index to Periodicals*, New York, N.Y.

Applications for permission to quote from this journal should be addressed to The University of Chicago Press, and will be freely granted.

Notice to subscribers: If you change your address, please notify us and your local postmaster immediately. The post office does not forward second-class mail.

Entered as second-class matter, July 21, 1900, at the Post-Office at Chicago, Ill., under the Act of March 3, 1879.
Acceptance for mailing at special rate of postage provided for in United States Postal Act of October 3, 1917, Section 1103, amended February 28, 1925.

[PRINTED IN U.S.A.]

THE ASTROPHYSICAL JOURNAL

AN INTERNATIONAL REVIEW OF SPECTROSCOPY AND ASTRONOMICAL PHYSICS

VOLUME 111 MARCH 1950 NUMBER 2

A NEW STABLE STATE OF THE NEGATIVE HYDROGEN ION

EGIL HYLLERAAS

Institute for Theoretical Physics, University of Oslo

Received November 26, 1949

ABSTRACT

The existence of a second stable state of the negative hydrogen ion has been proved. It corresponds to the doubly excited $(2s)(2p)^3P$ state of *He* with energy -1.506 in Rydberg units. The energy of the state has been calculated both for *He* and H^- with neglect of the mutual polarization energy of the two electrons. As to the distortion of the electron orbits also, mainly that of the s-electron has been taken into account. The binding energy of the second electron is in this approximation about 0.29 e.v. but it may possibly be considerably larger.

As is well known, the negative hydrogen ion has become important in astrophysical problems, particularly for the explanation of the opacity of the sun's atmosphere.[1] The anomalous absorption in the infrared region is mainly due to an existing closed state of H^- corresponding to the ground of *He*.

The author has repeatedly examined various possibilities, among others also the doubly excited $(2p)^2\ ^3P$ state, which, with respect to energy calculations, is rather similar to $(1s)^2\ ^1S$ and whose energy value in the case of the *He* atom is easily calculated in the first approximations. It is, however, doubtful whether this state is stable at all for H^-. Its energy for the *He* atom is about -1.4218 *Rh*, which may be compared with the energy $-1.45175{\cdot}4$ *Rh* of the ground state. This means that the binding energy of the second electron is comparatively smaller in the $(2p)^2\ ^1S$ than in the ground state $(1s)^2\ ^1S$, and the result appears to be that there will be no binding energy left in the H^- ion.

Considering other doubly excited states of *He*, our attention has been directed toward the $(2s)(2p)^3P$ state with a considerably larger binding energy of the second electron. Its energy has been calculated by several authors[2] and is about -1.50 *Rh*. The larger binding energy of the second electron in this state suggests that there will be some binding energy left for the electron even in H^-. This suggestion is easily verified even in the first approximation, in contrast to the ground state for which the second and third approximations are needed to give negative energy for the second electron.

[1] R. Wildt, *Ap. J.*, **89**, 295, 1939; J. A. Wheeler and R. Wildt, *Ap. J.*, **95**, 281; 1942; S. Chandrasekhar, *Ap. J.*, **100**, 176, 1944, **102**, 395, 1945, and **104**, 430, 1946.

[2] F. G. Fender and J. P. Vinti, *Phys. Rev.*, **46**, 77, 1934; Ta-You-Wu, *Phys. Rev.*, **46**, 239, 1934; W. S. Wilson, *Phys. Rev.*, **48**, 536, 1935. I am indebted to my students, Th. Rasmussen and G. Marthinsen, for suggesting the existence of the new state on the basis of the large binding energy of the second electron in the corresponding state of *He*.

THE WAVE FUNCTION AND THE SECULAR EQUATION

The state $(2s)(2p)^3P$ is the second state in the series $(ns)(2p)^3P$, beginning with the ordinary singly excited state $(1s)(2p)^3P$. Therefore, if we want to define the energy of the state as the minimum of some variational integral, we must not forget to take care of some additional condition for the eigen-function, as, for instance, that it must be orthogonal to the eigen-function of the lowest state. However, as is well known, an equivalent procedure is to expand the eigen-function in terms of some complete system of functions and take the second root in the resulting secular equation for the energy. By this procedure it is perfectly immaterial whether the first root is a good approximation or not for the lowest state.

As often used in the treatment of many-electron states, we shall also here introduce an expanding or contracting parameter k and write

$$\psi = \varphi(kr_1, kr_2) \tag{1}$$

for the eigen-function. The general form for a ^3P eigen-function, then, is

$$\varphi = \phi\cos\vartheta_2 - \Phi\cos\vartheta_1\,, \qquad \phi = \phi(r_1, r_2, r_{12})\,, \qquad \Phi = \phi(r_2, r_1, r_{12})\,. \tag{2}$$

If in the function ϕ we disregard its dependence on r_{12}, we lose the polarization energy of the state. Still, by writing $\phi = \phi(r_1, r_2)$ or $\phi = \varphi_1(r_1)\varphi_2(r_2)$, we can take care of other parts of the mutual distortion of the two electronic states. The whole problem will be discussed in greater detail later. In this paper we shall consider only the distortion of the (2s) state of the first electron by a second electron in the (2p) state. The (2p)-state function is varied only by the general contraction parameter k for the whole two-electron eigen-function.

The function ϕ is therefore written

$$\phi(r_1, r_2) = \sum_{n=1}^{\infty} \varphi_{n0}(r_1)\varphi_{21}(r_2)\,, \tag{3}$$

where φ_{nl} are hydrogen wave functions. However, whereas in the true hydrogen wave functions as expressed by Laguerre functions the argument depends on the quantum number n, we shall here use arguments independent of n. This may be expressed by putting

$$\varphi_{n0}(r) = \frac{1}{\sqrt{2n^2}}\frac{1}{2\pi i}\int^{(0+)}\frac{ds}{s^n}\frac{e^{-r(1+s)/2(1-s)}}{(1-s)^2}\,, \qquad \varphi_{21}(r) = \frac{r}{\sqrt{24}}\,e^{-r/2}. \tag{4}$$

By this supposition we expect suitable values for the parameter k to be a little smaller than $k = 1$ for He and $k = 0.5$ for H^-.

Because of the orthogonality properties of the functions $\varphi_{n_0}(r)$, the energy secular equation becomes rather simple and may be written

$$\begin{gathered}|\,N_{nn'}E - k^2M_{nn'} + k\,[ZL_{nn'} - (L'_{nn'} - L'_{nn'})]\,| = 0\,,\\ N_{nn'} = \delta_{nn'} - \tfrac{1}{2}\,\delta_{1|n-n'|}\,, \qquad M_{nn'} = 2\,\delta_{nn'}\,, \qquad L_{nn'} = \left(1+\frac{2}{n}\right)\delta_{nn'} - \tfrac{1}{2}\,\delta_{1|n-n'|}\,.\end{gathered} \tag{5}$$

The only quantities which need a more careful examination are $L'_{nn'}$ and $L'_{nn'}$, the ordinary perturbation integral and the exchange integral of the electrons in the state n and n'.

It is found that

$$L'_{nn'} = \frac{2}{n}\,\delta_{nn'} - \frac{(n+n'-1)!}{24n!\,n'!\,2^{n+n'+2}}\,f(n,n'),$$

$$\begin{aligned} f(n,n') = {} & (10-n-n')\,[(n+n'-18)(n+n'-5)+6] \\ & + \frac{12(n+n'-9)(n+n'-16)(n-1)(n'-1)}{(n+n'-1)} \\ & + \frac{48(14-n-n')(n-1)(n-2)(n'-1)(n'-2)}{(n+n'-1)(n+n'-2)} \\ & + \frac{64(n-1)(n-2)(n-3)(n'-1)(n'-2)(n'-3)}{(n+n'-1)(n+n'-2)(n+n'-3)}, \end{aligned} \tag{6}$$

and

$$L'_{nn'} = \frac{1}{48nn'}\left(\frac{1}{2\pi i}\right)^2 \int^{(0+)} \frac{ds}{s^n} \int^{(0+)} \frac{dt}{t^{n'}} F(s,t),$$

$$\begin{aligned} F(s,t) = {} & 7\left[1-\frac{s+t}{2}\right]^3 - 24\left(\frac{s-t}{2}\right)^2\left[1-\frac{s+t}{2}\right] \\ & + \frac{30(s-t/2)^4}{[1-(s+t/2)]} - \frac{16(s-t/2)^6}{[1-(s+t/2)]^3} + \frac{3(s-t/2)^8}{[1-(s+t/2)]^5}. \end{aligned} \tag{7}$$

In this way the following perturbation matrices are obtained:

$$L'_{nn'} = \begin{vmatrix} \frac{7}{8} & -\frac{21}{64} & -\frac{5}{64} & -\frac{5}{512} & \frac{1}{256} \\ & \frac{83}{128} & -\frac{49}{256} & -\frac{5}{64} & -\frac{3}{128} \\ & & \frac{185}{384} & -\frac{63}{512} & -\frac{33}{512} \\ & & & \frac{781}{2048} & -\frac{357}{4096} \\ & & & & \frac{101}{320} \end{vmatrix}; \tag{8}$$

$$L'_{nn'} = \begin{vmatrix} \frac{7}{48} & -\frac{7}{64} & -\frac{1}{192} & \frac{17}{1536} & \frac{1}{128} \\ & \frac{15}{128} & -\frac{5}{256} & -\frac{5}{256} & -\frac{3}{512} \\ & & \frac{5}{192} & \frac{5}{1536} & -\frac{3}{512} \\ & & & \frac{55}{6144} & \frac{11}{4096} \\ & & & & \frac{9}{2048} \end{vmatrix}; \tag{9}$$

$$(L'-\bar{L}')_{nn'} = \begin{vmatrix} \frac{35}{48} & -\frac{7}{32} & -\frac{7}{96} & -\frac{1}{48} & -\frac{1}{256} \\ & \frac{17}{32} & -\frac{11}{64} & -\frac{15}{256} & -\frac{9}{512} \\ & & \frac{175}{384} & -\frac{97}{768} & -\frac{15}{256} \\ & & & \frac{143}{384} & -\frac{43}{512} \\ & & & & \frac{3187}{10240} \end{vmatrix} - \frac{1}{256}\,0. \tag{10}$$

These matrices up to $n = n' = 5$ are sufficient for calculating energy values to the degree of accuracy wanted.

NUMERICAL ENERGY VALUES

The results of the calculations for *He* and H^- are summarized in Tables 1 and 2. We restrict ourselves to energy values in various approximations and the corresponding k-values. The expansion coefficients are given in Table 2. However, the eigenfunction is still far from its final shape. When applying it for other purposes than for the calculation of the energy, one should re-examine the function to see what degree of accuracy is needed and what will be the most suitable form. We begin with the doubly excited $(2s)(2p)^3P$ state of *He* (Table 1).

TABLE 1

Approx.	E	k	Approx.	E	k
	He, $Z = 1$			H^-, $Z = 1$	
1	−1.50403	0.867	1	−0.26965	0.367
2	−1.50121	.882	2	− .26702	.380
3	−1.50231	.854	3	− .26765	.360
4	−1.50581	.856	4	− .27091	.362
5	−1.50616	0.854	5	−0.27123	0.356

TABLE 2

EXPANSION COEFFICIENTS FOR NORMALIZED FUNCTIONS

	k	c_1	c_2	c_3	c_4	c_5
He	0.854	−0.060216	1.0	0.085951	0.067936	0.020406
H^-	0.356	−0.145745	1.0	0.177454	0.158407	0.056738

As seen, the approximate values both of E and k are running in a strictly parallel way in the various approximations, the difference in k being nearly $\frac{1}{2}$ all the way. The excess of binding energy above 1 and 0.25, respectively, which we attribute to the second electron, varies with nearly the same amount.

The first-approximation energy value is not reliable, since there is no orthogonality restriction on the eigen-function. In the second approximation, however, the orthogonality property has been accounted for by taking the second root of the secular equation, and the effect is a raising of the approximate energy value, which is now known to be above the true value. By this stage of the calculation we see that the $(2s)(2p)^3P$ state is really a closed state for the negative hydrogen ion with a binding energy of at least 0.017 $Rh = 0.23$ e.v.

The third approximation points toward a rapid convergence, which, however, is spoiled by the next approximation. A true convergence appears first in the fifth approximation. The energy differences in the fourth and fifth approximations can be rather well accounted for by considering only the $(L' - \bar{L}')_{25}$ term, together with an approximate value of the (55) matrix element of the secular equation in the sense of ordinary second-order approximations. In the same way the contributions from the sixth and seventh approxi-

mations can be estimated. To this end the two figures outside the matrix (9) have been added.

In this way it is found that the contribution from the sixth approximation probably cannot exceed more than 1 and 2 in the fifth decimal place. Hence, as a result of the independent distortion of the (2s) function, together with a contraction or dilatation of the (2p) function, we obtain the approximate energy values, say,

$$He: E = -1.50619\,Rh\,,$$

$$H^-: E = -0.27124\,Rh\,.$$

Thus the binding energy of the second electron in the $(2s)(2p)^3P$ state and H^- is at least

$$E = 0.02124\,Rh = 0.2876 \text{ e.v.}$$

EQUATION OF STATE OF HYDROGEN, HELIUM, AND RUSSELL MIXTURE AT HIGH TEMPERATURES AND PRESSURES*

R. E. MARSHAK, P. M. MORSE, AND H. YORK
University of Rochester, Massachusetts Institute of Technology, University of California
Received November 14, 1949

ABSTRACT

Several improved tables of the equation of state of a Russell mixture of elements with and without hydrogen and helium have been computed. Account has been taken of electron screening and the conversion of bound states into free states due to the proximity of neighboring atoms at sufficiently high densities.

It has been shown[1] that the central temperatures and densities in stars are appreciably altered by taking account of the variation of guillotine factor throughout the star as compared with previous simplified models which had assumed a constant guillotine factor. For this reason, one of us prepared improved tables[2] of the opacity for mixtures of elements likely to occur in stars. Thus far, most calculations on stellar interiors have assumed the constancy of the average molecular weight. While the effect of the variation of the molecular weight on the central temperatures and densities will probably not be so important as the variation of the guillotine factor, nevertheless improved tables of the equation of state of mixtures of hydrogen, helium, and Russell combination of heavy elements may prove useful for future astrophysical calculations. It is the purpose of the present note to supply several such improved tables.

Many years ago Strömgren[3] made simplified calculations of the equation of state for a Russell mixture for a limited range of temperature and density. He used hydrogenic wave functions and did not correct for the presence of other electrons in the atomic orbit (screening) and for the conversion of bound states into free states by the proximity of other atoms (at high densities). These quantum-mechanical refinements are troublesome to introduce but appreciably alter previous results in certain regions of temperature and density. We proceed to outline briefly the rather "hybrid" method[4] used to obtain improved tables of the equation of state for a rather wide range of temperature and density.

The pressure (cf. n. 2; we restrict ourselves to electron pressure, since the heavy-particle pressure is easy to compute and is merely additive) due to a mixture of elements, each having a charge Z, is written as follows:

$$p = \frac{R\rho T}{\mu}, \tag{1}$$

* This is a brief report of work carried out in 1941; while the tables are not so extensive as originally planned, they seem of sufficient interest to publish at the present time.

[1] G. Blanch, A. Lowan, R. Marshak, and H. Bethe, *Ap. J.*, **94**, 37, 1941; cf. also L. Henrich, *Ap. J.*, **96**, 106, 1942; and M. Schwarzschild, *Ap. J.*, **104**, 203, 1946.

[2] P. M. Morse, *Ap. J.*, **92**, 27, 1940.

[3] *Zs. f. Ap.*, **4**, 118, 1932.

[4] A completely consistent method would be to use the Thomas-Fermi method to determine the pressure, not merely the cutoff energy (cf. R. E. Marshak and H. A. Bethe, *Ap. J.*, **91**, 239, 1940; and more recently R. Feynman, N. Metropolis, and E. Teller, *Phys. Rev.*, **75**, 1561, 1949). Or another method would be to write down the complete partition sum and evaluate the pressure from it. We have adopted a "hybrid" approach, using features of both methods, in order to avoid extremely laborious calculations.

with

$$\frac{1}{\mu} = \sum_Z \left\{ \frac{\sigma_Z}{M_Z} \sum_{n_Z} \left[\frac{2n_Z^2}{1 + A\, e^{\chi_n^{(Z)}/kT}} \right] \right\}. \tag{1a}$$

In equations (1) and (1*a*) T is the temperature, ρ the density, R the gas constant, σ_Z the concentration of element Z by weight, M_Z the atomic weight of Z, n_Z the principal quantum number, $kT \log A$ the Fermi energy, and, finally,

$$\frac{\chi_n^{(Z)}}{kT} = \left[\left(\frac{Z_e}{n_Z} \right)^2 - E_c^{(Z)} \right] \cdot \frac{0.157}{T},$$

where Z_e is the effective nuclear charge, E_c^Z is the Thomas-Fermi correction (discussed below) in atomic units, and T is measured in millions of degrees. The summation over n_Z is over all bound states of all atoms of the mixture. The quantity μ is essentially the average molecular weight.

The calculation of μ proceeds in successive steps as follows:

1. Approximate values of $[\chi_n^{(Z)}/kT]$ are chosen. $E_c^{(Z)}$ is determined as a function of temperature and density in a manner described below, while Z_e is taken as Z for low densities and high temperatures and as Z_{eff} for the normal atom for high densities and low temperatures. An approximate value of A is found from the implicit equation

$$\frac{2}{\sqrt{\pi}} \int^{\infty} \frac{\sqrt{x}\, dx}{(1 + e^x/A)} = 1.21 \cdot 10^8 \frac{\rho}{T^{3/2}} \sum_Z \left\{ \frac{\sigma_Z}{M_Z} \sum_{n_Z} \left[\frac{2n_Z^2}{1 + A\, e^{\chi_n^{(Z)}/kT}} \right] \right\}. \tag{2}$$

Equation (2) is rigorous if the $\chi_n^{(Z)}$'s are exact and follows from the fact that the electrons obey Fermi-Dirac statistics.

2. Once approximate values of $\chi_n^{(Z)}/kT$ and A are given, the probability, P_n, that an electron is in a certain orbit is found from

$$P_n^{(Z)} = \frac{1}{1/A\, e^{\chi_n^{(Z)}/kT} + 1}. \tag{3}$$

3. Using these $P_n^{(Z)}$'s, the Z_e's are recomputed for the various states on the basis of Slater's screening constants[5]—weighing each screening constant by the appropriate $P_n^{(Z)}$ and distinguishing among s, p, d, . . . , electrons.

4. New values of $\chi_n^{(Z)}/kT$ are computed and thereby a new A (from eq. [2]).

5. The process is continued until there is no appreciable change in the $\chi_n^{(Z)}/kT$'s and A.

Utilizing the procedure outlined above, we have computed $(1/\mu)$ for the following four mixtures (the concentrations are all by weight): (I) pure Russell mixture; (II) Russell mixture 64 per cent, hydrogen 36 per cent; (III) Russell mixture 15 per cent, hydrogen 45 per cent, helium 40 per cent; (IV) Russell mixture 35 per cent, hydrogen 35 per cent, helium 30 per cent. The first two cases were investigated for a range of T from $10^{5.6}$ to $10^{7.6}$ and of ρ from 10^{-3} to $10^{2.5}$. The results are given in Tables 1 and 2, respectively. The results for Mixtures III and IV are presented in Tables 3 and 4, respectively. The last two cases were not investigated so thoroughly because hydrogen and helium are almost always completely ionized, and for an arbitrary mixture it almost suffices to use the formula

$$\frac{1}{\mu} = \sigma_H + 0.5\sigma_{He} + \frac{\sigma_R}{\mu_R}, \tag{4}$$

[5] J. C. Slater, *Phys. Rev.*, **36**, 57, 1930.

TABLE 1

log ρ	log T 1/μ										
	5.6	5.8	6.0	6.2	6.4	6.6	6.8	7.0	7.2	7.4	7.6
2.5	0.370	0.370	0.370	0.370	0.370	0.375	0.386	0.391	0.426	0.457	0.476
2.0	.335	.335	.335	.335	.337	.352	.390	.395	.456	.469	.484
1.5	.250	.252	.258	.266	.219	.366	.411	.445	.469	.478	.493
1.0	.059	.097	.142	.211	.300	.381	.431	.470	.484	.492	.495
0.5	.092	.131	.209	.276	.348	.398	.461	.478	.492	.495	.495
0	.119	.160	.253	.297	.375	.444	.473	.485	.496	.496	.496
−0.5	.169	.228	.291	.358	.417	.461	.480	.488	.496	.496	.496
−1.0	.206	.261	.333	.389	.444	.478	.488	.491	.496	.496	.496
−1.5	.238	.300	.350	.398	.455	.485	.489	.492	.496	.496	.496
−2.0	.253	.338	.370	.412	.464	.488	.489	.494	.496	.496	.496
−2.5	.280	.339	.391	.425	.477	.492	.492	.494	.496	.496	.496
−3.0	0.314	0.356	0.402	0.439	0.485	0.492	0.492	0.496	0.496	0.496	0.496

TABLE 2

log ρ	log T 1/μ										
	5.6	5.8	6.0	6.2	6.4	6.6	6.8	7.0	7.2	7.4	7.6
2.5	0.597	0.597	0.597	0.597	0.598	0.600	0.607	0.610	0.636	0.652	0.665
2.0	.574	.574	.574	.574	.576	.585	.610	.613	.652	.660	.670
1.5	.520	.521	.525	.530	.500	.594	.623	.645	.660	.666	.675
1.0	.398	.422	.451	.495	.552	.604	.636	.661	.670	.675	.677
0.5	.419	.444	.494	.537	.583	.615	.655	.666	.675	.677	.677
0	.372	.422	.508	.550	.600	.644	.663	.672	.677	.677	.677
−0.5	.439	.492	.537	.589	.627	.655	.667	.672	.677	.677	.677
−1.0	.481	.521	.571	.607	.644	.666	.672	.674	.677	.677	.677
−1.5	.506	.550	.583	.614	.651	.670	.673	.675	.677	.677	.677
−2.0	.522	.574	.597	.624	.657	.673	.673	.676	.677	.677	.677
−2.5	.539	.577	.610	.632	.665	.675	.675	.676	.677	.677	.677
−3.0	0.561	0.588	0.617	0.641	0.670	0.675	0.675	0.677	0.677	0.677	0.677

TABLE 3

log ρ	log T	1/μ	log 0	log T	1/μ	log ρ	log T	1/μ
−3.0	5.8	0.702	−1.0	6.4	0.717	1.0	6.8	0.716
	6.0	.710		6.6	.720		7.2	.723
−2.5	5.8	.700	−0.5	6.4	.708	1.5	7.0	.717
	6.2	.716		6.8	.721		7.4	.722
−2.0	6.0	.706	0	6.6	.718	2.0	7.2	.716
	6.4	.721		7.0	.720		7.6	.725
−1.5	6.2	.709	0.5	6.8	.716	2.5	7.2	.714
	6.6	0.724		7.2	0.725		7.6	0.721

where $1/\mu_R$ is obtained from Table 1. The extensive values of $1/\mu$ given in Table 2 and the scattered values of $1/\mu$ found in Tables 3 and 4 show up the slight deviations and make interpolation easier for an arbitrary combination of hydrogen, helium, and Russell mixture.

Several remarks should be made about Tables 1 and 2. In general, as T increases, ρ increases because both A and $\chi_n^{(Z)}$ decrease until, at the lower R.H.S. of each table, the maximum value is attained, i.e., complete ionization. As ρ increases, the region of complete ionization decreases in extent (with respect to T); this is due to the rapid increase of A with ρ. Eventually, for sufficiently large ρ (higher than that covered in the two tables), complete ionization is attained for all T, owing to the extremely large values of $E_e^{(Z)}$ (i.e., pressure ionization). As the temperature is lowered for moderate densities, the tendency to ionize diminishes. At first, the K-shell of *Fe* is filled, then other shells of other atoms are filled, and $1/\mu$ becomes quite small. This effect is due partly to increasing A and partly to increasing $\chi_n^{(Z)}$. As ρ is increased at the lower temperatures, $E_e^{(Z)}$ increases and finally overtakes $(Z_e/n_Z)^2$, first for the lightest element and then for the

TABLE 4

log ρ	log T	$1/\mu$	log ρ	log T	$1/\mu$	log ρ	log T	$1/\mu$
−3.0	5.8	0.607	−1.0	6.4	0.653	1.0	6.8	0.653
	6.0	.640		6.6	.666		7.2	.670
−2.5	5.8	.620	−0.5	6.4	.645	1.5	7.0	.658
	6.2	.642		6.8	.669		7.4	.665
−2.0	6.0	.628	0	6.6	.649	2.0	7.2	.661
	6.4	.657		7.0	.664		7.6	.671
−1.5	6.2	.644	0.5	6.8	.659	2.5	7.2	.651
	6.6	0.672		7.2	0.668		7.6	0.669

heavier ones. This causes a sudden jump from practically zero ionization for a certain shell clear up to complete ionization. This effect is due to the fact that all negative values of $\chi_n^{(Z)}$ are taken as $-\infty$, so that, no matter how large A is, $Ae^{\chi_n^{(Z)}/kT} = 0$. Thus, for low temperatures $2n_Z^2/[1 + Ae^{\chi_n^{(Z)}/kT}]$ is equal to 0 or $2n_Z^2$, and, since $E_e^{(Z)}$ does not change with T at these low temperatures, $1/\mu$ stays constant over a wide range of values from $T = 0$ up to a maximum T where the ionization of other shells starts to play a role; $1/\mu$ then begins its usual increase with increasing T. It sometimes happens that as T and Z_e increase, $(Z_e/n_Z)^2$ becomes larger than $E_e^{(Z)}$, in which case $1/\mu$ suddenly falls and then recommences its usual slow increase. It is this phenomenon which is responsible for the fluctuations in value of $1/\mu$ at the L.H.S. of each table.

We must now discuss how $E_e^{(Z)}$ is determined, where $E_e^{(Z)}$ is the depression in atomic energy units of the lower limit of the continuum of free states (and therefore the amount which must be subtracted from the energy of the bound states). To determine $E_e^{(Z)}$, we use the Thomas-Fermi model of the atom, generalized to include the effect of high temperatures and subject to finite boundary conditions as for electrons in metals.[6] Using the same notation as in the quoted reference, the Thomas-Fermi equation with finite temperature may be written

$$\frac{d^2\phi}{dx^2} = \frac{\phi^{3/2}}{x^{1/2}}\left(1 + \beta\,\frac{x^2T^2}{\phi^2}\right), \tag{5}$$

[6] Marshak and Bethe, *op. cit.*

where

$$\phi = \frac{r}{Ze^2}(\zeta + eV),$$

$$x = \frac{r}{a}, \quad a = \left(\frac{9\pi^2}{128}\right)^{1/3} a_0 Z^{-1/3} \qquad (a_0 = \text{Bohr radius}),$$

$$\beta = \frac{3^{4/3}\pi^{10/3}}{2^{29/3}Z^{8/3}}\left(\frac{k}{Ry}\right)^2 \qquad (Ry = \text{Rydberg energy}).$$

In equation (5), r is the distance of an electron from the nucleus, ζ the Fermi energy, and eV the potential energy. Equation (5) must be solved subject to the boundary conditions:

$$(A) \quad \phi(0) = 1; \qquad (B) \quad \phi' = \frac{\phi}{x} \text{ at } x = X,$$

TABLE 5

ρ	B	T (in Units of 10^6)	X	ϕ_X	$\phi^X/X = \phi'_X$
10	0	$\frac{1}{3}$	0.785	2.164	2.75
10	0	1	.635	1.978	3.12
10	0	3	.375	1.636	4.36
10	0	9	.202	1.451	7.19
25	−2	0.6	.574	3.098	5.40
25	−2	1	.524	2.916	5.56
25	−2	3	.370	2.392	6.46
25	−2	9	.229	2.075	8.76
25	−2	15	.170	1.889	11.12
52.6	−5	1	.451	4.139	9.19
52.6	−5	3	.387	3.724	9.63
52.6	−5	9	.217	2.615	12.02
52.6	−5	25	.126	2.127	16.78
121	−10	2	.346	5.208	15.05
121	−10	10	.214	3.730	17.41
121	−10	25	0.121	2.613	21.54

where X is the boundary of the atom. Sixteen numerical integrations of equation (5) were carried out for various values of B ($-B$ is the derivative of ϕ with respect to x at $x = 0$ and is a measure of the density ρ; cf. Table 5) and T. It was assumed that $Z = 1$; however, from the relations given after equation (5) it is possible to interpret the results for different Z, provided that one assigns a different ρ to the specified B and scales the temperature according to $Z^{4/3}$. The results are tabulated in Table 5.

The quantity in which we are interested, namely, $E_c^{(Z)}$, is related to the quantities given in Table 5 as follows:[2]

$$E_c^{(Z)} = 2.26Z^{4/3}(\phi'_X - \Delta B). \tag{6}$$

In equation (6), ϕ'_X is the derivative of ϕ with respect to x at the boundary of the atom X, and ΔB is the difference between the value of B found from Table 5 and 1.588—the

TABLE 6

LOG $\rho = 1.0$

LOG T	$E_c^{(Z)}$			
	$Z=1$	$Z=2$	$Z=8$	$Z=12, 14, 20, 26$
6.4	5.6	6.3	7.8	8.2
6.6	7.6	8.3	9.8	10.2
6.8	10.3	11.0	12.5	13.0
7.0	13.4	14.1	15.6	16.0
7.2	16.0	16.7	18.2	18.7
7.4	18.5	19.2	20.7	21.2
7.6	20.5	21.2	22.7	23.2

LOG $\rho = 1.5$

LOG T	$E_c^{(Z)}$			
	$Z=1$	$Z=2$	$Z=8$	$Z=12, 14, 20, 26$
6.8	9.3	10.8	14.7	17.0
7.0	12.4	13.9	17.8	20.1
7.2	15.9	17.4	21.3	23.6
7.4	23.7	25.2	29.1	31.4
7.6	45.0	46.5	50.4	52.7

LOG $\rho = 2.0$

LOG T	$E_c^{(Z)}$			
	$Z=1$	$Z=2$	$Z=8$	$Z=12, 14, 20, 26$
6.8	10.1	13.0	19.8	23.6
7.0	12.6	15.5	22.3	26.1
7.2	15.9	18.8	25.6	29.4
7.4	22.2	25.1	31.9	35.7
7.6	39.1	42.0	48.8	52.6

LOG $\rho = 2.5$

LOG T	$E_c^{(Z)}$			
	$Z=1$	$Z=2$	$Z=8$	$Z=12, 14, 20, 26$
6.8	11.6	15.6	28.1	36.6
7.0	13.6	17.6	30.1	38.6
7.2	16.4	20.4	32.9	41.4
7.4	21.2	25.2	37.7	47.2
7.6	33.0	37.0	49.5	58.0

value of B for the free atom ($\rho = 0$). We must still show how to evaluate the X_Z's (and therefore ϕ'_{X_Z} and B_Z), once ρ is specified. We have, rigorously, for a mixture of elements,

$$\rho = \frac{3\, m_H}{4\pi \sum_Z \sigma_Z R_Z^3 / M_Z}, \tag{7}$$

where m_H is the mass of the hydrogen atom, σ_Z is the concentration by weight of element Z, and R_Z is the radius of the atom Z. In the Thomas-Fermi model R_Z is roughly proportional to $Z^{1/3}$, so that we may substitute

$$R_Z = \left(\frac{9\pi^2}{128}\right)^{1/3} a_0 X_1 Z^{1/3}$$

($[9\pi^2/128]^{1/3} a_0 X_1$ is the radius of the hydrogen atom) into equation (7), yielding

$$\rho = \frac{32\, m_H}{3\pi^3 a_0^3 X_1^3 \sum_Z \sigma_Z Z / M_Z}. \tag{8}$$

Now, for hydrogen $Z/M_Z = 1$, while for helium and the heavier elements $Z/M_Z = \frac{1}{2}$; therefore, to a good approximation, equation (8) becomes

$$\rho = \frac{64\, m_H}{3\pi^3 a_0^3 X_1^3 (1 + \sigma_H)}. \tag{9}$$

Equation (9) determines X_1 and hence ϕ_{X_1}; if we further require that the Fermi energy and the potential be the same at the edge of each atom, we have

$$Z^{1/3} \phi'_{X_Z} = \phi'_{X_1}. \tag{10}$$

Equation (10) enables us to find X_Z and hence the quantities needed in equation (6) to determine $E_c^{(Z)}$. In this fashion, we have calculated the $E_c^{(Z)}$'s for hydrogen, helium, and the elements of the Russell mixture for a wide range of ρ and T. The results are given in Table 6 and were fed into the calculations on the equation of state discussed earlier. It might be remarked that the $E_c^{(Z)}$'s for densities below 10 need not be corrected for the temperatures contemplated in investigations of stellar structure and so may be taken from earlier work on the subject.[2]

We wish to thank Mr. W. Pratt and Miss M. Ramsey for assistance with the numerical calculations. One of the authors (R. E. M.) acknowledges with gratitude the receipt of a Sigma Xi grant-in-aid (1941) in support of the present work.

RADIAL VELOCITIES OF 2111 STARS

RALPH E. WILSON AND ALFRED H. JOY
Mount Wilson and Palomar Observatories
Received December 19, 1949

ABSTRACT

Herein are presented radial velocities and spectral classifications of 2111 stars, determined from observations with the 60-inch and 100-inch reflectors of the Mount Wilson Observatory.

Since the erection of the 60-inch telescope in 1908 a considerable portion of its time has been devoted to observations for determining stellar radial velocities. Beginning with the stars with measured parallaxes, the program was early expanded to include all the stars fainter than 5.5 visual magnitude of spectral classes F–M in the Boss *Preliminary General Catalogue* and all other stars with proper motions known to exceed 0".1 per year. In 1934 the Mount Wilson Observatory agreed to determine the velocities of 437 stars in Kapteyn's Selected Areas. Less extensive programs added at various times covered the stars in the four moving clusters, Hyades, Pleiades, Praesepe, and Perseus, and visual double stars in which the separation is large enough to permit observation of both components. Since 1918 the use of the 100-inch telescope has facilitated the observation of the fainter stars.

The more extensive lists of radial velocities resulting from these programs are as follows:

W. S. ADAMS and A. KOHLSCHUTTER. 100 stars with measured parallaxes. *Mt. W. Contr.*, No. 79; *Ap. J.*, **39**, 341, 1914.
W. S. ADAMS. 500 stars. *Mt. W. Contr.*, No. 105; *Ap. J.*, **42**, 172, 1915.
W. S. ADAMS and A. H. JOY. 1013 stars. *Mt. W. Contr.*, No. 258; *Ap. J.*, **57**, 149, 1923.
W. S. ADAMS, A. H. JOY, R. F. SANFORD, and G. STRÖMBERG. 741 stars. *Mt. W. Contr.*, No. 387; *Ap. J.*, **70**, 207, 1929.
W. H. CHRISTIE and O. C. WILSON. 600 stars. *Mt. W. Contr.*, No. 593; *Ap. J.*, **88**, 34, 1938.
A. H. JOY. 181 dwarf stars. *Mt. W. Contr.*, No. 726; *Ap. J.*, **105**, 96, 1947.
R. E. WILSON. 204 stars in the Hyades. *Mt. W. Contr.*, No. 741; *Ap. J.*, **107**, 119, 1948.

By 1942 there had accumulated in our files one or more plates of a large number of stars taken for a variety of reasons, but the observations had not been completed, and none of the work on the Kapteyn areas had been published. At that time the unfinished work was incorporated in one general program under the supervision of R. E. Wilson.

The observations from 10 to 24 hours of right ascension and from declination $-25°$ to the pole are now complete. Some work remains to be done from 0 to 10 hours of right ascension, mainly in 6–8 hours, the region covered during our poorest observing season, but the accumulation of velocities has become so great that it seems advisable to make the results available now.

Most of the velocities are based upon plates taken with dispersions of 38 or 75 A/mm at $H\gamma$. For a few of the faintest stars we have also used 120 A/mm, and for a few of the brightest stars the 10 A/mm of the coudé spectrograph at the 100-inch. All the members of the spectrographic department have shared in securing the spectrograms, but since 1942 R. E. Wilson has taken most of them. The completion of the measures of the plates obtained during the war years and those taken since is principally due to the valued assistance of Mary F. Coffeen, A. Louise Lowen, and Sylvia Burd. The classifications of spectra were made by A. H. Joy. The velocities of the early B stars and the interstellar velocities are mainly from the work of P. W. Merrill and R. F. Sanford.

The columns of the table need but little explanation. In the first column, "A" denotes Aitken's *New General Catalogue of Double Stars;* "B," Boss's *Preliminary General Catalogue;* "C," *Publications of the Cincinnati Observatory*, Volume **18;** and "G," the Boss *General Catalogue of Positions and Proper Motions*. For stars not in one of these four catalogues the BD numbers are given, the initials being omitted. The principal source of the magnitudes is the *Henry Draper Catalogue;* that of the proper motions, the Boss *General Catalogue*. In the tenth column, "r" denotes a revision of an earlier published value on the basis of additional plates or measures, and an asterisk calls attention to the notes following the table. In the last column, which gives radial velocities published by other institutions, and in the notes the following symbols are used: "B," Bonn; "D," Dunlap (Toronto); "L," Lick; "M," Moore's *General Catalogue;* "Md," McDonald; "Mi," Michigan; "O," Ottawa; "S," Simeis (Pulkova); "V," Victoria; "W," Mount Wilson; "Y," Yerkes. Velocities from the individual plates of spectroscopic binaries, interstellar (IS) velocities, and comments on the spectra are given in the notes.

TABLE I

RADIAL VELOCITIES OF 2111 STARS

STAR	H.D.	1950 R.A.	Decl.	Vis. Mag.	P.M.	Spec.	Vel.	P.E.	No. Pl.	Others
		h m	° ′		″		km	km		
B 6176	225009	0 00.0	+65 49	6.0	0.011	gG5	- 17.6	1.0	5r	
G 17	225094	00.8	+63 22	6.3	.062	cB2e	- 39.4	1.3	7•	- 47.9 V
G 24	225136	01.3	+66 26	6.6	.021	gM4	+ 13.6	0.9	2	+ 17.6 D
B 6182	225212	01.9	-10 47	5.2	.010	gK5	- 42.0	2.1	4	- 41.9 L
G 61	26	02.8	+ 8 30	8.2	.258	sgG2p	-213.4	0.7	3•	
G 98	203	0 04.3	-23 23	6.1	.116	dA7	- 2.9	1.7	3	
72° 1140	219	04.5	+72 56	8.0	---	dF2n	- 20.8	2.2	4	
G 118	245	05.4	+86 31	9.2	.329	dF7	- 80.3	1.9	3	
G 126	360	05.7	- 9 06	6.1	.064	gG8	+ 20.9	0.1	3	
G 131	400	06.1	+36 21	6.1	.179	dF5	- 14.0	1.2	3	- 14.5 SV
G 139	404	0 06.3	+66 11	8.4	.176	dK2	- 59.2	1.7	3	
G 181	645	08.2	-12 51	5.9	.155	dK1	+ 4.9	0.1	3	
B 26	877	10.5	-22 45	6.7	.018	gG4	- 16.	var	4•	
ι Peg	886	10.7	+14 54	2.9	.010	B2	+ 2.9	0.6	12•	+ 4.8 L
G 268	1015	11.9	-14 42	7.0	.140	dF8	- 1.0	0.6	3	
G 273	1037	0 12.1	-15 05	6.9	.097	gG8	- 29.3	0.9	3	
G 278	1051	12.3	-14 27	6.9	.090	gA8	- 9.0	1.5	3	
15° 30	1213	14.0	+15 34	8.2	.032	gFo	- 4.6	1.1	3	
A 237A	1309	14.8	+16 14	8.4	.044	dG4	- 3.	var	4•	
A 237B	----	14.8	+16 14	9.0	---	dG5	- 2.8	0.8	3	
σ And	1404	0 15.7	+36 30	4.5	.074	A2n	- 3.5	2.1	4r	- 9.9 M
A 252A	1429	15.9	+25 52	7.6	.055	dA6n	- 11.2	0.7	3•	
A 252B	----	15.9	+25 52	8.0	---	dF2	- 9.2	1.5	3	
A 257A	1450	16.1	+15 42	9.0	.042	dF4	+ 10.2	1.0	3	
A 257B	----	16.1	+15 42	9.0	---	dF4	+ 10.2	0.8	4	
A 285A	1641	0 18.3	+32 42	7.0	.063	dF4	- 6.4	1.0	2	- 3.0 D
49° 73	----	22.5	+49 50	8.6	.104	dK3	- 64.6	0.3	3	
B 75	2140	23.1	+ 7 25	7.2	.062	gK3	- 17.2	2.0	4	
30° 60	2343	24.8	+30 28	8.4	.025	gG7	- 22.2	2.5	4•	
G 550	2454	25.7	+ 9 55	6.0	.207	dF3	- 11.5	0.9	4r	- 9.4 V
74° 14	2520	0 27.0	+74 58	8.2	---	dGo	- 61.6	1.1	3	
B 88	2629	27.4	- 1 24	7.5	.167	dF1	- 0.2	1.1	3	
G 600	2663	28.2	+69 31	7.4	.309	dF8	+ 10.6	0.6	3	
G 611	2767	28.8	+33 18	6.1	.048	gG8	+ 5.3	0.1	3	+ 11.6 D
G 633	2880	29.6	- 5 27	8.7	.272	dG8	- 10.1	0.9	3	
K Cas	2905	0 30.1	+62 39	4.2	.000	cBoe	- 1.1	2.1	3•	- 4.1 M
G 650	2952	30.4	+54 37	6.1	.079	gG8	- 34.1	0.3	3	- 34.5 D
G 685	----	32.2	+78 59	9.0	.167	dG7	+ 14.0	2.2	4	
A 486A	3165	32.5	+36 33	6.8	.020	gK1	- 8.4	0.9	3	
A 486B	----	32.5	+36 33	8.8	---	gG5	- 7.4	1.9	2	
B 117	3229	0 33.0	- 0 47	5.9	.144	dF7	+ 7.2	1.4	3	+ 4.3 S
B 126	3440	35.9	+82 13	6.4	.143	dF8	- 33.6	0.9	3	- 34.6 V
13° 26	----	36.2	+74 29	9.1	---	dG4	+ 0.1	0.5	3	
62° 130	3637	36.8	+62 57	7.7	.304	dF5	- 28.1	1.9	3	
A 562A	3743	37.7	+23 47	7.2	.034	dA5	- 3.5	1.7	3	
A 562B	----	0 37.7	+23 47	8.6	---	dF2n	- 1.8	1.7	2	
G 800	3765	38.1	+39 55	7.5	.752	dK5	- 62.7	0.4	7r	
G 825	3856	39.1	+65 52	5.9	.006	gKo	- 4.2	0.4	3	- 1.0 D
A 608A	4096	40.9	- 1 10	9.2	.312	dG3	- 52.6	1.2	3	
39° 166	4143	41.5	+40 25	8.8	.023	gM1	- 55.4	1.2	3	
G 926	4362	0 43.8	+59 18	6.5	.009	cF9	- 14.3	1.8	2	- 15.5 D
G 943	4440	44.9	+72 24	6.0	.134	sgKo	+ 3.6	0.7	3	+ 0.9 D
45° 202	4514	44.9	+45 28	8.4	.022	gK2	- 13.9	0.2	3	
G 950	4585	45.2	-18 20	5.9	.054	gK3	+ 2.1	1.3	3	
B 174	4676	46.3	+16 40	5.2	.201	dF6	+ 4.7	2.3	3	+ 4.6 L
A 679A	4732	0 46.8	-24 24	6.1	.088	gK2	+ 23.4	1.9	3	
B 179	4775	47.7	+63 59	5.4	.033	dF1	+ 4.8	1.6	4	+ 2.2 LV
73° 39	----	48.0	+74 12	9.4	---	gG5	+ 17.0	1.9	3	
G 1012	4741	48.1	+78 21	8.2	.228	dG7	+ 4.9	1.4	3	
G 1017	4841	48.4	+63 31	7.1	.030	cB5	- 22.3	2.6	5•	- 29.6 V
A 716A	5058	0 49.8	-22 53	7.6	.229	dGo	- 22.8	2.0	4	
55° 191	5005	50.0	+56 21	7.7	---	O6	- 26.2	2.9	7	- 21.1 V
G 1066	5129	50.8	+43 06	7.2	.286	dGo	- 10.	var	4•	
A 735A	5128	50.9	+52 25	6.2	.076	gA8	- 4.4	0.5	2	- 1.2 V
A 735B	----	50.9	+52 25	9.2	---	dG4	- 2.0	2.0	2	

TABLE I (Cont'd)

STAR	H.D.	1950 R.A.	1950 Decl.	Vis. Mag.	P.M.	Spec.	Vel.	P.E.	No. Pl.	Others
		h m	° ′		″		km	km		
G 1103	5384	0 53.2	- 7 37	6.0	0.043	gK5	+ 2.4	1.6	3	
-0° 145	5520	54.5	+ 0 11	8.0	.008	dF3	+ 8.4	2.5	4	
G 1141	5543	54.7	+ 1 07	8.0	.018	dF2	+ 0.3	1.1	3	
-0° 146	5544	54.7	+ 0 04	7.7	.021	dK1	- 12.7	2.0	3	
A 806A	5659	55.7	-15 57	7.7	.027	dF6	+ 0.1	0.4	3	
A 806B	----	0 55.7	-15 57	7.8	.025	dF7	- 2.6	2.0	3	
G 1190	5715	57.1	+70 43	6.5	.087	A4n	+ 9.	5.7	4	+ 2.1 V
59° 163	5797	57.5	+60 11	8.8	.014	gA8	- 8.6	1.9	5	
G 1212	5839	58.2	+69 05	6.7	.002	B9	+ 4.9	1.0	3	
60° 145	5890	58.4	+60 47	8.9	.049	dF1n	+ 1.5	1.8	4	
G 1232	5817	0 59.1	+81 50	8.4	.190	dG2	- 51.2	0.9	3	
B 222	6077	59.5	+ 7 40	7.8	.041	gG9	+ 24.	var	4•	
G 1244	5996	59.6	+68 58	8.1	.278	dG7	- 20.2	1.1	3	
G 1271	6226	1 01.0	+47 22	6.7	.003	B6	- 52.	var	5•	- 56.v VS
G 1279	6210	01.2	+61 19	5.9	.071	dF5	- 19.2	0.8	3	- 14.8 D
A 875A	6288	1 01.2	+ 1 06	6.1	.123	dA8n	+ 8.0	1.4	2	+ 3.5 V
A 875B	----	01.2	+ 1 06	9.0	---	dG8	+ 6.4	0.1	3	
G 1290	6301	01.7	+29 24	6.1	.139	dF6	- 5.0	0.7	3•	+ 4.1 S
B 234	6397	02.4	+14 41	5.6	.052	dF0	- 1.6	0.7	3•	+ 5.9 V
A 903A	6479	03.2	+ 4 39	6.8	.117	dF4	- 5.5	0.5	3	- 9.9 V
A 903B	6480	1 03.3	+ 4 39	7.6	.117	dF5	- 14.3	2.2	3	- 7.8 D
A 918AB	6586	04.3	+38 23	7.3	.046	dF8	+ 13.9	1.0	3	
A 923A	6651	04.6	- 2 00	7.5	.066	dF6	- 6.8	0.8	3	
A 923B	----	04.6	- 2 00	8.3	.062	dG3	- 1.5	1.8	3	
G 1415	6955	07.6	+25 12	6.1	.112	gK5	+ 4.6	0.8	4	+ 6.4 D
B 265	6972	1 08.4	+64 45	5.5	.026	B8n	+ 5.0	2.0	6	- 7. LY
A 988A	7215	10.1	+31 49	6.6	.008	•	- 2.	var	4•	
G 1472	7252	10.9	+60 37	7.3	.048	B3	- 1.4	1.2	2•	- 3. V
G 1475	7307	11.1	+26 52	8.7	.043	gM5	+ 27.5	1.3	4	
A 1023A	7651	13.8	- 7 25	9.8	.036	dG0	+ 9.2	0.9	3	
A 1023B	----	1 13.8	- 7 25	9.9	---	dG0	+ 9.2	2.3	3	
G 1562	7623	15.1	+76 32	7.6	.024	gK0	- 77.2	1.7	3	
B 292	7732	16.1	+77 18	6.4	.092	gG4	- 71.9	0.8	3	- 75.6 D
14° 252	7920	16.2	-13 40	8.1	.032	dK2	+ 14.5	1.5	3	
75° 58	7924	17.8	+76 26	7.3	---	dK0	- 22.2	1.9	3	
G 1626	8142	1 18.2	-14 09	7.0	.057	gG4	+ 7.6	1.6	5	
C 175	8249	19.3	+14 56	8.3	.276	dG2	+ 9.9	0.4	3	
C 176	8249	20.2	+67 51	8.8	.14:	dG5	+ 8.6	2.2	4	
13° 249	8389	20.6	-13 13	8.3	---	dK0	+ 31.1	1.5	3	
G 1697	8556	21.8	- 7 10	6.0	.038	dF2	+ 28.1	0.8	3	
G 1729	8671	1 23.4	+43 12	6.1	.116	dF6	+ 31.7	0.2	2	+ 30.0 DV
B 320	8779	23.9	- 0 39	6.5	.040	gK0	- 5.9	0.7	6r	
29° 240	8806	24.7	+30 15	8.5	.066	dF0	- 8.6	0.3	3	
G 1762	8730	25.0	+73 57	7.3	.229	dG5	+ 24.4	1.7	3	
30° 230	9023	26.6	+30 38	8.3	.112	dF3	+ 4.2	1.9	3	
G 1804	9070	1 27.0	+30 45	8.2	.226	dG5	+ 12.3	1.7	3	
29° 252	----	27.3	+30 06	8.5	.013	gM2.5	- 19.1	0.7	3	
AA Psc	9138	27.6	+ 5 53	5.1	.292	gK4	+ 36.8	0.9	6r	+ 36.0 M
G 1825	9105	27.9	+63 05	7.5	.019	e8Se	- 38.6	1.8	10•	- 38.8 V
29° 256	9269	28.9	+30 22	8.4	.073	gK0	+ 43.7	1.1	7	
29° 260	9485	1 30.8	+30 09	8.1	.028	A4n	+ 13.	var	4•	
G 1883	9540	30.9	-24 26	7.0	.330	dG8	+ 0.4	0.6	3	
G 1888	9563	31.2	- 7 17	5.9	.198	dG2	- 15.1	0.9	3	
B 340	9631	31.4	+36 59	5.8	.015	B9n	- 4.	4.4	5•	
A 1227AB	----	31.6	+34 24	9.3	---	dG5	- 28.2	0.8	3	
G 1905	9990	1 32.2	+55 47	7.1	.023	B9	+ 6.0	0.7	6	
G 1977	9996	35.5	+45 09	6.3	.040	cA0	- 1.6	2.2	4•	+ 3.0 D
G 1986	10015	36.1	+64 54	8.4	.299	dG6	- 57.7	1.9	4	
53° 364	10031	36.1	+54 21	7.4	.010	A4n	- 3.4	1.3	6	
55° 375	10063	36.5	+55 32	7.6	.018	B8	- 31.8	1.0	6	
B 364	10148	1 36.5	-21 32	5.7	.126	A4n	+ 18.	3.4	5•	
G 2003	10126	36.8	+27 51	7.9	.534	dG6	+ 55.1	1.3	4r	
44° 547	10212	37.8	+44 45	8.2	.079	gK0	- 26.5	2.3	4	
44° 552	10322	38.8	+45 20	8.8	.014	cK3	- 26.4	0.5	3	
B 374	10332	39.2	+60 18	7.4	.007	gK1	+ 5.5	2.1	4r	+ 3. V

TABLE I (Cont'd)

STAR	H.D.	1950 R.A.	1950 Decl.	Vis. Mag.	P.M.	Spec.	Vel.	P.E.	No. Pl.	Others
		h m	° ′		″		km	km		
G 2103	10495	1 40.5	+55 38	7.4	0.028	dA6	- 19.0	1.8	6	
A 1369A	10668	41.6	+ 9 14	8.3	.157	dF3	+ 2.8	1.1	4	
A 1369B	----	41.6	+ 9 14	8.7	.194	dF4	+ 4.1	1.5	3	
G 2127	10718	42.0	-20 51	7.8	.315	dG4	+ 0.9	1.8	3	
C 242	10785	42.8	-16 09	8.5	.331	dG4	- 7.4	2.0	3	
B 398	10845	1 43.9	+17 10	6.5	.053	dA7n	+ 3.	var	6•	- 8.1 S
G 2196	11037	45.8	+ 3 26	6.0	.023	gG6	+ 2.4	1.0	3	+ 4.0 D
A 1457B	11154	47.4	+22 02	7.4	----	gG5	+ 1.8	1.4	4r	
B 409	11151	47.7	+51 41	5.9	.125	dF3	- 15.5	0.3	2	- 18.4 V
54° 393	11187	48.2	+54 40	7.1	.015	Ao	+ 5.0	0.4	6	
G 2236	11161	1 48.4	+66 12	8.9	.285	dGo	- 3.0	1.1	3	
A 1500A	11430	50.2	+37 05	7.0	.055	dF4	- 13.9	0.9	3	
A 1500B	----	50.2	+37 05	8.4	----	dF6	- 11.0	1.0	3	
B 435	11803	53.3	+ 1 36	6.2	.246	dGo	+ 29.1	1.1	5	+ 30.0 V
G 2357	11928	54.9	+27 34	6.0	.062	gM2	- 4.1	1.7	3	
A 1613AB	12376	1 59.2	+36 29	8.0	.174	dG5	+ 16.8	1.2	3	
B 457	12301	59.3	+64 09	5.6	.006	cB8	- 21.1	0.7	10r•	- 19. V
G 2471	12583	2 00.6	-15 33	5.9	.021	gG5	+ 6.4	1.5	3	
B 470	12558	00.8	+25 42	5.7	.134	dF4	+ 15.8	1.9	3	+ 14.4 S
G 2485	12642	01.2	- 4 21	5.9	.061	cK5	+ 25.0	1.5	3	
G 2489	12509	2 01.3	+64 09	8.0	.006	cB2	- 17.2	1.9	4	
56° 424	12709	02.6	+57 03	8.0	.003	B3	- 19.6	1.9	3	
44° 422	----	03.9	+44 57	9.5	----	dGo	- 11.	3.0	3•	
A 1683A	13294	07.8	+38 48	6.0	.022	Aon	0.	3.6	3	+ 1. V
A 1683B	13295	07.9	+38 48	6.7	.026	Aon	+ 15.6	0.5	2	+ 14. V
B 488	13267	2 08.0	+57 25	6.4	.015	cB8	- 35.2	1.3	8r	- 32.0 V
A 1689A	13357	08.2	+13 27	8.4	.158	dG4	+ 23.7	0.3	3	
A 1689B	----	08.2	+13 27	8.9	.115	dG8	+ 23.1	1.3	5	
G 2623	13456	08.9	-10 17	6.1	.171	dF2	+ 10.9	0.5	3	
G 2631	13403	09.4	+56 58	7.0	.347	dG1	- 34.3	1.8	3r	
B 499	13520	2 10.1	+44 00	5.1	.025	gK3	- 48.3	1.9	3	- 45.8 LV
G 2654	13449	10.3	+66 30	7.7	.127	dKo	- 27.5	1.3	3	
57° 521	13543	10.5	+57 41	8.9	.089	gG6	- 20.4	0.3	3r	
G 2662	13692	10.7	-21 14	6.0	.063	gG6	+ 38.9	1.1	3	
57° 526	13744	12.4	+58 04	7.8	.004	Ao	- 52.0	2.5	5r	
55° 554	13745	2 12.4	+55 46	8.0	.010	B2	- 29.5	1.3	6r•	
56° 469	13831	13.2	+56 30	8.6	.004	cB1	- 43.	var	4r•	
G 2724	13866	13.5	+56 29	7.7	.040	cB2	- 47.0	1.7	5r•	
55° 564	13970	14.3	+56 25	8.6	.006	B3	- 19.	var	6•	
A 1752A	14082	14.5	+28 31	6.6	.099	dF6	+ 5.8	1.5	3	
A 1752B	----	2 14.5	+28 31	7.6	.100	dGo	+ 3.4	0.9	3	
G 2758	14039	14.9	+56 20	8.6	.412	dKo	+ 3.7	1.9	3	
56° 527	----	15.7	+56 54	8.4	.009	B3	- 33.4	1.7	4	
14° 423	14284	15.8	-14 21	8.1	.056	gM5.5	+ 28.1	0.2	3	
B 522	14212	16.0	+47 09	5.1	.059	Aon	- 29.2	1.6	8r	- 29.5 M
G 2786	14262	2 16.1	+22 56	6.4	.004	dA7n	- 8.	3.0	5	- 22. V
56° 543	14210	16.3	+57 06	8.0	.013	Aon	- 39.0	1.5	3r	
A 1780AB	14394	16.9	+29 33	8.5	.038	dF3	- 9.4	1.5	3	
G 2800	14322	17.2	+55 41	6.8	.014	cB9	- 35.0	2.1	7•	
56° 555	14357	17.7	+56 38	8.9	.008	B3	- 41.1	1.5	5	
57° 550	14404	2 18.0	+57 38	8.6	.008	gM2	- 38.5	2.8	3	
56° 570	14443	18.4	+56 56	8.6	.011	cB2	- 39.5	1.7	4	
B 534	14489	18.9	+55 37	5.2	.003	cA2	- 16.2	0.7	7r•	- 14.0 M
56° 591	14535	19.2	+57.01	7.5	.010	cA2	- 53.5	1.9	4	
15° 331	14610	19.2	+15 47	8.1	.116	dA9	- 21.	var	4•	
B 535	14542	2 19.4	+57 10	7.0	.002	cB8	- 47.4	0.5	7r•	
55° 600	14543	19.4	+56 24	8.4	.006	gG9	- 38.6	2.7	4r	
G 2847	14692	19.4	-14 31	7.4	.035	dA3n	+ 5.5	1.8	4	
56° 595	----	19.7	+56 58	8.6	.008	gM1	- 46.6	0.1	2	
56° 609	14826	21.7	+57 13	8.5	.012	gM4	- 41.6	1.3	3	
14° 392	14887	2 21.7	+15 18	7.8	.036	dFo	- 39.	var	5•	
G 2925	14956	23.2	+57 27	7.3	.034	cB1	- 25.	var	6•	- 30.3 V
B 553	15144	23.6	-15 34	5.8	.074	A4	- 8.3	2.5	6r	
G 2941	15220	24.3	-20 16	6.0	.129	gK3	+ 42.9	1.5	3	
56° 630	15124	24.6	+57 03	8.2	----	B4n	- 10.3	1.9	3	

TABLE I (Cont'd)

STAR	H.D.	1900 R.A.	1900 Decl.	Vis. Mag.	P.M.	Spec.	Vel.	P.E.	No. Pl.	Others
		h m	° ′		″		km	km		
B 561	15355	2 25.9	+29 42	5.9	0.103	dGo	+ 37.1	0.8	3	+ 40.6 V
G 2973	15316	26.4	+57 36	7.3	.029	cA2	- 43.8	0.6	4r	
G 2974	15385	26.4	+23 15	6.1	.084	gA5	+ 20.2	1.9	4	+ 21.1 V
G 2992	15555	27.3	-24 20	7.5	.359	dKo	+ 29.4	1.0	3	
B 565	15524	27.7	+25 01	5.9	.100	dF4	- 10.1	1.9	4	- 12.8 V
B 571	15656	2 29.0	+35 56	5.4	.049	gK5	- 36.2	1.0	2	- 35.8 L
B 574	15779	29.6	- 1 15	5.5	.042	gG3	- 5.5	1.2	3	
B 573	15703	29.9	+52 05	6.5	.013	A2	- 12.8	1.9	2	- 11.6 V
B 584	16074	32.2	- 8 05	5.8	.088	gK4	+ 25.4	0.4	3	
30° 417	16090	32.9	+30 56	7.9	.095	dGo	- 7.4	2.0	4	+ 2. L
68° 176	15948	2 33.1	+68 51	7.4	---	gG9	- 41.3	0.8	3	
G 3125	16024	33.5	+65 32	6.1	.050	cK5	+ 43.7	0.5	3	+ 41.6 D
B 590	16212	33.5	- 8 03	5.7	.066	gMo	+ 14.6	0.5	3	
B 595	16400	35.2	- 3 37	5.8	.055	gG5	+ 8.2	0.8	3	
ε Cet	16620	37.1	-12 05	5.0	.274	dF5	+ 11.0	1.6	3	+ 15.6 L
G 3203	16619	2 37.3	- 0 04	8.2	.178	dG4	+ 39.4	0.6	3	
B 608	16673	37.8	- 9 40	5.9	.196	dF6	- 4.1	2.8	4•	
B 610	16739	39.1	+39 59	5.0	.186	dF9	- 18.8	1.5	3	- 22.5v L
G 3247	16825	39.2	-14 46	6.0	.055	dF5	+ 1.9	1.1	3	
G 3249	16824	39.3	- 3 26	6.1	.020	gG9	+ 4.7	1.3	3	
B 599	16458	2 40.4	+81 14	5.9	.070	gG9	+ 13.0	0.3	3•	+ 23.5 D
τ Cet	16970	40.7	+ 3 02	3.6	.203	A2n	- 3.	3.5	6	- 5.4 M
44° 573	17115	42.0	+45 15	8.1	.017	B9	- 0.1	1.8	4	
G 3315	17163	42.7	+ 4 30	6.0	.078	gFon	+ 22.	var	3•	+ 18.4 SV
G 3325	17190	43.3	+25 27	8.1	.276	dG8	+ 8.9	0.7	3	
G 3418	17656	2 48.3	+46 38	6.0	.038	gG5	- 13.7	1.7	3	- 10.0 D
G 3439	17743	49.3	+52 48	6.4	.011	B9	+ 1.3	1.4	3	
τ Per	17878	50.7	+52 34	4.1	.004	gG1	+ 1.	var	5	+ 2.2v M
B 656	17948	52.0	+61 19	5.6	.152	dF4	+ 28.2	0.6	2	+ 28.4 V
-0° 451	18175	52.3	+ 0 15	7.2	.074	gK1	- 33.0	0.6	4	
B 666	18331	2 54.1	- 3 55	5.3	.050	A3n	- 9.	3.9	7r	- 17. LVY
G 3549	18369	54.6	+ 0 15	6.7	.033	dA5n	- 4.1	2.4	4	
A 2237A	18384	54.6	- 0 47	7.1	.022	gG5	+ 10.8	0.7	3	
G 3556	18339	54.9	+38 25	6.1	.016	gK3	- 39.3	1.3	3	- 41.6 D
A 2270A	18537	57.3	+52 09	5.4	.038	B8n	- 3.	3.0	4r	- 4.1 M
A 2270B	18538	2 57.3	+52 09	6.8	.026	A1n	+ 0.8	2.7	4	
B 688	18784	58.7	- 7 52	5.9	.118	dG6	+ 14.7	0.8	3	
G 3642	18885	59.5	-10 09	6.0	.050	gG6	+ 12.0	1.0	3	
B 692	18883	59.8	+ 4 09	5.6	.017	B5	+ 11.8	1.7	3	
B 695	18953	3 00.2	- 7 53	5.5	.048	gG5	+ 25.2	0.3	3	
6° 594	19034	3 01.1	- 5 50	8.3	.42:	dG5	- 19.4	0.7	3	
B 697	18970	01.8	+56 31	5.1	.077	gG8	- 44.9	1.1	3	- 44.8 M
G 3683	19121	02.0	+ 1 40	6.0	.031	gG6	+ 4.6	1.2	3	+ 0.3 D
B 715	19548	06.6	+28 53	5.6	.021	B9n	- 2.	3.1	6	
G 3785	19536	07.5	+60 27	7.3	.044	A3	+ 11.2	2.5	3	+ 12.8v D
15° 554	19934	3 09.4	-15 07	7.9	---	gG5	+ 36.	var	4•	
15° 450	20086	11.3	+15 23	7.3	.035	A3n	+ 17.	3.1	4•	
B 724	20041	12.0	+56 57	5.9	.006	cAo	- 12.6	0.7	8r•	- 11.6 V
59° 616	20040	12.2	+59 56	7.8	.018	gG1	- 35.0	1.5	4	
G 3884	20162	12.7	+45 10	6.4	.069	gM2	- 3.8	1.0	2	- 0.9 D
14° 629	20268	3 12.7	-14 01	7.5	---	gG5	+ 26.2	2.1	3	
G 3904	20277	13.5	+32 00	6.0	.108	gG8	+ 22.5	2.4	3	+ 17.5 D
G 3907	20319	13.5	- 6 06	6.0	.007	B9n	+ 6.9	2.9	4	
B 721	19978	13.9	+77 33	5.5	.086	A4n	+ 1.	4.2	7•	+ 6.8 LY
14° 646	20622	16.2	-14 28	7.9	---	agK2	+ 84.8	2.0	4r	
G 3961	20619	3 16.5	- 3 01	7.1	.273	dG2	+ 20.1	1.7	3	
64° 385	20535	18.0	+64 56	8.6	---	gKo	+ 0.3	1.3	3	
G 4009	20507	18.5	+74 00	6.9	.244	dF4	- 28.	var	4•	
B 771	20894	19.2	-23 49	5.7	.033	gG3	+ 6.2	0.3	2	+ 11. L
B 777	21050	21.6	+20 38	5.9	.006	B9	- 8.6	2.9	4	
G 4072	21110	3 22.3	+31 33	7.5	.025	gK4	+ 19.5	0.9	4	
G 4083	21252	22.9	-15 13	8.0	.330	dGo	+ 44.2	2.0	3	
B 781	21291	25.0	+59 46	4.4	.002	cB9	- 5.5	1.5	4•	- 7.2 M
B 783	21362	25.3	+49 41	5.6	.040	B6n	0.	4.2	4	0. M
G 4131	21483	25.7	+30 12	7.1	.018	B3	- 4.	4.1	5	- 6.5 V

TABLE I (Cont'd)

STAR	H.D.	1950 R.A.	1950 Decl.	Vis. Mag.	P.M.	Spec.	Vel.	P.E.	No. Pl.	Others
		h m	° ′		″		km	km		
A 2559A	21448	3 25.8	+44 53	7.4	0.018	B3	- 13.4	1.1	4•	- 10.6 V
A 2559B	----	25.8	+44 53	8.5	---	g05	- 15.0	0.9	3	
B 786	21389	25.9	+58 42	4.8	.009	cAoe	- 5.9	1.1	3•	- 7.7 M
29° 568	21611	27.2	+29 52	7.5	.008	Aon	+ 4.	3.9	4•	+ 13. D
G 4183	21755	28.1	+ 6 01	6.1	.032	g05	+ 10.2	0.6	2	+ 12.4 S
44° 732	21771	3 28.9	+44 40	7.3	.010	gK3	- 10.0	2.9	4•	
B 805	21770	29.0	+45 53	5.4	.086	dA9	- 46.1	1.5	2	- 45.4 LV
C 463	21854	31.2	+72 56	9.2	.31:	dK2	- 45.7	1.9	3	
G 4340	22675	36.0	- 7 33	5.9	.052	g05	- 29.1	0.3	3	
B 839	22951	39.2	+33 48	5.0	.010	B2	+ 35.	var	8•	+ 12.v M
C 495	23065	3 39.4	-10 51	8.8	.408	dG4	+ 1.4	0.9	3	
22° 535	23133	40.6	+22 35	9.2	.067	dFo	- 3.7	0.1	2•	
G 4459	23139	41.2	+45 57	6.1	.037	gA6	+ 3.1	1.3	3	+ 10.1 D
B 840	23005	41.3	+67 03	5.8	.146	dF4	+ 5.0	0.3	2	+ 4.7 V
B 845	23193	41.3	+36 18	5.6	.059	cA3	+ 21.5	0.4	5•	+ 22. V
44° 790	23256	3 41.5	+45 11	7.7	.073	dFo	+ 13.8	1.0	4	
45° 808	23287	42.4	+45 26	7.5	.028	Ao	+ 1.5	1.6	3	
B 853	23300	42.5	+45 32	5.6	.031	B8	+ 4.0	0.5	3	+ 0.3 V
A 2768AB	23524	44.6	+51 53	8.4	---	dG6	- 3.3	1.6	3	
44° 797	23566	44.6	+45 12	7.7	.038	gA6n	- 6.3	2.9	4	
A 2772A	23625	3 44.7	+33 27	6.4	.004	B3	+ 33.	var	5•	+ 36. V
21° 530	23792	45.8	+21 47	8.3	.065	dA8n	- 2.2	1.0	2•	
G 4584	23887	46.1	+ 0 05	6.1	.058	gK3	+ 64.8	0.5	3	+ 68.5 D
G 4593	23978	46.4	-21 03	6.1	.025	gK5	+ 3.4	1.8	3	
G 4598	23800	46.6	+52 20	6.9	.009	B2n	- 16.	6.	4•	- 19.7 V
B 876	23838	3 46.6	+44 49	5.8	.037	g05	+ 24.	var	4•	+ 12.v D
B 886	24131	48.7	+34 13	5.7	.010	B3n	+ 17.6	0.9	6	+ 17.9 LV
I Per	24398	51.0	+31 44	2.9	.015	cB1	+ 20.4	1.1	5•	+ 20.9 M
A 2850B	24554	51.8	- 3 06	6.3	.030	Aln	+ 17.	var	5•	+ 18.v VS
G 4707	24616	51.8	-23 17	6.8	.421	dG6	+100.3	0.5	3	
4° 601	24550	3 51.9	+ 5 02	7.8	.043	gA8n	+ 15.	4.3	5	
G 4729	24712	52.9	-12 15	5.9	.067	gA9	+ 21.9	0.9	3	
ε Per	24760	54.5	+39 52	3.0	.036	B1n	+ 10.	var	9•	- 6.v M
ξ Per	24912	55.7	+35 39	4.0	.009	O7n	+ 70.	var	5•	+ 67. M
G 4785	25069	56.4	- 5 37	6.0	.184	dG9	+ 36.7	1.5	3	
B 931	25457	4 00.0	- 0 24	5.4	.289	dF7	+ 17.0	2.0	4	+ 17.4 M
G 4874	25274	01.0	+68 33	6.1	.018	gMo	- 46.6	1.8	3	- 45.5 Md
G 4877	25173	01.1	+75 03	7.3	.342	dF5	+ 35.9	0.7	6r	
B 933	25555	01.4	+23 58	5.7	.014	dF4	+ 17.3	1.1	4r	
G 4919	25616	02.4	+46 47	6.6	.074	Aln	+ 44.	4.9	4•	
B 947	25940	4 05.0	+47 35	4.0	.040	B3ne	+ 0.8	1.7	6•	+ 4. M
B 952	26162	06.2	+19 29	5.7	.114	gK1	+ 27.1	0.6	6r	+ 24.0 M
G 5018	25311	07.8	+33 27	5.9	.016	cK5	+ 22.3	1.3	3	+ 19.9 D
G 5035	26464	08.4	- 8 57	5.9	.039	gG9	+ 30.1	0.7	3	
75° 167	26047	08.8	+75 42	8.6	.001	dF8	- 7.	var	4•	
B 963	26574	4 09.4	- 6 58	4.1	.088	dF1	+ 2.0	0.9	3•	+ 14.4 L
B 971	26690	10.9	+ 7 35	5.4	.009	gF2	+ 3.	var	4	+ 4.v M
B 974	26764	12.8	+53 29	5.1	.009	Aln	- 13.	3.8	6•	+ 4. M
A 3093B	----	13.0	- 7 44	9.6	---	wA	- 53.	2.	4•	- 20. Md
15° 754	27064	13.8	-15 03	8.1	---	gG9	- 5.8	2.5	4•	
A 3102AB	27028	4 14.1	+19 33	7.6	.066	dF5	- 3.7	0.5	3	
G 5183	27179	14.9	- 6 36	6.1	.020	gG8	- 1.2	0.8	3	
G 5198	27325	15.9	-14 46	6.9	.031	gG6	+ 15.4	1.8	3	
G 5220	27278	16.8	+41 41	6.1	.030	gG5	+ 25.1	1.7	3	+ 23.1 V
15° 765	27467	17.3	-15 18	8.9	.033	gFo	+ 21.2	2.9	4•	
4° 801	27485	4 17.8	- 3 52	8.0	.30:	dG2	- 36.3	1.5	3	
B 1019	27778	21.0	+24 11	6.2	.014	B6	+ 13.4	2.9	7•	
G 4521	28322	25.5	+ 1 45	6.1	.028	gG8	+ 29.4	0.9	3	+ 31.1 D
B 1042	28292	25.6	+16 15	5.3	.028	gK1	+ 20.2	1.1	4	+ 17.0 VL
A 3243	28271	25.7	+30 15	6.5	.027	gF6	- 39.3	2.9	4•	- 35.4 D
A 3274B	----	4 28.0	+53 48	6.6	.016	B1	- 0.6	1.7	8r•	- 1.2 LV
29° 716	28592	28.4	+29 50	8.4	.056	dFon	+ 29.3	2.7	4	
α Tau	29139	33.0	+16 25	1.1	.202	gK5	+ 54.8	0.2	28	+ 54.1 M
A 3353S	29364	35.4	+26 51	7.2	.076	dF3	+ 3.0	var	29•	
B 1091	29503	35.9	-14 24	4.0	.174	gK4	+ 43.3	0.4	4	+ 41.8 M

TABLE I (Cont'd)

STAR	H.D.	1950 R.A.	1950 Decl.	Vis. Mag.	P.M.	Spec.	Vel.	P.E.	No. Pl.	Others
		h m	° ′		″		km	km		
B 1095	29573	4 36.6	-12 13	5.0	0.055	A2	+ 9.	3.2	3	+ 5.6 LYV
Q 5692	29587	38.1	+42 02	7.3	.687	dG2	+112.1	0.3	7r	
B 1099	29646	38.2	+28 31	5.7	.053	A1n	+ 26.2	1.6	5	+ 23.8 DV
Q 5701	29645	38.4	+38 11	5.8	.260	dG3	+ 45.6	2.4	2	+ 46.1 V
56° 964	29599	38.7	+57 07	8.0	.056	dF5	- 40.6	0.9	3	
C 607	29713	4 41.2	+70 00	8.8	.122	dKo	+ 13.4	1.2	3	
B 1100	29678	42.1	+75 51	6.0	.138	dA6n	- 9.	var	5•	- 4.4 D
Q 5794	30238	42.9	-21 22	6.0	.028	gK2	+ 22.6	2.3	3	
Q 5803	30138	43.3	+40 13	6.1	.030	gG5	+ 33.1	1.5	2	+ 35.9 D
Q 5822	30221	44.3	+45 24	7.7	.042	A2n	+ 7.8	0.9	3	
Q 5860	30562	4 46.1	- 5 46	6.0	.388	dGo	+ 77.7	1.5	3r	
Q 5863	30097	46.2	+75 38	7.2	.193	dG7	- 42.2	0.4	3	
B 1144	30794	49.0	+36 34	6.9	.054	gK1	- 36.6	0.7	3	
B 1139	30614	49.1	+66 16	4.4	.009	O9e	+ 15.9	2.9	4•	+ 6.0 M
B 1124	30338	50.9	+81 07	5.3	.029	gK4	- 11.4	1.0	2	- 7.9 L
64° 487	30957	4 51.7	+64 20	8.6	.099	dKo	- 6.7	1.8	3	
B 1156	31189	52.7	+55 45	6.9	.029	gK5	- 0.6	1.7	3	
Q 6005	31358	52.7	+19 56	8.0	.371	dKo	+ 27.6	1.4	3	
B 1166	31362	53.2	+24 31	6.3	.028	gFo	- 5.3	0.7	3	- 12.1 V
Q 6079	31499	56.7	+69 05	7.1	.131	dF5	+ 17.3	1.2	3	
B 1186	31925	4 56.8	-16 27	5.5	.206	dF2	+ 30.7	1.1	3	
Q 6132	31865	58.9	+63 01	8.6	.330	dG4	- 24.2	1.4	3r	
37° 1031	32270	5 00.2	+37 12	7.5	.028	B6	+ 8.8	1.1	6	
Q 6167	32393	00.3	- 4 17	6.1	.057	cK3	+ 38.8	1.3	3	
38° 1012	32316	00.6	+38 48	8.2	.016	B6n	- 3.	3.8	6•	
38° 1020	32672	5 03.2	+38 28	7.7	.031	B5	+ 4.8	1.0	6	
Q 6245	32518	04.1	+69 35	6.6	.096	gKo	- 8.1	0.3	3	- 6.1 D
37° 1046	32827	04.2	+37 35	8.2	.020	dA5n	- 23.9	2.5	5	
Q 6260	32715	04.9	+64 52	6.4	.170	dF3	+ 2.3	1.9	4r	- 4.7 V
B 1215	32991	04.9	+21 38	6.0	.011	B3ne	+ 28.	var	5•	+ 22.v V
Q 6268	33093	5 05.1	-12 33	6.1	.160	dF9	+ 49.2	1.8	3	
B 1219	33054	05.2	+ 8 26	5.5	.069	gF0	+ 10.5	1.5	5	+ 4.v M
B 1224	33256	06.2	- 4 31	5.2	.047	dF1	+ 10.0	0.3	2	+ 9.5 M
Q 6348	33608	08.8	- 2 33	5.9	.073	dF5	+ 30.4	0.7	3	
C 674	33725	09.5	- 9 09	8.0	.573	dK1	+ 6.2	0.7	9r	
Q 6377	33533	5 10.4	- 6 07	6.0	.040	gG7	+ 23.7	0.6	3	
B Ori	34085	12.1	- 8 15	0.3	.001	cB8	+ 21.0	0.7	21	+ 22.6v Q
C 677	34101	12.1	-15 53	8.0	.316	dG6	+ 33.1	1.9	3	
B 1248	34053	12.5	+22 14	6.2	.014	A0n	- 4.	var	3•	- 9.v D
Q 6428	33924	13.0	+60 08	7.2	.130	dF5	+ 16.8	1.6	4	
B 1249	34078	5 13.0	+34 15	5.8	.030	O9	+ 58.6	1.5	11r•	+ 59.4 VLY
29° 849	34114	13.1	+29 18	9.0	.081	dF5	- 33.9	1.2	3	
A 38648	----	14.3	+79 11	9.0	---	dF5	- 45.3	1.3	3	
Q 6486	34427	15.3	-15 16	6.7	.014	A0n	+ 67.	var	4•	
B 1271	34658	16.6	+ 2 33	5.4	.049	dF3	+ 6.3	1.8	3	+ 13.0 L
B 1268	34678	5 16.7	+33 54	5.2	.013	cA5	- 3.0	0.8	7r	- 3.5 YLV
15° 787	34636	16.8	+15 44	7.9	.029	A2n	- 7.	3.9	4•	
14° 881	34792	17.0	+15 00	8.2	.013	B9n	+ 18.0	2.7	4	
14° 1094	34796	17.2	-14 48	8.2	---	dGo	+ 48.0	1.5	4	
Q 6546	34575	17.9	+59 14	7.3	.372	dG6	- 22.7	0.1	3	
Q 6571	34664	5 18.8	+64 05	8.0	.222	dF8	- 15.3	1.4	3	
14° 1103	35041	18.9	-14 11	8.0	---	dG1	- 5.0	0.7	3	
B 1282	34989	19.0	+ 8 23	5.7	.002	B2	+ 32.	4.1	5•	+ 21.0 V
B 1284	35039	19.2	- 0 26	4.6	.003	cB2	+ 28.9	1.6	8•	+ 28.8 M
14° 1117	35307	21.0	-14 52	7.9	.014	gK4	+ 50.3	1.4	3	
B 1272	34653	5 21.7	+77 56	6.5	.017	dA5n	- 14.9	2.9	5	- 19.0 D
B 1300	35410	21.9	- 0 56	5.2	.133	gKo	+ 21.6	0.8	5r	+ 20.6 M
γ Ori	35468	22.4	+ 6 18	1.7	.015	B2	+ 20.8	0.9	8•	+ 18.0 M
Q 6672	35536	22.7	-10 22	5.9	.027	gK5	+ 57.1	1.1	3	
B 1316	35736	23.8	-19 44	5.8	.022	dF4	+ 5.6	1.7	3	
B 1310	35600	5 23.9	+30 10	5.7	.018	cB9	+ 16.7	0.5	7r•	
Q 6719	34712	24.5	+81 40	8.7	.194	dGo	+ 1.8	0.9	3	
Q 6733	35802	25.1	+17 12	6.0	.057	gM1	- 22.5	1.1	3	- 22.0 D
Q 6760	35956	26.0	+12 31	6.8	.238	dGo	+ 7.2	0.4	2	+ 9.0 D
Q 6797	36040	27.3	+41 25	6.1	.045	gG6	+ 15.4	1.0	3	+ 14.5 D

TABLE I (Cont'd)

STAR	H.D.	1950 R.A.	Decl.	Vis. Mag.	P.M.	Spec.	Vel.	P.E.	No. Pl.	Others
		h m	° ′		″		km	km		
B 1328	36166	5 27.3	+ 1 45	5.7	0.009	B3	+ 10.	3.1	5	+ 15.1 V
G 6808	35863	27.8	+67 59	6.9	.180	dF8	+ 31.0	0.3	3	
29° 921	36281	28.6	+29 24	8.6	.026	gG7	- 22.4	0.5	3	
29° 923	36335	29.0	+29 10	7.8	.058	dF3	- 31.1	1.7	4	
A 4134C	36485	29.5	- 0 19	6.9	.009	B6	+ 15.8	1.5	6	+ 23.3 V
G 6883	36130	5 31.0	+74 40	7.5	.181	dG2	- 61.9	1.8	3	
B 1346	36653	31.1	+14 16	5.6	.008	B3	+ 20.	5.	3	+ 18.9 VY
B 1353	36822	32.1	+ 9 27	4.5	.006	Bo	+ 32.9	0.8	4•	+ 33.2 Y
A 4179A	36861	32.4	+ 9 54	3.7	.006	O8	+ 37.4	2.7	3•	+ 33.0 M
A 4179B	36862	32.4	+ 9 54	5.6	---	B2	+ 38.4	1.1	5•	+ 35.4 M
B 1361	36960	5 32.6	- 6 02	5.6	.010	B1	+ 28.2	1.9	3•	+ 29.4 LYV
B 1362	36960	32.6	- 6 02	4.7	.006	B1	+ 26.5	2.5	4•	+ 28.1 M
B 1368	37077	33.2	- 4 53	5.3	.014	gF0	- 8.4	1.7	3	- 8.7 L
ε Ori	37128	33.7	- 1 14	1.8	.000	cBo	+ 25.3	0.9	5•	+ 26.2 M
G 6975	37171	34.3	+11 00	6.1	.049	gMo	-106.	var	4•	-118.8 S
ζ Tau	37202	5 34.7	+21 07	3.0	.023	B3e	+ 27.	var	7•	+ 29.8v M1
B 1367	37070	34.9	+56 20	6.9	.135	dF2	+ 16.	var	4•	+ 20.v V
G 7030	37387	36.2	+23 18	7.8	.011	gKo	+ 6.5	1.5	3	
1° 1005	37776	38.4	- 1 30	8.2	---	B5	+ 29.	3.4	3	+ 25.5 L
44° 1270	37736	39.3	+44 49	7.7	.016	A2	+ 5.9	0.8	3	
44° 1278	38188	5 42.5	+44 47	7.8	.029	B9n	+ 6.7	1.6	4	
G 7226	38529	44.0	+ 1 09	6.1	.165	dG4	+ 29.1	0.6	3	+ 30.1 D
G 7228	38527	44.1	+ 9 30	5.9	.073	gG7	- 24.7	0.7	3	- 25.4 D
B 1423	38545	44.4	+14 28	5.7	.044	A2n	+ 19.	3.2	4	+ 21.7 D
B 1443	38710	45.3	+ 6 26	5.3	.021	gA6n	+ 51.8	1.9	3•	+ 39.0 LYV
29° 1004	38688	5 45.7	+29 44	8.2	.032	dF4	+ 30.6	2.0	3	
G 7286	38858	46.1	- 4 06	6.0	.231	dG4	+ 29.7	0.7	3	
G 7320	39051	47.6	+ 4 25	6.1	.047	gK2	+ 23.5	1.1	2	+ 29.6 D
G 7335	39169	48.1	- 1 27	7.9	.044	gKo	+ 3.4	2.3	4•	
G 7463	39910	53.0	- 4 37	6.0	.042	gK2	+ 26.1	1.3	3	
G 7483	39970	5 53.9	+24 15	6.0	.007	cB9	+ 1.7	2.2	9•	- 2.7v V
G 7494	40151	54.1	-22 51	6.0	.122	dKo	+ 34.5	1.8	3	
G 7496	40040	54.1	+15 44	7.9	.267	dG4	- 24.5	1.1	3	
G 7523	40084	55.5	+49 55	6.1	.013	gG4	- 5.0	1.5	3•	
G 7537	40298	55.8	+21 14	8.6	.008	B9	- 3.4	1.6	6	
G 7583	40202	5 57.4	+64 58	8.8	.204	dG3	- 25.9	1.2	3	
22° 1147	40897	59.7	+22 03	8.4	.021	B9n	+ 6.2	1.7	6	
19° 1182	40910	59.7	+19 56	8.6	---	A1	+ 16.1	1.7	6	
G 7655	39861	6 00.2	+81 31	8.9	.381	dG5	- 26.5	1.8	3	
G 7664	40647	00.6	+69 29	8.1	.124	dG6	- 16.9	0.5	3	
G 7671	40708	6 00.8	+67 39	8.8	.310	dG6	+ 48.	var	4•	
21° 1099	41140	01.1	+21 30	8.1	.015	dA5n	+ 31.0	2.6	6	
B 1519	41547	03.1	-10 14	5.8	.027	dF4	+ 32.0	1.9	3	
B 1518	41543	03.8	+23 39	6.9	.006	gK5	- 16.	3.1	3•	- 14.4 V
G 7740	41593	03.8	+15 33	7.6	.156	dKo	- 11.2	0.5	3	
G 7769	41690	6 04.6	+21 53	8.0	.016	B2	+ 15.5	1.9	6	
20° 1284	42088	06.7	+20 31	7.4	.017	O6	+ 21.8	2.7	3	+ 24.1 V
G 7947	43028	11.2	-15 22	6.9	.014	gKo	- 2.7	2.3	3	
G 7951	42983	11.3	+ 2 50	7.9	.282	dKo	- 25.8	1.3	3	
G 7952	43023	11.4	- 3 44	5.9	.028	gG7	+ 49.5	1.6	3	
B 1562	----	6 12.3	+36 10	7.5	.064	dF3	+ 8.1	1.0	2	
B 1563	43017	12.3	+36 10	6.7	.061	dF2	+ 7.4	0.7	2	+ 5.3 V
B 1567	43112	12.3	+13 52	5.8	.034	B2	+ 40.2	0.9	3	+34.4 V
B 1578	43384	13.9	+23 46	6.3	.006	cB3	+ 13.2	0.7	10r•	
15° 1328	43670	14.6	-15 06	7.9	---	gK5	+ 39.2	1.6	3	
G 8076	43297	6 15.4	+65 31	8.6	.284	dG3	- 16.8	0.8	3	
B 1591	43827	15.5	-16 48	5.3	.012	gK2	- 9.2	1.3	2	- 7.8 M
B 1584	43740	15.9	+23 37	6.6	.012	gG3	+ 39.7	0.5	2	+ 41.0 V
B 1595	43993	16.5	- 9 22	5.7	.033	gK1	+ 7.6	0.2	3	
14° 1399	44007	16.5	-14 49	8.3	---	sdGo	+166.4	1.0	3	
G 8108	44021	6 16.5	-15 00	6.3	.022	gM1	+ 51.5	1.1	4	
B 1585	43749	17.5	+64 47	7.2	.112	dF2	+ 3.2	0.3	2	+ 8.2 V
14° 1260	44414	19.5	+14 54	8.4	.073	gGo	+ 18.8	0.7	3	
G 8203	44497	19.8	+12 36	6.0	.051	dFo	+ 23.2	1.9	4	+ 18.2 D
G 8304	45289	22.9	-42 50	6.8	.772	dG4	+ 47.8	1.4	2	

TABLE I (Cont'd)

STAR	H.D.	1950 R.A.	1950 Decl.	Vis. Mag.	P.M.	Spec.	Vel.	P.E.	No. Pl.	Others
		h m	° ′		″		km	km		
B 1628	45415	6 24.7	+ 2 56	5.8	0.047	gG9	+51.6	0.9	2	+ 53.1 V
29° 1231	45336	24.9	+29 16	7.6	.029	gMo	- 1.6	2.7	4•	
30° 1240	257670	25.6	+30 20	8.5	.017	gPon	- 4.8	1.6	4	
29° 1241	45541	26.2	+29 32	8.0	.032	A2m	+43.7	1.8	3	
30° 1245	258213	27.1	+30 30	8.4	.034	gKo	+15.	var	4•	
B 1651	46184	6 29.1	-12 21	5.3	.043	gK2	+10.8	0.3	2•	+ 17.9 M
5° 1262	46149	29.3	+ 5 04	7.7	.022	O8	+38.	4.7	3•	+ 38.9 V
G 8477	46150	29.3	+ 4 59	6.8	.007	O6	+39.	6.	3•	+ 35.9 V
A 51668	-----	29.4	+17 49	7.8	.056	dF6	+ 7.1	0.3	3	- 3. V
B 1654	46229	29.4	- 8 07	5.6	.015	gK2	+ 3.4	1.4	3	
B 1667	46300	6 30.2	+ 7 22	4.5	.008	cAo	+15.0	0.8	5•	+ 11.9 LYV
29° 1264	259274	30.3	+29 43	8.2	.016	gF2	- 0.9	1.1	3	
C 809	45821	30.7	+72 06	7.8	.26:	dG1	+40.8	1.5	3	
G 8540	45947	31.6	+73 44	6.2	.147	dF4	+ 5.6	1.1	2	+ 5.0 D
G 8567	46709	32.5	+10 02	6.1	.013	gK5	+40.4	1.8	4	+ 38.7 D
6° 1303	46966	6 33.8	+ 6 08	7.3	.043	O8	+43.5	1.7	2•	+ 42.3 V
B 1692	47138	34.2	-18 37	5.8	.019	gG2	+24.3	1.0	3	
G 8630	46509	34.6	+71 48	6.1	.021	gG9	-21.1	0.6	3	- 23.6 D
64° 596	46606	34.6	+64 15	8.0	---	gK2	+28.8	0.3	2	
45° 1330	47019	35.0	+45 07	8.8	---	gM3	-29.7	1.6	4	
G 8686	47335	6 36.6	+44 23	6.8	.039	gG8	-13.	var	4•	
G 8791	48270	41.1	+44 33	6.8	.016	gKo	+20.4	0.7	3	
B 1735	49098	43.5	-31 44	5.9	.392	dF5	+31.	3.8	3	
B 1743	49331	45.2	- 8 57	5.3	.018	cM2.5	+29.8	2.5	4•	+ 23.4 M
7° 1457	49409	46.0	+ 7 42	8.3	.320	dG3	-87.1	1.6	3	
18° 1365	49635	6 47.2	+18 51	7.7	---	cF5	+27.4	2.2	5•	
G 8954	49933	48.3	- 0 29	5.8	.187	dF2	-15.2	1.0	8r	
1° 1409	50040	48.8	- 1 54	8.3	---	Aon	+ 8.7	2.5	5	
B 1762	50018	49.6	+38 56	6.1	.009	dA7n	- 2.1	2.5	3	+ 2.7 S
-0° 1468	50209	49.7	- 0 14	8.3	.010	B8ne	+17.1	2.2	6	
-0° 1479	50583	6 51.3	- 0 15	7.8	.062	B9	+22.7	1.8	5	
G 9063	50820	52.2	- 1 42	6.2	.008	•	+11.6	1.2	2	+ 13.4 V
1° 1449	50846	52.3	- 1 19	8.3	---	B6p	+13.9	2.3	5	+ 15.8 L
G 9070	50890	52.5	- 2 44	6.0	.018	gG6	+20.0	0.9	3	
G 9081	50551	53.0	+57 38	6.1	.027	gK3	-53.2	2.5	3	- 53.9 D
G 9089	50763	6 53.2	+46 46	6.0	.138	gKo	+40.3	0.1	2	+ 40.0 D
G 9098	48974	53.6	+83 41	8.6	.240	dG5	-28.6	1.2	3	
G 9101	51000	53.7	+33 45	6.0	.016	gG2	-10.6	0.8	3	- 10.1 D
2° 1483	51565	55.3	+ 2 24	7.7	---	•	-20.	var	4•	
G 9152	50885	55.7	+70 53	5.8	.028	gK4	-17.1	0.6	3	- 15.8 D
G 9175	51814	6 56.3	+ 3 40	6.0	.014	gG7	+17.8	0.3	2	+ 17.4 D
A 56698	-----	57.5	+75 18	7.6	.277	dG8	+16.3	1.8	3	
G 9265	52556	59.4	+15 25	5.9	.021	gK1	-11.6	0.8	2	- 13.1 D
G 9275	52609	59.7	+16 45	6.0	.028	gM2	+34.0	1.2	3	+ 36.9 D
B 1817	53136	7 00.9	-23 46	3.1	.000	cB3	+45.2	2.7	3•	+ 48.6 M
B 1814	268518	7 01.1	+20 40	8.6	.107	dGo	+19.7	0.4	3	
G 9355	53510	02.9	+ 9 16	6.0	.052	gMo	+44.2	1.5	3	+ 48.7 D
B 1834	54153	04.3	-38 18	6.1	.016	gGo	+21.4	1.8	4	
B 1825	53683	05.3	+60 49	8.7	.060	gG9	+37.0	1.7	3	
A 5816A	54244	05.9	+16 59	7.6	.025	gK5	+38.6	1.8	3	
A 58168	-----	7 05.9	+16 59	8.4	---	gK5	+36.7	0.8	2	
60° 1034	54122	07.0	+60 20	7.3	.033	gG6	+ 5.6	1.3	3	
B 1850	55052	09.4	+24 13	5.8	.055	gF4	+10.6	1.7	4	+ 13.3 V
G 9570	55178	11.2	+59 52	7.3	.030	gG6	+ 8.2	0.4	3	
A 5911A	55775	11.7	- 3 49	6.1	.017	gK5	+22.4	2.1	4	
B 1864	55730	7 11.8	+12 12	5.8	.058	gG6	+31.8	0.1	2	+ 28.8 V
G 9600	55832	11.9	- 9 52	6.1	.007	gK3	+43.9	1.5	3	
G 9628	56031	12.9	+ 8 04	6.0	.028	gM4	-10.4	0.5	2	- 6.6 D
G 9642	55866	13.6	+52 13	6.0	.030	gK1	- 6.3	1.1	3	
14° 1810	56617	14.8	-14 45	8.1	---	dF5	+33.7	1.9	3	
B 1876	56099	7 14.9	+59 13	7.6	.083	dF7	-54.9	1.9	3	
A Gem	56537	15.2	+16 38	3.6	.061	A3n	+ 0.3	1.8	6•	- 13.8 M
67° 483	56168	16.0	+67 45	8.6	.089	dK1	- 8.3	0.9	3	
B 1893	56790	16.4	+22 07	8.0	.010	gG8	+ 7.	var	4•	
15° 1537	56888	16.6	+15 18	8.3	.017	gA8	+ 4.8	1.6	3	

TABLE I (Cont'd)

STAR	H.D.	1950 R.A.	1950 Decl.	Vis. Mag.	P.M.	Spec.	Vel.	P.E.	No. Pl.	Others
		h m	° ′		″		km	km		
G 9739	56989	7 16.8	+ 2 50	6.1	0.018	gG8	+25.7	0.4	2	+ 23.9 D
B 1908	57146	16.8	-26 30	5.4	.020	cO5	+31.3	2.5	3	+ 33.1 L
G 9752	57006	17.1	+ 7 14	6.0	.098	dF8	+22.7	0.6	3	+ 21.3 S
15° 1544	----	17.8	+15 00	8.5	.018	gG9	-41.2	0.7	3	
B 1902	57067	18.4	+50 15	7.4	.060	dA5n	+ 5.	var	3	+ 5.v V
B 1903	57066	7 18.4	+50 15	7.3	.061	dA5n	+14.5	2.4	3•	- 2.0 V
14° 1644	57496	19.2	+14 45	8.6	.062	gG2	+25.3	0.9	3	
14° 1649	57675	19.9	+14 24	8.3	.017	gF4	+31.6	1.5	3	
B 1921	57727	20.4	+25 09	5.1	.070	gG2	+ 4.2	0.3	2	+ 6.4 L
B 1871	55966	20.7	+82 31	5.1	.041	gM4	+24.0	1.5	3•	+ 12.4 M
G 9860	57646	7 21.1	+51 59	5.9	.044	gK5	+20.3	1.9	3	+ 18.0 D
π CMa	58350	22.1	-29 12	2.4	.008	cB7	+49.8	1.8	2•	+ 40.4 M
B 1935	58343	22.4	-16 06	5.2	.017	cB5e	- 5.9	0.5	5r•	- 3.8 L
ι Gem	58207	22.6	+27 54	3.9	.147	sgG7	+ 6.4	1.1	4	+ 8.7 M
B 1941	58579	24.0	+20 22	5.9	.023	gA7n	+14.	var	6•	- 0.2 S
G 9956	58683	7 24.7	+27 24	8.1	.122	gG6	+54.7	1.3	3	
B 1957	59067	25.5	-11 27	5.9	.007	•	+14.1	0.9	4	
B 1948	58855	26.1	+49 47	5.4	.144	dF5	-27.9	2.3	3	- 26.6 M
B 1964	59380	27.0	- 7 27	6.0	.144	dF9	+ 8.6	1.2	3	
B 1965	59438	27.1	-14 53	5.9	.316	dF4	- 9.6	2.8	4	- 1. Md
B 1984	60357	7 31.6	+ 3 29	5.8	.020	Aon	+35.1	2.7	3	+ 32.0 D
G 10288	61294	36.9	+38 28	5.9	.049	gMo	+47.2	1.1	3	+ 47.1 D
G 10304	61606	37.5	- 3 29	7.2	.298	dK3	-20.6	0.4	3	
70° 471	61091	37.8	+69 50	8.3	---	gK1	+ 3.5	0.6	3	
B 2016	61772	38.1	-15 09	5.2	.026	gK5	- 3.0	2.5	4	+ 0.6 M
B 2035	62623	7 41.8	-28 50	4.1	.010	cA2e	+30.6	0.5	7•	+ 23.6v L
G 10433	61994	42.2	+70 20	7.1	.173	dG5	-23.4	2.0	4	
β Gem	62509	42.3	+28 09	1.2	.625	gG8	+ 4.7	0.5	12	+ 3.3 M
B 2040	62721	43.2	+18 38	5.0	.097	gK5	+84.7	2.5	3	+ 80.v M
B 2037	62647	43.3	+37 38	5.4	.026	gM3	-30.4	1.8	3	- 36.0 L
A 6381B	----	7 45.6	-12 04	8.2	.142	dG2	+24.5	1.9	3	
88° 39	57535	45.9	+87 51	8.9	---	dA5	+ 4.	var	4•	
C 928	63103	46.7	+64 14	8.0	.11:	dG7	+12.2	1.4	3	
B 2077	64152	49.5	-21 03	5.8	.066	gG8	+32.4	1.2	3	
B 2074	64092	50.0	+22 28	7.1	.012	gG7	- 8.2	1.1	3	
B 2078	64145	7 50.4	+26 54	5.0	.048	A4n	+ 6.3	1.8	4	+ 3. LYV
B 2076	64106	50.8	+47 31	6.4	.015	gK2	-63.3	1.1	6	- 60.6 D
G 10682	64324	51.6	+34 45	7.7	.218	dG3	+14.0	1.2	3	
G 10694	64606	52.0	- 1 17	7.5	.271	dG5	+93.8	2.0	4	
G 10699	64385	52.4	+50 41	8.5	.246	dF5	+ 6.9	0.9	3	
B 2084	64307	7 54.3	+74 03	5.6	.039	cK5	+35.6	1.2	3r	
G 10751	65066	54.6	+ 8 47	6.1	.021	gG6	-35.2	1.2	3	- 35.1 D
C 946	65277	55.4	- 0 42	8.3	.177	dK5	- 3.2	2.7	4•	
G 10821	65583	57.4	+29 22	6.9	1.178	dG7	+13.0	0.4	7r	
B 2106	65448	58.0	+63 14	6.0	0.025	gG1	+22.2	2.2	3	+ 18.2 D
B 2107	65429	7 58.0	+61 08	6.7	.026	dF3	-20.5	0.8	3	
B 2122	65873	58.7	+16 36	5.9	.012	Aon	-18.	var	4•	- 15.v SD
B 2121	65856	58.7	+25 14	6.2	.024	Aln	- 9.	6.	4	- 9.1 SV
B 2133	66347	8 00.9	+22 13	6.8	.041	gK3	- 3.0	1.0	3	
B 2129	66138	01.1	+57 55	6.8	.122	dF3	+10.4	1.8	3	
B 2139	66751	8 05.2	+69 52	6.6	.189	dF8	- 6.	var	4•	
G 11028	67404	05.2	- 3 16	6.8	.009	gM4	+24.0	2.0	3	
74° 348	66633	05.4	+74 31	8.2	.059	gFon	+ 3.	3.4	3	+ 6. L
G 11050	67294	06.0	+58 24	6.0	.082	gK4	+33.5	0.9	3	+ 36.2 D
G 11073	67587	06.9	+35 36	6.6	.314	dGo	-55.3	0.8	3	
B 2159	67880	8 07.2	-16 06	5.5	.018	cB3	+32.9	1.5	5r	
B 2162	68077	09.9	+56 36	5.9	.040	gG9	+ 7.4	1.2	3	+ 8.3 D
B 2173	68351	10.1	+29 48	5.6	.024	Aop	+22.	3.1	4•	+ 18. V
A 6659A	68433	10.2	+ 9 44	7.6	.054	gA5	+32.	var	4•	
A 6659B	----	10.2	+ 9 44	9.3	---	dF5	+38.1	0.6	3	
G 11211	68638	8 12.1	+57 15	7.8	.396	dG6	+17.4	1.3	4r	
74° 350	67739	12.2	+74 39	8.5	.015	gK3	-12.1	0.7	3	
G 11220	68579	12.4	+64 45	8.6	.099	gG5	+11.2	2.3	4	
B 2185	68930	13.7	+59 44	5.5	.001	A4n	-14.3	1.5	7	- 19.6 Y
15° 2351	69371	13.9	-15 32	7.3	---	gKo	+28.3	1.1	3	

TABLE I (Cont'd)

STAR	H.D.	1950 R.A.	1950 Decl.	Vis. Mag.	P.M.	Spec.	Vel.	P.E.	No. Pl.	Others
		h m	° ′		″		km	km		
G 11280	69530	8 14.6	-15 00	7.3	0.010	gK5	- 4.7	0.9	3	
B 2197	69548	16.4	+57 54	5.9	.062	dF2	-13.5	2.2	3	- 16.9 V
14° 1872	69809	16.4	+14 21	8.2	.038	dG6	+16.6	0.4	3	
14° 1878	70319	19.0	+14 29	7.9	.055	gK0	+73.1	1.1	3	
B 2212	70442	19.1	-19 55	5.6	.022	gG0	- 9.	var	6•	
15° 1809	70594	8 20.5	+15 26	8.4	.034	A2	-16.1	1.3	3	
70° 510	70311	21.4	+70 19	7.5	---	sgG3	-63.1	0.5	3	
G 11478	70923	22.0	- 0 59	6.8	.227	dG0	+ 8.7	0.8	3	
G 11493	71095	23.0	+ 2 16	5.9	.029	gK5	+12.1	1.3	3	+ 13.1 D
B 2237	71155	23.2	- 3 45	4.0	.071	Aon	+ 5.4	1.4	4	+ 10.1 M
B 2245	71250	8 24.0	+12 49	5.8	.108	gM3	- 6.8	0.8	4r	
29° 1759	71594	26.2	+29 38	8.3	.023	Aon	+23.	3.7	4•	
30° 1719	72052	28.8	+29 53	8.2	.025	gF2	-22.8	1.9	3	- 26. L
29° 1770	----	29.2	+29 38	8.5	.066	gF5	+10.3	2.0	3	
G 11372	72561	31.1	+ 4 56	6.1	.017	gG5	+ 1.3	1.5	3	+ 1.6 D
22° 2317	72769	8 31.6	-23 11	7.4	.368	dG5	+18.6	1.3	3	
G 11769	72846	32.9	+19 57	8.3	.053	dA5n	+30.3	1.0	3	
20° 2125	72942	33.5	+20 32	8.2	.034	A3	+30.4	1.5	4	
19° 2047	73045	34.1	+19 05	8.5	.040	A4	+22.8	0.9	4	
20° 2129	73142	34.7	+20 39	8.1	.039	dF8	-16.2	1.9	4	
20° 2131	73161	8 34.7	+20 12	9.1	.038	dF0	+34.1	2.8	3	
G 11815	73174	34.7	+19 54	8.3	.046	dF2p	+33.9	2.0	3	
G 11818	73210	34.9	+19 27	6.7	.034	sgA7n	+27.4	0.8	4	
20° 2133	73175	35.0	+19 41	8.2	.040	dA6n	+31.0	0.3	3	
b Hya	73262	35.0	+ 5 53	4.2	.070	Aon	+21.0	2.6	4•	+ 10.3 M
20° 2136	73294	8 35.7	+20 23	8.1	.025	dF6	- 9.9	2.5	3	
20° 2138	73345	35.9	+20 10	8.6	.038	dA8	+34.8	1.7	3	
21° 1880	73425	36.2	+20 59	8.6	---	gG5	-22.1	1.1	3	
20° 2141	73430	36.2	+20 10	8.7	.035	dA6	+28.4	1.6	3	
B 2300	73449	36.2	+19 51	8.1	.037	dA6n	+30.	var	5•	
B 2301	73450	8 36.3	+19 46	8.6	.038	dA7n	+31.8	2.5	4	
G 11873	73574	36.8	+20 16	8.1	.031	dFon	+36.5	2.9	3	
B 2305	73575	36.8	+19 57	6.7	.039	sgA7n	+30.6	1.2	4	+ 29.8 V
19° 2064	73576	37.0	+19 27	7.8	.043	A4	+32.	3.1	3	
G 11879	73598	37.0	+19 43	6.7	.037	gG8	+34.3	0.6	3	
G 11881	73618	8 37.1	+19 44	6.9	.044	gA5	+39.3	2.2	4	
G 11886	73696	37.2	+32 07	6.1	.047	gF3	+12.	var	4•	+ 12.0 D
G 11893	73711	37.4	+19 43	7.4	.040	sgA6n	+38.5	1.6	4	
G 11895	73712	37.5	+19 32	6.8	.057	sgA5n	+30.7	1.0	4	
20° 2168	73730	37.5	+20 02	8.7	.039	dA9	+27.3	0.4	3	
20° 2169	73739	8 37.6	+20 22	9.1	.035	dA5n	- 6.	var	4•	
B 2311	73771	37.6	+19 43	6.3	.039	gA6n	+21.	var	8•	+ 38.1 V
B 2313	73765	37.9	+19 54	6.7	.037	gA8n	+36.8	1.1	3	+ 26.6 V
19° 2075	73783	38.0	+19 24	8.0	.044	A4	+37.1	2.3	3	
B 2314	73819	38.1	+19 46	6.8	.038	sgA5n	+27.6	1.5	6	
20° 2179	73872	8 38.3	+20 06	8.8	.035	A4n	+30.3	2.9	3	
45° 1620	73769	38.4	+45 04	7.9	.035	gF2	+21.0	2.0	3	
19° 2078	73890	38.4	+19 27	8.7	.039	dA5n	+39.	var	3•	
G 11950	73978	39.0	+20 03	7.0	.039	gG7	+31.0	0.6	3	
19° 2083	74028	39.4	+19 35	7.9	.041	dA5	+30.0	1.9	3	
44° 1783	74327	8 41.6	+44 22	8.5	.040	gF5	+22.9	1.9	5	
a Pyx	74575	41.6	-33 00	3.7	.019	B1	+11.8	1.5	2	+ 15.6 M
B 2343	74591	42.4	+ 5 52	6.0	.009	A3n	0.	4.3	4•	
B 2346	----	42.8	- 2 25	7.5	.024	dF6	-18.3	0.6	3	
67° 559	74463	43.8	+67 38	8.5	---	sdGo	-168.6	1.3	3r	
ε Hya	74874	8 44.1	+ 6 36	3.5	.198	dF8	+30.4	0.5	7	+ 36.8 L
B 2353	74873	44.2	+13 17	5.7	.090	Ao	+28.3	1.8	2	+ 21.0 D
B 2357	74988	44.7	- 1 43	5.2	.033	Ao	- 0.3	2.0	5r	0. M
G 12154	66368	45.9	+88 46	7.0	.011	A2	- 8.	3.1	4	
G 12155	75157	45.9	+10 37	7.1	.029	gM4	-12.2	1.7	4	
G 12156	75156	8 45.9	+12 44	6.8	.023	gM3.5	+67.1	0.6	3	
45° 1642	75135	46.4	+44 52	7.7	.031	Ao	+ 2.6	1.9	3	
45° 1643	75172	46.7	+45 10	8.6	.015	dA6n	-22.2	2.0	4	
64° 710	75073	47.0	+64 37	8.5	---	dG3	-43.5	1.5	3	
B 2370	75558	48.4	+16 11	7.2	.031	sgG3	+89.5	1.0	3	

TABLE I (Cont'd)

STAR	H.D.	1950 R.A.	1950 Decl.	Vis. Mag.	P.M.	Spec.	Vel.	P.E.	No. Pl.	Others
		h m	° ′		″		km	km		
C 1039	75596	8 48.4	- 0 28	8.6	0.194	dF7	+ 36.0	1.3	3	
G 12226	75523	48.8	+45 30	6.1	.051	gK1	+ 12.2	0.7	3	+ 13.7 D
G 12228	75556	48.9	+42 12	6.1	.086	gK2	+ 54.5	0.4	3	+ 58.9 D
G 12234	75487	49.2	+59 15	6.1	.015	gF2	+ 8.3	0.4	3	+ 9.1 D
B 2367	75486	49.3	+62 09	5.7	.022	gFon	- 31.1	1.1	3	- 31.3 D
B 2383	75958	8 52.4	+64 48	5.6	.088	gG3	+ 9.1	1.1	3•	- 0.1 V
B 2385	75972	52.6	+65 43	7.4	.019	gG6	- 33.2	1.5	3	
G 12341	76292	53.3	+40 24	5.9	.098	gF3	+ 25.4	0.7	3	+ 25.4 D
B 2413	76943	57.4	+41 59	4.1	.505	dF2	+ 23.5	1.1	5r	+ 26.3 M
G 12441	76539	57.7	+76 36	7.8	.193	dG4	+ 14.3	1.2	3	
G 12468	77236	8 58.7	- 2 22	7.9	.149	sgKo	+142.5	0.3	3	
G 12499	77445	9 00.1	+ 7 30	6.1	.020	dK3	+ 26.4	0.7	3	+ 28.0 D
B 2429	77557	01.2	+28 06	6.3	.007	Aon	- 22.	4.3	5	- 26. S
B 2432	77601	02.0	+48 44	5.6	.026	gF1	- 15.	var	6•	0.v VL
G 12551	77692	02.9	+59 33	6.2	.031	Ao	+ 5.6	2.6	5	+ 3. DV
B 2439	77996	9 03.3	+ 5 18	5.4	.019	gK2	+ 17.8	1.5	5•	+ 25.8 M
G 12613	78366	05.8	+34 05	6.0	.222	dGo	+ 26.3	1.1	3	+ 27.6 S
G 12638	78274	06.6	+67 40	8.1	.237	dF5	+ 9.1	1.0	3	
59° 1223	78364	06.6	+59 29	8.2	.082	dF4	- 1.1	1.7	3	
B 2446	78362	06.8	+63 43	4.7	.120	gF6	- 8.8	0.1	2	- 6.5 L
A 7213AB	78608	9 06.8	+16 19	9.0	.031	A2	+ 21.6	2.8	4	
B 2476	79439	12.6	+54 14	4.9	.078	dA5n	- 7.6	2.2	4	- 17.v M
G 12774	79752	13.1	-14 49	6.2	.033	Aon	+ 32.4	1.2	3	
G 12779	79726	13.4	+14 20	8.3	.256	dG1	- 45.4	0.8	3	
G 12785	79765	13.6	+19 01	6.9	.159	dFo	+ 30.0	1.5	4	
A 7281A	79872	9 14.4	+23 52	7.8	.089	dF5	+ 12.1	1.5	3	
A 7281B	----	14.4	+23 52	8.1	.081	dF6	+ 6.3	1.4	3	
G 12811	80050	14.8	-14 22	6.0	.050	gKo	- 36.1	0.9	3	
G 12816	79969	14.9	+28 47	7.3	.511	dK4	- 17.5	1.9	4r	
B 2496	80105	15.1	-11 45	7.3	.057	gG6	+ 9.2	1.3	3	
G 12838	79968	9 16.1	+65 14	7.6	.331	dG4	+ 22.	var	5•	
B 2498	80130	16.7	+60 00	7.5	.044	gKo	- 32.5	1.1	3	
B 2505	80479	17.2	-15 37	5.9	.071	gK4	- 29.1	1.9	4	
B 2510	80550	17.9	- 9 24	6.9	.041	gFo	+ 15.5	2.9	4•	
B 2511	80586	18.0	- 9 21	5.0	.037	gG9	+ 22.1	1.0	4	+ 25.5 L
G 12883	80390	9 18.1	+56 55	6.0	.013	gM4	+ 23.0	1.6	4	+ 21.0 D
G 12897	80719	18.6	-15 24	6.3	.123	dM6	- 1.	var	4•	
G 12947	81028	20.8	+ 7 56	7.2	.037	gM4	+ 57.8	1.7	2	+ 58. L
B 2520	81058	21.2	+26 08	6.8	.049	gK3	- 15.6	1.1	4	
G 12967	80768	21.6	+76 09	9.1	.375	dK5	- 1.6	2.0	3	
G 12987	81265	9 22.5	+30 43	7.8	.198	sgG8	- 1.0	0.8	3	0. L
B 2528	81361	22.8	+16 48	6.3	.089	gG9	+ 13.6	1.1	4	+ 8.5 V
G 13010	81567	23.8	- 1 15	6.1	.007	gK3	- 14.3	0.7	3	
G 13013	81540	23.9	+16 55	7.9	.014	gM2.5	+ 67.5	0.7	3	
29° 1903	81594	24.5	+29 28	8.9	.016	gK3	+ 3.7	0.9	3	
B 2530	81688	9 25.4	+45 49	5.6	.131	gG5	+ 39.4	1.0	2	+ 37.9 V
B 2531	81701	25.4	+45 48	8.1	.052	gGo	+ 8.6	0.3	2	+ 8. L
G 13088	82077	26.9	-20 32	6.0	.025	gM1	- 8.	var	4•	
G 13122	82232	28.0	-15 21	6.1	.087	gK3	+ 24.4	1.6	3	
ψ Vel	82434	28.7	-40 15	3.6	.207	dA7n	+ 11.	4.5	3	+ 12.4 L
B 2547	82189	9 30.2	+72 26	5.8	.110	dF6	- 37.8	0.9	3	- 38.9 D
B 2582	83240	34.6	+ 7 04	5.1	.060	gG9	+ 20.	var	3•	+ 20.4 L
G 13388	83951	39.7	+35 19	6.0	.057	dF1	- 8.2	1.3	4	- 8.4 D
A 7500A	84184	40.9	+ 2 51	7.3	.033	gF7	- 3.1	1.4	4•	
B 2611	84179	42.1	+63 53	6.5	.049	dA8n	- 25.	var	8•	- 32.5 V
B 2623	84607	9 43.8	+ 2 01	5.7	.074	gFo	+ 13.	var	5•	+ 16.3 S
13° 2946	84636	43.9	-14 22	8.0	.044	gK2	+ 22.7	1.0	3	
C 1161	----	44.0	-14 17	9.2	.306	dG4	- 4.7	0.4	3	
12° 2093	----	44.6	+11 40	9.4	---	gK4	+ 97.3	1.6	3•	
B 2625	84739	44.9	+20 50	7.8	.079	dF2	- 15.9	2.0	3	
G 13512	84937	9 46.2	+13 59	8.1	.877	sdA4p	- 18.1	1.9	5r	- 15.3 Md
B 2634	85040	47.0	+21 25	6.0	.048	gFo	+ 22.	var	3•	var L
G 13531	85091	47.1	+11 20	7.5	.311	dGo	+ 40.	var	4•	
G 13544	85162	47.8	+31 38	7.3	.018	gM2.5	- 33.4	0.2	2	- 34. L
B 2641	85364	48.7	- 4 00	6.0	.033	gA5n	- 10.0	2.7	5	

TABLE I (Cont'd)

STAR	H.D.	1950 R.A.	1950 Decl.	Vis. Mag.	P.M.	Spec.	Vel.	P.E.	No. Pl.	Others
		h m	° ′		″		km	km		
B 2644	86373	9 49.3	+38 09	6.7	0.048	A3n	+ 14.0	2.7	2	+ 16.v V
G 13579	86441	49.6	+27 13	8.1	.220	dKo	- 11.6	0.7	3	
G 13607	86515	51.0	+65 29	9.1	.188	dG5	- 16.7	1.9	4	
G 13608	86709	51.1	+ 6 12	6.3	.014	gM2.5	+ 0.4	2.5	2	- 0.3 D
+0° 2582	86904	52.4	+ 0 03	8.1	.015	gM4	+ 30.	var	4•	
-0° 2270	86990	9 53.1	- 0 53	8.1	.071	gKo	+ 1.6	1.0	3	
+0° 2588	86135	54.1	- 0 14	8.3	.014	gK5	- 6.4	1.7	3	
A 7589A	86133	54.3	+20 00	7.7	.231	dF8	+ 27.2	0.6	3	
A 7589B	----	54.3	+20 00	9.2	.221	dG3	+ 28.7	1.7	3	
B 2670	86359	55.5	+15 28	7.6	.044	sgG7	+ 17.7	0.5	3	
G 13732	86535	9 56.2	+56 43	7.3	.012	gKo	+ 13.8	0.9	3	
G 13733	86476	56.2	+ 5 03	7.3	.037	gM3.5	- 26.5	1.9	3	- 32. L
B 2673	86378	56.4	+57 03	5.7	.046	gK5	- 12.4	1.3	8	- 14.2 V
G 13748	86590	57.2	+24 48	7.9	.242	dG5	0.	var	4•	
G 13790	86966	59.8	+14 48	7.9	.266	A2	+ 12.6	0.6	3	
B 2683	87096	10 00.1	-13 03	7.0	.138	dF9	+ 16.	var	4•	
B 2685	87301	01.6	+ 3 27	6.4	.126	dF3	+ 4.0	0.8	2	- 2.4 V
η Leo	87737	04.6	+17 00	3.6	.008	oAo	+ 3.2	0.5	11•	+ 2.2 M
G 13901	87598	04.7	+68 41	9.0	.296	dKo	+ 32.4	1.4	3	
G 13902	87808	04.8	-16 54	5.9	.054	gK5	+ 11.4	0.4	3	
G 13941	88021	10 06.6	+20 35	6.6	.036	•	+ 9.2	1.5	4	
G 13949	88071	06.9	+ 9 50	7.5	.040	gM3	+ 6.1	0.7	3	
G 13951	88108	06.9	-13 07	7.3	.052	gM3	- 10.6	1.8	2	- 13. L
B 2701	88161	08.0	+40 54	6.5	.017	gK3	+ 14.3	1.0	3r	
G 13985	88231	08.3	+37 39	6.1	.043	gK3	+ 10.3	0.8	3	+ 9.7 D
C 1225	233719	10 10.8	+52 46	9.2	.75:	dMo	- 24.3	1.0	6r	
G 14037	88639	11.0	+27 23	6.1	.016	gG2	- 6.2	1.3	3	+ 21.v S
B 2717	88697	11.3	- 7 08	7.3	.192	dF6	+ 14.1	1.5	3	
B 2719	88764	11.6	- 7 45	7.1	.026	gG7	+ 9.8	1.8	4	
G 14056	88737	11.7	+21 25	6.1	.166	dF8	+ 14.9	1.3	3	+ 17.5 SV
B 2724	88960	10 13.4	+29 34	5.4	.079	Ao	+ 16.6	2.7	4	+ 16.7 VL
A 7705A	88849	13.9	+71 19	6.6	.062	gA8	+ 10.2	0.9	2	+ 10.0 V
A 7705B	88850	13.9	+71 18	7.2	.058	gFo	+ 13.5	1.6	2	+ 12.0 V
G 14106	89024	13.9	+25 37	6.0	.109	gK2	+ 34.4	0.4	5r	
ι Leo	89025	13.9	+23 40	3.6	.023	gFo	- 19.3	2.9	3	- 18.7 M
73° 491	88988	10 15.3	+72 42	7.7	---	gKo	+ 18.7	1.3	3	
B 2736	89269	15.8	+44 18	6.7	.307	dG5	- 10.1	0.7	5r	- 6.9 V
G 14167	----	16.9	+20 07	9.4	.491	dM4e	+ 10.4	1.6	5r	
B 2746	89619	17.9	+ 6 41	8.4	.058	gF7	+ 1.8	1.7	4	
G 14202	89707	18.4	-15 14	7.0	.358	dF8	+ 78.8	2.3	4r	
B 2748	89688	10 18.5	+ 2 33	6.5	.009	B3	+ 11.	3.3	6r•	- 1. V
B 2752	89774	19.2	+15 14	6.1	.041	B9	+ 7.3	2.7	5	+ 8.8 V
G 14237	89813	19.5	+11 34	8.0	.335	dG6	- 16.3	0.7	3	
B 2757	89962	20.4	+ 6 48	6.3	.106	dK3	- 24.1	1.9	7	
G 14292	90197	21.9	-24 21	7.0	.353	dGo	+ 57.4	2.4	4	
A 7762A	90204	10 22.8	+52 53	7.9	.129	dF5	+ 14.2	1.2	4	
A 7762B	----	22.8	+52 53	8.4	---	dF8	+ 16.4	1.4	3	
B 2769	90303	23.0	+ 9 02	7.7	.026	gA7	- 18.6	1.4	3	
G 14237	-----	23.7	+69 07	9.4	.169	dK4	- 53.0	0.6	3	
B 2772	90473	24.1	- 0 44	6.8	.050	gK3	+ 4.5	0.6	3	
G 14336	90441	10 24.2	+29 56	7.8	.075	gF2	+ 12.8	0.9	4	
A 7778A	90483	24.4	+18 19	8.7	.169	dG7	+ 15.1	0.9	3	
A 7778B	----	24.4	+18 19	8.7	.158	dG8	+ 6.7	2.4	3	
G 14346	90494	24.5	+20 04	8.9	.268	dGo	+ 3.9	1.5	3	
G 14355	90572	24.9	+ 3 49	7.2	.111	sgKo	+ 45.6	2.1	5	
30° 2022	----	10 26.6	+29 56	8.5	.005	gKo	+102.7	0.8	4	
B 2789	90957	27.2	-29 24	5.8	.061	gK5	- 4.2	2.4	5	
B 2797	91120	28.5	-13 20	5.5	.047	B9n	+ 8.	var	7•	var Y
B 2798	91130	29.0	+32 38	5.8	.015	B9n	- 14.	5.	4	- 10.9 D
ρ Leo	91316	30.2	+ 9 34	3.8	.009	oBo	+ 41.5	1.4	11•	+ 42.2 M
B 2810	91369	10 30.3	-16 42	7.6	.092	dGo	+ 11.9	2.2	5	
B 2818	91706	32.6	-22 55	6.2	.103	dF7	+ 11.6	1.3	4	
G 14569	91816	33.6	-11 39	7.9	.288	dK3	+ 4.0	1.1	3•	
B 2821	91880	33.8	-16 05	6.2	.027	gM1	+ 16.2	1.4	9	
B 2836	92214	36.1	-16 37	5.1	.104	gKo	+ 18.7	2.3	4	+ 16.8 M

TABLE I (Cont'd)

STAR	H.D.	1950 R.A.	1950 Decl.	Vis. Mag.	P.M.	Spec.	Vel.	P.E.	No. Pl.	Others
		h m	° ′		″		km	km		
B 2831	92168	10 36.3	+38 10	5.8	0.224	dF8	+ 4.	var	11•	+ 16.v V
A 7873A	92321	37.3	+38 40	8.0	.022	gK5	+ 25.8	2.6	3•	
A 7873B	----	37.3	+38 40	8.5	---	gK3	+ 26.1	3.1	4•	
B 2839	92371	37.6	+27 47	6.9	.010	Aon	- 9.	4.4	6•	+ 6. D
88° 60	90162	37.8	+88 08	8.7	---	dF8	- 23.	var	4•	
B 2841	92424	10 38.6	+65 59	5.1	.180	gK4	- 17.1	1.9	4•	- 8.8 L
B 2846	92588	38.9	- 1 29	6.4	.188	sgK1	+ 43.5	0.4	10r	
G 14698	92587	39.0	+14 14	7.9	.011	gM2.5	- 10.9	0.5	3	
G 14719	92668	39.8	+51 04	7.2	.017	dA7n	- 2.0	1.4	4	
45° 1857	92764	40.5	+45 12	8.8	.025	dA5n	- 8.	var	4•	
B 2855	92844	10 40.5	-23 17	6.9	.005	gG3	- 12.	var	4•	
B 2857	92855	41.1	+46 28	8.1	.286	dGo	+ 9.	var	10•	- 2.v L
A 7925A	93270	44.4	+65 43	7.6	.096	dF5	- 1.4	1.6	3	
B 2877	93527	45.2	-15 22	7.4	.128	dF5	+ 30.0	1.9	3	
G 14852	----	45.2	-15 21	8.3	.155	dF8	+ 21.0	1.5	3	
G 14877	93655	10 46.1	- 1 42	6.2	.014	gM1.5	+ 3.0	1.0	3	
B 2882	93704	46.5	- 8 50	7.2	.028	gG5	- 11.6	1.1	3	
G 14900	93833	47.2	- 9 35	6.0	.041	gG8	+ 40.8	1.0	4	
C 1304	93932	48.0	-14 50	8.1	.30:	dGo	+ 36.	var	4•	
B 2895	94083	49.5	+52 50	6.7	.036	gG8	- 4.1	1.7	4•	- 12.8 V
B 2897	94132	10 50.1	+70 07	6.1	.402	dG9	+ 15.8	1.1	4r	
G 14963	94340	50.6	-20 21	7.1	.315	dG3	- 13.6	1.9	3	
G 14968	94336	50.9	+26 28	7.3	.034	gM3	- 5.8	0.6	3	0. L
C 1318	94387	51.0	-15 33	8.3	.332	dKo	+ 30.	var	4•	
A 7979B	94602	52.9	+25 01	6.3	.080	Aln	- 3.3	2.3	2	- 2.v SV
G 15019	94549	10 53.0	+64 48	7.3	.140	dG8	+ 19.9	0.6	3	
B 2910	94600	53.0	+33 46	5.2	.114	gK1	- 22.3	0.8	4r	- 22.3 M
B 2914	94671	53.3	+18 25	7.6	.058	gG4	- 10.7	2.2	6r	
G 15034	94718	53.6	+28 01	8.6	.475	dG6	+ 5.9	1.3	8r	
-0° 2392	94808	54.1	- 0 53	8.1	.045	gA5	- 10.2	0.9	3	
G 15062	94791	10 55.3	+75 59	7.6	.159	dF6	+ 14.1	1.2	3	
G 15101	95234	57.0	-16 05	6.2	.052	gM2.5	+ 33.7	1.5	3	
G 15116	95314	57.7	-13 49	6.1	.035	gK5	- 5.9	0.5	3	
G 15144	95486	58.8	+15 17	7.9	.319	dG5	- 55.9	1.5	3	
B 2931	95578	59.3	- 2 13	5.0	.040	gM1	- 15.0	1.9	4	- 13.1 L
A 8022A	95577	10 59.4	+14 53	8.9	.066	dF4	+ 4.3	1.3	4	
B 2935	95735	11 00.6	+36 18	7.6	4.779	dM2	- 85.6	1.0	9r	
α UMa	95689	00.7	+62 01	2.0	0.138	gG7	- 10.4	0.5	3	- 8.6 M
B 2937	95808	00.7	-11 02	5.6	.135	gG6	- 7.0	1.5	5r	
G 15199	95544	01.1	+81 19	8.3	.226	dG4	+ 11.3	1.4	3	
B 2940	95934	11 01.7	+38 31	6.1	.074	dA5n	+ 6.5	2.5	3	+ 4.9 V
B 2941	95976	02.0	+38 31	7.4	.076	dF5	+ 4.3	2.1	5r	
χ Leo	96097	02.4	+ 7 36	4.7	.308	dF3	+ 3.0	0.8	4	+ 6.1 L
G 15275	96373	04.1	+15 27	7.6	.029	gM3	- 0.9	0.4	3	
B 2949	96418	04.4	+25 48	6.7	.071	dF6	- 7.4	2.7	4	
A 8061A	96478	11 04.6	+11 11	9.3	.061	gKo	+ 11.6	2.3	3	
A 8061B	----	04.6	+11 11	9.5	---	gKo	+ 8.8	1.5	2	
G 15294	96360	04.7	+68 38	8.4	.031	gM4	- 53.7	1.6	3	
G 15299	96553	04.9	-15 05	8.3	.296	dGo	+ 9.3	0.9	3	
59° 1351	96656	06.0	+59 29	7.3	.032	dG5	+ 7.5	0.8	4	
G 15327	96734	11 06.4	+51 39	7.1	.021	gM4	- 19.2	2.1	3	
66° 703	96972	07.9	+66 18	8.8	---	gG7	- 1.6	2.1	4•	
G 15361	97068	08.0	+11 34	7.5	.031	gM4.5	+ 0.4	1.1	3	
14° 3289	97635	11.6	-15 10	8.1	---	gFon	+ 6.3	2.1	4	
A 8100B	----	12.0	+73 45	7.5	---	gMo	+ 3.5	1.9	3	
C 1371	97783	11 12.3	-23 22	8.7	.309	dG2	+ 87.4	2.0	4	
G 15480	97918	13.1	-12 19	6.7	.037	gM4	- 0.8	1.7	3	
B 2979	97937	13.4	+13 07	6.5	.071	dA8n	- 20.	var	4•	- 20.7 V
G 15514	98088	14.4	- 6 52	6.0	.016	gFop	- 55.	var	5•	
A 8119A	98231	15.5	+31 49	4.4	.733	dGo	- 14.6	0.8	4	- 15.7 L
A 8119B	----	11 15.5	+31 49	4.9	---	dGo	- 16.0	0.6	4	
A 8131B	----	16.8	- 1 23	8.0	.282	dG3	+ 16.4	1.0	3	
σ Leo	98664	18.6	+ 6 18	4.1	.096	B9	- 3.2	1.5	3	- 5.3 M
15° 2325	----	19.8	+14 46	9.5	.567	dK5	+ 20.9	2.1	4	
15° 2326	98883	20.3	+14 36	8.3	.032	gK1	- 29.8	1.1	3	

TABLE I (Cont'd)

STAR	N.D.	1950 R.A.	1950 Decl.	Vis. Mag.	P.M.	Spec.	Vel.	P.E.	No. Pl.	Others
		h m	° ′		″		km	km		
L Leo	99028	11 21.5	+10 48	4.0	0.188	dM4	- 12.4	0.1	2	- 9.7 M
14° 2382	99088	21.7	+14 11	8.1	.151	dM7	+ 21.5	1.5	3	
B 3007	99285	23.1	+56 07	5.8	.082	gG6	- 4.7	1.3	3	- 6.7 V
B 3011	99329	23.5	+ 4 08	6.4	.093	dA6n	+ 2.1	2.3	3	- 6.v VS
B 3019	99625	25.1	-25 35	6.7	.068	dG7	- 14.1	1.5	3	
A 8175A	99787	11 26.4	+39 37	6.5	.052	A2n	- 3.	4.0	4	- 11.5 M
A 8175B	----	26.4	+39 37	8.4	---	dG5	- 3.2	0.7	2	
G 15790	100041	28.3	+28 44	7.0	.085	gM3.5	+ 85.3	2.4	4•	
A 8190A	100070	28.3	- 6 27	7.6	.040	dF3	+ 3.6	0.9	3	
B 3034	100238	29.4	- 6 12	6.9	.092	gK1	+ 4.2	0.6	3	
B 3039	100343	11 30.2	- 7 53	6.2	.012	gK4	- 0.8	1.8	4	
ζ Hya	100407	30.5	-31 35	3.7	.215	gG7	- 2.9	1.1	3	- 4.6 M
G 15847	100418	30.7	-16 00	6.0	.049	gG0	- 4.8	0.5	3	
A 8220B	-----	32.1	+17 04	7.3	.012	B6	+ 15.	5.	4	+ 14. V
B 3052	100808	33.7	+28 03	5.8	.023	A4n	+ 16.3	2.1	5	+ 3.7 DV
A 8236A	100831	11 33.9	+56 25	7.9	.208	dG2	- 15.7	0.7	3	
A 8236B	------	33.9	+56 25	8.4	---	dG6	- 17.6	0.9	3	
30° 2180	------	36.0	+30 03	8.1	.036	gF8	- 6.8	1.5	5	
C 1437	101227	36.5	+44 34	8.0	.240	dG4	+ 13.5	1.8	5	
45° 1951	101330	37.1	+44 48	8.2	.032	gG4	+ 3.1	0.9	4	
G 16008	101370	11 37.3	-16 21	6.5	.019	gM2.5	+ 26.4	2.5	4•	
44° 2115	101549	38.7	+44 17	7.8	.010	A3n	- 8.9	2.7	3	
68° 658	101656	39.6	+68 28	9.1	---	dG4	- 1.0	2.1	4	
44° 2118	101716	39.9	+44 03	8.0	.053	dF8	- 26.2	0.9	4	
G 16106	101967	41.6	+44 46	7.8	.209	dF4	+ 14.6	1.5	5	
ξ Vir	102124	11 42.7	+ 8 32	5.1	.066	A3n	- 2.	5.	5•	0. YLV
G 16127	102159	43.0	+36 10	7.2	.057	gM5	+ 61.2	1.1	2	+ 58. L
G 16138	102253	43.5	+ 7 27	7.1	.056	gM2	- 18.8	1.3	4	
G 16159	102326	44.6	+77 19	8.9	.207	dG7	- 92.1	2.5	4r	
B 3097	102510	45.3	+ 8 31	5.2	.057	A1	- 1.0	2.0	4	- 0.8 LYV
B Leo	102647	11 46.5	+14 51	2.2	.511	A4n	+ 4.9	1.8	5	- 2.3 M
B Vir	102870	48.1	+ 2 03	3.8	.792	dF8	+ 2.5	0.9	5	+ 5.0 M
G 16223	102942	48.6	+33 39	6.1	.024	dF1	+ 2.8	0.9	3	0.0 V
G 16227	102925	48.7	+69 07	7.1	.064	A2	+ 13.	var	4•	
B 3112	103095	50.1	+38 05	6.5	7.047	dG5	- 98.6	0.5	11r	- 97.2 L
23°10243	103191	11 50.1	-24 12	8.7	0.315	dG5	0.0	2.0	3	
G 16259	103126	50.7	+86 30	9.1	.326	dKo	+ 10.	var	4•	
A 8348A	103321	51.4	+72 12	7.5	---	dF5	- 7.8	1.3	3	
-0° 2507	103341	51.5	- 0 46	8.5	.021	gG7	+ 12.4	1.6	3	
G 16290	103459	52.3	- 1 10	7.9	.343	dG5	+ 18.8	1.4	3	
+0° 2858	103486	11 52.5	- 0 17	8.3	.050	gF2	0.	var	4•	
G 16299	103500	52.7	+37 02	6.5	.079	gM2.5	+ 18.8	0.8	2	+ 20.7 D
-0° 2512	103631	53.4	- 1 11	8.5	---	dF6	+ 1.3	0.8	3	
G 16322	103681	53.6	+16 00	8.5	.044	gM4.5	- 28.6	1.2	3	
G 16410	104207	57.5	+19 42	7.1	.104	gM4	+ 35.0	1.6	3	
B 3137	104304	11 58.2	-10 10	5.6	.498	dG7	+ 0.2	0.5	5r	+ 1.8 V
29° 2245	104319	58.3	+29 28	8.5	.059	dGo	+ 14.8	1.7	4	
G 16437	104456	59.1	+65 13	7.2	.062	gA8	- 5.4	1.9	4	
A 8395A	104435	59.1	+71 08	7.4	.011	gKo	+ 3.6	1.1	3	
30° 2212	104451	59.2	+29 50	8.4	.062	gF3	- 13.	var	4•	
B 3142	104453	11 59.2	+22 22	6.6	.043	gF8	+ 10.9	2.0	7	+ 9.8 V
29° 2251	104688	12 00.8	+29 25	8.5	.027	gK4	- 5.2	1.3	4	
B 3154	104904	02.2	+85 52	6.4	.103	dF6	+ 7.7	1.8	3	+ 7.0 D
A 8413A	105028	03.0	+69 04	7.6	.048	gKo	- 23.5	0.9	3	
A 8413B	105029	03.0	+69 02	8.1	.058	gM4	+ 12.7	1.5	3	
G 16520	105036	12 03.0	- 5 54	6.8	.012	gM3	- 18.3	0.8	3	
A 8414A	105031	03.0	+52 13	7.0	.014	gG5	- 17.5	1.3	5	
A 8414B	------	03.0	+52 13	8.0	---	gFo	- 17.2	0.4	3	
30° 2223	105182	04.1	+29 48	8.5	.060	gK4	- 16.2	1.7	4	
A 8434A	105421	05.6	+55 45	8.0	.187	dF8	+ 3.5	1.3	3	
A 8434B	105422	12 05.7	+55 45	8.4	.184	dG1	+ 7.0	1.6	4	
B 3173	105778	08.0	+17 05	6.3	.022	Aon	- 10.	3.3	5	- 12.8 V
G 16640	105901	08.8	- 5 39	8.2	.290	dG4	- 9.	var	4•	
B 3181	106057	09.6	+20 49	5.7	.034	gG8	- 23.3	1.4	4r	- 25.8 V
A 8470A	106365	11.6	+33 04	6.8	.113	gK3	- 9.8	0.9	4r	

TABLE I (Cont'd)

STAR	H.D.	1950 R.A.	1950 Decl.	Vis. Mag.	P.M.	Spec.	Vel.	P.E.	No. Pl.	Others
		h m	° '		°		km	km		
A 84708	------	12 11.6	+33 04	8.8	---	dF8	- 4.4	2.2	4	
G 16712	106384	11.7	- 5 26	6.5	0.141	dF3	+ 8.6	0.4	3	
G 16723	106485	12.4	-20 34	6.0	.003	gG7	+ 16.6	2.1	4	
δ UMa	106591	13.0	+57 19	3.4	.106	A2n	- 7.7	2.0	5	- 12. M
G 16745	------	13.4	+ 5 55	9.3	.301	dK6	+ 44.2	0.2	3	
B 3192	106661	12 13.5	+15 11	5.1	.091	A2n	+ 4.	var	5	+ 11.v M
A 84898	------	13.6	+40 56	8.0	---	dF6	- 17.3	0.2	2	
G 16759	106811	14.3	+63 54	8.4	.282	dG3	+ 52.3	2.5	4•	
B 3198	106887	15.0	+29 13	5.7	.054	gA5n	- 7.6	2.4	5	- 7.5 V
G 16773	106949	15.3	+15 18	8.3	.148	dF6	+ 7.3	0.7	3	
G 16784	107028	12 15.7	+69 04	7.8	.122	dG3	- 29.7	2.0	3	
A 8506A	107068	16.2	+12 04	9.1	.040	dGo	+ 12.5	2.5	5•	
A 8506B	------	16.2	+12 04	9.3	---	dG2	+ 16.1	2.2	3	
B 3211	107274	17.4	+49 16	5.6	.011	gM1	+ 7.8	0.9	6	+ 11.0 D
G 16822	107295	17.6	-21 54	6.1	.115	dG2	- 1.7	1.1	3	
G 16827	107326	12 17.8	+26 17	6.1	.146	dA8n	+ 4.0	2.6	4	+ 5. V
B 3213	107328	17.8	+ 3 35	5.1	.301	gK1	+ 35.5	0.3	5r	+ 35.4 M
C 1553	107632	19.6	+42 30	9.2	.30:	dG1	- 30.3	1.1	3	
G 16868	107642	19.7	-15 17	6.7	.030	gK2	+ 10.8	1.2	3r	
G 16886	107814	20.7	-11 32	6.7	.073	gM3	+ 4.0	1.6	4	
B 3228	107869	12 21.2	-30 03	6.6	.014	gMo	+ 68.	3.5	2	
B 3229	107904	21.3	+42 49	6.0	.077	gFon	- 11.	var	5•	- 4.v D
B 3230	107950	21.6	+51 50	5.0	.013	gG7	- 10.8	1.3	3	- 13.0 M
G 16907	107937	21.6	+ 6 15	8.0	.028	gM4	+ 26.	var	4•	
A 8539A	108007	21.9	+25 52	6.3	.018	dA6n	- 10.	3.6	7	- 15.5 V
G 16925	108081	12 22.4	- 3 57	8.3	.270	dG4	+ 47.	var	7•	
36° 2268	------	22.8	+36 16	9.1	---	B3	+ 43.3	1.1	5	
G 16960	108399	24.2	+72 12	6.4	.156	gG8	+ 3.9	0.2	3	+ 8.7 D
A 8553B	------	24.7	+27 18	9.5	---	dK6	- 0.3	2.7	3	
G 16978	108464	25.1	+41 38	6.8	.029	gF5	- 5.4	1.4	6	- 7.9 V
C 1576	108523	12 25.5	-15 23	8.3	.30:	dG4	+ 20.7	1.6	3	
A 8569A	108693	26.6	+31 40	8.1	.139	dF8	- 47.8	1.1	3	
B 3257	108765	27.2	+21 10	5.7	.046	Aln	- 4.8	1.8	8	- 8.1 V
A 8572B	------	27.3	-16 15	8.2	.249	dK2	+ 7.7	2.3	3	
B 3265	108907	27.9	+69 29	5.2	.082	gM4	- 8.4	0.6	3	- 14.v L
B 3262	108875	12 28.0	+10 00	7.9	.079	dF5	- 14.5	1.9	3	
A 8586A	109054	29.2	+27 18	9.2	.015	dG3	- 7.0	0.9	3	
G 17115	109282	31.0	+24 43	7.4	.021	gM3	- 5.	var	4•	
B 3276	109307	31.1	+24 34	6.1	.021	cA4	+ 1.4	2.0	2	+ 2.3 SV
B 3278	109317	31.2	+33 31	5.4	.045	gG7	- 15.5	2.1	4	- 20.8 M
B 3277	109309	12 31.2	- 9 11	5.4	.083	B9n	- 9.	5.	2	- 11. M
G 17125	109345	31.3	+33 40	6.4	.016	gG8	- 40.8	0.3	3	- 42.7 D
B 3288	109646	33.7	+80 32	7.4	.096	dF4	+ 34.8	0.5	3	
G 17165	109585	33.4	-20 15	6.1	.046	dFon	- 2.0	2.3	5	
A 8605A	109654	33.5	+56 51	8.0	.040	gK1	- 29.6	0.5	3	
G 17208	110010	12 35.7	+79 29	7.0	.122	dG2	- 19.0	1.2	4	
G 17216	109931	36.1	-17 59	6.1	.118	dA6n	- 13.4	2.0	4	
B 3299	110024	36.6	+21 20	5.5	.086	gG8	- 11.4	2.0	3•	- 26.1 V
75° 479	110312	38.1	+74 41	8.1	.004	gK4	- 40.8	2.1	5	
G 17273	110385	39.2	-19 29	6.0	.215	dF2n	- 3.3	0.3	3	
B 3308	110418	12 39.4	- 7 14	7.2	.048	gM1	- 1.1	0.5	11	
C 1612	------	40.2	+73 14	9.3	.30:	dG2	- 45.7	2.0	3	
76° 464	110611	40.2	+75 37	8.0	---	dG9	- 33.2	1.6	4	
G 17302	110612	40.7	+10 22	8.0	.063	gM3	- 13.6	2.0	4	
G 17326	110833	42.0	+52 02	7.0	.440	dKo	+ 9.1	1.3	3	
G 17344	------	12 42.9	+14 38	7.5	.092	dF5	- 44.6	0.3	3	
3 3326	111028	43.8	+ 9 49	5.9	.529	sgK1	+ 51.7	0.6	6r	+ 51.6 V
B 3327	111067	44.1	+16 51	5.3	.009	gK5	+ 56.8	2.9	6•	+ 50.7 L
B 3329	111164	44.7	+12 14	6.0	.048	Aon	0.	3.3	4	- 3.5 D
1° 2756	------	45.2	+ 1 28	9.5	---	dG8	- 12.1	1.3	3	
G 17392	111307	12 45.9	+19 36	7.8	.016	gM3	- 6.0	0.9	3	
G 17415	111499	47.2	-14 48	7.0	.014	gM5	- 13.9	1.2	3	
B 3343	111604	47.8	+37 47	5.9	.099	Aon	- 8.	3.9	3	- 14. V
B 3355	112033	50.8	+21 31	5.1	.055	gG8	- 3.8	1.1	4	- 6.6 M
G 17496	112082	51.0	+46 56	7.6	.013	gM4	- 25.1	1.7	4	

TABLE 1 (Cont'd)

STAR	H.D.	1950 R.A.	Decl.	Vis. Mag.	P.M.	Spec.	Vel.	P.E.	No. Pl.	Others
		h m	° ′		″		km	km		
G 17541	112278	12 53.0	+11 46	7.0	0.022	gM4	- 51.9	0.3	3	
A 8705AB	------	53.6	+70 10	9.0	---	dG8	- 27.6	1.4	3	
G 17582	112570	54.8	+46 27	6.2	.056	gG5	+ 7.5	0.3	4	+ 8.5 D
44° 2238	112610	55.2	+44 05	8.0	.056	dF4	+ 2.8	0.9	5	
13° 3627	112575	55.2	-14 12	8.9	.536	dK6	+ 5.6	1.6	4	
B 3407	114282	12 58.4	+87 55	7.6	.016	gK3	- 54.1	1.1	3	
A 8740A	113097	58.8	+16 08	9.5	.045	dM6	+ 7.0	1.8	3	
G 17676	113126	59.0	+ 1 47	7.9	.021	gM3.5	+ 9.5	2.1	4	
A 8749A	113303	13 00.1	+23 46	7.6	.049	dF2	+ 5.5	1.4	3	
G 17706	113406	00.8	+24 06	7.2	.043	gM2.5	+ 5.7	1.9	4	+ 1. L
B 3388	113459	13 01.3	- 3 24	6.5	.055	dA7n	+ 2.	3.1	6r	
85° 214	113826	01.5	+84 32	9.2	---	dG4	- 31.0	0.7	3	
G 17717	113496	01.5	+11 30	7.9	.014	gM4.5	- 2.0	0.7	3	
G 17722	113545	01.6	+43 17	7.0	.013	gM3	+ 18.5	1.0	3	
B 3392	113797	03.4	+36 04	5.1	.031	B9n	- 11.2	2.3	8	- 13.6 M
B 3394	113817	13 03.8	-14 39	7.2	.042	gG5	- 11.7	1.3	3	
A 8786A	113984	04.8	+ 0 51	7.2	.158	dF5	- 22.7	1.9	4r	
A 8786B	------	04.8	+ 0 51	7.6	.158	dGo	- 87.0	1.5	3	
G 17808	114159	06.0	+43 27	7.8	.043	gM3	- 17.0	1.7	3	
C 1688	114172	06.2	+29 39	8.6	.222	dGo	- 40.2	1.6	4	
G 17821	114300	13 07.0	+17 45	8.7	.035	gM1	- 24.6	1.3	4r	
G 17826	114357	07.3	+37 41	6.1	.103	gK4	- 17.3	0.7	4	- 18.7 D
B 3409	114330	07.4	- 5 16	4.4	.053	A2	- 5.9	1.2	3	- 3.4 YLV
29° 2374	114401	07.6	+29 06	8.8	.010	gK1	- 3.7	1.5	5	
30° 2372	114448	08.0	+29 42	8.6	.026	gKo	+ 2.6	2.2	3	
29° 2379	114635	13 09.1	+29 08	8.8	.043	dF7	- 11.4	2.3	4	
A 8814A	114723	09.7	+32 21	6.7	.043	dF4	- 14.9	2.3	5	- 12.7 D
G 17881	114762	09.9	+17 47	7.7	.576	dF7	+ 49.4	0.5	7r	
G 17911	115061	11.3	+67 34	7.0	.156	•gK2	+ 4.5	0.9	3	
57° 1424	115019	11.4	+56 56	8.6	.023	gKo	- 18.2	1.7	3	
B 3431	114960	13 11.4	+ 1 43	6.8	.076	gK5	+ 2.1	2.3	4	+ 9.5v V
B 3432	115004	11.4	+40 25	5.0	.050	gG8	- 20.1	0.8	4r	- 21.6 L
G 17919	115043	11.6	+56 58	6.7	.117	dG2	- 10.0	1.5	3	- 7.9 L
B 3433	115062	12.1	-10 06	7.2	.064	gM2	+ 27.8	1.8	3	
B 3435	115080	12.3	-11 06	6.9	.380	dG3	+ 7.7	0.8	6r	
B 3436	115079	13 12.4	-11 05	7.8	.007	gK2	+ 9.6	1.3	3	
G 17962	115322	13.9	+ 6 46	7.2	.056	gM4	- 20.4	1.0	2	- 24. L
G 17981	115404	14.4	+17 17	6.6	.686	dK3	+ 6.0	0.6	5r	
B 3445	115478	14.8	+13 56	5.4	.032	gK5	- 24.8	0.8	5r	- 25.6 L
G 17992	115467	14.9	-15 17	6.7	.083	gG5	+ 24.7	1.0	5	
G 18010	115723	13 16.2	+34 22	6.0	.042	gK3	- 18.0	0.4	4	- 19.6 D
A 8852A	115721	16.2	+40 10	8.1	.045	dG2	- 25.4	1.7	4	
22° 3557	------	16.5	-22 46	9.4	.340	dKo	- 57.6	1.1	3	
B 3465	116292	20.3	-17 28	5.4	.060	gG5	- 29.2	0.1	3	- 26.4 L
14° 3708	116332	20.5	-15 09	8.6	---	gK3	+ 30.6	1.8	4	
G 18112	116875	13 21.0	+47 16	6.9	.006	gM4	- 8.8	1.1	3	
B 3471	116568	22.0	- 4 54	5.8	.161	dF5	+ 14.4	2.4	4	+ 11.5v S
G 18158	116926	23.3	+68 26	9.7	.237	dG8	- 20.1	1.8	4	
23° 11071	116858	23.9	-24 02	8.4	.366	dKo	- 10.4	1.0	3	
23° 11076	116920	24.3	-24 02	8.6	.314	dK1	- 6.5	1.4	3	
A 8903AB	117173	13 24.3	+76 15	8.2	---	dF2n	- 11.4	2.0	3	
G 18201	117655	25.6	+83 34	7.3	.104	dG4	- 25.9	0.7	3	
B 3484	117104	25.7	-24 57	7.3	.058	dF7	- 34.3	2.2	4	
34° 2426	117262	26.4	+33 56	8.2	.042	gK2	- 7.4	1.3	4r	
B 3497	117566	26.5	+78 54	5.9	.138	gG4	+ 15.6	0.2	2	+ 14.3 V
G 18281	117673	13 29.0	+36 44	7.7	.015	gM3.5	- 1.4	1.3	3	
B 3500	117710	29.1	+42 22	6.2	.096	gK3	- 19.1	0.7	4r	- 19.7 D
B 3499	117675	29.4	- 6 00	4.8	.112	gM3	+ 18.4	1.5	4r	+ 18.3 M
A 8934A	117846	30.1	+37 05	7.3	.018	gG5	- 24.2	1.0	4	
A 8934B	------	30.1	+37 05	8.2	---	dF2	- 21.3	1.4	3	
o Vir	118022	13 31.6	+ 3 55	4.9	.050	gA2	- 8.4	0.6	5r	- 10.9 M
G 18377	118289	33.4	+ 8 33	7.1	.050	gM4	+ 23.6	1.3	3	
G 18399	118508	34.6	+24 52	5.9	.029	gK2	- 35.7	1.1	4•	- 26.1 D
+0° 3082	118526	34.9	+ 0 02	8.5	.010	gFo	+ 14.2	0.7	4	
A 8972A	118511	35.0	- 7 37	7.1	.013	gG5	- 4.3	1.2	4	

TABLE 1 (Cont'd)

STAR	H.D.	1950 R.A.	1950 Decl.	Vis. Mag.	P.M.	Spec.	Vel.	P.E.	No. Pl.	Others
		h m	° '		"		km	km		
A 8972B	------	13 35.0	- 7 37	7.6	---	gG4	- 1.2	0.9	3	
G 18429	118788	35.6	+67 17	6.8	0.083	gG4	- 1.1	0.5	3	
B 3523	118741	35.7	+50 58	6.8	.014	gM3	- 47.5	1.6	5	- 46.6 D
A 8981C	------	35.8	+39 26	9.6	.270	dG8	- 26.2	1.8	2	
G 18479	119035	38.0	+32 16	6.1	.112	gG3	- 17.8	1.2	3	- 17.6 SV
A 8991A	119055	13 38.3	+20 12	5.6	.051	A2	- 28.9	1.8	2	- 23.0 V
A 8991B	------	38.3	+20 12	9.1	---	dF8	- 26.8	1.8	3	
G 18523	119290	39.8	+ 1 15	7.9	.019	gM3.5	- 7.2	0.8	3	
B 3539	119476	40.0	+65 04	5.7	.055	B9n	+ 2.2	2.3	4•	- 15.4 V
G 18535	119392	40.2	+23 34	7.5	.068	gM4	- 35.7	1.2	3	
G 18539	119458	13 40.5	+35 14	6.0	.018	gG2	- 5.	var	4•	- 26. S
A 9000B	------	40.5	+ 3 47	8.2	---	dG5	- 41.2	0.6	2	
17° 3918	119608	41.8	-17 41	7.3	---	dBo	+ 25.3	2.4	5•	+ 19.9 L
B 3543	119706	42.3	- 7 23	7.1	.039	gK1	- 31.6	0.8	4	
G 18602	119850	43.2	+15 10	8.5	2.507	dM2	+ 15.7	0.9	5r	
B 3548	119853	13 43.3	-12 11	5.8	0.021	gG6	- 10.4	1.0	3	
G 18605	119992	43.4	+56 08	6.4	.382	dF4	- 2.9	1.1	3r	- 6.0 V
G 18621	120048	44.2	+38 45	6.0	.052	gG5	- 14.4	0.2	3	- 11.9 S
η UMa	120315	45.6	+49 34	1.9	.123	B3n	- 10.0	2.7	2	- 10.9 M
B 3563	120235	45.7	- 6 35	6.6	.045	gG4	- 1.4	1.6	4	
B 3568	120348	13 46.0	+42 18	6.8	.072	gK2	- 0.4	0.2	4r	
G 18704	120787	48.1	+61 44	6.0	.124	dG3	- 11.6	0.2	3	- 11.7 D
G 18705	120771	48.2	+55 07	8.2	.049	gM4.5	- 9.2	1.5	3	
42° 2444	120817	48.6	+42 23	7.5	.011	A2n	- 2.5	2.0	5•	- 16. D
G 18742	120950	49.6	+39 55	7.8	.026	gM4.5	+ 33.0	0.7	3	
G 18744	121146	13 49.8	+68 34	6.4	.202	sgK2	- 46.0	0.5	3	- 43.5 D
G 18747	120901	49.9	-18 28	7.0	.049	dF3	- 38.	var	3•	
B 3598	121457	50.2	+79 15	6.6	.046	gK1	- 3.6	1.1	3	- 3.8 V
G 18785	121297	51.5	+52 34	7.0	.016	gM4	- 18.4	1.7	3	
η Boo	121370	52.3	+18 39	2.8	.370	dF7	- 7.2	1.1	6	- 0.2v O
G 18864	121979	13 55.0	+67 11	8.2	.147	dG6	- 14.3	1.9	3	
A 9069A	122189	55.1	+78 39	7.9	.016	dF4	- 3.4	0.6	3	
A 9069B	------	55.1	+78 39	9.7	---	dGo	- 2.5	1.7	3	
B 3604	121847	55.7	-24 44	5.2	.061	B8n	+ 11.	4.1	4•	- 3.7 L
A 9072A	121906	55.8	+19 42	8.6	---	dFo	+ 3.2	2.3	4	
2° 2752	121908	13 55.8	+ 2 29	8.5	---	dF9	+ 8.1	1.8	3	
G 18910	122132	56.8	+46 50	7.2	.024	gM2	- 57.9	2.0	3	- 60. L
B 3609	122135	57.4	- 7 55	6.6	.061	gG5	- 3.	var	4•	
G 18965	122563	14 00.1	+ 9 56	6.1	.211	sdF5p	- 26.1	0.6	3•	- 21.1 S
73° 615	123154	01.3	+73 12	8.8	.12:	dG7	- 14.6	3.1	4r	
G 19040	123214	14 04.0	-13 58	6.7	.025	gM4	+ 8.7	1.7	3	
G 19043	123303	04.1	+17 12	6.8	.012	gM4	+ 14.3	1.4	3	
G 19067	123802	05.1	+74 57	7.6	.136	gK3	- 68.1	1.5	4r	
G 19088	123598	06.2	-19 01	7.2	.058	gM3	+ 52.0	1.3	2•	+ 65. L
B 3631	123782	06.4	+49 42	5.4	.084	gM2	- 11.5	1.0	5r	- 13.5 M
G 19105	123760	14 07.0	+10 29	7.9	.181	dG3	- 3.5	2.7	5•	+ 2. L
A 9136A	123963	07.9	+26 50	8.4	.188	dG4	- 24.6	2.1	4	
A 9136B	------	07.9	+26 50	9.4	---	dG7	- 26.2	0.6	3	
B 3649	124547	09.0	+77 47	5.0	.043	gK4	+ 10.	var	6	+ 9.5v V
G 19144	124106	09.1	-12 22	7.9	.309	dKo	+ 8.1	1.0	3	
B 3640	124248	14 09.2	- 9 40	7.3	.046	dA8	0.0	2.7	4	
G 19195	124752	11.4	+67 49	8.2	.154	dK1	- 7.6	1.7	3	
G 19223	124681	12.4	+ 3 34	6.6	.052	gM4	- 45.2	0.3	2	- 47.8 D
α Boo	124897	13.4	+19 26	0.2	2.284	gKo	- 5.0	0.1	76	- 5.1 M
A 9188A	124929	13.8	+ 6 19	7.9	0.014	A5	- 18.2	1.2	3	
A 9197A	125193	14 14.4	+56 55	6.6	.105	dG2	- 29.4	0.4	3	
B 3675	125377	16.4	+ 4 07	8.7	.065	gG5	- 44.4	0.2	3	
B 3678	125454	17.0	- 2 02	5.2	.141	gKo	- 26.9	1.1	5	- 27.2 M
15° 2695	125504	17.0	+15 10	8.1	.012	gK5	- 18.4	0.9	4	
G 19347	125796	18.5	+48 44	7.2	.057	dF8	- 18.3	1.1	3	
G 19385	126009	14 20.0	+29 36	6.6	.047	gM4.5	- 18.4	1.7	3	
B 3688	125823	20.0	-39 17	4.6	.048	B7	+ 5.2	1.4	2	+ 8.7 L
B 3694	126201	21.5	+ 6 03	7.7	.047	dG8	- 39.9	0.6	3	
G 19433	126271	21.8	+ 8 19	6.2	.152	gK4	- 31.0	1.1	3	- 29.0 D
B 3698	126251	22.0	-11 27	6.5	.083	dF2	- 36.3	2.0	4	

TABLE 1 (Cont'd)

STAR	H.D.	1950 R.A.	1950 Decl.	Vis. Mag.	P.M.	Spec.	Vel.	P.E.	No. Pl.	Others
		h m	° ′		″		km	km		
G 19438	126273	14 22.0	- 2 07	7.4	0.035	gM3	- 27.2	2.5	4•	
G 19475	126795	23.7	+65 23	9.1	.181	dG2	+ 20.3	0.3	3	
C 1898	126681	24.7	-18 11	9.1	.30:	dGo	- 47.7	1.3	3	
B 3708	126766	25.0	-13 08	6.7	.075	gF4	- 18.8	2.2	4	
G 19512	126947	26.0	+ 5 54	7.5	.033	gM3	+ 18.	var	4•	
G 19528	127093	14 26.5	+26 05	7.0	.031	gM4	+ 0.3	0.5	3	
G 19550	127334	27.6	+42 01	6.4	.273	dG4	- 1.6	0.7	3	0.0 D
G 19572	127537	28.2	+ 5 00	6.1	.021	gK4	+ 6.9	2.3	4•	
- 19598	127618	29.7	+ 4 22	7.4	.015	gM3	+ 0.8	2.1	4	
B 3723	127929	30.4	+60 27	6.2	.052	gFo	- 19.1	1.9	3	- 19.5 D
G 19627	128000	14 31.0	+55 37	6.0	.023	gK5	+ 2.4	0.8	3	+ 4.8 D
G 19705	129245	35.0	+79 53	6.4	.127	gK3	- 22.2	1.4	3	- 22.9 V
G 19724	128684	35.9	- 3 24	7.4	.022	gM3.5	- 2.0	1.6	3	- 11. L
B 3737	128756	36.5	-24 49	8.1	.042	gKo	+ 12.3	1.8	3	
G 19757	129333	37.9	+64 30	7.4	.148	dGo	- 31.0	1.3	3	
69° 765	130043	14 41.4	+69 19	9.2	---	dGo	- 6.6	1.5	3	
A 9366A	129868	42.3	+ 7 55	8.0	.016	gG4	- 15.2	0.7	3	
A 9366B	------	42.3	+ 7 55	8.5	---	dA8n	- 17.2	1.9	4	
G 19852	129902	42.6	+ 1 12	6.2	.057	gM1	- 46.7	0.3	3	
ε Boo	129989	42.8	+27 17	2.7	.051	gKo	- 14.3	1.3	4r	- 16.4 M
G 19867	130084	14 43.1	+33 00	6.5	.093	gM1	+ 27.5	1.8	3	+ 33.3 D
54° 2559	130083	43.2	+34 35	7.8	.005	gM2	- 24.	var	7r•	
G 19871	129944	43.2	-22 57	5.9	.069	gG5	+ 7.8	1.7	4	
A 9383A	130256	44.6	+ 1 11	6.8	.048	Ao	+ 3.	4.0	4•	
A 9383B	------	44.6	+ 1 11	9.1	---	dF3	- 7.6	1.9	4	
B 3775	130259	14 44.8	-25 53	5.4	.044	gG5	+ 0.1	0.4	3	- 0.9 M
G 19934	130604	46.4	+ 6 10	6.7	.093	dF5	- 1.5	0.7	3	
B 3778	130529	46.4	-24 03	5.8	.028	gK1	- 25.8	0.5	3	
A 9396A	130559	46.6	-13 57	5.4	.068	A3	- 10.8	1.6	4	- 2.0 LYV
A 9396B	------	46.6	-13 57	6.3	---	A3	+ 0.7	1.1	4	
G 19943	130669	14 46.8	+10 25	8.2	.229	dG9	- 91.1	1.5	3	
68° 801	131020	47.0	+68 10	9.2	---	dG8	+ 5.0	1.8	3	
B 3788	130917	47.8	+28 49	5.7	.022	B9n	+ 6.	var	6•	- 14.7 V
A 9406A	131040	47.9	+61 35	6.4	.011	dF4	- 5.9	1.6	3	- 6.0 V
G 19983	131023	48.6	+ 9 56	7.3	.230	dG5	- 35.1	1.8	3	
B 3791	130989	14 48.8	-17 35	6.7	.134	dF5	+ 25.3	1.2	3	
B 3801	131430	51.4	-24 26	5.4	.038	gK2	+ 9.7	2.1	3	+ 8.7 M
G 20049	131582	51.5	+23 33	8.8	.837	dK6	- 29.8	1.9	4r	
B 3817	135294	53.6	+87 25	7.2	.020	gK1	- 26.6	1.5	3	
B 3833	133002	53.6	+82 43	5.7	.340	dGo	- 42.4	1.0	4r	- 46.3 V
G 20124	132112	14 55.0	-12 14	7.6	.036	gM5	+ 4.7	1.0	3	
G 20131	132770	55.3	+75 05	7.0	.002	gM3	+ 30.4	1.3	3	
B 3820	132230	55.5	-10 57	6.4	.026	Aon	- 17.	var	4•	
B 3823	132345	56.2	-10 57	6.0	.125	gK4	- 11.0	1.9	8•	
B 3827	132813	56.8	+66 08	4.9	.082	gM5	+ 7.1	1.1	5	+ 6.8v V
B 3826	132772	14 57.7	+39 28	5.6	.044	gF3n	+ 10.6	0.4	4	+ 12.6 D
G 20204	132971	58.9	+31 34	8.0	.072	gM4	- 16.2	1.5	3	
B 3834	133124	59.9	+25 12	4.9	.055	gK5	+ 13.6	0.7	4	+ 13.5 L
G 20239	133254	15 00.4	+31 53	6.8	.026	gM4	- 27.4	2.2	4	
G 20249	133235	00.9	- 7 25	8.1	.016	gM2	+ 14.(	1.9	4	
B 3844	133604	15 03.3	-23 08	7.1	.052	gF5n	- 28.0	1.0	3	
29° 2621	------	03.9	+29 12	8.5	.013	gG4	- 8.0	1.3	3	
29° 2622	------	04.0	+29 37	8.5	.014	gFon	- 25.	3.9	5•	
G 20325	133894	04.5	- 8 44	8.3	.017	gM3.5	- 1.3	1.2	3	
B 3854	134044	04.6	+36 39	6.3	.068	dF7	- 4.4	1.0	3	- 6.5 V
30° 2611	------	15 04.8	+30 13	8.8	.018	dG2	-278.7	0.5	4	
G 20338	134319	05.0	+64 14	8.3	.159	dG5	- 3.8	0.9	3	
G 20361	134584	05.4	+74 05	7.2	.037	A3	- 16.4	1.8	3	
G 20362	134585	05.7	+72 04	7.6	.107	gK1	- 17.1	1.5	3	
A 9520A	134646	06.9	+63 18	7.0	.002	gF2	0.	var	4•	
A 9527A	134679	15 08.0	+39 10	7.9	.088	dF8	- 12.8	2.7	4•	
G 20402	134627	08.1	+11 52	7.1	.022	gM2.5	- 19.2	1.0	3	
ι Lib	134759	09.4	-19 36	4.7	.059	B9n	- 18.1	2.2	6	- 11.6v M
B 3870	135100	09.8	+48 53	8.2	.019	dF1	- 14.3	2.3	4•	
G 20444	134963	09.8	+22 30	6.8	.050	gM2.5	- 27.2	1.5	4	

TABLE 1 (Cont'd)

STAR	H.D.	1950 R.A.	1950 Decl.	Vis. Mag.	P.M.	Spec.	Vel.	P.E.	No. Pl.	Others
		h m	° ′		″		km	km		
A 9535B	------	15 10.5	+19 28	7.6	0.665	dG6	- 39.6	1.4	6r	- 38.4 V
A 9538A	135051	10.9	-26 00	6.0	.018	gG5	- 27.8	1.6	3	
A 9543A	135264	11.4	+14 38	8.4	.079	dF6	+ 29.0	0.8	4	
A 9543B	------	11.4	+14 38	9.2	---	dF8	+ 28.1	1.5	4	
3° 3746	------	11.4	- 3 37	9.2	.78:	dMo	-107.2	1.3	4r	
G 20478	135694	15 11.5	+72 02	8.9	.208	dG1	- 84.5	2.0	3	
G 20479	135207	11.6	-14 01	7.0	.029	gM2.5	+ 6.2	2.6	4•	
G 20494	135530	12.4	+42 21	6.4	.026	gM2.5	- 7.6	1.0	3	- 4.8 D
14° 4160	135485	13.0	-14 30	8.3	.015	cB5	- 5.6	1.8	4•	- 15.8 L
G 20536	135775	14.2	+ 9 54	6.6	.020	dF7	- 11.0	2.1	7r	- 7.6 V
G 20537	135725	15 14.2	- 8 06	8.0	.256	dG5	- 34.3	1.4	3	
B 3891	125758	14.8	-29 58	4.4	.019	gKo	- 6.2	2.1	2	- 3.3 L
G 20570	136028	15.9	- 0 17	6.0	.013	gK5	- 12.6	1.8	3	
G 20588	136140	16.7	- 8 58	7.5	.067	gM4	+ 10.7	1.0	3	
B 3912	136726	17.1	+72 00	5.1	.009	gK4	- 15.7	0.4	7	- 16.1 L
G 20623	136406	15 18.2	-15 12	7.5	.027	gKo	- 19.8	1.8	4	
B 3902	136407	18.2	-15 22	6.1	.029	gA8	+ 5.	3.4	5•	
B 3911	136729	18.6	+52 08	5.5	.011	A1n	+ 12.3	2.1	5	+ 6.3 M
B 3922	137071	20.8	+39 46	5.8	.022	gK4	- 10.6	1.5	2	- 11.1 S
η CrB	137107	21.1	+30 28	5.0	.236	dF9	- 8.3	1.0	4	- 6.5v V
G 20757	137570	15 24.1	+10 13	7.1	.033	gM1.5	- 52.5	0.6	3	
B 3935	137744	25.4	-16 33	5.9	.040	gK5	- 20.9	2.0	4	
G 20819	138265	26.9	+60 51	6.1	.020	gK5	- 49.9	0.7	4	- 42.8 D
G 20843	139213	28.0	+82 04	8.0	.204	dG2	- 6.	var	5•	
A 9681A	138268	28.8	-20 00	6.1	.083	dA5n	- 40.	var	4•	
A 9681B	------	15 28.8	-20 00	8.7	.085	dF5	- 31.	var	4•	
B 3946	138527	29.8	+16 13	6.1	.001	B9	- 7.8	2.2	4	
G 20912	138648	31.1	-16 50	8.3	.358	dG9	+ 51.	var	4•	
B 3983	139777	32.0	+80 37	6.5	.253	dG3	- 14.1	1.5	4r	
A 9701A	138918	32.4	+10 42	4.2	.077	dA5n	- 43.7	1.5	3r	- 42.1 M
A 9701B	138917	15 32.4	+10 42	5.2	.078	dFo	- 36.6	2.0	3r	- 37.5 M
G 20968	139087	33.5	+11 26	6.1	.047	gKo	- 28.8	2.0	4r	- 23.8 S
28° 2447	139224	33.9	+28 35	8.3	.027	dF1	- 4.0	1.5	4	
G 20989	139586	34.2	+67 58	6.9	.151	dG5	- 33.9	1.8	3	
-0° 2990	139308	34.9	- 0 43	8.1	.029	gK1	- 24.2	1.5	4	
G 21033	139608	15 36.1	+24 41	7.1	.032	gM5	- 21.4	1.4	4	
B 3984	139780	36.7	+43 46	6.8	.013	A1n	+ 7.	3.2	4•	- 11.6 V
B 3981	139663	37.3	-23 39	5.1	.032	gK4	- 17.7	2.7	4	- 22.6 M
G 21071	140064	37.8	+57 37	7.6	.032	gM3	+ 1.6	0.8	3	
A 9740A	139862	37.8	+12 13	6.3	.018	gG5	- 19.9	1.4	3	- 20.5 D
-0° 2997	139840	15 37.8	- 0 45	8.3	.076	gKo	- 4.4	1.1	3	
B 3990	139997	39.1	-19 31	5.0	.120	gMo	+ 11.6	1.9	3	- 5.v M
C 2105	140611	40.1	+66 00	9.2	.27:	dG5	- 19.9	1.5	4	
G 21119	140590	40.3	+60 09	8.4	.276	dG6	+ 33.7	1.7	4	
G 21124	140283	40.4	-10 46	7.3	1.187	sdA5p	-171.0	1.0	10r	-175. V
γ CrB	140436	15 40.6	+26 27	3.9	0.111	Ao	- 10.9	2.2	6	- 10.4 M
B 4020	141652	42.3	+80 08	6.9	.051	gF3n	- 32.6	1.4	4	
B 4002	140687	42.8	-24 34	7.5	.110	sgKo	+ 2.2	0.1	3	
G 21233	141472	45.4	+59 38	5.9	.142	gK3	- 1.1	0.9	3	- 4.4 D
G 21239	141272	45.6	+ 1 44	7.9	.234	dG7	- 27.9	1.7	3	
A 9799A	141690	15 47.4	+25 37	8.2	.043	dG4	- 37.	var	4•	
44° 2511	141930	48.2	+44 40	7.6	.026	A2n	- 12.8	2.7	6•	- 20.2 D
B 4065	143173	48.5	+83 06	7.3	.007	dA6n	- 8.5	1.3	3	
81° 530	142653	48.5	+81 27	8.7	---	dF6	- 29.	var	4•	
B 4028	141851	48.6	- 2 56	5.2	.096	Aon	- 7.	3.4	4	- 7. M
G 21307	142474	15 49.0	+74 34	9.3	.332	dK6	- 27.	var	4•	
A 9816A	142282	49.8	+53 03	6.5	.019	A2	- 11.2	2.3	2	- 8.5 V
A 9816B	------	49.8	+53 03	8.8	---	dF5	- 16.	3.7	3•	
B 4047	142531	51.1	+55 58	5.9	.055	gG8	- 29.4	2.5	4•	- 28.6 D
G 21348	142357	51.3	+16 13	6.1	.037	dF2	- 2.3	0.3	3	+ 3.v VS
B 4043	142378	15 52.1	-19 14	5.9	.033	B5n	- 6.	var	4•	
A 9842A	142661	53.3	- 2 01	7.0	.120	dF7	- 38.5	0.6	8	
A 9842B	------	53.3	- 2 01	8.1	---	dG8	- 40.6	1.5	4	
B 4051	142640	53.4	-14 15	6.4	.086	dF5	- 7.	var	4•	
B 4057	142908	54.0	+38 05	5.5	.082	dFo	- 13.7	1.9	4	- 11.1 M

TABLE 1 (Cont'd)

STAR	H.D.	1950 R.A.	Decl.	Vis. Mag.	P.M.	Spec.	Vel.	P.E.	No. Pl.	Others
		h m	° ′		″		km	km		
B 4059	142983	15 55.4	-14 08	4.7	0.030	A2pe	- 27.	var	12•	- 12.1 M
17° 4461	143016	55.5	-17 38	8.7	.315	dG1	+ 16.0	2.3	4	
C 2141	143665	57.2	+65 32	9.1	.25:	dG8	- 8.	var	4•	
ρ Sco	143275	57.4	-22 29	2.5	.032	B1n	- 2.1	1.4	3•	- 16.v M
G 21499	143584	57.6	+50 01	5.9	.061	dA8	+ 2.1	1.7	3	+ 4.0 V
30° 2735	143586	15 58.2	+29 47	8.6	.013	gG8	- 20.7	1.1	4	
30° 2736	143585	58.2	+30 15	8.7	.020	gG5	+ 3.3	1.3	5	
G 21515	144061	58.6	+71 02	7.4	.261	dG2	- 9.7	1.3	3	
30° 2742	144044	16 00.8	+30 18	8.7	.022	gK1	+ 3.1	1.2	5	
B 4085	144204	00.8	+53 03	6.2	.041	gK5	- 6.3	0.5	6r	
29° 2758	144063	16 00.9	+29 05	8.7	.031	gG4	- 6.3	2.5	4•	
A 9913C	144218	02.5	-19 40	5.1	.034	B3	- 6.4	1.7	9r•	- 1.0 L
G 21618	------	03.1	+68 40	9.6	.287	dG8	+ 27.7	2.0	3	
G 21623	144579	03.2	+39 17	6.8	.573	dG8	- 59.2	0.6	11r	- 60.8 V
B 4093	144470	03.9	-20 32	4.1	.031	B2	+ 2.1	2.9	6•	- 6.4 M
G 21674	------	16 05.0	+66 55	9.8	.243	dGo	- 77.	3.4	3r	
A 9930A	144999	05.6	+29 08	7.7	.028	oFo	- 23.7	1.4	4	
B 4099	144937	05.7	+10 13	6.7	.046	A4n	- 22.3	2.7	4	
G 21706	145050	06.2	+ 8 45	6.7	.047	gM4.5	+ 52.9	2.1	4	
τ CrB	145328	07.1	+36 37	4.9	.328	sgK1	- 20.1	0.4	3	- 18.4 LBV
φ Her	145389	16 07.2	+45 04	4.3	.041	Ao	- 14.3	1.6	3	- 15.7 LYV
G 21781	145991	09.3	+65 58	9.3	.268	dKo	- 30.0	2.7	4•	
G 21792	145802	09.8	+33 28	6.4	.010	gK2	+ 2.0	1.7	3	- 1.5 V
G 21794	145730	09.8	+12 02	8.4	.065	dA5	+ 1.7	1.7	3	
Σ 2017pr	145743	09.8	+14 41	8.7	.044	gG9	- 46.8	1.3	4	
G 21802	145951	16 10.1	+42 30	6.0	.023	gK5	- 19.7	1.0	4	- 21.2 D
G 21811	145976	10.7	+26 48	6.4	.055	dF2	- 5.9	0.3	2	- 9.0 D
ρ Oph	146051	11.7	- 3 34	3.0	.156	gMo	- 19.4	0.6	8r	- 19.8 M
B 4151	146926	12.2	+76 00	5.5	.010	B9n	- 1.1	2.5	7	- 0.8 M
75° 585	------	12.6	+74 47	8.4	.025	gM5	- 30.1	0.7	4	
B 4137	146233	16 12.9	- 8 14	5.6	.556	dG1	+ 10.1	0.6	5r	
G 21867	146254	13.0	-14 44	6.1	.012	Aon	- 8.3	2.9	5	
B 4141	146452	13.6	+11 33	7.5	.059	gG7	- 25.4	2.0	4	
B 4142	146605	14.2	+23 15	6.6	.026	gG8	+ 12.4	1.5	6	+ 15.0 V
G 21895	146514	14.3	- 3 50	6.1	.037	dA6n	- 6.4	1.6	3	- 11.3 S
14° 4389	146543	16 14.5	-15 12	7.4	---	dA8n	+ 6.	var	5•	
G 21907	147231	15.2	+71 03	7.8	.299	dG5	- 17.0	0.6	3	
G 21958	147009	17.1	-19 56	8.8	.030	B9n	- 4.	var	3•	
G 21960	147010	17.2	-19 56	7.2	.025	A1	- 8.8	2.2	3	
G 21976	147266	17.9	+21 15	6.1	.057	dG7	- 24.6	1.3	3	- 23.9 S
B 4161	147365	16 18.2	+39 50	5.5	.127	dF2	- 28.0	2.6	4	- 30.7 V
C 2189	147676	18.3	+67 23	9.3	.117	dGo	+ 7.6	1.1	3	
G 21995	147395	18.5	+37 06	6.8	.038	gM2	- 15.	var	4•	
24° 12671	147284	18.9	-24 52	9.1	.296	dG3	- 23.0	2.1	4	
A 10030A	147735	20.8	+13 57	7.6	.037	dF2	- 42.	var	4•	
A 10030B	------	16 20.8	+13 57	9.9	---	dG2	- 43.1	2.3	3	
B 4176	147835	21.0	+32 27	6.2	.020	A1	+ 4.6	0.9	3•	- 7.3 V
G 22055	147776	21.5	-13 31	8.6	.320	dK2	+ 10.2	1.3	3	
B 4186	148295	21.9	+69 14	5.4	.023	gK2	- 8.6	1.0	6	- 7.8 M
B 4184	148283	23.6	+37 30	5.5	.017	Ao	+ 2.8	2.3	5	- 2.4 M
χ Oph	148184	16 24.1	-18 21	4.8	.034	B3e	- 1.8	2.6	7•	- 8.1 M
G 22125	148296	24.4	+11 06	7.0	.046	gM3.5	- 29.8	1.8	3	
α Sco	148478	26.3	-26 19	1.2	.029	aM1	- 3.6	0.4	11	- 3.2v C
A 10074B	------	26.3	-26 19	6.8	---	B4p	+ 1.8	2.0	4•	
A 10077A	148683	27.0	+10 42	7.7	.021	gG4	- 14.9	2.1	4	
A 10077B	------	16 27.0	+10 42	9.2	---	dF2	- 6.4	2.2	4	
B 4213	149212	28.1	+68 53	5.0	.041	B9	- 5.9	2.9	7	- 9.1 M
G 22199	149198	28.2	+67 09	6.7	.037	gM3	- 80.0	2.0	4	
G 22210	149222	28.7	+64 54	7.8	.204	dG2	- 34.0	1.1	3	
G 22216	149009	29.1	+22 18	6.0	.015	gK5	- 25.	var	4•	- 22.9 D
B 4211	149141	16 29.6	+33 27	6.7	.040	A2n	- 16.	4.6	4•	- 43. V
A 10113A	149394	31.3	+31 01	7.5	.010	dF2	- 12.9	1.6	3	
τ Sco	149438	32.8	-28 07	2.9	.030	Bo	- 1.3	1.5	4•	+ 0.6 M
G 22306	-------	33.0	+ 8 55	8.9	.256	dG2	+ 11.6	0.3	3	
G 22337	150706	34.5	+79 54	7.0	.118	dG3	- 14.1	2.9	4•	

TABLE 1 (Cont'd)

STAR	H.D.	1950 R.A.	1950 Decl.	Vis. Mag.	P.M.	Spec.	Vel.	P.E.	No. Pl.	Others
		h m	° ′		″		km	km		
G 22343	149956	16 34.7	+36 08	7.4	0.041	gM3	- 51.5	1.9	3	
G 22369	150102	35.8	+27 09	7.1	.040	gM2.5	+ 1.1	1.5	3	
G 22391	------	36.8	+38 25	9.2	.009	A3n	- 19.1	2.9	3	
A 10140A	150693	36.9	+69 52	7.9	---	dA8	- 0.2	1.4	2	
G 22404	150409	37.2	+48 58	6.7	.026	gM4	- 37.	var	4•	
B 4235	150365	16 38.4	-17 58	6.6	.058	gA6	- 2.8	1.8	3	
B 4241	150453	39.0	-19 50	5.6	.040	dF5	+ 4.4	0.4	3	
66° 969	------	39.1	+65 55	9.3	---	dF9	- 24.	var	4•	
I Her	150680	39.4	+31 42	3.0	.608	dGo	- 69.0	1.3	4	- 69.9v L
G 22491	151623	40.7	+79 01	6.4	.040	gG9	- 18.2	0.8	3	- 19.8 D
78° 565	151698	16 41.2	+77 57	8.2	---	gKo	- 59.2	1.7	4	
G 22511	151481	41.5	+72 46	6.9	.008	gM2	- 61.4	1.5	3	
B 4263	151199	42.0	+55 47	6.2	.092	A2p	- 42.	var	5•	- 49.9 V
B 4258	151087	42.0	+34 08	5.9	.087	dA8	- 10.7	1.9	3	- 11.2 V
G 22537	151061	42.6	- 3 00	7.2	.027	gM4.5	- 10.6	1.1	3	- 6. L
A 10194A	151237	16 43.1	+28 27	7.2	.033	gF5	- 48.7	2.5	4•	
G 22564	151388	43.6	+43 18	6.1	.056	gK4	- 16.9	1.7	3•	- 8.6 D
A 10201A	151367	43.8	+30 06	8.7	.063	dF1	+ 7.3	1.9	3	
B 4261	151179	43.8	-25 26	6.6	.022	gG6	+ 2.8	2.6	5•	
45° 2449	------	43.9	+45 43	8.1	.003	gM4	- 26.6	2.0	4	
A 10203A	151428	16 44.0	+35 43	7.3	.062	dF6	- 3.9	0.7	3	
A 10203B	------	44.0	+35 43	9.7	---	dKo	- 2.6	2.7	3	
B 4293	152303	45.3	+77 36	6.0	.212	dF4	+ 8.8	1.1	3	+ 5.5 D
G 22629	151658	46.6	-21 46	7.6	.026	gM2.5	-101.5	2.6	4•	
45° 2453	152030	47.7	+45 16	8.7	.050	dF3	- 6.7	1.8	4	
B 4278	151884	16 48.0	-16 28	7.0	.018	B6n	- 13.	5.	4•	
B 4274	151804	48.1	-41 09	5.9	.005	O9e	- 64.	3.4	3•	- 60.9 L
B 4288	152234	50.5	-41 44	5.3	.016	Bo	- 0.5	0.8	3•	- 8.7 LMd
B 4290	152311	50.5	-20 20	5.9	.061	dG5	- 17.2	1.3	3	
G 22743	153372	50.8	+79 35	6.9	.029	gK1	- 28.2	0.9	3	
B 4301	152601	16 51.9	- 6 04	5.4	.045	gK1	- 14.7	1.3	4	- 18.0 L
74° 690	153752	54.7	+74 24	7.6	---	dFo	- 21.7	1.9	3	
G 22852	153299	54.8	+50 07	6.7	.028	gM2	- 31.2	1.2	3	- 29.6 D
B 4325	153697	56.2	+65 07	7.0	.053	dFo	- 17.5	0.5	3	- 25.0 D
G 22890	------	56.5	+68 06	9.3	.262	dG4	- 16.3	1.6	3	
B 4319	153363	16 57.1	-24 55	5.8	.087	dF2	+ 18.8	1.3	3	
29° 2915	153650	57.6	+29 37	7.8	.015	A1	+ 3.	var	5•	
G 22923	153698	57.9	+27 23	7.3	.040	gM3.5	- 24.2	0.8	3	- 20. L
G 22924	154159	57.9	+71 32	8.0	.224	dGo	- 19.7	0.8	3	
G 22993	154100	17 00.5	+20 48	7.1	.010	gM3	- 12.6	1.5	4	
30° 2925	------	17 00.8	+29 54	8.4	.029	dF2	+ 13.6	0.6	4	
B 4434	154090	01.5	-34 03	4.9	.009	cB1e	+ 4.4	1.4	2•	+ 10.2 L
G 23035	154633	02.0	+64 40	6.1	.058	dG5	- 23.3	0.6	3	- 26.1 V
29° 2933	------	02.8	+29 44	8.0	.013	gK5	- 7.	var	4•	
A 10332A	154510	02.8	+28 09	7.2	.014	gKo	- 1.1	1.5	3	
B 4345	154445	17 03.0	- 0 50	5.6	.005	B3	+ 12.	3.3	7	+ 18.4 SV
29° 2935	154651	03.8	+29 42	7.6	.015	Ao	- 10.1	1.5	5	
B 4348	154660	04.3	- 1 35	6.2	.050	A2n	+ 7.	3.7	6	
7° 3303	154694	04.3	+ 6 54	9.8	---	dF8	- 41.3	1.1	3	
G 23095	------	04.5	+ 6 52	9.3	.091	dK2	- 30.7	1.7	3	
G 23097	154734	17 04.5	+ 6 52	9.1	.059	dK3	- 29.9	1.5	3	
B 4356	155078	07.0	-10 28	5.6	.124	dF5	- 3.8	1.1	3	
G 23181	155456	08.6	+24 35	8.3	.313	dKo	- 56.1	1.0	3	
81° 574	156648	09.2	+81 27	8.6	---	dG5	+ 4.4	1.9	3	
A 10394B	------	10.0	+21 17	8.5	.045	sgKo	+ 0.7	1.0	3	
G 23264	156162	17 12.0	+54 12	7.0	.100	dFo	- 18.8	1.5	3	
B 4371	155886	12.3	-26 32	5.3	1.240	dK2	- 1.5	0.6	3	- 0.6 L
α Her	156014	12.4	+14 27	3.5	0.032	gM5	- 32.8	0.9	8	- 32.5 M
G 23290	156558	12.8	+69 22	8.3	.185	dG4	- 55.3	0.5	3	
15° 3141	156144	13.2	+14 57	8.3	.034	gG8	- 16.4	2.4	4•	
G 23309	156284	17 13.6	+23 48	6.1	.032	gK2	- 43.9	0.6	3	- 39.0 D
14° 3213	156342	14.3	+14 44	8.0	---	dG1	- 63.4	0.7	5	
15° 3149	156431	14.8	+15 19	8.3	.020	A4	- 19.	3.1	4•	
14° 3215	156432	14.8	+14 43	8.4	.013	dF7	- 43.	var	4•	
15° 3153	156483	15.0	+15 13	8.3	.015	Ao	- 15.8	1.7	3	

TABLE 1 (Cont'd)

STAR	H.D.	1950 R.A.	1950 Decl.	Vis. Mag.	P.M.	Spec.	Vel.	P.E.	No. Pl.	Others
		h m	° '		"		km	km		
15° 4511	156461	17 15.4	-15 45	7.2	---	gdG3	+ 19.5	1.0	3	
B 4391	156729	16.0	+37 21	4.8	0.068	A2n	- 14.1	1.6	4	- 9.4 M
G 23390	156891	16.7	+38 52	6.0	.074	gG7	- 37.7	1.4	3	- 36.4 D
G 23404	156860	17.2	+ 2 11	6.9	.023	gM5	- 25.6	1.0	3	
G 23406	156802	17.3	- 7 58	8.0	.222	dGo	- 89.3	1.7	4	
G 23413	156966	17 17.4	+27 20	7.1	.035	gM2	+ 59.4	2.0	3	
A 10480AB	156952	18.0	- 7 04	8.8	---	dG4	- 1.6	1.5	3	
G 23438	157089	18.6	+ 1 29	7.0	.310	dGo	-162.5	2.1	5r	
B 4397	156992	18.6	-24 51	6.6	.057	gK1	- 11.5	2.3	3	
G 23466	157257	19.3	+16 47	6.6	.057	gM2	+ 39.2	0.9	2	+ 40.4 D
B 4411	157482	17 20.1	+40 01	5.7	.070	dGo	0.	var	4•	+ 3.v VS
G 23505	157681	20.7	+53 28	6.0	.020	gK5	- 6.0	1.3	4	- 8.2 D
G 23527	157617	21.6	+ 8 54	5.9	.009	gK1	+ 14.7	0.8	3	+ 17.9 D
G 23542	158209	21.9	+73 03	8.3	.222	dKo	- 23.	var	4•	
G 23572	------	22.7	+32 18	8.8	.035	gK5	- 3.7	1.7	3	
G 23573	------	17 22.8	+32 20	9.1	.002	gM3.5	- 2.3	1.3	3	
G 23583	------	23.1	+19 58	8.5	.016	gM3	- 40.6	1.5	3	
G 23599	158996	23.4	+80 11	5.9	.016	gK5	- 5.5	1.0	3	- 5.9 D
G 23608	157967	23.7	+16 58	6.3	.011	gM4.5	- 12.8	0.1	2	- 6.5 D
G 23623	158537	24.0	+71 55	7.0	.026	gM4.5	- 21.4	0.8	3	
A 10555B	------	17 24.3	+29 30	9.1	---	gK1	- 28.0	2.0	2	
A 10561AB	158122	25.3	-20 55	8.0	---	dP5	- 10.5	1.7	3	
G 23655	158228	25.3	+ 8 29	6.6	.054	gM4	+ 10.2	2.0	3	
B 4430	158414	25.4	+48 18	5.8	.010	A2n	- 0.7	2.9	7•	- 17.8 V
C 2329	158332	25.9	+26 49	8.0	.289	dG8	- 25.0	0.7	3	
B Dra	159181	17 29.5	+52 20	5.0	.019	cG2	- 20.9	0.8	7	- 20.1 M
59° 1823	159266	29.4	+59 44	8.4	.051	gK0	- 15.0	2.4	4•	
G 23805	159358	31.4	+14 53	6.7	.077	gM4.5	+ 30.0	0.3	2	+ 31.2 D
G 23811	159906	31.7	+69 38	7.3	.034	gG7	+ 6.8	0.4	3	
B 4464	159966	32.2	+68 10	5.2	.132	gG9	- 68.3	1.1	4	- 73.9 L
B 4450	159433	17 33.1	-38 36	4.3	.206	gKo	- 48.	3.3	3	- 48.8 M
G 23872	159968	34.4	+27 36	6.6	.079	gM4	- 35.7	2.0	3	
G 23929	160346	36.8	+ 3 35	6.6	.208	dK3	+ 19.6	1.9	4	
G 23939	160933	37.1	+69 36	6.5	.218	dGo	- 54.1	0.7	3	- 53.3 D
G 23953	160471	37.6	- 2 08	6.4	.033	gM4	- 48.2	2.5	4•	
ι Her	160762	17 38.0	+46 02	3.8	.007	cB3	- 21.7	1.1	4•	- 20.0 MV
G 23967	160677	38.1	+31 14	6.3	.020	gM2	- 7.0	2.2	2	- 8.9 D
G 23968	161178	38.1	+72 29	6.0	.026	gG8	+ 7.6	1.2	3	+ 9.0 D
G 23980	160529	38.7	-33 29	6.7	.009	cA4e	- 34.	3.1	4•	
A 10715B	------	39.0	+24 32	8.5	---	dPon	- 28.8	2.4	4	
G 23991	160781	17 39.1	+ 6 20	6.0	.016	gG7	- 28.2	0.8	3	- 31.2 D
G 23998	------	39.5	+71 21	9.2	.345	dMo	+ 2.1	1.8	3	
B 4484	161016	39.6	+41 41	7.0	.019	A2n	- 36.	var	7•	- 42.2 V
G 24025	161193	40.2	+51 50	6.1	.037	gKo	- 9.2	1.5	3	- 7.0 D
+0° 3763	161201	41.6	+ 0 23	8.1	.011	dP4	- 34.1	1.1	4	
A 10748A	161262	17 41.9	+ 2 59	8.6	.018	gKo	+ 12.4	0.8	3	
C 2367	161897	42.1	+72 26	8.4	.324	dG6	- 16.5	1.2	3	
-0° 3352	161304	42.3	- 0 06	8.5	.008	B9n	- 11.	3.6	6•	
B 4494	161693	42.9	+53 49	5.7	.028	B9n	- 0.4	2.2	6r	- 8.0 V
A 10765A	161550	43.0	+31 09	8.0	.022	dP5	- 37.3	0.9	3	
A 10765B	------	17 43.0	+31 09	8.5	---	dP6	- 37.1	0.2	2	
A 10775A	161589	43.8	- 4 27	9.3	---	dG2	- 14.3	1.5	3	
C 2370	------	44.0	+67 19	9.2	.30:	dG2	- 78.6	1.2	3r	
A 10777A	161865	44.0	+51 58	8.6	.012	gG5	- 48.8	1.7	4	
A 10781A	161623	44.1	- 1 12	8.2	.003	dGo	+ 15.4	0.8	3	
A 10781B	------	17 44.1	- 1 12	9.1	---	dG5	+ 15.8	0.3	2	
C 2368	------	45.7	+27 49	9.8	.25:	dG2	- 56.0	1.8	3	
2° 4458	161961	46.0	- 2 10	8.2	---	G9	- 6.0	2.0	2•	- 13.0 L
G 24180	163240	46.1	+80 18	7.1	.018	gM2.5	- 27.7	2.0	3	
G 24183	162159	46.2	+36 34	6.7	.030	gM3	- 14.3	0.6	3	
B 4503	161912	17 46.7	-40 05	4.9	.011	cA3	- 15.8	1.4	2	- 18.0 L
44° 2777	162751	49.0	+44 30	7.7	.027	A3	- 0.7	2.4	5	
78° 612	163859	49.8	+78 25	8.2	---	dG2	- 46.6	0.2	3	
B 4516	162917	50.8	+ 6 07	5.8	.144	dP4	- 35.5	2.7	4	- 31.7 V
G 24331	163077	51.3	+25 00	8.1	.111	sgG6	+ 6.3	1.9	3	

TABLE 1 (Cont'd)

STAR	H.D.	1950 R.A.	1950 Decl.	Vis. Mag.	P.M.	Spec.	Vel.	P.E.	No. Pl.	Others
		h m	° ′		″		km	km		
B 4522	163217	17 51.7	+40 01	5.1	0.048	gK4	- 36.1	2.1	3	- 34.7 M
G 24347	162978	51.8	-24 53	6.1	.010	Bon	- 11.	4.6	5•	
B 4521	163245	53.0	-18 48	6.4	.027	A2n	+ 4.	3.8	5	
G 24379	163608	53.3	+45 13	8.0	.013	A2n	- 25.6	1.9	5r	
B 4528	163506	53.4	+26 03	5.5	.004	cF5	- 32.2	1.4	6	- 29.4 L
B 4526	163428	17 54.1	-23 56	6.8	.008	cM1	- 12.	var	6•	
G 24439	163947	55.6	+33 48	8.7	.020	gM5	- 29.4	1.3	3	
33° 2997	163992	55.6	+33 50	7.9	.011	gKo	- 24.8	1.7	3	
G 24441	164446	55.6	+69 37	7.0	.026	gG8	- 7.4	1.4	4	
13° 4807	163810	55.9	-13 05	9.5	.825	dGo	+187.2	1.0	3	+198. M1
G 24454	163799	17 55.9	-22 33	8.6	.339	dF6	- 16.6	2.4	4	
4° 3562	------	56.0	+ 4 28	9.8	.062	dK5	- 11.6	1.1	3	
G 24464	163972	56.1	+14 37	8.4	.013	gK1	- 17.2	1.4	3	
G 24487	164064	57.0	- 4 49	6.0	.098	gK5	- 31.2	0.7	3	
G 24488	164280	57.0	+36 17	6.0	.060	gG5	+ 10.9	0.7	3	+ 10.5 D
G 24489	164394	17 57.0	+52 13	7.7	.029	A4	- 1.0	1.7	3	
B 4548	164353	58.1	+ 2 56	3.9	.011	cB7	- 4.6	0.8	5•	
G 24515	164432	58.4	+ 6 16	6.2	.006	B3	- 11.2	1.9	2•	- 24.v VS
B 4552	164577	59.2	+ 1 18	4.4	.018	B9	+ 17.1	2.1	7	- 6.v VLV
A 10991A	164492	59.4	-23 02	6.9	.005	07	- 1.	var	7•	+ 8.v V
A 10991C	------	17 59.4	-23 02	9.4	.028	B2	- 2.	var	3•	
22° 4510	164514	59.4	-22 54	7.3	---	cA5	- 1.6	2.0	3	
A 10993B	164668	59.4	+21 36	5.2	.028	gG3	- 32.2	0.5	6	- 30.6 LV
B 4562	164852	18 00.2	+20 50	5.1	.014	B4	- 14.0	1.3	6	- 15.1 YV
τ Oph	164764	00.4	- 8 11	4.9	.048	dF3	- 41.4	0.5	3	- 39.3 LV
G 24573	164924	18 00.8	+15 00	8.0	.014	gM4	- 29.2	0.8	3	
G 24589	165042	01.2	+19 33	7.2	.014	gM4	- 20.0	0.2	2	- 23. L
A 11016A	165522	01.3	+65 57	7.6	.037	gF5	- 20.9	1.3	3	
A 11016B	------	01.3	+65 57	9.2	---	dF6	- 22.5	1.5	3	
G 24637	165374	02.8	+16 55	7.2	.037	gM3	- 11.	var	4•	- 17.v L
A 11045A	165569	18 02.9	+21 26	8.2	---	dF8	- 8.	3.6	5•	
A 11046A	165341	02.9	+ 2 31	4.3	1.127	dK1	- 5.6	1.3	7	- 7.2v L
A 11046B	------	02.9	+ 2 31	6.0	---	dK6	- 14.9	1.0	9	- 6.5 LV
C 2393	165504	03.0	+33 16	7.6	0.191	dG2	- 7.7	1.3	3	
B 4603	166866	03.9	+80 00	5.8	.127	dF6	+ 11.4	1.4	6	+ 8.8v LV
G 24676	165626	18 04.1	+15 34	8.2	.222	dGo	+ 5.7	0.8	3	
B 4576	165516	04.2	-21 27	6.2	.011	Bo	- 5.2	1.0	4r•	- 13.9 L
49° 2728	166011	04.8	+49 27	7.7	.020	gA8n	- 14.9	1.3	3	
G 24699	165848	05.1	+15 55	6.8	.149	gK1	+ 18.0	0.5	3	
C 2402	166356	05.4	+65 04	7.4	.120	dG3	- 2.3	1.5	3	
G 24713	165784	18 05.6	-21 28	6.6	.017	cA2	- 15.5	2.3	5•	
B 4589	166208	06.0	+43 27	5.1	.064	gG9	- 17.6	1.2	3	- 15.5 M
G 24733	166253	06.3	+41 43	7.7	.050	gM3.5	- 16.3	1.9	4	
B 4590	166182	06.6	+20 48	4.3	.012	B2	- 15.8	1.3	3•	- 13.7 M
B 4594	166233	07.1	+ 3 59	5.7	.036	dFo	- 21.	3.3	6•	- 14.6 V
G 24793	166821	18 08.6	+48 23	8.0	.067	dF8	+ 7.8	0.8	3	
C 2407	167605	10.4	+69 39	9.1	.15:	dKo	- 7.7	1.5	3	
G 24852	------	10.7	+31 34	8.3	.008	gM1	- 15.4	1.1	3	
G 24855	167106	10.8	+22 49	7.1	.023	gM2	+ 17.2	1.7	3	
66° 1087	167779	11.8	+66 06	7.3	---	gG5	- 14.4	0.2	3	
G 24885	167278	18 12.0	+ 0 10	7.9	.030	dF5	- 8.1	1.2	3	
15° 4889	167246	12.1	-15 24	7.3	---	gK1	- 17.0	1.6	4	
G 24900	167356	12.6	-18 41	6.1	.013	cAo	- 1.0	2.1	4	
G 24914	167654	13.6	+ 2 22	6.3	.019	gM4	+ 22.8	2.5	2	+ 23.0 D
G 24955	167838	14.8	-15 27	6.6	.016	B4	- 3.4	1.7	5	- 6.6 L
A 11240AB	168021	18 15.8	-18 38	6.7	.011	Bo	+ 16.	var	4•	- 8.2 L
A 11240C	------	15.8	-18 38	8.0	.012	B2	+ 25.9	2.1	3•	
A 11257B	------	17.1	- 5 00	9.2	---	dG4	- 12.9	0.9	3	
B 4646	169027	17.3	+68 43	6.7	.096	Ao	- 25.5	0.7	3	
G 25009	168499	17.3	+10 15	8.2	.229	dG2	- 10.0	0.9	3	
G 25025	168694	18 17.9	+29 39	6.1	.007	gK4	- 36.0	0.5	3	- 34.8 D
G 25052	168701	18.9	-16 21	7.9	.013	gKo	+ 22.3	1.8	5•	
A 11282A	168815	19.4	-15 07	7.4	.025	cK5	- 28.1	0.9	3	
A 11282B	------	19.4	-15 07	8.0	---	gF5	- 25.8	0.5	2	
G 25071	169508	19.8	+67 25	7.1	.031	gM3	- 22.2	1.9	3	

TABLE 1 (Cont'd)

STAR	H.D	1950 R.A.	1950 Decl.	Vis. Mag.	P.M.	Spec.	Vel.	P.E.	No. Pl.	Others
		h m	° ′		″		km	km		
A 11292A	------	18 19.9	+11 24	9.4	0.061	gKo	- 15.5	1.8	3	
G 25151	169493	22.4	- 1 36	6.1	.023	dF2n	- 10.8	2.7	3	- 11.1 S
B 4655	169420	22.4	-20 34	5.0	.030	gK1	- 12.1	2.1	3	- 11.7 M
A 11353B	------	24.6	+ 0 10	7.8	---	A2	- 22.2	1.7	4	
G 25194	170157	25.4	+ 3 43	6.1	.011	gK3	- 20.4	0.2	2	- 17.7 D
G 25225	171299	18 26.6	+77 32	7.8	.048	dG8	- 6.4	1.5	3	
43° 2984	170594	26.7	+43 53	7.8	.007	A3	+ 2.7	2.1	3	
C 2425	170493	27.3	- 1 51	8.2	.252	dK5	- 52.8	0.7	3	
C 2433	171314	31.2	+22 17	9.3	.48:	dM1	+ 37.0	1.2	3	
G 25364	174878	31.8	+86 38	6.8	.030	gM3	- 35.8	1.8	3	
34° 3238	171568	18 32.3	+34 24	7.4	.046	gG8	+ 3.1	1.8	4	
C 2438	171620	32.3	+34 22	7.8	.268	dF7	- 32.8	1.1	3	
G 25382	171394	32.4	-19 19	7.2	.022	gM5	- 23.8	0.6	3	
G 25394	234677	32.8	+51 41	8.3	.365	dM1	- 23.0	1.5	3	- 39. Md
G 25404	171911	33.4	+51 44	6.7	.061	gM4	- 86.0	1.2	3	
A 11483A	171746	18 33.6	+16 56	6.8	.085	dGo	+ 9.1	0.9	4r	
B 4713	171834	34.2	+ 6 38	5.4	.146	dF2	- 26.6	2.9	6	- 30.1 V
B 4716	171893	35.0	-17 17	6.8	.001	dF2	- 5.2	2.0	4	
β Lyr	172167	35.2	+38 44	0.1	.345	A1	- 13.3	0.8	9	- 13.8 M
B 4720	172051	35.9	-21 06	5.9	.174	dG4	+ 35.1	0.1	3	
G 25498	172669	18 36.4	+66 52	7.6	.120	dG2	- 5.8	1.5	3	
G 25501	------	36.4	+20 35	9.2	.219	dG2	+ 28.5	1.1	3	
G 25503	172393	36.5	+42 37	8.7	.293	dKo	+ 32.5	0.9	3	
+0° 3989	172327	37.1	+ 0 07	8.2	.010	gKo	- 12.2	1.1	3	
G 25524	172348	37.3	- 7 50	6.1	.054	gK4	- 22.9	1.0	3	
B 4729	172711	18 37.6	+55 12	7.6	.062	dF5	- 13.3	1.9	3	
G 25551	173084	38.4	+67 05	8.5	.235	dG1	- 43.0	0.7	3	
B 4726	172546	38.8	-23 53	6.1	.040	dFo	+ 0.4	2.0	4r	
+0° 3993	172651	38.9	+ 0 32	7.8	.031	gK3	+ 13.1	2.1	4	
+0° 3995	172829	39.8	+ 0 07	9.1	.034	gK5	+ 18.9	1.9	4	
G 25603	173398	18 40.5	+62 42	6.0	.060	gKo	- 24.6	0.7	3	- 25.7 D
-0° 3540	173160	41.3	- 0 16	7.9	.028	Ao	- 24.	var	4•	
B 4742	173417	42.0	+31 53	5.5	.159	dFo	- 2.3	1.7	5	- 3.7 V
G 25654	173371	42.4	- 0 25	6.8	.015	B8n	- 18.2	1.7	4	
G 25677	173425	43.1	-19 40	6.6	.005	gM4.5	- 39.0	2.0	4	
-0° 3546	173514	18 43.2	- 0 19	8.3	.039	B9n	- 12.4	1.9	4	
B 4753	173667	43.5	+20 30	4.3	.338	dF5	+ 20.6	1.1	3	+ 23.6 M
G 25725	174156	44.3	+64 45	7.3	.105	gKo	+ 46.6	1.1	3	
B 4761	173880	44.8	+18 07	4.4	.129	A4	- 39.4	1.6	3	- 45.7 LYV
A 11685A	174022	45.3	+31 21	7.2	.012	gG5	- 21.9	1.2	3	
Anom.	------	18 45.9	+35 56	11.5	---	dKo	-178.8	1.9	3•	
+0° 4023	174066	46.2	+ 0 28	8.5	.018	gK1	+ 35.2	1.4	3	
B 4764	174116	46.7	-20 23	5.4	.034	gK4	- 15.4	2.1	4	- 18.6 M
10° 4819	174142	46.9	-10 26	7.9	.010	gK2	- 48.0	1.1	11r	
C 2464	174433	47.2	+34 28	8.4	.219	dF6	- 13.0	2.0	3	
45° 2779	174600	18 47.7	+45 15	8.6	.028	gK3	+ 12.8	0.4	3	
B 4767	174309	47.8	-22 13	6.2	.049	gA8n	- 35.9	1.5	3	
G 25844	174403	48.2	-20 22	7.6	.026	B9n	+ 12.	var	4•	
G 25846	174464	48.2	- 9 50	5.9	.006	gF2	- 18.8	2.1	4	
C 2469	175305	48.4	+74 40	7.3	.331	dF9	-181.2	2.9	4r	
G 25853	174512	18 48.4	- 6 20	8.0	.006	cA3	+ 28.	var	11•	
G 25886	174912	49.7	+38 34	7.2	.322	dF8	- 13.9	0.9	3	
44° 3003	175055	50.0	+45 04	7.2	.008	B9	- 22.	var	5•	
A 11773A	174897	50.0	+14 28	6.5	.040	gKo	+ 11.2	0.5	3	
B 4779	174933	50.1	+21 22	5.3	.016	Ao	- 21.	var	6•	- 19.8v L
G 25911	175018	18 50.9	+ 3 19	8.8	.041	dF3	- 24.7	1.3	3	
G 25926	175404	51.7	+40 56	6.6	.040	gM5	+ 9.6	1.0	3	
G 25942	175443	52.2	+27 51	5.8	.079	gK4	+ 15.7	0.6	3	+ 16.3 D
G 25968	175541	53.2	+ 4 12	8.1	.087	dKo	+ 18.9	1.8	3	
C 2474	175742	53.8	+23 29	8.4	.33:	dK1	- 6.	var	4•	
B 4813	175869	18 54.8	+ 2 28	5.6	.017	B9n	- 10.7	2.6	4	
C 2476	176213	56.0	+23 45	8.6	.12:	dF7	- 19.7	1.9	3	
C 2479	176252	56.4	+23 43	7.4	.12:	sgG6	- 35.1	0.8	3	- 37. V
B 4833	176668	56.8	+62 20	6.4	.041	gG6	- 7.2	1.3	3	- 8.6 V
G 26078	176377	56.9	+30 06	6.6	.206	dGo	- 39.2	0.8	4	- 38.2 D

TABLE 1 (Cont'd)

STAR	H.D.	1950 R.A.	1950 Decl.	Vis. Mag.	P.M.	Spec.	Vel.	P.E.	No. Pl.	Others
		h m	° ′		″		km	km		
G 26080	176304	18 56.9	+10 04	6.5	0.023	B4	- 23.	1.1	2•	- 22.5 V
B 4819	176246	57.4	-25 01	6.4	.066	gK1	- 24.0	0.5	3	
G 26118	176386	58.3	-36 58	6.9	.038	B9n	+ 7.3	0.9	3	
B 4842	177003	59.0	+50 28	5.2	.018	B3n	- 20.7	0.6	5r	- 19.0 M
G 26157	176938	59.4	+29 27	6.6	.017	A1n	- 14.3	2.2	3	- 20.6 D
B 4835	176704	18 59.4	-24 55	5.7	.181	gK4	+ 0.3	2.2	4	
B 4848	177249	59.7	+55 35	5.5	.021	gG2	+ 11.8	0.3	2	+ 8.6 V
B 4846	177196	19 00.0	+46 52	5.1	.089	dA5n	+ 5.2	1.8	4	+ 8.8 M
G 26184	176884	00.1	-19 19	6.0	.006	gG6	- 19.7	1.7	3	
30° 3392	------	00.2	+30 22	8.5	.012	gA5	- 5.6	1.8	6	
A 11977A	177279	19 00.8	+31 20	8.2	.001	gA5	- 15.1	2.1	8•	
A 11977B	------	00.8	+31 20	9.3	---	sgG7	- 13.	var	4•	
B 4856	177517	02.8	-15 44	5.9	.009	B9	- 20.	var	4•	- 37.v Y
65° 1319	178326	03.2	+65 30	7.2	---	sgG5	+ 20.9	0.5	3	
A 12040A	178091	04.2	+30 22	8.2	.059	dG5	- 45.6	1.1	3	
B 4865	178175	19 05.3	-19 22	5.4	.008	B3ev	- 20.	var	50•	- 27.8 L
C 2496	178450	05.6	+30 10	8.1	.167	dG6	+ 9.	var	4•	
B 4875	178596	06.6	+ 6 00	5.4	.079	dF2	- 50.9	1.6	5	- 45.4 M
G 26392	178849	06.9	+34 41	6.6	.008	B6	+ 3.1	1.0	3•	- 17.1 V
G 26397	179094	07.2	+52 21	5.9	.121	sgKo	+ 9.	var	5•	var D
G 26412	180427	19 08.2	+79 34	7.9	.088	gKo	- 71.5	1.0	3	
71° 933	179907	08.9	+71 13	9.0	---	dF5	- 27.0	1.3	3	
B 5140	190250	09.4	+88 56	8.4	.143	dG3	- 13.7	2.2	4	
G 26447	179343	09.5	+ 2 32	6.8	.010	B9e	- 10.7	0.5	3•	
B 4884	179497	10.5	-12 22	5.6	.028	gK4	- 17.0	0.2	3	
B 4892	179957	19 10.8	+49 46	6.8	.662	dG5	- 40.6	0.8	4r	
B 4893	179958	10.8	+49 46	6.6	.666	dG3	- 38.1	1.3	4r	
14° 3831	179786	11.1	+14 32	7.8	.031	gK2	+ 35.8	0.6	3	
G 26496	180841	11.3	+76 06	8.2	.174	dF8	- 43.8	1.2	3	
15° 3739	180080	12.2	+15 17	8.3	.011	Ao	- 19.4	1.7	5	
G 26529	180110	19 12.9	-14 56	7.9	.019	B9	- 8.8	1.6	4	
14° 3845	180243	13.0	+15 00	7.8	.021	Ao	- 27.	var	4•	
B 4898	180262	13.0	+15 00	5.7	.014	gG7	- 24.6	1.0	7r	
B 4907	180610	13.0	+57 37	5.3	.073	gK2	- 22.7	1.9	4	- 29.1 V
G 26549	181204	13.5	+73 48	8.1	.035	gM3	- 0.6	2.5	4•	
14° 3849	231014	19 13.5	+15 08	8.1	.027	dG6	+ 4.5	1.5	3	
A 12248B	------	14.2	+14 28	8.9	---	dG2	- 28.6	0.2	2	
15° 3752	231039	14.3	+15 16	8.2	.037	dF4	- 14.8	1.4	3	
B 4900	180416	14.3	-21 10	7.4	.015	gKo	- 3.9	1.2	3	
C 2525	------	15.4	+71 27	9.0	.22:	dK2	+ 7.2	1.5	4	
G 26616	181468	19 15.6	+66 11	8.7	.137	dF9	+ 11.7	0.6	3	
B 4916	180972	16.0	+ 1 00	5.3	.018	gK2	- 23.3	1.5	3	- 24.2 L
15° 3762	181120	16.4	+15 35	7.7	.040	Ao	- 22.	3.1	4	
τ Dra	181984	16.5	+73 16	4.6	.180	gK4	- 25.7	1.0	3	- 30.v M
14° 5387	181058	16.7	-14 15	8.3	---	gG6	+ 34.4	1.5	3	
41° 3306	------	19 17.3	+41 33	8.7	.662	dK1	-123.0	1.9	4r	
A 12322A	181386	17.7	+ 3 57	8.4	.020	gG5	+ 7.5	2.1	4	
A 12322B	------	17.7	+ 3 57	9.0	---	gG5	+ 19.	var	4•	
G 26708	182190	19.4	+57 33	6.1	.022	gM1	- 18.4	0.3	3	- 21.7 D
α Sgr	181369	20.4	-40 43	4.1	.124	B8	- 4.7	1.5	4	+ 4. L
C 2531	182712	19 20.7	+69 49	9.3	.24:	dK1	- 35.4	1.4	3	
71° 949	182951	21.4	+72 00	7.2	---	gKo	- 11.5	1.6	3	
B 4952	182629	23.3	-21 53	5.6	.032	gK3	- 19.6	0.2	3	
26° 3549	------	23.4	+26 14	8.2	.064	gKo	- 63.3	1.5	4	
V Aql	182835	24.0	+ 0 14	4.9	.004	oFo	- 3.2	1.3	2	- 0.6 M
B 4965	182919	19 24.0	+20 00	5.6	.038	B9n	- 13.1	2.3	7•	- 29.7 V
B 4964	182926	24.8	-18 27	7.3	.020	dF5	- 0.4	1.8	5	
G 26873	183143	25.2	+18 12	6.9	.015	cB8e	+ 12.5	0.9	13•	+ 13.0 V
12° 3913	183145	25.3	+12 23	7.8	.026	gK1	- 0.2	0.9	3	
49° 3009	183255	25.4	+49 21	8.0	.846	dK1	- 65.4	1.8	3	
B 4980	183534	19 26.2	+52 13	5.7	.032	Ao	+ 4.6	2.1	7	+ 0.5 V
12° 3923	183401	26.6	+12 21	7.7	---	gA8n	- 31.8	0.8	6	
α Vul	183439	26.6	+24 34	4.6	.176	gM1	- 85.7	0.8	4r	- 85.6 M
12° 3925	183421	26.7	+12 45	7.2	---	Aop	- 22.3	1.7	6	
C 2537	183536	26.8	+34 30	8.2	.220	dF8	- 50.4	1.8	3	

TABLE 1 (Cont'd)

STAR	H.D.	1950 R.A.	1950 Decl.	Vis. Mag.	P.M.	Spec.	Vel.	P.E.	No. Pl.	Others
		h m	° ′		″		km	km		
12° 3926	183460	19 26.9	+13 04	7.9	---	dPpn	- 51.6	1.6	6	
12° 3929	183512	27.2	+12 18	7.7	---	gA5	- 16.6	0.6	6	
G 26923	183650	27.4	+31 31	7.0	0.419	dG5	- 11.3	1.6	3	
12° 3932	183615	27.6	+13 02	7.6	---	gFo	- 35.3	0.6	6	
B Cyg	183912	28.7	+27 51	5.2	.009	gK1p	- 23.6	0.8	5	- 23.9 M
G 26968	184010	19 29.3	+26 31	6.0	.038	sgG8	+ 2.6	0.6	4•	- 5.0 S
B 4994	184293	30.0	+50 12	5.7	.056	gK1	- 8.4	2.4	2	- 9.3 V
G 26996	184467	30.3	+58 29	6.7	.606	dK5	+ 11.6	0.7	9r	
C 2545	184152	30.5	+ 7 19	9.1	.33:	dG6	- 12.8	1.8	4	
71° 956	184824	30.6	+72 10	7.8	---	sgKo	- 26.6	1.1	3	
G 27003	184201	19 30.6	+ 4 55	6.8	.008	gM2.5	+ 1.6	1.5	3	
A 125948	------	31.1	+20 18	8.9	---	dF?	- 42.6	1.1	3	
G 27016	184279	31.1	+ 3 39	6.8	.016	cB3e	- 15.	3.4	4•	- 2.9 V
27° 3428	184384	31.2	+27 17	8.5	---	gF3	+ 1.7	1.1	3•	
G 27028	184926	31.6	+67 36	8.1	.143	sgG7	- 39.2	1.3	3	
G 27042	184590	19 32.2	+25 15	7.2	.026	gM2	+ 24.0	1.0	2•	+ 15. L
G 27045	184786	32.3	+49 09	6.2	.006	gM4	- 10.2	1.6	3	- 7.8 D
B 4998	184606	32.4	+19 40	4.9	.003	B3n	+ 1.	5.	4	+ 7. M
B 5000	184759	32.9	+29 21	5.4	.025	dF4	- 12.5	1.9	3	- 14.3 M
G 27076	184700	33.2	- 0 21	9.1	.344	dG2	- 22.3	1.0	3	
G 27082	184768	19 33.4	- 0 01	7.9	.406	dG4	- 14.6	1.6	6	
G 27083	184767	33.4	+ 0 08	7.1	.016	A1	- 17.6	0.5	3	
B 5007	185037	34.0	+36 50	5.9	.006	B9n	- 15.2	2.3	7	
B 5011	185264	34.6	+50 08	6.6	.036	gG8	+ 8.3	1.1	3	+ 9.3 D
B 5020	185713	34.9	+71 30	6.7	.131	dF4	+ 16.0	2.1	4	
G 27136	185090	19 35.0	- 0 15	7.4	.035	gA3n	+ 7.0	1.5	3	
G 27154	185799	35.6	+69 42	7.1	.034	gM5	- 10.1	0.4	3	
G 27160	185297	35.8	+ 0 14	7.4	.017	dA5n	+ 2.7	2.5	5	
A 12730A	185855	36.5	+63 43	8.7	.038	gF5	- 34.7	1.6	4	
A 12730B	------	36.5	+63 43	10.2	---	dF?	- 22.7	1.4	4	
G 27195	185622	19 37.2	+16 27	6.6	.006	cK5	- 5.9	0.8	3	- 0.4 D
G 27226	185859	38.3	+20 22	6.4	.026	cB5	+ 4.4	1.7	5•	+ 5.6 V
+0° 4270	185823	38.4	+ 0 35	7.9	.013	gK2	- 2.2	1.9	4	
G 27240	186121	39.1	+42 58	6.4	.009	gM2.5	- 1.8	1.8	2	- 4.2 D
G 27288	186922	40.7	+76 18	8.0	.202	dKo	- 8.2	1.5	3	
G 27294	186552	19 41.0	+55 21	6.5	.043	gM5	- 28.7	1.6	3	- 25.7 D
G 27296	186379	41.0	+24 29	6.8	.283	dF9	- 8.8	0.6	4	
G 27321	186587	42.6	+10 39	7.4	.012	B5	- 1.7	1.9	3	+ 3.4 V
3° 4698	186610	42.9	- 3 17	9.1	---	B3n	+ 27.7	2.5	2•	+ 21.5 L
G 27341	186776	43.1	+40 36	6.4	.074	gM4	- 92.6	1.6	2	- 98.1 D
γ Aql	186791	19 43.9	+10 29	2.8	.012	cK4	0.0	0.8	15	- 2.0 M
G 27356	187053	43.9	+55 44	7.8	.005	gM4	- 5.4	0.7	3	
27° 3507	186884	43.9	+28 12	8.8	.045	Ao	- 10.8	2.1	3	
G 27402	187193	45.7	+25 16	6.0	.081	gKo	- 17.3	0.3	3	- 16.7 S
G 27406	187257	46.0	+27 44	6.8	.224	dG5	- 32.8	0.7	3	- 35.9 D
G 27407	187372	19 46.0	+47 47	6.2	.046	gM1	- 1.6	2.3	4•	+ 7.8 D
B 5061	187532	48.0	-10 54	5.6	.048	dF2n	+ 5.6	2.3	3	
B 5065	187691	48.6	+10 17	5.2	.275	dF8	- 0.4	0.5	13r	- 0.5 M
G 27498	187880	49.0	+37 42	6.3	.020	gM3	- 16.8	2.0	2	- 14.2 D
B 5066	187739	49.3	-19 10	6.0	.058	gG5	- 26.	var	4•	
A 13038A	187981	19 49.7	+31 01	6.9	.024	gA8n	+ 6.	var	3•	+ 7. DV
B 5073	188001	50.1	+18 33	6.3	.009	G7	- 1.1	1.9	10r•	+ 11.1 M
G 27552	188268	51.7	+ 1 49	8.5	.283	dKo	+ 11.7	1.7	3	
G 27560	188311	51.9	+ 1 49	8.8	.272	dK1	+ 9.3	1.5	3	
45° 3001	188637	52.2	+45 20	7.8	.007	gG9	- 17.8	0.6	3	
B 5092	188486	19 52.4	+24 11	5.5	.020	A1n	- 9.	5.	6	- 8. M
C 2597	188427	52.6	+ 3 55	9.5	.39:	dK3	+ 50.2	2.1	4	
G 27579	188442	52.6	+ 3 52	8.7	.111	dG8	+ 1.3	0.8	3	
A 13125A	188753	53.3	+41 44	7.4	.306	dKo	- 20.4	0.8	3	
G 27608	188875	53.9	+40 02	6.7	.017	gK5	- 17.0	1.8	3	
G 27628	189344	19 54.7	+66 37	7.2	.039	gKo	+ 0.8	1.5	3	
A 13156AB	188914	54.8	+ 5 05	8.6	---	dF8	- 11.6	2.2	4	
C 2605	189087	55.2	+29 40	8.2	.26:	dG7	- 29.2	1.1	3	
B 5121	189377	56.2	+42 07	6.5	.006	Ao	- 5.	var	3•	- 7. DV
A 13196A	189378	56.6	+33 08	7.5	.072	dF2	- 22.4	0.5	3	

TABLE 1 (Cont'd)

STAR	H.D.	1950 R.A.	1950 Decl.	Vis. Mag.	P.M.	Spec.	Vel.	P.E.	No. Pl.	Others
		h m	° ′		″		km	km		
B 5130	189775	19 57.9	+51 55	6.0	0.011	B5n	- 17.8	1.5	5	- 15.1 V
B 5124	189561	58.4	-22 53	6.1	.017	dG7	+ 8.7	0.5	3	
G 27739	189695	58.6	+ 8 25	6.1	.009	gK5	- 40.5	0.9	3	- 36.8 D
29° 3844	189779	58.6	+29 46	8.2	.011	B2	- 5.0	2.1	3•	
A 13256B	------	59.1	+10 37	7.8	---	dF6	- 39.3	1.6	2	
G 27776	190066	20 00.2	+22 01	6.6	.001	cBe	+ 14.9	0.2	2•	+ 16.1 V
G 27782	190007	00.3	+ 3 11	7.8	.147	dK4	- 30.8	1.3	3	
5° 4393	190073	00.6	+ 5 36	7.9	---	Ape	- 0.7	0.1	7•	
B 5135	190009	00.8	-22 44	6.5	.048	dF6	+ 6.0	2.4	4	
29° 3871	------	01.4	+29 49	8.5	.011	gK4	- 8.7	0.3	3	
29° 3875	------	20 01.8	+29 56	8.5	.005	dA8n	- 13.	3.6	4•	
A 13323A	------	01.9	+16 51	8.7	.016	gF2	+ 5.9	0.9	3	
A 13323B	------	01.9	+16 51	9.4	---	dA8n	- 4.8	1.3	3	
36° 3841	190467	01.9	+36 16	8.0	.012	cB4	+ 29.	var	6•	
B 5141	190283	02.0	-21 27	7.1	.056	dG4	- 20.7	2.1	3	
G 27849	190513	20 02.2	+30 24	8.2	.011	gFo	- 18.0	2.1	4	
B 5145	190390	02.3	-11 45	6.5	.014	gF4	- 12.6	1.0	3	
36° 3848	190570	02.4	+37 02	8.1	.001	Ao	- 6.7	1.7	6	
B 5150	190603	02.6	+32 05	5.7	.021	cBoe	+ 18.8	2.2	13r•	+ 18.0 M
C 2625	190605	02.8	+25 55	7.8	.40:	dG5	+ 23.3	1.9	3	
54° 2281	190780	20 02.9	+54 20	8.0	.154	dKo	- 8.5	0.5	3	
G 27872	190658	03.1	+15 21	6.6	.032	gM2.5	-110.9	1.1	2	-110.v D
35° 3949	190864	03.8	+35 27	8.2	.016	O6	- 4.0	1.9	5•	+ 3. V
B 5161	191096	04.2	+56 12	6.2	.078	gF4	- 12.6	1.3	3	- 12.2 D
G 27926	191633	05.3	+72 51	8.1	.220	dGo	- 36.2	1.8	3	
37° 3772	191176	20 05.4	+37 35	8.2	.02:	Ao	- 1.3	1.3	6	
16° 5509	191069	05.7	-15 52	8.2	.44:	dG4	- 1.0	2.0	3	
G 27940	191178	05.8	+16 31	6.7	.004	gM3	+ 10.4	1.3	3	+ 13.4 D
B 5164	191250	06.6	-20 44	7.3	.080	dF2	- 7.3	1.5	3	
B 5167	191571	07.7	+20 45	7.3	.009	gK2	- 4.4	0.9	34r	
36° 3916	191720	20 08.2	+36 50	8.0	.02:	Aon	- 14.8	1.7	6	
G 28008	191707	08.7	+ 6 12	7.8	.013	gM4	+ 15.7	2.5	4•	
B 5172	191709	08.8	- 0 17	7.1	.033	gF3	- 19.6	1.8	3	
14° 4223	192126	10.5	+15 18	8.5	.012	gKo	- 3.1	0.1	3	
15° 5584	192031	10.6	-15 30	8.6	.26:	dG8	+ 23.1	1.9	3	
G 28070	192575	20 10.7	+68 07	6.8	.013	B2	- 35.9	0.1	2•	- 38.1 V
36° 3937	192382	11.4	+36 35	8.7	.01:	A3	+ 15.	var	6•	
B 5182	192425	12.0	+15 03	5.0	.075	A2n	- 16.9	2.7	3	- 24.5 M
66° 1276	192800	12.2	+66 19	7.9	---	gKo	- 50.	var	4•	
14° 4240	192686	13.2	+15 17	8.5	.021	Aop	- 13.1	1.8	4	
31° 4013	------	20 14.0	+32 12	9.1	---	dF7	- 17.4	2.0	4	
15° 5606	192700	14.0	-15 20	7.8	---	gK2	- 20.8	2.0	3	
A 13611AB	192911	14.0	+43 30	8.1	.018	dFo	- 9.1	1.5	3	
A 13611C	------	14.0	+43 30	10.0	---	dF5	- 4.7	1.9	3	
G 28188	192954	14.9	+15 43	7.3	.020	cAoe	+ 20.3	2.2	5	
74° 854	193591	20 15.0	+75 15	8.5	.032	gM3	- 16.8	1.0	4	
G 28207	193216	15.5	+50 08	8.2	.304	dG7	- 33.	var	4•	
15° 4124	193097	15.7	+15 51	8.6	.017	gK5	+ 32.7	1.1	3	
G 28225	193102	16.2	-14 27	7.4	.033	gKo	- 47.3	1.4	3	
B 5206	193150	16.5	-19 17	5.5	.008	gK4	- 10.6	1.9	9	- 10.2 M,
G 28243	193347	20 16.8	+26 50	6.7	.025	gM1.5	- 35.5	0.6	3	
G 28257	193373	17.1	+13 04	6.5	.036	gM1	+ 22.2	1.9	3	+ 25.9 D
B 5212	193353	17.3	- 0 48	7.4	.012	gK1	+ 4.6	1.5	3	
G 28292	193579	18.1	+17 38	6.0	.038	gK5	- 33.6	0.8	3	- 30.0 D
D 28303	193793	18.8	+43 42	6.8	.012	O5	- 10.	8.	3•	+ 2. M
γ Cyg	194093	20 20.4	+40 06	2.3	.001	cF7	- 6.3	0.3	12r	- 7.6 M
B 5230	194152	20.4	+45 38	5.9	.048	gKo	- 28.4	1.3	3	- 24.v M
G 28340	194298	20.5	+63 49	5.9	.025	gK5	+ 30.4	1.2	3	+ 31.9 D
3° 4888	194454	23.1	- 3 11	6.1	.159	gK1	+ 24.0	1.2	3	
74° 859	195121	23.4	+75 17	8.9	.073	gKo	+ 1.0	1.1	4	
75° 739	195191	20 23.8	+75 53	8.0	.006	gK3	+ 10.4	2.5	4•	
9° 4529	194598	23.8	+ 9 18	8.5	.57:	dF5	-246.8	1.1	3	
ρ Cap	194943	26.0	-17 59	5.0	.028	dFo	+ 14.6	1.6	5	+ 19.5 L
B 5254	195135	27.0	- 3 03	5.1	.068	gK3	- 20.8	1.6	4	- 23.8 M
B 5261	195527	27.0	+68 36	7.2	.014	gG5	+ 8.4	2.4	4•	

TABLE 1 (Cont'd)

STAR	H.D.	1950 R.A.	Decl.	Vis. Mag.	P.M.	Spec.	Vel.	P.E.	No. Pl.	Others
		h m	° ′		″		km	km		
G 28546	195592	20 28.9	+44 09	7.2	0.016	cB0	- 40.0	1.8	2•	- 24. V
B 5273	195838	31.4	-13 54	6.2	.101	dF8	- 43.2	0.4	3	
B 5308	196787	31.5	+81 15	5.6	.033	gK0	- 6.8	1.6	4	- 3.9 D
B 5279	196093	32.0	+35 05	4.8	.007	cK4	- 3.0	1.9	6	- 4.4 L
G 28720	196610	35.6	+18 06	6.3	.099	gM6	- 67.0	0.9	4	- 63.3 D
G 28745	196753	20 36.4	+23 30	6.1	.012	cK0	+ 11.	var	5•	- 1. V
G 28760	196950	36.8	+38 28	6.8	.264	dG2	- 21.1	1.1	3	
G 28765	196794	36.9	+ 9 53	8.9	.310	dK1	- 52.4	0.5	3	
G 28797	196857	37.7	-16 18	5.9	.101	gG7	- 3.2	0.5	3	
B 5314	197039	38.2	+15 28	6.8	.096	dF6	- 31.0	0.9	4r	
A 14152A	197042	20 38.6	- 1 16	8.7	.010	gK1	- 6.7	1.8	3	
A 14158A	197177	39.0	+32 08	6.0	.015	cK2	- 28.2	0.4	5r	
A 14158B	197178	39.0	+32 08	8.1	---	A1	- 31.	var	3•	
G 28859	------	40.3	+15 57	8.9	.006	gMe	- 29.9	1.6	4	
G 28861	197419	40.4	+35 17	6.5	.025	B3	- 7.2	1.8	6	- 6.2 V
45° 3245	197488	20 40.7	+45 38	7.6	.191	dG2	+ 10.3	1.7	4	
-0° 4076	197409	41.0	+ 0 18	8.7	.011	A2	- 19.2	1.9	4	
G 28905	197795	42.1	+55 07	7.6	.010	Ao	+ 0.8	1.8	4	
G 28912	197623	42.4	+ 0 07	7.4	.186	dG3	- 71.2	2.2	5•	
A 14238AB	197685	42.6	+12 35	8.0	---	dF5	+ 16.1	1.1	6	
A 14238C	197704	20 42.6	+12 33	7.3	---	dF2	- 24.9	0.4	3	
G 28926	197939	43.1	+56 18	6.2	.015	gM3	- 25.0	1.8	2	- 27.3 D
ε Cyg	197989	44.2	+33 47	2.6	.481	gK0	- 8.3	0.8	2	- 10.5 M
A 14278A	198180	44.4	+63 21	8.5	---	dA6n	- 8.0	2.7	4•	
G 28988	198385	45.4	+68 22	8.5	.186	dG5	- 18.5	0.8	3	
B 5359	198044	20 45.4	-22 55	7.3	.172	dF5	+ 12.	var	4•	
A 14299A	198063	45.6	-18 23	6.7	.020	gG7	- 9.0	1.3	3	
A 14299B	------	45.6	-18 23	7.2	.013	gG6	- 7.4	1.1	3	
G 29020	198188	46.4	-20 49	8.2	.305	dG3	- 82.6	1.9	3	- 90. L
B 5351	198208	46.5	-18 13	6.4	.034	gK2	+ 44.6	1.9	3	
B 5361	198478	20 47.2	+45 56	4.9	.001	cB2e	- 9.7	1.3	5•	- 6.6 M
A 14355A	198626	48.5	+30 43	6.8	.060	gFo	- 26.6	0.5	2	- 30.4 D
G 29104	198729	49.8	- 3 25	8.0	.042	gM4	- 29.7	1.7	3	
B 5368	198732	50.1	-23 58	6.4	.110	sgG5	- 39.9	0.5	3	
A 14382A	198896	50.2	+43 34	8.5	---	sgG8	+ 4.	var	5•	
A 14382B	------	20 50.2	+43 34	8.8	---	A3	- 10.6	2.2	4	
44° 3621	199138	51.9	+44 59	8.3	.033	A1	- 43.9	1.1	4	
A 14412AB	199306	52.6	+59 07	6.8	.058	dA8n	+ 7.6	2.0	3	- 0.8 V
C 2711	------	52.8	+74 24	9.9	.120	dG5	- 74.1	2.1	3	
G 29194	199221	52.9	+27 54	8.0	.124	dG2	+ 4.9	0.4	3	
G 29195	199251	20 52.9	+33 34	7.4	.020	gM3	- 6.6	0.7	3	
B 5389	199478	54.1	+47 14	5.8	.007	cB8e	- 14.2	0.9	8r•	- 21.0 Y
B 5392	199611	54.8	+50 32	5.8	.038	dA8n	- 7.6	1.0	3•	- 19.6 D
V Cyg	199629	55.3	+40 58	4.0	.018	B9n	- 29.	6.	3	- 27. M
G 29285	200099	56.7	+68 52	7.1	.074	gK4	- 39.9	0.3	3	
B 5405	199955	20 56.9	+50 16	5.5	.013	B8n	- 14.	3.5	5	- 25.0 M
G 29292	199802	56.9	+ 0 54	8.7	.157	dF9	- 17.4	0.9	3	
G 29294	199803	57.0	+ 0 52	8.7	.244	dG4	- 20.2	0.9	3	
G 29309	199942	57.6	+ 7 19	6.0	.033	A3n	- 20.4	1.0	4	- 23. V
B 5405	199947	58.0	-17 44	6.5	.030	gK2	+ 1.6	0.7	3	
C 2716	199976	20 58.1	- 8 32	8.2	.240	dG7	- 37.4	0.5	3	
B 5412	200205	58.2	+59 15	5.8	.041	gK4	- 18.6	1.7	8	- 14.2 V
G 29350	200253	59.2	+35 50	6.1	.019	gG5	- 12.	var	4•	- 7.4 S
29° 4283	------	59.7	+30 20	8.5	.033	dF5	+ 4.4	1.1	4	
29° 4284	200390	21 00.2	+30 20	7.8	.036	A2n	- 23.	3.7	4	
G 29407	200494	21 01.1	+ 2 44	7.9	.188	gK2	+ 6.0	0.8	3	
G 29413	200563	01.3	+23 48	7.4	.017	gM5	- 8.4	0.5	3	
1° 4492	200535	01.4	+ 3 54	8.5	---	gK2	- 27.8	1.7	3	
30° 4299	200631	01.6	+30 51	7.8	.018	gK2	- 14.0	1.7	4	
G 29421	200565	01.6	+ 3 47	8.5	.173	dG3	- 7.3	1.1	3	
B 5425	200733	21 02.0	+41 26	6.3	.054	gF2n	- 5.1	2.6	4	- 11.5 V
30° 4307	------	02.6	+30 43	8.3	.016	gKo	- 22.6	1.8	4	
B 5428	200790	03.0	+ 5 46	6.0	.159	dF7	- 27.2	2.4	2	- 23.4 V
26° 4070	200860	03.2	+27 06	8.6	.235	dG5	- 26.6	1.1	3	
30° 4314	------	03.6	+30 34	8.5	.022	Aon	- 6.4	2.0	3	

TABLE 1 (Cont'd)

STAR	H.D.	1950 R.A.	Decl.	Vis. Mag.	P.M.	Spec.	Vel.	P.E.	No. Pl.	Others
		h m	° ′		″		km	km		
29° 4307	------	21 03.7	+30 00	8.5	0.021	gM5	- 13.3	0.3	3	
B 5433	201091	04.7	+38 30	5.6	5.204	dK6	- 63.1	0.9	13r	- 66.1 M
B 5436	201251	04.9	+47 27	4.9	0.005	cK5	- 24.2	0.4	2	- 26.1 M
G 29550	201636	06.1	+71 14	6.0	.121	dFon	+ 0.7	0.9	2	+ 1.5 V
G 29560	201651	06.4	+69 28	8.1	.131	dG8	- 13.2	1.5	3	
B 5437	201301	21 06.4	-20 24	6.9	.025	gG7	- 45.6	0.9	3	
B 5438	201352	06.7	-20 46	6.2	.170	dF1	- 43.2	1.1	3	
G 29578	201479	07.1	+17 08	9.4	.007	dF6	- 15.2	0.3	3	
14° 4550	201640	08.1	+15 02	8.1	.030	gK3	+ 10.9	1.2	3	
G 29598	201733	08.2	+45 18	6.5	.002	B5ne	+ 8.5	0.3	2	+ 9.2 V
14° 4552	201706	21 08.6	+15 14	9.2	.033	dGo	+ 10.9	1.3	4	
15° 4362	201751	08.8	+15 40	8.7	.028	gK1	- 13.4	1.1	3	
G 29612	201707	08.9	-14 41	6.4	.036	gFon	- 39.7	1.4	3	
B 5449	201921	10.4	-25 03	7.5	.031	gK2	- 7.1	0.5	3	
14° 4556	202017	10.5	+15 23	8.1	.057	dF7	- 69.3	1.4	5	
δ Equ	202275	21 12.0	+ 9 48	4.6	.306	dF5	- 16.8	2.1	4	- 15.4 L
τ Cyg	202444	12.8	+37 50	3.8	.464	dFon	- 22.1	1.9	3	- 22.0 Y
15° 5938	202495	13.8	-15 02	8.0	.016	Aln	- 9.	3.5	4	
B 5465	202671	15.2	-18 12	5.4	.014	B8	- 10.8	2.6	4	- 11.3 L
σ Cyg	202850	15.4	+39 11	4.3	.006	cAo	+ 1.5	1.2	6•	- 3.8 M1
A 14839A	202908	21 16.2	+11 22	7.0	.039	dF8	+ 5.7	0.7	12•	
B 5470	202890	16.5	-16 23	6.9	.036	gG7	- 35.4	1.7	3	
B 5474	203064	16.6	+43 44	5.1	.009	O8n	- 19.	var	5•	+ 4.v M
A 14843A	------	16.6	+33 35	9.0	---	gF5	- 29.2	1.9	4	
B 5509	204149	17.4	+84 03	7.1	.022	gKo	+ 5.0	1.8	3	
G 29855	203400	21 17.7	+65 57	8.1	.162	dG6	- 35.7	0.7	3	
B 5475	203142	18.2	-21 02	7.1	.067	dFo	- 7.5	2.0	3	
B 5490	203525	20.2	- 9 32	6.2	.040	gMo	+ 18.7	1.0	7r	
B 5495	203644	20.3	+49 10	5.9	.073	gKo	- 1.6	0.4	2	- 2.1 V
B Equ	203562	20.4	+ 6 36	5.1	.052	A2	- 10.4	0.9	3	- 10.4 M
G 29941	203712	21 20.9	+40 43	7.3	.012	gM6	- 47.4	1.5	2	- 53. L
B 5500	203843	22.2	- 3 37	6.4	.051	gA9	- 23.7	1.0	3	
G 30078	204585	26.7	+21 58	6.2	.042	gM4	- 21.4	0.2	2	- 20.5 D
B 5525	204770	26.8	+66 35	5.4	.023	B7n	+ 6.2	2.9	6	+ 1. M
G 30083	204734	26.9	+64 10	8.8	.282	dKo	- 9.2	0.4	3	
C 2791	204627	21 27.0	+25 13	8.6	.23:	dG5	- 15.0	0.2	3	
B 5520	204577	27.2	-19 22	6.5	.053	gF2	- 12.4	1.5	3	
B 5528	204905	28.2	+52 43	7.2	.017	Ao	- 19.8	0.9	3	- 11.v V
59° 2387	204964	28.4	+60 09	7.5	.022	B3	- 18.7	2.7	6r•	
G 30129	204832	28.6	+ 5 21	8.5	.018	gM3	- 5.2	1.3	3	
B 5535	205139	21 29.6	+60 14	5.5	.004	B1	- 13.6	2.0	5r	- 15.7 M
G 30162	205196	30.1	+57 17	7.4	.010	Bo	- 20.5	2.2	7r	- 10.0 V
B 5534	205132	30.9	-16 25	7.1	.110	dF4	- 40.1	1.0	3	
B 5537	205289	32.0	-20 18	5.8	.051	dF2	+ 5.5	1.1	3	
B 5538	205306	32.1	-20 29	7.0	.061	dF6	- 13.2	0.7	4	
B 5540	205342	21 32.4	-23 41	6.4	.074	gG7	- 14.4	1.9	4	
B 5548	205551	32.7	+51 28	6.0	.005	B9n	- 22.	4.0	5•	
G 30237	205741	33.4	+66 30	7.0	.042	gK1	- 12.7	1.8	4	
G 30240	205776	33.6	+66 33	7.2	.016	gK2	- 12.1	1.3	3	
B 5554	205850	34.5	+57 15	8.8	.020	gF2	- 15.5	0.9	3	
G 30283	205941	21 35.8	+32 58	7.5	.113	dG8	- 29.1	0.5	3	
B 5556	205924	36.0	+ 5 33	5.8	.112	A2n	- 16.6	2.6	4	- 21.0 D
B 5563	206165	36.6	+61 51	4.9	.004	cB2	- 11.0	1.5	5r	- 14.3 M
B 5559	206058	37.0	- 0 17	6.8	.229	dF7	- 28.	var	6r•	
A 15136A	206224	37.5	+41 30	8.1	---	dG9	- 14.8	1.9	3	
A 15136B	206225	21 37.5	+41 30	8.7	---	dG7	- 17.9	0.1	3	
60° 2776	206327	37.6	+61 19	8.5	.006	B2	- 29.6	2.5	3r	
B 5577	206554	38.5	+71 05	7.1	.131	dF5	- 7.8	1.0	4	
B 5568	206356	39.2	-23 29	5.3	.133	gG9	- 39.3	2.5	3•	- 44.9 M
G 30371	206404	39.4	+ 0 07	7.7	.063	dF7	+ 16.7	0.3	3	
G 30407	206731	21 40.8	+49 22	6.1	.008	gG5	+ 0.6	0.7	3	- 3.4 D
-0° 4257	206660	41.1	+ 0 18	7.1	.035	gG8	- 29.4	1.3	3	
A 15267AB	206792	41.7	+27 37	8.0	.102	dF5	- 57.3	0.3	3	
ε Peg	206778	41.7	+ 9 39	2.5	.025	cKo	+ 4.0	0.5	7r	+ 5.2 M
μ Cep	206936	42.0	+58 33	var	.002	gM2	+ 23.	var	3	+ 20.v M

TABLE 1 (Cont'd)

STAR	H.D.	1950 R.A.	Decl.	Vis. Mag.	P.M.	Spec.	Vel.	P.E.	No. Pl.	Others
		h m	° ′		″		km	km		
G 30443	206860	21 42.1	+14 33	6.1	0.277	dGo	- 20.1	1.4	3	- 18.4 S
B 5586	206833	42.2	- 9 16	7.1	.049	gK3	- 25.3	1.6	3	
C 2830	------	42.7	+74 13	9.4	.23:	dG7	- 29.6	1.6	4	
A 15300AB	207033	43.5	+11 39	8.5	---	dGo	- 28.1	1.9	3	
G 30473	207198	43.5	+62 14	6.0	.009	G9	- 15.	5.	2•	- 19.8 V
V Cep	207260	21 44.0	+60 53	4.5	.003	cA2	- 18.4	0.1	2•	- 21.5 M
B 5597	207061	44.0	-11 56	7.0	.131	dF6	+ 1.6	0.9	3	
61° 2194	207308	44.3	+62 04	7.9	.017	B3	- 22.6	2.1	2•	
B 5610	207436	46.4	- 5 38	6.8	.065	gKo	+ 0.8	1.7	4	
B 5613	207503	47.0	-12 57	6.1	.018	gA8	- 1.	4.	4•	
G 30566	207673	21 47.6	+40 55	6.5	.009	cAo	- 1.9	1.5	4r•	- 6.6 V
B 5619	207780	47.8	+61 02	6.4	.021	gM1.5	- 18.3	0.7	3	- 19.7 V
G 30585	207692	48.6	-23 30	6.8	.352	dF5	- 49.0	0.6	3	
B 5618	207760	48.9	-18 51	6.1	.165	dF1	- 42.2	1.7	3	
C 2845	207992	50.2	+39 34	8.7	.46:	dG5	- 51.2	0.8	3	
B 5623	207598	21 50.6	-13 47	5.2	.308	dFo	- 23.8	0.8	5	- 21.0 L
G 30643	208011	51.0	-20 15	8.1	.131	dF2	- 10.0	1.1	3	
G 30645	208218	51.2	+62 29	6.8	.020	B1	- 23.6	1.0	2	- 20.9 V
G 30661	208174	51.7	+28 06	6.7	.197	dA5n	- 5.6	2.6	3	- 8.4 D
67° 1370	208376	51.9	+67 51	9.6	---	A2	- 8.9	1.8	3	
G 30666	208411	21 52.0	+67 52	7.6	.014	gG4	- 2.9	1.2	3	
44° 3980	208310	52.3	+45 19	8.5	.007	Aon	- 1.6	2.9	4	
C 2850	208313	52.5	+32 06	7.6	.33:	dKo	- 15.4	1.4	4	
A 15442A	208395	52.9	+45 33	8.5	.006	Ao	0.	var	4•	
44° 3985	208513	53.5	+44 42	7.8	.014	Ao	- 16.	var	5•	
B 5641	208565	21 54.5	+11 50	5.6	.035	Ao	+ 13.0	2.9	7	+ 18. V
B 5643	208703	55.6	- 5 40	6.2	.102	dF2	+ 0.1	2.4	4	+ 0.6 S
B 5644	208704	55.7	-12 54	7.0	.068	dG2	+ 2.6	1.5	3	
B 5649	208808	56.5	-23 07	7.4	.061	dF5	- 10.9	1.5	3	
G 30774	209112	57.4	+62 27	6.2	.029	gM3	- 16.4	1.6	3	- 14.5 D
B 5653	209008	21 57.6	+ 6 29	6.0	.006	B5	- 6.	3.4	3	- 7.3 V
B 5661	209369	58.5	+72 57	5.2	.172	dF3	- 21.3	1.5	8	- 21.2 M
30° 4587	209206	58.8	+30 31	8.7	.017	dA5n	- 0.6	1.8	4•	
B 5659	209240	59.4	-18 09	6.4	.127	dG7	- 16.0	0.6	3	
30° 4591	209440	22 00.6	+30 32	8.2	.007	A3	+ 4.5	1.9	4•	
G 30849	209484	22 01.0	+29 58	7.0	.014	B9	- 3.	var	4•	- 7.v D
30° 4594	209516	01.1	+30 45	8.2	.011	A1	+ 3.4	1.8	4	
29° 4570	209517	01.1	+29 48	7.9	.028	B9n	+ 1.	3.2	3	+ 1. D
G 30851	209675	01.4	+68 01	8.8	.196	dG8	+ 56.0	1.2	3	
B 5671	209625	02.2	- 1 09	5.2	.052	gA8	+ 16.9	2.0	6	+ 20.4v L
G 30883	209709	22 02.6	+14 34	6.7	.018	gM2.5	- 3.2	0.7	3	
A 15610A	209745	02.9	+29 57	8.7	.045	dF8	- 25.2	1.3	3	
B 5681	209833	03.3	+28 43	5.6	.023	Aon	- 5.7	1.8	5	- 15.8 DV
B 5687	209975	03.6	+62 02	5.2	.003	G9	- 11.3	1.6	7•	- 12.8 M
G 30929	209977	04.6	+11 31	7.3	.039	gM1	- 63.9	2.4	4•	- 68. L
B 5692	210129	22 05.5	+21 28	5.7	.071	B8ne	- 52.	4.	4r	
B 5700	210353	06.7	+47 41	6.8	.034	A1	+ 6.	3.1	3•	- 7.v V
B 5696	210269	06.8	- 8 26	7.0	.077	gG4	- 46.2	0.6	3	
B 5704	210422	07.9	-11 04	7.0	.055	gG7	+ 1.1	0.8	3	
G 31026	210502	08.2	+11 23	5.9	.063	gM1	+ 11.8	0.4	3•	+ 21.7 D
B 5716	210807	22 08.8	+72 06	5.0	.031	gG3	- 9.6	2.3	3•	- 15.9 M
B 5712	210705	09.7	-14 26	6.2	.045	dF3	+ 14.7	1.2	3	
A 15729A	210885	10.1	+59 28	7.6	.017	gKo	- 3.9	1.8	4	
A 15729B	------	10.1	+59 28	9.5	---	A2	+ 1.3	2.5	3	
B 5715	210763	10.1	- 4 58	6.4	.065	dF4	+ 2.	var	6•	
69° 1229	211003	22 10.4	+70 07	8.3	---	dFo	- 5.0	2.0	4	
B 5727	210959	10.4	+60 31	5.5	.024	gG9	- 2.0	0.9	2	- 3.8 V
B 5717	210845	10.8	-12 10	7.1	.029	gGo	- 8.8	2.5	4•	
G 31086	211029	10.8	+63 03	6.1	.010	gM3	- 13.8	1.0	3	- 12.3 D
G 31087	210925	10.9	+25 42	6.8	.154	dG6	- 68.4	0.3	3	
B 5735	211140	22 12.6	- 5 50	8.2	.020	gG7	- 0.2	1.7	4	
15° 6174	211234	13.3	-14 43	8.0	---	gK3	- 20.	var	4•	
14° 6764	211286	13.4	+15 11	8.6	.023	dF5	+ 4.7	2.5	4•	
15° 6604	211381	13.7	+15 46	8.2	.013	dF6	+ 6.4	1.3	4	
B 5743	211361	14.1	-13 05	5.6	.013	gKo	+ 13.8	2.2	4	

TABLE 1 (Cont'd)

STAR	H.D.	1950 R.A.	Decl.	Vis. Mag.	P.M.	Spec.	Vel.	P.E.	No. Pl.	Others
		h m	° '		"		km	km		
G 31156	211380	22 14.2	-14 54	7.1	0.077	dF8	+ 18.6	1.7	3	
G 31201	211733	16.4	+16 00	6.9	.023	A3n	- 30.0	1.5	3	- 24.1 D
15° 4618	------	16.6	+15 41	8.4	.030	gG6	- 18.3	1.3	4	
B 4754	211797	16.7	+37 31	6.1	.071	dF2	+ 6.7	0.9	3	+ 6.5 V
15° 4620	211837	17.2	+15 55	8.6	.014	dA8n	+ 13.	4.9	4•	
53° 2844	211868	22 17.5	+54 19	8.0	---	A4	- 60.4	1.4	6	
B 5787	212774	17.8	+85 58	6.8	.038	gK0	- 9.3	1.0	3	
B 31242	212047	18.7	+26 41	6.5	.013	gM4	- 0.2	0.8	3	- 4.8 D
B 5760	212022	18.8	- 6 30	7.5	.030	A4	- 11.2	2.8	4	
G 31260	212081	19.2	- 6 26	8.1	.007	gM3	+ 11.4	1.1	3	
B 5767	212247	22 19.8	+43 30	8.0	.038	gK2	- 22.4	2.0	4	
A 15881A	212391	20.3	+66 27	7.2	.034	gG6	- 2.8	1.5	5r	- 1.5 V
A 15881B	212392	20.3	+66 27	8.0	.028	A3	- 8.	var	4•	- 10.v V
G 31288	212291	20.6	+ 9 12	7.8	.307	dG6	- 7.5	1.0	3	
54° 2756	212455	21.2	+55 29	8.4	---	cB5	- 59.4	2.3	6r•	
G 31312	212470	22 21.6	+31 00	7.5	.017	gM4.5	- 4.0	1.2	3	
51° 3359	212510	21.7	+52 13	8.6	---	A2	- 38.4	1.3	6	
B 5774	212430	21.8	-13 47	5.9	.047	gG6	- 20.6	1.9	4	
B 5779	212593	22.5	+49 13	4.6	.010	cB8	- 22.7	1.3	2•	- 26.4 M
B 5780	212643	23.4	-23 56	6.2	.006	Ao	- 15.3	2.3	4	
51° 3372	212791	22 23.8	+52 11	8.2	.016	B4ne	- 13.0	0.7	6•	
74° 964	212955	23.8	+74 35	8.0	---	gG5	- 3.3	1.1	3	
74° 965	213021	23.9	+74 34	8.0	---	cGo	- 23.1	0.8	3	
G 31350	212810	23.9	+53 41	7.4	.061	dF1	- 15.3	2.4	3	
53° 2882	212898	24.5	+53 51	7.6	.007	Aon	- 4.	5.	6•	
B 5790	212943	22 25.3	+ 4 27	4.9	.318	sgKo	+ 53.9	0.3	13r	+ 53.9 M
G 31388	213014	25.8	+17 00	7.5	.022	gG8	- 39.2	0.7	9r	
B 5804	213310	27.4	+47 27	4.6	.005	cMop	- 0.8	1.5	11r•	- 11.6 M
σ Aqr	213320	28.0	-10 56	4.9	.028	Ao	+ 5.0	1.7	6	+ 13.v LV
G 31451	213470	28.4	+56 58	6.7	.012	cA3	- 61.9	1.0	3	- 61.2 V
B 5812	213464	22 29.0	-11 10	6.4	.081	dF2	+ 4.	var	4•	
B 5817	213789	31.5	- 1 50	5.9	.046	gG6	- 7.5	0.7	3	
B 5816	213780	31.5	- 9 52	6.8	.010	gK2	+ 5.1	1.9	4	
B 5823	213973	31.6	+69 39	6.0	.135	dF2	+ 1.0	0.7	3	- 5.5 V
B 5821	213930	31.7	+56 22	5.8	.086	gG9	- 10.1	1.8	6•	
A 16095A	214168	22 33.6	+39 23	5.8	.005	B3ne	- 8.	6.	6•	- 1. M
A 16095B	214167	33.6	+39 22	6.6	.012	cB2	- 11.4	1.0	4•	- 15.1 V
53° 2931	214357	34.5	+53 32	8.6	---	Ao	- 5.9	0.9	6	
B 5838	214470	34.5	+73 23	5.2	.172	gF3	+ 2.3	0.9	8r	+ 0.7 M
A 16111AB	214511	34.9	+72 37	7.5	.009	dF6	- 12.	var	4•	
A 16111D	------	22 35.0	+72 37	8.3	.098	dF7	- 5.0	1.1	3	
G 31604	214710	36.2	+75 07	6.1	.046	gM1	- 5.7	0.7	3	- 5.3 D
G 31608	214547	36.4	+ 2 16	10.1	.013	dF2	+ 6.	3.1	6•	
B 5839	214572	36.6	-10 17	7.2	.049	dGo	+ 11.4	1.5	3	
A 16145pr	214615	36.9	-12 52	8.6	.269	dKo	- 10.8	0.6	3	
A 16145fo	------	22 36.9	-12 52	8.6	---	dKo	- 6.8	0.6	3	
B 5844	214680	37.1	+38 47	4.9	.006	O9	- 12.	3.3	2•	- 9.5 M
G 31632	214714	37.3	+37 20	6.1	.004	gGo	- 7.7	0.3	3	- 6.5 D
B 5845	214690	37.6	-30 55	6.0	.234	gK2	+ 79.8	0.6	2	
G 31650	214878	38.3	+53 35	6.1	.013	gG4	- 6.3	1.0	3	- 5.7 D
54° 2836	214956	22 38.8	+54 45	8.8	---	Aon	+ 1.4	2.5	6•	
G 31689	215093	40.2	- 0 02	6.9	.006	dF2	- 16.2	2.2	4	
B 5859	215081	40.3	-21 55	7.3	.028	gG3	+ 7.5	0.3	4	
B 5861	215097	40.4	-10 22	7.2	.018	gKo	+ 14.6	1.3	3	
O 31694	215110	40.4	+ 0 09	8.0	.226	dG4	- 9.5	1.2	3	
G 31695	215129	22 40.4	+ 0 57	6.9	.015	A3	- 9.0	0.5	3	
G 31739	215500	42.3	+64 19	7.8	.297	dG5	- 41.4	2.5	4•	
C 2972	215696	44.6	-16 24	7.4	.358	dG4	- 30.4	1.7	4	
B 5879	215766	45.1	-14 19	5.7	.029	Aon	+ 15.	var	5•	
B 5883	215907	45.4	+58 13	6.3	.005	Ao	+ 6.4	2.6	5	- 0.6 D
B 5882	215874	22 45.9	-10 49	6.2	.030	dFo	- 6.3	0.5	3	
G 31824	215943	45.9	+37 09	6.0	.084	gG8	- 25.9	0.7	3	- 23.2 D
G 31825	215953	46.0	+49 19	7.2	.035	gM4	- 56.0	2.2	4	- 52. L
G 31880	216720	49.3	+84 31	7.1	.049	gKo	+ 2.4	0.9	3	
B 5894	216385	49.9	+ 9 34	5.3	.520	dF5	+ 8.6	1.5	7	+ 12.8 L

TABLE 1 (Cont'd)

STAR	H.D.	1950 R.A.	1950 Decl.	Vis. Mag.	P.M.	Spec.	Vel.	P.E.	No. Pl.	Others
		h m	° ′		″		km	km		
G 31927	------	22 51.2	+75 46	9.3	0.330	dK1	+ 39.3	1.8	3	
H 5902	216567	51.5	-12 27	7.2	.062	gK2	+ 5.3	0.5	3	
B 5918	217050	54.9	+48 25	5.2	.014	B3ne	- 17.4	1.0	3•	- 10.9 M
A 16407A	217294	55.6	+78 14	8.0	.148	gG5	- 21.8	0.7	3	
A 16407B	------	55.6	+78 14	9.0	.135	dF6	- 25.1	1.5	3	
B 5920	217166	22 56.0	+ 9 05	6.5	.420	dG1	- 27.0	0.6	4r	
B 32067	217459	58.2	+ 2 45	6.0	.082	gK4	+ 17.5	0.7	3	+ 21.4 D
o And	217675	59.6	+42 03	3.6	.022	B7n	- 18.3	0.9	3•	- 13.9 M
56° 2933	240170	23 00.2	+56 48	8.6	---	dG6	- 38.7	0.7	3	
B Peg	217906	01.4	+27 49	2.6	.234	gM2	+ 9.5	0.6	6r	+ 8.6 M
B 5945	218060	23 02.6	- 7 58	5.6	.124	dFon	- 8.1	1.0	4	- 19. S
b 5946	218081	02.7	- 8 01	7.6	.012	gKo	- 23.	var	4•	- 25. L
G 32173	218209	03.1	+68 09	7.5	.623	dG3	- 18.7	0.7	8r	
29° 4856	218199	03.4	+30 27	8.3	.013	gG7	- 5.6	2.2	4	
29° 4858	218301	04.1	+30 21	8.0	.020	dA8n	- 3.0	2.1	5	
B 5954	218356	23 04.7	+25 12	5.0	.031	gKo	- 26.	3.4	2	- 26.8 LV
G 32217	218454	05.4	+30 10	7.5	.024	gK4	- 19.9	1.0	3	
29° 4867	------	05.9	+29 57	8.5	.050	gKo	+ 4.1	1.3	4	
30° 4885	------	06.3	+30 35	9.0	.046	gA8	+ 1.1	1.7	4	
G 32299	218853	08.7	+ 4 44	6.9	.007	gM5	- 5.7	0.5	3	
G 32331	219139	23 10.9	+10 48	5.9	.017	gG5	+ 16.2	1.9	4	+ 18.0 D
14° 6429	219364	12.7	-14 18	7.6	---	dG9	+ 9.5	1.8	3	
G 32395	219642	14.0	- 1 52	8.3	.177	dG4	- 17.0	1.4	3	
G 32412	219617	14.5	-14 06	8.3	1.292	sdA8p	+ 8.0	1.4	8r	+ 23. Md
γ Peg	219615	14.6	+ 3 01	3.8	0.756	gG6	- 15.0	0.9	3	- 13.4 M
G 32420	219657	23 15.0	- 1 48	8.2	.265	dG4	- 47.8	2.0	3	
G 32430	219702	15.3	-14 04	6.8	.012	gK2	- 9.6	2.7	4•	- 5.5 L
14° 6467	219758	15.6	+15 19	8.2	.084	dF8	- 52.8	1.1	3	
G 32467	219879	16.8	-18 21	6.1	.026	gK3	+ 5.2	1.0	3	
G 32486	220007	17.6	+56 58	7.2	.007	gMo	+ 1.7	1.8	3	
G 32489	219983	23 17.7	- 4 11	6.6	.302	dGo	- 14.6	1.6	3	
G 32493	220140	17.8	+78 44	7.7	.166	dKo	- 15.1	1.3	3	- 19. L
14° 4974	220078	18.2	+14 46	7.6	.036	dA5	- 16.1	1.0	4	
G 32532	220382	20.0	+75 31	8.0	.017	gK1	- 14.4	0.6	3	
A 16713B	------	20.3	+20 17	9.5	---	dK6	- 21.6	0.2	2	
B 6012	220321	23 20.4	-20 22	4.2	.158	gKo	- 10.6	2.8	3	- 6.0 M
G 25345	220373	20.6	+15 48	8.6	.138	dGo	+ 4.1	0.7	3	
B 6019	220466	21.4	-22 03	6.5	.112	dF2	+ 24.0	1.8	3	
A 16730A	220512	21.7	+ 3 26	6.8	.033	gK2	- 13.0	1.0	3	
A 16730B	------	21.7	+ 3 26	8.8	---	dF4	- 19.9	1.9	4	
G 32589	------	23 23.0	+69 41	9.2	.185	dG4	- 12.1	2.0	3	
G 32611	220819	24.1	+60 49	6.7	.007	gA5	+ 0.9	1.6	3	
58° 2595	220999	25.6	+59 25	7.4	.041	A3n	- 26.2	2.5	4	
B 6041	221147	26.9	- 2 04	6.6	.025	gG8	+ 12.2	2.4	4	
B 6056	221525	27.6	+87 02	5.6	.082	dA8	- 11.4	1.1	3	
B 6045	221251	23 28.0	-24 28	7.5	.068	dG3	- 25.0	0.3	3	
B 6050	221357	29.1	-21 39	6.2	.008	gA8n	- 8.	var	5•	
A 16819A	221445	29.7	+ 6 49	6.8	.055	dF6	- 12.7	1.0	3	
17° 6769	221503	30.1	-17 07	8.6	.35:	dK5	- 1.9	1.9	3	+ 3. Md
G 32767	------	31.3	+70 05	8.6	.035	gM1	- 32.7	1.0	3	
G 32771	221668	23 31.4	+20 34	6.3	.022	gM3	+ 5.6	1.0	3	+ 6.7 D
G 32793	221861	32.8	+71 22	6.1	.008	dK1	- 1.4	1.3	3	- 2.4 D
B 6064	221833	32.9	+ 1 02	6.6	.056	gK4	+ 7.8	1.9	4	+ 5.3 V
B 6065	221855	33.0	- 7 44	6.5	.025	gG5	+ 5.2	1.0	3	
18° 6342	221974	34.1	-17 31	9.1	.44:	dKo	- 22.8	1.2	3	
B 6069	222093	23 35.1	-13 20	5.7	.043	gG6	- 12.1	0.7	3	
G 32872	222387	37.2	+73 44	6.1	.013	gG5	+ 4.	var	4•	+ 14.6 D
G 32907	222589	38.9	+74 07	8.8	.218	dG7	- 24.3	1.1	3	
B 6082	222547	39.0	-18 18	5.6	.079	gK5	+ 25.6	0.9	3	
B 6083	222574	39.2	-18 06	5.0	.014	cG1	- 2.2	2.5	4•	+ 4.8 L
B 6086	222641	23 39.8	+44 43	6.7	.018	gK5	- 9.9	1.4	4r	
G 32961	222860	41.7	+ 0 26	8.0	.040	dF8	+ 4.2	1.4	3	
B 6100	223029	43.4	- 0 01	7.8	.050	dF8	- 33.0	1.7	4	
B 12558A	------	44.6	+68 47	9.2	---	dF6	- 45.3	1.5	3	
B 12558B	------	44.6	+68 47	9.3	---	dF6	- 41.0	0.8	3	

TABLE 1 (Cont'd)

STAR	H.D.	1950 R.A.	1950 Decl.	Vis. Mag.	P.M.	Spec.	Vel.	P.E.	No. Pl.	Others
		h m	° ′		″		km	km		
B 6109	223311	23 46.0	- 6 39	6.3	0.019	gK4	- 20.0	0.7	11r	
A 17022A	223385	46.4	+61 56	5.6	.007	cA2e	- 45.3	1.8	11r•	- 47.0 V
A 17022B	------	46.4	+61 56	8.0	---	cAo	- 43.6	1.5	2•	
B 6112	223421	46.7	+58 41	6.4	.038	dF3	+ 29.0	1.9	4	+ 29.4 V
B 6116	223524	47.7	-10 15	6.1	.155	sgKo	- 17.2	1.5	4	
B 6118	223559	23 48.0	-14 41	5.9	.043	gK5	- 57.9	1.9	3	
A 17052AB	223688	49.2	- 6 53	8.9	---	dG2	+ 11.5	0.9	3	
B 6126	223744	49.9	-14 32	6.0	.104	gK3	+ 2.5	0.2	3	
B 6128	223781	50.1	+10 40	5.4	.026	A2n	+ 3.	3.7	7	- 7. M
B 6131	223807	50.3	- 9 16	6.0	.061	gKo	- 17.6	1.3	3	
B 6132	223825	23 50.4	- 3 26	6.1	.080	gG9	- 5.7	1.7	5	
19° 6533	223932	51.2	-18 39	7.4	---	dG6	- 19.7	1.8	3	
G 33149	223960	51.3	+60 35	7.0	.010	cAoe	- 48.7	1.5	5•	- 48. V
60° 2637	223987	51.6	+61 20	7.6	.031	Bo	- 44.8	2.0	5•	
G 33163	224055	52.2	+61 34	7.2	.036	cB3e	- 41.9	2.5	7•	- 42.7 V
G 33191	224186	23 53.4	+14 57	6.6	.100	gM3.5	+ 4.2	0.7	3	
A 17107A	224253	53.8	- 9 47	8.5	.279	dG3	+ 36.9	0.9	3	
A 17107B	------	53.8	- 9 47	9.0	---	dK3	+ 40.5	1.8	2	
G 33208	224303	54.1	+20 22	6.3	.023	gM2.5	+ 2.0	1.5	3	+ 1.8 D
47° 4331	224380	54.8	+48 00	7.5	.012	B9n	+ 2.	4.3	5•	- 12.2 D
58° 2676	224424	23 55.2	+59 26	7.8	---	cB1e	- 70.9	2.7	5•	
B 6152	224481	55.8	-16 08	6.4	.078	gG8	+ 4.8	2.0	3	
G 33252	224559	56.2	+46 08	6.5	.017	B3ne	+ 0.3	1.0	7•	- 3.0 V
σ Cas	224572	56.5	+55 29	4.9	.008	B3n	- 16.9	2.5	2•	- 9.9 M
A 17140B	------	56.5	+55 29	7.0	---	B3	- 5.	var	4•	
17° 6856	224618	23 56.8	-17 13	8.5	1.145	dG6	- 42.3	1.3	4r	
G 33276	224677	57.2	- 0 33	7.0	0.026	gM2	- 30.4	1.9	3	
G 33283	------	57.5	+19 46	9.5	.288	dKo	+ 8.5	1.3	4	
59° 2813	224905	59.1	+60 11	9.2	---	B3n	- 16.9	1.1	3r•	
B 6168	224906	59.2	+42 05	6.1	.002	B9	- 7.	3.0	5	- 15. S
B 6175	225003	23 59.9	+ 8 12	5.8	.111	dFo	+ 9.5	0.9	5	+ 8.2 S

NOTES

STAR	R.A. h m	
G 17	0 00.8	IS -17.0 +2.6, 5.
G 61	02.8	Hydrogen faint; λ4215 and λ4077 strong.
B 26	10.5	-2, -22, -15, -23.
γ Peg	10.6	IS -5.2 +1.1, 2.
A 237A	14.8	-21, -18, +48, -23.
A 252A	15.9	Lines may be double on one plate.
30° 60	24.8	Velocity probably variable; -21, -27, -12, -29.
κ Cas	30.1	IS -16.5 +1.2, 6.
G 1017	48.4	IS -16.5 +0.7, 5.
G 1066	50.8	-8, -18, -23, +9.
B 222	59.5	+35, +19, +25, +17.
G 1271	1 01.0	IS -25.0 +2.1, 5; IS lines may be double.
G 1290	01.7	Large difference, S-W; Velocity probably variable.
B 234	02.4	Velocity variable; lines are double on two plates.
A 988A	10.1	Spectrum is composite, A2 + A1; lines are double on one plate.
G 1472	10.9	IS -16.3 ±0.6, 3.
G 1825	27.9	IS -19.2 ±1.1, 3.
29° 260	30.8	+20, +23, -12, +22.
B 340	31.4	Lines are poor but velocity is probably variable; -20, -21, +5, +9, +6.
G 1977	35.5	Fine spectrum; velocity is probably variable; -6, 0, +11, -6.
B 365	36.5	Lines are poor.
B 398	43.9	-14, +19, +7, +16, -7, -2.
B 457	59.3	IS -10.7 ±1.5, 7.
44° 422	2 03.9	All plates with dispersion of 130A.
55° 554	12.4	IS -19.9 ±2.7, 3.
55° 469	13.2	-32, -46, -32, -64; IS -30 ±3.4, 4.
G 2724	13.5	IS -14 ±4.6, 2.
55° 564	14.3	-34, -19, -35, -25, +14, -16; lines are double on second plate.
G 2800	17.2	IS -23.3 ±2.1, 4.
B 534	18.9	IS -16.9 ±2.1, 4.
15° 331	19.2	-10, -16, -30, -28.

STAR	R.A. h m	
B 535	2 19.4	IS -20.6 ±2.5 4.
14° 392	21.7	-51, -48, -17, -38, -40.
G 2925	23.2	-38, -17, -35, -19, -29, -10.
G 2973	26.4	IS -26.4 ±2.3 4.
B 608	37.8	Fine spectrum; velocity probably variable; +5, -10, -12, +1.
B 599	40.4	Large difference, D-W; velocity probably variable.
G 3315	42.7	+33, +25, +8.
15° 554	3 09.4	+54, +37, +30, +23.
15° 450	11.3	Velocity probably variable; +9, +5, +28, +27, +17.
B 724	12.0	IS -10.8 ±1.7 6.
B 721	13.9	Lines are poor but velocity probably varies; range -23 to +21.
G 4009	18.5	-28, -10, -26, -46.
B 781	25.0	IS -8.3 ± 0.7 4.
A 2559A	25.8	IS +0.3 ± 1.5 3.
B 786	26.9	IS -7.7 ± 1.5 3.
29° 568	27.2	Velocity probably variable; -2, +16, +12, -8.
44° 732	28.9	Velocity probably variable; -14, -1, -5, -19.
B 839	39.2	Range +50 to +14.
22° 535	40.6	In Pleiades.
B 845	41.3	IS +22.6 ±1.7 2.
A 2772A	44.7	Lines double on two plates; IS +18.0 ±2.5 5.
21° 550	45.8	In Pleiades.
G 4598	46.6	IS -4.7 ±0.9 5.
B 876	46.6	+34, +18, +15, +31.
I Per	51.0	IS +12.9 ±0.6 9.
A 28508	51.8	+8, +14, +8, +31, +27.
ε Per	54.5	IS +10.8 ±0.8 8.
ε Per	55.7	IS +10.5 ±0.3 7.
G 4919	4 02.4	Lines are poor.
B 947	05.0	IS +3.8 ±1.0 4.
75° 167	08.8	-14, -14, +5, -6; lines are double on third plate.
B 963	09.4	Large difference, L-W; velocity probably variable.
B 971	10.9	-12, +3, +15, +7.
B 974	12.8	Lines are poor; but velocity is probably variable.
A 30958	13.0	Companion to 32 Eri; velocities depend upon measures of one hydrogen line on each plate; the small p.e. is accidental.
15° 754	13.8	Velocity probably variable; -17, -4, -3, +1.
15° 765	17.3	Velocity probably variable; +23, +31, +10, +22.
B 1019	21.0	Velocity probably variable; range +30 to -6.
A 32434	25.7	Velocity probably variable; -28, -46, -46, -37.
A 32748	28.1	IS +0.6 ±0.9 5.
A 33535	35.4	Sanford's orbit of the N star of this pair gives V_o = +3.4.
B 1100	42.1	-8, -30, -12, -2, +7.
B 1139	49.1	IS -8.6 ±0.6 5.
38° 1012	5 00.6	Ca+ lines give +4.7 ±0.6 6; Hydrogen lines are fair and velocity is probably variable; range +10 to -30.
B 1215	04.9	IS +15.1 ±2.1 2.
B 1248	12.5	+12, -18, -7.
B 1249	13.0	IS +14.9 ±0.6 6.
G 6486	15.3	+71, +71, +96, +29.
15° 787	16.8	Lines are poor; they appear double on one plate.
B 1282	19.0	IS +20.0 ±1.5 3.
B 1284	19.2	IS +12.8 ±1.2 2.
γ Ori	22.4	IS +21.6 ±1.5 4.
B 1310	23.9	IS +14.8 ±0.4 4.
B 1353	32.1	IS +15.9 ±1.8 4.
A 41794	32.4	IS +17.0 ±1.2 4.
A 41798	32.4	IS +15.8 ±1.6 5.
B 1361	32.6	IS +27. ±3.1 2.
B 1362	32.6	IS +25.2 ±1.9 4.
ε Ori	33.7	IS +18.5 ±0.5 12; IS lines are double on four high dispersion plates, +3.1 ±0.8; +25.2 ±0.5.
G 6975	34.3	-96, -118, -114, -96.
ι Tau	34.7	IS +19.8 ± 0.4 4.
B 1367	34.9	+7, +26, +25, +8.
B 1443	45.3	Velocity probably variable.
G 7335	48.1	Velocity probably variable; +10, +7, -6, +2.
G 7483	53.9	IS +8.0 ±1.2 9.
G 7523	55.5	Dunlop calls this a binary with two spectra showing on one plate, the other three agree and give a velocity -3.7 ± 0.7.

STAR		R.A. h m	
G	7671	6 00.8	+58, +48, +32, +56.
B	1518	03.8	Velocity probably variable; -15, -25, -9.
B	1578	13.9	IS +12.4 ±0.8 6.
29°	1231	24.9	Velocity probably variable; +7, -3, -11, -8.
30°	1245	27.1	+21, +26, +3, +11.
B	1651	29.1	Velocity probably variable in long period.
5°	1282	29.3	IS +24.8 ± 1.5 3.
G	8477	29.3	IS +22. 1 plate.
B	1657	30.2	IS +11.6 ± 1.0 5.
6°	1303	33.8	IS +19. ±3.2 2.
G	8686	36.6	-21, +4, -15, -22.
B	1743	45.2	Velocity probably variable; +39, +29, +30, +21.
18°	1365	47.2	Velocity probably variable; +22, +32, +32, +17, +34.
G	9063	52.2	Spectrum composite, B_3 + F_3.
2°	1483	55.3	Spectrum composite, gF5 + A5; -14, -45, +24, -44.
B	1817	7 00.9	IS +17.4 ±2.5 2.
A	Gem	15.2	Lines are broad and ill-defined but velocity may be variable, as announced by Hnatek at Vienna.
B	1893	16.4	-12, +11, +14, +14.
B	1903	18.4	Lines are poor but large difference, V-W, suggests that the velocity is probably variable.
B	1871	20.7	Velocity probably variable.
η	CMa	22.1	IS +21.4 ±1.3 2.
B	1935	22.4	IS +15.2 ±2.5 2.
B	1941	24.0	+24, +32, +23, +9, +4, -4.
B	1957	25.5	Spectrum composite, gF8 + B3n.
B	2035	41.8	IS +29.5 ±1.9 2.
88°	39	45.9	+16, +5, -7, +3.
C	946	55.4	Velocity probably variable; +4, -2, +1, -15.
B	2122	58.7	-35, -9, -27, -2.
B	2139	8 05.2	0, +4, -13, -16.
B	2173	10.1	λ4128 and λ4130 strong.
A	6659A	10.2	+41, +12, +52, +22.
B	2212	19.1	+2, -28, +1, -16, -13, 0.
29°	1759	26.2	Velocity probably variable; +30, +8, +20, +33.
δ	Hya	35.0	Velocity probably variable; +25, +26, +9, +23.
B	2300	36.2	+45, +28, +19, +34, +23.
G	11886	37.2	+20, -12, +21, +18.
20°	2169	37.6	Double-lined binary; range -95 to +84.
B	2311	37.6	Range +89 to -21.
19°	2078	38.4	+30, +28, +60; lines may be double on last plate.
B	2343	42.4	Lines are poor.
B	2383	52.4	Large difference, V-W; velocity probably variable.
B	2432	9 02.0	-6, +4, -15, -30, -8, -34.
B	2439	03.3	Large difference, M-W; velocity probably variable.
G	12838	16.1	+16, -1, +59, +1, +34.
B	2510	17.9	Good lines; velocity probably variable; +28, +12, +13, +9.
G	12897	18.6	+6, +16, -30, +5.
G	13088	26.9	+19, -74, +5, +18.
B	2582	34.6	+32, +18, +10.
A	7500A	40.9	Lines are double on two plates.
B	2611	42.1	Range -10 to -41.
B	2623	43.8	+26, +15, 0, +6, +20.
12°	2093	44.6	Companion to R Leo.
B	2634	47.0	+27, +8, +25; lines fuzzy or double on two plates.
G	13531	47.1	+35, +8, +45, +72.
+0°	2582	52.4	+37, +38, +14, +30.
G	13748	57.2	+30, -52, +69, -51.
B	2683	10 00.1	+19, +28, +12, +4.
η	Leo	04.6	IS +2.9 ±0.8 6.
G	13941	06.6	Spectrum composite; gF5 + A2.
B	2748	18.5	IS +5.6 ±0.8 9.
B	2797	28.5	Range +35 to -4.
ρ	Leo	30.2	IS lines are double; -10.1 ±0.2 10; +15.1 ±0.6 10.
G	14569	33.6	Lines are abnormally wide for the type.
B	2831	36.3	Range +30 to -15.
A	7873	37.6	Velocities of both components are probably variable.
B	2839	37.6	Lines are poor.

STAR	R.A. h m	
88° 60	10 37.8	-58, -28, +30, -36.
B 2841	38.6	Large difference, L-W; velocity probably variable.
46° 1857	40.5	-33, +3, -6, +5.
B 2855	40.5	-21, +3, +2, -30.
B 2857	41.1	Range +23 to -22.
C 1304	48.0	+32, +44, +42, +24.
B 2895	49.5	Large difference, V-W; velocity probably variable.
C 1318	51.0	+30, +20, +33, +39.
66° 703	11 07.9	This velocity was ascribed (MWC N° 387) to C 1359 = Lal. F 1822A = BD 66° 704. BD 66° 703 is Lal.F 1822 C. For velocity of C 1359 see MWC N° 726.
B 2797	13.4	-20, -21, -6, -35; lines are double on first plate.
G 15514	14.4	-54, -74, -54, -9, -89; lines are double on fourth plate; λ4077 is strong.
G 15790	28.3	Velocity probably variable; +83, +96, +83, +79.
G 16008	37.3	Velocity probably variable; +31, +15, +30, +30.
G 16227	48.7	-28, +30, +24, +24.
G 16259	50.7	+25, +4, +12, +1.
+0° 2868	52.5	+16, +4, -16, -4.
30° 2212	59.2	-56, +23, -13, -7; lines are double on all except third plate.
G 16640	12 08.8	-5, -16, -18, +2.
B 3192	13.5	+17, -15, -2, +11, +7.
G 16759	14.3	Velocity probably variable; +63, +46, +48, +53.
A 8506A	16.2	Velocity probably variable; +17, -1, +10, +14, +21.
B 3229	21.3	-17, -3, -12, -25, 0.
G 16907	21.6	+14, +42, +19, +17.
G 16295	22.4	Range +65 to +31.
G 17115	31.0	-12, +7, +14, -14.
B 3299	36.6	Large difference, V-W; velocity probably variable.
B 3327	44.1	Velocity probably variable; +54, +52, +69, +68, +52, +46.
G 18399	13 34.6	Large difference, D-W; velocity probably variable.
B 3539	40.0	Large difference, V-W; velocity probably variable.
G 18539	40.5	-28, -7, +10, +7.
17° 3918	41.8	IS -4.2 ±2.0 3.
G 18747	49.9	-22, -40, -43, -22, -63.
B 3609	57.4	0, -19, +3, +4.
G 18965	14 00.1	Hydrogen and metallic lines weak.
G 19088	06.2	Large difference, L-W; velocity probably variable.
G 19105	07.0	Velocity probably variable; -4, -1, -18, +6, -1.
G 19438	22.0	Velocity probably variable; -21, -30, -37, -21.
G 19512	26.0	+6, +25, +25, +15.
G 19572	28.2	Velocity probably variable; -2, +14, +7, +10.
34° 2559	43.2	Range +3 to -41.
A 9383A	44.6	Lines are poor.
B 3788	47.8	+27, -4, +6, -5, +4, +12.
B 3820	55.5	+11, -19, -29, -33.
B 3823	56.2	Velocity probably variable; range +2 to -20.
29° 2622	15 04.0	Velocity probably variable; -34, -20, -39, -29, -9.
A 9520A	06.9	+74, -55, +13, -33.
A 9527A	08.0	Velocity probably variable; -18, -12, -2, -19.
B 3870	09.8	Velocity is variable; lines are double on one plate.
G 20479	11.6	Velocity probably variable; +17, +7, 0, +1.
14° 4160	13.0	IS -10.8 ±1.2 4.
B 3902	18.2	Velocity probably variable; +5, -4, +25, 0, +2.
G 20843	28.0	-1, -9, +12, -24, -7.
A 9681A	28.8	-42, -38, -61, -20; lines are double on first two plates.
A 9681B	28.8	-34, +3, -12, -82.
G 20912	31.1	+44, +67, +41, +51.
A 9799A	47.4	-46, -54, +2, -49.
44° 2511	48.2	Velocity probably variable; -26, -14, 0, -21, -11, -4.
81° 530	48.5	-17, -6, -66, -26.
G 21307	49.0	-8, -42, -23, -34.
A 9816B	49.8	Velocity probably variable; -16, -6, -27.
B 4047	51.1	Velocity probably variable; -32, -26, -38, -20.
B 4043	52.1	+6, -19, +10, -22.
B 4051	53.4	-5, -19, -7, +3.
B 4059	55.4	Range +1 to -77.
C 2141	57.2	-21, +10, -2, -19.
B Sco	57.4	IS -12.2 ±0.4 6.

STAR	R.A. h m	
29° 2758	16 00.9	Velocity probably variable; -17, -4, -2, -1.
B 4093	03.9	IS -15.0 +2.7 5.
G 21781	09.3	Velocity probably variable; -23, -28, -42, -27.
14° 4389	14.5	-7, +5, +25, -17, +22; lines are double on second and third plates.
G 21958	17.1	+23, -27, -9.
G 21995	18.6	-25, -5, -10, -18.
A 10030A	20.8	-47, -31, -49, -41.
B 4176	21.0	Lines are double on one plate; large difference, V-W. Velocity is variable.
χ Oph	24.1	IS -14.5 ±1.5 6.
A 10074B	26.3	IS -16.2 ±1.7 4.
G 22216	29.1	-19, -39, -21, -27.
B 4211	29.6	Lines are very poor, but velocity is probably variable.
τ Sco	32.8	IS -12.2 +2.2 3.
G 22337	34.5	Velocity probably variable; -3, -16, -19, -19.
G 22404	37.2	-27, -30, -53, -38.
66° 969	39.1	-3, -36, -48, -7.
B 4263	42.0	λ4077 and λ4215 strong.
A 10194A	43.1	Lines abnormally wide, but velocity is probably variable; -39, -46, -58, -51.
G 22564	43.6	Large difference, D-W; velocity probably variable.
B 4261	43.8	Velocity probably variable; +15, +8, -7, +1, -3.
G 22629	46.6	Velocity probably variable; -101, -105, -91, -109.
B 4278	48.0	Lines are very poor.
B 4274	48.1	IS -8.9 ±2.1 2.
B 4288	50.5	IS -8.6 ±0.9 3.
29° 2915	57.6	+15, +14, -11, -13, +12.
B 4434	17 01.5	IS -2.5 ±0.8 2.
29° 2933	02.8	-21, -6, -2, 0.
15° 3141	13.2	Velocity probably variable; -8, -19, -25, -13.
15° 3149	14.8	Velocity probably variable; -30, -18, -8, -19.
14° 3215	14.8	-26, -52, -62, -29.
B 4411	20.1	Lines are fuzzy and appear double on two plates.
G 23542	21.9	-36, -16, -8, -31.
B 4430	25.4	Velocity probably variable; range -18 to 12.
59° 1283	29.4	Velocity probably variable; -22, -11, -7, -21.
G 23953	37.6	Velocity probably variable; -50, -37, -51, -54.
ι Her	38.0	IS -20.0 ±1.5 4.
G 23980	38.7	IS -22.2 ±1.6 2.
B 4484	39.6	Range -52 to -10.
-0° 3352	42.3	Lines are poor.
2° 4458	46.0	IS -13.5 ±1.0 2.
G 24347	51.8	IS -11.2 ±1.7 3; stellar lines are very poor.
B 4526	54.1	-22, -9, -26, -24, -9, +6.
B 4548	58.1	IS -14.2 +0.3 6.
G 24515	58.4	IS -10.5 ±3.0 3.
A 10991A	59.4	IS -12.8 ±1.8 3; Lick records five plates but no velocities.
A 10991C	59.4	+17, +28, -49.
G 24637	18 02.8	-28, -25, +50, -41.
A 11045A	02.9	Plates are too poor to substantiate possible velocity variation.
B 4576	04.2	IS -12.2 +2.2 3.
G 24713	05.6	IS -3.0 ±1.9 4.
B 4590	06.6	IS -22.4 ±0.5 4.
B 4594	07.1	Velocity probably variable; -30, -1, -29, -33, -17, -16.
A 11240AB	15.8	+34, +12, -1, +20; IS -16.4 ±2.4 3.
A 11240C	15.8	IS -12 ±3.7 3.
G 25052	18.9	Hydrogen strong.
Anon.	45.9	8′ distant from EZ Lyr.
G 25844	48.2	-5, +12, +37, +4.
G 25853	48.4	Range +77 to -131; lines are double on four plates.
44° 3003	50.0	-4, -73, +6, -21, -19.
B 4779	50.1	-35, -10, -12, -17, -26, -24.
C 2474	53.8	-25, -11, -54, -42.
G 26080	56.9	IS -4.8 ±1.5 2.
A 11977A	19 00.8	Velocity variable; lines are double on four plates.
A 11977B	00.8	+1, -18, -36, +12.
B 4856	02.8	-30, -26, -2, -24; lines are double on fourth plate.
B 4865	05.3	Range +18 to -60; lines appear double on several of the plates; IS -4.6 ±2.0 4.

STAR	R.A. h m	
G 2496	19 05.6	+05, -18, +15, +11.
G 26392	06.9	Large difference, V-W; velocity probably variable.
G 26397	07.2	-3, -4, +9, +18, +26.
G 26447	09.5	IS -11.7 ±0.7 3.
14° 3845	13.0	-27, -44, -52, -5.
G 26549	13.5	+7, +4, -4, -10.
A 125228	17.7	+19, +36, -3, +24.
B 4966	24.0	Large difference, V-W; velocity probably variable.
G 26673	25.2	IS +0.3 ±0.8 6.
G 26688	29.3	Large difference, S-W; velocity probably variable.
G 27016	31.1	IS -8.1 ±0.6 3.
21° 5428	31.2	This star is identified as C 2551 in Cincinnati 18 with a proper motion of 0".190. Such a motion would be surprising for a giant star of the magnitude and type.
G 27042	32.3	Large difference, L-W; velocity probably variable.
G 27226	38.5	IS -9.9 ±1.1 5.
1° 4698	42.9	IS +3.1 ±2.3 3.
G 27407	46.0	Large difference, D-W; velocity probably variable; +7, -10, -14, -3.
B 5066	49.3	-38, -20, -19, -26.
A 130384	49.7	+8, +14, -5.
B 5073	50.1	IS -5.8 ±1.0 3.
B 5121	56.2	+19, -44, +10.
29° 3844	58.6	IS -18.1 ±1.4 3.
G 27776	20 00.2	IS -6.0 ±0.8 3.
1° 4393	00.6	All plates with dispersion of 10 A/mm.
36° 3841	01.9	-42, +59, +49, +43, +12, +53; IS -9.0 ±1.7 5.
B 5150	02.6	IS-12.5 ±0.9 12.
35° 3949	03.8	IS -12.4 ±2.2 4.
G 28008	08.7	+21, +11, +6, +24.
G 28070	10.7	IS -20.2 ±1.0 2.
36° 3937	11.4	+65, -64, -4, +78, +62, -45.
66° 1776	12.2	-59, -53, -48, -39.
G 28207	15.5	-32, -31, -47, -22.
G 28303	18.8	IS -12.4 ± 1.3 9.
75° 739	23.8	Velocity probably variable; +17, +17, +5, +3.
B 5261	27.0	Velocity probably variable; +12, +6, -1, +15.
G 28546	28.9	IS -11.0 ±0.7 3.
G 28745	36.4	+17, +8, +29, -4, +5.
A 141538	39.0	-46, -28, -20; lines are double on the first two plates.
G 28912	42.4	Velocity probably variable; -61, -72, -82, -70, -70.
A 142728A	44.4	Lines are double on one plate; velocity probably variable.
B 5339	45.4	+12, +17, +26, -6.
B 5361	47.2	IS -15.4 ±0.9 6.
B 5389	54.1	IS -16.8 ±0.7 4.
B 5397	54.8	Lines are double on two plates.
B 5405	56.9	Velocity probably variable; -26, +1, -6, -24, -16.
G 29350	59.2	Velocity probably variable; -19, -14, -1, -14.
σ Cyg	21 15.4	IS -6.9 ±1.3 6.
A 143539A	16.2	V from approximate orbit by R. E. Wilson; double-lined binary; P = 3.97 days; $K_1 = K_2 = 65$ km/sec.
B 5474	16.6	IS -14.9 ±0.6 8.
59° 2387	28.4	IS -12.7 ±2.3 4.
B 5548	32.7	Velocity probably variable; -14, -29, -42, -18, -8.
B 5563	36.6	IS -22.2 ±1.5 8.
B 5559	37.0	-51, -44, -23, -19, -16, -17.
B 5568	39.2	Velocity probably variable; -47, -34, -37.
μ Cep	42.0	+33, +19, +16.
G 30473	43.5	IS -15. ±3.2 2.
ν Cep	44.0	IS -22.2 ±2.0 2.
61° 2194	44.5	IS -22. ± 4.2 2.
B 5613	47.0	Velocity probably variable; +5, +15, -16, -6.
G 30566	47.6	IS -11.8 ±2.7 3.
A 145424	52.9	-10, +13, -16, +16.
44° 3985	53.5	-9, -57, +12, -10, -18; two spectra suspected but not measured.
39° 4587	58.8	Lines are double on one plate.
30° 4591	22 00.6	Lines are double on one plate.
G 30849	01.0	+29, -21, -17, -3.
B 5687	03.6	IS -12.5 ±0.5 5.
B 5700	06.7	Lines are double on one plate.

STAR	R.A. h m	
G 31026	22 08.2	Large difference, D-W; velocity probably variable.
B 5716	08.8	Velocity probably variable; -11, -15, -3.
B 5715	10.1	-18, +6, +7, 0, -20, +40.
B 5717	10.8	Velocity probably variable; -6, -18, 0, -10.
15° 6174	13.3	-24, -29, -21, -4.
14° 4764	13.4	Velocity probably variable; -2, +2, +15, +4.
15° 4620	17.2	Lines are very poor.
A 15881B	20.3	-28, -20, -13, +29.
54° 2756	21.2	IS -3.+3.1 6.
B 5779	22.5	IS -17.6 ± 2.8 2.
51° 3372	23.8	IS - 3.6 ± 0.7 6.
53° 2882	24.5	Lines are poor but velocity is probably variable; +21, +3, -24, -19, +13, -18.
B 5804	27.4	Large difference, M-W; velocity probably variable; five late Coude plates give V = -0.6 ± 0.3; IS -12.8 ± 1.9 7.
B 5812	29.0	+1, +16, -6, +5.
B 5821	31.7	Announced binary, MWC N° 593.
A 16095A	33.6	IS -14.0 ± 1.3 7.
A 16095B	33.6	IS -14.0 ± 0.7 5.
A 16111AB	34.9	-14, -16, +7, -25.
G 31608	36.4	+14, -11, +19, -5, +10, +8.
B 5844	37.1	IS -13.6 ±0.6 4.
54° 2836	38.8	Velocity Is variable; lines are double on two plates.
G 31739	42.3	Velocity probably variable; -49, -35, -47, -35.
B 5879	45.1	+9, +12, +24, +28, 0.
B 5918	54.9	IS -11.6 ± 0.5 5.
o And	59.6	IS -12.2 ± 0.2 3.
B 5946	23 02.7	-26, -30, -8, -30.
G 32430	15.3	Velocity probably variable: - 8, 0, -20, -11.
B 6050	29.1	+22, -2, -46, -20, -17.
G 32872	37.2	-6, -1, +13, +12.
B 6083	39.2	Velocity probably variable; -11, -6, +8, +1.
A 17022A	46.4	IS -32.3 ± 1.3 8.
A 17022B	46.4	IS -34. ± 3.4 2.
B 6128	50.1	Velocity probably variable; +20, +21, 0, +8, -3, -19, -9.
G 33149	51.3	IS -33.7 ± 1.7 5.
60° 2637	51.6	IS -29.8 ± 0.6 4.
G 33163	52.2	IS -25.3 ± 1.3 7.
47° 4331	54.8	Velocity probably variable; +21, -4, -16, +11, -1.
58° 2676	55.2	IS -17.0 ± 2.2 4.
G 33252	56.2	IS -14.5 ± 0.7 2.
σ Cas	56.5	IS -12.8 ± 2.8 4.
A 171408	56.5	+5, -19, -9, +2; lines are double on first plate and suspected on the third.
59° 2813	59.1	IS -8.4 ± 0.4 3.

December, 1949.

AN ATLAS OF SPECTRA OF SIX STARS OF CLASSES R AND N

ROSCOE F. SANFORD
Mount Wilson and Palomar Observatories
Received November 17, 1949

ABSTRACT

Coudé spectra of two class R and four class N stars are reproduced in Figures 1–16. The shortward limits vary from λ 3600 for the bluest of the six stars to λ 5800 for the reddest. The longward limit for four of them is λ 8800.

Estimates of the intensities of prominent molecular band heads and of strong atomic lines have been made (Tables 3 and 6). Atomic-line intensities indicate a decreasing stellar temperature sequence that does not correspond to a sequence of increasing redness. This lack of correspondence, which probably results from some widespread absorption in the photographic region, varies from star to star but not linearly with temperature. Differences in the abundances of elements such as *Na* I, *Li* I, and *K* I relative to other elements are suggested by the run of the intensities of their lines.

The blue *CN* bands are found to be closely correlated with the red bands when the intensity of the blue *CN* bands is obtained from the 0, 2 band head at λ 4606 instead of from the 0, 1 head at λ 4216, which is interfered with by veiling from absorption shortward from λ 4382.

Large stellar velocities separate the stellar from the interstellar D lines in 4 stars (Fig. 16).

Spectrograms of much higher dispersion than hitherto possible can now be obtained with the 100-inch telescope and its coudé plane-grating spectrograph. This gain in dispersion is possible not only because of the greater light-gathering power of the aluminized 100-inch mirror, the improved spectrograph optics, and the efficient grating but also because of the greater speed of photographic plates for all spectral regions, especially for the visual and the near infrared.

The spectra of stars of classes R and N are now obtainable with dispersions of 10 A/mm in the photographic region and 20 A/mm in the visual and infrared regions with exposures no longer than were formerly necessary with very much lower dispersion. These new spectrograms provide an opportunity to study these stars in much greater detail than hitherto not only because of the greater resolution provided by the higher dispersion but also because of the greater wave-length range.

Since I shall not be able to study this material in great detail in the near future, it seems desirable to publish reproductions of spectrograms of some typical stars sufficiently enlarged for easy inspection and even moderately accurate measurement.

Spectra of six stars of classes R and N are reproduced in Figures 1–16. Table 1 gives the relevant data. The spectrograms of U Cyg, it should be noted, were near the phase of light-minimum. The photographic plates that my experience showed to be most suitable for stars of classes R and N are the following Eastman Kodak emulsions: II*a*-O, for the photographic region; 103*a*-D for λλ 5000–6200; 103*a*-E for λλ 6200–6600 (especially fast at *Hα*); 103*a*-F for λλ 6200–6800 (for uniform density); and I-N and IV-N hypersensitized with ammonia for λλ 6600–8800. The Eastman C emulsions, also hypersensitized with ammonia, were often used for the visual region before the 103*a*-D, 103*a*-E, and 103*a*-F emulsions became available. The last two columns in Table 1 show the exposure times and emulsions of the various spectrograms of the six stars. Although these spectrograms have not been studied exhaustively, some comments may be made upon prominent molecular bands and atomic lines.

MOLECULAR BANDS

The band heads listed in Table 2 appear upon at least some of the spectra in Figures 1–16. In order to make the identifications of the band heads of $C^{12}C^{12}$, $C^{12}C^{13}$, and $C^{13}C^{13}$

more convincing, positives of emission spectra obtained in the laboratory have been inserted between the strips for HD 156074 and HD 52432 at the Swan band sequences 1, 0; 0, 1; and 0, 2. The laboratory spectra were obtained by passing a high-voltage current through a vacuum tube which contained a mixture of C^{12} and C^{13} in the approximate ratio 2:1. This tube was prepared by Professor W. R. Smythe, of the physics department of the California Institute of Technology. His permission to use it is hereby gratefully acknowledged. The juxtaposition of laboratory spectrum and that of HD 52432 gives convincing evidence of the high ratio $C^{13}:C^{12}$ for HD 52432. This ratio was found by A. McKellar[1] to be 1:3 for HD 156074 instead of 1:90, as in terrestrial samples. The

TABLE 1

STELLAR SPECTROGRAMS IN FIGURES 1–16

Star	m_p	C.I.* (Mag.)	Spect. Class†			Figure	Coudé Plate No.	Date	Exposure (Minutes)	Emul.
			HD	Shane	KM					
HD 156074	7.3	1.4	R0	R1	$C1_2$	1– 6	3006	1943 Apr. 18	200	IIa-O
						7	5111‡	1948 Feb. 29	67	103a-D
						7– 9	5219‡	1948 June 23	(365)	103a-D
						10	1943‡	1939 Mar. 7	122	II-E+§
						11–15	5289‡	1948 Aug. 19	200	I-N+
HD 52432	7.5	1.7	R5	.....	$C4_4$	3– 6	3350	1944 Jan. 13	219	IIa-O
						7– 8	5057‡	1948 Jan. 19	120	103a-D
						9	4967	1947 Nov. 24	245	103a-D
						10–14	3350	1944 Jan. 13	219	IV-N+
HD 223075	5.3	2.8	Na	N0	$C6_2$	2– 3	3236	1943 Oct. 12	181	IIa-O
19 Psc						4– 6	3230	1943 Oct. 11	75	IIa-O
						7– 8	4964	1947 Nov. 3	10	103a-D
						9–10	2444‖	1940 Oct. 6	(90)	103-C+
						10–16	2857‖	1942 Sept. 22	210	IV-N+
HD 92055	4.5– 6.3	3.5±	Nb	N2	$C7_3$	3– 6	3005	1943 Apr. 17	193	IIa-O
U Hya						7– 8	2015	1939 May 3	95	1-C+
						9–16	3000	1943 Apr. 17	275	IV-N+
HD 1546	8.1– 9.5	4.6	Pec	N7	$(C4_2)$	5– 7	5405#	1948 Oct. 24	280	103a-D
VX And						7– 8	5337	1948 Sept. 18	(200)	103a-D
						8–10	4969	1947 Nov. 25	150	103a-D
						10–16	3272	1943 Nov. 11	198	IV-N+
HD 193680	6.1–11.8	5.6+	R8	Np	$C9_2$	9–11	3485‡	1944 July 5	170	103a-F
U Cyg (min.)						12–16	5742‡	1949 July 10	260	I-N+
HD 137613	7.4	.....	R0	R3	$C1_3$	16	2016	1939 May 3	182	1-C+
177336	6.5– 8.0	.....	Np	N6	$C6_4$	16	2602	1941 Aug. 12	70	103-E+
189711	8.7	.....	Nb	.....	.....	16	2017	1939 May 3	240	1-C+
209621	8.8	.....	R3	R3	$C3p_3$	16	2862	1942 Sept. 23	167	103-F+

* Color indices of 19 Psc, VX And, and U Cyg are from J. A. Parkhurst, *Ap. J.*, **35**, 132, 1912. Those of HD 52432, U Hya, and HD 156074 depend upon photographic magnitudes estimated on Franklin-Adams charts.

† C. D. Shane, *Pub. Lick Obs.*, **13**, 124, 1928. KM = Keenan and Morgan, *Ap. J.*, **94**, 501, 1941.

‡ Wide slit, no serious loss of detail.

§ The symbol + after an emulsion signifies hypersensitization with NH_3.

‖ Taken with a dispersion of 5.9 A/mm.

Very wide slit for coarse detail only.

[1] *Pub. A.S.P.*, **59**, 186, 1947.

$C^{12}C^{13}$ band λ 4744 can be well seen in the spectrum of HD 156074, where it is very much less striking than in HD 52432, in which, however, McKellar could not compare the $C^{12}C^{13}$ band with the $C^{12}C^{12}$ band on account of their extreme intensities.

Laboratory spectra of *CN* at λ 4216 in Figure 3 and in Figures 10–16 provide direct evidence that the detail in the stellar spectra for these regions is nearly all that of the *CN* spectrum.

Rough eye-estimates for the intensities of C_2 and *CN* band heads have been averaged as in Table 3. The star HD 52432 has the strongest $C^{12}C^{12}$,$C^{12}C^{13}$, and $C^{13}C^{13}$ bands, and 19 Psc has the strongest $C^{12}N^{14}$ bands. The $^2\Sigma \rightarrow {}^2\Sigma$ or blue *CN* 0, 1 bands have already been compared elsewhere[2] with the $^2\Pi \rightarrow {}^2\Sigma$ or red *CN* bands. From this comparison it was concluded that absorption affected the intensities of the blue band heads more

TABLE 2

MOLECULAR BANDS OBSERVED IN STELLAR SPECTRA

No.	$C^{12}C^{12}$	$C^{12}C^{13}$	$C^{13}C^{13}$	No.	$C^{12}N^{14}$	$C^{13}N^{14}$
v′, v″	C_2, $^3\Pi \rightarrow {}^3\Pi$ Transition			v′, v″	*CN*, $^2\Sigma \rightarrow {}^2\Sigma$ Transition	
3, 1	λ 4371			2, 2	λ 3862	
2, 0	4382	λ 4395	λ 4408	1, 1	3871	
6, 5	4669			0, 0	3883	
5, 4	4677			3, 4	4168	
4, 3	4685			2, 3	4181	
3, 2	4698	4706		1, 2	4197	
2, 1	4715	4723	4731	0, 1	4216	λ 4208
1, 0	4735	4744	4752	3, 5	4532	
0, 0	5165			2, 4	4553	
2, 3	5541	5534		1, 3	4578	
1, 2	5586	5577	5568	0, 2	4606	4588
0, 1	5636	5626	5617			
2, 4	6060			*CN*, $^2\Pi \rightarrow {}^2\Sigma$ Transition		
1, 3	6122	6101				
0, 2	6191	6168		4, 0	6206	6260
				3, 0	6954	6999
				2, 0	7874	7951

than it did the red ones and this produced a spurious decrease in the ratios of blue to red bands with advancing spectral type.

This regional absorption, extending shortward from λ 4382, is well seen in the spectrum of U Hya. My estimates for blue *CN* have been confined to the 0, 2 sequence with head at λ 4606 (fourth line, Table 3) in order to avoid this regional absorption. The last two lines of the table then show that the behavior of the blue and red *CN* is similar.

I have been impressed by the absorption shortward from λ 4382, as in the spectrum of U Hya, and the intense absorption shortward from λ 4736 in the much redder class N star, VX And. In U Hya the absorption begins abruptly so near the 2, 0 sequence of $C^{12}C^{12}$ and in VX And so near the 1, 0 sequence as to suggest that this absorption has some intimate relation to the $^3\Pi \rightarrow {}^3\Pi$ bands of C_2 (Swan bands).

A note has already been published[3] on the band heads at λ 4208 and at λ 4588 (Ta-

[2] Swings and King, *Mt. W. Contr.*, No. 700; *Ap. J.*, **101**, 13, 1945; Shajn and Struve, *Ap. J.*, **106**, 91, 1947.

[3] R. F. Sanford, *Pub. A.S.P.*, **52**, 204, 1940.

ble 2) of $C^{13}N^{14}$ and on the band at λ 6260 as possibly produced by that molecule.[4] McKellar[5] has noted that the intense absorption at λ 6260 differs in wave length from the mean position of the R_1 and Q_1 branches of the 4, 0 sequence of red *CN* by about the expected isotopic shift (54 A). Later I found intense molecular absorption at λ 6999 and λ 7951 in stars with a high ratio of C^{13} to C^{12}. Upon receiving this information, McKellar called my attention to the relationships shown in Table 4.

The relationships in Table 4 are the reason for including the $C^{13}N^{14}$ bands of ($^2\Pi \rightarrow {}^2\Sigma$) *CN* in Table 3. It is not clear, however, that in the R and N stars the most intense absorptions of $C^{12}N^{14}$ of this band system are always in the mean position of the R_1 and Q_1 branches, as in the *CN* emission spectrum,[6] and this may be an argument against identifying the bands in the third column of Table 4 with $C^{13}N^{14}$.

TABLE 3

INTENSITY ESTIMATES OF C_2 AND *CN* BANDS

MOLECULE	TRANSITION	STAR*					
		HD 156074	HD 52432	19 Psc	U Hya	VX And	U Cyg
$C^{12}C^{12}$	$^3\Pi \rightarrow {}^3\Pi$	1.5	6.1	5.3	5.4	4.3	3.0
$C^{12}C^{13}$	$^3\Pi \rightarrow {}^3\Pi$	0.3	3.8	2.7	2.0	1.0	.....
$C^{13}C^{13}$	$^3\Pi \rightarrow {}^3\Pi$	0.0	3.0	0.0	0.0	0.0	.....
$C^{12}N^{14}$	$^2\Sigma \rightarrow {}^2\Sigma$	0.8	3.5	4.5	2.0	.....	.....
$C^{12}N^{14}$	$^2\Pi \rightarrow {}^2\Sigma$	0.9	4.4	4.8	4.2	2.2	3.5

* Blank spaces indicate no observations.

TABLE 4

POSSIBLE ISOTOPIC BANDS IN ($^2\Pi \rightarrow {}^2\Sigma$) *CN*

v', v''	$C^{12}N^{14}(R_1+Q_1)/2$	$C^{13}N^{14}$	Δ	Isotopic Δ
4, 0	λ 6210	λ 6260	50 A	54 A
3, 0	6950	6999	49	51
2, 0	7907	7951	44	44

Besides C_2 and *CN* bands, the 0, 0 band of *CH*, λ 4315, is present in the spectra of HD 156074, HD 52432, 19 Psc, and U Hya with their intensities estimated to be in the ratio 5:4:2:1. These values may, however, be more or less influenced by veiling.

U Cyg has the P_1, P_2, Q_1, and Q_2 branches of the 0, 0 band of *CaCl*. The Q_2 branch, λ 6185, is the strongest and seems to be present in HD 52432, 19 Psc, U Hya, and VX And, as well as in U Cyg, with the strength estimated to be in the ratio 1:1:2:2:5.

The three band heads λλ 4867, 4905, and 4977 (degraded to the red) announced by P. W. Merrill and by Sanford[7] are well shown in the spectrum of VX And. Of three band heads discovered by C. D. Shane,[8] only the one of longest wave length, λ 4640, has enough background of continuous spectrum to be seen in the spectrum of VX And. None

[4] R. F. Sanford, *Pub. A.S.P.*, **53**, 255, 1941.

[5] *Pub. A.S.P.*, **61**, 34, 1949.

[6] Herzberg and Phillips, *Ap. J.*, **108**, 163, 1948.

[7] *Pub. A.S.P.*, **38**, 175 and 177, 1926.

[8] *Lick Obs. Bull.*, **13**, 127, 1928.

of these four band heads has been definitely identified with any molecule, although general suggestions are given in a discussion by A. McKellar.[9]

In rich stellar spectra like those of spectral classes R and N, only those bands with very pronounced heads are easily recognized. Hence it is to be expected that bands of other molecules will be identified when careful search is made either by detailed measures or, better, by direct comparison with laboratory spectra. Either process will require care and patience.

The close correspondence between stellar and laboratory *CN* in the figures is, of course, much interfered with by the atmospheric bands B, a, and A, and to some extent by atmospheric lines in the region from λ 7800 to λ 8300.

ATOMIC ABSORPTION LINES

W. C. Rufus[10] has identified absorption lines of the following elements in the spectra of class R stars: *H*, *Mg*, *Ca*, *Ti*, *V*, *Cr*, *Fe*, and *Ni*. C. D. Shane[11] listed the lines of the following elements for spectral class N: *Na*, *Ca*, *Sc*, *V*, *Cr*, *Ti*, *Mn*, *Fe*, *Zr*, *Cd*, *Ba*, and *La*. McKellar[12] has found the lines of *Li* very strong in the spectrum of the very red star W Cas; and I have found them in the spectrum of WX Cyg near its light-minimum (see Fig. 11). Lines of *Li* I of moderate strength seem to me to be present in the spectra of all the stars in the *Atlas* except HD 156074. Besides the elements already mentioned, I would add *Al* I, *K* I, *Sr* I, *Sr* II, and *La* II for both classes R and N, and *Mg* I, *Rb* I, and *Cs* I for class N. I would question the presence of *Ni* listed by Rufus and of *Cd* by Shane. But it is highly probable that careful scrutiny of these spectrograms will reveal the lines of still other elements.

The three systems of spectral classification given in Table 1 arrange the six stars in about the same order, which is also the order of increasing redness or color index and presumably of decreasing temperature. But the classifications of both the *Henry Draper Catalogue* and of C. D. Shane are to some extent dependent upon the intensity of one spectral region relative to that of another region, a relationship that could be greatly affected by molecular bands, as well as by the effective temperature of the source. The classification of Keenan and Morgan depends, in part at least, upon the strength of atomic lines and therefore perhaps approaches more nearly a temperature sequence.

The spectrograms in Figures 1–16 have so much greater dispersion than those hitherto used for classification that they should provide a much better approximation to a true temperature sequence. At the same time, they reveal more clearly the difficulties that may arise from blending of atomic lines with band lines. Furthermore, worth-while estimates of equivalent widths cannot be made in regions that are affected by veiling any more than on spectrograms of low dispersion.

Estimates of the equivalent widths of certain of the strong atomic lines have been attempted with the foregoing considerations in mind. Measurement by microphotometer tracings becomes very difficult in class R and N stars, whose spectra are much cut up by heavy absorption. Hence it was decided to depend upon eye-estimates referred to a sequence of spectral lines of the desired range of intensity chosen from the spectra in the *Atlas*. Approximate values of their equivalent widths were obtained from microphotometer tracings and are given in Table 5. Appropriate factors convert estimates by means of these standards into equivalent widths for dispersions other than 10 A/mm.

It is recognized that these equivalent widths in Table 5 are rough approximations and that their use as standards for other lines on plates of quite different characteristics and processing is beset with uncertainties. It is hoped, however, that, in spite of these difficulties, estimates of equivalent width may still be obtained that are relatively dependable for the same line throughout the stellar sequence, even though the values of

[9] *Pub. A.S.P.*, **58**, 240, 1946.

[10] *Pub. U. Michigan Obs.*, **2**, 103, 1915.

[11] *Lick Obs. Bull.*, **10**, 79, 1920.

[12] *Pub. A.S.P.*, **52**, 407, 1940.

the estimated equivalent width of one line cannot with safety be compared directly with those of another line in the same spectrum, especially if it is in quite a different spectral region.

Table 6 gives the equivalent widths of lines estimated by means of the lines in Table 5. When blending seemed to interfere with a line, other lines in its multiplet served to establish the equivalent width. For *Na* I the equivalent width is for the sum of D2 and D1, since they could not be separated in the spectrum of U Cyg. The estimates are rough for all but HD 156074 and U Cyg. For HD 156074 the equivalent width was derived from a comparison with the solar D lines on a moon spectrum by assuming their combined equivalent widths to be 1.3 A.[13] The equivalent width of (D2 + D1) for U Cyg was measured from a microphotometer tracing of Ce 5742.

Table 6 shows that the ground-state lines of the neutral atoms increase in strength, on the average, from HD 156074 through HD 52432 to 19 Psc, have about the same equivalent widths in U Hya as in 19 Psc, become definitely weaker in VX And, and then again in U Cyg recover or exceed their strength in 19 Psc.

TABLE 5

EQUIVALENT WIDTHS OF INTENSITY STANDARDS (DISPERSION 10 A/MM)

No.	λ	Element	Star	Plate Ce	E.W. (A)
1	4406.641	*V* I	HD 156074	3006	0.1
2	4407.637	*V* I	HD 156074	3006	0.2
3	4408.204	*V* I	HD 156074	3006	0.3
4	4427.312	*Fe* I	HD 156074	3006	0.4
5	4415.125	*Fe* I	HD 156074	3006	0.5
6	4404.752	*Fe* I	HD 156074	3006	0.7
7	4404.752	*Fe* I	HD 52432	3350	1.1
8	4454.033	*Ba* II	19 Psc	3230	1.7

The equivalent widths for the neutral atomic lines of the higher states of excitation show, on the average, a less pronounced increase but one in the same order as the ground-state lines. Unfortunately, the equivalent widths of only two lines of this kind were obtained for U Cyg. The one line, *Hα*, λ 6562.8, with 10.2 volts for its lower excitation potential, quite naturally does not show in a star as cool as U Cyg. The other line, *La* I λ 6249.92, on the other hand, appears only in U Cyg. However, the lower E.P. of this line is only 0.5 volts.

The average equivalent widths of lines of the ionized atoms increase in a manner similar to the average for the equivalent widths of the neutral lines of the higher states of excitation. The equivalent widths of the three kinds of lines in Table 6 would, on the average, be in smoother sequences if the six stars were arranged in the order HD 156074, HD 52432, VX And, U Hya, 19 Psc, and U Cyg. Ground-state lines of the neutral atom would then increase in equivalent width fairly consistently, and neutral lines of higher-excitation potentials and the lines from ionized atoms would give an increase through the first five stars and a decrease thereafter.

If this revised sequence of the six stars really represents a sequence of decreasing surface temperature, it would seem that some kind of absorption takes place in the photographic region and that this absorption does not increase linearly with declining temperature. This would explain why the color indices do not increase progressively in the suggested new order for the six stars.

In addition to the tendency for all lines in Table 6 to strengthen in the order just de-

[13] Merrill, Sanford, Wilson, and Burwell, *Mt. W. Contr.*, No. 576; *Ap. J.*, **86**, 279, 1937.

scribed, it should be noted that in U Cyg the lines of *Na* I and *K* I are markedly stronger than those of the other five stars; this is not true of the *Li* I doublet. Four stars which have strong *Na* I lines and equivalent widths of the *Li* I and *K* I lines, either estimated or measured, are collected in Table 7. They include a nonvariable, BD +38°955, an irregular variable WZ Cas, and two periodic variables, WX Cyg and U Cyg. The stars are listed in the order of increasing equivalent width of the *Na* I lines. It is evident that the equiva-

TABLE 6

ESTIMATED EQUIVALENT WIDTHS OF LINES IN SPECTRA OF CLASSES R AND N

ELEMENT	λ	MULT. NO.	LOW E.P.	EQUIVALENT WIDTH (IN Å)					
				HD 156074 C1₂	HD 52432 C6₄	19 Psc C6₂	U Hya C7₂	VX And C4₂	U Cyg C9₂
	Neutral Lines from the Ground Level								
Li I	6707.815	1	0.0	0.0	0.6	0.8	0.6	0.6	0.8
Na I	D lines	1	0.0	3.0	5.0	15.0	15.0	4.0	65.0
Mg I	4571.096	1	0.0	0.2	0.3	0.5	0.3	.....	.....
K I	7698.979	1	0.0	0.4	0.4	1.0	0.8	0.8	6.4
Ca I	6572.781	1	0.0	0.2	0.6	0.8	1.0	0.4	0.6
Sc I	6305.671	1	0.0	0.0	0.6	0.8	1.0	0.6	1.0
V I	4881.554	3	0.1	0.3	0.4	0.7	0.7	.....	.....
Cr I	4254.346	1	0.0	0.3	0.7	0.7	0.5	.....	.....
Fe I	4427.312	2	0.0	0.4	0.7	0.7	0.4	.....	.....
Rb I	7800.227	1	0.0	0.0	0.0	0.8	1.0	0.2	0.4
Sr I	4607.331	2	0.0	0.1	0.2	0.4	0.4	.....	.....
Y I	6687.57	1	0.0	0.2	0.4	1.4	1.4	0.4	1.4
Zr I	6762.36	1	0.0	0.0	0.4	0.8	0.6	0.2	0.6
Zr I	6134.58	2	0.0	0.0	0.0	0.2	0.4	0.0	0.4
	Neutral Lines from Higher Levels								
H I	6562.817	1	10.2	2.2	0.8	0.0	0.0	0.0	0.0
Mg I	5183.604	2	2.7	2.2	0.6	1.0	0.6	0.4	.....
Sc I	5671.805	12	1.4	0.2	0.4	0.4	0.4	0.8	.....
Ti I	4533.238	42	0.8	0.3	0.1	0.2	0.1	.....	.....
Cr I	5208.436	7	0.9	0.6	0.6	1.4	0.8	0.4	.....
Fe I	4957.603	318	2.8	0.7	(0.5)	0.5	0.3	0.1	.....
Fe I	5232.946	383	2.9	0.6	0.4	0.4	0.4	.....	.....
Zr I	4739.48	43	0.7	0.1	0.3	0.4	0.3	0.1	.....
La I	6249.92	7	0.5	0.0	0.0	0.0	0.0	0.0	1.4
	Ionized Lines								
Ca II	8542.089	2	1.7	0.3	.....	1.7	1.4	0.8	0.8
Sc II	4246.829	7	0.3	0.2	0.3	0.2	0.1	.....	.....
Ti II	4468.493	31	1.1	0.2	0.3	0.4	0.3	.....	.....
Ba II	4934.086	1	0.0	0.4	0.5	1.7	0.5	0.1	.....
Ba II	6141.718	2	0.7	0.2	0.0	0.9	0.1	0.0	0.0
La II	4899.92	7	0.0	0.2	0.3	0.4	0.3	0.0	.....

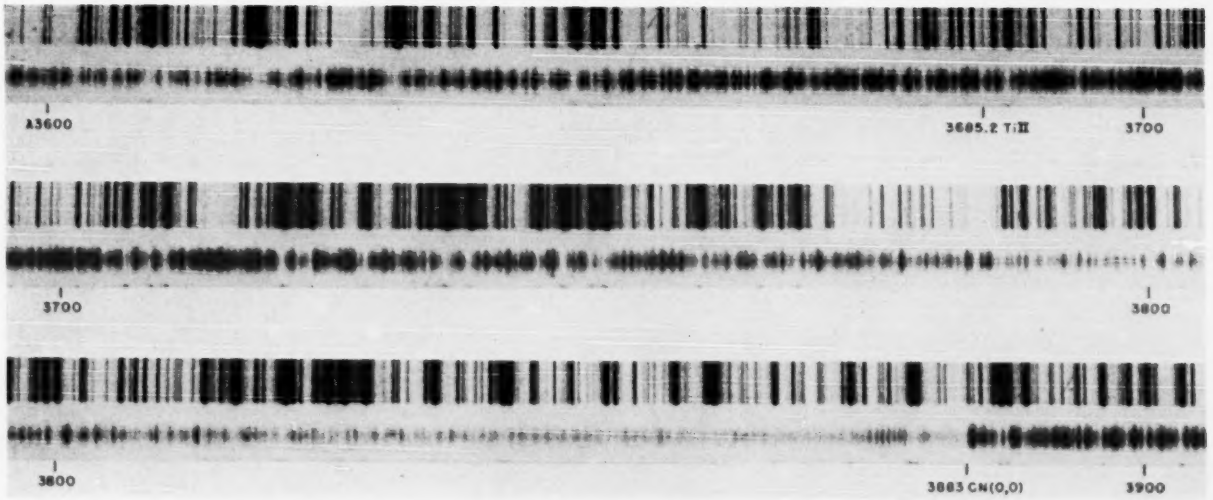

FIG. 1.—The spectrum of HD 156074, type $C1_2$. Iron comparison spectrum, λλ 3600–3900

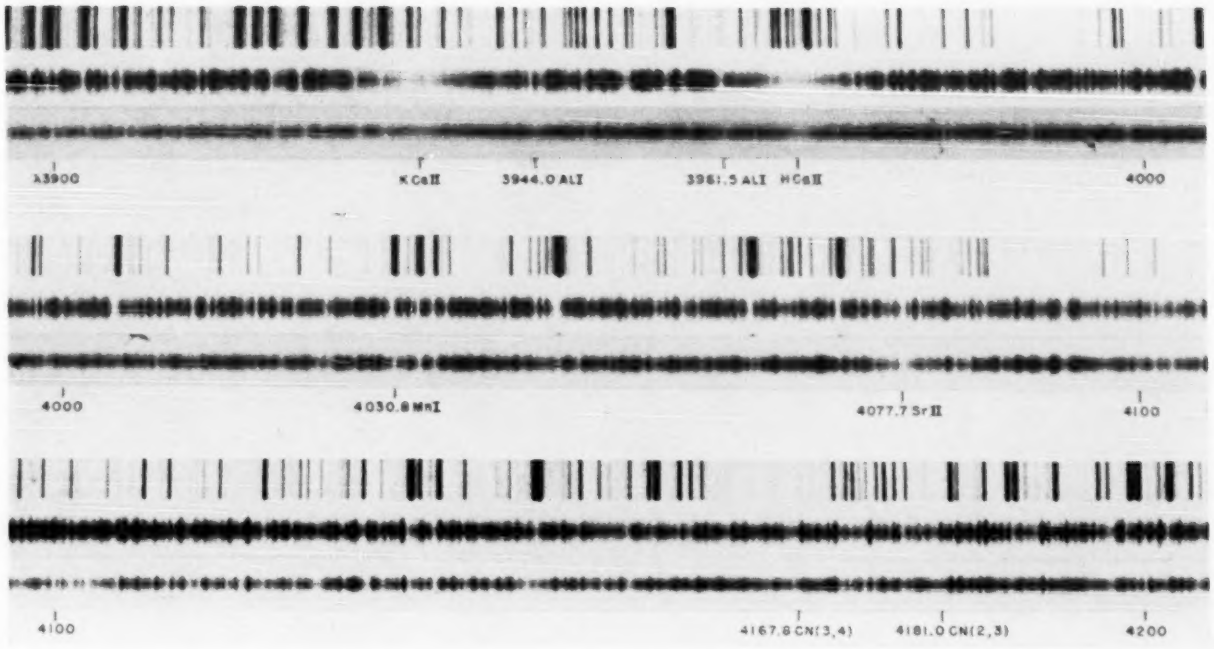

FIG. 2.—Spectra of HD 156074, type $C1_2$ (upper star spectrum in each section), and 19 Piscium, $C6_2$. λλ 3900–4200

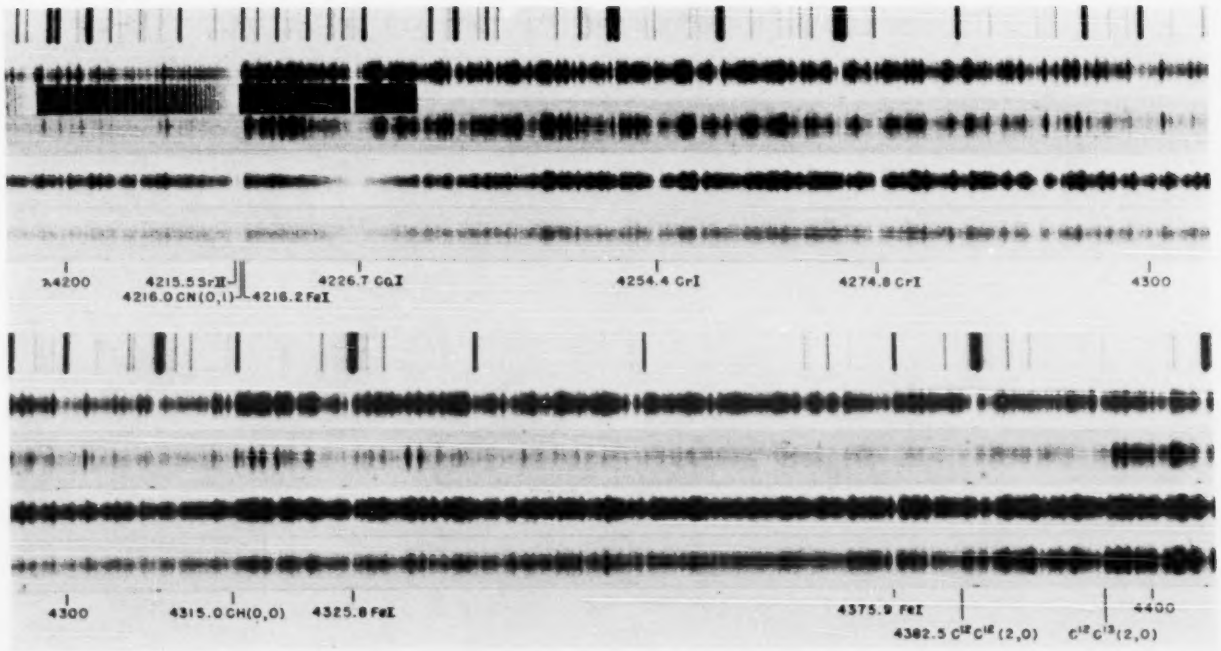

FIG. 3.—Spectra of R- and N-type stars. λλ 4200–4400. Top to bottom in each section: HD 156074, type $C1_2$; HD 52432, $C4_4$; 19 Piscium, $C6_5$; U Hydrae, $C7_3$. In upper left-hand corner, the carbon-arc spectrum, showing the 0, 1 band of *CN*, is placed between the spectra of HD 156074 and HD 52432.

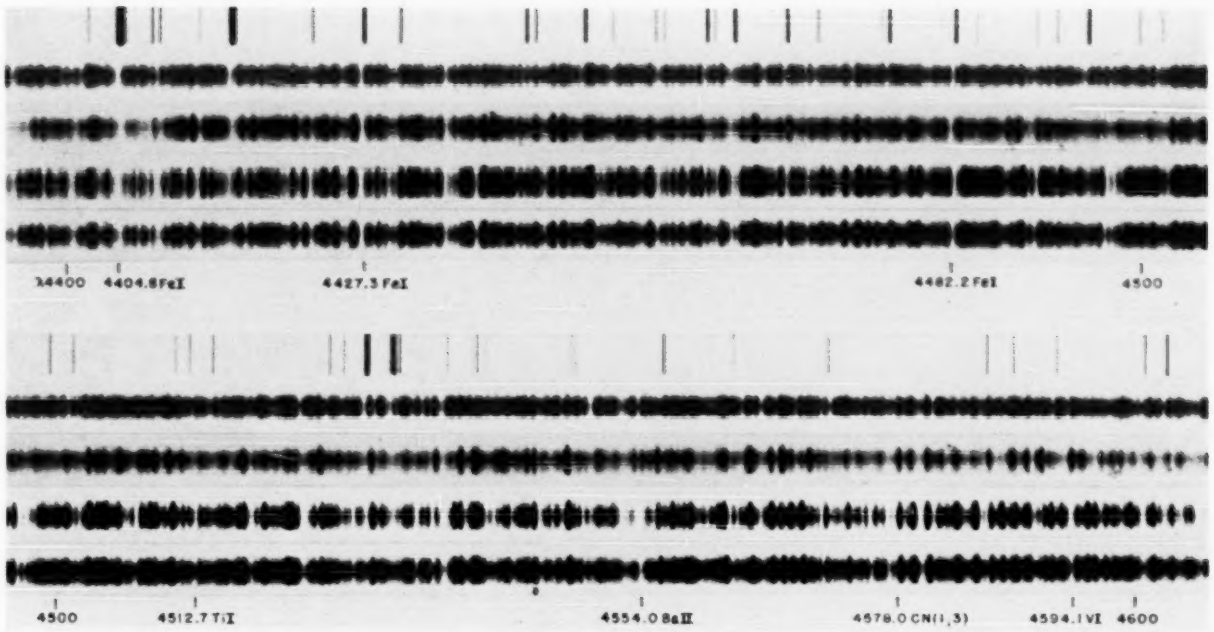

FIG. 4.—Spectra of R- and N-type stars, λλ 4400–4600. Top to bottom in each section: HD 156074, HD 52432, 19 Piscium, U Hydrae

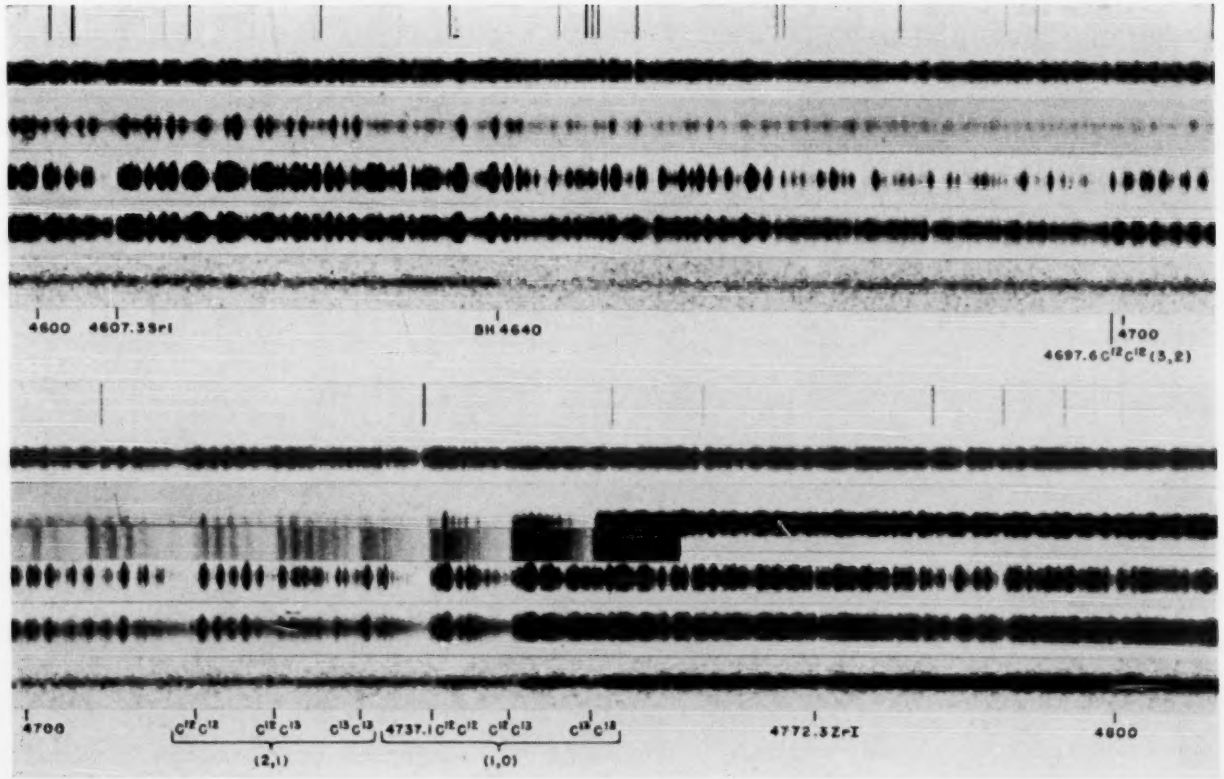

FIG. 5.—Spectra of R- and N-type stars. λλ 4600–4800. Top to bottom in each section: HD 156074, type $C1_2$; HD 52432, $C4_4$; 19 Piscium, $C6_2$; U Hydrae, $C7_3$; VX Andromedae, $C4_2$. In the lower section, a positive copy of a laboratory emission spectrum showing the 1, 0 bands of $C^{12}C^{12}$, $C^{12}C^{13}$, $C^{13}C^{13}$, is placed between the spectrum of HD 52432 and that of 19 Piscium.

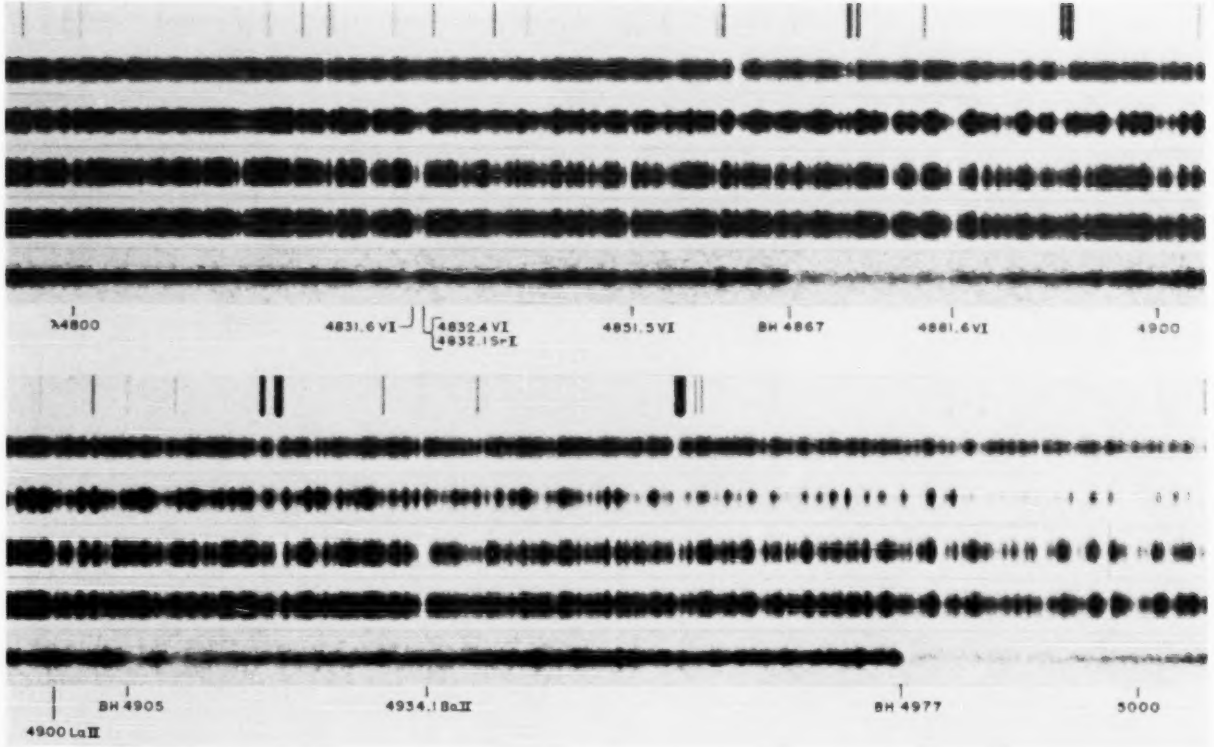

FIG. 6.—Spectra of R- and N-type stars. λλ 4800–5000. Top to bottom in each section: HD 156074, HD 52432, 19 Piscium, U Hydrae, VX Andromedae.

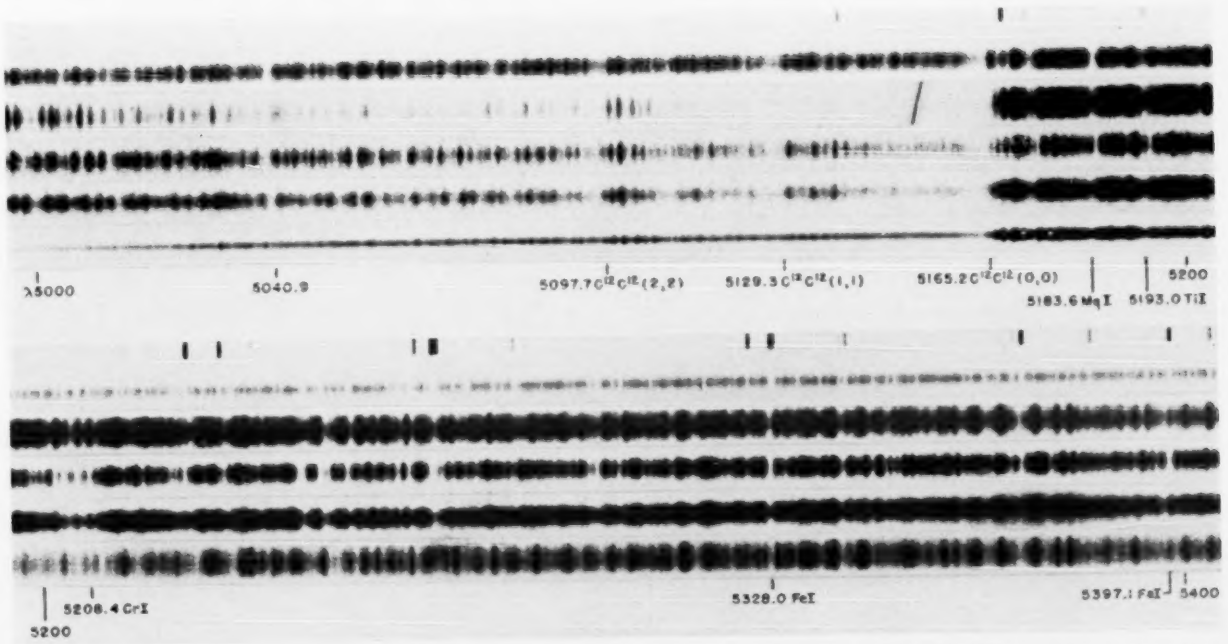

FIG. 7.—Spectra of R- and N-type stars. λλ 5000-5400. Top to bottom in each section: HD 156074, HD 52432, 19 Piscium, U Hydrae, VX Andromedae.

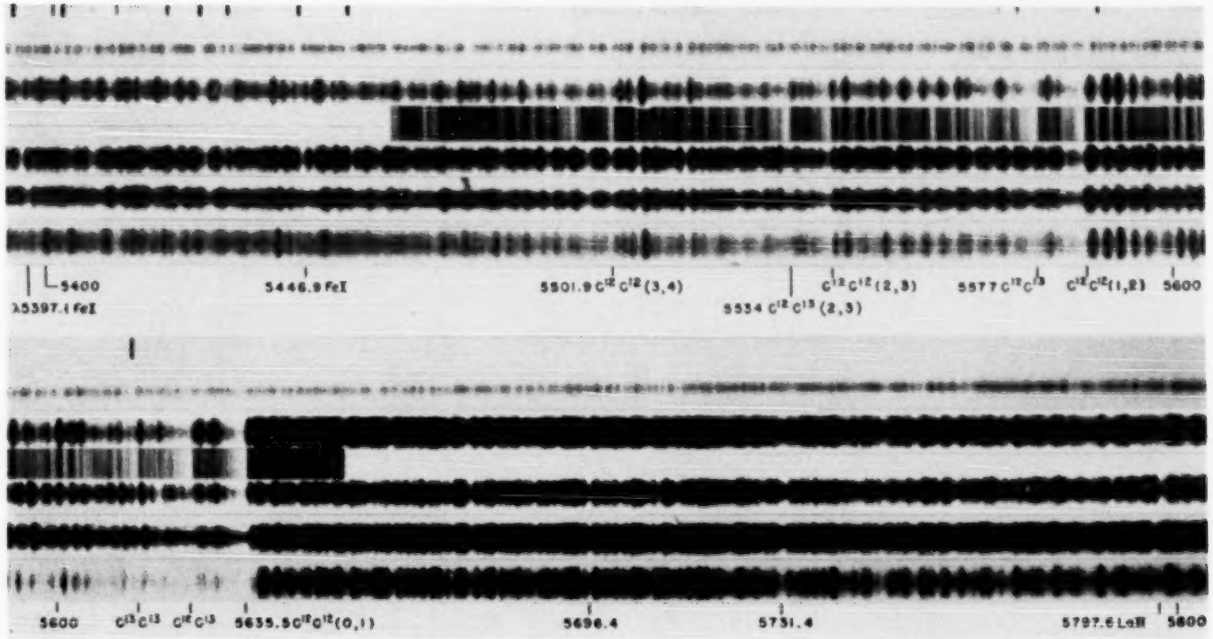

FIG. 8.—Spectra of R- and N-type stars. λλ 5400–5800. Top to bottom in each section: HD 156074, HD 52432, 19 Piscium, U Hydrae, VX Andromedae. The laboratory spectrum of the 0, 1 bands of $C^{12}C^{12}$, $C^{12}C^{13}$, and $C^{13}C^{13}$ is placed between the spectrum of HD 52432 and that of 19 Piscium.

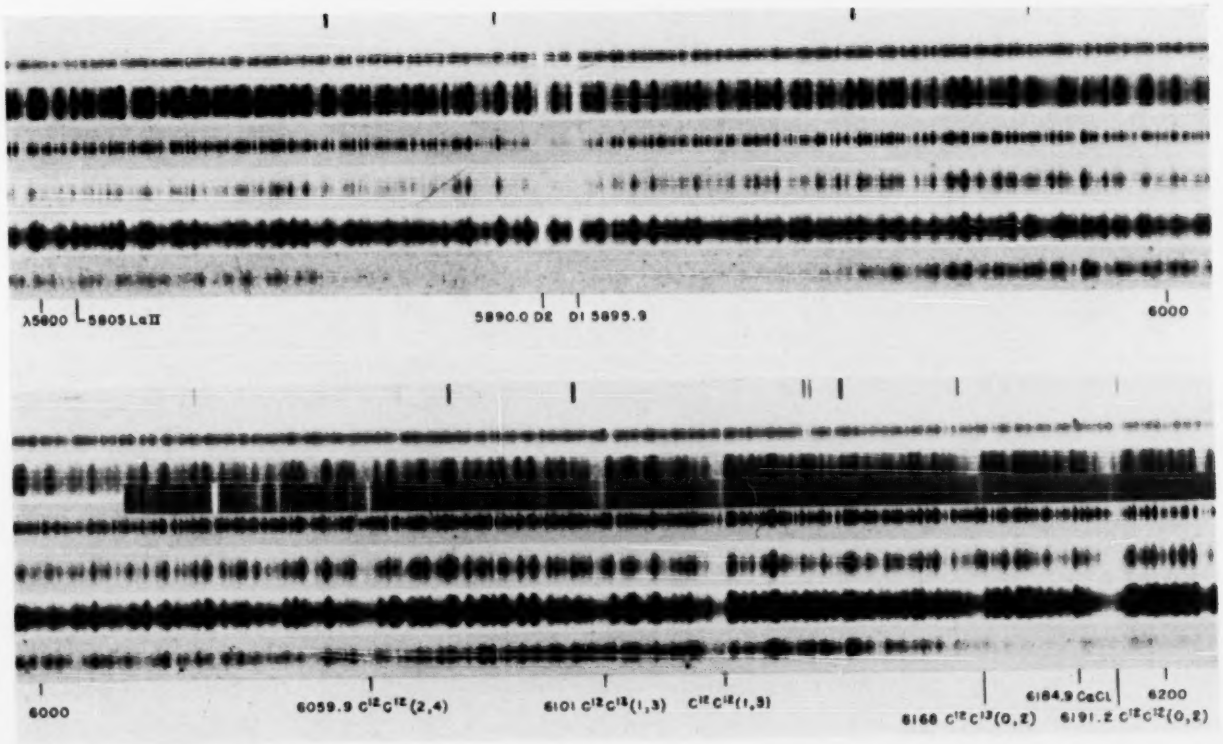

FIG. 9.—Spectra of R- and N-type stars. λλ 5800–6200. Top to bottom in each section: HD 156074, type $C1_2$; HD 52432, $C4_4$; 19 Piscium, $C6_2$; U Hydrae, $C7_2$; VX Andromedae, $C4_2$; U Cygni, $C9_2$. In the lower section the laboratory spectrum of the 0, 2 bands of $C^{12}C^{12}$ and $C^{12}C^{13}$ is placed between the spectrum of HD 52432 and that of 19 Piscium. Neon comparison spectrum.

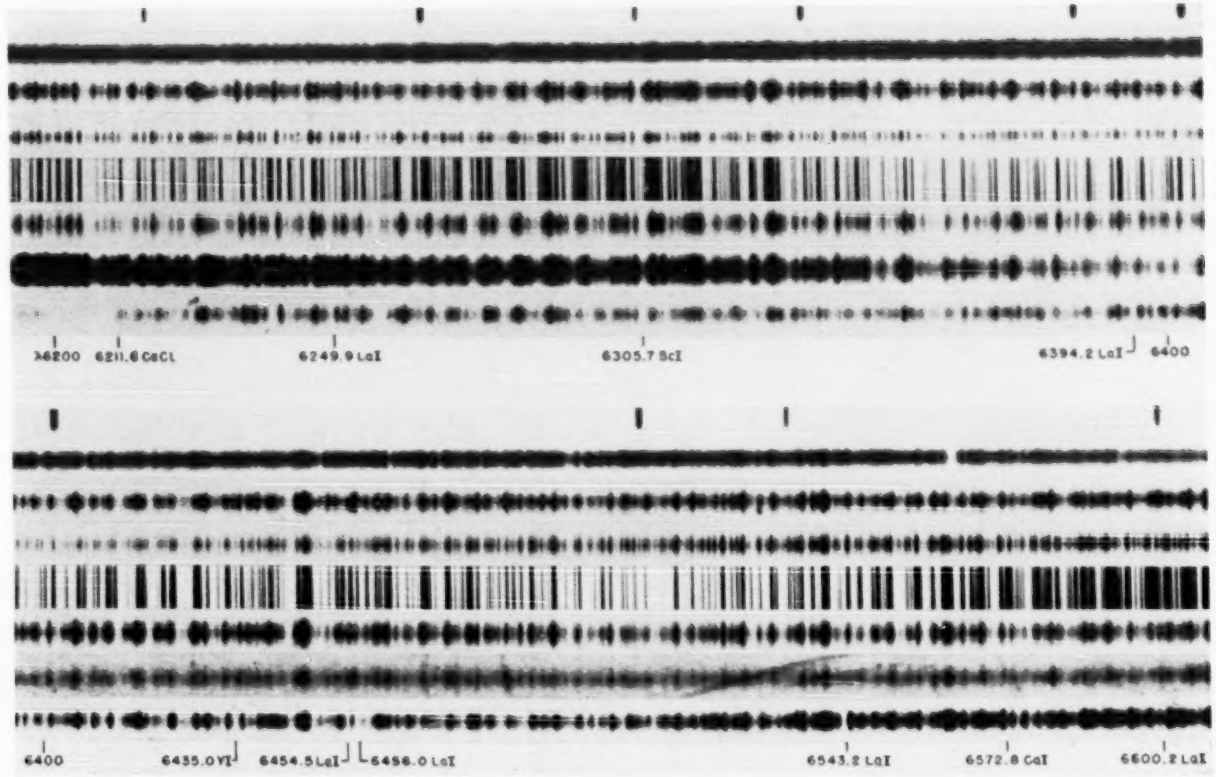

FIG. 10.—Spectra of R- and N-type stars. λλ 6200–6600. Top to bottom in each section: HD 156074, HD 52432, 19 Piscium, laboratory spectrum of *CN*, U Hydrae, VX Andromedae, U Cygni, Neon comparison spectrum.

FIG. 11.—Spectra of R- and N-type stars. λλ 6600–7000. Top to bottom in each section: HD 156074, HD 52432, 19 Piscium, laboratory spectrum of *CN*, U Hydrae, VX Andromedae, U Cygni. Neon comparison spectrum. At the bottom of the upper section is added a small portion of the spectrum of WX Cygni, type $C9_2$, near minimum light, showing the very strong line *Li* I, λ 6708.

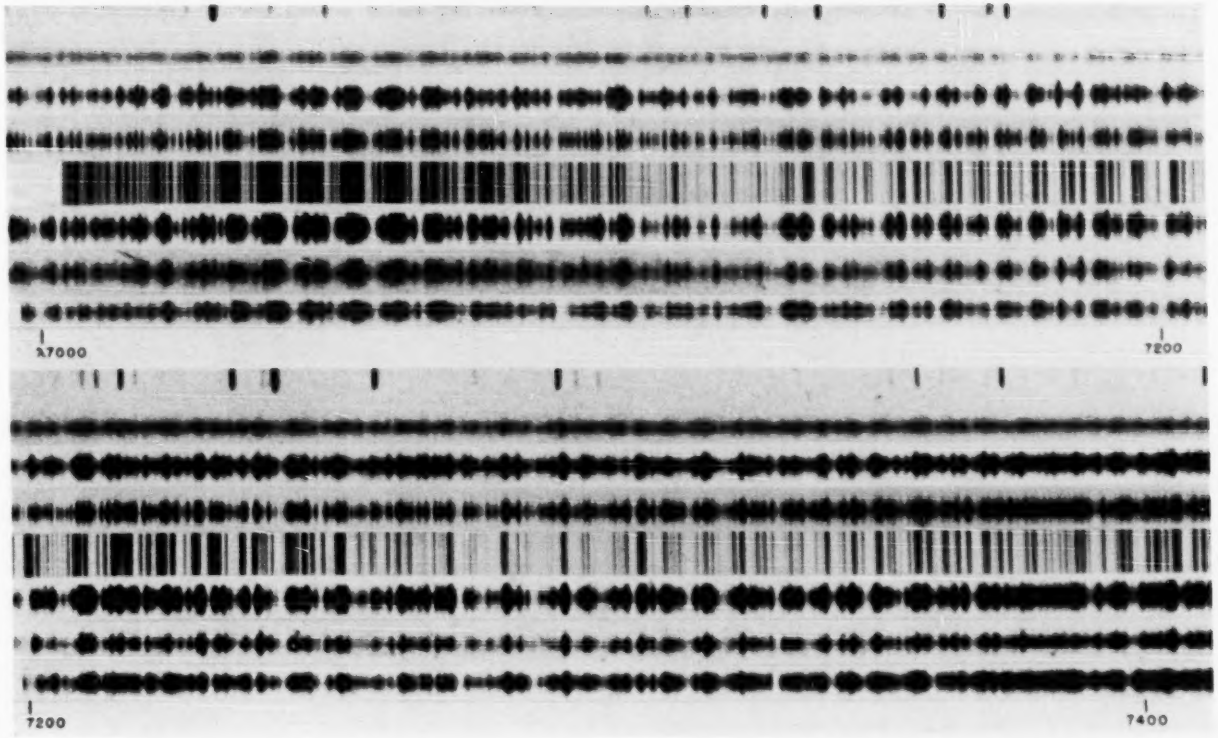

FIG. 12.—Spectra of R- and N-type stars, λλ 7000–7400. Top to bottom in each section: HD 156074, HD 52432, 19 Piscium, laboratory spectrum of CN, U Hydrae, VX Andromedae, U Cygni. Second-order iron comparison spectrum.

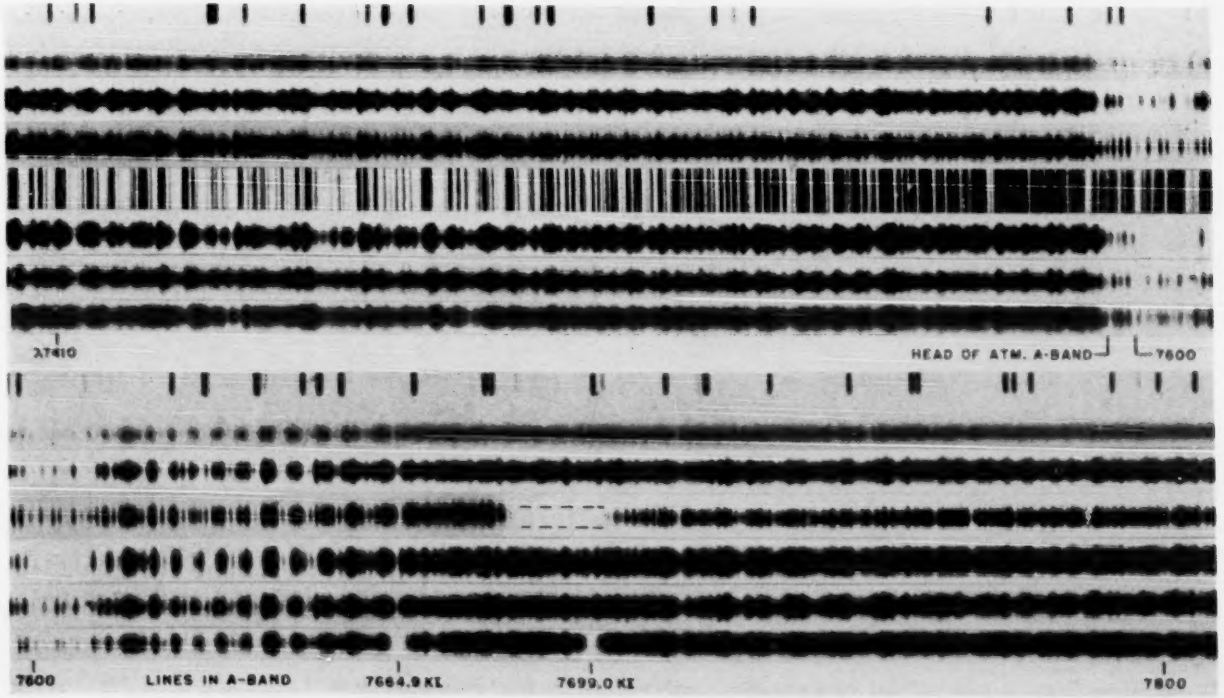

FIG. 13.—Spectra of R- and N-type stars. λλ 7400–7800. Top to bottom in each section: HD 156074, HD 52432, 19 Piscium, laboratory spectrum of *CN* (upper section only), U Hydrae, VX Andromedae, U Cygni. Second-order iron comparison spectrum.

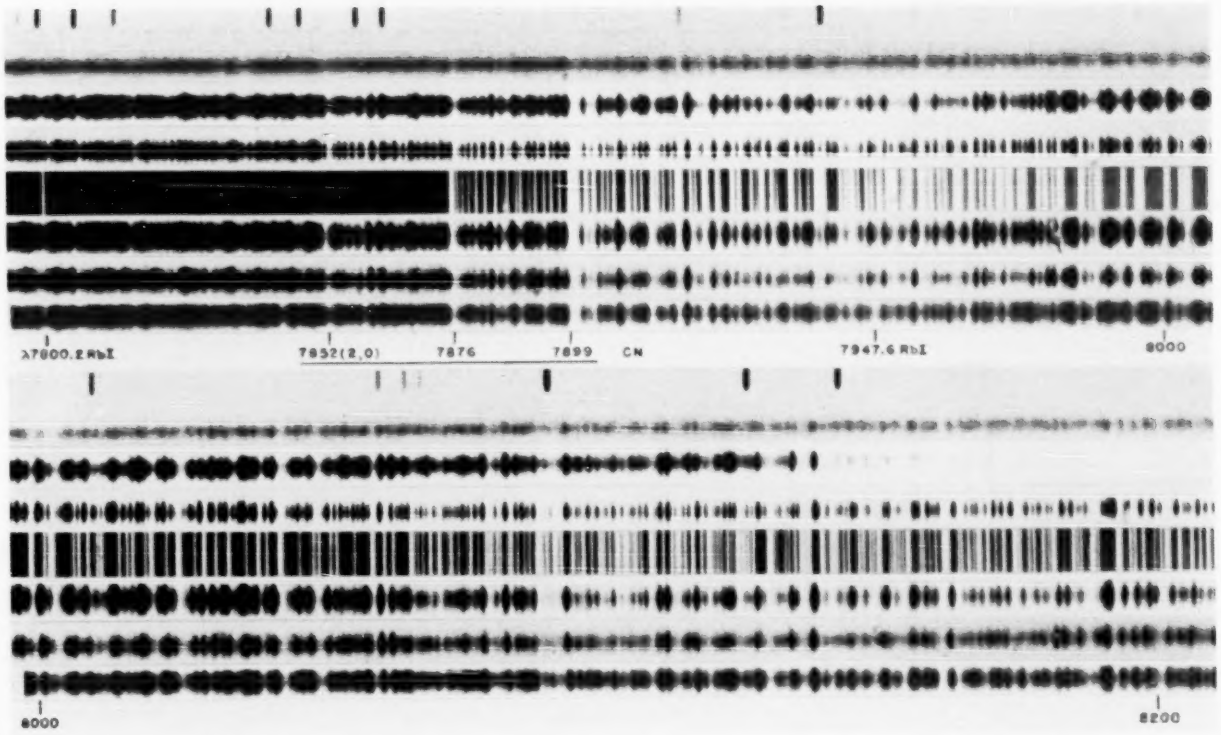

FIG. 14.—Spectra of R- and N-type stars, λλ 7800–8200. Top to bottom in each section: HD 150074, HD 52432, 19 Piscium, laboratory spectrum of *CN*, U Hydrae, VX Andromedae, U Cygni. Second-order iron comparison spectrum.

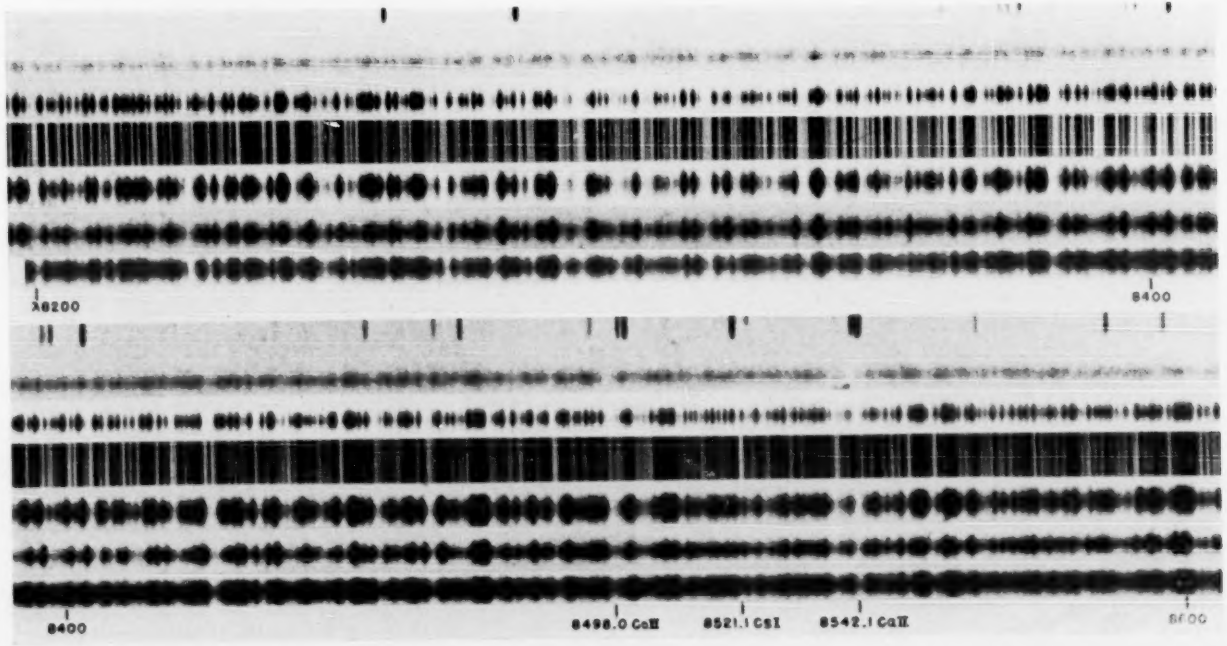

FIG. 15.—Spectra of R- and N-type stars, λλ8200–8600. Top to bottom in each section: HD 156074, 19 Piscium, laboratory spectrum of *CN*, U Hydrae, VX Andromedae, U Cygni, Second-order iron comparison spectrum.

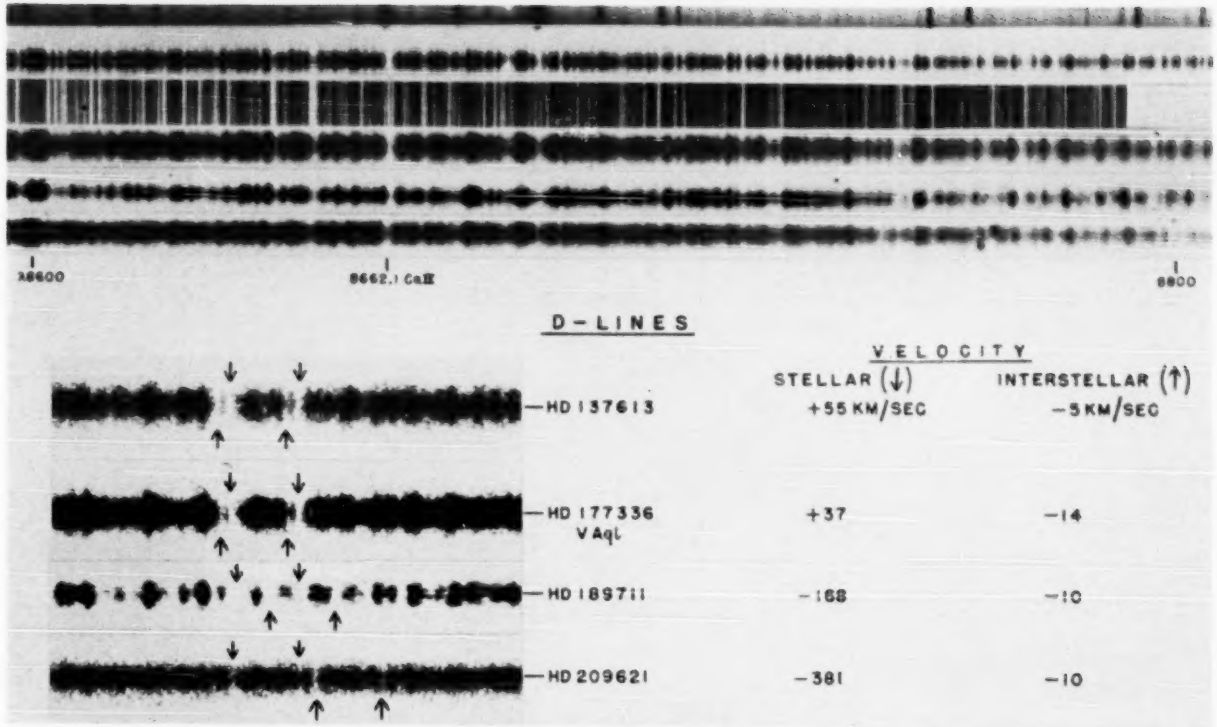

FIG. 16.—Spectra of R- and N-type stars, λλ 8600–8800. Top to bottom: 19 Piscium, laboratory spectrum of *CN*, U Hydrae, VX Andromedae, U Cygni. First-order iron comparison spectrum. *Below:* Stellar and interstellar D lines in the spectra of four stars.

lent widths of the lines of *Li* I and *K* I are not correlated with those of lines of *Na* I. For each of the periodic variables, WX Cyg and U Cyg, Table 7 has equivalent widths for two different phases, one of which has very strong *Na* I lines. In WX Cyg, the *Li* I and the *K* I lines tend to strengthen mildly with the lines of *Na* I, whereas this is true only for the *K* I line in U Cyg. It should be remarked that WX Cyg and WZ Cas, with equivalent widths of 10 A and 8 A, respectively, for the *Li* I doublet, are exceptional among class N stars with strong *Na* I lines. Of all stars observed in the region of the *Li* I doublet, none except the two mentioned above has an equivalent width of this doublet much exceeding 1 A.

The data in this table appear to support the conclusion that the relative abundances of *Na* I, *Li* I, and *K* I may vary from one class N star to another. The table further suggests, by the evidence of the two periodic variables, that the *Li* I and *K* I lines are less sensitive to temperature changes than are lines of *Na* I.

TABLE 7

EQUIVALENT WIDTHS IN ANGSTROMS OF *Li* I AND *K* I LINES IN SPECTRA WITH STRONG *Na* I LINES

Star	Date	Phase	*Na* I(D2+D1)	*Li* I λ 6708	*K* I λ 7699
WX Cyg	1949 July 11	29d	15*	3*	0.5*
U Cyg	1947 Sept. 5	70	15*	1*	4 *
BD+38°955	1948 Nov. 9		35*	1*	4 *
WX Cyg†	1948 July 25	83	45‡	10‡	1.5*
WZ Cas			55§	8§	2 *
U Cyg	1948 July 10	−216	65‡	1‡	6 *

* Estimates by Sanford.

† See first section of Fig. 2.

‡ Microphotometer measures by Sanford.

§ Microphotometer measures by McKellar, *Pub. A.S.P.*, **52**, 407, 1940.

STELLAR EMISSION LINES

Emission lines of *H* are in the spectra of many long-period variables of spectral class N for approximately one half-period, and this phase interval is centered near light-maximum. These emission lines have a rapid decrement with increasing quantum number. U Cyg is such a variable, but its spectrum in the *Atlas* belongs to the phase interval without *H* emission lines.

There is one poor spectrogram of U Cyg near maximum light, Ce 4859, and one fairly good one near minimum light, Ce 5742 (Figs. 12–16). At maximum, *Hα* is in emission, and the *Ca* II triplet lines λλ 8498.018, 8542.089, and 8662.140 are absorption lines with shortward emission components, while at minimum no *Hα* emission or emission components of the *Ca* II triplet lines appear. These two observations do not, of course, suffice to establish whether the emission for *Hα* and that for the *Ca* II lines both bear the same relation to phase or not.

INTERSTELLAR D LINES

The second section of Figure 16 reproduces the D lines in the spectra of two stars of class R and two of class N which have sufficiently high stellar radial velocities to separate the stellar from the interstellar D lines. These spectra and two others have already been used to derive values of absolute magnitude.[14]

[14] R. F. Sanford, *Mt. W. Contr.*, No. 689; *Ap. J.*, **99**, 145, 1944.

VARIATIONS IN VELOCITY AND SPECTRUM OF EIGHT N-TYPE LONG-PERIOD VARIABLE STARS

ROSCOE F. SANFORD
Mount Wilson and Palomar Observatories
Received December 16, 1949

ABSTRACT

Coudé spectrograms have been obtained of the following variables: R Leporis, UV Aurigae, T Cancri, V Hydrae, V Coronae Borealis, RR Herculis, V Ophiuchi, and U Cygni.

The absorption-line velocities depend upon lines of the *CN* molecule. Small variations have been found for all eight variables; these variations have the periods of the light-variations but phases 0.25 earlier.

If pulsation is assumed to explain the velocity variation, maximum diameter approximates the phase of minimum light; minimum diameter, the phase of maximum light. On such an assumption the average change in diameter of these variables may not exceed 3 per cent, i.e., less than the percentage change in the diameters of cepheid variables.

Emission Hα has been observed in the spectra of all these variables except T Cnc. The weighted mean velocity difference (*Hα* — Abs.) from the seven variables is −20.3 km/sec compared with the best previous determination, −20.5 km/sec. No certain variation of velocity with phase is shown by *Hα*.

Spectral changes. Emission *Hα* is present from 0.25*P* before to 0.25*P* after maximum light and disappears for the remaining phase interval. There is marked enhancement of absorption lines of *Na* I, *Sc* I, *La* I, and *V* I and of the bands of *CaCl* near minimum light for R Lep, UV Aur, RR Her, and U Cyg.

UV Aur is the only known class N variable with the bright [*Ne* III] and [*O* III] lines which characterize gaseous nebulae and, as postmaximum features, the emission lines of *Si* I, *Fe* I, *In* I, and *Mg* I, which characterize long-period Me variables.

Radial velocities for 283 stars of spectral classes R and N have already been published.[1] A number of these stars are long-period variables about as regular as the well-known long-period Mira variables of spectral class Me. Although there was a considerable range of individual velocities for some of these long-period variables of class N, it was uncertain whether this variation meant more than errors of measurement with the dispersion used (largely 65 A/mm). Hence in the catalogue only mean velocities were given for such variables.

But now the very fast Eastman 103*a*-E emulsion permits spectrograms (20 A/mm) to be obtained of some of these variables at all phases of their light-changes. The higher accuracy of the velocities with this greater dispersion made it worth while to reobserve a few of the brighter variables. A well-exposed coudé spectrogram of a class N star with the 103*a*-E emulsion gives good density from λ 6100 to λ 6700. Frequently, the D lines also are well shown.

The eight long-period variables of class N used for this study are in Table 1. The columns for maximum and minimum magnitudes give the extreme values observed for each; as with Me variables, different maximum and minimum magnitudes may occur in different cycles.

Except for those of the two variables UV Aur and RR Her, the spectrograms have been referred to the epochs of current maxima, by means of photometric data kindly supplied by Professor Leon Campbell, of the Harvard College Observatory. UV Aur has received scant attention from variable-star observers in recent years. It was therefore necessary to assume the period best fitting the two series of observations by M. Luizet[2] and by W. Doberck.[3] The Julian day of maximum and the period for RR Her are from the *Katalog und Ephemeriden veränderlicher Sterne* for 1940.

[1] *Mt. W. Contr.*, No. 689; *Ap. J.*, **99**, 145, 1944.

[2] *A.N.*, **196**, 399, 1913. [3] *J. des observateurs*, **7**, 85, 1924.

RADIAL VELOCITIES

ABSORPTION-LINE VELOCITIES

Certain atomic lines are fairly well seen in the spectra of some class N variables at all phases; other atomic lines may be strong at minimum and weak or absent at maximum light, but the details of the molecular absorption spectrum of *CN* are always prominent. Hence, for uniformity, it seemed best to base the radial velocities upon suitable lines chosen from the ever present spectrum of *CN*.

To this end, isolated lines of good quality were selected in the region from λ 6100 to λ 6700 on spectra of the carbon arc photographed with the same spectrograph as that used for the stars. The wave lengths of these lines were then derived by reference to an accompanying comparison spectrum of neon. Experience with these *CN* wave lengths led to the rejection of some lines that seemed to give erratic values of velocity from star to star. The remaining lines were retained after small systematic differences had been

TABLE 1

EIGHT LONG-PERIOD VARIABLES OF CLASS N

NAME	1900		MAG.		SPEC.	PHASE OF MAX. JD	PERIOD	γ (KM/SEC)	γ FROM *MT. W. Contr.*, NO. 689 (KM/SEC)	*K* (KM/SEC)
	R.A.	Decl.	Max.	Min.						
R Lep	4^h55^m0	−14°57′	4.5–5.8	8.0–10.7	N6e	2429908.4	447.45	+ 32.4	+ 34	5.9
UV Aur*	5 15.3	+32 24.7	7.9–	<10	Npe	2423336	395	− 5.6	− 3	7.0
T Cnc	8 51.0	+20 13.9	7.6–9.2	9.1–10.5	N6	2431523	498.5	+ 6.2	+ 7	3.8
V Hya	10 46.8	−20 43.2	6.0–	–12.5	N6e	2430920.5	539	− 15.2	− 8	3.8
V CrB	15 46.0	+39 52.5	6.8–9.1	9.9–12.4	N2e	2429823.5	361	−115.0	−115	5.7
RR Her	16 1.5	+50 46.3	7.8–	– 8.8	Npe	2421508	238.8	− 37.2	− 37	5.8
V Oph	16 21.2	−12 12.0	6.9–8.1	9.2–10.8	N3e	2429896	300.8	− 37.4	− 40	5.0
U Cyg	20 16.5	+47 34.7	6.1–9.0	8.9–12.2	Npe	2429963.7	480	+ 10.0	+ 13	9.0

* Primary of visual double star A.D.S. 3934. Secondary is distant 3″4; its magnitude is 11.6, spectrum A0. No changes in position angle or distance have been observed. Five spectrograms of the secondary give the radial velocity +0.1 ± 2.8 km/sec.

smoothed out. The final test of the lines on this list is the accordance of their velocities with the velocities from atomic lines, when observable on the same plates. The mean of thirty-two differences is

$$\text{Vel. } (CN) - \text{Vel. (atomic)} = -1.3 \text{ km/sec},$$

which was deemed satisfactory accordance. The *CN* wave lengths were therefore adopted for velocity determinations of the class N stars whenever observed within their wave-length range with the dispersion of 20 A/mm.

The first and second columns of Table 2 list the *CN* lines, and the third column the atomic lines sometimes available. *Hα*, given among the latter, appears as an emission line at certain phases in many class N long-period variables.

Table 3 is the journal of observations, with phases expressed in decimals of the period. The absorption-line velocities in the fourth column and the velocities from bright *Hα* in the fifth column (T Cnc has no bright *Hα*) are plotted for each variable in Figures 1 and 2, with filled circles and open circles, respectively. Values of $M - m$ from *Geschichte und Literatur des Lichtwechsels der veränderlichen Sterne* provide the vertical lines indicating the phases of light-minima in Figures 1 and 2.

The absorption-line velocities of all eight variables show variations in which the

minimum velocity anticipates minimum light and the maximum velocity anticipates maximum light by roughly $0.25P$.

The ninth and eleventh columns of Table 1 are estimates of the systemic velocity and the semiamplitude of velocity variation. No solution has been made for spectroscopic binary elements, since it was very doubtful whether these would have any significance except as a formal way of describing the variation. The tenth column contains the velocities previously published in *Mt. W. Contr.*, No. 689.[3]

The intervals for the observations range from 3 cycles for T Cnc to 7.4 cycles for V Oph. Nevertheless, fairly consistent results for the variations are shown by throwing all the observations into single cycles. This does not, of course, rule out the possibility that inconsistencies may appear in abnormal cycles, as in a star like V Hya, for which Leon Campbell[4] finds an 18-year period in addition to the period of 539 days. Extra deep minima in the light-curve of V Hya were reached in 1889, 1908, 1925, and 1943. It is to be

TABLE 2

ABSORPTION LINES FOR DETERMINATION OF RADIAL VELOCITY

CV	*CV*	Atomic
λ 6195.62	λ6438.03	λ 6102.72 *Ca* I
6201.08	78.71	03.64 *Li* I
04.95	6522.79	22.22 *Ca* I
18.05	36.99	41.72 *Ba* II
37.45	6692.89	43.20 *Zr* I
6310.48	97.76	62.17 *Ca* I
6408.15	6707.73 with *Li* I	6496.90 *Ba* II
10.52		6562.82 *Hα*
31.91		72.78 *Ca* I

noted that the discordant velocities for V Hya are the first two in Table 3. The first (early in 1940) precedes and the second (early in 1944) follows the low light-minimum of 1943. The remaining radial velocities (1945–1947) are mutually consistent.

If pulsation is assumed, the velocity-curves show a rough correspondence of maximum of light with minimum of diameter and minimum of light with maximum of diameter. The mean change in diameter for the eight stars is about 60,000,000 km. The percentage change in the diameter by the pulsation of such a variable is largely guesswork. However, a reasonable guess for the average diameter of one of these variables is of the order of 12 A.U. based upon a surface temperature of about 2150° K[5] and an absolute magnitude of about −2.[6] The average change in diameter of 60,000,000 km would, accordingly, be about 3 per cent of the diameter itself. This is less than the percentage change of diameter for pulsation in cepheid variables.

EMISSION *Hα* VELOCITIES

The velocities from *Hα* plotted in Figures 1 and 2 are algebraically less than the absorption-line velocities, but they are not sufficiently accurate to settle whether their variation parallels the variation for the absorption-line velocities. In deriving the mean value of the difference between the velocity from emission *Hα* and that from the absorption lines (Table 4), no distinction for phase has been made. The mean value of this difference for

[3] *Pop. Astr.*, **51**, 400, 1943.

[5] Nicholson and Pettit, *Mt. W. Contr.*, No. 369; *Ap. J.*, **68**, 91, 1928.

[6] R. E. Wilson, *Mt. W. Contr.*, No. 618; *Ap. J.*, **90**, 492, 1939; Sanford, *Mt. W. Contr.*, No. 689; *Ap. J.*, **99**, 365, 1944.

TABLE 3

JOURNAL OF OBSERVATIONS

Plate Ce	JD	Phase	Radial Velocity	
			Absorption (Km/Sec)	Emission $H\alpha$ (Km/Sec)
	R Leporis			
2674	2430308	0.895	+36.0	.....
2692	0325	.950	+35.3	+12.6
2853	0624	.600	+35.6	.....
2885	0658	.677	+36.7	+ 4.6
2949	0773	.935	.....	+18.7
3208	0988	.414	+29.0	.....
3238	1010	.463	+30.7	.....
3240	1010	.463	+30.1	.....
3263	1038	.525	+34.2	.....
3321	1063	.581	+35.2	.....
3346	1101	.666	+36.1	+ 7.8
3392	1132	.735	+39.4	+13.5
3584	1365	.256	+23.1	.....
3617	1393	.319	+23.2	.....
3622	1394	.321	+23.2	.....
3675	1454	.455	+28.1	.....
3734	1539	.638	+38.1	.....
3981	1717	.042	+30.6	+ 8.1
4086	1806	.242	+28.5	+ 9.8
4160	1865	.374	+30.4	.....
4589	2224	.176	+23.2	.....
4625	2258	0.252	+23.2	.....
	UV Aurigae			
3207	2430988	0.364	−11.5	.....
3232	1009	.417	−10.4	.....
3268	1039	.493	− 6.9	.....
3320	1073	.580	− 2.5	.....
3347	1102	.652	− 1.4	.....
3393	1132	.730	+ 0.5	−23.1
3413	1194	.885	+ 1.8	−26.9
3519	1300	.154	−10.3	−21.0
3583	1365	.319	−10.3	.....
3624	1393	.390	− 9.7	.....
3682	1456	.549	− 5.3	.....
3867	1655	.053	−18.4	−35.6
3980	1717	.210	−15.3	.....
4020	1748	.288	−13.4	.....
4082	1805	.432	−10.5	.....
4391	2070	.104	−13.0	−25.5
4856	2433	.023	− 7.3	−28.3
4872	2456	.081	−12.1	−20.7
4970	2515	0.230	−12.5	.....

TABLE 3—*Continued*

Plate Ce	JD	Phase	Radial Velocity	
			Absorption (Km/Sec)	Emission $H\alpha$ (Km/Sec)
	T Cancri			
2962	2430804	0^{p}558	+ 8.4	
3684	1456	.866	+ 6.6	
3716	1484	.921	+ 7.1	
3735	1539	.032	+ 9.1	
3750	1572	.098	+ 7.6	
3800	1604	.163	+ 3.3	
3817	1622	.199	+ 2.4	
4027	1751	.458	+ 8.6	
4083	1805	.565	+ 6.1	
4112	1831	.618	+ 8.3	
4158	1864	.685	+10.0	
4187	1895	.745	+ 8.8	
4220	1927	.810	+ 9.6	
4273	1956	.870	+ 5.1	
4539	2195	.348	+ 4.6	
4595	2227	.413	+ 5.4	
4621	2257	.474	+ 5.9	
4668	2308	0.576	+ 7.6	
	V Hydrae			
2274	2429687	0.712	− 2.6	
3352	2431103	.339	−12.6	
3681	1455	.993	−15.4	−43.3
3710	1483	.044	−18.3	−44.1
3751	1572	.209	−17.6	
4163	1865	.752	−12.0	−27.4
4188	1895	.810	−10.2	−33.6
4212	1925	.865	−14.2	−38.2
4267	1954	.917	−16.0	−45.0
4540	2195	.365	−18.6	
4622	2257	.480	−17.2	
4659	2306	.571	−16.6	
4708	2342	0.638	−13.6	
	V Coronae Borealis			
2012	2429386	0.790	−112.3	−136.8
3105	2430924	.041	−114.1	−129.0
3204	0988	.218	−118.3	−134.8
3398	1134	.622	−110.6	
3415	1195	.790	−107.2	−137.1
3429	1230	.887	−110.5	−133.3
3489	1278	.019	−118.8	−138.0
3515	1300	.080	−118.9	−131.8
3541	1334	.174	−123.8	−133.8
3581	1365	.259	−122.9	−138.8
3752	1572	.831	−109.0	−141.0
3832	1625	.978	−110.6	−129.7
3863	1655	0.061	−115.7	−136.1

TABLE 3—*Continued*

Plate Ce	JD	Phase	Radial Velocity	
			Absorption (Km/Sec)	Emission $H\alpha$ (Km/Sec)
	RR Herculis			
3155	2430955	0^{p}595	−31.3	−47.6
4196	1897	.505	−33.2	−67.6
4221	1927	.630	−32.2	−49.3
4272	1956	.750	−35.6	−52.5
4284	1983	.860	−37.3	−51.6
4344	2023	.033	−40.2	−62.4
4660	2306	.218	−43.5	.....
4709	2342	0.368	−40.6	.....
	V Ophiuchi			
2039	2429418	0.411	−44.3	.....
2968	2430806	.025	−36.2	−54.8
3002	0832	.112	−40.6	−58.8
3042	0866	.225	−41.5	−57.6
3062	0889	.302	−42.1	−61.5
3102	0923	.414	−41.0	.....
3492	1279	.597	−36.3	.....
3516	1300	.667	−36.2	−62.7
3542	1335	.783	−34.8	−59.0
3578	1363	.875	−30.6	−52.8
3833	1625	.748	−31.8	−57.5
3862	1655	0.848	−35.7	−50.5
	U Cygni			
2438	2429918	0.676	+17.5	+ 0.8
2809	2430539	.970	+ 2.3	− 9.0
2855	0625	.150	+ 0.8	.....
2889	0659	.221	+ 1.2	.....
3050	0869	.658	+18.5	− 6.2
3063	0889	.700	+19.5	− 8.7
3104	0923	.770	+19.5	− 5.4
3157	0955	.837	+17.9	− 8.6
3234	1010	.951	+ 7.0	− 7.4
3260	1038	.011	+ 0.7	− 8.4
3319	1073	.084	+ 2.4	− 9.8
3427	1229	.408	+ 5.2	.....
3430	1230	.411	+ 9.3	.....
3451	1249	.450	+ 8.6	.....
3485	1277	.509	+11.7	.....
3517	1300	.556	+16.4	.....
3540	1333	.625	+20.1	− 2.2
3579	1363	.688	+17.2	− 5.3
3830	1624	.232	+ 5.5	−11.6
3869	1656	.298	+ 6.0	.....
3969	1716	.422	+12.6	.....
3983	1718	.427	+12.9	.....
4859	2433	0.918	+ 9.7	− 8.1

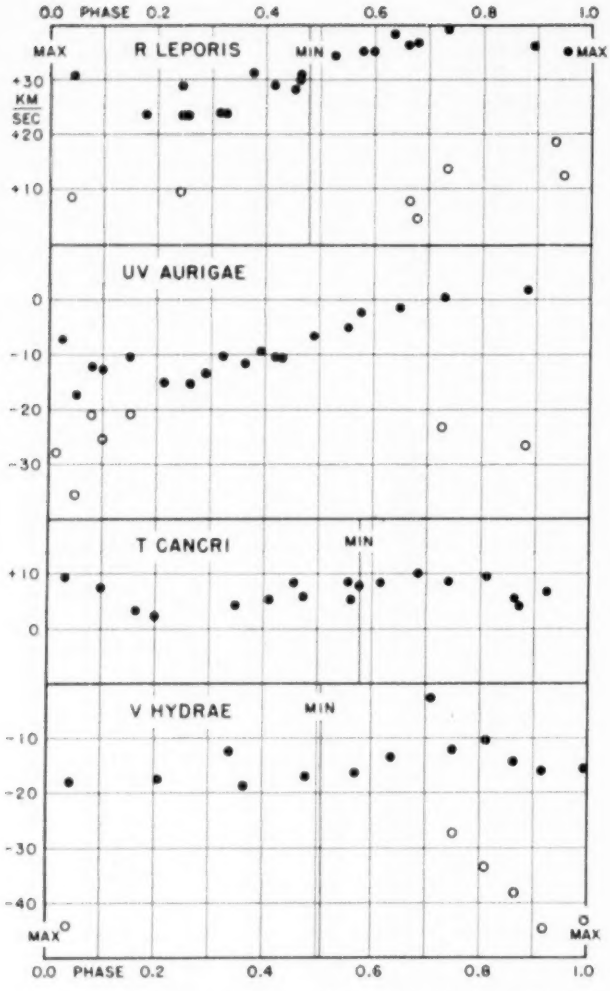

FIG. 1.—Velocities for the first four variables of Table 3 plotted with phases derived from the epoch of maximum light and the period as in Table 1. Solid circles are absorption-line velocities; open circles, emission $H\alpha$ velocities.

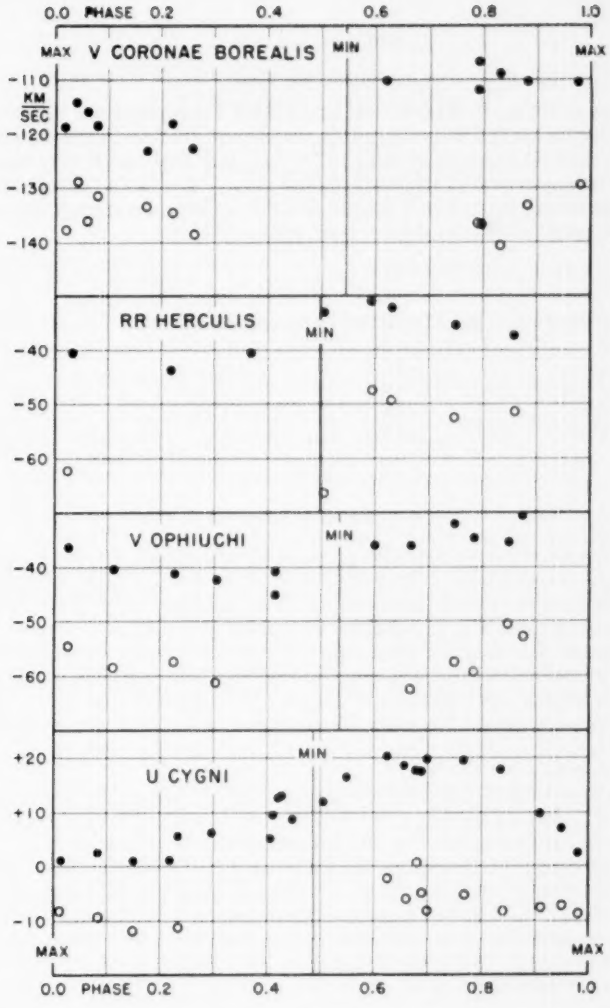

FIG. 2.—Velocities for the last four variables of Table 3 plotted with phases derived from the epoch of maximum light and the period as in Table 1. Solid circles are absorption-line velocities; open circles, emission $H\alpha$ velocities.

all the stars, weighted according to the number of separate determinations for each, is −20.3 km/sec, agreeing with the value (−20.5 km/sec) derived previously in *Mt. W. Contr.*, No. 689.[1]

SPECTRAL CHANGES

ABSORPTION LINES

The spectra of T Cnc, V Hya, V CrB, and V Oph in passing from maximum to minimum light show no conspicuous changes in the absorption lines in the part of the visible region that is used. The spectra of R Lep, UV Aur, RR Her, and U Cyg show, however, considerable enhancement of the lines of *Na* I, *Sc* I, *V* I, and *La* I at minimum as compared with maximum light. The 0, 0 band of *CaCl*, λ 6185, also strengthens at light-minimum as compared to light-maximum, especially in U Cyg.

TABLE 4

DIFFERENCES (*Hα* VELOCITIES *minus* ABSORPTION-LINE VELOCITIES)

	Km/Sec		Km/Sec
R Lep	−25.0	RR Her	−20.2
UV Aur	−18.0	V Oph	−19.5
V Hya	−24.2	U Cyg	−19.0
V CrB	−18.9		
		Weighted Mean	−20.3

EMISSION LINES

Emission *Hα* occurs in the spectra of all the stars except T Cnc. It is strongest at maximum light, being visible from phase $-0.25P$ to $+0.25P$. Limited observations of other *H* emission lines in these variables indicate that they are probably present at the same phases as emission *Hα*. The Balmer decrement is rapid.

A spectrogram of U Cyg, Ce 4859, September 5, 1947, phase 70 days, has the triplet lines of *Ca* II λλ 8498.018, 8542.089, and 8662.140 in absorption with shortward emission borders, while another spectrum, Ce 5742, July 10, 1949, at phase −216 days has only the absorption components. Emission *Hα* is present on the first spectrogram but not on the second. Nothing is known about the *Ca* II triplet emission lines for any of the other stars here concerned.

The only emission lines regularly observed in long-period variables of spectral class N are those of *H* and of *Ca* II (in U Cyg). In UV Aur, however, there also appear the lines of [*Ne* III] and [*O* III], characteristic of gaseous nebulae, and lines of *Si* I, *Fe* I, *In* I, and *Mg* I as in long-period Me variables. This unusual array of bright lines in the spectrum of UV Aur has already been described.[2] The mean velocity from all measurable [*Ne* III] and [*O* III] lines is −4.7 km/sec; and from the *Fe* I lines (λ 4202 and λ 4308), −5.7 km/sec. Both these velocities agree well with the systemic velocity −5.6 km/sec for the absorption lines (Table 2). In Me stars, however, the velocities from emission lines of *Fe* I, like those from emission lines of *H*, are algebraically less than the velocities from the absorption lines.

[2] *Pub. A.S.P.*, **61**, 261, 1949.

A SURVEY OF INTERNAL MOTIONS IN THE PLANETARY NEBULAE

O. C. WILSON
Mount Wilson and Palomar Observatories
Received December 6, 1949

ABSTRACT

Slit spectrograms (dispersion 10 A/mm) of twenty-six bright planetary nebulae have been obtained with the coudé spectrograph of the 100-inch telescope. For thirteen of the nebulae, slitless spectrograms have been secured with the same instrument.

The main observational results are the separations of the components of the double nebular lines and the dimensions of corresponding slitless images. Analysis of these data leads to the following principal conclusions:

1. There is no correlation between the relative intensities (V/R) of the red and violet components of the nebular lines and the general level of nebular excitation.

2. The number of nebulae with $V/R > 1$ is about equal to the number with $V/R < 1$; hence the nebulae are probably transparent in the observed wave-length range.

3. The most reliable measure of expansion velocity is shown to be the mean of the values given by lines of *H*, [*O* III], and [*Ne* III]. There may be a very weak positive correlation between this quantity and the level of excitation.

4. Where differences in component separation exist in the spectrum of a planetary nebula (and they are quite common), the high-excitation particles show smaller separations than the low-excitation particles. Extreme examples are [*Ne* V], for which the separations are often close to zero, and [*O* II] and [*N* II], which sometimes show large separations. Hydrogen presents an outstanding exception to the general run of separation with excitation, agreeing closely with [*O* III] and [*Ne* III]. Available evidence is against any marked dependence of component separation upon transition probability.

5. There is generally a positive correlation between component separation and monochromatic image size. Usually, though not always, differences in image size are much less than differences in separation.

6. Components of the nebular lines are often quite sharp, their apparent width being frequently determined by the resolving power of the emulsion; but components of *H* lines are noticeably diffuse in all nebulae.

By-products of the investigation include improved wave lengths of twenty nebular lines and radial velocities of twelve nebulae.

Two models have been investigated in attempting to explain the observations. The basic assumption of the first model is that the velocity given by the lines of any ion is a measure of the velocity of the abundant *H* and *He* in the region where the lines in question are produced. In this model the material is supposed to have originally a velocity equal to that measured for [*Ne* V], which is, in some nebulae, probably less than 5 km/sec. The increments in velocity between [*Ne* V] and *He* II and between *He* II and *H* are assumed to be due to the increases in momentum flux carried by the gas upon absorption of nuclear radiation below λ 228 A and between λ 912 and λ 228 A, respectively. Reasonable values of the radius and temperature of the central star lead, on this model, to the correct orders of magnitude both for the velocity changes and for the total nebular brightness.

The second model assumes that measured velocity differences are due to selective forces acting upon some of the rare ions and maintaining them in relative motion with respect to the abundant *H* and *He*. It appears possible in this fashion to construct a model which can account for the [*Ne* V] anomaly on the basis of an inward flux of Lyman continuum from the bright hydrogen shell. This model leads, however, to nebulae about 5 mag. too faint, and for this reason the first one seems preferable.

I. INTRODUCTION

Planetary nebulae, though fairly scarce objects, have presented many fascinating problems to the astrophysicist. During the last twenty-odd years some of these problems, namely, those dealing with the origin and manner of production of the nebular radiations, have been solved to a high degree of completeness.[1] Likewise, some of the

[1] I. S. Bowen, *Ap. J.*, **81**, 1, 1935; *Rev. Mod. Phys.*, **8**, 55, 1936.

physical processes occurring in the planetaries are now understood fairly well, though certain simplifying assumptions necessarily underlie the theoretical discussions.[2,3]

This pleasant picture of steady progress does not, however, hold true in all fields of nebular research. Very little is known of the dynamics, or even of the kinematics, of the nebular material. Such knowledge as we have of the internal motions in the planetaries rests entirely upon work done at the Lick Observatory more than thirty years ago. At that time Campbell and Moore[4] showed that in several nebulae the λ 4959 and λ 5007 lines, since identified with forbidden transitions in *O* III, consisted of two components, most widely separated near the centers of the nebulae and converging in the outer regions. Somewhat later, Wright and Moore[5] noted a difference in the appearance of λ 4686 *He* II as compared to the [*O* III] lines in NGC 7662. Finally, R. H. Stoy[6] reexamined the Lick plates and noted a considerable variation in the degree of widening of the nebular lines among those nebulae in which the lines had not been resolved into components.

These three papers contain, as far as I am aware, all the factual data on the internal motions in the planetary nebulae. Some theoretical work bearing on the subject has been done, based upon general considerations of transformation of ultraviolet nuclear radiation into Lyman-α with resultant internal radiation pressure.[7] There was, however, no adequate observational basis for theoretical studies, and I suspect that the theories are incapable of accounting for some of the phenomena to be described below.

Gaseous nebulae offer the great observational advantage of permitting investigation of spatial distribution of both matter and velocity. In fact, the two kinds of study necessarily go hand in hand. For the planetaries, basic data on the sizes and intensities of the monochromatic nebular images were obtained at the Lick Observatory, by W. H. Wright,[4] who utilized the Crossley reflector with a slitless quartz spectrograph which gave images on a scale of about 39″ per millimeter. Probably because of this rather small scale, some of the relative image dimensions differ from those derived in the present investigation.

The work described below was thus undertaken with the idea of extending the pioneering researches of Campbell and Moore and of Wright by making use of the more powerful telescopic and spectrographic equipment and faster photographic emulsions now available, with the hope of laying the observational foundation necessary for theoretical studies of the dynamics of planetaries.

The coudé spectrograph of the 100-inch telescope, with a Schmidt camera of 32″ focus, was used throughout. In the blue-violet, from λ 5100 to λ 3200, spectra were photographed in the second order with a dispersion of 10.3 A/mm. It is possible with this instrument to obtain spectra of the *Hα* region in the first order simultaneously with the blue-violet in the second, by inserting a short length of red-sensitive plate at one end of the plateholder. Most of my spectrograms were taken in this fashion. Baked Eastman 11*a*-O or 103-O plates were used for the blue, Eastman 103*a*-E for the red. All the spectrograms were obtained in the period April, 1946—February, 1949. Exposure times of three to four hours were most frequent, but ranged from a few minutes to about ten hours.

At the coudé focus the 100-inch telescope has an equivalent focal length of 250 feet,

[2] H. Zanstra, *Ap. J.*, **65**, 50, 1927; *Zs. f. Ap.*, **2**, 1, 329, 1931.

[3] D. H. Menzel and colleagues, eighteen papers in the *Astrophysical Journal* on the general subject "Physical Processes in Gaseous Nebulae." The last of the series, *Ap. J.*, **102**, 239, 1945, includes references to the others.

[4] *Pub. Lick Obs.*, Vol. **13**, 1918.

[5] *Pub. A.S.P.*, **41**, 307, 1929.

[6] *Pub. A.S.P.*, **51**, 233, 1939.

[7] S. Chandrasekhar, *Ap. J.*, **102**, 402, 1945. This paper gives references to earlier work by Ambarzumian and Zanstra.

and a scale of 2".7 to the millimeter. With a collimator of 290-cm focus, the scale of images on the plate is 9".64 per millimeter, about four times that of Wright's slitless spectra. In order to take slitless spectra, the slit of the spectrograph was replaced by a hinged mirror. With the mirror in position, the nebular image was centered with respect to a reticle in the usual manner, the mirror was raised, and the light was allowed to enter the spectrograph for a time, after which the mirror was lowered again and the centering process repeated. Such intermittent guiding is not ideal, of course, but it appears to give fairly satisfactory results when conditions are good. The proportion of total exposure time consumed by guiding is estimated to vary from 10 to 20 per cent.

Some weaknesses of the present work should be pointed out. First, some large regions of the spectrum have not been covered. Between λ 5100 and λ 6200 I do not have a single exposure, nor has the red beyond λ 6600 been photographed. More spectrograms, both slit and slitless, will be needed for some of the nebulae in the survey, even in the spectral regions already investigated. The most serious weakness in the observations is, however, the rotation of the image on the slit. For a fairly symmetrical nebula with a more or less definite "center," the image rotation is probably not a very serious drawback in the determination of the separations of the components of the nebular lines. Even if the true center of expansion rotates through a circle of small radius during the exposure, all lines will, to the first approximation, undergo similar amounts of distortion, and the relative separations for different lines should not be appreciably affected. For unsymmetrical nebulae, however, or for off-center studies of symmetrical ones, an image rotator is absolutely necessary; without one the guiding is hopeless.

For slitless work, also, an image rotator is of prime importance. Most slitless spectrograms are exposed at least an hour, corresponding to a 15° rotation of the image. Thus only large-scale radial structure can be seen on the slitless plates, all fine structure being lost. On the other hand, even without an image rotator, especially for images of approximately the same shape, differences in size along any specified diameter can be determined with fair accuracy.

In view of the above statements, the present work should be considered as a preliminary survey rather than as a definitive investigation. A number of new facts have come to light, and the direction of some future, more precise, investigations is clearly indicated. It will be evident to the reader, however, that much remains to be done.

Following this introduction, Section II*a* contains a number of measured nebular wave lengths (some of which are probably improvements on current values) and radial velocities of a few nebulae. These items are by-products of the investigation.

The observations of internal motions are in Section II*b*, where a small amount of material relating to the spectra of the central stars is included, where available.

Section III contains correlations, generalizations, conclusions, discussion of a few specialized observations, and some preliminary calculations on the dynamics of the planetary nebulae.

II. OBSERVATIONS

a) NEBULAR WAVE LENGTHS AND VELOCITIES

Although on most of the spectrograms only the separations of the components of the lines were measured, twenty plates were measured, completely or partially, for wave length. Of these, twelve plates of six nebulae were considered satisfactory for wavelength determination, the criterion being that enough lines with laboratory wave lengths (chiefly those of *H* and *He* I) should be measurable to provide a good nebular velocity. The nebulae employed for this purpose and the numbers of plates of each are: NGC I 418 (2), NGC 2392 (1), NGC 3242 (2), HD 184738 (2), NGC 7009 (2), NGC 7662 (3). Resulting wave lengths are in Table 1.

For most of the stronger nebular lines the agreement between Miss Moore's tabulation and the measured values is very good. For the weaker lines and for the stronger ones

where there are considerable differences, I believe that the wave lengths of the first column are to be preferred. Two lines in Table 1 are unidentified. The line at λ 4090 was apparently attributed by Wyse[8] to transitions in *O* II, although this identification seems incorrect in view of the present more accurately determined wave length. The identification by Wyse of the line at λ 4699 with transitions in [*Fe* III] and *O* II also appears incorrect for the same reason. It is possible that this line is λ 4699.3 [*Mn* IV], although other lines of the same multiplet have not been seen. The close agreement between the line measured at λ 4571.11 and the wave length of 4571.10 *Mg* I seems to make this identification certain in spite of the fact that the line was measured on only one plate of NGC I 418.

TABLE 1

MEASURED NEBULAR WAVE LENGTHS

I.A.	No. Plates	Mean Dev.	Ident.	Revised Mult. Table*
3345.82	(1)		[*Ne* V]	45.9
3425.86	(3)	±0.01	[*Ne* V]	25.8
3726.06	(7)	± .02	[*O* II]	26.16
3728.82	(7)	± .05	[*O* II]	28.91
3868.77	(7)	± .01	[*Ne* III]	68.74
3967.48	(6)	± .02	[*Ne* III]	67.51
4068.62	(3)	± .03	[*S* II]	68.62
4076.36	(1)		[*S* II]	76.22
4090.83	(1)			
4267.20	(1)		*C* II	67.27
4363.22	(7)	± .02	[*O* III]	63.21
4571.11	(1)		*Mg* I	71.10
4699.28	(3)	± .03		
4711.36	(4)	± .04	[*A* IV]	11.4
4740.22	(3)	± .04	[*A* IV]	40.3
4958.91	(6)	± .05	[*O* III]	58.91
5006.85	(4)	± .03	[*O* III]	06.84
6300.27	(1)		[*O* I]	00.23
6548.06	(2)	± .03	[*N* II]	48.1
6583.43	(2)	±0.02	[*N* II]	83.6

* *Contr. Princeton U. Obs.*, No. 20, 1945.

Radial velocities have been measured for twelve nebulae. For the nebulae used in determining the wave lengths of Table 1, the velocities depend chiefly upon lines of *H* and *He* I. The wave lengths of Table 1 were then used to find the velocities of the other nebulae (Table 2). The agreement with the Lick observations is reasonably good, although the present measures appear in the mean to be algebraically smaller. Some large differences, notably in NGC 2392, are probably due to the fact that the two components of the nebular lines are of very unequal intensity.

b) COMPONENT SEPARATIONS AND MONOCHROMATIC IMAGE DIMENSIONS

Much of the information derived from the slit spectrograms is summarized in Table 3. The nebulae have here been divided into three groups of high, medium, and low excitation. There is no doubt that the nebulae in the first and third groups are properly placed; some of those in the medium group might be put elsewhere, however, were more complete observations available.

[8] *Ap. J.*, **95**, 356, 1942.

In the third column of Table 3 an attempt has been made to indicate roughly the morphology of the nebulae: "R" = ring; "DR" = double ring; "A" = amorphous, i.e., neither ringlike nor highly irregular; "Irreg." = irregular structure. These data are based mostly on my own slitless spectrograms, supplemented in one or two instances by statements in Wright's paper, and are probably correct as far as they go. In the fourth column is a qualitative estimate of the relative intensities of the components of the double nebular lines.

The fifth to seventeenth columns inclusive contain the condensed results on the separations of the components of the lines arising from the various ions and atoms. At the head of each column is the designation of the particle with the ionization potential of the next lowest stage of ionization. Each ΔV entry is the mean of all measures of all lines produced by the various particles, the total number of lines used in forming each mean ΔV being given in parentheses.

TABLE 2

MEASURED NEBULAR RADIAL VELOCITIES

Nebula	Measured Velocity (Km/Sec)	No. Plates	No. Lines	M.D.	Velocity from Campbell and Moore (Km/Sec)
NGC I 418	+61.1	1	15	±1.9	+62.5
NGC II 2149	−34.8	1	17	±2.4	−32.5
II 2165	+50.0	1	5	±1.0	+55.3
NGC 2392	+71.0*	1	9	±1.8	+84.2
3242	+ 4.2	2	10, 5	±1.6	+ 4.6
6210	−48.0	1	5	±1.0	−36.0
6741	+39.7	1	5	±2.8	+42.9
HD 184738	−32.9	2	9, 7	±1.8	−30.4
NGC 6818	−16.9	1	7	±2.4	−13.5
6886	−34.1	1	8	±2.8	−36.4
7009	−46.3	2	16, 7	±1.4	−46.0
7662	−16.5	3	12, 8, 5	±0.6	−12.3

* Includes velocity from three stellar emission bands.

For many of the nebulae the values of ΔV show surprisingly large variations from one particle to another. It is therefore not possible to specify unambiguously a ΔV for each object. The ΔV's for *H*, [*O* III], and [*Ne* III] are, however, always in close agreement; for statistical discussion of expansion velocities, therefore, the mean ΔV for these three particles has been entered in the eighteenth column. The mean of the mean deviations for all lines measured on more than one plate is given in the last column as a rough measure of the precision attained. In those instances where only one plate has been measured, the mean of the mean deviations of the various lines arising from common origins has been entered.

Further details on some of the nebulae listed in Table 3 follow.

1. *NGC I 418.*—In addition to the double lines given in Table 3, λ 4571 *Mg* I was measured as double on one plate with ΔV = 37.5 km/sec.

The *H* and *He* I lines are slightly diffuse, but none is resolved into components. Other lines appear narrower, ranging down to λ 3868 [*Ne* III], which is as fine and sharp as the resolving power of the plate will allow. This line is noticeably shorter than the others. A special graded series of exposures for the [*N* II] lines λ 6548, λ 6584 and for [*O* II] λ 3726, λ 3728 shows that these lines, too, are single with no trace of resolution into components. The appearance of the various lines is illustrated in Figure 1*a*.

TABLE 3

MEAN SEPARATIONS OF DOUBLE LINES IN PLANETARY NEBULAE
(Km/Sec)

Nebula NGC	Excitation	Form	V/R	[O I] 0.0	[S II] 10.3	H 13.5	[O II] 13.6	[N II] 14.5	He I 24.5	N III 29.5	[O III] 35.0	O III 35.0	[Ar IV] 40.8	[Ne III] 40.9	He II 54.2	[Ne V] 96	Mean ΔV H, [Ne III], [O III]	Mean M.D.
II 2165*	H	R	>1	.....	.....	.....	106.0(2)	.....	.....	.....	40.0(1)	.....	.....	39.9(2)	.....	0: (1)	40.0	1.7
2392*		DR	<1	.....	.....	.....	65.6(1)	61.5(1)	.....	.....	105.3(2)	.....	.....	113.9(1)	.....	0: (2)	107.3	11.4
2440		Irreg.	†	.....	.....	.....	.....	.....	.....	.....	44.6(2)	.....	.....	44.8(1)	.....	0: (1)	44.6	2.0
3242*		DR	1	.....	.....	40.8(22)	.....	.....	.....	.....	39.6(24)	32.5(3)	35.6(2)	39.0(13)	33.6(8)	.....	39.8	1.6
6741*		R?	†	.....	.....	.....	44.2(2)	42.1(6)	.....	.....	41.6(6)	.....	.....	41.0(3)	.....	0: (1)	41.4	3.3
6818*		R	<1	.....	.....	55.5(5)	60.2(2)	.....	.....	.....	56.2(12)	.....	.....	58.0(5)	42.4(4)	32.6(2)	56.5	1.8
6886*		A	>1	.....	.....	34.4(1)	45.3(2)	.....	.....	.....	32.8(1)	.....	.....	40.6(2)	.....	0: (2)	37.1	1.4
7009*		R	1	.....	.....	42.1(20)	40.9(2)	.....	44.1(4)	41.1(4)	41.1(11)	32.9(3)	39.7(3)	38.7(7)	35.8(4)	.....	41.2	1.5
7027		Irreg.	.....	45.5(1)	42.7(2)	42.4(4)	47.2(2)	41.6(2)	.....	.....	40.9(5)	41.4(1)	.....	44.7(4)	39.6(2)	38.2(1)	42.7	2.8
7662*		DR	<1	.....	.....	51.9(21)	58.0(2)	.....	.....	47.7(1)	52.7(15)	50.6(11)	46.0(5)	51.8(12)	46.1(5)	38.6(2)	52.2	1.5
I 351	M		>1	.....	.....	.....	.....	.....	.....	.....	29.0(2)	.....	.....	.....	.....	.....	29.0	0.2
1535		DR	1	.....	.....	.....	.....	.....	.....	.....	40.0(2)	.....	.....	39.0(2)	.....	.....	39.5	0.3
J 320			>1	.....	.....	.....	.....	.....	.....	.....	.....	.....	.....	34.6(1)	.....	.....	34.6	
II 2149*		A	>1	.....	.....	.....	40.3(2)	.....	.....	.....	.....	.....	.....	.....	.....	.....	0:	2.7
J 900			<1	.....	.....	.....	50.4(2)	45.0(1)	.....	.....	35.8(1)	.....	.....	35.2(4)	.....	.....	35.4	0.8
II 4593*		A		.....	.....	.....	.....	.....	.....	.....	.....	.....	.....	.....	.....	.....	0:	
6210*		A	<1	.....	.....	42.1(13)	71.1(5)	71.1(3)	38.3(1)	.....	42.8(9)	.....	.....	41.6(8)	.....	.....	47.2	1.6
II 4634		A	1	.....	.....	.....	.....	.....	.....	.....	29.8(4)	.....	.....	28.6(1)	.....	.....	29.6	1.0
6567		A	†	.....	.....	35.6(4)	.....	71.5(2)	.....	.....	36.9(6)	.....	.....	29.8(1)	.....	.....	35.8	2.6
6572		A	<1	32.0(1)	31.0(1)	.....	33.7(3)	29.5(1)	.....	.....	.....	.....	.....	.....	.....	.....	.....	2.5
6720		R	1?	.....	.....	.....	.....	.....	.....	.....	.....	.....	.....	60:	.....	.....	60:	
6803		.....	1	.....	.....	.....	.....	40.1(4)	.....	.....	29.0(3)	.....	.....	26.6(2)	.....	.....	28.0	0.6
6884		.....	†	.....	.....	45.6(1)	.....	.....	.....	.....	45.5(4)	.....	.....	42.0(1)	.....	.....	44.9	1.7
7026		Irreg.	.....	.....	.....	81.7(1)	.....	.....	.....	.....	.....	.....	.....	.....	.....	.....	81.7	
I 418*	L	R	>1	49.9(2)	34.7(7)	0:	0:	0:	0:	.....	0:	.....	.....	0:	.....	.....	0:	1.2
HD 184738 = BD+ 30°3639*		R	†	.....	43.2(7)	52.8(32)	59.6(17)	51.9(13)	.....	.....	.....	.....	.....	.....	.....	.....	52.8	4.3

* Further information will be found in the text.

† Red components stronger at one end of line; violet components stronger at other end.

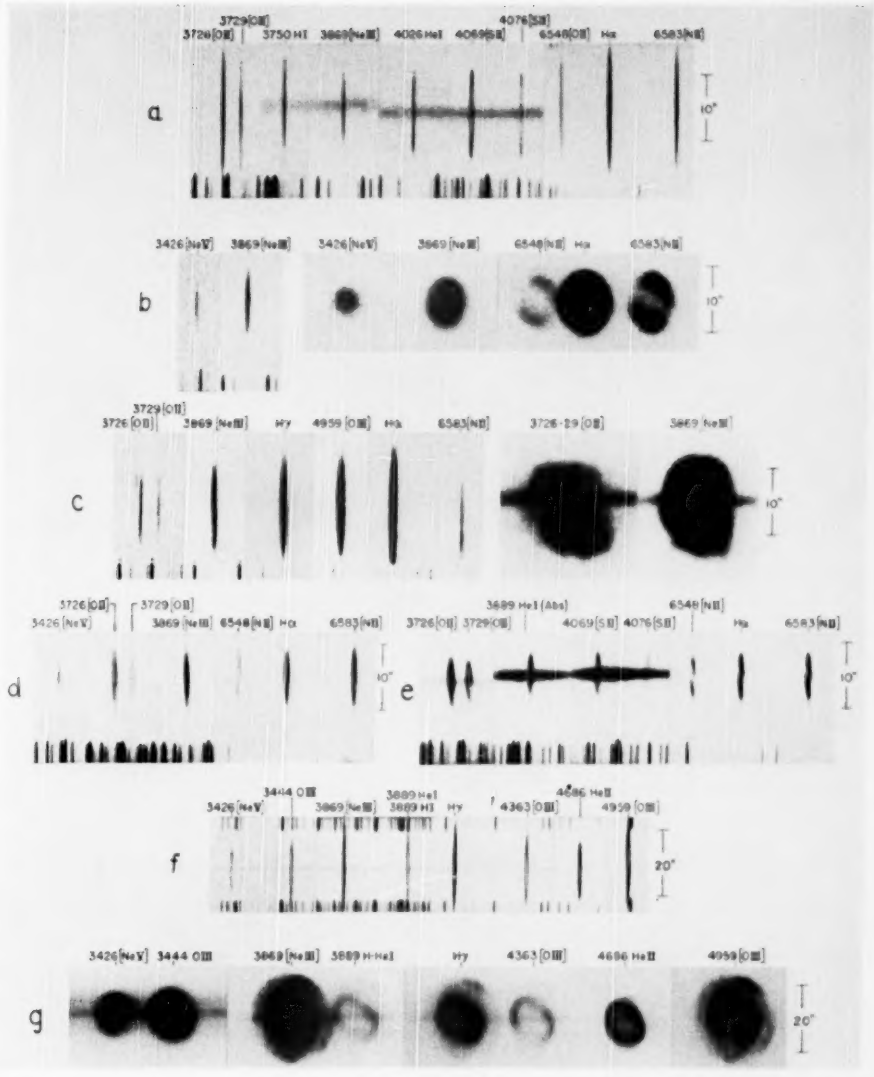

FIG. 1.—Slit and slitless spectra of planetary nebulae. *a*, NGC I 418; *b*, NGC II 2165; *c*, NGC 6210; *d*, NGC 6741; *e*, HD 184738 (BD+30°3639); *f* and *g*, NGC 7662. In *a*, 6548 [O II] should read 6548 [*N* II].

To the red of λ 4000 the nuclear spectrum is well shown on one plate. *H* and *He* I appear to be present in absorption, but the presence of the strong nebular emissions precludes measurement for velocity. The only absorption lines free of nebular emission are λ 4199 and λ 4542 *He* II; both are exceedingly diffuse and shallow.

Five emission bands in the λ 4600 region are easily measurable in the nuclear spectrum and are readily identified as λλ 4634, 4640 *N* III; 4647, 4650–51 *C* III; and 4686 *He* II. Widths of emission bands are in Table 4.

TABLE 4

NUCLEAR BAND WIDTHS IN NGC I 418

Band	Width (Km/Sec)
4634 *N* III	104
4640 *N* III	98
4648 *C* III	116
4686 *He* II	161

The mean radial velocity from four bands is +63.7 km/sec compared to +61.1 from the nebular lines. Thus, as in NGC 2392, the bands do not appear to be shifted appreciably from their normal positions, and, in particular, no occultation effect is observable.

Only one good slitless spectrogram of NGC I 418 has been obtained. A number of the nebular images are overexposed, especially the earlier members of the Balmer series. The weaker hydrogen lines appear as rings; the contrast between the ring itself and its interior is not, however, so great as in [*S* II] and [*O* I]. Measures of the slitless images in the direction of dispersion are in Table 5.

TABLE 5

SLITLESS IMAGE DIAMETERS IN NGC I 418

Line	Outer Diam.	Line	Outer Diam.	Inner Diam.
Hβ	13".0	4471 *He* I	10".5	.....
γ	12.7	5007 [*O* III]	10.9	.....
δ	12.1	4959	10.5	.....
ε	11.7	6300 [*O* I]	11.8	7".2
8	11.6	4076 [*S* II]	12.0	5.3
9	11.2			
10	10.5			
11	10.6			
12	10.5			

The apparent variation in diameter among the hydrogen images is doubtless due to overexposure of the earlier series members. Image densities of the last three hydrogen lines are comparable to those of λλ 4076, 4471, and 6300. The lines λ 5007 and λ 4959 are slightly stronger. Hence it appears that the true diameters for *H*, *He* I, and [*O* III] are about 10".5, while those of [*S* II] and [*O* I] are slightly larger, about 12".0.

The slitless image of λ 3868 [*Ne* III], although too faint for measurement, appears as a faint, hazy blob and is, I believe, considerably smaller than the other images.

2. *NGC II 2149.*—The red components of the [*O* II] lines are very much weaker than the violet; nevertheless, the mean radial velocity from the two components, −36.2 km/sec, agrees well with that of the single lines, −34.8 km/sec. The [*N* II] lines λ 6548 and λ 6584 are suspected of being double, with relative intensities in the same sense as for [*O* II]. Single nebular lines are rather diffuse; the hydrogen lines are the widest; those of [*Ne* III] sharpest.

On one spectrogram the nuclear spectrum is fairly well shown. A number of diffuse, difficult features were measured, with the results indicated in Table 6. In spite of the very poor quality of these lines, they agree roughly in velocity with the nebular lines, and I am inclined to consider them real.

3. *NGC II 2165.*—The mean radial velocity from three double nebular lines is +50.4 km/sec, compared to +49.5 km/sec for λ 3426 [*Ne* v].

One slitless spectrogram has been measured in the direction of dispersion, with the results shown in Table 7. All nebular images except that of λ 3426 [*Ne* v] appear to have a ring structure, although the degree of contrast between the ring and its interior is not the same for all images. The image of λ 3426 [*Ne* v] is a small round blob without visible

TABLE 6

ABSORPTION LINES IN NUCLEUS OF NGC II 2149

Meas. λ Rel. to ⊙	Ident.	Vel. (Km/Sec)
3753.99	54.67 *O* III	−54.4
3756.92	57.21 *O* III	−23.3
3759.33	59.87 *O* III	−43.2
3790.88	91.26 *O* III	−29.9
4068.37	68.97 *C* III	−43.9
4074.32	74.71 C II Bl	−28.4
4198.98	99.83 *He* II	−60.5
4541.09	41.59 *He* II	−33.1

TABLE 7

SLITLESS IMAGE DIAMETERS IN NGC II 2165

Line	Outer Diam.	Inner Diam.	Line	Outer Diam.	Inner Diam.
Hβ	5".3		λ 4959 [*O* III]	5".7	2".2
γ	5.5		λ 4363	5.1	
δ	5.7		λ 4686 *He* II†	4.4	
λ 6584 [*N* II]*	6.4	2".6	λ 3426 [*Ne* V]	3.4	
λ 3868 [*Ne* III]	5.9	2.0			

* Ring not complete, measures approximate. † Ring structure, but not measurable.

structure. Table 7 shows unquestionably that the [*Ne* v] image is smaller than those of *H*, [*O* III], and [*Ne* III]. The line *He* II λ 4686 is probably smaller also and λ 6584 [*N* II] probably larger, although these conclusions are less certain. Some of the slit and slitless images are shown in Figure 1*b*.

4. *NGC 2392.*—Observations of this very interesting object have been fully covered in a separate publication,[9] and no new material has since been obtained. A slight error affecting the data in Table 5 of the paper cited has been found. All dimensions in Table 5 should be multiplied by 1.06. A remeasure of the same slitless spectrogram leads to the data in Table 8. It is probable that λ 3426 [*Ne* v] gives an image very slightly smaller than the others.

5. *NGC 3242.*—This nebula has a bright inner ring surrounded by a fainter outer ring. Two slitless spectrograms have been measured in the direction of dispersion, with the results given in Table 9, where the mean deviations and numbers of measured images

[9] *Mt. W. Contr.*, No. 749; *Ap. J.*, **108**, 201, 1948.

are included. It is barely possible that the *He* II and *O* III images are a trifle smaller than the others, but the differences are nearly the same as the mean deviations.

6. *NGC II 4593.*—No lines in this nebula are resolved into components. The only trace of structure is in λ 3726 and λ 3728 [*O* II], which have the appearance of consisting of three blended components with the center one considerably the stronger. Other nebular lines are somewhat diffuse. As usual, the *H* lines are most diffuse, while the lines of [*Ne* III] are fairly sharp.

On a slitless spectrogram the images are rather amorphous, with no clearly defined edges. Measured diameters on such images depend so strongly on image density as to have little significance unless made on a graded series of exposures so that images of equal density can be compared.

TABLE 8

SLITLESS IMAGE DIAMETERS IN NGC 2392

Line	Outer Diam.	Inner Diam.	Line	Outer Diam.	Inner Diam.
Hβ	13".0	7".0	λ 4957	13".5	6".8
γ	13.3	6.6	λ 4363	12.4	6.5
δ	12.5	6.0	λ 3868 [*Ne* III]	13.6	6.8
λ 4686 *He* II	12.8	6.8	λ 3426 [*Ne* V]	11.8	5.0
λ5007 [*O* III]	14.2	7.1			

TABLE 9

SLITLESS IMAGE DIAMETERS IN NGC 3242

Element	Outer Ring Outer Diam.	Inner Ring	
		Outer Diam.	Inner Diam.
H	33".7±0.5 (2)	15".2±0.1 (7)	9".2±0.2 (6)
He I		15.2 (1)	
He II		14.8±0.2 (2)	9.4±0.3 (2)
O III		14.8±0.4 (2)	9.6±0.6 (2)
[*O* III]	33.0±0.2 (3)	15.0±0.0 (3)	9.4±0.4 (3)
[*Ne* III]	34.7 (1)	15.2±0.5 (2)	9.7 (1)
[*A* IV]		15.2±0.1 (2)	

7. *NGC 6210.*—In view of the large excess velocities of [*O* II] and [*N* II] in this nebula, it is especially important to examine slitless spectrograms. The slitless images are somewhat disappointing; they possess some structure but not of the roughly circular-symmetric type often observed. An image rotator will be required for best results. Nevertheless, it is possible to show that there are no major differences in image size between [*O* II] and the other nebular emissions. On the best slitless spectrogram the diameters of λλ 3726–28 [*O* II] and 3868 [*Ne* III] were measured in the direction perpendicular to the dispersion, with the following results: Outer diam. [*O* II] = 13".0; outer diam. [*Ne* III] = 12".6. Images of the [*N* II] lines could not be measured with accuracy because of their extremely broken structure. Inspection shows, however, that they are certainly of very nearly the same over-all dimensions as the other nebular images of the same density. Slit and slitless images are illustrated in Figure 1*c*.

8. *NGC 6741.*—Radial-velocity measures of one plate give +45.6 km/sec for λ 3426 [*Ne* V] compared to +38.2 km/sec from four double lines. Hence the displacement for

[*Ne* V] agrees at least approximately with the mean displacements for the components of the double lines. The nebular lines are illustrated in Figure 1*d*.

9. *HD 184738 (BD+30°3639).*—For this object the rather large mean deviation in Table 3 is due to the influence of seeing and guiding errors combined with the small diameter, about 5″, of the nebula. On the best plates the lines are of good quality. A graded series of four slitless exposures made on a single plate under excellent conditions permits measures of images of various lines with approximately equal image density. The results are in Table 10. The differences in image size shown in this table are

TABLE 10

SLITLESS IMAGE DIAMETERS IN HD 184738

Line	Outer Diam. (M. D.)
	A. Parallel to Dispersion
λ 3726 [*O* II]	4.″69 ± 0.12 (3)
Hε[a]	4.60 ± 0.11 (4)
	B. Perpendicular to Dispersion
λ 4068 [S II]	6.65 (1)
Hε	6.75 (1)
λ 3726 [*O* II]	6.75 ± 0.00 (2)
λ 6548 [*N* II]	6.26 (1)

[a] Mean of *Hβ*, γ, δ, ε.

TABLE 11

NUCLEAR BAND WIDTHS IN HD 184738

Band	Width (Km/Sec)	Total Excitation (Volts)
3920 C III	850	35.5
3961 *O* III	410	103.3
4026 *He* I	660	24.5
4056 C III	700	83.2
4187 C III	690	83.2
4200 *He* II	410	78.7
4267 C II	950	35.5
4441 C IV	480	147.4
4542 *He* II	430	78.7

probably no larger than the errors of measurement, and, to within the accuracy obtained, all images may fairly be said to have the same diameters.

The nuclear spectrum of this object is most interesting and will be investigated in detail in the future. For the present, only two features will be noted. The widths of a few unblended nuclear emission bands have been measured on a spectrogram of smaller dispersion than the spectrograms used for the nebular lines, with the results given in Table 11. Total excitations tabulated are the sums of the various ionization potentials required to produce one higher stage of ionization than that for a given band. In other words, it is assumed that the bands result from cascading after recombination. The run of band width with excitation is shown in Figure 2.

The most interesting feature of the nuclear spectrum revealed by the high-dispersion plates is a pair of sharp absorption lines just to the violet of the $H\zeta$ nebular emission, which are probably to be attributed to absorption of λ 3888.65 by *He* I atoms in the metastable 2^3S state.[10] Measures of the two sharp *He* lines from two plates give velocities of −56.0 and −89.0 km/sec. The velocity from the violet components of the nebular emission lines is −60.2 km/sec. Probably, therefore, the *He* absorption line at −56.0 km/sec is to be attributed to the same portion of the nebula responsible for the emission lines. The other, somewhat weaker, component has no analogue in emission. Various features of HD 184738 are shown in Figure 1*e*.

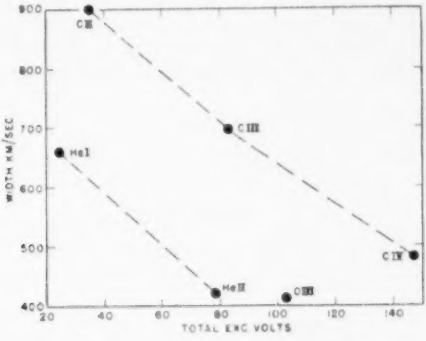

FIG. 2.—Dependence of nuclear band width upon total excitation in HD 184738 (BD+ 30°3639)

TABLE 12

SLITLESS IMAGE DIAMETERS IN NGC 6818

Line	Diameter	
3426 [*Ne* V]	10".8	(1)
3868 [*Ne* III]	19.2 ± 0.8	(2)
4101 *Hδ*	17.8	(1)
4340 *Hγ*	17.9	(1)
4363 [*O* III]	16.7	(1)
4686 *He* II	14.4 ± 1.2	(2)
4861 *Hβ*	17.6	(1)
4959 [*O* III]	19.0 ± 1.0	(2)
5007 [*O* III]	19.7 ± 1.0	(2)

10. *NGC 6818.*—One plate measured for radial velocity gives −11.3 km/sec for λ 3426 [*Ne* V], as compared to a mean of −17.9 for six other lines. Slitless images of this nebula do not have a very sharp boundary; hence measured diameters depend somewhat on image density. Two slitless spectrograms were measured in the direction of dispersion, with the results given in Table 12. Some of the scatter in the table is certainly due to variation in image density. Nevertheless, the λ 3426 and λ 4686 images are strong enough to insure the reality of their smaller diameters.

11. *NGC 6886.*—Radial velocities from λ 3345 and λ 3426 [*Ne* V] are −34.2 ± 0.2 km/sec; from six double nebular lines −34.1 ± 3.6 km/sec. One slitless spectrogram has been obtained. The images are small and without sharply defined boundaries. A

[10] This line is found also in absorption in the spectra of stars imbedded in the Orion nebula (*Pub. A.S.P.*, **49**, 338, 1937).

faint wing or extension projects out from one side and seems to be present in all lines, at least in all that are of sufficient strength to show it. Measures of the slitless images in the direction of dispersion are in Table 13.

Most of the apparent variation in diameter is doubtless an effect of image density. Images of λλ 3426, 4101, 4363, and 4686 are of fairly comparable density. Hence one may conclude that [*Ne* v] probably gives a slightly smaller image than the other lines do, although there are no major differences in size.

TABLE 13

SLITLESS IMAGE DIAMETERS IN NGC 6886

Line	Diameter
3426 [*Ne* v]	3".1
4101 *Hδ*	3.7
4363 [*O* III]	3.3
4340 *Hγ*	4.0
4686 *He* II	3.4
4861 *Hβ*	3.9
4959 [*O* III]	5.0

TABLE 14

SLITLESS IMAGE DIAMETERS OF NGC 7662

Line	Outer Ring Outer Diam.	Inner Ring	
		Outer Diam.	Inner Diam.
3312 *O* III		13".0 ± 0.6 (2)	7".4 ± 0.1 (2)
3340 *O* III		12.3 ± 0.4 (3)	7.2 ± 0.1 (2)
3426 [*Ne* v]		9.1 ± 0.2 (3)	4.4 ± 0.2 (3)
3444 *O* III		12.8 ± 0.4 (4)	8.0 ± 0.6 (4)
3760 *O* III		12.7 ± 0.4 (3)	7.5 ± 0.5 (3)
3797 *H*10		13.6 ± 0.4 (2)	6.6 (1)
3835 *H*9		13.5 ± 0.7 (3)	6.9 ± 0.5 (3)
3868 [*Ne* III]	24".3 ± 0.3 (3)	14.7 ± 0.3 (3)	8.4 ± 0.8 (3)
Hζ		13.0 (1)	8.1 (1)
Hδ	23.7 ± 0.6 (3)	14.1 ± 0.6 (4)	8.3 ± 0.4 (4)
Hγ	23.9 ± 0.4 (3)	14.3 ± 0.5 (4)	8.3 ± 0.6 (3)
4363 [*O* III]		13.7 ± 0.5 (4)	8.5 ± 0.4 (4)
4471 *He* I		14.8 ± 0.6 (2)	9.2 (1)
4542 *He* II		11.8 (1)	
4640 *N* III		13.3 (1)	
4686 *He* II		12.2 ± 0.3 (3)	7.0 ± 1.0 (3)
4699		12.3 ± 0.4 (2)	7.4 (1)
4711 [*A* IV]		13.1 ± 0.6 (2)	6.5 (1)
4740 [*A* IV]		12.4 ± 0.3 (2)	6.2 (1)
Hβ	24.0 ± 0.1 (2)	14.1 ± 0.6 (4)	8.0 ± 0.5 (4)
4958 [*O* III]	23.9 ± 0.3 (3)	14.8 ± 0.4 (3)	8.1 ± 0.8 (3)

12. *NGC 7009.*—Slitless spectrograms of this nebula show so much structure that no attempt has been made to measure them. An image rotator will be required for satisfactory study of the distribution of the various ions and atoms.

13. *NGC 7662.*—Four slitless spectrograms have been measured in the direction of dispersion. This nebula is an especially favorable one in which to look for small differences in image diameter, since the images of both the inner and the outer ring are relatively sharply bounded. Accordingly, the measures are given in Table 14 in considerable detail,

to illustrate the order of accuracy attainable. Mean deviations and numbers of images measured are given in the table.

The mean image diameters for lines having a common source are given in order of total excitation in Table 15 for the inner ring only. Some features of NGC 7662 are shown in Figures 1*f* and 1*g*.

While both inner and outer diameters of slitless images have been measured wherever possible, the results should not be taken too literally. The mean of the inner and outer diameters for a given image probably yields a good value of the mean diameter. However, the cumulative errors of seeing and guiding, as judged by the widths of the spectra of the central stars, apparently amount to about 2 or 3 seconds of arc. Thus, for example, the fact that the measured outer diameters of the [*Ne* v] images exceed the measured inner diameters of the [*Ne* III] images is probably to be attributed to lack of resolution rather than to a physical overlapping of *Ne* v and *Ne* III in the nebulae. Also, the differences of measured outer and inner radii cannot be used to derive the true thicknesses of the nebular shells.

TABLE 15

SLITLESS IMAGE DIAMETERS OF INNER RING IN NGC 7662 AS A FUNCTION OF TOTAL EXCITATION

Element	Outer Diam.	Inner Diam.	Total Excitation (Volts)
H	13".9 (18)	7".9 (15)	13.5
He I	14.8 (2)	9.2 (1)	24.5
[*O* III]	14.1 (7)	8.3 (7)	48.6
[*Ne* III]	14.7 (3)	8.4 (3)	62.4
He II	12.1 (4)	7.0 (3)	78.6
[*A* IV]	12.7 (4)	6.4 (2)	84.0
O III	12.7 (12)	7.6 (11)	85.6
[*Ne* V]	9.1 (3)	4.4 (3)	222

Because it was convenient to do most of the measuring of slitless spectrograms in the direction of dispersion, there are few data on image sizes of [*O* II] and [*N* II]. For the ring nebulae, pending a more exact investigation, the following statements may, however, be made: The general patterns of the [*O* II] and [*N* II] images are very similar, if not identical. In some double-ring nebulae these radiations appear in both inner and outer rings (e.g., NGC 2392); in others only in the outer ring (NGC 7662). The general patterns in the outer rings are the same for all radiations, but more detail appears in [*N* II] and [*O* II] lines than in any others. There are, moreover, no significant differences in diameter of the outer rings between any of the particles emitting there.

III. DISCUSSION

a) FREQUENCY DISTRIBUTION OF RELATIVE INTENSITIES OF COMPONENTS OF DOUBLE LINES

Data on the distribution of V/R extracted from Table 3 are summarized in Table 16. Although the numbers involved are too small to have much statistical significance, no correlation between V/R and the degree of excitation is evident. If there were any appreciable general absorption in the nebulae, one would expect a preponderance of nebulae with $V/R > 1$. Since the number with $V/R > 1$ equals that with $V/R < 1$, the proper conclusions probably are that the nebulae are transparent in the observable spectral

range and that the value of V/R observed in any particular case depends upon nonuniform distribution of the nebular material and upon the direction of the observer.

b) FREQUENCY DISTRIBUTION OF $\overline{\Delta V}$

The eighteenth column of Table 3 contains the mean ΔV for H, [*O* III], and [*Ne* III]. This quantity, here referred to as $\overline{\Delta V}$, is apparently the most reliable measure of the velocity of expansion. Its frequency distribution is indicated roughly in Table 17. While the numbers of nebulae involved are again too small for reliable conclusions, there may be a trend toward smaller velocities of expansion as the nebular excitation decreases.

c) ANOMALOUS ΔV VALUES

In a simple expanding shell or cloud of gas, all particles should yield the same value of ΔV. Table 3 shows, however, that for many nebulae the ΔV's for different particles

TABLE 16

FREQUENCY DISTRIBUTION OF V/R

V/R	Excitation			Total	V/R	Excitation			Total
	High	Med.	Low			High	Med.	Low	
>1	2	3	1	6	1	2	3	0	5
<1	3	3	0	6	*	2	2	1	5

* Violet components stronger at one end; red components at the other.

TABLE 17

FREQUENCY DISTRIBUTION OF $\overline{\Delta V}$ IN VARIOUS NEBULAE

$\overline{\Delta V}$ (Km/Sec)	Excitation			Total	$\overline{\Delta V}$ (Km/Sec)	Excitation			Total
	High	Med.	Low			High	Med.	Low	
<20	0	2	1	3	40–60	6	4	1	11
20–40	3	6		9	>60	1	1		2

often differ considerably. The most outstanding anomalies are the low values of [*Ne* V], on the one hand, and the high values of [*O* II], [*N* II], and a few other low-excitation particles, on the other.

Analysis of the data indicates the following nearly general rule: Where differences in component separation exist in the spectrum of a planetary nebula, the high-excitation particles show smaller separations, and the low-excitation particles higher separations, than [*O* III] and [*Ne* III]. To this rule there is one universal exception: Hydrogen, which requires less excitation than either [*O* II] or [*N* II], always agrees closely in separation with the much more highly excited ions [*O* III] and [*Ne* III].

For five of the high-excitation nebulae, ΔV is plotted against excitation in Figures 3–6. In every instance there is an unmistakable, though irregular, trend downward toward the right. An isolated exception to the general relationship between component separation and excitation is offered by HD 184738, where the [*S* II] lines exhibit con-

siderably less separation than do those of *H*. This behavior, which seems to be real, is opposite that in NGC I 418.

In five out of eight nebulae in which at least one of the [*Ne* v] lines has been observed, these lines are not resolvable into components, although for the same nebulae the $\overline{\Delta V}$ values range from 37 to 107 km/sec. An inspection of close pairs of lines in the iron-arc comparison shows that, under favorable circumstances of image density and nearly equal intensity, pairs separated by as little as 0.015 mm can clearly be distinguished as double on fast plates. Thus, for the most favorable cases, unresolved [*Ne* v] lines probably indicate a corresponding ΔV of not over 10 km/sec. Where the lines are inherently somewhat diffuse or short (small nebulae), the limiting ΔV must be greater, and spectra of higher dispersion will be required to gain further information.

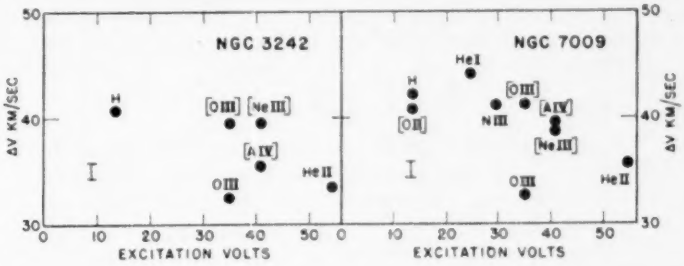

FIG. 3.—Separations of components of nebular lines as a function of excitation for NGC 3242 and NGC 7009. In this and the next three figures the short vertical lines indicate the mean mean deviations.

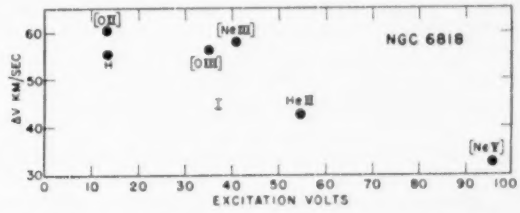

FIG. 4.—Separations of components of nebular lines as a function of excitation for NGC 6818

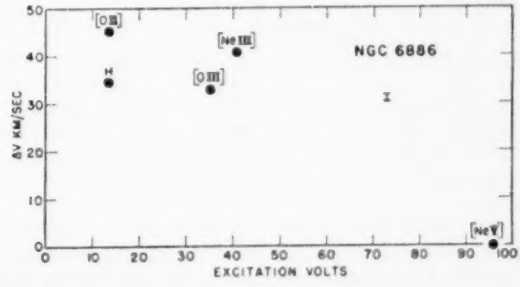

FIG. 5.—Separations of components of nebular lines as a function of excitation for NGC 6886

Among the forbidden lines there is no evidence for any major correlation of component separation with transition probability. The [*O* II] lines λ 3726 and λ 3728, which often show larger ΔV's than those of any other lines, have very small transition probabilities of the order of 8×10^{-5}, while those of λ 3346 and λ 3426 of [*Ne* V], which yield small ΔV's, are 0.11 and 0.31, respectively.[11] The transition probabilities for the [*S* II] lines are, however, almost identical with those of [*Ne* V], and in NGC I 418 the ΔV for [*S* II] greatly exceeds that for [*O* II].

Further data bearing on this question are available from the forbidden lines of *O* III (Table 18). In every nebula the lines λ 4959 and λ 5007 agree more closely with each

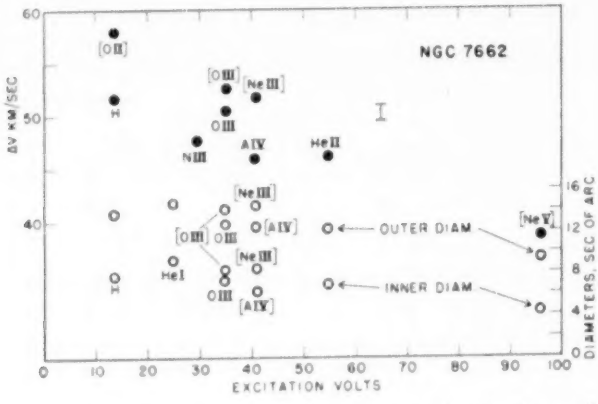

FIG. 6.—Separations of components of nebular lines (*above*) and inner and outer diameters (*below*) as a function of excitation for NGC 7662.

TABLE 18

COMPONENT SEPARATIONS FOR [*O* III] LINES
(Km/Sec)

λ	Trans. Prob.	NGC 3242	NGC 6210	NGC 6818	NGC 7009	NGC 7662
4363	2.8	38.0 ± 1.2 (7)	40.3 ± 0.8 (3)	62.0 ± 2.0 (2)	38.8 ± 1.3 (4)	53.2 ± 1.9 (5)
4959	0.0056	39.7 ± 1.0 (9)	44.3 ± 2.5 (4)	55.3 ± 1.9 (5)	42.4 ± 2.2 (4)	52.4 ± 1.1 (6)
5007	0.016	40.7 ± 1.2 (9)	43.6 ± 1.2 (2)	54.9 ± 1.8 (5)	42.5 ± 1.3 (3)	52.6 ± 2.4 (4)

other than they do with λ 4363. Since the latter is always much weaker on the spectrograms, the apparent differences may be due merely to a systematic error in measuring, or they may be traceable to the fact that λ 4363 requires over twice as much energy from electron impact as do the other lines. In any event, while the reality and significance of the differences shown in Table 18 are a subject for future investigation, it seems safe to conclude that transition probability, by itself, is not a major factor in determining ΔV.

d) COMPONENT SEPARATION AND MONOCHROMATIC IMAGE SIZE

Since large differences in component separation have been demonstrated for some of the nebular constituents, it becomes important to see whether the separations and the

[11] S. Pasternack, *Ap. J.*, 92, 129, 1940. All transition probabilities quoted here are from this paper.

dimensions of the corresponding monochromatic nebular images are correlated. The greatest leverage will be obtained by examining images for which ΔV differs most widely from $\overline{\Delta V}$. For the high-excitation nebulae this requires a comparison of the images of [*Ne* v] with those of *H*, [*O* III], and [*Ne* III].

Data assembled from the various tabulations in Section II*b* are given in Table 19. It must be realized that this material is not highly accurate. Much of it is based on measures of single spectrograms, and some error has been introduced by unavoidable comparisons between images of unequal density. To minimize this effect, only means of *Hδ* and λ 4363 [*O* III] have been utilized to form $\bar{D}$ in several instances.

Table 19 shows that in the high-excitation group [*Ne* v], which always has a smaller component separation, also always gives a smaller monochromatic image. Numerically, however, no close correlation between differences of ΔV and differences of image size is apparent. The best data are for NGC 2392 and NGC 7662. In the former a very large difference in ΔV corresponds to a small difference in image diameter. Just the reverse is true for NGC 7662.

TABLE 19

COMPARISON OF IMAGE DIAMETERS OF [*Ne* V] WITH MEANS FOR *H*, [*O* III], AND [*Ne* III]

NEBULA NGC	ΔV (KM/SEC)		DIAMETERS (SEC. OF ARC)			
			[*Ne* v]		$\bar{D}$	
	[*Ne* v]	$\overline{\Delta V}$	In	Out	In	Out
2165	0:	40.0	.....	3.4	.....	5.5
2392	0:	107.3	5.0	11.8	6.2	12.4
6818	32.6	56.5	.....	10.8	.....	17.3
6886	0:	37.1	.....	3.1	.....	3.5
7662	38.6	52.2	4.4	9.1	8.1	14.0

In the medium-excitation group data are available only for NGC 6210. As pointed out in Section II*b*, this nebula gives a ΔV for [*O* II] nearly 30 km/sec greater than $\overline{\Delta V}$, yet the [*O* II] and [*Ne* III] images differ in diameter very slightly, if at all.

For the low-excitation nebulae, similar results hold. In NGC I 418 the slitless images of [*O* I] and [*S* II] are only about 10 per cent larger than those of *H* and [*O* III], whereas the ΔV's must differ by a factor of at least 3 or 4. Again, in HD 184738, slitless images of [*O* II], [*S* II], and *H* differ inappreciably in size, although there is a range of 13 km/sec in the corresponding ΔV's.

To sum up the evidence, there is generally a positive correlation between component separation and monochromatic image size for nebulae of all degrees of excitation. Usually, though not always, differences in image size are much less than differences in separation.

In NGC 7662—the only nebula for which the data justify a detailed comparison of ΔV with image diameter—the ratio of the diameters of the *H* and [*Ne* v] images considerably exceeds the corresponding ratio of the ΔV's. Component separations and inner and outer diameters of slitless images (*inner ring*) are plotted against excitation for this nebula in Figure 6.

e) VELOCITY DIFFERENCES AND THE FLUORESCENT EXCITATION OF *O* III AND *N* III

The fluorescent mechanism proposed by Bowen[1] to account for the production of the permitted lines of *O* III and *N* III requires an intimate connection between these particles and *He* II. It is generally believed that there are large differences in monochromatic image size between *He* II and [*O* III] and that the *O* III images agree in size with those of *He* II. If this were true, it would, of course, provide strong evidence for the mechanism proposed by Bowen, but my observations do not bear out the previously observed differences.

Permitted lines of *O* III are found only in high-excitation nebulae, most of which show a ring or double ring structure (Table 3). In the double ring nebulae, the dimensions of the bright inner rings are nearly the same for *He* II, [*O* III], and *O* III (Tables 9 and 15). The outer, fainter rings are generally missing in *He* II and *O* III but quite strong for [*O* III], as illustrated for NGC 7662 in Figure 1*g*. Presumably, on small-scale slitless spectrograms, the distinction between inner and outer rings has not been clear, and this fact has led to the misconception noted in the preceding paragraph.

The wave length of Ly-α of *He* II is 303.779 A, while that of the most nearly coincident line of *O* III is 303.799 A. Hence the most favorable situation for the fluorescent

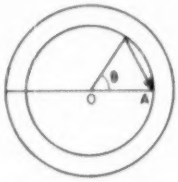

FIG. 7.—Excitation of *O* III by *He* II in absence of thermal motions or velocity gradients

exchange of energy would be that in which the *O* III ion has a velocity of recession of 20 km/sec from the *He* II. If all *He* II and *O* III ions had the same outward velocity, the operation of the process would be severely limited. In fact, the only *He* II capable of exciting *O* III at point *A* (Fig. 7) would be located in a zone such that θ is equal to 60° if the common outward velocity is 20 km/sec.

Thermal motions and velocity gradients within the various nebular shells can greatly increase the effectiveness of the exchange mechanism. At 10,000°, the mean thermal velocities of *He* and *O* are about 6 and 3 km/sec, respectively, and, in addition, there are probably outward velocity gradients of several km/sec through the *He* II and *O* III zones.

From Table 15, it is probable that the permitted oxygen shell is intermediate in size between those of *He* II and of forbidden oxygen. Moreover, the data of Table 3 indicate that the *O* III velocities agree more closely with those of *He* II than do the [*O* III] velocities. Apparently, therefore, the velocity increases outward through the region where *O* III can exist, and it is in the *inner* portion of this region, adjacent to the bright *He* II shell, that the fluorescent mechanism operates. Since the velocity gradients by themselves would be most effective in causing excitation of the *outer* portions of the *O* III region, it seems probable that they are not of much consequence in the process and that thermal motions are largely responsible. This would be even more likely if the temperature in the bright *He* II zone were higher than 10,000°.

f) CHARACTER OF THE NEBULAR LINES

In many of the nebulae the components of the nebular lines are quite sharp. In fact, where the image density is favorable, many of the nebular lines are as well defined as those in the *Fe* comparison spectrum, and their apparent width must depend largely

upon the resolving power of the emulsion. This observation, though only qualitative as yet, eliminates the possibility of any large-scale turbulence. It eliminates also the possibility that the regions of line formation contain any large velocity gradients. These statements must not be taken as applying equally to all the nebulae or to all lines. There are some real, though not large, differences in line quality whose quantitative investigation is a task for the future.

There is, moreover, one general exception to the sharpness of the nebular lines. In every instance the components of the hydrogen lines are noticeably more diffuse than those of any other element. The line λ 4686 of *He* II often appears somewhat diffuse also, although the fine structure of this line (about 0.1 A between the main components) may be responsible. From the few examples of *He* I lines of adequate strength, I suspect that they, too, show some lack of sharpness.

g) NEBULAR DYNAMICS

A successful theory of the dynamics of the planetaries must be able to account for the anomalous component separations of various lines and for the correlations between component separation and image size discussed in Sections III*c* and *d* and for the differences in line quality noted above.

Two additional points should be kept in mind while considering nebular dynamics. The first is that amorphous (i.e., neither ring nor highly irregular) forms seem to be restricted to the planetaries of moderate excitation. Among the high-excitation nebulae of Table 3, only one, NGC 6886, has been classified as amorphous. This is a very small nebula, however (Table 13), and may well have a ring structure which has been lost in the errors of seeing and guiding.

The second point is that measured displacements of absorption lines in the nucleus of NGC 2392 almost certainly require the interpretation that this object is ejecting matter at the present time.[9] While this knowledge is restricted to one nucleus, which may or may not be typical, it should not be entirely disregarded.

Cosmological determinations of abundances of the chemical elements indicate that a fair estimate of relative masses of atomic species in the nebulae would be: *H* ∼ 60 per cent, *He* ∼ 40 per cent, all others together about 1 or 2 per cent.[12] With such a distribution, one would expect *H* and *He* to exert an overwhelming influence in determining the motions of the nebular material. Therefore, when it is observed that some relatively rare ion has an expansion velocity differing widely from that of *H-He*, there are two possible conclusions: (1) The velocity given by the lines of the rare ion is the same as that of *H-He* in the region where the lines of the rare ion are produced, where, for some reason such as level of excitation, the *H-He* velocity is not directly observable; or (2) selective forces act upon the rare ion and maintain it in relative motion with respect to *H-He*.

Possibility 1 carries the implication that the true expansion velocity (of *H-He*) is far from constant throughout many of the nebulae, while under 2 the *H-He* velocity may or may not be constant. In this respect the two possibilities do not seem to be necessarily mutually exclusive; both effects might contribute to give a resultant observed ΔV for a specific ion, or the first effect might predominate for some ions and the second for others. For simplicity we shall, however, investigate the two possibilities separately.

Consider the high-excitation ring nebulae. In a typical object of this group, there is a shell of matter, evidenced by the [*Ne* V] lines, which lies just inside the bright *He* II and *H* shells but which has a much smaller expansion velocity. How can this situation, which constitutes the outstanding anomaly of the high-excitation nebulae, have arisen?

Under 1 there are two distinct possibilities. The first is based on the assumption that the high-excitation ring nebulae are the result of two separate ejections of shells of dif-

[12] See, e.g., Aller and Menzel, *Ap. J.*, **102**, 239, 1945.

ferent velocity. If the matter represented by [*Ne* v] was ejected later and at a higher velocity than that in the bright *H* and *He* II shells, it must have been slowed down greatly as it overtook the first shell. It is difficult to think of a mechanism which could have brought about this result. If the bright shells of *H* and *He* II represent a second, faster ejection, it must be concluded that the second shell penetrated through the first without much interaction between the two. This could happen only if the shells were not much thicker than the mean free paths of the particles, which are of the order of 10^{12} cm or less, with the usually accepted nebular densities; and such thin shells seem to be entirely inconsistent with observed nebular magnitudes. Moreover, in either form of the two-shell hypothesis, one might reasonably expect to find more of a range in relative radii of the two shells than is observed. Altogether, the assumption of two distinct shells does not look promising.

The second possible explanation under 1 is based on the assumption of a single thick shell and is illustrated by the schematic cross-section shown in Figure 8, in which *A* represents the inner boundary of the thick shell. The innermost *observable* zone is that of [*Ne* v] at *B*. Emission of *H* and *He* II must be very slight in the region from *A* through *B*, and the most likely reason is that the electron temperature, as well as the degree of

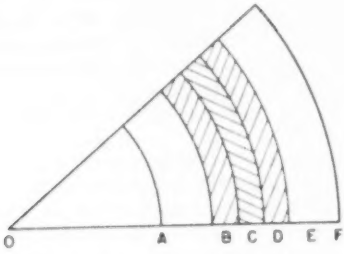

FIG. 8.—Schematic hypothetical cross-section of high-excitation planetary nebula

ionization, is very high. In fact, in this region conditions must resemble those in the solar corona, although they are less extreme, since *Fe* X does not appear to be present in the planetaries.

Inward from *B* one would expect zones of more highly excited ions in this order: *Mg* V, *Al* V, *Ne* VI, *Na* VI, *Mg* VI, *Al* VI, *Na* VII, *Mg* VII, *Al* VII, etc. Some of these ions, notably *Na* VI, *Mg* V, VI, and VII, *Al* VI and VII, possess metastable levels yielding forbidden lines in the unobservable 2000 A region. It is possible, therefore, that these ions could exert a cooling effect on the electrons in their respective zones. The actual amount of such cooling would depend upon unknown parameters: the collisional cross-sections, the abundances of the ions in question, and the electron temperature and density. There is at least a possibility, therefore, that *Te* increases inward from the [*Ne* v] zone.

The material from *A* through *B* has an outward velocity equal to that measured for [*Ne* v], which, in some cases, is very low, probably not more than 5 km/sec. Moreover, owing to the scarcity of ground state *H* and *He* II in this region, the opacity for nuclear radiation below λ 912 A is low, and the matter acquires but little momentum from the outflowing radiation.

Ions of *Mg* V should occur just inside the *Ne* V zone and those of *Ne* IV just outside. All three of these ions can cause cooling of the electrons, and it must be supposed that the reduction in *Te* in this general region is sufficient to produce a large increase in the recombination rate of *He* II, which results in the bright *He* II shell at *C*. As soon as this occurs, the opacity short of λ 228 A rises, and *He* II picks up momentum from the nuclear radiation and is accelerated outward. Since *He* is very abundant, collisions probably in-

sure that in zone C the momentum acquired by *He* II is shared by H and the other nebular constituents.

Nuclear radiation passing through zone C is considerably depleted or, in some cases, eliminated entirely for wave lengths below 228 A, and this depletion permits formation of *O* III and *Ne* III in appreciable quantity in zone D. These two ions, particularly *O* III, are very effective electron cooling agents. T_e, therefore, is further reduced in zone D to the point where there is a large increase in recombination rate for H. Most of the nuclear radiation between λ 912 A and λ 228 A is therefore absorbed in zone D and produces here the bright inner rings of H, [*O* III], and [*Ne* III]. At the same time, the momentum of the radiation is transferred to the gas, which thereby acquires a further increase in outward velocity.

Finally, zone E, with outer boundary at F, is the faint outer ring. It is not clear whether F is a real physical boundary marking the limit of the nebular material or whether it is determined by quenching of the exciting radiation somewhat in the manner discussed by B. Strömgren for interstellar hydrogen.[13] If the absorption of nuclear radiation is incomplete in zones C and D, there may be enough leakage to account for the excitation in zone E. This is probably the case for nebulae in which λ 4686 *He* II occurs in the outer ring, e.g., NGC 2392. In NGC 7662, on the other hand, even long exposures fail to show a trace of λ 4686 in the outer ring. For such nebulae the outer rings are probably excited by radiations such as Ly-α of *He* II produced in zone C.

While the foregoing picture does not appear unreasonable, a detailed analysis would be required in order to see whether the various processes would actually occur in the manner indicated. Without attempting such an analysis, however, a rapid check may be obtained from momentum considerations in the following way:

The total number of quanta emitted per second by the central star of radius R and temperature T in the frequency interval $d\nu$ is given by

$$\frac{8\pi^2R^2k^3}{c^2h^3}T^3\frac{x^2}{e^x-1}\,dx\,, \qquad x=\frac{h\nu}{kT}. \tag{1}$$

For the same frequency interval the total momentum flux is found by multiplying equation (1) by $h\nu/c$, which gives

$$\frac{8\pi^2R^2k^4}{c^3h^3}T^4\frac{x^3}{e^x-1}\,dx\,. \tag{2}$$

The total radiative momentum flux from x_0 to ∞, then, is

$$F_0=\frac{8\pi^2R^2k^4}{c^3h^3}T^4\int_{x_0}^{\infty}\frac{x^3}{e^x-1}\,dx\,, \tag{3}$$

the integral in which has been tabulated by Zanstra.[14]

In equation (3) let $R=R_\odot=7\times10^{10}$ cm, $T=10^5$. Then, for frequencies short of λ 228,

$$F_0(H\epsilon)=1.4\times10^{26}\ \text{gm}\cdot\text{cm}\cdot\text{sec}^{-2}$$

and for frequencies between λ 912 and λ 228,

$$F_0(H)=9.0\times10^{26}\ \text{gm}\cdot\text{cm}\cdot\text{sec}^{-2}\,.$$

In the foregoing model, continuity requires that the total number of particles flowing across any spherical surface concentric with the nucleus be constant. Let such a surface

[13] *Ap. J.*, **89**, 526, 1939.

[14] *Pub. Dom. Ap. Obs. Victoria*, **4**, 209, 1929.

have radius r_1, where the outward gas velocity is V_1. Then the total number of particles flowing across the surface per second is $4\pi r_1^2 n_1 V_1$, and the momentum carried by the particles is

$$4\pi r_1^2 n_1 m V_1^2 , \tag{4}$$

where n_1 is the number of particles per cubic centimeter and m is their average mass. Across some adjacent spherical surface, where the particle density and velocity are different, the momentum flux will be

$$4\pi r_2^2 n_2 m V_2^2 . \tag{5}$$

Since r_2 is not much different from r_1, the change in the momentum flux carried by the gas may be written

$$\Delta F_G = 4\pi r^2 m (n_2 V_2^2 - n_1 V_1^2) ,$$

or, since $n_1 V_1 = n_2 V_2$,

$$\begin{aligned} \Delta F_G &= 4\pi r^2 n_2 V_2 m (V_2 - V_1) \\ &= 4\pi r^2 n_2 m V_2 \Delta V . \end{aligned} \tag{6}$$

According to the model under discussion, ΔF_G should be comparable in magnitude with the radiative momentum fluxes F_0 found above. From the data of Table 3 it is evident that for a rough calculation both ΔV and V_2 may be taken as being of the order of 10 km/sec. We also adopt the values $r = 10^{17}$ cm, $n_2 = 10^3$ cm^{-3}, and $m = m_H = 1.7 \times 10^{-24}$ gm and find, from equation (6),

$$\Delta F_G = 2 \times 10^{26} \text{ gm} \cdot \text{cm} \cdot \text{sec}^{-2} .$$

The agreement between ΔF_G and F_0 is close enough, considering the very approximate character of the calculations, to lend considerable weight to the belief that the processes considered in this model may be essentially correct.

From Table 3 it is seen that [O II] gives a larger expansion velocity than *H* for some of the high-excitation ring nebulae, although the differences are much less than some of those found in nebulae of lower excitation. If these [O II] velocities are a measure of the general motion of the nebular material in the region where the [O II] lines are formed, they can perhaps be interpreted in the following way:

Presumably O II occurs in the outer portion of zone *D*. In this region the hydrogen, which has been undergoing acceleration throughout the entire zone, has attained a velocity greater than that given by the separations of the components of the hydrogen lines, which measures the mean velocity for the zone. If this is indeed true, then the widths of the components of the hydrogen lines should be great enough to include the separations of the [O II] lines. I should be inclined to guess that this will prove to be the case, judging by the diffuse character of the hydrogen components; but accurate photometry of the lines of specific nebulae will be required to settle the point.

In the preceding paragraph it was implied that the widths of the hydrogen components are caused by a velocity gradient through the hydrogen emission zone which is due to a gradual increase in outward velocity as the nuclear radiation is depleted. Another possible source of velocity gradient is the pressure of Ly-α resonance radiation. For *He* II and *H* the widths, $\Delta\lambda_D$, of the Ly-α lines, λ 304 and λ 1215, are 13 and 26 km/sec, respectively, at $T = 10^4$. According to Chandrasekhar,[7] if the differential velocities between the inner and the outer boundaries of a nebular shell are about 3.5 times the widths of the undisplaced lines, the pressure of resonance-line radiation is reduced by a factor of the order of 10^4 and becomes unimportant through much of the shell. For this to be true in the planetaries would require that the widths of the components of the *H*

and the *He* II lines be about 83 and 46 km/sec, respectively. Both the *He* II and the *H* lines are widened appreciably, but the amount of widening can hardly exceed about half the above values at most.

More recent work by Zanstra[15] indicates a further reduction in the Ly-α pressure by a factor of the order of 300, owing to the fact that the scattering of resonance radiation must take place with an almost complete redistribution of frequency. Under these circumstances an exact evaluation of the role of Ly-α pressure does not at present appear possible, although the indications are that it is probably not of very great importance.

In this connection a suggestion by Bowen is of interest. *He* II near the inner boundary of the shell, in the [*Ne* V] zone, can absorb Ly-α originating in the corresponding region on the opposite side of the nebula because of the low expansion velocity. Such ions are thus subject to an outward radiative pressure due to Ly-α. They may also, however, absorb to some extent the inward-flowing Ly-α flux originating in the bright *He* II shell. It is possible that this may result in a self-regulating mechanism which is, indeed, responsible for the fact that low expansion velocities are observed to be common in the [*Ne* V] zones of the high-excitation ring nebulae. There are at least two possible difficulties involved in this idea. First, the density of *He* II in the [*Ne* V] zone may be quite low; second, if *Te* is high, the majority of captures will tend to take place directly to the ground state, and the production of Ly-α may not be sufficiently large. A detailed analysis of the feasibility of this mechanism is necessary but is outside the scope of this paper.

The probable time sequence of development of a nebula of the type considered here is of interest. If the widths of the nuclear emission bands are a measure of the outward velocities near the central star, the material must be ejected at velocities of the order of 50–100 km/sec. These velocities are subsequently reduced, perhaps by gravity, in some cases to very low values, probably less than 5 km/sec. Presumably, after a time the ratio of the forces of gravitation and radiation pressure will become and remain constant as long as the physical state of the nebular material does not change, and the gas will drift slowly outward. During this stage the excitation and electron temperature are both so high that the nebula emits very little visible radiation and is, indeed, fairly transparent to the ultraviolet nuclear radiation. It may be possible, in this way, to account for the scarcity of high-excitation amorphous nebulae.

Finally, the ejection of matter from the nucleus must be supposed to cease, for reasons which will be made clear later, and the thick nebular shell expands slowly. Ultimately, perhaps because of the decrease in dilution factor, the general excitation level in the outer portion of the shell decreases to the point where *Ne* V and ions of similar ionization potential become common. The nebular material continues to flow through the *Ne* V zone, and thereafter the processes assumed previously produce the various bright shells of *He* II, *H*, [*O* III], etc. This stage of the nebula would be semipermanent. The inner boundary (*A*, Fig. 8) continues to move outward with a low velocity; the various bright shells maintain a constant distance from the nucleus while the gas flows through them. The outer boundary, *F*, will move outward with a large velocity if it is the real physical terminus of the nebular matter; otherwise, if it is a Strömgren boundary, it, too, will remain fixed in space.

Eventually, the inner boundary of the shell, *A*, arrives at the [*Ne* V] zone, *B*. By this time the real physical extent of the shell is much greater than the radius of zone *B*. The next stage, therefore, is probably a large nebula of reduced surface brightness and lower excitation, perhaps resembling the ring nebula in Lyra.

The lower-excitation amorphous nebulae are presumably those in which the central star does not have enough ultraviolet radiation to produce particles of excitation higher than *Ne* III and in which the nebular material extends to the surface of the nucleus, or

[15] *B.A.N.*, 11, 401, 1949.

nearly so. Because of the presence of *O* III throughout the nebula, *Te* is everywhere low, and the opacity of the material for the ultraviolet nuclear radiation is fairly high throughout. Under these circumstances it is not immediately evident what the resultant motion will be. If the momentum acquired from the radiation per unit time by a given element of mass varied as r^{-2}, the velocity would be uniform. In these objects also, however, it appears likely that the widths of the hydrogen lines are sufficient to include the separations of [*O* II] and [*N* II]. If so, the ΔV's for these particles presumably indicate the hydrogen expansion velocity in the outer fringes of the nebulae, and it is probable that the hydrogen velocity increases outward.

While the foregoing model appears promising, it offers many difficulties. In equation (3) the rather arbitrary choices of $R = R_\odot$ and $T = 10^6$ gave a momentum flux of the right order, but such a value of T is much too low to account for the suppression of emission of *H* and especially of *He* II inward of zone *C*. A decrease of R to $1/10\ R_\odot$ or less and a corresponding increase in T would maintain the momentum balance and might be carried to the point where a sufficiently high electron temperature would exist in the inner layers of the nebular shell. Such high effective temperatures for the nuclei are, however, entirely inconsistent with what is known of their spectra. For example, the absorption lines in the nucleus of NGC 2392 are an excellent match, both in shape and in intensity, with those of 10 Lacertae, a star whose effective temperature is generally considered to be about 30,000°.[16] This discrepancy may, of course, merely be additional strong evidence that the planetary nuclei radiate in a manner widely different from a black body.

Another difficulty involves the widths of the [*Ne* V] lines. According to the above model, these lines are formed in a region where *Te* is still high enough to suppress emission of *He* II, i.e., where *Te* must be well in excess of 10^6 degrees. Such high kinetic temperatures should be sufficient to widen the [*Ne* V] lines appreciably; yet no widening is apparent by inspection. The slit width used for the spectrograms employed in this investigation corresponds, however, to 15 km/sec at λ 3500. This is also about the smallest line width which can be recorded by the emulsions used. Hence the intrinsic width of a [*Ne* V] line would probably have to be greater than 20 km/sec before it would appear appreciably widened. The apparent sharpness of the [*Ne* V] lines may thus offer no difficulty, but the matter requires careful future investigation.

While the nebular model based on the assumption that expansion velocities of all ions really measure the *H-He* velocities in the zones where the ions radiate is successful to some degree, it encounters the difficulties noted above and, in addition, provides no logical place for the observations of the nucleus of NGC 2392. This nucleus is at present ejecting matter, according to the simplest interpretation of the observed absorption-line displacements, a fact which suggests the desirability of a brief investigation of a model based on the following assumptions:

The nuclear star ejects continuously, and the expansion velocity is approximately constant throughout the nebula except, perhaps, in the immediate vicinity of the nucleus. To account for the [*Ne* V] anomaly on this basis, it is evident that hypothesis 2 will be employed, namely, a selective force must be found which can maintain *Ne* V in relative motion with respect to *H* and *He*.

For steady outward flow,

$$n V r^2 = \text{Const.}, \tag{7}$$

where n is number of particles per cubic centimeter, V is velocity, and r distance from the center. If the velocity is constant,

$$n r^2 = C\ . \tag{8}$$

[16] L. H. Aller, *Ap. J.*, **109**, 179, 1949.

The total number of particles between inner and outer radii, r_1 and r_0, then, is

$$N = 4\pi C \int_{r_1}^{r_0} dr = 4\pi C (r_0 - r_1), \tag{9}$$

and the total number per square centimeter radial column is given by

$$\frac{N}{\text{cm}^2} = C \int_{r_1}^{r_0} \frac{dr}{r^2} = C \left(\frac{1}{r_1} - \frac{1}{r_0} \right). \tag{10}$$

The formation of bright rings in such a nebula must be supposed to result from processes much like those discussed for the preceding model. Although the ionization is presumably very high in the inner portions of the nebula, the opacity below λ 912 will build up gradually and, together with decreasing dilution factor, will finally reduce the level of ionization to the point where *Ne* V, etc., can exist. From that point on, bright rings of *He* II, *H*, [*O* III], etc., will presumably be formed. In the present model, however, the expansion velocity is approximately constant throughout, and there is no place for zones where large fractions of the nuclear ultraviolet energy are absorbed with resultant major velocity changes. In fact, it must be assumed that the energy which is transformed in, say, the bright hydrogen ring into observable radiation is mostly transported by inflowing highly ionized material rather than by the flux of ultraviolet radiation from the nucleus. This could be true only if the absorption of nuclear radiation below λ 912 were already fairly complete at the radius of the bright hydrogen ring.

If the ring nebulae are hollow shells, then, as was shown by Milne, the net flux of any radiation originating in the nebula is zero at the inner surface of the shell.[17] But, if the space within the bright rings is filled with matter and if the opacity within the Lyman continuum is considerable at the radius of the hydrogen ring, the conditions on which Milne's theorem is based no longer hold. In fact, the result must be that there is an inward flux of Lyman continuous radiation near the inner boundary of the hydrogen shell because the outward flux from the opposite side of the nebula is cut down by the intervening opacity. This inward flux would have little influence on the hydrogen approaching it from inside, since very few of these particles are in the ground state. However, for *Ne* V or similar ions having strong resonance lines within the Lyman continuum, such a flux might conceivably be the source of the required selective forces. If so, the momentum acquired per unit time by a *Ne* V ion from the inward flux of Lyman continuum must approximately equal the outward momentum transfer due to collisions with the outflowing *H-He*.

If a neon ion is held approximately stationary against an outward flux of ionized hydrogen of density n cm^{-3} and velocity V, the number of collisions per second with hydrogen ions will be

$$N_c = n \sigma V, \tag{11}$$

where σ is the effective cross-section. Ordinary kinetic-theory values of σ for uncharged particles are about 10^{-16} cm^2. Because of coulombic interactions, one would expect a rather larger value of σ for encounters between ions. In fact, the Rutherford expression for the cross-section for scattering,

$$\sigma = \frac{(e_1 e_2)^2}{4 m^2 V^4 \sin^4 (\theta/2)},$$

gives $\sigma \sim 10^{-14}$ cm^2 with $e_1 = 4e$, $e_2 = e$, $V = 10^6$ cm/sec, and $\theta = \pi/2$; and this value is adopted for an approximate calculation. If it be further assumed that each collision

[17] *Zs. f. Ap.*, **1**, 98, 1930.

results in complete transfer of the proton momentum to the *Ne* v, in order to err on the side of overestimating the effect, one finds that the momentum transfer per *Ne* v ion per second is

$$m_H V_H N_e \sim 10^{-23}\ \text{gm} \cdot \text{cm} \cdot \text{sec}^{-1}$$

for a relative velocity of 10 km/sec.

Ne v has several strong resonance lines in the λλ 500–600 region of the spectrum. Each quantum of energy absorbed in one of these lines from the inward flux of Lyman continuum provides a *Ne* v ion with about 10^{-21} c.g.s. momentum units. The ion would therefore have to absorb about one quantum every 10^2 seconds to balance the outward collisional momentum transfer.

For a hydrogen density of 10^3 cm^{-3} and outward velocity 20 km/sec, the flux of hydrogen ions into the zone of hydrogen emission amounts to 2×10^9 ions per square centimeter per second. In the limiting case each ion would produce one quantum of Ly-α on recombining, and the maximum flux of Ly-α from the bright hydrogen zone would be of the order of 10^9 quanta per square centimeter per second, in the steady state, if there were no flux from the opposite side of the nebula.

Suppose, for the moment, that *Ne* v possesses a resonance line of the same wave length as Ly-α, and let τ and τ^1 be the mean lifetimes in the upper state and in the ground state of the line, respectively. Then, for an atom exposed to radiation from one side only, it follows that[18]

$$\frac{\tau}{\tau^1} = \tfrac{1}{2} I \frac{c^2}{2h\nu^3},$$

and, since I = flux $\div \pi \sim 10^9$ quanta per second,

$$\frac{\tau}{\tau^1} \sim \frac{10^9 h\nu c^2}{2h\nu^3} \sim 10^{-1}.$$

Since $\tau \sim 10^{-10}$ sec, $\tau^1 \sim 10^{-9}$ sec, i.e., the *Ne* v ion would make about 10^9 absorptions per second, under the conditions of maximum Ly-α flux, if it had a resonance line coinciding with Ly-α. Since only about 10^{-2} absorptions per second are required in order to balance the outward momentum transfer by collisions, it would appear that the process considered here is a feasible one if only a very modest fraction of the total radiation from the hydrogen zone appears in the form of Lyman continuum.

While this second model may be a physically possible one, it runs into precisely the same difficulties as those noted previously for the first model, even including the one concerning the observations on the nucleus of NGC 2392. From equation (8), for $n = 10^3$ cm^{-3} and $r = 10^{17}$ cm, one finds $C = 10^{37}$. Then, from equation (10), the number of particles per square centimeter radial column is $N/\text{cm}^2 = 10^{37}([1/r_1] - [1/r_0])$. If the material is highly ionized inward of the bright hydrogen ring, the number of free electrons may be taken to be equal to the number of particles, and, moreover, the only important source of general opacity will be electron scattering whose coefficient is 7×10^{-25}. Hence the distance to which one may see inward along a radius from the hydrogen shell is determined approximately by the expression

$$10^{37}\left(\frac{1}{r_1} - \frac{1}{10^{17}}\right) \times 7 \times 10^{-25} = 1,$$

which gives $r_1 = 7 \times 10^{12}$ cm for the radius down to which the line of sight can penetrate. Since this radius must be at least 10^2 or 10^3 times larger than the nucleus, the latter

[18] E. A. Milne, *M.N.*, **84**, 354, 1924.

should not be directly observable. At least, its absorption lines should be completely washed out by the Doppler effect of electron scattering at the high electron temperatures which have been required for other reasons. Hence it does not seem that continuous nuclear ejection will yield a satisfactory model, and the observations of the nucleus of NGC 2392 cannot be made to fit into either of the models investigated, in neither of which can the nebula be allowed to extend all the way into the nucleus.

As a final comparison between the two models, it is instructive to calculate roughly the nebular brightness to which they lead and to see which is in closer agreement with observation. For the first model the energy available for dissipation in the nebula is given simply by multiplying $Fo\ (H) + Fo\ (He)$ by c; with the values of the parameters used, this gives about 10^{37} erg/sec. This energy will be distributed in some fashion among all the line and continuous radiations of the nebula. We shall probably be within an order of magnitude if we assume that 10 per cent of the available energy goes into radiations which contribute to the photographic magnitude. It is assumed, therefore, that the absolute photographic magnitude of a nebula operating according to the first model corresponds to the radiation of 10^{36} erg/sec in the photographic region.

In the second model the energy dissipated in the nebula is carried by the ionized particles and consists of ionization energy plus kinetic energy. With the same figures used previously, $n = 10^3\ \text{cm}^{-3}$, $V = 20$ km/sec, and $r = 10^{17}$ cm, the rate of flow of ionization energy into the bright hydrogen shell will be $4\pi r^2 nVE = 5.4 \times 10^{33}$ erg/sec, where E is the ionization energy per particle, 2.05×10^{-11} ergs. Doubly ionized helium with fewer particles but a higher ionization potential will carry a similar amount of energy, and an additional amount of the same size seems to be a generous allowance for the kinetic energy of the particles. For this model, then, the total energy available to the nebula is about 10^{34} erg/sec, and again, on the assumption that 10 per cent of the total contributes to the photographic nebular magnitude, the latter will correspond to a rate of radiation of about 10^{33} erg/sec in the photographic region.

According to Berman,[19] the mean absolute photographic magnitude of the planetary nebulae is close to -1, which makes them about 6 mag., or 2.5×10^2, brighter photographically than the sun. Equation (3) applied to the sun, with $T = 6000°$, shows that the solar radiation between 5000 A and 3000 A amounts to 1×10^{33} erg/sec. Multiplication of this value by 2.5×10^2 indicates that a radiation rate of about 2.5×10^{35} erg/sec in the photographic region by a typical planetary is required by Berman's data. This result, in spite of the crudity of the computations, appears to be decisively in favor of the first model.

Many points require further investigation, and the difficulties mentioned above will have to be resolved satisfactorily before knowledge of the planetaries can be considered even reasonably complete. Nevertheless, the simple straightforward model, which basically assumes that the expansion velocity given by any line is the same as the *H-He* velocity in the region where the line is produced, appears quite promising.

It is a pleasure to acknowledge many helpful and stimulating discussions with Drs. R. Minkowski, L. H. Aller, and D. H. Menzel, and especially with Dr. I. S. Bowen.

[19] *Lick Obs. Bull.*, No. 486, 1937.

THE BAND SPECTRUM OF CO^+. II. COMET-TAIL SYSTEM ($A^2\Pi - X^2\Sigma$)

K. NARAHARI RAO
Yerkes Observatory
Received December 9, 1949

ABSTRACT

Three comet-tail bands ($A^2\Pi - X^2\Sigma$) of CO^+ in the red and near infrared are photographed in the first and second orders of a 21-foot grating spectrograph. Their fine-structure analysis is given in Table 1. All the available data concerning these comet-tail bands are examined in the light of the results obtained in a previous investigation for the ground state of CO^+. The rotational constants B_v for the $A^2\Pi$ state can be represented by the relation $B_v = 1.58940 - 0.09142(v + \frac{1}{2})$. Arguments are advanced for revising the vibrational numbering of these bands by a lowering of the v' values by three units.

A. INTRODUCTION

Astronomers as well as laboratory spectroscopists evinced great interest in the $A^2\Pi - X^2\Sigma$ bands of the ionized carbon monoxide molecule ever since their identification in the cometary spectra by A. Fowler.[1] The upper state of these bands is an inverted $^2\Pi$ state and the lower state the ground state of CO^+. In a previous investigation[2] from a comprehensive study of the first negative carbon bands accurate values were derived for the molecular constants of the ground state of CO^+. It was considered profitable to examine all the available material concerning the comet-tail bands in the light of these revised results for the ground state of CO^+. Further, the laborarory work carried out at the Yerkes Observatory afforded an opportunity to extend the experimental data concerning these bands and to improve our knowledge of their rotational and vibrational structures. It was found that the vibrational numbering available in the literature for the comet-tail system needs to be revised by a lowering of the v' values by three units. In other words, what was considered to be the (3, 0) band is actually the (0, 0) band, etc.

B. EXPERIMENTAL

The apparatus used to excite the comet-tail bands was precisely the same as that described previously.[2] The measurement and the reduction of these bands were also carried out as before. A survey was made of the spectral region from λ 3000 to λ 9000 in the first and second orders of a 21-foot grating spectrograph with a view to reproducing all the known comet-tail bands and also to look for any interesting members of the system that had not been previously mentioned in the literature. Figure 1 gives a reproduction of the band at λ 7200, which was first observed by R. K. Asundi[3] about ten years ago. This was photographed in the first order of the 21-foot grating spectrograph (dispersion 2.5 A/mm).

C. ROTATIONAL STRUCTURE

The fine-structure analysis of three comet-tail bands in the red and the photographic infrared (at λλ 6200, 7200, and 8400) is given in Table 1. These three bands have never been analyzed before, and the band at λ 8400 does not seem to have been even observed. The designation of the branches of these bands can easily be understood from the energy-level diagram given in Figure 2. In the past[4] the nomenclature that is applicable for a

[1] A. Fowler, *M.N.*, **70**, 484, 1909–1910.

[2] K. N. Rao, *Ap. J.*, **111**, 50, 1950.

[3] R. K. Asundi, *Current Science*, **9**, 503, 1940.

[4] H. Bulthuis, *Groningen Diss.*, 1935.

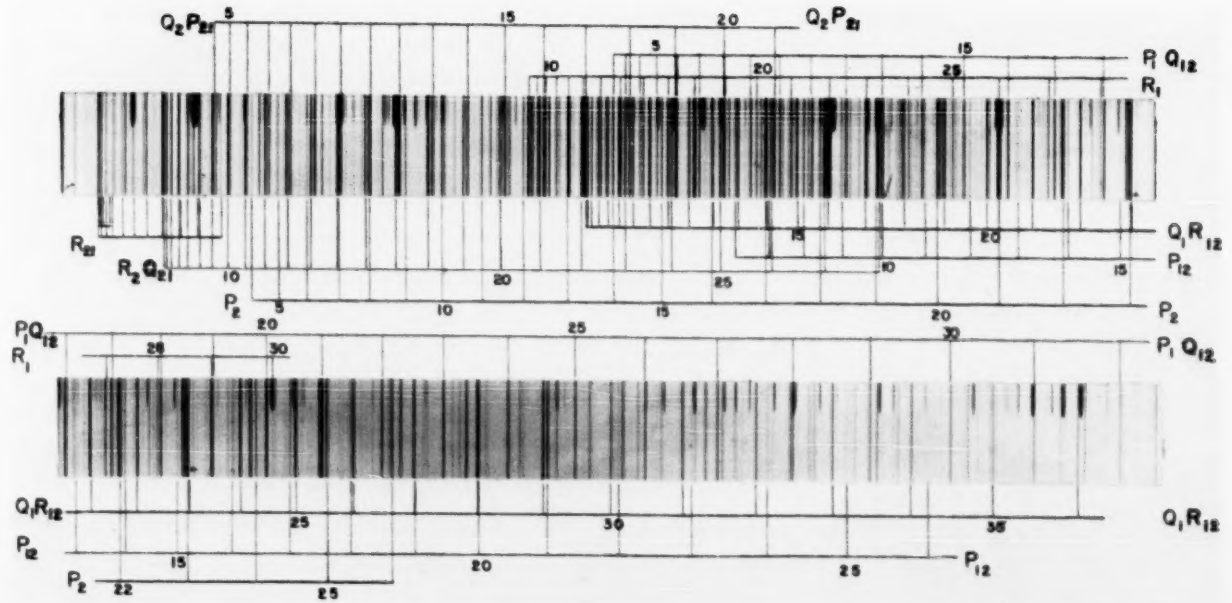

FIG. 1.—The (0, 3) comet-tail band of CO^+ at λ 7230

$^2\Pi - {}^2\Sigma$ transition when the $^2\Pi$ state is normal appears to have been used to describe the structure of the comet-tail bands of CO^+, which have as their initial state an *inverted* $^2\Pi$. The difference in the designations of the branches is due to the fact that for an inverted $^2\Pi$ state the $^2\Pi_{1/2}$ component corresponds to the term series F_2 and the $^2\Pi_{3/2}$ component to F_1, whereas for a normal $^2\Pi$ state the $^2\Pi_{1/2}$ component is F_1 and the $^2\Pi_{3/2}$ component is F_2. The data of the previous investigators[4,5,6] were reduced to the scheme presented in the energy-level diagram given in Figure 2 before using them for the evaluation of the rotational constants. The designations used by the previous authors along with those adopted in the present work are summarized in Table 2.

Whereas a $^2\Sigma$ state belongs strictly to Hund's case *b*, a $^2\Pi$ state can belong either to case *a* or to case *b* or to cases intermediate between *a* and *b*. The form of the rotational

TABLE 1

WAVE NUMBERS OF THE LINES IN THE COMET-TAIL BANDS OF CO^+

(0, 2) BAND

K	R_{21}	$R_{21}+Q_{21}$	$Q_{21}+P_{21}$	P_{21}	R_1	Q_1+R_{12}	P_1+Q_{12}	P_{12}
0	.....	.....	.....	.....	.....	.....	.....	.....
1	.....	.....	16128.87	.....	.....	.....	.....	.....
2	.....	16133.98	125.89	.....	.....	.....	16000.20	.....
3	.....	133.63	122.48	16114.39	.....	.....	15996.88	.....
4	.....	132.59	118.38	106.80*	.....	.....	992.35	.....
5	16151.38	130.89	113.42	098.90	.....	16004.25	987.10	.....
6	152.52*	128.53	107.91	090.17	.....	001.37	981.11	.....
7	152.52*	125.51	101.23	080.77	.....	15997.73	974.37	.....
8	152.01	121.81	094.49	070.72*	16023.01	993.38	966.91	.....
9	150.85	117.46*	086.99	060.02	021.03	988.30	958.71	.....
10	149.01	112.46	078.81	048.61	018.30	982.46	949.81	.....
11	146.48	106.80*	069.95	036.59	014.85	975.89	940.08	.....
12	143.32	100.46	060.43	023.89	010.59*	968.61	929.67	.....
13	139.48	093.46*	050.23	010.59*	005.71	960.57	918.55	.....
14	134.94	085.76	039.38	15996.47	000.05	951.79	906.65	.....
15	129.77	077.42	027.88	981.77	15993.64	942.28	894.01	.....
16	123.90	068.40	015.67	966.42	986.50	932.05	.....	.....
17	117.46*	058.77	002.81	950.38	978.63	921.09	.....	.....
18	110.14	048.29	15989.27	933.71	970.04	909.40	.....	.....
19	102.27	037.36	975.08	916.37*	960.66	896.98	.....	.....
20	093.46*	025.52	960.20	898.36	950.65	.....	.....	.....
21	084.41	013.29	944.66	.....	939.85	.....	.....	.....
22	070.72*	.....	928.40*	.....	928.40*	.....	.....	.....
23	063.88	.....	911.58	.....	916.37*	.....	.....	.....
24	052.62	.....	.....	.....	.....	.....	.....	.....

* Blend.

energy function is complicated in a $^2\Pi$ state because of the spin uncoupling which occurs as the rotation increases. Hill and Van Vleck[7] computed theoretically the rotational term values of the components of the doublet states for any magnitude of the coupling between S and Λ, S being the resultant spin and Λ the component of the electronic orbital angular momentum along the internuclear axis. They obtained for the rotational energy in the case of a $^2\Pi$ state

$$F_1(J) = B_v\{(J+\tfrac{1}{2})^2 - \Lambda^2 - \tfrac{1}{2}\sqrt{4(J+\tfrac{1}{2})^2 + Y(Y-4)\Lambda^2}\},$$
$$F_2(J) = B_v\{(J+\tfrac{1}{2})^2 - \Lambda^2 + \tfrac{1}{2}\sqrt{4(J+\tfrac{1}{2})^2 + Y(Y-4)\Lambda^2}\}, \quad (1)$$

[5] D. Coster, H. H. Brons, and H. Bulthuis, *Zs. f. Phys.*, **79**, 787, 1932.

[6] R. Schmid and L. Gerö, *Zs. f. Phys.*, **86**, 297, 1933.

[7] E. L. Hill and J. H. Van Vleck, *Phys. Rev.* **32**, 250, 1923.

TABLE 1—*Continued*

(0, 3) BAND

K	R_{21}	$R_{21}+Q_{21}$	$Q_{21}+P_{21}$	P_2	R_1	Q_1+R_{12}	P_1+Q_{12}	P_{12}
0	.....	.....	.....	.....	.....	.....	.....	.....
1	.....	.....	.....	.....	.....	13885.23*	.....	.....
2	.....	.....	.....	.....	.....	885.23*	13877.12*	.....
3	.....	14010.49	.....	.....	.....	884.66	873.67	.....
4	14027.38	009.60	13995.42	13984.06	.....	883.43	869.39	.....
5	028.61	008.12	990.68	976.16	.....	881.46	864.33	.....
6	029.77	005.97*	985.39	967.63	.....	878.82	858.61	13841.50
7	030.13*	003.24	979.01	958.64*	.....	875.45	852.07	831.88
8	030.13*	13999.88*	972.52	948.79	13901.01	871.41	844.80*	821.60
9	029.23	995.89	965.36	938.37	899.35	866.61	837.07	810.66
10	027.78	991.22	957.56	927.36	896.00	860.12	828.51	798.72*
11	025.69	986.02	949.16*	915.75	894.01	855.07	819.26	786.59
12	022.99	980.10	940.05	903.50	890.25	848.25*	809.28	773.42
13	019.61	973.59	930.35	890.62	885.82	840.69	798.72*	759.77
14	015.63	966.43	920.03	877.12*	880.72	832.46	787.33	745.30
15	010.99	958.64*	909.06	862.99	874.89	823.56	775.28	730.18
16	005.97*	950.23	897.50	848.25*	868.38	814.09	762.57	714.35
17	13999.88*	941.20	885.23	832.88	861.15	803.49*	749.12	697.85
18	993.37	931.55	872.45	816.91	853.30	792.62	734.99	680.63
19	.....	921.23	858.94	800.31	844.80*	780.92	720.23	662.55*
20	.....	910.26	844.80*	783.01	835.34	768.56	704.70	644.04
21	.....	898.69	830.16	764.99*	825.35	755.44	688.55	624.80
22	.....	886.46	.....	746.67	814.76	741.71	671.67	604.94
23	.....	873.67	.....	727.37*	803.49*	727.37*	654.10	584.25
24	.....	860.12	.....	707.67	791.24	712.09	635.84	562.94
25	.....	845.94	.....	687.34	778.46	696.22	616.85	540.96
26	.....	831.20	.....	666.26	764.99*	679.80	597.25	518.27
27	.....	815.83	.....	.....	750.88	662.55*	576.97	.....
28	.....	799.74	.....	.....	736.05	644.59	555.97	.....
29	.....	.....	.....	.....	720.50	625.99	534.32	.....
30	.....	.....	.....	.....	704.38	606.79	511.98	.....
31	.....	.....	.....	.....	.....	586.84	488.91	.....
32	.....	.....	.....	.....	.....	566.20	465.24	.....
33	.....	.....	.....	.....	.....	544.90	440.86	.....
34	.....	.....	.....	.....	.....	522.92	415.80	.....
35	.....	.....	.....	.....	.....	500.25	390.07	.....
36	.....	.....	.....	.....	.....	476.91	363.72	.....
37	.....	.....	.....	.....	.....	452.86	.....	.....
38	.....	.....	.....	.....	.....	428.17	.....	.....
39	.....	.....	.....	.....	.....	402.78	.....	.....
40	.....	.....	.....	.....	.....	376.72	.....	.....

where $Y = A/B_v$; A (negative for inverted $^2\Pi$) is the coupling constant which is a measure of the strength of the interaction between the orbital and the spin angular momenta; $F_1(J)$ is the term series that forms for large rotation the levels with $J = K + \frac{1}{2}$, while $F_2(J)$ is that which forms for large rotation the levels with $J = K - \frac{1}{2}$, K being the total angular momentum apart from spin and J the total angular momentum including spin. The other symbols have the usual meaning.

From these relations it is easy to show that for $^2\Pi - {}^2\Sigma$ transitions

$$\tfrac{1}{2}(Q_1 + Q_2) = \nu_0 - B'_v + (B'_v - B''_v)(J + \tfrac{1}{2})^2 \ldots . \qquad (2)$$

By plotting the observed $\frac{1}{2}(Q_1 + Q_2)$ values against $(J + \frac{1}{2})^2$, straight lines were obtained, the slopes of which gave the values of $(B'_v - B''_v)$. Using the rotational constants ob-

TABLE 1—*Continued*

(0, 4) BAND

K	R_{21}	R_2+Q_{21}	Q_2+P_{21}	P_2	R_1	Q_1+R_{12}	P_1+Q_{12}	P_{12}
0								
1								
2						11792.43		
3		11917.95*				791.93*		
4	11934.85	917.13	11902.95			790.92	11776.90	
5	936.25	915.82	898.38			789.17	772.02	
6	937.72	913.92	893.29	11875.54		786.68*	766.50	
7	938.49*	911.43	887.17	866.75*	11810.10	783.66	760.14*	
8	938.49*	908.35	881.03	857.26	809.49	779.93	753.45	
9	938.06	904.73	874.21	847.21	808.16	775.54	745.94*	
10	937.00	900.50	866.75*		806.26	770.46	737.74	
11	935.34	895.64	858.77	825.46*	803.61	764.76	728.94	
12	933.09	890.23	850.17	813.64	800.40	758.37	719.45	
13	930.24	884.21	840.99	801.25	796.48	751.34	709.29	
14	926.83	877.61	831.20	788.30	791.93*	743.64	698.45	
15	922.76	870.39	820.83	774.75	786.68*	735.30	687.03	
16		862.60	809.88	760.62	780.70	726.28	674.90	
17		854.23	798.30	745.94*	774.17	716.58*	662.13	
18		845.27	786.17	730.61	766.93	706.30	648.71	
19			773.43	714.71	759.08	695.33	634.66	
20		825.46*	760.14*	698.20*	750.55	683.71	619.90	
21		814.73	746.16	681.14	741.37	671.44	604.54	
22		803.34	731.61*	663.45	731.61*	658.52	588.50	
23		791.42	716.58*	645.16	721.06	644.95	571.79	
24			700.83	626.36	709.89	630.72	554.48	
25			684.48		698.20*	615.85	536.57	
26			667.56		685.64	600.35		
27			650.04		672.51	584.17		
28			631.92		658.74	567.35		
29			613.22		644.42	549.90		
30			593.88		629.34	531.81		
31			573.95		613.66			
32			553.42		597.35			
33			532.26		580.33			
34					562.70			

TABLE 2

DESIGNATIONS OF COMET-TAIL BANDS OF CO^+

	D. Coster, H. H. Brons, and H. Bulthius* and R. Schmid and L. Gerö†	H. Bulthuis‡	Present work
$^2\Pi_{1/2}-{}^2\Sigma$	R_2	R_{11}	R_{21}
	Q_2R_1	$Q_{11}R_{12}$	R_1Q_{21}
	Q_1P_1	$P_{11}Q_{12}$	Q_2P_{21}
	P_1	P_{12}	P_2
$^2\Pi_{3/2}-{}^2\Sigma$	R_2	R_{21}	R_1
	Q_2R_1	$Q_{21}R_{22}$	Q_1R_{12}
	Q_1P_2	$P_{21}Q_{22}$	P_1Q_{12}
	P_1	P_{22}	P_{12}

* *Zs. f. Phys.*, **79**, 787, 1932.

† *Zs. f. Phys.*, **86**, 297, 1933.

‡ *Groningen Diss.*, 1935.

tained previously[2] for the ground state, the B'_v values could easily be computed. The final results, evaluated partly from the new bands measured here (Table 1) and partly from those measured by earlier investigators, are summarized in Table 3. Their accuracy is estimated to be ± 0.00025 cm^{-1}. The data given in the above table can be represented by the following formula

$$B_v = 1.58940 - 0.01942\,(v + \tfrac{1}{2})\,. \qquad (3)$$

A value of $6.6_9 \times 10^{-6}$ cm^{-1} was estimated for the rotational constant D of the upper state. The V in equation (1) was evaluated by using differences of the wave numbers of

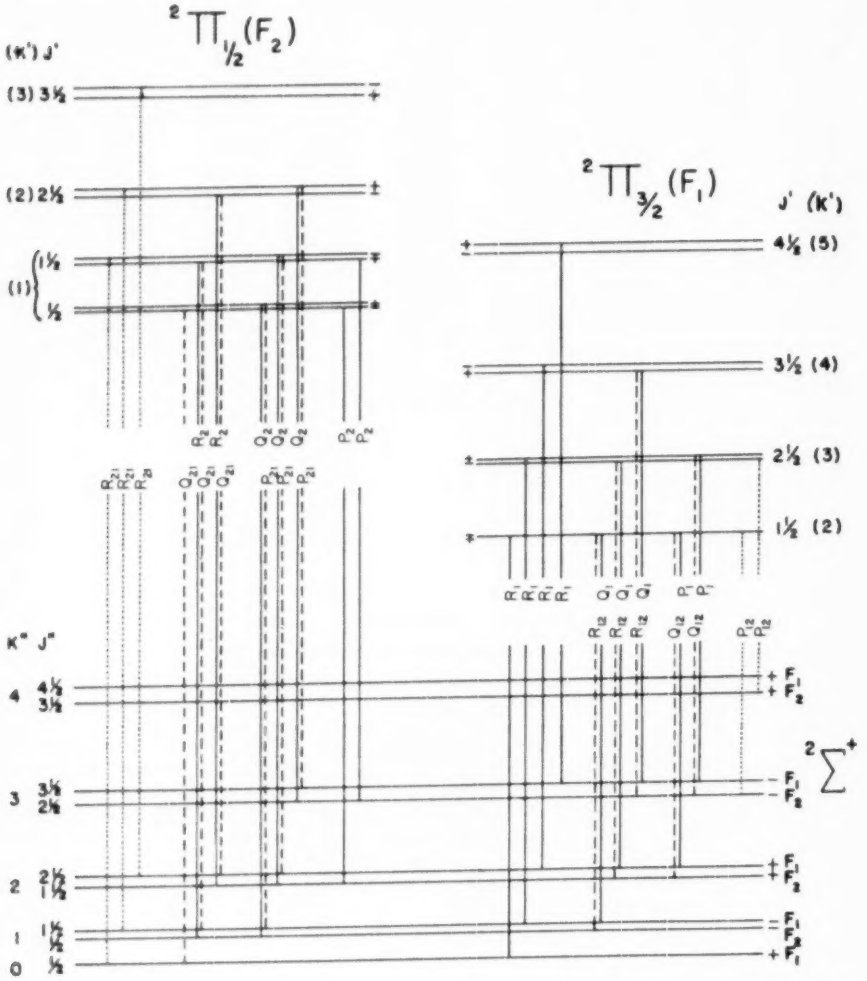

FIG. 2.—Energy level diagram for the first lines of a $^2\Pi(a) - {}^2\Sigma^+$ transition when the $^2\Pi$ state is inverted.

the lines in the appropriate branches. An average value of $117._5$ cm^{-1} was derived for the coupling constant A.

D. VIBRATIONAL STRUCTURE

The vibrational analysis available in the literature[8] for the comet-tail system of CO^+ was the result of an attempt to represent all the observed data of Baldet.[9] In this scheme four weak bands at λλ 6400, 5800, 5300, and 6000, which were estimated to be of intensity ½ by Baldet, were assigned the transitions (0, 0), (1, 0), (2, 0), and (2, 1). This scheme, however, meets with the following difficulties:

1. On the plates obtained in this laboratory the above bands did not occur. Also there was no evidence for the presence of other bands in the v'' progression with $v' = 0$, 1, and 2. Some of these, if real, would have occurred in the infrared region covered by the present survey. The bands at λ 7200 and λ 8400, whose fine-structure analysis has been

TABLE 3

ROTATIONAL CONSTANTS

v*	B_v†	v*	B_v†
0	1.5797_1	6	1.4631_9
1	1.5602_2	7	1.4437_5
2	1.5407_0	8	1.4240_9
3	1.5215_2	9	1.4050_9
4	1.5020_2	10	
5		11	1.3651_5

* The numbering is according to the revised scheme (see Sec. D).

† Table 4 shows the bands studied by the different authors. The measurements given in their papers were used in the evaluation of these B_v values.

TABLE 4

ORIGINS OF THE COMET-TAIL BANDS

v' \ v''	0	1	2	3	4
0			16070.11	13946.74	11853.88*
1	21942.73	19758.78†			
2	23450.59	21266.74			
3	24931.68‡				
4	26386.23				
5					
6	29214.02				§
7	30588.61				
8		29752.85			
9		31074.41			
10					
11			31484.55		

* Present work.

† Computed from the data of Schmid and Gerö (*Zs. f. Phys.*, **86**, 297, 1933).

‡ Computed from the data of Coster, Brons, and Bulthuis (*Zs. f. Phys.*, **86**, 297, 1933).

§ Computed from the data of Bulthuis (*Groningen Diss.*, 1935).

[8] G. Herzberg, *Zs. f. Phys.*, **52**, 815, 1928.

[9] F. Baldet, *C.R.*, **180**, 271 and 820, 1925.

discussed in Section C, could be assigned the transitions (3, 3) and (3, 4) in this scheme. This can easily be verified by forming appropriate combination relations.

2. In the Deslandres table of the Baldet-Johnson bands[8] no bands with $v'' = 0, 1$, or 2 have ever been observed either by the earlier workers or on the plates obtained at this institution.

3. It is also obvious that in the above assignments of the comet-tail and Baldet-Johnson bands no normal Condon parabolae are obtained.

From all these reasons it seems definite that the old numbering has to be revised. The scheme given in Table 4 avoids the difficulties discussed above and represents the ob-

TABLE 5

VIBRATIONAL QUANTA OF THE UPPER STATE OF THE COMET-TAIL BANDS

v'	$\Delta G_{v'+1/2}$ (Observed)	$\Delta G_{v'+1/2}$ (Computed)	O−C
0	1535.23	1535.04	+0.19
1	1507.86	1508.09	−0.23
2	1481.09	1481.22	−0.13
3	1454.55	1454.44	+0.11
6	1374.59	1374.54	+0.05
7	1348.11	1348.07	+0.04
8	1321.56	1321.67	−0.11

TABLE 6

MOLECULAR CONSTANTS OF THE $A^2\Pi$ STATE OF CO^+

Rotational constants:	
B_e	1.5894_0 cm^{-1}
α_e	0.0194_2 cm^{-1}
D	$6.6_0 \times 10^{-6}$, cm^{-1}
β	Negligibly small (computed from the theoretical formula[9])
I_e	17.606_0 gm/cm^2
r_e	$1.2436_7 \times 10^{-8}$ cm
Coupling constant A	$117._5$ cm^{-1}
Vibrational constants:	
ω_e	1562.0_6 cm^{-1}
$\omega_e x_e$	13.53_7 cm^{-1}
$\omega_e y_e$	0.013_1 cm^{-1}

[9] See, e.g., G. Herzberg, *Molecular Spectra and Molecular Structure*, Vol. I: *Diatomic Molecules* (New York: Prentice Hall Book Co., Inc., 1939), p. 116.

servations satisfactorily. The values given in this table are the band origins which were evaluated from the intercepts of the straight lines obtained in the plots of relation (2). In the new scheme the previous (3, 0) Baldet-Johnson band is the (0, 0) transition of the $B^2\Sigma - A^2\Pi$ system of CO^+, and a normal Condon parabola is obtained for the observed bands of this system.

Next the vibrational constants of the $A^2\Pi$ state were evaluated. It is customary to represent the vibrational term values by the relation

$$G(v) = \omega_e(v + \tfrac{1}{2}) - \omega_e x_e(v + \tfrac{1}{2})^2 + \omega_e y_e(v + \tfrac{1}{2})^3 \ldots \quad (4)$$

where $\omega_e x_e \ll \omega_e$ and $\omega_e y_e \ll \omega_e x_e$ the separation of successive vibrational levels is designated by

$$\Delta G_{v+1/2} = G(v+1) - G(v). \tag{5}$$

From the band origins given in Table 4 and using the vibrational quanta of the lower state, which were obtained from a study of the first negative carbon bands, the $\Delta G'_{v+1/2}$ values were derived as shown in Table 5. A least-squares solution through all the above observations for $\Delta G'_{v+1/2}$ values gives the following formula for the vibrational term values:

$$G(v) = 1562.06\,(v+\tfrac{1}{2}) - 13.532\,(v+\tfrac{1}{2})^2 + 0.0131\,(v+\tfrac{1}{2})^3 \ldots. \tag{6}$$

The computed values given in Table 5 are obtained by using this formula. The difference between the observed and the computed values is a little large for $v' = 0$ and $v' = 1$. When combining the work of different authors, as was done here, one has to bear in mind that a constant shift of the lines in the bands relative to the comparison spectrum between the observations of different authors may give rise to such discrepancies. Table 6 summarizes the molecular constants for the $A^2\Pi$ state of CO^+.

My thanks are due to Dr. G. Herzberg under whose supervision this work was carried out and to the government of India for the award of a fellowship. Some of the computations were done at the National Research Council, Ottawa, Canada, during the winter months of 1949. I wish to express my gratitude to the officials of that institution for providing me with all the required facilities. I am grateful to Miss Irene Hansen for drawing the energy-level diagram given in Figure 2.

SINGLET ELECTRONIC STATES OF THE *TiO* MOLECULE

JOHN G. PHILLIPS
Yerkes Observatory
Received October 27, 1949

ABSTRACT

Rotational analyses of the bands in the spectrum of the *TiO* molecule at 8859 A and 5597 A have made it possible to identify the corresponding electronic transitions as $^1\Pi - {}^1\Delta$ and $^1\Phi - {}^1\Delta$, respectively. The two transitions have a common lower state. The resulting rotational constants are presented in Table 3. It is shown that the two bands are the (0-0) bands of the respective systems. Additional bands of the two systems are listed in Tables 5 and 6. The excitation energies, ν_{00}, of the $^1\Pi$- and $^1\Phi$-states are 11,272.77 and 17,840.60 cm^{-1}, above the $^1\Delta$-state, respectively.

A. INTRODUCTION

Up to the present time, three band systems have been identified in the spectrum of the *TiO* molecule: (1) the α-system ($^3\Pi - {}^3\Pi$) in the blue-green region, analyzed by Christy;[1] (2) the β-system in the yellow; and (3) the γ-system in the infrared. A vibrational analysis carried out by Lowater[2] showed that the γ-system was associated with a $^3\Sigma - {}^3\Pi$ transition, the lower ($^3\Pi$) state being the same as the lower state of the α-system. The β-system consists of a single sequence of bands degraded to the red, with the head of the most intense band at 5597 A. Each band in the sequence has an intense *Q* head and a weaker *R* head. From the appearance of the bands Lowater has suggested that they constitute the main sequence of a $^1\Pi - {}^1\Sigma$ transition, the most intense band at 5597 A being the (0-0) band. All three of these band systems are present in the spectra of M-type stars.

The γ-system has been found by Wurm and Meister[3] to extend to 8646 A. They have also found a large number of additional bands extending to 11,238 A. Recently, Kiess[4] reported on a series of improved measurements of the heads of a number of these bands, extending to 9602 A. The most intense of these new bands are also found in the spectra of M-type stars.[5] Of particular interest is a sequence of intense bands, starting at 8859 A and degrading to the red.

No positive identifications of any of the bands beyond 8646 A have been made up to the present time, although some suggestions have been offered. Dobronravin[6] has attempted to place the sequence at 8859 A, together with others in the same region of the spectrum, into a new triplet system ($^3\Sigma - {}^3\Pi$), with the same lower state as the α-system, while Wurm and Meister have suggested that this sequence might be associated with a singlet system. This latter suggestion raises an interesting possibility. The sequence of bands at 8859 A has a general appearance which is quite similar to that of the β-system. Furthermore, just as in the case of the β-system, no additional sequences of comparable intensity and appearance are found in the same region of the spectrum. Therefore, if the suggestion of Wurm and Meister is valid, it is likely that the 8859 A sequence is a main sequence of a new singlet transition, with the (0-0) band at 8859 A. Both the 8859 A

[1] Andrew Christy, *Phys. Rev.*, **33**, 701, 1929.

[2] F. Lowater, *Proc. Phys. Soc. London*, **41**, 557, 1927.

[3] Karl Wurm and H. J. Meister, *Zs. f. Ap.*, **13**, 199, 1936.

[4] C. C. Kiess. Paper read before the American Astronomical Society, Pasadena, Calif., 1948.

[5] See, e.g., Paul W. Merrill, *Ap. J.*, **79**, 183, 1934.

[6] P. P. Dobronravin, *C.R. Acad. Sci. U.S.S.R.*, **17**, 399, 1937.

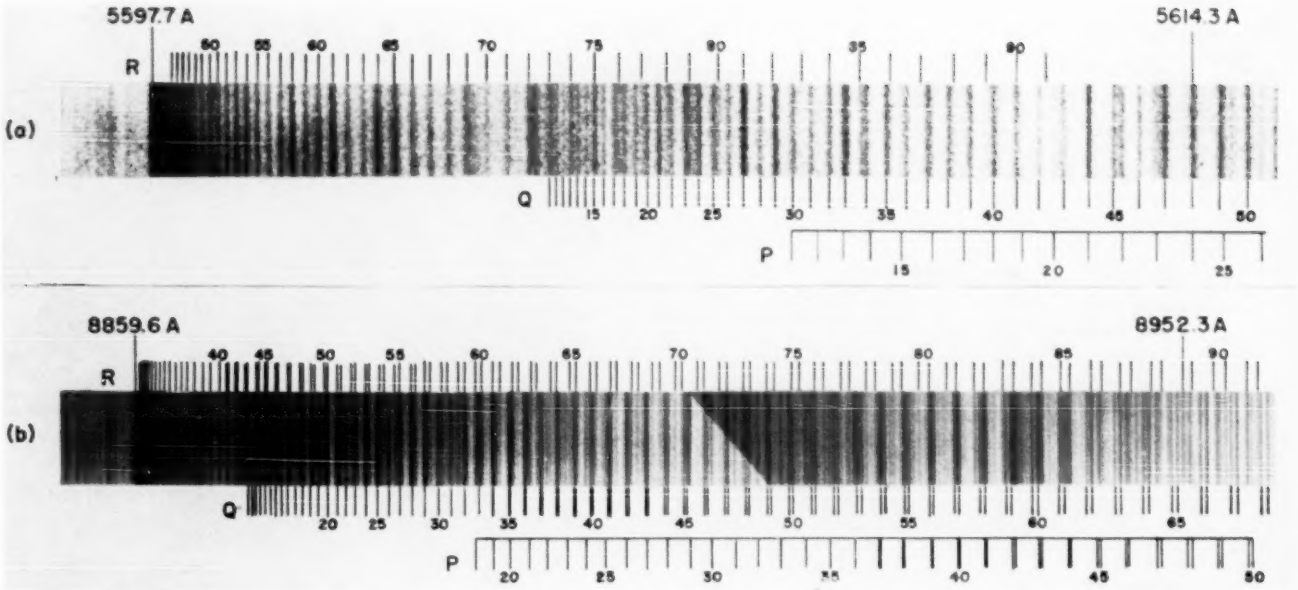

FIG. 1.—The spectra of two singlet bands of TiO. *a*, the (0, 0) band of the $^1\Phi - {}^1\Delta$ system at 5597 A; *b*, the (0, 0) band of the $^1\Pi - {}^1\Delta$ system at 8859 A. In each spectrum the leading lines show the positions of the lines in each of the three branches.

band and the 5597 A band are present in absorption in the spectra of M-type stars, so that their lower states are certainly not greatly different in energy. Indeed, the possibility exists that the two bands have a lower state in common.

It is important to show which of the two suggestions mentioned above is correct. This may be done by carrying out a rotational analysis of the band at 8859 A. A comparison of combination differences with those of the a-system would then show whether or not the suggestion of Dobronravin is correct. Also, by carrying out a rotational analysis of the 5597 A band, a similar comparison of the combination differences of the 8859 A band and the 5597 A band would show whether these two bands have a state in common.

These two investigations were accordingly undertaken, in the hope that they would result in the determination of the transition associated with the sequence at 8859 A.

B. EXPERIMENTAL

The source that was used to produce the spectrum of *TiO* was a high-tension a.c. arc. The arc consisted of two carbon electrodes, with a piece of titanium metal in a depression in the top of the lower electrode. The arc was connected directly to the secondary of a 4800-volt, 5-kva transformer. A 7-ohm resistance was placed in series with the 220-volt primary of the transformer. It was found, quite by accident, that, if an ordinary Bunsen flame fed with natural gas was played on the burning arc from the side and the spectrum taken of the extremity of the bow formed by the arc as a result of the blast of the burner, the atomic lines of titanium were considerably reduced in intensity, while the spectrum of the oxide was greatly enhanced. This technique was followed in obtaining all the exposures used in this study.

The spectrograms were taken with the 21-foot grating spectrograph. The 5597 A band was photographed in the second order with a dispersion of 1.25 A per millimeter. Exposure times ranged from 20 seconds to 1 minute with 103a-F emulsions. The 8859 A band was photographed in the first order, with a dispersion of 2.5 A per millimeter. Using sensitized I-N plates, the exposure times that were required ranged up to 25 minutes in duration.

C. ROTATIONAL ANALYSIS OF THE 8859 A BAND

The measurements made of the 8859 A and 5597 A bands are presented in Tables 1 and 2, respectively. The method used to obtain the correct J values of the 5597 A band will be described later. In the case of the 8859 A band the analysis was carried out in the following manner: As can be seen in Figure 1, the band degrades to the red, has an intense Q branch, and weaker R and P branches. No difficulty was experienced in obtaining the correct rotational numbering. In the case of the Q and P branches, this was obtained immediately, since only short extrapolations to the band origin were required. In the case of the R branch, lines with low J were masked by the more intense lines in the part of the branch returning from the head, so the following procedure was used to obtain the J values. It will be noticed in Figure 1 that each of the branches experiences a splitting into two components for large J. When the magnitude of the doubling in the Q and P branches was plotted against $J(J + 1)$, the plot presented in Figure 2 was obtained. The points exhibited considerable scatter, but a straight line through the origin represented the observations quite well. This shows that the splitting is caused by Λ-type doubling and not by spin doubling, because in the latter case a plot of splitting versus J would be a straight line through the origin. Furthermore, for a given J, the doubling is the same for the Q and P branches, within the error of observation. Therefore, as will be shown in greater detail later, one of the two electronic levels involved in the transition must have negligible Λ-type doubling. This circumstance makes it possible to use the Q and P

TABLE 1

WAVE NUMBERS OF THE LINES IN THE 8859 A BAND

J	$R_{aa}(J)$	$R_{bb}(J)$	$Q_a(J)$	$Q_b(J)$	$P_{aa}(J)$	$P_{bb}(J)$
7				11271.49 cm^{-1}		
8				271.06		
9				270.67		
10				270.13		
11				269.60		
12				268.96		
13				268.37		
14				267.67		
15				267.01		
16				266.19		
17				265.36		
18				264.46		
19				263.58		11244.09 cm^{-1}
20				262.56		242.14
21				261.51		240.11
22				260.51		238.01
23				259.43		235.89
24				258.28		233.70
25		11283.62 cm^{-1}		257.05		231.47
26		283.37		255.76		229.13
27		283.06		254.48		226.74
28		282.71		253.12		224.52
29		282.34		251.65		222.03
30		281.90		250.24		219.63
31		281.40		248.73		217.06
32		280.85		247.22		214.46
33		280.31		245.60		211.88
34		279.61	11243.88	11244.09	11209.12	11209.32
35		278.98	242.14	242.33	11206.53	
36		278.13	240.38	240.59	203.79	
37		277.35	238.56	238.79	11200.81	11201.03
38		276.52	236.69	236.96	198.10	198.42
39		275.74	234.76	235.06	194.89	195.38
40	11274.66	11274.95	232.84	233.16	192.06	192.37
41	273.69	273.95	230.86	231.13	189.04	189.26
42	272.62	272.89	228.81	229.13	185.92	186.31
43	271.49	271.82	226.74	226.98	182.86	183.19
44	270.41	270.67	224.52	224.88	179.72	180.02
45	269.28	269.60	222.34	222.68	176.49	176.82
46	267.99	268.37	220.09	220.44	173.30	173.60
47	266.66	267.01	217.80	218.16	169.93	170.27
48	265.36	265.71	215.46	215.83	166.53	166.94
49	263.92	264.26	213.06	213.44	163.19	163.54
50	262.56	262.91	210.63	211.02	159.75	160.20
51	261.05	261.51	208.11	208.54	156.20	156.57
52	259.43	259.89	205.58	206.02	152.65	153.07
53	257.86	258.28	202.97	203.42	149.12	149.50
54	256.22	256.68	200.34	200.81	145.48	145.88
55	254.48	255.02	197.63	198.10	141.73	142.20
56	252.73	253.31	194.89	195.38	138.04	138.48
57	250.99	251.65	192.06	192.61	134.22	134.72
58	249.14	249.75	189.26	189.77	130.31	130.89
59	247.22	247.79	186.31	186.87	126.49	127.00
60	245.23	246.08	183.38	183.96	122.59	123.10
61	243.27	243.88	180.38	180.95	118.52	119.13
62	241.22	241.82	177.36	177.96	114.49	115.05
63	239.14	239.76	174.22	174.85	110.37	110.99
64	236.96	237.60	171.08	171.73	106.11	106.80

TABLE 1—*Continued*

J	$R_{ab}(J)$	$R_{ba}(J)$	$Q_a(J)$	$Q_b(J)$	$P_{ab}(J)$	$P_{ba}(J)$
65	11234.76 cm^{-1}	11235.43 cm^{-1}	11167.90 cm^{-1}	11168.55 cm^{-1}		
66	232.48	233.16	164.65	165.35		
67	230.18	230.86	161.34	162.03		
68	227.85	228.53	158.00	158.69		
69	225.39	226.19	154.62	155.34		
70	222.95	223.74	151.14	151.89		
71	220.44	221.20	147.65	148.44		
72	217.80	218.65	144.18	144.87		
73		216.15	140.52	141.31		
74	212.58	213.44	136.87	137.67		
75	209.86	210.63	133.18	133.99		
76	207.08	208.11	129.42	130.31		
77	204.32	205.14	125.60	126.49		
78	201.34	202.34	121.75	122.59		
79	198.42	199.35	117.79	118.75		
80	195.38	196.44	113.86	114.79		
81	192.37	193.37	109.85	110.77		
82	189.26	190.30	105.77	106.80		
83	185.92	187.30				
84	182.86	183.96				
85	179.72	180.75				
86	176.14	177.36				
87	172.98	174.22				
88	169.63	170.77				
89	166.19	167.29				
90	162.54	163.88				
91	159.04	160.20				
92	155.34	156.57				
93	151.89	153.07				

branches to derive two sets of combination differences, $\Delta_1 F_r''(J)$ and $\Delta_1 F_v''(J)$, using the equations

$$\Delta_1 F_r''(J) = Q_r(J) - P_r(J+1),$$

$$\Delta_1 F_v''(J) = Q_v(J) - P_v(J+1),$$

where the subscripts r and v refer to the components of each doublet to long and short wave lengths, respectively. The combination differences $\Delta_1 F_r''(J)$ and $\Delta_1 F_v''(J)$ derived in this way were then used to compute an R branch. It was found that the computed and observed R branches agreed within the error of measurement, so that the corresponding numbering could be assigned to the observed R branch. The doublet splitting of the R branch is also plotted in Figure 2. The resulting points fall on the same straight line as do the Q and P branches. The final rotational numbering of the three branches is included in Table 1.

As mentioned above, for a given J the doublings of the R and P branches are the same as that of the Q branch, within the accuracy of the measurements. Now, if both the upper and the lower states involved in the transition exhibited Λ-type doubling of comparable magnitude, then the doublet separation, in the case of the Q branch, would be equal to the sum of the Λ-type doublings of the corresponding upper and lower rotational levels, and equal to their difference in the case of the R and P branches. The fact that the R and P branches exhibit the same amount of splitting as does the Q branch shows that one of the electronic states must have negligible Λ-type doubling, as compared with that of the other state. Furthermore, the presence of a strong Q branch shows that $\Delta\Lambda$

between the upper and lower state must be ± 1. These two facts together show that the transition is between a Π- and a Δ-state, since a Δ-state usually has a negligibly small Λ-type doubling as compared with that of a Π-state.

Without further information it cannot be ascertained whether the Π-state is the upper or the lower state. The relative intensities of the *R* and *P* branches cannot be used, since the I-N emulsion changes rapidly in sensitivity through this region of the spectrum. The two possibilities are illustrated in Figure 3, which shows the nomenclature to be used in the two cases. For simplicity, singlet states are shown in Figure 3. A similar nomenclature can be used in the case of a sub-band of a triplet system. Since it is impossible to apply the criteria proposed by Mulliken[7] for designating the two series into which the

TABLE 2

WAVE NUMBERS OF THE LINES IN THE 5597 Å BAND

J	*R*(*J*)	*Q*(*J*)	*P*(*J*)	*J*	*R*(*J*)	*Q*(*J*)	*P*(*J*)
9		17839.28 cm^{-1}		51	17856.30 cm^{-1}	17802.39 cm^{-1}	
10		838.98		52	855.85	800.86	
11		838.61	17826.93 cm^{-1}	53	855.37	99.35	
12		838.24	825.66	54	854.84	797.81	
13		837.85	824.27	55	854.32	796.26	
14		837.47	822.89	56	853.73	794.68	
15		837.02	821.44	57	853.13	793.06	
16		836.53	819.84	58	852.52	791.35	
17		836.02	818.33	59	851.85	789.75	
18		835.51	816.75	60	851.15	787.96	
19		834.94	815.15	61	850.44	786.28	
20		834.34	813.43	62	849.69	784.50	
21		833.78	811.89	63	848.87	782.72	
22		833.11	810.14	64	848.11	780.85	
23		832.41	808.30	65	847.28	779.05	
24		831.69	806.61	66	846.35	777.18	
25		830.99	804.97	67	845.46	775.21	
26		830.21	803.06	68	844.53	773.27	
27		829.42	801.36	69	843.59	771.28	
28		828.58	799.35	70	842.56	769.26	
29		827.84	797.57	71	841.56	767.27	
30		826.93	795.60	72	840.47	765.20	
31		826.04	793.69	73	839.28	763.08	
32		825.10	791.84	74	8.8 .4	760.93	
33		824.27	789.75	75	837.02		
34		823.20	787.74	76	835. .3		
35		822.17	785.76	77	834.00		
36		821.14	783.62	78	833.34		
37		820.08	781.59	79	832.00		
38		819.01	779.45	80	830.69		
39		817.87	777.18	81	829.42		
40		816.75	775.21	82	827.84		
41		815.56	772.89	83	826.47		
42		814.35	770.66	84	825.10		
43		813.12	768.42	85	823.48		
44		811.89	766.13	86	821.91		
45	17858.41 cm^{-1}	810.61	763.87	87	820.40		
46	858.15	809.29	761.56	88	8.8.70		
47	857.82	807.97		89	817.10		
48	857.47	806.61		90	815.56		
49	857.12	805.19		91	813.99		
50	856.75	803.78					

[7] Robert S. Mulliken, *Rev. Mod. Phys.*, **3**, 89, 1937.

rotational levels of the Π-state are split as *c* or *d* levels, the temporary symbols *a* and *b* must be used. The lower series is designated by the symbol *a* and the upper series by the symbol *b*. For the Δ-state these two series are superimposed.

The first few members of each of the six branches are shown in Figure 3. In the case of a Π − Δ transition, the violet components of the doublet are $R_{ba}(J)$, $Q_b(J)$, and $P_{ba}(J)$, and the red components $R_{ab}(J)$, $Q_a(J)$, and $P_{ab}(J)$. The violet components all arise from the *b* series, and the red components from the *a* series. An analogous situation arises in the case of a Δ − Π transition.

In the case of a Π − Δ transition, the combination differences $\Delta_2F'_a(J)$ and $\Delta_2F''_a(J)$ are found by combining the $R_{ab}(J)$ and $P_{ab}(J)$ components of the doublets, and, similarly, the $R_{ba}(J)$ and $P_{ba}(J)$ components are to be combined to find the differences $\Delta_2F'_b(J)$ and $\Delta_2F''_b(J)$. Similar relationships can be derived in the case of a Δ − Π transition.

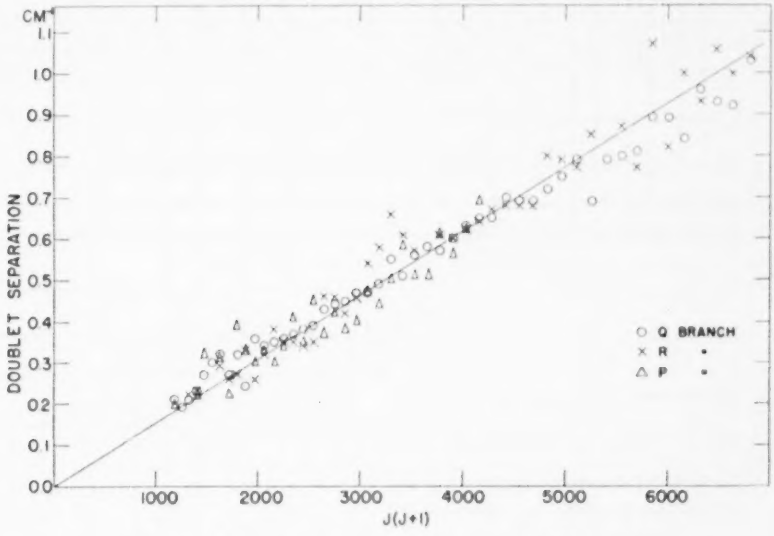

FIG. 2.—Doublet separations of the lines of the 8859 A band

The usual methods were used to derive the approximate rotational constants B', B'', D', and D''; the band origin, ν_0; and the differences $(B' - B'')$ and $(D' - D'')$, from which more accurate constants could be derived. The details will not be presented here.[8] The differences $(B' - B'')$ and $(D' - D'')$ between the rotational constants B'_a, B'_b, D'_a, and D'_b of the upper state and B''_a, B''_b, D''_a, and D''_b of the lower state could be determined quite accurately. However, on account of the observational scatter of the measurements, the determination of the approximate constants could not be carried out accurately enough to make it possible to decide from this one band whether the Δ-state was the upper or the lower state. Both interpretations led to a set of rotational constants which represented the observations equally well. It will be shown later, however, that it can be ascertained that the Δ-state is the lower state, so that the band is associated with a Π − Δ transition. With this interpretation, it was possible to derive the constants found in the second and third columns of Table 3. In the case of the Π-state, the constant

[8] See, e.g., G. Herzberg, *Molecular Spectra and Molecular Structure*, I (New York: Prentice-Hall Book Co., Inc., 1939), 183 ff.

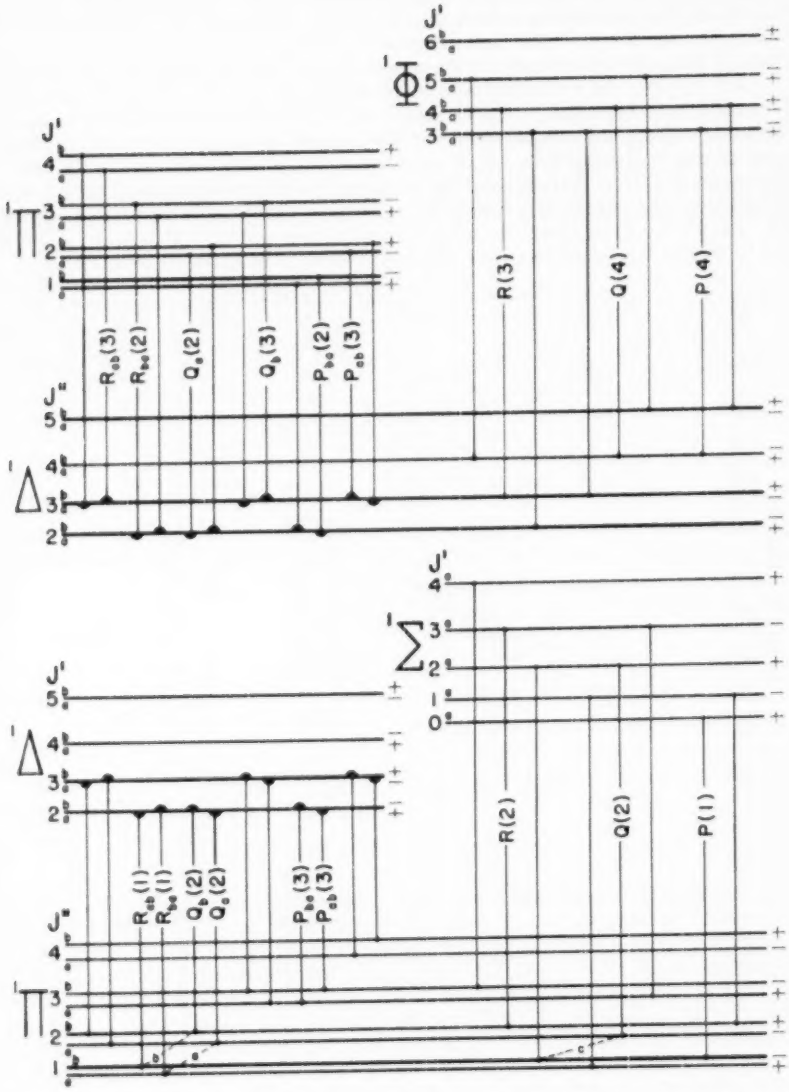

FIG. 3.—*Above*, permitted rotational transitions in the case of a $^3\Pi - {}^1\Delta$ and a $^1\Phi - {}^1\Delta$ transition; *below*, permitted rotational transitions in the case of a $^1\Delta - {}^1\Pi$ and a $^1\Sigma - {}^1\Pi$ transition.

B in Table 3 is the mean of B_a and B_b, and the Λ-type doubling constant, q, is the difference $(B_b - B_a)$.

D. COMPARISON OF THE 8859 A BAND AND THE α-SYSTEM

The combination differences $\Delta_2 F(J)$ of the 8859 A band were compared with those obtained from the published measurements on the α-system made by Christy. No agreement could be found with any of the three sub-bands of each of the (0–0), (1–0), and (0–1) bands. Also, the constants given in Table 3 are different from those computed for the α-system by Budó,[9] in a rediscussion of Christy's measurements. These constants are: $B_0'' = 0.5340$, $B_1'' = 0.5309$, $B_0' = 0.4884$, and $B_1' = 0.4855$ cm^{-1}. The differences are larger than the errors in the determinations.

Thus it can be said definitely that the 8859 A band does not have a state in common with a substate of the α-system, so that the suggestion made by Dobronravin, which was mentioned in the introduction, is untenable. This does not exclude the possibility that the 8859 A band is a sub-band of a $^3\Sigma - {}^3\Pi$ transition to a lower state which is quite different from the lower state of the α-system. However, if the 8859 A band is such a sub-

TABLE 3

MOLECULAR CONSTANTS OF THE SINGLET STATES OF *TiO*

Electronic State	$^1\Pi$	$^1\Delta$	$^1\Phi$
B_v	0.5120_0 cm^{-1}	0.5362_0 cm^{-1}	0.5211_5 cm^{-1}
D_v	$0.63_3\times10^{-6}$ cm^{-1}	$0.59_4\times10^{-6}$ cm^{-1}	0.30×10^{-6} cm^{-1}
H_v			2.76×10^{-11} cm^{-1}
r_0	1.6567$_9$ A	1.6188$_8$ A	1.6420$_9$ A
q_v	0.00016 cm^{-1}		
Excitation energy, ν_{00}	11,272.77 cm^{-1}		17,840.60 cm^{-1}

band, one should expect the other two sub-bands of the triplet system to appear in its neighborhood in the spectrum and to be of comparable intensity. Such bands are not found. It should be mentioned that Dobronravin did, indeed, call attention to this anomalous intensity distribution, but he did not consider that it invalidated his suggestion.

E. COMPARISON OF THE 8859 A BAND AND THE 5597 A BAND

As was pointed out in the introduction, if the 8859 A band is a member of a singlet system, then there is a possibility that it would have a lower electronic state, in common with the 5597 A band.

The suggestion was tested by making another comparison of combination differences. The usual methods were used to find the rotational numbering of the branches of the 5597 A band. It was then found that there does exist a close agreement between corresponding combination differences of the lower states of the 8859 A band and the 5597 A band. A partial list in Table 4 illustrates the agreement that was found.

The relationships illustrated in Table 4 have an important implication when the types of electronic states involved in the two transitions are considered. As can be seen from the table, the combination differences $\Delta_1 F''(J)$ of the 5597 A band agree with the differences $\Delta_1 F_a''(J)$ and $\Delta_1 F_r''(J)$ of the 8859 A band. These latter two quantities were defined above in Section C. Now it was also shown in Section C that the lower state of the 8859 A band must be either a Π- or a Δ-state. It is now possible to state definitely that the lower state must be a Δ-state, since otherwise the particular relationships illustrated in Table 4

[9] A. Budó, *Zs. f. Phys.*, **98**, 437, 1936.

would not be found. This can be demonstrated by a process of elimination, as follows: Assume for a moment that the lower state of the 8859 A band is a Π-state, as illustrated in the lower part of Figure 3. The difference $R_e(J) - Q_e(J+1)$ then is the difference between two successive rotational levels in the *a* series, shown by the dotted line *a* in the figure, and, similarly, the difference $R_f(J) - Q_f(J+1)$ is the difference between two successive levels in the *b* series, shown by the dotted line *b*. Now the 5597 A band has an intense *Q* branch, so that if its lower state is a Π-state, its upper state must be a Σ- or a Δ-state. However, the upper state cannot be a Σ-state, since the resulting combination

TABLE 4

COMPARISON OF COMBINATION DIFFERENCES OF THE 5597 A BAND AND THE 8859 A BAND

J	5597 A Band	8859 A Band			
	$\Delta_1F''(J) = R(J-1) - Q(J+1)$	$\Delta_1F''(J) = R(J-1) - Q(J+1)$		$\Delta_1F''(J) = Q(J-1) - P(J+1)$	
		$\Delta_1F''_e(J)$	$\Delta_1F''_f(J)$	$\Delta_1F''_e(J)$	$\Delta_1F''_f(J)$
46	50.18 cm^{-1}	50.21 cm^{-1}	50.19 cm^{-1}	50.17 cm^{-1}	50.16 cm^{-1}
47	51.21	51.18	51.20	51.22	51.27
48	52.28	52.27	52.30	52.29	52.27
49	53.34	53.24	53.29	53.24	53.31
50	54.36	54.37	54.45	54.45	54.43
51	55.44	55.49	55.47	55.47	55.46
52	56.50	56.47	56.46	56.52	56.46
53	57.56	57.47	57.52	57.54	57.49
54	58.58	58.58	58.59	58.61	58.61
55	59.64	59.64	59.59	59.62	59.59
56	60.67	60.70	60.67	60.66	60.67
57	61.78	61.88	61.73	61.72	61.75
58	62.77	62.88	62.83	62.77	62.77
59	63.89	63.83	63.84	63.77	63.72
60	64.87	65.13	64.85	64.83	64.86
61	65.94	65.92	65.91	65.90	65.89
62	66.97	66.97	67.00	66.97	66.99
63	68.02	68.03	68.06	68.05	68.11
64	69.06	69.05	69.06		
65	70.10	70.08	70.11		
66	71.14	71.13	71.14		
67	72.19	72.17	72.18		
68	73.25	73.19	73.23		
69	74.33	74.30	74.25		
70	75.29	75.30	75.30		
71	76.36	76.33	76.26		

differences, $\Delta_1F''(J)$, would be differences between an *a* sublevel of a given rotational level and the *b* sublevel of the neighboring rotational level, or vice versa, as shown by the dotted line *c* in the lower part of Figure 3. This is not what is actually observed. On the other hand, the upper state of the 5597 A band cannot be a Δ-state, since such a state would have a negligibly small Λ-type doubling, so that the resulting spectrum would exhibit a doubling similar to that observed in the 8859 A band. It can be seen from Figure 1 that this is not the case. These objections eliminate the possibility that the 8859 A band is associated with a $\Delta - \Pi$ transition.

As can be seen from the upper part of Figure 3, no similar objection can be raised against the assumption that the 8859 A band is part of a $\Pi - \Delta$ band system, the lower state being the one held in common with the 5597 A band.

Corresponding to the identification of the lower state of the 5597 A band as a Δ-state, it is quite definite that the upper state is a Φ-state, in view of the fact that the R branch of this band is more intense than the P branch and also that this upper state must exhibit negligible Λ-type doubling. Both these considerations would seem to eliminate a Π-state as the upper state, although there is a possibility, as has been pointed out by Herzberg,[10] that the Π-state involved in the 8859 A band might have an abnormally large Λ-type doubling as the result of perturbations caused by a close Σ-state. However, the observed intensities of the R and P branches would still favor a Φ-state as the upper state.

As far as the multiplicities of the electronic states involved in these transitions are concerned, the appearance of the bands and the sequences associated with them favor the interpretation that they are singlet states. There is no evidence to indicate that the bands are sub-bands of triplet transitions. This is especially true of the sequence at 5597 A, which is not complicated by the superposition of any extraneous bands.

The results of this section may be summarized by stating that it has been shown that the 8859 A band is associated with a $^1\Pi - {}^1\Delta$ transition, and the 5597 A band, at the head of the β-system, with a $^1\Phi - {}^1\Delta$ transition, the $^1\Delta$-state being common to both systems. As mentioned in the introduction, Lowater has suggested that the β-system is associated with a $^1\Pi - {}^1\Sigma$ transition. The general appearance of the bands of this system would indeed suggest a $^1\Pi - {}^1\Sigma$ transition as the most probable. It is only the fact that another band system has been found to have an electronic state in common with the β-system that makes it possible to be more definite in the identification.

F. THE ROTATIONAL CONSTANTS OF THE $^1\Phi$ STATE

Since the upper ($^1\Phi$) state of the 5597 A band has been shown to have negligible Λ-type doubling, it is permissible to use the combination differences $\Delta_1 F'(J)$ to obtain the rotational constants. These combination differences can be derived from the R, Q, and P branches of Table 2 through the use of the equations:

$$\Delta_1 F'(J) = R(J) - Q(J) = Q(J+1) - P(J+1).$$

By inserting these combination differences into the usual equation,

$$\frac{\Delta_1 F'(J)}{J+1} = 2B' - 4D'(J+1)^2,$$

and plotting the left side of the equation against $(J+1)^2$, we obtain a straight line. The constant B' can then be derived from the intercept and the constant D' from the slope of the straight line. When this procedure was followed, the following constants were obtained: $B' = 0.5222$ cm^{-1} and $D' = 0.61 \times 10^{-6}$ cm^{-1}. These constants can be regarded as only provisional, in view of the scatter of the points on the plot.

The next step was to find the band origin, ν_0. To do this, the measured positions of the lines of the Q branch were introduced into the equation

$$Q(J) - \overline{(B' - B'')}\, J(J+1) = \nu_0 + (B' - B'')_{corr}\, J(J+1),$$

where, as usual, the difference $(B' - B'')$ is the difference between the provisional rotational constants and $(B' - B'')_{corr}$ is the correction to be applied to $(B' - B'')$. When the left side of this equation is plotted against $J(J+1)$, the curve shown in Figure 4 was obtained.

The curve in Figure 4 is quite anomalous. Normally, the plotted points would define either a straight line or a curve which deviated from a straight line only for large values

[10] Private communication.

of J, the deviation being explainable by the fact that the approximate equation that is used does not take into account the influence of centrifugal force on the magnitude of the rotational quanta. But the points in Figure 4 exhibit a double curvature, with a point of inflection. The best that could be done was to draw as smooth a curve as possible through the observed points and determine the band origin from the point where this curve intersected the ordinate. In this way it was found that the origin was located at 17,840.60 cm^{-1}.

The anomaly mentioned above may be illustrated in another way. The rotational quanta $F'(J)$ of the upper state can be found from the lines in the three branches, through the use of the following equations:

$$F'(J+1) = R(J) - \nu_0 + F''(J)$$

$$F'(J) \quad = Q(J) - \nu_0 + F''(J),$$

$$F'(J-1) = P(J) - \nu_0 + F''(J),$$

all the quantities on the right sides of these equations being known. The quanta $F''(J)$ can be computed from the rotational constants of the $^1\Delta$-state, and the band origin has been found above.

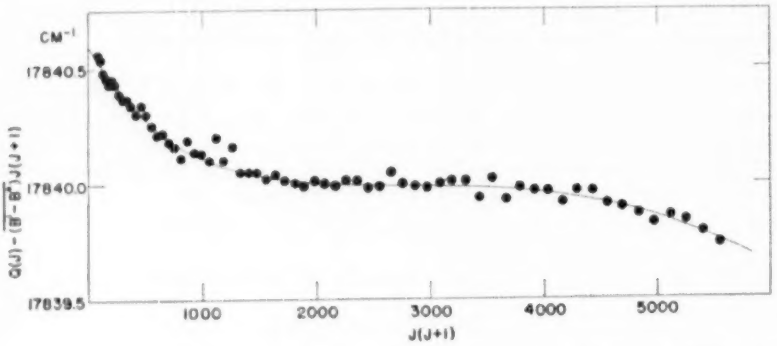

FIG. 4.—Determination of the origin of the 5597 A band. The quantities $Q(J) - \overline{(B' - B'')}J(J+1)$ are plotted as ordinates and $J(J+1)$ as abscissae.

If the quanta $F'(J)$ found in this way are then introduced into the usual equation,

$$\frac{F'(J)}{J(J+1)} = B' - D'J(J+1),$$

and the left side of the equation plotted against $J(J+1)$, the curve shown in Figure 5 is obtained. Normally, this curve is a straight line, whereas in Figure 5 the plot shows a definite downward curvature. The curvature is greatest for small values of $J(J+1)$, while for large values of $J(J+1)$ the curve approaches a straight line.

The most likely explanation for this curvature is that additional rotational terms are required in the equation for $F'(J)$. Accordingly, the following equation was used:

$$F'(J) = B'J(J+1) - D'J^2(J+1)^2 - H'J^3(J+1)^3.$$

By the use of graphical methods, the constants in the fourth column of Table 3 were obtained.

The constants found in this way were then used, together with those of the $^1\Delta$-state, to compute the wave numbers of the lines in the three branches. The differences (O − C) between the computed and observed wave numbers are plotted in Figure 6. It can be seen that, to about $J = 60$, the differences are small, but, nevertheless, systematic. Beyond $J = 60$, the differences are much larger. These differences could be reduced still more by adding more terms to the equation for $F'(J)$ used above, but several would have to be added to make the differences (O − C) as small as the error of measurement over the whole range of J values.

G. ADDITIONAL BANDS OF THE $^1\Pi - {}^1\Delta$ AND $^1\Phi - {}^1\Delta$ SYSTEMS

a) THE $^1\Pi - {}^1\Delta$ SYSTEM

Among the bands found by Wurm and Meister and Kiess in the neighborhood of the 8859 A band, there are three which form, together with the 8859 A band, a definite sequence. The three bands are on the long-wave-length side of the 8859 A band, their separations are the same, within the error of measurement, and there is a regular decrease in

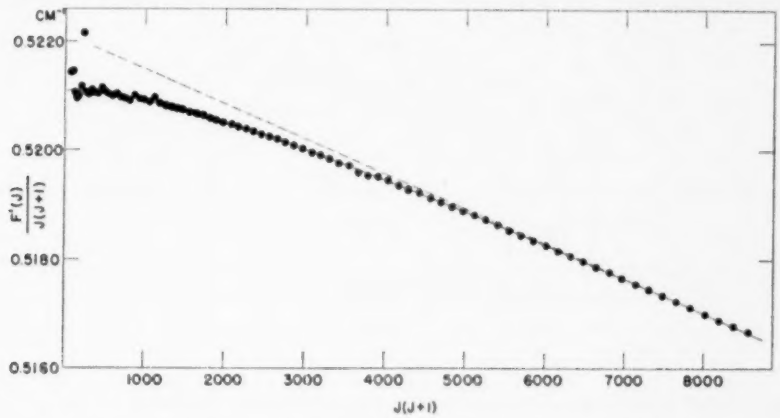

FIG. 5.—The quantities $[F'(J)]/[J(J+1)]$ of the 5597 A band plotted against $J(J+1)$

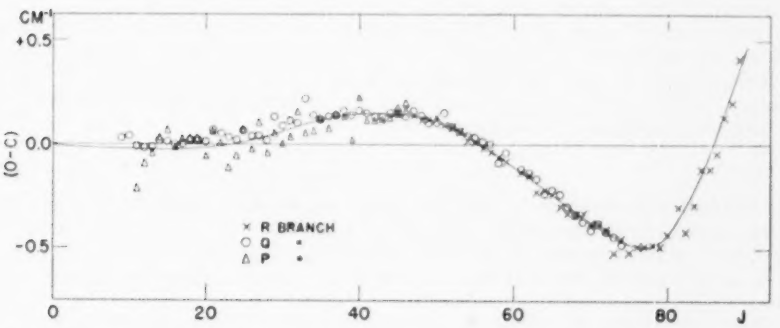

FIG. 6.—The differences (O − C) between the observed and the computed wave numbers of the lines of the 5597 A band.

intensity from one to the next. They are all degraded to the red. The most intense of the three bands, at 8937 A, has an observable Q branch, whose head is 15.5 cm^{-1} from the head of the R branch. This compares favorably with the analogous separation in the 8859 A band (11.3 cm^{-1}), when one considers that the Q head is quite weak, making accurate measurement impossible. Thus it is probable that these three bands, together with the 8859 A band, form a sequence of the $^1\Pi - {}^1\Delta$ system.

One may determine approximately where additional sequences of this band system should be located in the spectrum. As is well known, there is an approximate proportionality between the magnitudes of the rotational and vibrational constants for a given electronic state of a given molecule. Thus, since the rotational constants B of the $^1\Pi$- and $^1\Delta$-states are approximately the same as the rotational constants of the lower ($^3\Pi$) state of the a-system ($B_0'' = 0.5340$ cm^{-1}), then the vibrational constants, ω_e, should be approximately the same also, or about 1000 cm^{-1}. Therefore, in angstroms, one might expect additional sequences to appear at about 8139 A and 9721 A. The spectrum in the neighborhoods of both these wave lengths is very complex, and it is possible that some of the fainter band heads may be members of the $^1\Pi - {}^1\Delta$ system. This cannot be determined definitely, however, until better observational material is available. However, it

TABLE 5

BANDS OF THE $^1\Pi - {}^1\Delta$ SYSTEM

v', v''	λ_{air}		ν_{vac}	Int.	$\Delta\nu_{head}$
0, 0	8859.64 A	R	11,284.04 cm^{-1}	50	
	8868.49	Q	11,272.77	10	98.1 cm^{-1}
1, 1	8937.38	R	11,185.9	15	
	8949.8	Q	11,170.4	3	95.9
2, 2	9014.6	R	11,090.0	2	97.4
3, 3	9094.5	R	10,992.6	2	

is certain that no additional sequences are present which are similar in intensity to the 8859 A sequence. Therefore, it is highly probable that the 8859 A sequence is the main sequence of the $^1\Pi - {}^1\Delta$ system and that the 8859 A band is the (0-0) band. One may, accordingly, assign vibrational quantum numbers to the other members of the sequence, as shown in Table 5. Except for the 8859 A band, the measurements presented in Table 5 are those of Kiess,[11] as are also all the estimates of relative intensity. In the last column is shown the separation of successive band heads in wave numbers. These are all the bands which may be definitely assigned to the $^1\Pi - {}^1\Delta$ system at the present time, although, as mentioned above, additional work on the fainter bands in the spectrum will probably yield additional members.

b) THE $^1\Phi - {}^1\Delta$ SYSTEM

As was first pointed out by Lowater, a series of bands extending from the 5597 A band to longer wave lengths are undoubtedly further members of the same band system, since they constitute a sequence, with the 5597 A band at its head. Up to the present time, no additional sequences of this system have been found. By an argument similar to the one

[11] The author wishes to acknowledge the generosity of Dr. Kiess for permitting the use of these unpublished measurements.

used above in the case of the $^1\Pi - {}^1\Delta$ system, it is highly probable that this sequence at 5597 A is the main sequence of the $^1\Phi - {}^1\Delta$ system and that the 5597 A band is the (0-0) band of the system. This is in agreement with the suggestion made by Lowater. For the sake of completeness, Table 6 has been included here. All the measurements and identi-

TABLE 6

BANDS OF THE $^1\Phi - {}^1\Delta$ SYSTEM

V', V''	λ_{air}		ν_{vac}	Int.	$\Delta\nu_{band}$
0, 0	5597.68 A	*R*	17,859.60 cm^{-1}	8	
	5603.64	*Q*	17,840.60	3	101.3 cm^{-1}
1, 1	5629.28	*R*	17,759.3	7	
	5635.27	*Q*	17,740.4	2	101.2
2, 2	5661.55	*R*	17,658.1	7	
	5667.59	*Q*	17,639.3	2	101.9
3, 3	5694.42	*R*	17,556.2	4	
	5700.61	*Q*	17,537.1	2	101.2
4, 4	5727.43	*R*	17,455.0	3	
	5733.40	*Q*	17,436.8	2	

fications in Table 6 are those of Lowater, with the exception of the measurements of the heads of the (0-0) band, which have been taken from the present study.

I wish to acknowledge several helpful suggestions made by G. Herzberg during the course of this investigation and also his generosity in reading the manuscript.

THE INTERSTELLAR λ 4430 BAND

JESSE L. GREENSTEIN AND LAWRENCE H. ALLER
Mount Wilson and Palomar Observatories and Observatory of the University of Michigan
Received December 9, 1949

ABSTRACT

Measured equivalent widths of the interstellar λ 4430 band made on spectrograms taken at the McDonald Observatory are given in Table 1. The profile is found symmetric and smooth. Correlations of λ 4430 with other interstellar features are given in Table 2. The band is most strongly correlated with the interstellar λ 6284, fairly well correlated with interstellar reddening, and may be well correlated with interstellar polarization. Diffuse absorption bands occur in the solid and liquid states in molecules which have incomplete inner shells of electrons. Such substances are often paramagnetic, as in the case of iron alums and salts of the rare earths. It is possible that the compounds responsible for the diffuse interstellar bands also are active in the orientation of small, elongated paramagnetic grains and thus produce the interstellar polarization.

The broad, shallow absorption feature near λ 4430, detected by P. W. Merrill[1] and definitely shown to be interstellar by Merrill and Humason,[2] was observed in the spectra of numerous early-type stars by Beals and Blanchet.[3] It is conspicuous on low-dispersion spectra of highly reddened B stars. While the equivalent width, W, is large, the actual width is so great that the central absorption, A_c, is in all cases small. On high-dispersion spectra the band is seen only on microphotometer tracings. Thus the determination of W is necessarily inaccurate. Beals and Blanchet used spectra of late O and early B stars; they found a correlation of λ 4430 with the K line and with apparent distance modulus. It has since become clear that the correlation of λ 4430 with color excess is high and that the older apparent distance moduli need correction for interstellar absorption. In late O and early B stars the λ 4430 band is blended with many stellar lines, particularly *O* II. Between spectral types B3 and B8 the stellar lines are weak or absent. The extensive list[4] of accurate photoelectric color excesses, E_1, and approximate distance moduli, $(m_0 - M)$, corrected for interstellar absorption, provided a new choice of objects for study of the λ 4430 band. The program was initially confined to supergiants between B3 and B8, but a few stars of earlier and later types have been added. Stars were selected to provide reddened objects of both large and small true distance. New spectra were taken with the Cassegrain spectrograph of the 82-inch reflector at the McDonald Observatory. The *f*/2 Schmidt camera gave a dispersion of 70 A/mm; the 500-mm camera gave 30 A/mm and was used for a few highly reddened bright stars (HD 147889, 147933, 164353, 167971, 170740, 183143, 193514). A tube photometer provided calibration. The IIa-O emulsion was used. Spectra of the near ultraviolet longward of 3200 A, taken with quartz prisms, showed no strong additional interstellar bands.

Table 1 gives the HD designation, the equivalent width, W, in angstrom units, and n the number of spectra. Intensities of the interstellar D lines were taken from Merrill, Sanford, Wilson, and Burwell,[5] and of the diffuse interstellar band at λ 6284 from Merrill and Wilson.[6] Figure 1 gives the profiles of λ 4430 in three stars. Four plates were avail-

[1] *Mt. W. Contr.*, No. 536; *Ap. J.*, **83**, 126, 1936.

[2] *Pub. A.S.P.*, **50**, 212, 1938.

[3] *M.N.*, **98**, 398, 1938.

[4] Stebbins, Huffer, and Whitford, *Mt. W. Contr.*, No. 621; *Ap. J.*, **91**, 20, 1940.

[5] *Mt. W. Contr.*, No. 576; *Ap. J.*, **86**, 274, 1937.

[6] *Mt. W. Contr.*, No. 582; *Ap. J.*, **87**, 9, 1938.

able for HD 183143; no asymmetry or structure was detected. Since the profiles are similar in the three stars, W must be approximately proportional to A_c; the bands are unsaturated. Figure 2 shows a correlation of our measures of λ 4430 with E_1; the measures of Beals and Blanchet ("BB") are included. Only two stars are common to our list ("AG") and theirs, and for these our W (AG) = 0.87 W(BB). This correlation diagram seems to show that the regression line W(BB) on E_1 has a steeper slope than that of W(AG) on E_1; since completely different stars are involved and since the intrinsic spread in W is large, no inference as to scale error can be drawn. Measurement of λ 4430 is very difficult. Even with relatively fine-grain IIa-O film and widened spectra analyzed with a broad, long microphotometer slit, the fluctuation of the tracing of the continuous background is usually of the order of ±0.02; a single difference of intensity, A, has an error of nearly ±0.03. Only the strongest bands had A_c exceeding this error by a factor of 3.

TABLE 1

EQUIVALENT WIDTHS OF λ 4430

HD	W	n	HD	W	n	HD	W	n
108	1.65	2	15497	2.63	5	193514	2.26	3
698	0.92	2	16778	3.59	3	194279	3.00	2
2905	1.77	4	17505	2.45	6	194839	2.82	3
3940	3.10	5	34085	0.34	3	198895	2.42	2
4768	2.2	1	147889	2.71	2	199478	1.30	4
4841	2.20	5	147933	1.77	3	208501	1.50	4
7902	1.4	1	164353	0.5	1	218376	0.90	5
9105	2.97	4	164359	0.9	1	223960	1.80	2
MWC 14	1.80	4	164402	1.26	2	E227460	1.0	1
13267	2.57	4	164865	1.9	1	E228548	1.6	1
14010	2.26	4	167971	2.10	2	+31°643	2.70	5
14322	1.48	3	170740	1.72	2	+46°3474	2.50	3
14542	2.18	2	183143	4.92	4			

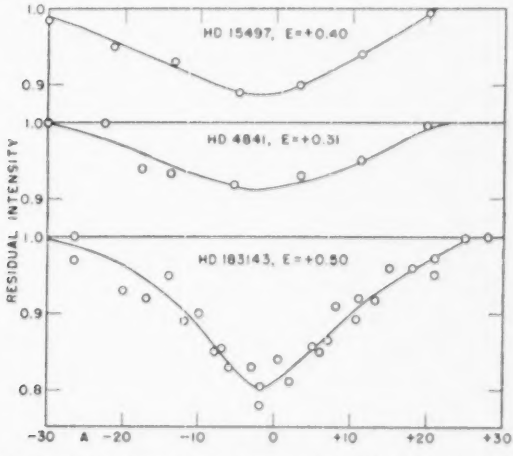

FIG. 1.—The profile of λ 4430 in three stars. Measures of individual points are plotted for HD 183143; normal places for the other stars.

An error of 0.01 in drawing the level of the continuous spectrum yielded an error of about 0.3 A in W. It is not surprising that even in stars of small E_1 an appreciable W is measured; for four stars of $E_1 \leqslant +0.10$, we find $W = 0.90$ A and, from Beals and Blanchet's measure, $W = 0.86$ A. A certain prejudice may exist, tending to put the continuum too high or to include weak stellar lines in both these investigations. The effect of such an error is to reduce the correlation coefficients. Figure 3 shows the correlation of the measures of λ 4430 with those of the diffuse interstellar band, λ 6284. This band[6] is relatively sharp and has A_v of 0.20 for $W = 1.0$ A; λ 4430 has A_v near 0.04 for $W = 1.0$ A. In spite of the large accidental error in W(4430), there is an excellent correlation and perhaps even a one-to-one correspondence between the intensities of λ 4430 and λ 6284.

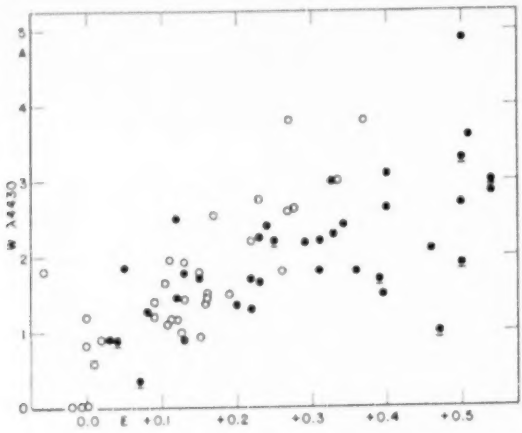

FIG. 2.—Correlation of the equivalent widths of λ 4430 with photoelectric color excess, E_1. *Solid dots*, this investigation, underlined when only one plate available; *open circles*, Beals and Blanchet.

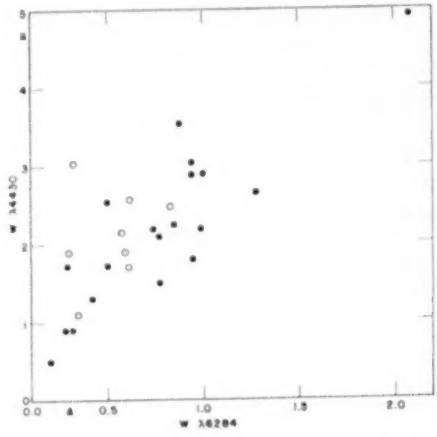

FIG. 3.—Correlation of the equivalent width of the diffuse interstellar bands at λ 4430 and λ 6284. *Solid dots*, this investigation; *open circles*, Beals and Blanchet.

A number of linear correlation coefficients were computed and are given in Table 2, together with their mean errors. Only stars for which we had two or more plates were used in the correlation of $W(4430, AG)$ with other quantities. In the correlation of λ 4430 with the interstellar D lines, the quantity $\frac{1}{2}(D_1 + D_2)$ is used, and stars are omitted for which a zero or no intensity is given. As the figures indicate, the correlation of λ 4430 with λ 6284 is excellent, and of λ 4430 with color excess, E_1, fairly good; that of λ 4430 with the D lines is barely significant. There is no correlation of λ 4430 with $m_0 - M$. Previous investigations suggested a correlation of λ 4430 with distance, as derived from the uncorrected distance modulus, $m - M$. Since these moduli differ by about $7E_1$, the correlation of λ 4430 with E_1 appears as a spurious correlation of λ 4430 with $m - M$. The list of stars for which λ 6284 was measured includes about one hundred objects; for these the corrected distance modulus has no correlation with space reddening ($r = +0.06 \pm 0.11$). Similarly, in our list, which deliberately includes many near-by highly reddened stars, the correlation of λ 4430 with corrected distance modulus is small but actually negative (-0.26 ± 0.18). The available values for $m_0 - M$ have unnecessarily large scatter, since they still include errors of luminosity classification; for example, HD 15497,

TABLE 2

CORRELATION COEFFICIENTS

Correlation	r	Remarks	Correlation	r	Remarks
λ 4430—E_1	$+0.72 \pm 0.10$	W(AG)	λ 6284—E_1	$+0.77 \pm 0.04$	
λ 4430—E_1	$+0.78 \pm 0.08$	W(BB)	λ 6284—(m_0-M)	$+0.27 \pm 0.10$	
λ 4430—D	$+0.38 \pm 0.20$	W(AG)	E_1—(m_0-M)	$+0.06 \pm 0.11$	Stars in λ 6284 list
λ 4430—λ 6284	$+0.84 \pm 0.08$	W(AG)			
λ 4430—(m_0-M)	-0.26 ± 0.18	W(AG)			

B7s, has strong interstellar lines and bands and must be a supergiant with a true modulus of 10 rather than 5.5. Several of the correlations in Table 2 are thus subject to improvement.

Regional analysis of the data does not seem profitable. We cannot find any significant statistical weakening of the λ 4430 band in O stars. Our accuracy, however, is sufficient to indicate that stars of the same E_1 may have different strengths of λ 4430. Thus HD 183143, $E_1 = +0.50$, has the strongest measured λ 4430 (4.9 A) and λ 6284 (1.9 A). Other stars of the same reddening have $W(4430)$ between 2.7 and 3.6 A. This cB9 supergiant occurs in a region of the Milky Way, at $l = 21°$, where few other distant and highly reddened stars are known. The region $0° < l < 40°$ is that of the near-by complex of dark nebulae in the rift in Scutum, Aquila, and the southern part of Cygnus. It is very opaque and relatively free of emission nebulae, hence probably a neutral hydrogen region. The Stebbins, Huffer, and Whitford catalogue[4] shows only four other highly reddened stars in this region which have E_1 of the order of +0.30. From unpublished data kindly communicated by Dr. John S. Hall, HD 183143 appears to have the highest known polarization, nearly 7 per cent.[7] Another star with $E_1 = +0.50$ is HD 147889, which has $W(4430)$ of 2.7 A and a polarization near 4 per cent. It seems possible that ultimately a correlation of λ 4430 and polarization might yield valuable results. For example, both HD 147889, which illuminates a reflection nebula at a distance of 100 parsecs, and HD 183143, at a distance of nearly 1000 parsecs, seem to suffer absorption in neutral hydrogen regions. Nevertheless, the λ 4430 intensity and polarization differ for the two stars.

The hypothesis has been advanced that the diffuse interstellar bands arise either from absorption bands present at low temperature in the solids forming the absorbing par-

[7] Also Hall and Mikesell, *A.J.*, **54**, 187, 1949.

ticles or from gases commonly associated with these particles. H. C. van de Hulst[8] has shown that, if a band is to arise from the solid state, the particles must be small, and the physical process one of pure absorption. Then, if the "molecule" producing the λ 4430 band originates in either the solid or the gaseous state,

$$W = 2 \times 10^{-13} N f ,$$

where N is the number of molecules per square centimeter between us and the star. The mass per square centimeter is $N\mu m_H$, where μ is the molecular weight; this mass per square centimeter is $8 \times 10^{-12} W\mu/f$. The molecular weight must be at least 50 unless H_2 is involved, and the f-value for the whole band is probably not greater than 0.01. Thus, if the band arises from the ground state of the molecule, the mass per square centimeter should exceed $4 \times 10^{-8} W$; for HD 183143 this is 2×10^{-7} gm/cm². HD 183143 suffers about 4.5 mag. photographic absorption, equivalent to perhaps 4.5 kpc of interstellar gas and dust at average space density. (We assume that the ratio of gas to dust remains constant, the mean absorption coefficient is 1 mag. per kiloparsec, and the mean space density of hydrogen is one atom per cubic centimeter.) Thus there is about 0.02 gm/cm² of interstellar hydrogen in the same line of sight, and the molecule producing λ 4430 should have an abundance by weight greater than 10^{-5} that of hydrogen. This is close to the generally accepted value for the interstellar molecules *CN* and *CH*. Complex compounds of the metals are obviously excluded as a source of λ 4430; compounds involving *Fe*, *Si*, *Mg*, *S*, and the common gases *C*, *N*, *O*, and *H* are possible. The surface density of the interstellar dust necessary to produce absorption of 1 mag. has been estimated to be near 3×10^{-4} gm/cm². Van de Hulst[8] has given a theoretical value as low as 2×10^{-5} gm/cm². If we adopt 10^{-4} gm/cm², we find that the molecule should have an abundance near 2×10^{-3} that of the solid absorbing matter. Again, only a common substance seems possible; a concentration of 10^{-3} might exist in dust for compounds of *Fe*, *Si*, *Mg*, and *S*, with greater concentrations for CH_4, NH_3, H_2O, O_2, and possibly even H_2. While van de Hulst[8] finds theoretical difficulties in the production of absorption bands in scattering dust grains, it is possible that absorbing substances play a larger role than he has assumed. The theories[9] of the origin of interstellar polarization require paramagnetic or ferromagnetic substances to be present in concentrations of about 10^{-3} or greater. One of the most suggestive features of a possible correlation of λ 4430 and interstellar polarization is that paramagnetic substances have incomplete inner shells of electrons. Such incomplete shells may produce in molecules in the solid state relatively sharp absorption bands. Examples occur in the rare-earth and uranyl compounds; neodymium liquid filters have been used to produce absorption bands for objective-prism radial velocities. The rare-earth and metallic alums form highly paramagnetic crystals. It is, of course, not suggested that interstellar dust has a large proportion of rare earths but rather that it contains paramagnetic compounds of other common substances with relatively sharp absorption bands.

This investigation was begun by Mr. Greenstein at the Yerkes and McDonald observatories and by Mr. Aller at Indiana University under a co-operative arrangement with the McDonald Observatory.

[8] *Rech. Astr., Obs. Utrecht*, Vol. 11, Part 2, 1949.

[9] Davis and Greenstein, *Phys. Rev.*, **75**, 1605, 1949; Spitzer and Tukey, *Science*, **109**, 461, 1949.

THE PECULIAR STAR HD 30353*

WILLIAM P. BIDELMAN
Yerkes and McDonald Observatories
Received October 25, 1949

ABSTRACT

The spectrum of HD 30353 is shown to possess characteristics similar to those of the well-known peculiar star υ Sagittarii, but at a somewhat lower temperature. From the comparative weakness of the lines of neutral iron and of ionized calcium, the spectral type of HD 30353 may be estimated as near A5, but the hydrogen lines are extremely weak, and there is no measurable Balmer discontinuity. The spectrum is a most complex one, containing very strong lines of the ionized metals, as well as many additional lines which do not appear strongly in normal stellar spectra. The *Hα* line appears in emission. A table of wave lengths covering the region λλ 3517–6678 A is contained in the paper.

It has been found that the radial velocity of HD 30353 is variable in a period of the order of 1 year. The value of *K* appears to be at least 50 km/sec.

The paper closes with some general remarks concerning the stars whose spectra give evidence of low hydrogen content.

I. INTRODUCTION

A number of stars are known whose spectra show abnormally weak absorption lines of hydrogen, compared with those in the spectra of other stars of similar temperature. Most of these have proved to be normal supergiants of classes B and A, and the weakness of their hydrogen lines has been ascribed to the very low pressures in their atmospheres. There exist, however, several stars in whose spectra the hydrogen lines are so weak that the stellar atmosphere appears to be actually deficient in hydrogen. The most recently discovered of these, HD 30353, is the subject of the present paper. The known members of this "hydrogen-poor" group and their approximate spectral classes are the following: (*a*) HD 124448, B2; (*b*) υ Sgr, A0; (*c*) HD 30353, A5; (*d*) the stars of the R CrB type, F5. A brief description of the spectra of these objects follows:

a) The far-southern star HD 124448 was recently found by Popper to show no observable Balmer lines, even on moderately high dispersion. All other lines commonly found in B2 stars are considerably enhanced, while the opacity usually due primarily to neutral hydrogen atoms is so lacking that Popper was able to measure the helium discontinuity at λ 3420 A.[1]

b) The spectrum of the single-lined spectroscopic binary υ Sagittarii has long been known to show anomalously weak hydrogen lines, strong helium lines, and numerous lines which do not appear in normal stellar spectra. It has been thought by some investigators merely to show, to an exceptional degree, the usual characteristics of the A-type supergiant stars.[2] Greenstein, however, has pointed out that the weakness of the hydrogen lines relative to those of the ionized metals cannot be explained in this way.[3] The low opacity of the atmosphere of υ Sagittarii is revealed by the great strength of absorption lines of high excitation potential, and the abnormally small number of absorbing hydrogen atoms in the second level is emphasized by the negligible value of the Balmer discontinuity. The *Hα* line appears in emission in υ Sagittarii and has occasionally shown a P Cygni structure.[4]

* *Contributions from the McDonald Observatory, University of Texas*, No. 184.

[1] *Pub. A.S.P.*, **54**, 160, 1942; **58**, 370, 1946; **59**, 320, 1947.

[2] C. H. Payne, *The Stars of High Luminosity* ("Harvard Monographs," No. 3 [1930]), p. 146.

[3] *Ap. J.*, **91**, 438, 1940.

[4] W. P. Bidelman, *Ap. J.*, **109**, 544, 1949.

c) As will be shown later, the star HD 30353 appears to be a lower-temperature analogue of υ Sagittarii. It is also the brighter component of a spectroscopic binary system.

d) The stars of the R Coronae Borealis type present unsolved problems of extreme interest, and it is not certain that they should be included in the present discussion, although their spectra show practically no evidence of hydrogen, either at maximum or at minimum light. The uncertainty on this point arises from the presence in their spectra of strong high-excitation lines of neutral carbon, as well as moderately strong bands due to C_2. It is difficult to avoid the conclusion that carbon is abnormally abundant in the R CrB stars, while the other three objects do not show evidence of an overabundance of carbon. The cooler carbon star, HD 182040, though unvariable, also appears to be deficient in hydrogen.[5]

II. THE SPECTRUM OF HD 30353

Attention was called to the unusual spectrum of HD 30353[6] many years ago in the *Henry Draper Catalogue*, and the star is also included in Miss Payne's c-star catalogue.[2] The description of its spectrum given in the *Henry Draper Catalogue* is as follows: "The spectrum has narrow lines and shows very little absorption at the band G. In that respect it resembles the spectrum of HD 18474[7] and of R Coronae Borealis." Apparently, no slit-spectrograph observations of this star had been made previous to the writer's observation in October, 1946. A low-dispersion spectrogram was obtained at that time, which was the basis of a preliminary report given at the September, 1947, meeting of the American Astronomical Society.[8] A more detailed study has awaited further spectroscopic material, which has since been obtained for the writer by Drs. J. L. Greenstein, O. Struve, and G. H. Herbig.

The spectrum of HD 30353 on low dispersion (76 A/mm at $H\gamma$) is reproduced in Figure 1, together with the spectra of two supergiant stars of luminosity class Ia of types A2 and A5—α Cygni and φ Cassiopeiae.[9] It is apparent that the G band is indeed weak or missing in the spectrum of HD 30353, but it is also evident that the H and K lines are more consistent with a spectral type of about A5 than with one of G0. The spectrum is very complex and filled with strong absorption lines of the ionized metals, in which respect it resembles to some extent the F5 supergiant α Persei; but the comparative weakness of the lines of neutral iron and of ionized calcium make it necessary to classify HD 30353 as an A-type star, although, properly speaking, it cannot be given a spectral type at all. The most remarkable feature of its spectrum, however, is the extreme weakness of the lines of hydrogen. They are far weaker than those of normal A-type supergiants and, for that matter, far weaker than those of F- or G-type stars as well.

A number of higher-dispersion spectrograms of HD 30353 have been recently obtained at the McDonald Observatory, and a study of its spectrum has been made, covering the wave-length range $\lambda\lambda$ 3517–6678 A. The results of this study may be summarized as follows: (*a*) The $H\alpha$ line appears in emission on the only spectrogram available in this region. The higher members of the Balmer series weaken greatly as the series limit is approached, and no Balmer discontinuity is measurable. (*b*) Lines of helium are certainly present, although only a few are unblended. (*c*) Many other high-excitation lines appear in unusual strength, and many unclassified and predicted lines of the ionized metals, espe-

[5] K. Wurm, *Naturw.*, **29**, 686, 1941.

[6] $\alpha = 4^h41^m8$, $\delta = +43°6'$ (1900); $m_v = 7.7$, HD spectrum G0p. The galactic co-ordinates are: $l = 129°$, $b = 0°$.

[7] HD 18474, which is HR 885, $m_v = 5.6$, is a peculiar star which has not been carefully studied. It exhibits the unique peculiarity of a spectrum resembling that of a giant G-type star but with no observable *CH* or *CN* absorption.

[8] *A.J.*, **53**, 110, 1948.

[9] W. W. Morgan, P. C. Keenan, and E. Kellman, *An Atlas of Stellar Spectra* (Chicago: University of Chicago Press, 1943).

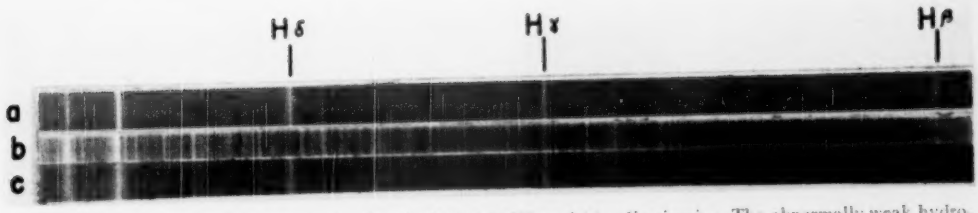

FIG. 1.—Low-dispersion spectra of (*a*) α Cygni, (*b*) HD 30353, and (*c*) φ Cassiopeiae. The abnormally weak hydrogen lines and complex nature of the spectrum of HD 30353 are apparent.

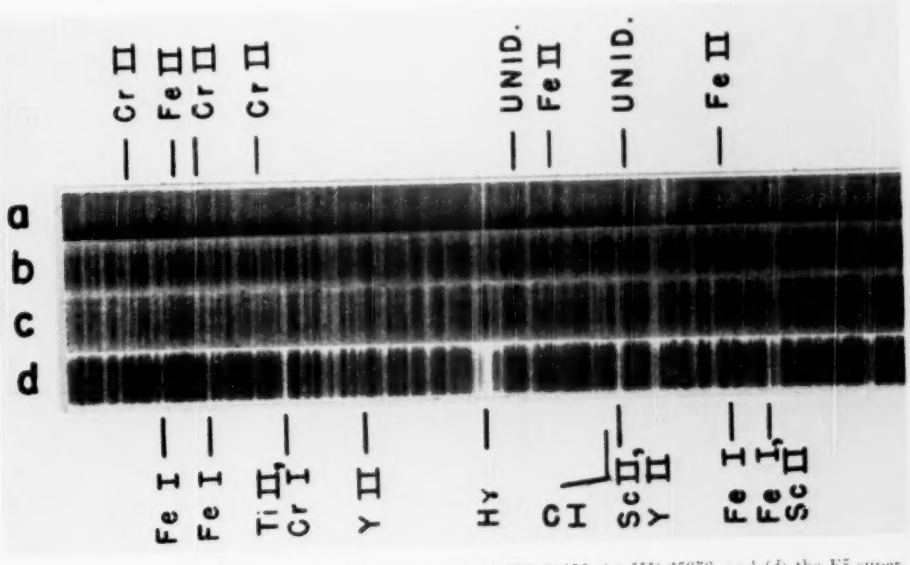

FIG. 2.—A portion of the spectra of (*a*) υ Sagittarii, (*b*) HD 30353, (*c*) HD 25878, and (*d*) the F5 supergiant star α Persei. Lines which are much stronger in HD 30353 than in α Persei are indicated above the spectra; those stronger in α Persei are indicated below. The lines due to *Cr* II arise from 3.85 electron volts, while those due to *Fe* II are unclassified. The C I line at 4371 A is very strong in the spectrum of HD 25878.

cially *Fe* II, are strongly present. An extremely large number of unidentified lines occur. Of nearly 800 lines measured, about 120 have not been satisfactorily identified, many of these lines being found also in υ Sagittarii. About half the unidentified lines are found between $H\beta$ and $H\alpha$. (*d*) The visual region of the spectrum of HD 30353 resembles that of υ Sagittarii much more than it does that of any normal star.

It seems clear from the study of the spectrum of HD 30353 on moderately high dispersion that the distinguishing characteristics of the spectrum of υ Sagittarii, hitherto considered unique, are present to a somewhat less marked degree in the spectrum of HD 30353. However, the conditions of ionization and excitation are both less extreme in the latter star.

The appearance of the spectrum of HD 30353 on moderate dispersion (27 A/mm at $H\gamma$) may be judged from an inspection of Figure 2, which shows a small region surrounding $H\gamma$. Together with the spectrum of HD 30353 are shown the spectra of υ Sagittarii, HD 25878, which has a spectrum similar to that of R Coronae Borealis,[10] and α Persei. Lines which appear much stronger in HD 30353 than in α Persei are marked above the spectra, and those which are stronger in α Persei are marked below. The similarity of the spectra of HD 30353 and HD 25878, except for the presence in the latter of lines of neutral carbon and those which strengthen with lower temperature, is remarkable. Both spectra are considerably more complex than that of α Persei.

TABLE 1

SPECTROGRAMS OF HD 30353 MEASURED FOR WAVE LENGTH

Region Å	Plate No.	Date	Type of Plate	Dispersion (A/Mm)
3517–3896	CQ 7208	Nov. 21, 1948	103*a*-O plate	27– 39
3896–4855	CG 6260	Nov. 12, 1947	IIa-O film	16– 41
4855–6678	CG 6228	Nov. 5, 1947	103*a*-F film	41–120

The line at $H\gamma$ is of special interest. In υ Sagittarii and α Persei it is overwhelmingly due to hydrogen, but in HD 30353 the line is obviously a blend, with the violet component due to hydrogen and the red component due, probably, to a blend of a *Ti* II and a *Cr* II line. In HD 25878 the component due to hydrogen appears to be completely absent.

In view of the unusual nature of HD 30353, wave lengths in the entire spectral region available have been measured. Data on the spectrograms used are given in Table 1, and the derived wave lengths and identifications are listed in Table 2.

Although only one spectrogram was used for each region, it is hoped that few spurious lines appear in the final wave-length table. Errors in wave length corresponding to more than 3 or 4 μ should be rare, since the lines are quite sharp with the dispersion used. Plate CG 6260 was of excellent quality, but the use of fine-grained emulsions in the ultraviolet and visual regions would have permitted the measurement of many more lines.

In view of the moderate dispersion, no attempt has been made to give a complete list of contributors to the stellar lines. Only lines which are felt to be major contributors have been included in Table 2. The isolation of even major contributors, however, is a difficult task in a spectrum which contains many unidentified lines. The procedure in making the identifications was as follows:

a) First, the *Revised Multiplet Table*[11] was used to make a complete list, multiplet by multiplet, of tentative identifications, bearing in mind both the relative intensities within

[10] W. P. Bidelman, *Ap. J.*, **107**, 413, 1948.

[11] C. E. Moore, *A Multiplet Table of Astrophysical Interest, Revised Edition* (*Contr. Princeton U. Obs.*, No. 20 [1945]).

TABLE 2

WAVE LENGTHS MEASURED IN THE SPECTRUM OF HD 30353

λ	Int.	Identification		λ	Int.	Identification	
3517	37(1)	*V* II-6	7.30(800)	3602	25(0)	*Co* I-4	2.08(40)
3520	28(5)	*Ti* II-98	0.25(20)			*V* II-9	1.93(100)
3521	88(4)	*Fe* II-10	1.64(p)			*Fe* II-101	2.60(p)
		Fe II-10	2.05(p)	3603	73(7)	*Cr* II-13	3.80(40)
3523	68(3)	*v* Sgr	3.45(2)			*Cr* II-13	3.86(20)
3524	78(4)	*V* II-5	4.71(200)			*Cr* II-13	3.61(20)
		Ni I-18	4.54(200)	3606	27(3n)	*Fe* II-175	6.18(p)
3526	45(7)	*v* Sgr	6.36(8)			*Fe* I-294	6.68(20)
3530	84(5n)	*V* II-5	0.76(500)			*Fe* I-294	5.45(15)
3533	12(4)	*Fe* II-132	2.65(2)	3608	76(5)	*Ni* II-4	8.7(p)
		Ti II-98	3.87(2)			*Fe* I-23	8.86(100)
3535	69(8)	*Ti* II-98	5.41(40)	3610	36(3)	*Fe* II-112	0.33(p)
3538	55(4)	*v* Sgr	8.67(2)	3613	52(12n)	*v* Sgr	3.11(3)
3540	05(0)	*v* Sgr	0.02(1)			*Sc* II-2	3.84(60)
3541	33(3)	*V* II-145	1.34(50)	3614	71(4)	*Fe* II-112	4.87(5)
3543	39(3)	*v* Sgr	3.24(3)	3619	01(6)	*V* II-158	8.92(200)
3545	23(7)	*V* II-5	5.19(1000)			*Fe* I-23	8.77(125)
3548	33(3n)	*Mn* I-18	7.80(50)			*Ni* I-35	9.39(150)
		Mn I-18	8.03(40)	3621	41(5)	*Fe* II-144	1.27(6)
		Mn I-18	8.20(30)			*Co* II-1	1.22(100)
		Fe II	9.03(1)	3622	97(0)	*v* Sgr	3.19(2)
3551	89(1)	*Zr* II-1	1.94(18)			*Fe* II-175	2.81(p)
3553	63(4N)	*Mg* II-11	3.51(5)	3624	84(6)	*Ti* II-52	4.83(70)
		He I-34	4.39(1)			*Fe* II-144	4.89(5)
		He I-34	4.52(1)	3627	37(6)	*Mn* II?	7.46(1)
		ϵ Aur	2.64(1)			*Fe* II-193	7.17(1)
3556	93(3n)	*V* II-5	6.80(1500)	3631	53(15n)	*Cr* II-12	1.49(50)
		Fe II-176	7.55(2)			*Cr* II-12	1.72(40)
		Zr II-9	6.61(30)			*Sc* II-2	0.74(50)
3558	71(1)	*Sc* II-3	8.54(20)			*Fe* II-112	2.29(3)
		Fe I-24	8.52(30)	3634	32(3n)	*He* I-28	4.24(2)
3561	11(12n)	*v* Sgr	1.22(4)			α Cyg	4.98(2)
3565	12(5N)	*V* II-4	6.18(200)			*Cr* II-147	4.04(10)
		Fe II-132	6.15(3)	3638	28(0)	*v* Sgr	8.48(1)
		Fe II-113	4.54(p)	3641	33(4)	*Ti* II-52	1.34(100)
		Ti II-42	6.00(6)	3643	11(5)	*Sc* II-2	2.78(40)
3567	62(0?)	*Sc* II-3	7.70(20)			*Cr* II-1	3.22.10)
3569	74(3n)	*Fe* II-113	8.97(p)	3645	04(6)	*Cr* II-1	4.70(10)
		Fe I-24	0.10(100)			*Sc* II-2	5.31(30)
		Co I-35	9.37(80)	3647	47(4)	*Cr* II-1	7.40(8)
3573	51(5N)	*Ti* II-15	3.74(20)			*Fe* I-23	7.84(100)
		Sc II-3	2.52(50)	3648	88(0)	*Mn* II?	8.72(1)
		v Sgr	5.29(3)	3650	18(2)	*Cr* II-156	0.37(40)
		Zr II-1	2.47(30)	3651	81(4)	*Cr* II-1	1.68(12)
3576	73(5)	*Ni* II-4	6.76(3)			*Sc* II-2	1.80(25)
		Sc II-3	6.34(35)	3655	34(1)	*Al* II-12	5.00(14)
3578	14(3)	*Co* II-1	8.03(30)	3656	61(0)	*Fe* II-111	6.50(p)
3581	06(8)	*v* Sgr	1.11(2)	3658	01(1)	*Cr* II-98	8.19(20)
3585	18(6)	*Cr* II-13	5.31(60)	3659	75(2)	*Ti* II-75	9.76(60)
		Cr II-13	5.54(40)	3662	30(6)	*Ti* II-75	2.24(40)
3587	38(6)	*Ti* II-15	7.13(12)	3664	84(3)	*Cr* II-156	4.95(30)
		Al II-7	6.56(10)	3666	77(1)	*v* Sgr	7.08(2)
		Al II-7	7.07(9)	3669	38(4)	*V* II-116	9.41(300)
		Al II-7	7.45(8)	3674	22(2n)	*Zr* II-9	4.74(40)
3589	74(5)	*V* II-4	9.74(1000)			*Fe* II-131	3.77(p)
3591	93(3)	*V* II-4	2.01(800)	3677	76(8)	*Cr* II-12	7.86(50)
3593	42(4)	*V* II-4	3.32(600)			*Cr* II-12	7.69(40)
3596	19(5)	*Ti* II-15	6.05(60)	3679	74(2)	*Ti* II-75	9.67(3)
3597	84(2)	*v* Sgr	7.63(3)			*Fe* I-5	9.92(40)
3600	66(1)	*Y* II-9	0.74(300)	3681	36(0)	*Fe* II-111	0.98(p)

TABLE 2—*Continued*

λ	Int.	Identification		λ	Int.	Identification	
3685.70	(15N)	*Ti* II-14	5.19(250)	3765.72	(0)	*Cr* II-20	5.62(8)
		Cr II-145	4.25(25)			*Fe* I-608	5.54(20)
		Mn II-8	6.20(1)	3767.25	(3)	*Fe* I-21	7.19(80)
		Cr II-118	6.67(20)			*Mn* II?	7.54(1)
3690.32	(1n)	*Fe* I-369	9.46(12)			*Zr* II-7	6.83(25)
		H 18	1.56	3769.57	(5)	*Ni* II-4	9.46(5)
3693.35	(0n)	*v* Sgr	3.28(1)	3770.68	(4)	*H* 11	0.63
		Fe I-394	4.00(20)			*V* II-21	0.97(400)
		O I-6	2.44(7)	3774.15	(3n)	*v* Sgr	3.66(2)
3696.50	(2)	*Cr* II-131	6.78(8)			*Ti* II-12	4.65(3)
		v Sgr	5.84(2)			*V* II-7	4.33(300)
3697.84	(4)	*Cr* II-118	8.00(35)	3776.16	(3)	*Ti* II-72	6.06(6)
		Zr II-71	8.17(100)	3779.00	(4n)	*Fe* II-23	9.58(p)
3700.87	(3n)	*V* II-116	0.34(200)			*V* II-21	8.36(100)
		v Sgr	0.94(2)			*Fe* II-192	8.37(p)
3703.45	(1)	*v* Sgr	3.59(1-0)	3781.38	(2)	*Fe* II-130	1.51(1)
3705.94	(8)	*Ca* II-3	6.03(10)	3783.38	(5)	*Fe* II-14	3.35(4)
		Ti II-73	6.22(20)	3786.94	(5N)	*Fe* II-15	6.37(p)
3709.82	(2)	*V* II-7	0.30(500)			*V* II-100	7.24(150)
		Fe I-21	9.25(75)			*Fe* I-21	7.88(50)
		Zr II-45	9.27(60)			*Ti* II-12	6.33(p)
3712.82	(7)	*Cr* II-12	2.97(35)	3791.57	(0)	ε Aur	1.43(0)
		Cr II-12	3.04(15)	3794.80	(3)	*Fe* I-21	5.00(60)
3715.30	(6)	*V* II-15	5.48(1200)	3796.85	(3)	*Ti* II-12	6.90(2)
		Cr II-20	5.19(20)	3798.32	(5)	*H*10	7.90
		Cr II-145	5.45(20)			*Fe* II-14	8.36(p)
3717.87	(1)	*Mn* II-8	7.53(1)	3801.70	(0)	*Mn* II-14	1.63(3)
		V II-21	8.16(60)	3806.14	(3n)	*He* I-63	5.76(1)
3720.04	(3)	*Fe* I-5	9.94(250)			*Fe* II-153	6.82(p)
		Fe II-23	0.17(p)	3809.88	(2n)	*v* Sgr	9.54(4)
3721.90	(4)	*Ti* II-13	1.63(15)			α Cyg	0.02(1-0)
		*H*14	1.94	3814.23	(12)	*Ti* II-12	4.58(4)
3723.56	(2)	*Cr* II-144	3.40(15)			*Fe* II-153	4.12(4)
3725.31	(2)	*Fe* II-130	5.30(3)	3817.46	(1)	*v* Sgr	7.37(2)
		Mn II-8	5.29(1)	3820.01	(4)	*He* I-22	9.61(4)
3727.48	(6)	*V* II-21	7.35(1000)			*Fe* I-20	0.43(250)
		Cr II-117	7.37(40)	3821.79	(3)	*Fe* II-14	1.92(p)
3732.71	(7)	*V* II-15	2.76(800)	3824.88	(6)	*Fe* II-29	4.91(4)
3734.96	(3)	*Fe* I-21	4.87(300)			*Fe* I-4	4.44(50)
3737.53	(7n)	*Ca* II-3	6.90(12)	3827.37	(3)	*Fe* II-153	7.08(4)
		Cr II-20	8.38(25)			*Fe* I-45	7.82(75)
3741.59	(4)	*Ti* II-72	1.63(50)	3829.67	(2)	*Mg* I-3	9.35(40)
3743.41	(4)	*Fe* II or III	3.40(8)	3832.86	(4)	*Fe* II-23	3.02(p)
3746.06	(6)	*V* II-15	5.81(800)			*Mg* I-3	2.30(80)
		Fe II-14	6.56(p)	3834.51	(3)	*Fe* I-20	4.22(100)
		Fe I-5	5.56(100)			*Fe* II-129	4.81(p)
3748.62	(7)	*Fe* II-154	8.49(8)	3835.94	(4)	*H*9	5.39
3750.97	(5)	*V* II-21	0.88(600)			*Ti* II-12	6.08(1)
		Cr II	0.56(12)	3838.18	(2)	*Mg* I-3	8.29(100)
3754.98	(7)	*Fe* II-154	5.56(4)			*He* I-61	8.09(1)
		Cr II-20	4.59(20)	3840.63	(3)	*Fe* I-20	0.44(80)
3757.72	(3)	*Ti* II-72	7.68(30)			*Fe* I-45	1.05(80)
3759.61	(3)	*Fe* II-154	9.46(6)	3844.89	(7)	*Fe* II-127	5.18(p)
		Ti II-13	9.29(200)			*v* Sgr	4.18(3)
3761.53	(5)	*Ti* II-13	1.32(200)	3847.96	(0)	*V* II-156	7.32(100)
		Ti II-107	1.87(15)			*Mg* II-5	8.24(7)
		Cr II-11	1.90(8)	3849.82	(6)	*Ni* II-11	9.58(2)
		Cr II-11	1.69(7)			*Mg* II-5	0.40(6)
3763.79	(5)	*Fe* II-192	2.89(5)	3853.67	(5)	*Si* II-1	3.66(3)
		Fe I-21	3.79(100)	3856.06	(6)	*Si* II-1	6.02(8)
		Fe II-29	4.09(p)	3859.85	(4)	*Fe* I-4	9.91(300)

TABLE 2—*Continued*

λ	Int.	Identification	
3862.97(8n)		*Si* II-1	2.59(6)
		Fe II-127	3.95(1)
3866.33(6n)		*Cr* II-167	5.59(75)
		He I-20	7.48(2)
3872.44(5)		*Fe* I-20	2.50(60)
		Fe II-29	2.76(p)
3875.78(0)		υ Sgr	5.75(1-0)
3878.49(6)		*V* II-33	8.72(300)
		Fe I-4	8.58(100)
3882.39(3)		*Ti* II-34	2.28(p)
3884.81(1)		*V* II-33	4.85(50)
3886.85(2)		*Fe* I-4	6.28(40)
		Fe I-20	7.05(15)
3888.38(6)		*He* I-2	8.65(20)
		υ Sgr	7.57(3)
		*H*8	9.05
3892.36(1)		υ Sgr	2.30(4)
3895.75(4)		*Fe* I-4	5.66(25)
		Fe II-23	6.11(p)
3898.04(1n)		*Mn* II?	7.60(1)
		υ Sgr	8.61(2)
3899.13(2)		*V* II-33	9.14(200)
3900.64(7)		*Ti* II-34	0.55(70)
		Al II-1	0.68(10)
3902.08(1)		α Cyg	1.62(1)
		υ Sgr	2.50(1)
3903.18(7)			
3905.85(8)		*Fe* II-173	6.04(5)
		Cr II-167	5.64(25)
		Si I-3	5.53(100)
3908.17(2)		υ Sgr	8.10(2)
3909.48(0)		υ Sgr	9.64(0)
3911.24(5)		υ Sgr	1.43(3)
3913.50(7)		*Ti* II-34	3.46(60)
3914.21(6)		*Fe* II-3	4.48(2)
		V II-33	4.33(250)
3916.32(5)		*V* II-10	6.42(200)
		Zr II-17	5.94(25)
3918.40(4)		*Fe* II-191	8.51(p)
3920.52(3)		υ Sgr	0.67(3)
		Fe I-4	0.26(20)
3922.90(1)		*Fe* I-4	2.91(25)
3926.23(3)		*He* I-58	6.53(1)
		Fe I-364	5.95(6)
3927.89(2)		*Fe* I-4	7.92(30)
3930.08(5n)		*Fe* II-3	0.31(p)
		V II-10	9.73(50)
3932.18(3)		*Ti* II-34	2.01(2)
3933.62(15)		*Ca* II-1	3.66(400)
3935.94(4)		*Fe* II-173	5.94(6)
3938.47(7n)		*Fe* II-3	8.29(2)
		Fe II-190	8.97(4)
3941.20(1)		*Mn* II?	1.21(1)
3942.29(2)		υ Sgr	2.35(2)
3943.76(5)		*Mn* II?	3.85(1)
		Al I-1	4.01(10)
3945.19(7)		*Fe* II-3	5.21(p)
3947.24(1n)		*O* I-3	7.30(10)
		O I-3	7.49(7)
		Fe I-561	7.00(4)

λ	Int.	Identification	
3948.86(3)		*Fe* I-604	8.78(10)
		A I-2	8.98(100)
3950.20(3)		*Y* II-6	0.35(200)
		Fe I-72	9.95(10)
3951.99(7)		*V* II-10	1.97(500)
3954.27(3n)		*O* I-30	4.69(10)
		υ Sgr	3.67(1-0)
3956.72(2n)		*Fe* I-278	6.68(12)
3958.20(2)		*Zr* II-16	8.24(50)
3959.17(1)		υ Sgr	9.18(1)
3960.98(7n)		*Fe* II-212	0.90(3)
		Al I-1	1.52(10)
3962.86(2)		υ Sgr	2.71(1-0)
3964.56(6)		*He* I-5	4.73(4)
		Fe II-29	4.57(p)
3966.33(3)		*Fe* II-3	6.43(p)
3968.57(15)		*Ca* II-1	8.47(350)
3973.86(7)		*V* II-9	3.64(300)
		Fe II-29	4.16(3)
3975.03(3)		*Fe* II-191	5.03(2)
3976.24(0)		α Cyg	6.11(1)
3977.73(3)		*V* II-10	7.73(60)
		Fe I-72	7.74(12)
3979.48(5)		*Cr* II-183	9.51(20)
3981.91(10)		υ Sgr	2.28(2)
		Fe II-3	1.61(p)
3983.91(0)		*Fe* I-277	3.96(10)
3986.06(4n)		*Mn* II?	6.01(1)
3987.66(4)		*Ti* II-11	7.63(p)
3989.73(4)		υ Sgr	9.82(0)
3991.23(3)		*Zr* II-30	1.14(40)
3995.05(0)		*N* II-12	5.00(10)
		Co I-31	5.31(60)
3997.12(4)		*V* II-9	7.13(200)
3999.05(3)		*Zr* II-16	8.98(30)
4002.48(12n)		*Fe* II-29	2.07(2)
		Cr II-194	3.33(25)
		Fe II-190	2.55(3)
4005.50(7)		*V* II-32	5.71(800)
		Fe I-43	5.25(25)
4008.35(0N)		*Fe* II-189	7.72(p)
		He I-55	9.27(1)
4012.45(7)		*Ti* II-11	2.37(4)
		Cr II-183	2.50(30)
4013.79(1n)		*Mg* II-22	3.80(2)
4015.45(4)		*Ni* II-12	5.50(1)
4016.83(1n)		υ Sgr	6.45(1)
		Fe I-527	7.16(6)
4019.48(1)		*P* II-30	9.45(4)
		υ Sgr	9.72(2)
4021.98(2)		*Fe* I-278	1.87(12)
		Cr II-183	2.36(3)
4023.37(5)		*V* II-32	3.39(600)
4024.60(5)		*Fe* II-127	4.55(5)
		Ti II-11	5.14(2)
4026.30(3)		*He* I-18	6.19(5)
		He I-18	6.36(1)
4028.38(7)		*Ti* II-87	8.33(7)
4030.29(3N)		*Zr* II-41	9.68(20)
		Mn I-2	0.76(200)
4031.41(2)		*Fe* II-151	1.46(1)

TABLE 2—*Continued*

λ	Int.	Identification		λ	Int.	Identification	
4032.87	(5)	*Fe* II-126	2.95(3)	4121.07	(1)	*He* I-16	0.81(3)
4034.21	(1)	υ Sgr	4.25(1)			*Co* I-28	1.32(60)
4035.56	(3)	*V* II-32	5.63(400)	4122.66	(7)	*Fe* II-28	2.64(4)
		Fe II-22	5.54(p)	4124.76	(4)	*Fe* II-22	4.79(1)
4036.85	(2)	*V* II-9	6.78(60)	4128.36	(10n)	*Si* II-3	8.05(8)
4038.07	(3)	*Cr* II-194	8.03(25)			*Fe* II-27	8.74(3)
4039.67	(2)	α Cyg	9.61(1)	4130.79	(6)	*Si* II-3	0.88(10)
4041.43	(3)	*Mn* I-5	1.36(50)	4132.37	(4)	*Cr* II-26	2.41(7)
		Fe II-172	1.64(p)			*Fe* I-43	2.06(25)
4043.96	(2)	*Fe* II-172	4.01(p)	4136.92	(0)	*Mn* II?	6.91(2)
4045.89	(5)	*Fe* I-43	5.82(60)			*Fe* I-726	7.00(7)
4048.90	(7)	*Fe* II-172	8.83(3)	4138.32	(3)	*Fe* II-39	8.40(p)
4051.14	(2)	*Fe* II-172	1.21(p)			*Fe* II-150	8.21(p)
4051.94	(5)	*Cr* II-19	1.97(12)	4139.71	(1)	υ Sgr	9.74(1)
4053.74	(8)	*Ti* II-87	3.81(3)	4143.64	(5)	*He* I-53	3.76(2)
4056.17	(3)	*Ti* II-11	6.21(1)			*Fe* I-43	3.87(30)
4057.35	(3)	*Fe* II-212	7.46(2)	4145.85	(3)	*Cr* II-162	5.77(25)
		Mg I-16	7.51(5)	4147.31	(1)	*Fe* I-42	7.67(10)
4058.43	(1)	υ Sgr	8.7(2)			*Fe* II-141	7.26(p)
		Fe I-558	8.23(4)	4149.04	(4)	*Zr* II-41	9.22(75)
4061.55	(3)	*Fe* II-189	1.79(1)	4150.48	(3)	υ Sgr	0.38(2)
		Sc III-1	1.3(2)	4151.08	(3)	*N* I-6	1.46(12)
4063.63	(3)	*Fe* I-43	3.60(45)	4152.81	(2)	*Fe* II-45	2.98(p)
4066.97	(6)	*Ni* II-11	7.05(3)	4154.41	(1n)	*Fe* I-355	4.50(12)
4068.37	(1)	α Cyg	8.19(1)			*Fe* I-695	3.91(10)
		Sc III-1	8.7(2)			*Fe* I-694	4.81(9)
		Fe I-559	7.98(8)	4156.19	(1n)	*Zr* II-29	6.24(15)
4069.78	(3)	*Fe* II-188	9.88(1)			*Fe* I-354	6.80(12)
4070.90	(3)	*Cr* II-193	0.90(10)	4158.40	(3n)	*Fe* II-12	8.45(p)
		Ni II-11	1.0(p)			*A* I-2	8.59(100)
4071.81	(1)	*Fe* I-43	1.74(40)			*Fe* I-695	7.79(8)
4072.68	(3)	υ Sgr	2.65(3)	4161.02	(6d)	*Fe* II-39	0.62(p)
4073.95	(0)	*Mn* II?	4.02(1)			*Ti* II-21	1.52(1)
		Fe I-558	3.76(4)	4163.68	(5)	*Ti* II-105	3.64(40)
4075.58	(4)	*Si* II	5.45(2)	4167.12	(2)	*Mg* I-15	7.27(10)
4077.65	(5)	*Sr* II-1	7.71(400)	4168.63	(2)	*Fe* II-22	8.66(p)
4079.41	(0)	*Mn* I-5	9.24(12)	4170.73	(1)	*Fe* I-482	0.91(5)
		Mn I-5	9.42(10)	4171.87	(4)	*Ti* II-105	1.90(30)
4081.49	(0)	*Fe* II-188	1.42(p)	4173.66	(5)	*Fe* II-27	3.45(8)
4082.17	(3)	*Cr* II-165	2.30(10)	4175.90	(0)	*Fe* I-354	5.64(10)
4083.65	(0)	*Mn* II-2	3.67(p)	4177.79	(5)	υ Sgr	7.67(10)
4085.46	(3n)	*Cr* II-26	6.14(8)	4178.87	(10)	*Fe* II-28	8.86(8)
		Fe I-698	4.50(6)	4181.90	(0?)	*Fe* I-354	1.76(15)
4087.39	(5)	*Fe* II-28	7.27(p)			*A* I-7	1.88(80)
4089.01	(3)	*Fe* II-39	8.75(p)	4183.19	(1)	*Fe* II-21	3.20(p)
4093.58	(4n)	*Fe* II	3.24(0)			*V* II-37	3.44(250)
		Mg II-29	3.90(1)	4184.24	(3)	*Ti* II-21	4.33(0)
4097.00	(3)	*Ca* II-17	7.12(1)			α Car	4.00(2)
4098.40	(3)	*Cr* II-165	8.44(8)	4186.77	(2)	*Fe* I-152	7.04(20)
4099.81	(3)	*N* I-10	9.94(9)	4187.58	(3)	*Ni* II?(•)	7.6
4101.69	(5)	*Hδ*	1.74			*Fe* I-152	7.80(20)
4104.50	(3n)	*Fe* II-39	4.18(p)	4189.04	(0)	*Fe* II or III	9.10(7)
		Mn II?	5.01(2)	4190.23	(3)	*Mn* II?	0.04(4)
4106.99	(1n)	*Fe* I-354	7.49(12)			*Si* II	0.74(3)
4109.55	(5)	*Mg* II-21	9.54(3)	4191.93	(3)	*Ni* II-10	2.07(1)
4110.92	(4)	*Cr* II-18	1.01(18)			*Fe* I-152	1.44(15)
4113.28	(1)	*Cr* II-18	3.24(5)	4193.47	(2)	*Mg* II-28	3.44(2)
4116.77	(1)	*Cr* II-181	6.66(2)	4195.54	(4)	*Cr* II-161	5.41(10)
4118.40	(0n)	*Fe* I-801	8.55(15)	4198.17	(3)	*Si* II	8.17(2)
		υ Sgr	8.00(0)			*Fe* I-152	8.31(20)
4119.55	(3)	*Fe* II-21	9.53(p)	4199.21	(2)	*Fe* I-522	9.10(20)

TABLE 2—*Continued*

λ	Int.	Identification		λ	Int.	Identification	
4200.58(4)		*υ* Sgr	0.77(6)	4287.82(2)		*Ti* II-20	7.89(2)
4202.35(6)		*υ* Sgr	2.60(5)	4290.15(5)		*Ti* II-41	0.22(50)
		Fe I-42	2.03(30)	4292.09(1)		*Mn* II-6	2.25(0)
4205.13(4)		*V* II-37	5.08(250)	4294.14(6)		*Ti* II-20	4.10(40)
4207.37(2)		*Mn* II-2	7.23(p)	4296.56(4)		*Fe* II-28	6.57(6)
		Cr II-26	7.35(4)	4300.03(6)		*Ti* II-41	0.05(60)
4209.41(2n)		*Zr* II-41	8.99(30)	4301.86(3)		*Ti* II-41	1.93(15)
		Fe I-152	0.35(15)	4303.27(5)		*Fe* II-27	3.17(8)
4211.86(1)		*Mn* II?	1.77(2)	4305.64(1)		*Sr* II-3	5.45(40)
		Zr II-15	1.88(12)			*N* I	5.46(6)
4213.61(2)		*υ* Sgr	3.57(1)	4306.91(0)		*Cr* II?(•)	7.0
4215.64(6)		*Sr* II-1	5.52(300)	4307.90(3)		*Ti* II-41	7.90(40)
4217.33(1)		*Fe* I-693	7.55(7)	4312.80(4)		*Ti* II-41	2.86(35)
4219.68(1n)		*Fe* I-800	9.36(12)	4314.63(6n)		*Ti* II-41	4.98(40)
4221.73(2)		*υ* Sgr	1.46(1)			*Sc* II-15	4.08(60)
		Fe I-152	2.22(12)			*Fe* II-32	4.29(4)
4222.89(0)		*O* I-33	2.78(5)	4316.72(2)		*Ti* II-94	6.81(1)
		N I-5	3.04(5)	4318.07(0)		*N* I	7.70(5)
4224.84(5)		*Cr* II-162	4.85(20)			*Fe* II-220	8.22(0)
4227.27(4)		*Ca* I-1	6.73(500)	4319.45(1)		*Fe* II-220	9.72(1)
		Fe I-693	7.43(30)	4320.99(4)		*Ti* II-41	0.96(1)
4229.84(2)		*N* I-5	0.35(4)			*Sc* II-15	0.74(50)
		N I	9.59(2)	4325.45(7)		*υ* Sgr	5.59(4)
4233.21(8)		*Fe* II-27	3.17(11)			*Sc* II-15	5.01(40)
4236.23(3n)		*υ* Sgr	6.58(1)			*Fe* I-42	5.76(35)
		Fe I-152	5.94(25)	4330.48(4)		*Ti* II-41	0.71(0)
4238.96(3)		*Mn* II-2	8.79(p)			*Ti* II-94	0.26(0)
		Fe I-693	8.82(10)	4331.78(0)		*Mg* II-27	1.93(3)
4240.36(1)		*υ* Sgr	0.49(1)			*Fe* II	1.53(3)
4242.43(6)		*Cr* II-31	2.38(30)	4337.90(10)		*Ti* II-20	7.92(50)
		Mg II-20	2.47(4)	4340.77(3n)		*Hγ*	0.47
4244.49(4)		*Ni* II-9	4.80(1)			*Ti* II-32	1.37(1)
		Mn II-7	4.26(1)			*Cr* II-179	1.09(7)
4246.85(5)		*Sc* II-7	6.83(100)	4343.44(1)		*υ* Sgr	3.32
4250.38(3)		*Fe* I-42	0.79(25)	4344.01(3)		*Mn* II-6	3.99(2)
		Fe I-152	0.12(12)			*Ti* II-20	4.29(2)
4251.62(1)		*Mn* II?	1.76(2)	4348.16(1)		*υ* Sgr	8.21(2)
		Fe II-12	1.49(p)	4351.69(4n)		*Fe* II-27	1.76(9)
4252.82(4)		*Cr* II-31	2.62(10)			*Ti* II-94	0.83(1)
		Mn II-7	3.02(2)			*Mg* I-14	1.90(30)
4254.54(3)		*Cr* I-1	4.35(1000)	4354.39(3)		*Fe* II-213	4.36(2)
		V I-4	4.7(4)	4357.54(4)		*Fe* II	7.57(4)
4256.13(1)		*Cr* II-192	6.16(5)	4359.35(0)		*Mn* II?	9.61(1)
4258.34(6)		*Fe* II-28	8.16(3)	4361.87(2n)		*Ni* II-9	2.10(1)
4259.04(0)		*Mn* II-7	9.20(0)			*Fe* II	1.25(2)
4260.46(3)		*Fe* I-152	0.48(35)	4363.05(1)		*Cr* II-179	2.93(3)
		Mn II-2	0.47(p)			*Mn* II?	3.25(1)
4261.91(4)		*Cr* II-31	1.92(20)	4365.26(0n)		*Mn* II?	5.28(1)
4263.87(2)		*Fe* II	3.90(1)	4367.70(3)		*Ti* II-104	7.66(15)
4266.32(0)		*Al* I-4	6.29(100)	4369.49(3)		*Fe* II-28	9.40(2)
4269.22(4)		*Cr* II-31	9.28(10)	4370.86(1)		*υ* Sgr	0.95(3)
4271.52(3n)		*Fe* I-42	1.76(35)	4372.23(0)		*Fe* II-33	2.22(p)
		Fe I-152	1.16(20)	4374.70(5)		*Sc* II-14	4.46(40)
4273.34(4)		*Fe* II-27	3.32(3)			*V* II-13	4.94(300)
4275.59(3)		*Cr* II-31	5.57(30)	4377.07(3)		*υ* Sgr	6.96(3)
4278.29(4n)		*Fe* II-32	8.13(1)	4379.97(2)		*Mn* II?	9.73(1)
4280.55(0)				4384.64(10n)		*Fe* II-27	5.38(7)
4282.25(1)		*Fe* I-71	2.41(12)			*Fe* II-32	4.33(p)
4284.16(4)		*Cr* II-31	4.21(20)	4386.60(2)		*Ti* II-104	6.86(10)
4285.89(1n)		*υ* Sgr	5.41(1)			*Fe* II-26	6.57(p)
		Fe II	6.31(1)	4390.73(4)		*Mg* II-10	0.58(10)

TABLE 2—*Continued*

λ	Int	Identification		λ	Int	Identification	
4395.06	(7n)	*Ti* II-19	5.03(60)	4507.00	(1)	*Fe* II-213	7.20(0)
		Ti II-61	5.85(2)	4508.28	(4)	*Fe* II-38	8.28(8)
		Ti II-51	4.06(2)	4510.45	(0)	α Cyg	0.40(0)
4398.17	(3)	υ Sgr	7.97(1-0)	4512.13	(3)	υ Sgr	2.14(3)
4399.97	(5)	*Ti* II-51	9.77(35)	4515.37	(6)	*Fe* II-37	5.34(7)
		Sc II-14	0.36(30)	4518.57	(0)	*Ti* II-18	8.30(p)
4402.85	(3)	*Fe* II	2.88(2)	4520.29	(5)	*Fe* II-37	0.22(7)
4404.79	(1)	*Fe* I-41	4.75(30)	4522.63	(5)	*Fe* II-38	2.63(9)
4409.21	(2)	*Ti* II-61	9.22(tr)	4524.73	(2)	υ Sgr	4.6(1)
		Ti II-61	9.52(tr)	4526.49	(2)	*Fe* II-171	6.58(p)
4411.30	(3)	*Ti* II-115	1.08(15)	4529.19	(3n)	*Ti* II-82	9.46(1)
		Ti II-61	1.94(1)			*V* II-56	8.51(300)
4413.54	(3)	*Fe* II-32	3.60(0)			*Fe* I-68	8.62(18)
4415.30	(2)	*Sc* II-14	5.56(20)	4532.21	(0)	υ Sgr	2.31(2)
		Fe I-41	5.12(20)	4534.07	(6)	*Ti* II-50	3.97(30)
4417.57	(6n)	*Fe* II-27	6.82(7)			*Fe* II-37	4.17(2)
		Ti II-40	7.72(40)	4539.32	(3n)	*Cr* II-39	9.62(2)
4421.93	(3)	*Ti* II-93	1.95(1)			υ Sgr	8.82(1)
4427.78	(3)	*Mg* II-9	8.00(7)	4541.39	(5)	*Fe* II-38	1.52(4)
4431.07	(3n)	*Fe* II-222	1.63(1)	4545.10	(3)	*Ti* II-30	5.14(tr)
4433.86	(3)	*Mg* II-9	3.99(8)	4549.48	(8)	*Fe* II-38	9.47(10)
4436.29	(3n)	*Mg* II-19	6.48(5)			*Ti* II-82	9.62(60)
		Ca I-4	5.69(40)	4552.18	(1)	*Si* III-2	2.65(9)
4440.28	(0)	υ Sgr	0.60(2)			α Cyg	1.62(0)
4441.77	(2)	*Ti* II-40	1.73(p)	4555.57	(6n)	*Fe* II-37	5.89(9)
4443.98	(7)	*Ti* II-19	3.80(50)			*Cr* II-44	5.02(20)
4446.11	(0)	*Fe* II-187	6.25(1)	4558.66	(6)	*Cr* II-44	8.66(100)
		α Cyg	5.82(0)	4563.83	(5)	*Ti* II-50	3.76(30)
4447.58	(0)	*Fe* I-68	7.72(9)	4565.69	(2)	*Cr* II-39	5.78(10)
4450.30	(2)	*Ti* II-19	0.49(10)	4568.73	(1n)	*Co* II?(*)	9.3
		Fe II-222	9.66(1)			*Si* III-2	7.87(7)
4451.40	(1)	*Fe* II	1.54(4)	4571.93	(6)	*Ti* II-82	1.97(50)
4453.13	(1)	υ Sgr	3.31(2)	4576.25	(5)	*Fe* II-38	6.33(4)
4455.51	(3n)	*Fe* II	5.26(3)	4577.90	(0)	*Fe* II-54	7.78(p)
		Ca I-4	4.78(80)	4579.88	(5)	*Fe* II-26	0.06(1)
		Ca I-4	5.89(40)			*Fe* II	9.52(1)
4458.95	(0)	*Fe* I-68	9.12(10)	4583.46	(10d)	*Fe* II-38	3.83(11)
4461.46	(5)	υ Sgr	1.63(7)			*Fe* II-37	2.84(3)
4464.30	(3)	*Ti* II-40	4.46(1)	4588.09	(3)	*Cr* II-44	8.22(75)
4468.58	(6)	*Ti* II-31	8.49(50)	4589.82	(2)	*Ti* II-50	9.96(2)
4471.15	(3)	*Ti* II-40	0.86(tr)	4592.08	(2)	*Cr* II-44	2.09(20)
		He I-14	1.48(6)	4593.72	(1)	υ Sgr	3.77(3)
4472.62	(1)	*Fe* II-37	2.92(2)	4595.89	(4)	υ Sgr	6.02(6)
		Ca II-6	2.09(0)	4598.49	(2)	*Fe* II-219	8.53(1)
4474.21	(0)	*Fe* II-171	4.19(0)	4601.73	(1n)	*Fe* II-43	1.34(p)
4475.78	(1)	υ Sgr	6.06(0)			*N* II-5	1.48(8)
		P II-24	5.27(7)			*P* II-15	1.97(8)
4478.45	(0)	*Mn* II?	8.73(1)	4605.47	(2n)	υ Sgr	5.35(1)
4481.21	(10)	*Mg* II-4	1.33(100)	4614.23	(1)	*N* II-5	3.87(6)
			1.13			υ Sgr	4.63(1)
4488.77	(5)	*Fe* II-37	9.18(4)	4616.60	(4)	*Cr* II-44	6.64(18)
		Ti II-115	8.32(15)	4618.78	(4)	*Cr* II-44	8.83(35)
4491.31	(3)	*Fe* II-37	1.40(5)	4620.79	(4n)	*Fe* II-38	0.51(3)
4494.08	(2n)	*Ti* II-18	3.53(1)			υ Sgr	1.61(7)
		Fe II-222	3.58(1)	4625.78	(4)	*Fe* II-186	5.91(1)
		N I	4.67(5)			*Fe* II-219	5.55(tr)
		Fe I-68	4.57(12)	4629.29	(5)	*Fe* II-37	9.34(7)
4497.29	(1)	*Zr* II-40	6.96(15)	4631.80	(1)	*Fe* II-219	1.90(0)
4499.58	(2)	*Fe* II	9.71(0)	4634.72	(5d)	*Cr* II-44	4.11(25)
4501.23	(5)	*Ti* II-31	1.27(40)			*Fe* II-186	5.33(5)
4504.41	(3n)	*Cr* II-16	4.52(p)	4638.00	(2)	υ Sgr	8.10(2)

TABLE 2—*Continued*

λ	Int.	Identification		λ	Int.	Identification	
4640.79	(1n)	*Fe* II	0.84(0)	4876.5	(5)	*Cr* II-30	6.41(50)
4648.95	(3)	*Fe* II-25	8.93(p)	4880.8	(1)		
4651.96	(2)	*Fe* II-219	2.28(tr)	4884.0	(7)	*V* II-22	3.69(200)
4654.41	(0)	*Fe* I-554	4.63(5)			*Cr* II-30	4.57(10)
4657.08	(5)	*Fe* II-43	6.97(1)	4893.0	(1N)	*Fe* II-36	3.78(0)
		Ti II-59	7.21(tr)			*Fe* I-318	1.50(50)
4660.44	(3)	υ Sgr	0.54(2)	4901.0	(3n)	*V* II-22	0.13(150)
4663.43	(4)	υ Sgr	3.02(6)			*Cr* II-190	1.65(15)
		Fe II-44	3.70(0)	4907.8	(1n)	*Fe* II	8.21(0)
4666.85	(4)	*Fe* II-37	6.75(2)			*Si* II	6.88(1)
4670.21	(5)	*Fe* II-25	0.17(0)	4911.9	(5n)	*Ti* II-114	1.20(0)
4673.36	(2)	υ Sgr	3.28(4)			*Cr* II-190	2.49(12)
4679.06	(3)	*Ni* II?(*)	9.2	4917.4	(1)		
4685.15	(0n)	υ Sgr	4.8(1-0)	4920.8	(3)	*Fe* I-318	0.51(60)
		Fe II-50	5.95(p)	4924.2	(7)	*Fe* II-42	3.92(12)
4697.98	(2)			4927.4	(1)	*P* II-13	7.17(4)
4702.73	(0n)	*Mg* I-11	2.98(40)	4934.4	(3n)	*Ba* II-1	4.09(700)
		A I-9	2.32(100)			*N* I-9	5.03(10)
4708.93	(2)	*Ti* II-49	8.66(tr)	4938.8	(2)	*Ne* I	9.04
4713.42	(2)	*He* I-12	3.14(3)	4948.5	(2)	*Fe* II	8.85(1)
		Fe II-26	3.18(p)			*Fe* II	8.13(0)
4719.93	(2)	*Fe* II-54	0.15(p)	4952.4	(3)	*Cr* II	2.78(10)
4723.55	(1)	υ Sgr	3.4(1)			*Fe* II	1.65(1)
4727.77	(3)	*Mn* II-5	7.9(p)	4957.7	(1n)	*Fe* I-318	7.60(60)
4731.48	(5)	*Fe* II-43	1.44(3)	4971.0	(0)		
4736.80	(1)	*Fe* I-554	6.78(12)	4977.3	(2n)	*Fe* II	7.10(0)
4739.28	(1n)	*Mg* II-18	9.59(5)	4983.3	(3n)	*Fe* I-1066	3.86(6)
		Mn II-5	8.29(p)			*Fe* I-1067	2.51(8)
4742.76	(0)	υ Sgr	2.44(1-0)	4990.9	(5)	*Fe* II-25	1.11(p)
4755.59	(3)	*Mn* II-5	5.73(0)	4993.1	(4)	*Fe* II-36	3.36(1)
4764.44	(6)	υ Sgr	4.74(3)	4996.0	(1)		
4779.90	(4)	*Ti* II-92	9.99(1)	4998.9	(0?)		
4785.35	(0n)	υ Sgr	4.64(2)	5001.5	(4)	*Fe* II or III	2.02(8)
		Ni I-98	6.54(15)	5004.5	(3)	*Fe* II	4.26(3)
4791.98	(2n)	*Ti* II-48	2.39(p)	5007.3	(1)		
		υ Sgr	1.31(2)	5010.1	(3)	*Fe* II	0.02(0)
4799.31	(1n)	*Ti* II-17	8.54(2)			*Fe* II	0.18(0)
		υ Sgr	0.00(1)	5013.4	(4)		
4805.22	(4)	*Ti* II-92	5.10(2)	5018.5	(5)	*Fe* II-42	8.43(12)
4806.67	(1)			5022.3	(3)	*Fe* II	2.87(1)
4811.76	(2n)	*Cr* II-30	2.35(25)			*Fe* I-965	2.24(6)
		Fe II-169	0.76(0)	5026.7	(3)		
4824.35	(5)	*Cr* II-30	4.13(75)	5031.0	(4)	*Fe* II	0.74(3)
4825.98	(1)	*Fe* II-30	5.71(p)			*Sc* II-23	1.02(40)
4830.87	(1)	*Fe* II-54	1.11(p)	5035.8	(4)	*Fe* II	5.77(3)
4833.34	(2)	*Fe* II-30	3.21(p)	5040.9	(4)	*Si* II-5	1.06(8)
4836.43	(3)	*Cr* II-30	6.22(25)	5044.7	(0)	*N* II-4	5.10(8)
4840.04	(1)	*Fe* II-30	0.00(p)	5047.8	(3n)	*Fe* II	7.69(1)
4842.49	(0)	υ Sgr	2.50(1)	5052.9	(1)		
4848.13	(4)	*Cr* II-30	8.24(60)	5055.9	(6)	*Si* II-5	6.02(10)
4851.25	(3n)	*Mg* II-25	1.10(5)	5058.7	(1)	*Cu* II	8.90
4855.95	(6)	*Cr* II-30	6.19(20)	5062.0	(1)	*Fe* II	1.79(1)
		Fe II-25	5.54(p)	5065.6	(3)	*Fe* I-1094	5.02(6)
				5070.7	(1n)	*Fe* II	0.96(2)
4860.8	(6n)	*Hβ*	1.33	5075.8	(2)	*Fe* II	5.83(1)
		Cr II-30	0.20(20)	5081.9	(0)	*Fe* II-221	1.92(tr)
4864.6	(4)	*Cr* II-30	4.32(50)	5086.8	(4)	*Fe* II	7.25(3)
4865.9	(3)	α Cyg	5.85(1-0)	5089.2	(0)	*Fe* II	9.28(0)
4868.6	(0)	*Fe* II-30	8.82(p)	5093.7	(3)	*Fe* II-205	3.47(1)
4871.3	(4)	*Fe* II-25	1.27(p)				
4873.9	(4)	*Ti* II-114	4.02(tr)				

TABLE 2—*Continued*

λ	Int.	Identification	
5096.8	(3)	*Fe* I-1092	7.00(6)
		Fe II	7.38(1)
5100.6	(3)	*Fe* II	0.95(15)
		Fe II-185	0.84(4)
5102.6	(2)		
5106.8	(3n)		
5110.1	(0?)	*Cr* II-199	0.43(2)
5112.6	(2)	*Fe* II	1.90(0)
		Fe II	3.05(tr)
5120.3	(2)	*Fe* II-35	0.34(p)
5123.5	(1)	*Y* II-21	3.21(50)
5127.8	(4n)	*Fe* II-167	7.87(1)
		υ Sgr	7.09
5132.3	(2)	*Fe* II-35	2.67(p)
5136.7	(3)	*Fe* II-35	6.79(tr)
5140.1	(2)		
5145.0	(3n)	*Fe* II	4.41(1)
		Fe II	4.77(0)
		Fe II	5.87(0)
5148.8	(2)	*Fe* II	9.54(3)
		Fe II	7.09(2)
5154.0	(4n)	*Ti* II-70	4.06(0)
		Cr II-24	3.49(15)
5157.4	(1)	*Fe* II	7.38(0)
5161.1	(2)	*Fe* II-167	0.82(1)
		Fe II-35	1.18(p)
5163.0	(0)	*Fe* I-1089	2.29(10)
5168.7	(3)	*Fe* II-42	9.03(12)
5172.6	(1)	*Mg* I-2	2.68(80)
5178.6	(3n)	*Fe* II	7.48(0)
		Fe II-35	8.71(p)
		Fe II-35	8.95(p)
5183.8	(1)	*Mg* I-2	3.60(125)
5186.8	(3)	*Fe* II	6.81(tr)
5188.7	(2)	*Ti* II-70	8.70(6)
5194.9	(0)		
5201.0	(2)	*Fe* II	0.83(0)
		Fe II	0.97(0)
5204.4	(4n)		
5208.1	(1)	*Cr* I-7	8.44(500)
5211.5	(4)		
5216.6	(5n)	*Fe* II or III	6.99(8)
5222.1	(0)		
5227.2	(8N)	υ Sgr	7.30
		Fe II	7.0(15)
		Ti II-70	6.53(5)
5232.0	(3)	*Cr* II-43	2.50(15)
5234.8	(2)	*Fe* II-49	4.62(7)
5237.4	(3)	*Cr* II-43	7.34(75)
5240.0	(2)	*Sc* II-26	9.82(15)
5257.3	(1)	*Fe* II-41	6.89(1)
5260.8	(0)	*Fe* II	1.0(15)
		Fe II or III	0.25(10)
5264.0	(4)	*Mg* II-17	4.14(5)
5270.1	(2)	*Fe* I-15	9.54(60)
		Fe I-37	0.36(30)
5272.8	(1)	*Fe* II-185	2.41(2)
5275.5	(4)	*Fe* II-49	5.99(7)
		Cr II-43	4.99(20)
5280.2	(3)	*Cr* II-43	9.92(15)
		Cr II-43	0.08(10)
5284.2	(4)	*Fe* II-41	4.09(3)
5291.6	(2)	*Fe* II or III	1.75(2)
5299.2	(3)	*O* I-26	9.00(5)
5306.9	(3N)	*Cr* II-24	5.85(25)
		Cr II-43	8.44(20)
		Fe II	6.23(0)
5313.4	(2)	*Cr* II-43	3.59(25)
5316.4	(4n)	*Fe* II-49	6.61(8)
		Fe II-48	6.78(4)
5325.2	(3n)	*Fe* II-49	5.56(2)
		Fe I-553	4.18(30)
5328.8	(2)	*N* I-13	8.70(5)
		Fe I-15	8.04(50)
5334.3	(3)	*Cr* II-43	4.88(40)
5337.0	(4)	*Fe* II-48	7.71(0)
		Ti II-69	6.81(4)
5340.2	(4)	α Cyg	9.53(2)
		Ne I-9	1.10(20)
5346.5	(6)		
5353.2	(2)		
5358.9	(1)		
5363.0	(4)	*Fe* II-48	2.86(5)
5367.0	(1)	*Fe* I-1146	7.47(20)
5370.6	(2)	*Fe* I-1146	9.96(25)
5375.6	(0)	*Fe* II or III	5.68(5)
5381.9	(3n)	*Ti* II-69	1.02(1)
5386.9	(3)	*Fe* II	7.14(2)
5390.7	(2)		
5393.4	(2)	*Fe* I-553	3.17(10)
5396.0	(3)	*Fe* II	5.86(1)
5399.1	(0)		
5402.0	(4)	*Fe* II	2.11(2)
5405.4	(2)	*Fe* I-1165	4.14(30)
		Fe I-15	5.78(40)
5408.2	(0)	*Fe* II-184	8.84(1)
		Cr II-23	7.62(10)
5411.4	(2)	*Fe* I-1165	0.91(15)
5414.6	(3)	*Fe* II-48	4.09(2)
		Fe I-1165	5.20(35)
5419.3	(2)	*Ti* II-69	8.80(0)
5425.0	(4)	*Fe* II-49	5.27(2)
		Fe I-1146	4.07(45)
5427.8	(1)	*Fe* II	7.83(30)
5429.7	(1)	*Fe* I-15	9.70(40)
5433.1	(3)	*Fe* II-55	2.98(p)
5439.8	(1)		
5445.1	(4n)		
5451.0	(1)	*P* II-23	0.66(6)
5455.9	(4n)	*Si* II	6.11(2)
		Fe I-15	5.61(40)
5462.0	(2n)		
5466.7	(7)	*Fe* II	6.94(20)
5473.3	(1)		
5478.2	(3)	*Cr* II-50	8.35(15)
		Fe II-49	7.67(p)
5482.3	(3)	*Fe* II	2.40(2)
5487.8	(5)	α Cyg	7.63(1)
5493.0	(5)		
5498.1	(2)	*Fe* II-24	8.19(p)
5502.7	(6)		
5506.2	(4)	*Fe* II	6.27(3)

TABLE 2—*Continued*

λ	Int.	Identification		λ	Int.	Identification	
5510.2	(5)			5834.9	(3)	*Fe* II-57	4.93(p)
5520.3	(3)	*Fe* II-52	9.83(p)	5844.8	(3n)		
5526.1	(3)	*Sc* II-31	6.81(75)	5853.3	(4n)	*Fe* II or III	4.1(5)
		Fe II-56	5.14(p)			*Ne* I-6	2.49(50)
5529.5	(3)	*Fe* II-224	9.94(2)	5861.4	(0)	*Fe* I-1180	2.36(8)
5534.9	(3)	*Fe* II-55	4.86(4)			*Fe* I-1181	9.61(5)
5544.3	(6)			5869.2	(3)		
5548.7	(3)			5875.2	(3)	*He* I-11	5.63(10)
5554.9	(0)	*O* I-24	4.94(6)	5882.7	(2n)	*Ne* I-1	1.90(20)
		Fe I-1183	4.90(4)	5890.5	(10)	*Na* I-1	9.95(10)
5559.9	(4n)	*N* I-25	0.37(9)	5896.4	(10)	*Na* I-1	5.92(10)
5564.4	(4)	*N* I-25	4.37(9)	5903.1	(3)	*Fe* II	3.6(8)
5569.7	(3n)	*Fe* I-686	9.62(20)	5908.0	(0x)	*Fe* II-57	9.38(p)
5575.5	(1)	*Fe* I-686	6.10(10)	5914.3	(4)		
5578.1	(2)	*Mn* II?	8.13(1)	5922.2	(2)		
5582.8	(1)			5929.7	(3n)	*V* II-98	8.86(100)
5587.1	(4)	*Fe* I-686	6.76(40)			*Fe* I-1180	0.17(8)
5592.5	(2)	*Al* II-16	3.23(10)	5936.7	(0)		
		Fe II-55	1.38(p)	5944.3	(2)	*Ne* I-1	4.83(10)
5601.5	(0)			5955.8	(3)	*Fe* II	6.5(4)
5605.9	(2)	*Fe* II-51	5.91(p)	5965.2	(1)	*Ne* I-39	5.47(10)
5616.2	(2)	*Fe* I-686	5.65(50)	5979.0	(4)	*Si* II-4	8.97(7)
		N I-24	6.54(5)	5987.9	(3)		
5620.7	(0)	*Cr* II-189	0.63(12)	5999.4	(2)	*N* I-16	9.47(6)
5624.6	(1)	*N* I-24	3.20(4)	6008.0	(2)	*N* I-16	8.48(10)
		N I-24	5.43(2)	6018.4	(1)		
		Fe I-686	4.55(10)	6024.0	(0)	*Fe* I-1178	4.07(15)
5628.1	(0)			6029.5	(2)	*Ne* I-3	0.00(10)
5640.1	(4)			6033.4	(2)		
5646.0	(3)			6045.7	(3N)	*O* I-22	6.46(10)
5658.8	(6)					*O* I-22	6.26(8)
5668.6	(3)					*Fe* II-200	5.50(6)
5675.9	(2)	*N* II-3	6.02(6)			*Fe* II-46	4.53(p)
5679.5	(2)	*N* II-3	9.56(10)	6053.4	(1)	*Cr* II-105	3.48(10)
5684.3	(1)	*Si* I-11	4.52(50)	6060.8	(3)	*Fe* II-217	1.04(3)
		Sc II-29	4.19(15)	6070.0	(3n)		
5689.3	(2n)	*Si* II	8.86(2)	6078.5	(1)	*Fe* I-1259	8.50(4)
		Si I-10	0.47(40)	6084.5	(2)	*Fe* II-46	4.11(5)
		Na I-6	8.20(10)	6088.8	(2)	*Cr* II-187	9.69(15)
5695.6	(1)			6095.5	(2n)		
5702.6	(1n)	*Si* II	1.38(1)	6103.5	(2)	*Fe* II-200	3.54(8)
5708.7	(0)	*Si* I-10	8.44(75)	6108.5	(0)		
		Fe I-686	9.38(10)	6113.2	(3)	*Fe* II-46	3.33(2)
5715.9	(1)			6124.5	(3n)	*Mn* II-13	2.44(40)
5726.7	(2)					*Mn* II-13	5.86(25)
5730.5	(0n)			6130.5	(2)	*Mn* II-13	0.79(15)
5739.7	(2n)	*Si* III-4	9.76(8)			*Mn* II-13	1.92(15)
5747.2	(3)					*Fe* II-46	9.71(p)
5753.4	(2)			6138.2	(1)	*Fe* I-207	7.70(18)
5761.4	(1n)	*Fe* I-1107	2.99(10)	6142.5	(2)	*Ne* I-1	3.06(12)
5770.1	(0?n)					*Ba* II-2	1.72(600)
5780.4	(2)	α Cyg	0.41(1)	6148.8	(5)	*Fe* II-74	7.74(30)
5784.3	(3)	*Fe* II-215	5.0(5)			*Fe* II-74	9.24(20)
5791.0	(1)			6158.2	(3)	*O* I-10	8.19(18)
5796.4	(1n)	*Fe* II-211	5.87(4)	6162.3	(1n)	*Ca* I-3	2.17(150)
		Fe II-165	7.81(p)			*Ne* I-5	3.59(12)
5805.4	(0)	*Fe* II-165	4.91(p)	6173.2	(2)		
5812.5	(3n)	*Fe* II-24	1.93(p)	6185.9	(0n)	*Fe* II-46	5.34(p)
		Fe II-163	3.67(3)	6192.6	(0)	*Fe* I-169	1.56(20)
5822.4	(0?)	*Fe* II-164	3.17(3)	6198.4	(2)		
5829.8	(3)	*N* I-32	9.53(6)	6204.2	(1)		
				6217.1	(2n)	*Ne* I-1	7.28(15)

TABLE 2—*Continued*

λ	Int.	Identification		λ	Int.	Identification	
6225.0	(1)			6468.2	(1)	*N* I-22	8.32(4)
6231.9	(2)	*Al* II-10	1.78(9)	6482.7	(10)	*N* I-21	2.74(9)
6238.7	(5)	*Fe* II-74	8.38(20)			*N* I-21	4.88(9)
6247.9	(6)	*Fe* II-74	7.56(80)			*N* II-8	2.07(8)
6254.8	(1)			6491.2	(0)	*Fe* II	1.28(4)
6271.4	(1)					*N* I-21	1.28(3)
6279.0	(2)	Atm?	9.11	6496.7	(1)	*Ba* II-2	6.90(600)
		Atm?	8.10			*Fe* I-1258	6.46(20)
6285.7	(1)					Atm?	5.86
6304.9	(0n)	*Fe* II-200	5.32(15)	6508.2	(2)		
6317.8	(3)	*Fe* II	7.40(3)	6516.9	(4)	*Fe* II-40	6.05(20)
6327.1	(2)					*Fe* II	7.01(5)
6334.3	(1)	*Ne* I-1	4.43(10)	6532.4	(0)		
6347.0	(8)	*Si* II-2	7.09(10)	6556.0	(1)		
6363.0	(1)			6563.8	(em)	*Hα*	2.82
6370.4	(8)	*Si* II-2	1.36(8)	6586.7	(1)	*Fe* II	6.69(5)
		Fe II-40	9.45(4)	6599.1	(1n)	*Ne* I-6	8.95(15)
6384.4	(4)	*Fe* II	3.75(15)	6613.7	(0)		
		Fe II	5.47(5)	6636.0	(1)	*N* I-20	7.01(4)
6397.5	(1)			6645.5	(4)	*N* I-20	4.96(9)
6402.6	(1)	*Ne* I-1	2.25(20)	6666.3	(1)	*v* Sgr	5.12(2)
6415.9	(1n)	*Fe* II-74	6.90(20)	6672.9	(2)	*Si* II	1.88(3)
6433.0	(2)	*Fe* II-40	2.65(8)			*v* Sgr	3.7(0-1)
6445.9	(2)	*Mn* II-19	6.28(50)	6678.6	(3)	*He* I-46	8.15(6)
		Fe II-199	6.43(20)				
6456.2	(4)	*Fe* II-74	6.38(200)				
		O I-9	6.01(17)				

each multiplet and the difference in excitation temperature between star and laboratory source.

b) This list was then examined to note cases in which the stellar lines appeared to be considerably too strong for the laboratory intensity, as judged by the strength in the star of other lines of the same multiplet or of other multiplets at the same level of excitation. In these cases it was generally assumed that the tentative identification could not be a major contributor to the stellar line, and it was dropped from the identification column of the wave-length table.

c) Finally, it was desirable to check the identifications against those for other stars. The most useful source in this connection was the work of Greenstein and Adams on *v* Sagittarii,[12] but a number of other sources were also used.

In addition to the *Revised Multiplet Table*, the lists of lines given by Kayser and Konen,[13] Dobie,[14] and King[15] were consulted, and a few identifications were taken from the *MIT Wavelength Table*[16] and the *Table of Enhanced Lines* of the Solar Physics Committee.[17] The lines found only in the last source are starred in Table 2. Lines which appear to be identical with unidentified or questionably identified lines in the spectra of other stars are so indicated, along with the wave lengths measured in the cited stars.

Successive columns of the table of wave lengths give the wave length, the estimated

[12] *Mt. W. Contr.*, No. 738; *Ap. J.*, **106**, 339, 1947.

[13] *Handb. d. Spectroscopie*, Vols. **7** and **8**, 1922–1934.

[14] *Ann. Solar Phys. Obs., Cambridge*, Vol. **5**, Part I, 1938.

[15] *Mt. W. Contr.*, No. 584; *Ap. J.*, **87**, 109, 1938.

[16] Cambridge, Mass.: Technology Press, 1939.

[17] London, England: Wyman & Sons, 1906.

intensity, the element and multiplet number in the *Revised Multiplet Table*, the laboratory wave length, and the intensity. The intensities given to the stellar lines are rough eye-estimates, and those in the visual region are probably not strictly comparable with those in the photographic region. The letter "n" signifies a somewhat broad line, "N" a very broad line, "d" a line clearly double but with the components not measured separately. It appears that the intensities of blended features have been estimated somewhat too high, but no corrections have been made to the original estimates.

The following remarks pertain to the elements which have been identified in the spectrum of HD 30353. It should be noted that, since the wave-length table lists only the major contributors to the stellar lines, the discussion below refers only to such contributors.

H.—The measured wave length of the emission *Hα* line is shifted about 1 A to the red of the laboratory position, which perhaps indicates an asymmetrical structure for this line, similar to that found in υ Sagittarii.[18] All the other Balmer lines are very weak and narrow absorption lines and give no indication of Stark broadening. The higher members are badly blended, but several are doubtfully present up to *H*18. As previously mentioned, no Balmer discontinuity can be seen in the spectrum.

He.—Although only λ 4026 and λ 5875 are sensibly unblended, the presence of helium lines is certain. Nineteen lines are listed in Table 2; their relative intensities appear to be normal.

N I.—One of the strongest features in the visual spectrum of υ Sagittarii is a blend due to *N* I at λ 6483.8.[18] This blend also appears strongly in HD 30353, and many other lines from levels of *N* I at 10 and 11 volts are also present, mainly in the visual region.

N II.—Several of the strongest lines appear rather weakly.

O I.—Eleven high-excitation lines contribute to blends. As in υ Sagittarii, the neutral oxygen lines are definitely weaker than the neutral nitrogen lines.

Ne I.—The presence of moderately strong lines in the visual region is certain. These lines, arising from 16 to 18 volts, are very strong in υ Sagittarii.[19]

Na I.—The D lines are very strong, but, to judge from the measured wave lengths, mainly of interstellar origin.

Mg I.—A few lines are present.

Mg II.—The lines are very strong, including λ 4481. There is no evidence of dilution of radiation in the spectrum of HD 30353.

Al I.—The resonance lines are probably present, though blended.

Al II.—Seven of the stronger lines, arising from levels up to 13 volts, are present. The somewhat weaker *Al* II line at λ 4026 is probably not an appreciable contributor to the helium line at that wave length.

Si I.—Four lines, of which three are from 5 volts, are listed in Table 2.

Si II.—The lines are very strong. Nine unclassified lines are also present.

Si III.—Three lines, arising from 19 volts, may contribute to blends.

P II.—Though several lines from 13 volts are listed in Table 2, the evidence is rather weak.

A I.—Several lines are probable contributors to stellar lines.

Ca I.—A few lines are present.

Ca II.—Four fairly high-excitation lines appear, in addition to the H and K lines.

Sc II.—The lines are well marked, though not so strong as in α Persei.

Sc III.—The two lines from 14 volts given in the *Revised Multiplet Table* may be present as important contributors to blends.

Ti II.—The lines are numerous, and many are very strong.

V II.—Many lines are strong, especially in the ultraviolet.

[18] J. L. Greenstein, *Ap. J.*, **97**, 252, 1943.

[19] P. W. Merrill, *Pub. A.S.P.*, **51**, 218, 1939.

Cr I.—Only two lines are listed in Table 2.

Cr II.—The lines are very numerous, and many high-excitation lines are considerably stronger than in α Persei. Lines from levels up to 6.6 volts are present in HD 30353.

Mn I.—Even the resonance triplet is quite weak.

Mn II.—Many classified lines, including predicted lines, are quite strong. A rather large number of lines probably due to *Mn* II, which have been observed by Exner and Haschek[18] as spark lines, are given in Table 2 as *Mn* II?

Fe I.—The lines of neutral iron are relatively weak, being of similar strength to those of φ Cassiopeiae, an A5 supergiant. It is difficult to determine when the numerous lines of *Fe* I should be included as contributors to blends, especially in the visual region. A rather large number of the higher-excitation lines of *Fe* I have been included in Table 2, even though the laboratory intensities of some are quite low.

Fe II.—This spectrum is the major contributor of lines to the spectrum of HD 30353. A great number of predicted lines are surprisingly strong. Classified lines are present up to 8.2 volts, and a large number of unclassified lines are also present in considerable strength. Many of the identifications in the visual region are tentative. Lines listed in Table 2 as due to *Fe* II or III are those given in the *Revised Multiplet Table* as unclassified lines of *Fe* III, with the remark that some may be due to *Fe* II. Most of these, if the identification is correct, would hence probably be due to *Fe* II.

Co I.—A few lines are probably present.

Co II.—Two ultraviolet lines are given in Table 2.

Ni I.—Several lines appear to be present, though blended.

Ni II.—The lines are very strong.

Sr II.—The resonance doublet is well marked, though much weaker than in α Persei.

Y II.—Nine lines appear in Table 2. The unidentified line near λ 4178 A, which has been thought to be due to *Y* II, is strong in HD 30353.

Zr II.—A number of low-lying lines are fairly strong.

Ba II.—Three lines are listed in Table 2. The lines are weak.

There are a number of spectra which might be expected to appear but which have not been found. A discussion of these follows:

C I.—The high-excitation lines of neutral carbon which are very strong in the spectrum of R Coronae Borealis are not seen in the present spectra of HD 30353. The abundance of carbon must be considerably lower in HD 30353.

S II.—The lines of ionized sulphur were found by Morgan[20] to be very strong in the spectrum of υ Sagittarii, but they are not visible with certainty in the blue region of the spectrum of HD 30353. Perhaps the excitation potential of these lines (13.5–14 volts) is responsible for their failure to appear in HD 30353.

A II.—Morgan[20] has also called attention to the unprecedented strength of the *A* II lines in the spectrum of υ Sagittarii. In the spectrum of HD 30353 a line appears at λ 4348 A which may be due to *A* II, but the writer prefers to consider it an unidentified line because of the high excitation potential of the *A* II line.

Fe III.—Though fairly strong lines from 8.2 volts are present in υ Sagittarii, they are not found in the present spectra of HD 30353.

No lines of neutral scandium, titanium, vanadium, or zirconium have been identified in the present spectra of HD 30353.

III. INTERPRETATION OF THE SPECTRUM OF HD 30353

Since spectrophotometric measures are not available, no detailed discussion of the characteristics of the atmosphere of HD 30353 can be carried out. The presence of a large number of high-excitation, unclassified, and unidentified lines which are not seen in normal stellar spectra makes it clear that the opacity in the stellar atmosphere is very

[20] *Ap. J.*, **79**, 513, 1934.

low. Since a deficiency of hydrogen is strongly indicated by the anomalous weakness of the Balmer lines, it is natural to attempt to explain the low opacity by the same hypothesis. With a great deficiency of hydrogen in the atmosphere of the star, the only sources of opacity operative in the outer layers of HD 30353 would be electron scattering and the discontinuities at the ionization edges of the other elements. These would produce far less opacity than would a normal number of neutral hydrogen atoms. The great complexity of the visual region of the spectrum might also be explained by the fact that in a "hydrogen-poor" star the continuous absorption coefficient would not increase with increasing wave length as it does in normal stars in which either neutral hydrogen or the negative hydrogen ion provides the main source of opacity.

Whether HD 30353 is a supergiant star is not definitely known. Spectroscopically it resembles an extreme supergiant, but the application of absolute-magnitude criteria to peculiar stars is of doubtful validity. We may obtain some indication of the luminosity of

TABLE 3

RADIAL VELOCITIES OF HD 30353

Plate No.	Date	Radial Velocity (Km/Sec)	Dispersion at $H\gamma$ (A/Mm)
f/2 8529	Oct. 31.41, 1946	−35	76
CG 6228	Nov. 5.42, 1947	−30	27
CG 6260	Nov. 12.34, 1947	−33	27
CG 6932	Apr. 27.12, 1948	+43	27
CQ 7208	Nov. 21.20, 1948	−58	55
7251	Nov. 29.13, 1948	−61	55
7286	Dec. 2.19, 1948	−59	55
7332	Dec. 7.09, 1948	−62	55
7398	Dec. 15.14, 1948	−60	55
7421	Dec. 20.08, 1948	−64	55
7455	Dec. 28.14, 1948	−57	55
7486	Jan. 6.07, 1949	−54	55
7553	Feb. 1.13, 1949	−42	55
7557	Feb. 8.06, 1949	−36	55
7559	Feb. 14.06, 1949	−22	55
7577	March 7.08, 1949	+ 7	55
7578	March 7.15, 1949	+13	55
CQ 7579	Apr. 10.11, 1949	+30	55

the star from its distance as indicated by its interstellar reddening. The color index of HD 30353, on the International System, has been measured by O. J. Eggen as 0.54 mag.[21] If we assume a normal color index of 0.10 mag., then we obtain an interstellar reddening of 0.44 mag. Such a value is consistent with a distance of perhaps 2000 parsecs, which would make the star a rather luminous supergiant. Yet the star may be intrinsically reddened, as is P Cygni.

IV. THE RADIAL-VELOCITY VARIATION OF HD 30353

On the basis of a number of spectrograms taken over a period of two and one-half years, it has been found that the radial velocity of HD 30353 is variable. This is of special interest in view of the fact that υ Sagittarii is a single-lined spectroscopic binary with a period of 137 days and a mass function of 1.6. The radial velocities of HD 30353 obtained from the material at hand are given in Table 3. No variations have been seen in the spectrum of HD 30353, and no trace of the other component has been found.

[21] This value is unpublished and was kindly obtained for the writer by Dr. Eggen.

The values of the velocity given by the first four plates of Table 3 are to be given less weight than the series with the 55-A/mm dispersion, since the velocities were determined from different sets of lines in these four cases. In measuring the 55-A/mm plates, an attempt was made to measure the same lines on all plates. Also only those lines were used whose wave lengths were known with certainty. Because of the great complexity of the spectrum, the lines which proved suitable were few. Those used are given in Table 4.

Despite the fact that so few lines were measured, the quality of the lines is such that the mean error of a single plate is probably only 2 or 3 km/sec. The velocities given in Table 3 may be represented by an orbital motion with a period of the order of 1 year, and a value of K of about 50 km/sec. These values give the large mass function f of 4.7, but an orbital eccentricity of $\frac{1}{2}$ would reduce this value to 3.1. This is still very large, but not unprecedented: μ Sagittarii has a mass function of 4.0 and ϵ Aurigae one of 3.3. We can now, however, place a lower limit to the mass of the invisible component of the system of HD 30353; for, from the definition of the mass function, it follows that f is the lower limit of the mass of the secondary star. In normal cases, of course, we always observe the more massive star, so that m_2 is very much larger than f. We cannot be certain that the observed component in the case of HD 30353 is, in fact, the more massive component; for, if the star is deficient in hydrogen, it will be considerably overluminous for

TABLE 4

LINES USED FOR RADIAL-VELOCITY DETERMINATIONS OF HD 30353

Wave Length (A)	Identification	Wave Length (A)	Identification
3951.97	*V* II	4122.64	*Fe* II
4028.33	*Ti* II	4233.20	*Fe* II + *Cr* II
4067.05	*Ni* II	4246.83	*Sc* II
4101.74	*Hδ*	4481.23	*Mg* II

its mass. In any case, however, it is certain that the unobserved component of the system of HD 30353 must be more massive than, say, three solar masses, if the observed radial-velocity variation is due to orbital motion.

V. GENERAL REMARKS ON THE PROBLEM OF THE "HYDROGEN-POOR" STARS

In the case of HD 30353 and the other stars mentioned in the first section of this paper, one observes a spectrum which strongly suggests that the abundance of hydrogen in the stellar atmosphere is abnormally low. This fact raises questions of great cosmogonical importance. If the atmospheres of these stars are actually deficient in hydrogen, the conclusion might be drawn that they have largely used up their originally normal supply of hydrogen and that the rarity of this element in their atmospheres is a direct result of this situation. However, according to recent work in the theory of stellar structure, this conclusion appears unjustified. Ledoux[23] and others have pointed out that no mixing can be expected to take place between the convective core of a star and its radiative envelope. Consequently, if a star did use up a large fraction of the original supply of hydrogen in its core, we could not expect to become aware of that fact solely by spectroscopic observations, unless a nova-like outburst occurred.

If Ledoux's conclusions are correct and if the atmospheres of these stars are truly deficient in hydrogen, then it would seem that only two possibilities remain: (*a*) the *entire star* has possessed a deficiency of hydrogen *throughout its lifetime*, or (*b*) the star originally had a normal supply of hydrogen, but its *atmosphere* has subsequently lost most of its most abundant constituent.

[23] *Ann. d'ap.*, **11**, 174, 1948.

Present astrophysical ideas do not provide any mechanism by which the latter process could occur. Thus one is forced to alternative *a*, and we must postulate the existence of regions of the universe of low hydrogen content.

However, the writer feels that there may still be another possibility, namely, that the spectroscopic observations have been misinterpreted and that these stars have, contrary to the appearance of their spectra, a normal atmospheric hydrogen content. We know that many stellar spectra present unsolved problems. For example, the spectra of slow novae near maximum light often show abnormally weak hydrogen lines, both in emission and in absorption. Also some of the RV Tauri stars pass through a stage in which the hydrogen lines are scarcely visible in their spectra. Sanford[23] writes of U Monocerotis: "The hydrogen lines change from strong absorption lines through a stage in which the lines are practically obliterated, to fairly strong emission." In view of the occasional P Cygni structure of *Hα* in *υ* Sagittarii, we may also call to mind the unusual spectra of the supergiant shell stars, such as P Cygni a..d HD 160529.[24] Nevertheless, the assumption that this group of apparently "hydrogen-poor" stars is actually deficient in hydrogen seems to be the most reasonable one which can be made at the present time.

The writer wishes to express his obligation to Dr. G. Münch for many helpful discussions of topics related to this paper.

[23] *Mt. W. Contr.* No. 465; *Ap. J.*, **77**, 120, 1933.

[24] P. Swings and O. Struve, *Ap. J.*, **91**, 592, 1940; O. Struve, *Ap. J.*, **99**, 206, 1944.

ON THE TURBULENT VELOCITIES OF SOLAR GRANULES*

R. S. Richardson and M. Schwarzschild
Mount Wilson and Palomar Observatories and Princeton University Observatory
Received December 30, 1949

ABSTRACT

With the 150-foot solar tower of the Mount Wilson Observatory, a spectrum of the solar granulation was obtained, showing individual granules with good definition. The Doppler shifts shown by this plate were measured and the corresponding turbulent velocities determined. From these data, together with the turbulent velocities determined from other solar observations, a tentative turbulence spectrum is derived for the solar photosphere. This spectrum suggests the possible existence of turbulent elements only 100–200 km in diameter, with velocities of the order of 2 km/sec and brightness contrasts much exceeding those of the directly observable larger granules.

I. INTRODUCTION

The photosphere of the sun seems to be in a state of turbulence. This is indicated directly by the appearance of the granules on the solar surface and is corroborated by the theory of the hydrogen convection zone. The velocities of the photospheric turbulence have thus far been derived from two sources: the solar curve of growth and solar-line profiles. Both sources indicate turbulent velocities of the order of 1 km/sec. From these data one might assume that the visible granules have velocities as high as 1 or 2 km/sec. If this is the fact, it should be possible to measure the Doppler shifts in the spectra of individual granules.

On the basis of this consideration the first tests for obtaining spectra of individual granules were made in the summer of 1948 at the 150-foot tower of the Mount Wilson Observatory. The central portion of the large solar image was focused on the spectrograph slit. Since a long slit was used, a wide spectrum was obtained. This spectrum was not of uniform density across its width; the granules and the intergranule spaces, as they happened to fall side by side along the slit, produced bright and dark parallel strips in the spectra (see Fig. 1). Most important, each solar absorption line, instead of being straight, crossed these strips in a wavy line, directly indicating turbulent Doppler shifts.

Though the plates of 1948 showed the looked-for phenomena, the definition of the granules in the spectra did appear rather poor. In May, 1949, a new grating, ruled at the Mount Wilson Observatory under the supervision of H. W. Babcock, was placed in the spectrograph of the 150-foot tower. This grating has a high light-concentration in the red of the second order and thus permitted a very appreciable reduction in the exposure time needed for the granule spectra. Late in May, Richardson took several exposures of granule spectra under fine seeing conditions. All exposures show the granules in the spectra with good definition, one, indeed, with excellent definition.

In August and September, approximately three hundred more exposures were taken on fifteen mornings, setting both on the center and near the limb of the sun. For none of these exposures, however, were the seeing and the state of the two coelostat mirrors simultaneously of that high quality necessary for reaching the granule definition obtained in May. Accordingly, the measurements of turbulent velocities reported in the following section are based entirely on the one exposure of exceptional quality obtained in May.

* This investigation was made possible by a co-operative arrangement between the Princeton University Observatory and the Mount Wilson and Palomar Observatories.

II. MEASUREMENTS OF TURBULENT VELOCITIES

The 150-foot tower, as used for the granule spectra, is described by the following data:

Aperture of the tower telescope	12 inches
Diameter of the solar image	422 mm
Length of slit	34 mm
Width of slit	0.125 mm
Dispersion	1 mm = 0.532 A = 25.3 km/sec
Scale of plate perpendicular to dispersion	1 mm = 4".50 = 3280 km on sun

The data for the one exposure used for the present velocity measurements are as follows:

Date: May 24, 1949, P.S.T., 8:03 A.M.
Exposure time: 3 seconds
Wave-length region: λλ6292–6307
Type of plate: Eastman IV-F
Type of filter: Eastman No. 3480 (3 ft. above slit)
Developed 7 minutes in Eastman X-ray developer with brushing

The wave-length region chosen contains not only solar lines but also several atmospheric lines, which can be used as comparison standards. Thus the results are unaffected if the slit is not exactly straight or if it was unevenly illuminated at any one place.

Test measurements showed that the Doppler shifts varied so strongly along the slit that independent measurements had to be made every tenth of a millimeter. Spectral strips only one-tenth of a millimeter wide seemed hardly sufficient for visual measurements, particularly since the absorption lines appeared fairly wide because of the high dispersion. Therefore, all measurements were made with the old microphotometer of the Mount Wilson Observatory. This photometer has an accurate measuring screw to move the plate in the direction of dispersion. It also has a second screw to displace the plate by measurable amounts in the direction perpendicular to the dispersion.

Measurements were made every tenth of a millimeter, i.e., at 340 positions, across the entire width of the spectrum. At each position seven lines were measured, three solar lines (λλ 6297.80, 6301.52, and 6302.51) and four atmospheric lines (λλ 6295.18, 6295.96, 6298.46, and 6299.23). The measurement of each line consisted of two settings made in the following way: While the galvanometer was being watched, the measuring screw was turned until the movement of the galvanometer indicated that the edge of the line had entered the photometer slit. When the galvanometer had reached a scale reading approximately midway between continuum and the central depth of the line, the position of the measuring screw was read. Then the turning of the screw was continued in the same direction while the galvanometer was watched as it went through the center of the line. When the galvanometer on its way back toward the continuum had reached exactly the same intermediate scale reading, a second screw reading was taken. The average of the two screw readings thus obtained was used as representing the position of the center of the line.

The length of the photometer slit was chosen to correspond to one-tenth of a millimeter on the plate, so that the measurements on neighboring positions were just independent of one another. The width of the photometer slit was chosen so that at each of the two measuring positions the slit contained the major portion of the descending or ascending part of the line profile, respectively. Accordingly, additional settings at different galvanometer readings would have added little to the resulting accuracy.

The settings of the screw were made by hand, the motor used for driving the screw having been uncoupled. The galvanometer beam was watched visually rather than re-

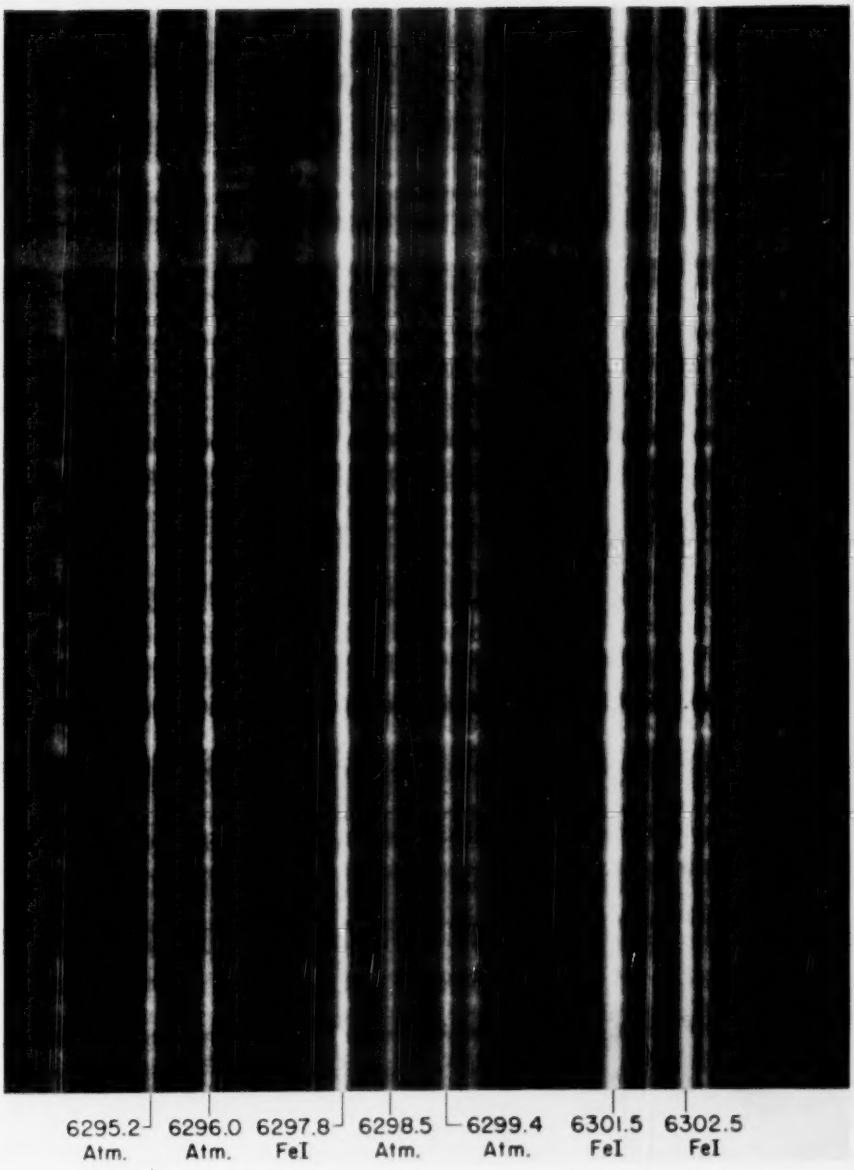

FIG. 1.—Granule spectrum taken at the 150-foot tower of the Mount Wilson Observatory

corded, as in the common use of the photometer. During the entire measurements the plate was never inspected directly.

The time interval between the two readings on the two sides of one line averaged approximately 10 seconds. Only during these very short time intervals was high stability of the photocell, amplifier, and galvanometer required, since changes of the sensitivity while moving from one line to another or from one position to another did not affect the screw readings for the line centers. The measurements of all seven lines at one position took approximately 4 minutes. For such limited time intervals the stability of the mechanical parts of the photometer—in particular, the supports of the microscope objectives—was found sufficient for the accuracy required.

The measurements were reduced in the following sequence: For each position an average was formed from the readings for the centers of the three solar lines. A similar mean was formed at each position for the four atmospheric lines. Then the atmospheric mean was subtracted from the solar mean, thus obtaining one such difference for each of the 340 positions. The 340 values were averaged, and the average was subtracted from the individual values. The residual differences were then multiplied by the dispersion constant (25.3 km/sec/mm). Thus 340 velocity values were obtained, listed in Table 1. In this reduction procedure the zero value for the velocity scale was automatically chosen so that the mean of the 340 resulting velocities was zero.

The accuracy of the measurements was determined in the following way: The measurement for each solar line at each position was subtracted from the average of the three solar lines at that position. The resulting values from the 340 positions for one line were compared with one another and their dispersion determined. Since the Doppler shifts do not enter into this dispersion, all three solar lines having the same shifts at any one position, the accuracy of an individual line measurement could be derived from this dispersion. The measurements of the atmospheric lines could be similarly analyzed. The resulting probable errors are:

P.E. for 1 solar line at 1 position = ± 0.0015 mm ,

P.E. for 1 atmospheric line at 1 position = ± 0.0022 mm ,

P.E. for the velocity at 1 position based on 3 solar lines and 4 atmospheric lines = ± 0.035 km/sec .

The probable errors of the velocities thus found are much smaller than the measured velocity fluctuations.

The measured velocities are plotted in Figure 2. Their frequency distribution is given in Figure 3. The distribution is closely represented by an error-curve.

The random turbulent velocity[1] comes out:

$$\pm 0.37 \text{ km/sec} .$$

This turbulent velocity is much smaller than the values previously found from other sources.

III. THE TURBULENT SPECTRUM OF THE SOLAR PHOTOSPHERE

The turbulent velocity found from direct measurements of Doppler shifts, as described in the preceding section, should be compared with the values for the turbulent velocity obtained from the solar curve of growth and from solar-line profiles.

[1] The term "random" is here used throughout to designate the root mean square of one velocity component multiplied by the square root of 2. In this definition the random turbulent velocity is identical with Unsöld's ξ (*Physik der Sternatmosphären* [1938], p. 158).

TABLE 1

MEASUREMENTS OF VELOCITY AND BRIGHTNESS OF GRANULES

Scale (Mm)	Velocity (Km/Sec)	Brightness (Mag.)	Scale (Mm)	Velocity (Km/Sec)	Brightness (Mag.)	Scale (Mm)	Velocity (Km/Sec)	Brightness (Mag.)
24.0	+0.08	+0.040	30.0	−0.32	+0.035	36.0	+0.04	+0.005
.1	+ .01	+ .035	.1	− .38	+ .040	.1	+ .10	.000
.2	+ .01	+ .040	.2	−. 16	+ .045	.2	− .04	+ .005
.3	+ .01	+ .035	.3	− .24	+ .055	.3	− .04	+ .015
.4	+ .23	+ .030	.4	− .24	+ .070	.4	− .05	+ .015
.5	+ .38	+ .025	.5	− .28	+ .075	.5	− .08	+ .005
.6	+ .41	+ .020	.6	− .04	+ .060	.6	+ .05	− .005
.7	+ .47	+ .030	.7	+ .03	+ .045	.7	+ .08	.000
.8	+ .29	+ .045	.8	+ .11	+ .035	.8	+ .16	.000
.9	+ .08	+ .060	.9	+ .10	+ .035	.9	− .01	+ .010
25.0	− .15	+ .050	31.0	+ .04	+ .035	37.0	+ .11	+ .005
.1	− .13	+ .030	.1	− .22	+ .030	.1	+ .27	− .015
.2	− .20	− .005	.2	− .30	+ .030	.2	+ .25	− .025
.3	− .06	− .040	.3	− .43	+ .020	.3	+ .08	− .015
.4	− .08	− .045	.4	− .33	+ .010	.4	− .18	+ .010
.5	− .16	− .030	.5	− .11	+ .005	.5	− .30	+ .030
.6	− .37	− .010	.6	− .03	+ .005	.6	− .29	+ .020
.7	− .56	+ .005	.7	+ .03	+ .005	.7	− .13	+ .010
.8	− .70	+ .005	.8	+ .09	+ .010	.8	+ .04	+ .010
.9	− .77	+ .005	.9	+ .06	+ .030	.9	+ .14	− .005
26.0	− .75	+ .005	32.0	− .03	+ .035	38.0	+ .19	− .005
.1	− .68	+ .005	.1	+ .05	+ .035	.1	+ .19	+ .005
.2	− .49	+ .005	.2	+ .08	+ .030	.2	+ .16	+ .010
.3	− .47	+ .005	.3	+ .04	+ .025	.3	+ .13	+ .010
.4	− .41	+ .015	.4	− .01	+ .025	.4	+ .20	+ .010
.5	− .47	+ .020	.5	.00	+ .010	.5	+ .27	+ .005
.6	− .47	+ .005	.6	.00	.000	.6	+ .41	− .010
.7	− .29	− .010	.7	− .24	+ .010	.7	+ .56	− .020
.8	+ .01	− .005	.8	− .37	+ .020	.8	+ .44	− .015
.9	+ .01	− .020	.9	− .32	+ .015	.9	+ .38	− .005
27.0	− .16	− .005	33.0	− .22	.000	39.0	+ .51	+ .010
.1	− .24	+ .020	.1	− .25	− .015	.1	+ .35	+ .015
.2	− .54	+ .035	.2	− .23	− .020	.2	+ .32	+ .005
.3	− .48	+ .045	.3	− .24	− .005	.3	+ .35	− .005
.4	− .33	+ .035	.4	− .14	+ .005	.4	+ .22	− .010
.5	− .28	+ .025	.5	− .06	− .010	.5	− .06	.000
.6	− .11	+ .015	.6	+ .18	− .020	.6	− .06	+ .005
.7	+ .04	+ .015	.7	+ .08	− .015	.7	+ .03	− .005
.8	+ .24	.000	.8	+ .08	− .005	.8	+ .28	.000
.9	+ .51	− .020	.9	+ .05	+ .015	.9	+ .33	+ .015
28.0	+ .60	− .020	34.0	+ .05	+ .010	40.0	+ .16	+ .005
.1	+ .75	− .020	.1	+ .30	− .005	.1	− .18	+ .005
.2	+ .77	− .015	.2	+ .28	− .005	.2	− .46	+ .035
.3	+ .67	.000	.3	+ .16	.000	.3	− .51	+ .025
.4	+ .52	+ .010	.4	+ .09	+ .015	.4	− .47	.000
.5	+ .35	.000	.5	+ .03	+ .015	.5	− .15	− .035
.6	+ .42	− .010	.6	+ .08	+ .010	.6	+ .13	− .040
.7	+ .28	− .010	.7	+ .11	+ .015	.7	+ .28	− .035
.8	+ .35	− .010	.8	+ .13	− .005	.8	+ .09	+ .010
.9	+ .24	− .020	.9	+ .04	− .020	.9	+ .13	+ .020
29.0	+ .19	− .020	35.0	+ .09	− .035	41.0	+ .05	+ .025
.1	+ .04	− .010	.1	− .05	− .035	.1	+ .06	+ .020
.2	− .13	+ .005	.2	− .22	− .035	.2	+ .08	+ .020
.3	− .18	+ .005	.3	− .01	− .040	.3	− .04	+ .015
.4	− .01	− .010	.4	+ .19	− .045	.4	− .22	+ .015
.5	+ .10	− .015	.5	+ .30	− .045	.5	− .13	+ .010
.6	+ .15	− .015	.6	+ .15	− .035	.6	+ .05	− .005
.7	+ .24	.000	.7	− .03	− .005	.7	+ .32	− .015
.8	− .13	+ .015	.8	− .27	+ .025	.8	+ .09	− .010
.9	−0.25	+0.030	.9	−0.14	+0.025	.9	−0.09	+0.005

TABLE 1—*Continued*

Scale (Mm)	Velocity (Km/Sec)	Brightness (Mag.)	Scale (Mm)	Velocity (Km/Sec)	Brightness (Mag.)	Scale (Mm)	Velocity (Km/Sec)	Brightness (Mag.)
42.0	−0.24	+0.015	48.0	+0.14	−0.065	54.0	−0.18	+0.010
.1	− .11	+ .010	.1	+ .15	− .030	.1	− .09	+ .010
.2	+ .01	+ .005	.2	− .04	− .010	.2	+ .13	.000
.3	+ .19	+ .010	.3	+ .05	+ .005	.3	+ .18	− .010
.4	+ .29	+ .010	.4	− .14	+ .010	.4	+ .37	− .020
.5	+ .34	+ .015	.5	− .20	+ .010	.5	+ .51	− .030
.6	+ .47	+ .010	.6	− .37	+ .015	.6	+ .46	− .035
.7	+ .44	+ .005	.7	− .32	+ .015	.7	+ .54	− .035
.8	+ .30	+ .005	.8	− .27	+ .010	.8	+ .43	− .025
.9	+ .39	+ .010	.9	− .13	+ .005	.9	+ .38	− .015
43.0	+ .51	.000	49.0	− .14	.000	55.0	+ .42	− .005
.1	+ .52	− .010	.1	− .16	− .005	.1	+ .19	.000
.2	+ .35	− .010	.2	− .01	− .005	.2	+ .16	+ .005
.3	+ .32	− .005	.3	.00	− .015	.3	− .14	+ .015
.4	+ .44	− .015	.4	+ .04	− .015	.4	− .39	+ .025
.5	+ .34	− .010	.5	+ .18	− .025	.5	− .42	+ .025
.6	+ .29	− .005	.6	+ .16	− .015	.6	− .20	+ .010
.7	+ .19	+ .005	.7	+ .03	.000	.7	+ .14	− .010
.8	+ .04	+ .010	.8	− .16	+ .015	.8	+ .20	− .015
.9	.00	+ .015	.9	− .09	+ .005	.9	+ .14	− .010
44.0	+ .04	+ .010	50.0	− .05	− .010	56.0	+ .16	+ .005
.1	+ .16	.000	.1	− .03	− .010	.1	+ .10	+ .010
.2	+ .19	+ .010	.2	− .08	+ .005	.2	.00	+ .020
.3	+ .13	+ .015	.3	− .10	+ .020	.3	.00	+ .020
.4	.00	+ .010	.4	+ .04	+ .020	.4	− .03	+ .020
.5	+ .06	− .005	.5	+ .08	+ .010	.5	− .06	+ .010
.6	+ .18	− .025	.6	+ .05	+ .005	.6	− .05	− .005
.7	+ .25	− .030	.7	− .01	.000	.7	− .05	− .010
.8	+ .19	− .025	.8	− .05	.000	.8	− .05	− .010
.9	.00	− .020	.9	− .24	+ .015	.9	− .05	.000
45.0	− .11	− .015	51.0	− .46	+ .015	57.0	− .18	.000
.1	− .25	− .010	.1	− .42	+ .005	.1	− .13	.000
.2	− .13	− .015	.2	− .28	+ .010	.2	− .18	.000
.3	− .14	− .030	.3	− .28	+ .010	.3	− .13	.000
.4	+ .01	− .040	.4	− .23	+ .005	.4	− .06	+ .005
.5	.00	− .045	.5	− .27	.000	.5	− .14	+ .015
.6	− .11	− .025	.6	− .27	+ .005	.6	− .18	+ .020
.7	− .16	+ .005	.7	− .30	+ .005	.7	− .06	+ .025
.8	− .14	+ .020	.8	− .32	+ .005	.8	+ .13	+ .020
.9	− .10	+ .015	.9	− .06	.000	.9	+0.04	+0.020
46.0	− .11	+ .005	52.0	− .09	− .005			
.1	− .20	.000	.1	.00	− .005			
.2	− .22	− .005	.2	+ .03	.000			
.3	− .32	− .005	.3	+ .03	− .005			
.4	− .15	− .015	.4	+ .01	.000			
.5	− .15	− .020	.5	− .23	+ .015			
.6	− .15	− .015	.6	− .33	+ .030			
.7	− .25	.000	.7	− .32	+ .030			
.8	− .39	+ .020	.8	− .08	+ .020			
.9	− .54	+ .030	.9	+ .10	.000			
47.0	− .57	+ .040	53.0	+ .10	+ .005			
.1	− .56	+ .030	.1	+ .05	+ .015			
.2	− .48	+ .005	.2	+ .05	.000			
.3	− .10	− .035	.3	+ .19	− .010			
.4	+ .01	− .055	.4	+ .22	− .020			
.5	− .01	− .055	.5	+ .47	− .030			
.6	− .09	− .055	.6	+ .42	− .035			
.7	− .05	− .070	.7	+ .44	− .040			
.8	+ .05	− .080	.8	+ .28	− .025			
.9	+0.16	−0.080	.9	+0.04	0.000			

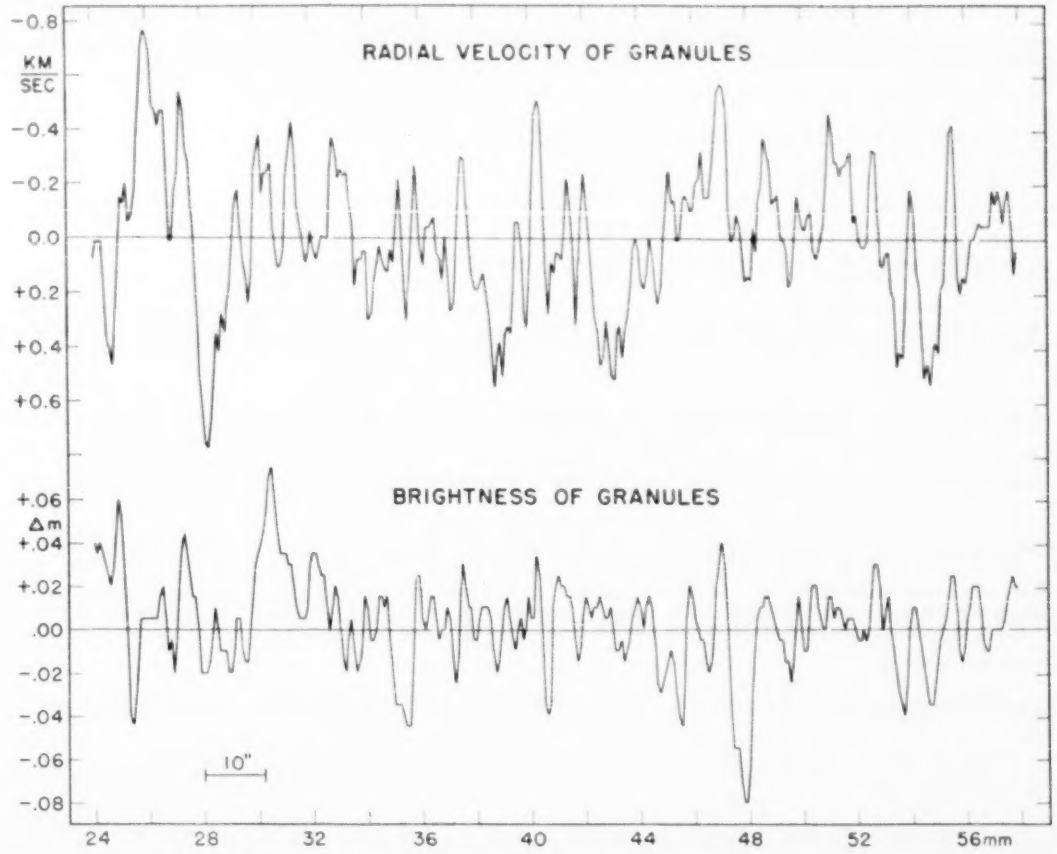

FIG. 2.—Radial velocity and brightness of granules

From the solar curve of growth the random turbulent velocity was found to be 0.9 km/sec by K. O. Wright,[2] 1.7 km/sec by Greenstein,[3] and 2.0 km/sec by Pierce and Goldberg.[4] Here the intermediate value of 1.7 km/sec will be adopted. From the profiles of faint solar lines, Allen[5] found for the random turbulent velocity 2.8 km/sec at the limb and 1.7 at the center of the solar disk. Here the higher limb value will be adopted, for reasons discussed in the next section.

The discrepancy between these velocity determinations and the measurements described in the previous section is large. It appears possible, however, that this discrepancy arises purely from a difference in size of the turbulent elements to which the different determinations refer.

Laboratory experiments have shown that the state of turbulence of a gas cannot be described well by one mean size of the turbulent elements but rather has to be described by a whole continuous spectrum of sizes. In every case of turbulence there appears to exist one size of elements which possesses the highest average velocity. Elements with

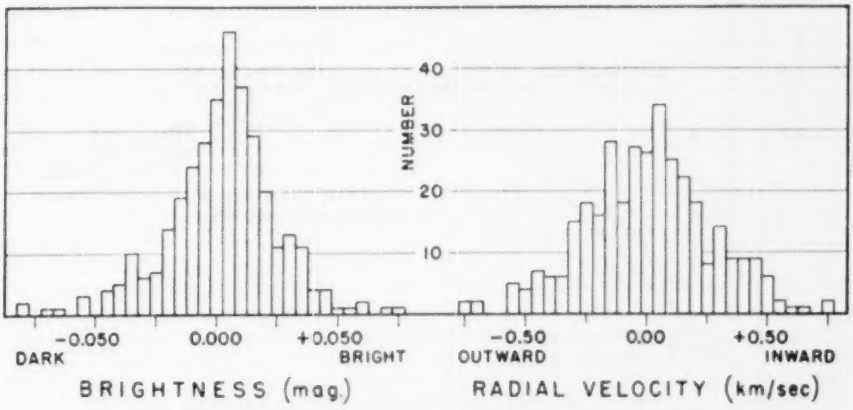

FIG. 3.—Frequency distribution of radial velocity and brightness of granules

sizes larger than those of the fastest elements show a rapid decrease of average velocity with element size. On the other hand, toward smaller element sizes the average velocity falls off slowly. More particularly, under conditions usually fulfilled in astronomical cases this fall-off is governed purely by the process of dissipation of bigger elements into smaller elements. In this process, according to Kolmogoroff,[6] the random turbulent velocity decreases as the reciprocal cube root of the element size.

Can the solar observations now be interpreted in terms of such a turbulence spectrum? To attempt this interpretation, one must determine the element sizes to which the three determinations of turbulent velocities refer. First, for the measurements reported in the preceding section the relevant element size is directly shown by Figure 2. There are approximately forty velocity maxima (not counting the small maxima of the order of the probable error) over a distance of 153″, which, according to Plaskett's definition, gives

[2] *Ap. J.*, **99**, 249, 1944.

[3] *Ap. J.*, **107**, 151, 1948.

[4] *Quarterly Progress Report, Project M 720-5, U. Michigan*, Ann Arbor, October 31, 1947.

[5] *M.N.*, **109**, 343, 1949.

[6] G. K. Batchelor, *Proc. Cambridge Phil. Soc.*, **43**, 533, 1947.

an average element diameter of 2″ or 1500 km. Second, the turbulent velocity determined from the curve of growth refers to elements smaller than the thickness of the effective reversing layer which forms the lines used in the curve of growth. If one estimates this effective thickness very roughly to be of the order of 50 km, then one obtains for the relevant element diameter approximately 20 km. Third, the turbulent velocities obtained from line profiles indicate the effect of elements of all sizes. The main effect for the profiles, however, will come from elements having the size corresponding to the highest average velocity. Hence, the turbulent velocity obtained from line profiles may be taken to give essentially the maximum for the curve relating velocity with element size.

Figure 4 shows the data from the three sources of turbulent velocities. The encircled point to the left represents the measurements described in the preceding section, the encircled point at the right, the data from the curve of growth, while the dotted horizontal line gives the velocity from the line profiles.

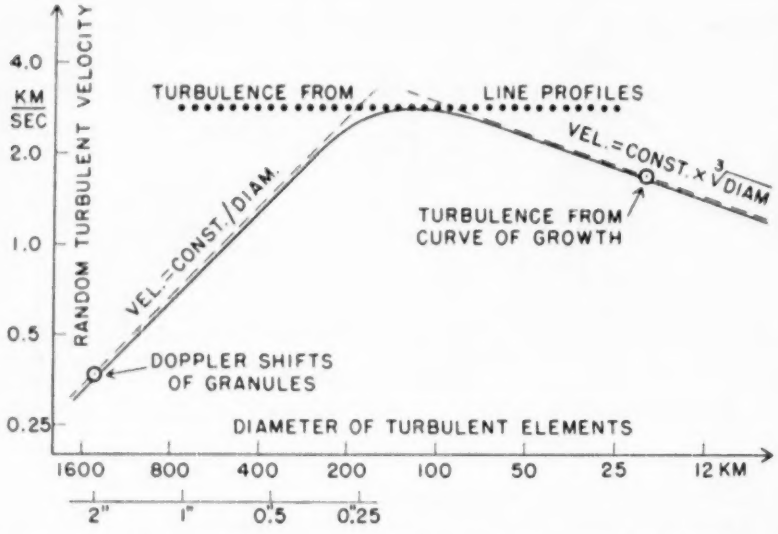

FIG. 4.—Dependence of turbulent velocity in solar photosphere on diameter of turbulence elements

It appears fairly certain that the element size of maximum average velocity is larger than 20 km, since the depth of the hydrogen convection zone, as well as the height over which the density drops by a factor e, exceeds this value. Hence the right-hand point, representing the data of the curve of growth, probably lies on the descending branch of the spectrum, which should follow Kolmogoroff's law. In Figure 4 this law is represented by the dashed line passing through the right-hand point.

On the other hand, the maximum average velocity can hardly occur for elements more than 2″ in diameter; if this were the case, Doppler shifts corresponding to more than 1 km/sec would have been found for the larger, easily resolvable elements. Under these circumstances it seems likely that the observed velocities described in the preceding section represent purely the statistical effect of the higher velocities of small unresolved elements. This statistical velocity effect should be proportional to the reciprocal square root of the number of unresolved elements. In turn, this number should be proportional to the area of the resolution circle. Thus the observed average velocity should be propor-

tional to the reciprocal of the linear scale of resolution. This relation is represented in Figure 4 by the dashed line passing through the left-hand point. The three straight lines of Figure 4 define fairly well the curve which relates the random turbulent velocity with the element diameter. The maximum and right-hand portions of this curve should represent the actual average velocities of turbulent elements of a given size. The left-hand portion of the curve, however, represents only the statistical effect of the elements of highest velocity. The actual velocities of the larger elements should be smaller than the values indicated by the curve.

From the above consideration of the observations of turbulent velocities in the solar photosphere the following main result appears: the diameter of the turbulent elements of highest average velocity is of the order of 100–200 km, i.e., about one-tenth the diameter of the granules thus far resolved. This small scale for the most active elements appears theoretically reasonable because it agrees closely with the height in which the density drops by a factor e in the photosphere.

IV. THE BRIGHTNESS DIFFERENCES OF GRANULES

The indications discussed in the preceding section point toward the possible existence of small, energetic granules. Since these suspected small elements should have velocities about seven times larger than those observed for the larger granules, the brightness differences of the small elements should also be much higher than those observed so far. Thus the question arises: Do the photometric observations permit the assumption that such small, highly contrasty granules exist?

Several series of photometric measurements on granules are available.[7] Of these, however, only the Potsdam series gives the random brightness differences, while others give the extreme values of contrast or the contrast in individual typical granules, neither of which is easily used for the comparison with other observational materials. To add to the Potsdam results for the random brightness differences, photometric measurements were made on two plates in the present investigation.

The first plate used for photometric purposes is the same granule spectrum already used for velocity measurements. The plate carrying this spectrum has, in addition, two exposures on the sky taken through a step-slit. These exposures provided the photometric calibration-curve for the plate. Further, the plate carries a second spectrum taken exactly like the granule spectrum and immediately preceding it, except that the image of the sun was trailed over the slit during the exposure. This spectrum does not show granule spectra but has a fairly even density across its whole width, with only minor fluctuations arising from variations in the slit-width and from dust on the slit. Both spectrum exposures were registered across their width with the recording microphotometer, and the two registered curves were measured at exactly the same 340 positions for which the velocities had been determined. The measurements were transformed into magnitudes with the help of the calibration-curve. Then each magnitude obtained from the trailed exposure was subtracted from the corresponding magnitude from the granule exposure. Thus magnitude differences were computed free of the effects of slit-width variation or dust. Finally, the average of the 340 magnitude differences was taken, and this average was subtracted from each of the individual values. The residual magnitude differences are listed in Table 1 and plotted in Figure 2, which shows that the correlation between the brightness fluctuations and the velocities is rather weak; only the narrow regions of high upward velocities appear to have systematically higher brightness than average. In Figure 3 the frequency distribution of the magnitude differences is given. As in the Pots-

[7] H. H. Plaskett, *M.N.*, **96**, 402, 1936; P. ten Bruggencate, W. Grotrian, E. von der Pahlen, *Zs. f. Ap.*, **16**, 51, 1938; P. C. Keenan, *Ap. J.*, **89**, 604, 1939. A later paper of P. ten Bruggencate and H. Müller (*Zs. f. Ap.*, **21**, 198, 1942) had not been noticed in time for this discussion. The results reported there are in close agreement with those obtained from the Mount Wilson plates.

dam material a slight asymmetry is indicated, showing a little excess of small positive and large negative values. The random brightness thus obtained from the 340 values came out to be ± 0.032 mag.

The second plate used for photometric measurements was a direct photograph of the sun taken from the routine solar program of the Mount Wilson Observatory. In this program two direct photographs of the sun are taken on every clear morning with the 60-foot tower. This instrument gives a solar image 17 cm in diameter ($1'' = 0.089$ mm). The exposures are taken through an orange filter on Solar Green A plates with an effective wave length of approximately 5800 A, with the objective diaphragmed down to 4 inches. The exposure taken on September 15, 1949, at P.S.T. 6:19 A.M. was found to be of excellent definition. On this plate a line 12.5 mm long across the center of the sun was registered with the recording photometer. The registration was measured at 250 equidistant points. The measurements were transformed into magnitudes with the help of a calibration-curve obtained from the limb darkening for which the intensities are known, and the corresponding photographic densities could be measured on the plate. The resulting 250 magnitude values were averaged, and the average was again subtracted from each individual value. The residual magnitudes gave for the random brightness difference: ± 0.054 mag.

To make possible a comparison of these two results with those from the Potsdam material, it is necessary to determine the average size of granules to which the three sets of data refer. Again using the frequency of maxima to determine the mean element diameter according to Plaskett's definition, one obtains for the Potsdam material approximately $5''$, while the two Mount Wilson plates both give very closely $2''$.

Comparing, first, the two Mount Wilson plates with each other, one finds that the spectrum plate gives for the random brightness differences about only two-thirds the value of the direct exposure, even though both appear to refer to identical granule sizes. This may be taken to indicate that spectrum plates, owing to greater light-scattering or other disturbances, are likely to be inferior to direct exposures for the purposes of measuring the brightness contrast in granules. Then, in comparing the direct exposures from Potsdam and Mount Wilson, one has to take into account the difference in effective wave length between the two materials. Assuming that the brightness differences in granules can be sufficiently well represented by black-body temperature differences, one finds from the Potsdam data (random brightness differences of ± 0.047 mag. at λ 3900) a random temperature difference of $\pm 37°$ K, while the Mount Wilson plate (± 0.054 mag. at λ 5800) gives $\pm 64°$ K. Although this comparison may not appear too certain, it seems to indicate that the increase of resolution from $5''$ to $2''$ has nearly doubled the random temperature differences.

However, not only the Potsdam plates but also the Mount Wilson plate most likely do not give the full brightness differences existing on the sun. This was shown by measurements on three individual granules picked for their sharpness and roundness. The photometric cross-section profiles determined from these three elements give a diameter of $1''.7$ at an intensity level halfway between center and base.[8] The corresponding diameter of the diffraction pattern of the 4-inch aperture is $1''.2$. Hence the smaller features shown by this Mount Wilson plate appear to be largely determined by the aperture diffraction, while the actual elements producing these visible features might well be much smaller—and hence brighter—than shown on the plate.

Accordingly, the present photometric material for the solar granulation does not appear to disagree with the possible existence of very small granules but rather suggests that the most contrasty features on the surface of the sun have not yet been resolved.

[8] Similar measurements on the Yerkes plate used by P. C. Keenan (*loc. cit.*) gave an appreciably smaller corresponding diameter, indicating a superior definition of this plate. The determination of the random brightness fluctuation on this plate would seem of great interest.

Indeed, it seems possible that the random temperature fluctuation increases, with decreasing element diameter, approximately proportionately to the random turbulent velocity, thus reaching perhaps $\pm 400°$ for the elements at the maximum of the turbulence spectrum.

If, in fact, such small elements of high brightness contrast exist in the solar photosphere, appreciable effects on the center-limb variation of line profiles and line centers might be expected from them. Regarding the profiles: Since the horizontal velocity components should not show any correlation with brightness, the line profiles at the limb should show the full range of turbulent velocities. On the other hand, for the vertical velocity component an appreciable correlation with brightness might be expected in the sense that the downgoing elements should be darker than the average. In this case, the integrated spectrum of the center of the sun should correspond chiefly to the rising elements, and the line profiles should tend toward giving only the spread in upward velocities, which would be smaller than the spread in all velocities. (This is the reason why the data from the limb profiles rather than from the center profiles were used in the preceding section.)[9] Similarly for the line centers: at the limb the line centers should remain unshifted by the turbulent velocities, while at the center the correlation between brightness and velocity, in the sense of high brightness for rising elements, should shift the line centers toward the violet. Both these effects are, as to sign, in agreement with observations. Whether these turbulence effects by themselves will fully explain the observed effects, future quantitative investigation will have to decide.

V. CONCLUSION

The velocity data discussed in Sections II and III indicate that the turbulent spectrum of the solar photosphere may have its maximum at a scale corresponding to element diameters of the order of 150 km. Further, the photometric measurements discussed in Section IV make it seem possible that these small elements may possess brightness contrasts far exceeding those found thus far from granule observations.

To obtain further data for the solar turbulence spectrum, two ways seem open at present. First, one might attempt to correlate the different values of turbulent velocities indicated by the curve-of-growth data for different types of lines, with the corresponding effective thicknesses of the reversing layer. Thus the curve-of-growth data might give not just one point (as used in Fig. 4) but also the slope of the turbulence spectrum in the range of small elements.

Second, one might attempt to obtain direct photographs of the sun with higher resolution than has been attained so far. Even though the most energetic elements suspected of being only one-fifth of a second in diameter probably cannot be resolved, it would seem important to see whether the random brightness differences really keep increasing with increasing resolution.

Both methods of obtaining additional data should greatly help in deciding how far the present tentative conclusions are correct.

[9] If, contrary to the present assumption, the increase of the line widths toward the limb is caused mainly by an anisotropy of the turbulence or by an increase in the turbulent velocity with height, then the turbulence spectrum should have a lower maximum than that shown in Fig. 4.

THE USE OF SAVART FRINGES IN THE OBSERVATION OF ZEEMAN EFFECTS IN SUNSPOTS

YNGVE ÖHMAN
Research Fellow, Harvard University, stationed at
High Altitude Observatory, Boulder, Colorado*
Received November 7, 1949

ABSTRACT

The use of Savart interference fringes to separate the polarized components in a Zeeman pattern is described. Preliminary results of observations of sunspots are presented. Various applications of the principle are suggested, and attention is drawn to the use of a subtractive double monochromator with narrow slit.

During a recent short visit to the Mount Wilson Observatory the writer had an opportunity to try a simple new method of observing Zeeman splitting in the spectra of sunspots with a Savart polariscope. This paper describes briefly the method and gives some illustrative results.

The Savart polariscope is generally composed of two plates of quartz or calcite of equal thickness, so figured that their optic axes are inclined about 45° to the end surfaces of the plates. Because the surfaces of the cleavage rhombohedron of calcite fulfil this condition, its use facilitates the construction of the instrument.[1] To use the instrument, we mount the plates in crossed positions and place behind them an analyzer with its vibrational direction adjusted to bisect the 90° angle between the principal sections of the plates. In this arrangement the polariscope gives a system of almost parallel dark interference fringes if the source observed is polarized. If the plane of vibration is the same for the source and the analyzer, the central strip in the field of view is bright. If, on the other hand, the planes of vibration are crossed, dark fringes appear in place of the bright. The Savart polariscope thus becomes a convenient instrument for the observation of Zeeman splitting in sunspot spectra.

When we observe a sunspot near the center of the sun, we can first transform the circularly polarized components of a Zeeman triplet in the spot to linearly polarized components having crossed vibrational directions by allowing the beam to traverse a quarter-wave plate before entering the polariscope. If we then place our Savart polariscope behind the eyepiece of the spectroscope and turn it so that it gives interference fringes perpendicular to the spectral lines, we can see the Zeeman splitting as waviness in a line which would be straight in the absence of the magnetic field splitting. If the dispersion of the spectrograph is very high, the wave-shaped line will be broken into a zigzag structure somewhat similar to that produced by mica strips when one observes Zeeman splitting in the conventional way.

When the polarity of the field changes, a wave toward the violet becomes a wave toward the red. We may easily introduce at the side of the spectral line a system of reference fringes produced by a strip of polaroid to facilitate the determination of the polarity of sunspots.

To observe a Zeeman triplet in a sunspot situated near the limb of the sun, we remove the quarter-wave plate; a double wave then appears at the spectral line if the spectrograph is properly adjusted. In this case the polariscope also produces a phenomenon similar to that observed with the mica strips generally used for such measurements.

* Astronomer, Stockholm Observatory, on leave for one year.

[1] Cf. F. E. Wright, *J. Opt. Soc. America*, **24**, 206, 1934.

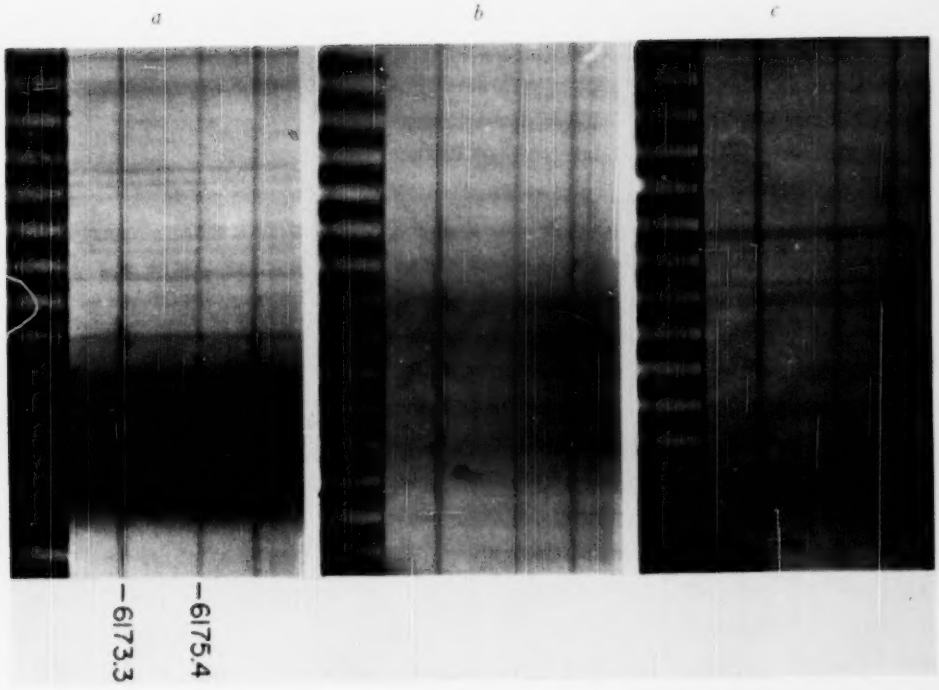

FIG. 1.—Zeeman splitting in sunspots observed with Savart polariscopes attached to the spectrograph of the 150-foot tower on Mount Wilson.

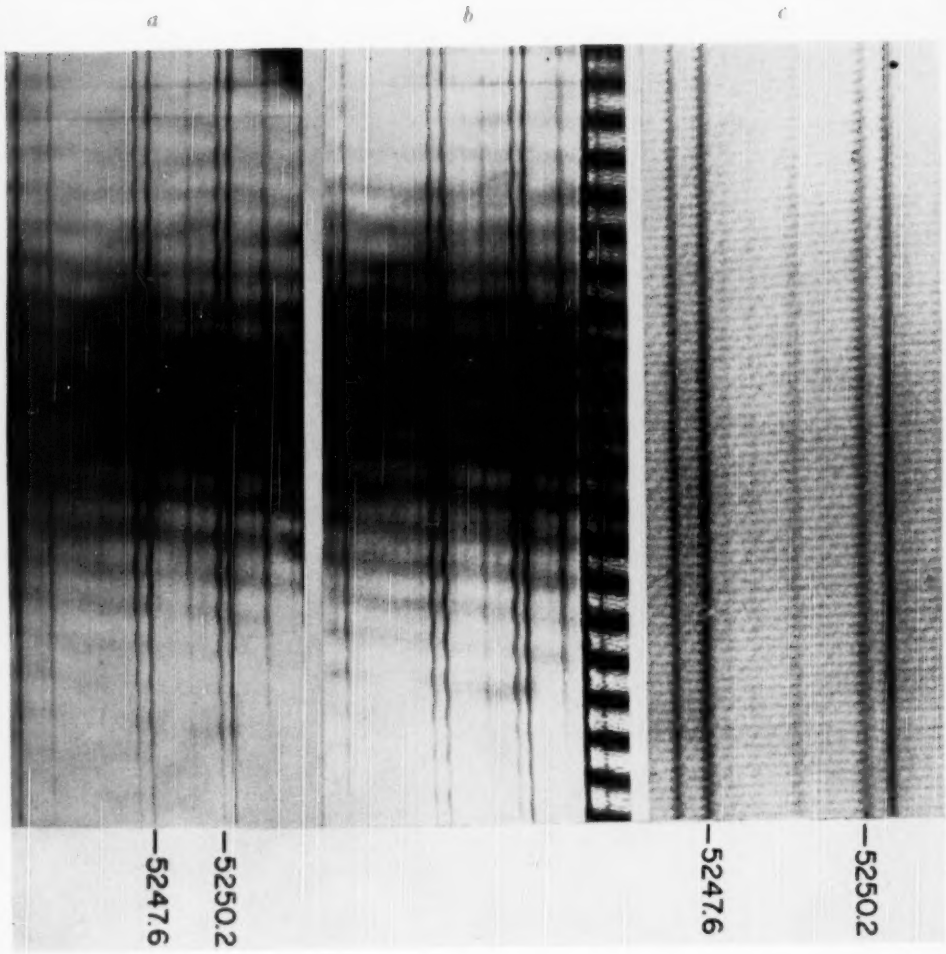

FIG. 2.—Zeeman splitting in a sunspot observed with a Savart polariscope attached to the concave grating spectrograph of Hale Solar Laboratory in Pasadena.

The polariscope will produce interference fringes not only for linear polarization but also for circular and elliptical polarization. Thus, when we observe a spot near the center of the sun without the quarter-wave plate, a wave-shaped line appears; but now the waves, in consequence of the superimposed phase difference, have intermediate positions between those of the corresponding waves produced when the quarter-wave plate is placed in front of the polariscope (in accordance with the well-known interference phenomena which appear in crystal plates when circular polarization is used). In general, the observations are more easily interpreted when a quarter-wave plate is used to transform the circular polarizations to linear ones.

The Savart polariscope should always be used in parallel beams of light, a condition easily satisfied for visual observation by placing the polariscope behind the eyepiece; in photographic observation by replacing the eye with a camera (the method used during my experiments at Mount Wilson Observatory). Or one may place the polariscope between a positive and a negative lens inside the collimating tube of the spectrograph or between a negative and a positive lens before the slit of the spectrograph. The interference fringes will then appear over the whole spectrum.[2] I have used arrangements of this kind to study the polarization of the solar corona with the Climax coronagraph. The angular separation of the fringes must be suitably adjusted for the different kinds of arrangement.

Figure 1 shows spectra obtained on August 23, 1949, with a polariscope attached to the grating spectrograph of the 150-foot tower. The dispersion in the original spectrum is 0.54 A/mm. The images *a* and *b* show Zeeman splitting in the large spot seen that day near the center of the sun. This spot was classified as violet, 3500 gauss, according to Mount Wilson measurements; *a* was taken with quarter-wave plate, and *b* without. At the side, reference fringes produced by a strip of polaroid appear. The image *c* shows, in its lower part, a neighboring spot classified as red, 1100 gauss. This spot was photographed with quarter-wave plate, and it is easy to recognize in the picture the different polarities of *a* and *c*. Because of the polarization produced by the mirrors and the grating, faint Savart fringes can be traced over the whole spectrum. A compensator, such as a tilted celluloid plate or similar unit, may be used to eliminate the faint fringes.

Figure 2 shows similar spectra of the large spot, which were obtained with the concave grating spectrograph of Hale Solar Laboratory in Pasadena. The dispersion in the original spectrum is 2.4 A/mm, and all spectra were obtained with a quarter-wave plate before the slit. Image *a* was taken on August 20, when the spot was 7′.5 from the center; *b* and *c* were taken on August 22, when the same spot was 1′.5 from the center; *c* was taken with only one-tenth the separation of the Savart fringes used in the other photographs. The background polarization is somewhat disturbing in this case; but the photograph indicates interesting inhomogeneities in the magnetic field. It is possible to study Zeeman splitting in sunspots with very narrow fringes, even when the solar image is of moderate size. In the study of the magnetic splitting in stellar spectra the use of narrow fringes may be of value.

Although the proposed method of observing Zeeman splitting in sunspots cannot be expected to give higher accuracy than that obtained with mica strips, it seems to possess several advantages. The joints between the mica strips, which are somewhat disturbing in the conventional method, do not appear; large fields of view may be covered more easily with the Savart-fringe method; a spectroheliographic recording of the magnetic structure of the solar disk is a promising possibility; for this purpose one could use a wide second slit and displace the image stepwise over the disk of the sun. The use of Savart fringes also offers a simpler way to determine polarities of sunspots from visual observations with instruments of moderate size.

For studies of Zeeman splitting in different parts of a sunspot a narrow-slit subtractive

[2] Cf. *Stockholms Obs. Ann.*, Vol. 15, No. 2, 1947.

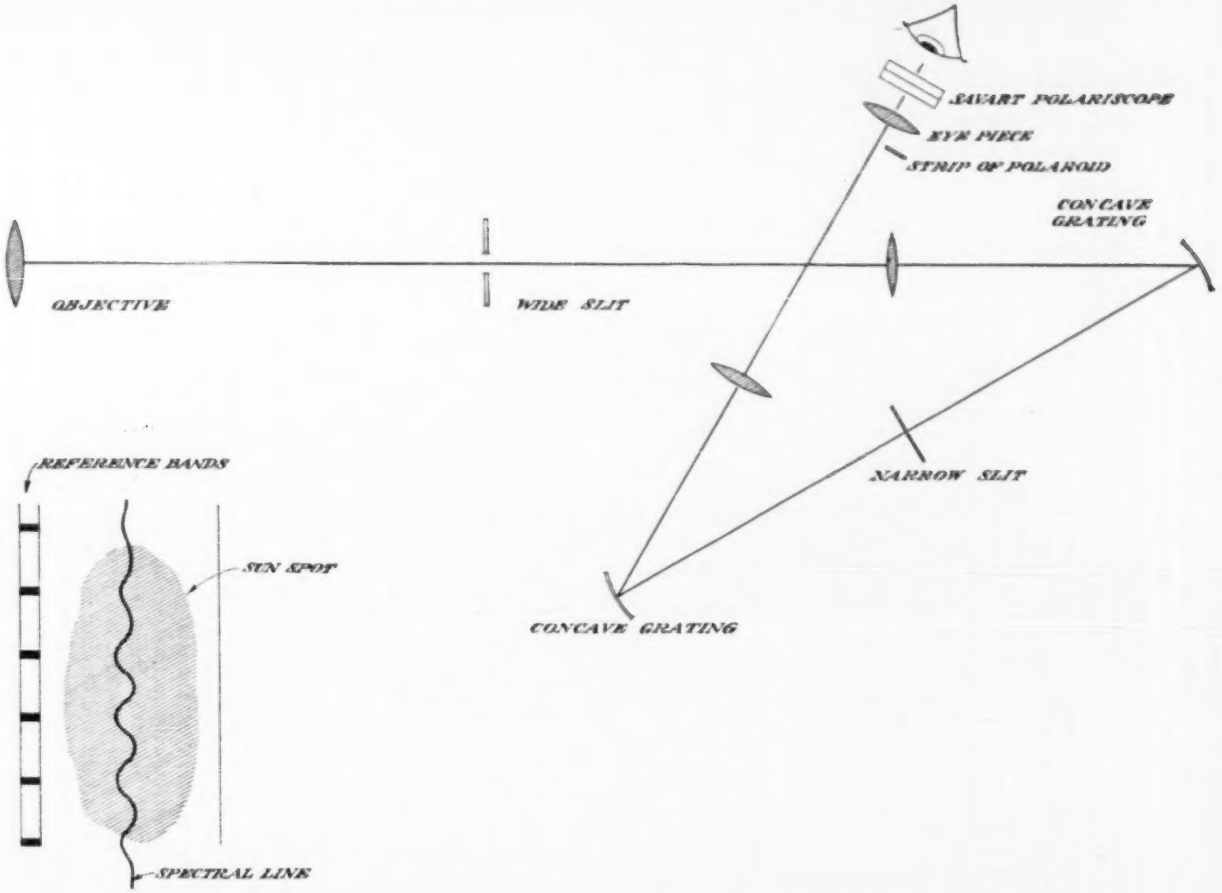

FIG. 3.—Tentative schematic diagram of a subtractive double monochromator for observing Zeeman splitting in sunspots

double monochromator[3] offers advantages. I have experimented with such an instrument at Boulder, assisted by Mr. J. Hood and Mr. L. Shaw. One form of the device is described in the *Upper Air Laboratory Progress Report No. 5* (1949), issued by the Physics Department of the University of Colorado. With a double monochromator with narrow slit, the solar disk is observed in a limited range of wave length, the spectral lines superimposed on the details of the disk; and different parts of a spot may be observed in any desired spectral line. With the use of a Savart polariscope, in addition, the observer may more easily follow the variations in the magnetic field from one point to another in a sunspot.

Figure 3 shows a tentative schematic diagram for an arrangement of a subtractive double monochromator and Savart polariscope. The light passes successively through (1) the objective, (2) a first wide slit, (3) a collimator, (4) a concave grating in Wadsworth mounting, (5) a narrow slit, (6) an identical concave grating in reversed Wadsworth mounting, (7) a telescope objective, (8) an eyepiece, (9) the Savart polariscope. Theoretically, the first concave grating may be used as an objective, but in practice the heating of the concave grating would probably be unfavorable and the image scale too small for observing small spots. The use, instead, of an objective prism and one spectrograph only looks more promising.

I am very much indebted to Dr. Bowen, who gave me permission to carry out these experiments during my short visit at the Mount Wilson Observatory, to Mr. Harold Babcock, who gave me much assistance and valuable advice during the work in the Hale Solar Laboratory, and to Messrs. Nicholson, Richardson, and Schwarzschild for important help during the work with the 150-foot tower on Mount Wilson. I wish also to express my great appreciation for the support of Harvard University Research Contract W19-122ac-17 with the Air Materiel Command, which has made this research possible.

[3] Cf. K. O. Kiepenheuer, *Naturforsch. u. Med. in Deutschland*, **20**, 236, 1947.

THE ROTATIONAL VELOCITIES OF GROUPS OF STARS, AS DETERMINED FROM THE APPARENT ROTATIONAL VELOCITIES

ARCHIBALD BROWN*
Yerkes Observatory
Received December 16, 1949

ABSTRACT

The frequency distribution of the apparent velocities of rotation of a group of stars is obtained for two different assumptions as to the form of the frequency distribution of the true rotational velocities. A comparison with observational material for the Be stars suggests that, provided the mean and the second moment about the mean are correctly evaluated, the shape of the frequency distribution of true rotational velocities can vary appreciably, yet still lead to distributions of the apparent rotational velocities which are compatible with the observations.

I

If the axis of rotation of a star is inclined at an angle i to the line of sight, then the apparent rotational velocity of the star is $v \sin i$, where v is the true (equatorial) rotational velocity. In general, the value of i is not known for individual stars and it is impossible to deduce the value of v from the observed $v \sin i$. Having conceded that it is impossible to deduce v in most individual cases, one can still attempt to derive group properties, such as the frequency distribution of true rotational velocities, from observations of the apparent rotational velocity for a number of stars. This requires some assumption as to the frequency of occurrence of a given angle of inclination among the group of stars under consideration and the assumption usually made is that the axes of rotation of the stars are randomly distributed in space. In that case the probability of occurrence of a value of the angle of inclination in the interval i to $i + di$ is $\sin i\, di$. This assumption is adopted for the remainder of the present paper.

Recently Chandrasekhar and Münch[1] pointed out that simple numerical relations exist between the moments of $\phi(v \sin i)$, the frequency distribution of the apparent rotational velocities, and the corresponding moments of $f(v)$, the frequency distribution of the true rotational velocities. Using these relations, the mean value of v and the second moment about the mean of $f(v)$ can be determined from the observed values of $v \sin i$. Chandrasekhar and Münch recognized that, although $f(v)$ and $\phi(v \sin i)$ are related by an integral equation, in cases where only a small number of observed values are available the mean and standard deviation might be the only properties of $f(v)$ that one could deduce reliably. (The results obtained below tend to confirm that view.) They suggested that, in general, instead of solving for $f(v)$ by numerical inversion of the integral equation, it would be better to assume a form for $f(v)$, work out the corresponding frequency distribution of $(v \sin i)$, and compare this with the observations. To illustrate this procedure, they used the form

$$f(v) = \frac{j}{\sqrt{\pi}} \left\{ e^{-j^2(v-v_1)^2} + e^{-j^2(v+v_1)^2} \right\}, \tag{1}$$

which gives a two-parameter family of frequency distributions. This led to satisfactory agreement with the observations, the only trouble about using this form of $f(v)$ being that the corresponding form for the distribution of the apparent rotational velocities is difficult to handle. In the present paper, two forms of $f(v)$ are considered which lead to more tractable forms of $\phi(v \sin i)$. Both these forms involve two parameters, which can

* Commonwealth Fund Fellow.

[1] *Ap. J.*, 111, 142, 1950.

be evaluated directly from the mean and standard deviation of $f(v)$, i.e., in practice, from the mean and second moment of the observed values of apparent rotational velocity.

In Section II, $\phi(v \sin i)$ is obtained for the first of these assumed forms of $f(v)$, while Section III gives the corresponding results for the other assumed distribution. Section IV gives details of a numerical comparison with the frequency distribution of apparent rotational velocity of Be stars, using the material recently published by Slettebak.[2] Since these stars have large rotational velocities, the effect of observational errors due to the difficulty of determining $v \sin i$ from line profiles will be relatively small. Indeed, this material is probably as homogeneous and reliable as any that is available, so it is of especial interest to see how much information about the distribution of the true rotational velocities can be extracted from it. The paper concludes with a short discussion of the results obtained.

II

For a random orientation of the axes of rotation of the stars under consideration, the equation relating f and ϕ is

$$\phi(y) = y \int_y^\infty \frac{f(v)\, dv}{v \sqrt{(v^2 - y^2)}}, \tag{2}$$

where $y = v \sin i$ = observed equatorial rotational velocity.[3] If $f(v)$ is of "rectangular" form, i.e.,

$$\begin{aligned} f(v)\, dv &= \text{Probability of occurrence of a value of } v \text{ between } v \text{ and } v + dv \\ &= \begin{cases} \dfrac{dv}{2a} & \text{for} \quad v_0 - a \le v \le v_0 + a \\ 0 & \text{for} \quad v < v_0 - a \quad \text{or} \quad v > v_0 - a\,, \end{cases} \end{aligned} \tag{3}$$

then it is easy to show that

$$\begin{aligned} \phi(y)\, dy &= \text{Probability of occurrence of a value of } y \text{ between } y \text{ and } y + dy \\ &= \frac{1}{2a}(\theta_1 - \theta_2)\, dy\,, \end{aligned} \tag{4}$$

where

$$\cos\theta_1 = \begin{cases} \dfrac{y}{(v_0 + a)} & \text{for} \quad 0 \le y \le v_0 + a \\ 1\,, & \text{for} \quad y \ge v_0 + a\,; \end{cases}$$

$$\cos\theta_2 = \begin{cases} \dfrac{y}{(v_0 - a)} & \text{for} \quad 0 \le y \le v_0 - a \\ 1 & \text{for} \quad y \ge v_0 - a\,. \end{cases} \tag{5}$$

However, for comparison with an observed frequency distribution we usually require the integral of $\phi(y)$ over finite intervals of y, corresponding to the intervals into which the observations have been grouped, e.g., we want to compute, say, the number of stars for which the apparent rotational velocity y should be between 200 and 250 km/sec and compare this with the observed number. So it is convenient to tabulate not $\phi(y)$ but the distribution function of y, written

$$F(y) = \int_0^y \phi(y)\, dy\,.$$

[2] *Ap. J.*, **110**, 498, 1949.

[3] For a derivation of this equation cf. Chandrasekhar and Münch. *op. cit.*, pp. 143–144.

Then the fraction of the stars with $200 \leq y \leq 250$ is simply

$$F(250) - F(200)$$

and the required values can be read off from a table of $F(y)$ or a graph of $F(y)$ against y. In this case,

$$F(y) = \frac{1}{2a}\int_0^y (\theta_1 - \theta_2)\, dy .$$

$$\int_0^y \theta_1 dy = \int_{\theta_1}^{\pi/2} \theta\,(v_0 + a)\sin\,\theta\, d\theta ,$$

putting $y = (v_0 + a)\cos\theta$ within the integral.
Hence,

$$\begin{aligned}\int_0^y \theta_1 dy &= (v_0 + a)\,[\sin\,\theta - \theta\cos\,\theta]_{\theta=\theta_1}^{\theta=\pi/2} \\ &= (v_0 + a)(1 - \sin\,\theta_1) + \theta_1 y .\end{aligned}$$

Similarly,

$$\int_0^y \theta_2 dy = (v_0 - a)(1 - \sin\,\theta_2) + \theta_2 y .$$

Hence,

$$F(y) = 1 + \frac{y}{2a}(\theta_1 - \theta_2) + \frac{1}{2a}\{(v_0 - a)\sin\,\theta_2 - (v_0 + a)\sin\,\theta_1\} . \tag{6}$$

[It will be evident that $F(y)$ can usually be obtained without evaluating $\phi(y)$ explicitly, since

$$F(y) = \int_0^y \phi(y)\, dy = \int_0^y \int_{v=y}^{v=\infty} \frac{f(v)\, y\, dv\, dy}{v\sqrt{(v^2 - y^2)}} .$$

If it is permissible to reverse the order of integration—and this will usually be the case—one can integrate immediately with respect to y. This can be used to check the algebra.]

III

If $f(v)$ has the "parabolic" form

$$f(v) = \begin{cases} \dfrac{3}{4b}\left[1 - \dfrac{(v - v_0)^2}{b^2}\right] & \text{for} \quad v_0 - b \leq v \leq v_0 + b \\ 0 & \text{for} \quad v < v_0 - b , \quad v > v_0 + b , \end{cases} \tag{7}$$

then

$$\phi(y)\, dy = y dy \int_y^\infty \frac{f(v)\, dv}{v\sqrt{(v^2 - y^2)}} \qquad \text{as before.}$$

For $y < v_0 - b$, the lower limit of the integral becomes $v_0 - b$. Hence, for $y \leq v_0 - b$,

$$\phi(y)\, dy = y dy \int_{v_0 - b}^{v_0 + b} \frac{3}{4b}\left\{1 - \frac{(v - v_0)^2}{b^2}\right\} \frac{dv}{v\sqrt{(v^2 - y^2)}} ,$$

and, for $v_0 - b \leq y \leq v_0 + b$,

$$\phi(y)\,dy = y\,dy \int_y^{v_0+b} \frac{3}{4b}\left\{1 - \frac{(v - v_0)^2}{b^2}\right\} \frac{dv}{v\sqrt{(v^2 - y^2)}}.$$

These integrals can be integrated immediately by the substitution $v = y \sec \psi$. If we define ψ_1 and ψ_2 similarly to θ_1 and θ_2 of Section II, i.e.,

$$\cos\psi_1 = \begin{cases} \dfrac{y}{v_0 + b} & \text{for} \quad 0 \leq y \leq v_0 + b \\ 1 & \text{for} \quad y > v_0 + b\,, \end{cases}$$

$$\cos\psi_2 = \begin{cases} \dfrac{y}{v_0 - b} & \text{for} \quad 0 \leq y \leq v_0 - b \\ 1 & \text{for} \quad y > v_0 - b\,, \end{cases}$$

then we obtain

$$\phi(y) = \frac{3}{4b}\left(1 - \frac{v_0^2}{b^2}\right)(\psi_1 - \psi_2) + \frac{3y^2}{4b^3}(\tan\psi_1 - \tan\psi_2) + \frac{3v_0 y}{2b^3}\log_e \frac{\sec\psi_1 + \tan\psi_1}{\sec\psi_2 + \tan\psi_2}. \quad (8)$$

The expression for $F(y)$ can be evaluated from this. In this case it is more convenient to evaluate

$$1 - F(y) = \int_y^{v_0+b} \phi(y)\,dy. \quad (9)$$

However, the method of integration is the same as before, i.e., put $y = (v_0 + b)\cos\psi$ within the integral where the integrand involves ψ_1 and put $y = (v_0 - b)\cos\psi$ within the integral where the integrand involves ψ_2. The typical terms are

$$\begin{aligned} I_1 &= \int_y^{v_0+b} \psi_1 dy \\ &= (v_0 + b)\int_0^{\psi_1} \psi \sin\psi\, d\psi \\ &= (v_0 + b)(\sin\psi_1 - \psi\cos\psi_1)\,; \end{aligned}$$

$$\begin{aligned} I_2 &= \int_y^{v_0+b} y^2 \tan\psi_1 dy \\ &= (v_0 + b)^3 \int_0^{\psi_1} \cos^2\psi \tan\psi \sin\psi\, d\psi \\ &= \tfrac{1}{3}(v_0 + b)^3 \sin^3\psi_1\,; \end{aligned}$$

$$\begin{aligned} I_3 &= \int_y^{v_0+b} y \log_e(\sec\psi_1 + \tan\psi_1)\,dy \\ &= (v_0 + b)^2 \int_0^{\psi_1} \cos\psi \sin\psi \log_e(\sec\psi + \tan\psi)\,d\psi \\ &= \tfrac{1}{2}(v_0 + b)^2\left[-\cos^2\psi_1 \log_e(\sec\psi_1 + \tan\psi_1) + \int_0^{\psi_1} \frac{\cos^2\psi}{\cos\psi}\,d\psi\right] \\ &= \tfrac{1}{2}(v_0 + b)^2\{\sin\psi_1 - \cos^2\psi_1 \log_e(\sec\psi_1 + \tan\psi_1)\}. \end{aligned}$$

Substituting these expressions in equation (9), together with the corresponding terms in ψ_2, leads to

$$1-F(y)=\frac{3(v_0+b)^2}{4b^3}\left\{b\sin\psi_1+(v_0-b)\psi_1\cos\psi_1-\frac{(v_0+b)}{3}\sin^3\psi_1\right.$$
$$\left.-v_0\cos^2\psi_1\log_e(\sec\psi_1+\tan\psi_1)\right\}$$
$$+\frac{3(v_0-b)^2}{4b^3}\left\{b\sin\psi_2-(v_0+b)\psi_2\cos\psi_2+\frac{(v_0-b)}{3}\sin^3\psi_2\right. \tag{10}$$
$$\left.+v_0\cos^2\psi_2\log_e(\sec\psi_2+\tan\psi_2)\right\}.$$

Since $(v_0+b)\cos\psi_1=(v_0-b)\cos\psi_2=y$, for $0\le y\le v_0-b$, this can be rewritten in different ways, e.g.,

$$1-F(y)=\frac{3y}{4b}\left[\frac{v_0}{b}(\tan\psi_1+\tan\psi_2)+(\tan\psi_1-\tan\psi_2)-\frac{y^2}{b^2}(\tan^3\psi_1-\tan^3\psi_2)\right.$$
$$\left.+(v_0^2-b^2)(\psi_1-\psi_2)+\frac{v_0y}{b^2}\log_e\left(\frac{\sec\psi_2+\tan\psi_2}{\sec\psi_1+\tan\psi_1}\right)\right]. \tag{11}$$

One can check this inelegant expression, (*a*) by reversing the order of integration and (*b*) by noting that $F(y)$ must be zero for $y=0$. For $y=0$,

$$\psi_1=\psi_2=\frac{\pi}{2},$$
$$y\tan\psi_1=(v_0+b)\sin\psi_1=(v_0+b),$$
$$y\tan\psi_2=(v_0-b)\sin\psi_2=(v_0-b),$$
$$y^2\log_e(\sec\psi_2+\tan\psi_2)\to 0 \quad \text{as} \quad y\to 0,$$

and

$$y^2\log_e(\sec\psi_1+\tan\psi_1)\to 0 \quad \text{as} \quad y\to 0.$$

Hence,

$$1-F(y)=\frac{3v_0}{4b^2}\{2v_0\}+\frac{3}{4b}\{2b\}-\frac{1}{4b^3}\{(v_0+b)^3-(v_0-b)^3\}$$
$$=\frac{3v_0^2}{2b^2}+\frac{3}{2}-\frac{3}{2}\frac{v_0^2}{b^2}-\frac{1}{2}$$
$$=1.$$

This checks that $F(y)$ is zero for $y=0$.

IV

Using the apparent rotational velocities given by Slettebak for the Be stars,[2] Chandrasekhar and Münch computed the mean and standard deviation of the distribution of true velocities as 348 and 50 km/sec, respectively. For the rectangular distribution of Section II, the mean is v_0 and the standard deviation is $a\sqrt{3}$; hence we can substitute $v_0=348$ km/sec and $a=50\sqrt{3}=87$ km/sec in equations (5) and (6) of Section II. It will be noted that $v_0=4a$; and, although this proportionality is purely fortuitous, one can take advantage of it to simplify the numerical work. If we write

$$z=\frac{y}{2a}=\frac{y}{174},$$

then

$$\cos\theta_1 = \begin{cases} \dfrac{y}{v_0 + a} = \dfrac{2}{3}z & \text{for} \quad 0 \le z \le 2.5 \\ 1 & \text{for} \quad z > 2.5\,, \end{cases}$$

$$\cos\theta_2 = \begin{cases} \dfrac{y}{v_0 - a} = \dfrac{2}{3}z & \text{for} \quad 0 \le z \le 1.5 \\ 1 & \text{for} \quad z > 1.5\,; \end{cases}$$

and we have

$$F(y) = 1 + z(\theta_1 - \theta_2) - \tfrac{5}{2}\sin\theta_1 + \tfrac{3}{2}\sin\theta_2\,. \tag{12}$$

Values of z were taken at intervals of 0.1 from $z = 0$ to $z = 2.5$, and $F(y)$ was computed for each value of z. A graph of $F(y)$ against y was drawn, and the value of $F(y)$ was read off for $y = 0, 50, 100, 150, \ldots, 450$ km/sec. These values are shown in Table 1. The first

TABLE 1

COMPARISON OF PREDICTED FREQUENCY DISTRIBUTION OF APPARENT ROTATIONAL VELOCITIES WITH OBSERVED DISTRIBUTION (FOR Be STARS)

Distribution Functions			Comparison: Observed vs Predicted Numbers			
	$F(y)$				Predicted Number	
y (Km/Sec)	Rectangular Form of $f(v)$	Parabolic Form of $f(v)$	Apparent Rotational Velocity y (Km/Sec)	Observed Number	Rectangular Case	Parabolic Case
0	0.000	0.000	0–50	1	0.6	0.6
50	0.012	0.012	50–100	1	1.6	1.7
100	0.045	0.047	100–150	3	3.0	2.9
150	0.106	0.106	150–200	4	4.6	4.5
200	0.199	0.198	200–250	8	7.2	7.5
250	0.346	0.351	250–300	9	11.5	11.2
300	0.581	0.580	300–350	13	10.4	10.8
350	0.793	0.800	350–400	6	7.5	7.4
400	0.947	0.952	$\geqslant 400$	4	2.6	2.4
450	1.000	0.998				
			Total	49	49	49
435	1.000					
464		1.000				

differences of this table of $F(y)$ give the expected proportion of stars having apparent rotational velocities between 0 and 50 km/sec, between 50 and 100 km/sec, and so on. (Because of the small number of observations available, the grouping had to be relatively coarse.) Multiplying by the number of stars in the group, in this case 49 stars, allows a direct comparison with the observed distribution (fifth and sixth cols. of Table 1).

For the parabolic distribution, the mean is again v_0 and the standard deviation is $b/\sqrt{5}$. Putting $b/\sqrt{5} = 50$ gives for the parameters,

$$v_0 = 348 \text{ km/sec} \qquad b = 112 \text{ km/sec}\,.$$

With these values of v_0 and b, the distribution function becomes

$$1-F(y) = 12.6515 \sin\psi_1 + 3.3300 \sin\psi_2 - 17.3205 \sin^3\psi_1 + 2.3390 \sin^3\psi_2 + 6.4908 \left(\frac{y}{112}\right)(\psi_1-\psi_2) - 5.3658 \left(\frac{y}{112}\right)^2 \log_{10}\left[\left(\frac{1+\sin\psi_1}{\cos\psi_1}\right)\left(\frac{\cos\psi_2}{1+\sin\psi_2}\right)\right], \tag{13}$$

where

$$\cos\psi_1 = \frac{y}{460} \qquad \text{for} \qquad 0 \le y \le 460,$$

$$\cos\psi_2 = \begin{cases} \dfrac{y}{236} & \text{for} \quad 0 \le y \le 236 \\ 1 & \text{for} \quad 236 \le y \le 460 \end{cases}$$

(y cannot exceed the maximum value of v, in this case 460 km/sec). As in the rectangular case, a graph of $F(y)$ against y was drawn, and the value of $F(y)$ was read off for $y = 0$, 50, 100, 150, . . . , 450. These values are shown in the third column of Table 1, and the seventh column gives the number of stars expected in each interval of y, for comparison with the observations.

V

Considering the application to the Be stars, certain aspects of the results require little explanation if the different forms of $f(v)$ are presented graphically, as in Figure 1. For the rectangular case, v can only have values between 261 and 435 km/sec, although between these values the distribution is uniform. The resulting distribution of the apparent rotational velocities, shown in Figure 2, extends from 0 to 435 km/sec with a long tail on the lower side and a sharper cutoff at the upper end. It will be seen that the agreement with the observed distribution in Table 1 is satisfactory.

For the parabolic case, v lies between 236 and 460 km/sec, with a maximum frequency at the mean value, 348 km/sec (Fig. 1). The form of $f(v)$ used by Chandrasekhar and Münch[1] is also shown in Figure 1. For the Be stars it is effectively a Gaussian distribution, with a mean of 348 km/sec and a standard deviation of 50 km/sec, since the second term in equation (1),

$$\frac{j}{\sqrt{\pi}}\, e^{-j^2(v+v_1)^2},$$

gives a negligible contribution to $f(v)$. The unit for the ordinate in Figure 1 is immaterial but the diagram has been drawn so that the area under each of the curves is the same. It will be seen that the parabolic case is intermediate between the rectangular form and the Gaussian form. As Chandrasekhar and Münch found that the frequency distribution of y derived from their form of $f(v)$ was in satisfactory agreement with the observed frequency distribution and as we have just seen that the rectangular form of $f(v)$ also leads to a distribution of y in agreement with the observations, it would be surprising if an intermediate form like the parabolic form *failed* to give agreement. Indeed, from this point of view, there was no need to consider the parabolic form. However, the fact that it *is* an intermediate form and that the corresponding $\phi(y)$ and $F(y)$ are known in terms of elementary functions may make it a suitable form to try in practical applications. The frequency distribution of apparent rotational velocities derived from the parabolic form is almost identical with that shown for the rectangular distribution in Figure 2. It was intended, at first, to show the two distributions together in Figure 2, but, in fact, they are so alike that it would be difficult to distinguish them clearly.

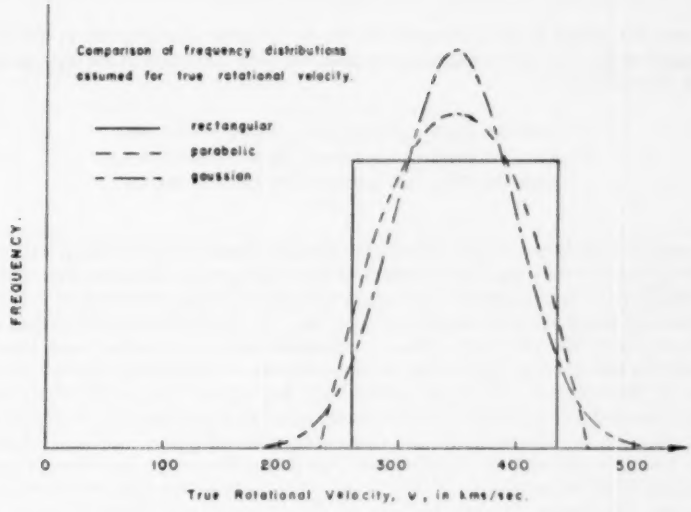

FIG. 1

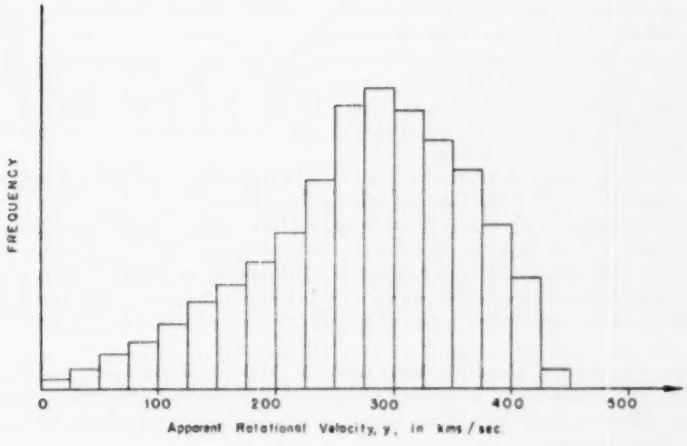

FIG. 2. Derived distribution of apparent rotational velocity when frequency distribution of true rotational velocities is assumed to be of rectangular form; the numerical case considered is that of the Be stars.

VI

In theory, one could apply the result for the rectangular distribution to obtain a numerical solution for $f(v)$. For example, suppose we take intervals of 50 km/sec and assume that $f(v)$ consists of

x_0 stars for which v is between 0 and 50 km/sec,
x_1 stars for which v is between 50 and 100 km/sec,
x_2 stars for which v is between 100 and 150 km/sec,
. . . . . .

and that within each interval the probability distribution is uniform. Then we could use equations (5) and (6) to give $F(y)$ for each of these subgroups, find out how much each would contribute to the number of stars observed within similar intervals of y, and so obtain a system of linear equations relating $x_0, x_1, x_2, \ldots$, to the observed number of stars for which $0 \leq y \leq 50$, $50 \leq y \leq 100, \ldots$. Numerically, the solution would be exact; there would be exactly the right number of equations to determine all the x's. But the exactness of the solution would be misleading, for, apart from other objections, we know that forms of $f(v)$ as different as the rectangular and the Gaussian distribution lead to agreement with the observations and there are presumably any number of intermediate forms which would also give agreement. Put in another way, the effect of the angle of inclination is to smooth out and blur any differences in the assumed forms of $f(v)$. For example, the frequency distributions of the apparent rotational velocity derived from the rectangular and parabolic forms of $f(v)$ are so alike for the Be stars that it would require something of the order of one thousand observations to have a reasonable chance of distinguishing between them.

There remains the possibility of stipulating the form of $f(v)$ from theoretical considerations, e.g., if the accretion of interstellar matter tends to increase the angular momentum of a star, subject to an upper limit at which the configuration becomes unstable, one might expect to have an asymmetrical distribution of v, with a sharp cutoff at the upper end of the frequency distribution. One check on such a form of $f(v)$ would be that the corresponding form of $\phi(y)$ give agreement with the observed distribution of y. However, although $f(v)$ would have to satisfy this test, it is evident from the results above that the test is not a sensitive one.

To conclude, by using the relations given by Chandrasekhar and Münch one can compute the moments of $f(v)$ from those of the observed distribution of y. Both sets of moments are determined with the same accuracy, which means in practice that only the lower moments will be reliably determined. Beyond being able to determine the moments, one cannot specify $f(v)$ too exactly, for the smoothing effect of having the axes of rotation randomly oriented with respect to the observer makes it hazardous to attempt to distinguish between different forms of the distribution of true rotational velocities.

I am grateful to Dr. Chandrasekhar and Dr. Münch, whose work stimulated this paper and with whom I had a number of helpful discussions during its preparation. I should also like to acknowledge their kindness in allowing me to consult their paper in advance of publication.

A COMET MODEL. I. THE ACCELERATION OF COMET ENCKE

FRED L. WHIPPLE
Harvard College Observatory
Received November 23, 1949

ABSTRACT

A new comet model is presented that resolves the chief problems of abnormal cometary motions and accounts for a number of other cometary phenomena. The nucleus is visualized as a conglomerate of ices, such as H_2O, NH_3, CH_4, CO_2 or CO, (C_2N_2?), and other possible materials volatile at room temperature, combined in a conglomerate with meteoric materials, all initially at extremely low temperatures ($< 50°$ K). Vaporization of the ices by externally applied solar radiation leaves an outer matrix of nonvolatile insulating meteoric material. Quantitative and qualitative study shows that heat transfer through thin meteoric layers in a vacuum is chiefly by radiation, that the heat transfer is inversely proportional to the effective number of layers, and that an appreciable time lag in heat transfer can occur for a rotating cometary nucleus. Because of the time lag, such a cometary nucleus rotating in the "forward" sense will emit its vaporized ices with a component toward the antapex of motion. The momentum transfer from the kinetic velocity of the emitted gas will propel the nucleus in the forward sense, reduce the mean motion, and increase the eccentricity of the orbit. Such orbital effects occur for Comet D'Arrest; the mean daily motion of Comet Wolf I also appears to be decreasing.

Retrograde rotation can produce an acceleration in mean motion and a decrease in eccentricity, as observed for Comet Encke. If the decelerating force component is taken as one-quarter its maximum theoretical value, the present observed acceleration in the mean motion of Comet Encke can be produced by a loss of 0.002 of its mass per revolution. The corresponding mass loss for Comet D'Arrest is 0.005. For both comets the observed changes in eccentricity are obtained if the force acts proportionately to the solar energy flux but is cut off at a solar distance of about 2 A.U.

A second paper (Part II) soon forthcoming will be concerned with the physical problems of comet structure, loss of meteoric and gaseous material, and correlations with observed meteoric phenomena.

A. INTRODUCTION

The recent and valuable contribution by A. J. J. van Woerkom[1] on the origin of comets has strengthened the growing confidence in the concept that comets are ancient members of the solar system. He has shown that the process of replenishment of the periodic comets from the extremely long-period comets via capture by Jupiter appears to be the most plausible, if not the only plausible, process for maintaining the supply of periodic comets. The remaining question as to the statistical stability of a solar family of comets with semimajor axes up to about 10,000 A.U. has been studied by E. Öpik.[2] The losses to such a system by the gravitational action of passing stars is not serious over a period of even 3×10^9 years. Only a close approach of a passing star to the sun would remove the sun from control of a large fraction of the comets. The loss by stellar attraction for individual comets with periods up to a million years is statistically unimportant over such a long interval of time; but comets with longer periods will suffer statistical increases in perihelion distance that will tend appreciably to place them beyond Jupiter's reach.

There still remains, however, a discrepancy of approximately 20 between van Woerkom's calculated number of Jupiter "captures" of long-period comets into short-period orbits (one per 650 years) and the estimated loss of three periodic comets per century. This discrepancy might be removed by assuming a greater number of comets with peri-

[1] *B.A.N.*, **10**, 445, 1948; see also H. N. Russell, *A.J.*, **33**, 49–61, 1921; and H. A. Newton, *Mem. Nat. Acad. Sci. Washington*, **6**, 1, 1893.

[2] *Proc. Amer. Acad. Arts and Sci.*, **67**, 169, 1932. In a recent and extremely important paper, J. H. Oort (*B.A.N.*, **11**, 91, 1950) has independently expanded the work of Öpik to demonstrate that an extended cloud of comets about the sun would be sufficiently stable, yet disturbed enough by passing stars to provide comets for Jupiter's capture after 3×10^9 years. The postulated cloud extends about 1 parsec about the sun.

helion in the neighborhood of Jupiter, by establishing more certainly the rate of disintegration of comets, or by accepting G. Fayet's[3] suggestion that, statistically, several short-period comets arise from each parent-comet.

In any case, the lifetime of a short-period comet must lie generally in the range of from 3000 (one hundred comets being lost at a rate of three per century) to possibly 60,000 years. Probably more important is the number of small perihelion passages that can be weathered by a comet—of the order of several hundreds, at least, for perihelion distances as small as 0.5–1.0 A.U. For considerably greater perihelion distances the number probably increases to several thousand, thus permitting comets with periods up to 10^6 years to persist throughout all or most of the past history of the solid earth.

Even though parts of the preceding discussion are somewhat conjectural, we must certainly accept the conclusion that individual short-period comets cannot exist indefinitely in their present orbits and also that they must previously have existed at great distances from the sun, where their temperature throughout remained at extremely low values. K. Wurm[4] has discussed certain effects of such low temperatures in cometary phenomena. N. T. Bobrovnikoff[5] and P. Swings[6] have pointed out that certain possible parent-compounds, such as CO_2, H_2O, and NH_3, may be responsible for the observed radicals, such as CO, OH, and NH, in cometary spectra; Swings has suggested that these materials would exist in the solid state within the nuclei of comets.

In the present discussion I propose to investigate the possibility that the molecules responsible for most of the light of comets near perihelion arise primarily from gases long frozen in the nuclei of comets. Furthermore, I propose that these primitive gases constitute an important, if not a predominant, fraction of the mass of a "new" or undisintegrated comet.

On the basis of these assumptions, a model comet nucleus then consists of a matrix of meteoric material with little structural strength, mixed together with the frozen gases—a true conglomerate. Since no meteorites are known certainly to arise from cometary debris, we know very little about the physical structure of the meteoric material except that the pieces seem generally to be small. Hence we assume that the larger pieces are perhaps a few centimeters in radius and the smallest are perhaps molecular. As a convenience in terminology, the term "ices" will be used in referring to substances with melting points below about 300° C and "meteoric material" to substances with higher melting points.

Our only chemical knowledge of the meteoric material comes from the spectra of meteors,[7] which tell us that *Fe*, *Ca*, *Mn*, *Mg*, *Cr*, *Si*, *Ni*, *Al*, and *Na*, at least, are present. Physically the meteoric material is strong enough to withstand some shock in the atmosphere, but more than 3 per cent of the Harvard photographic meteors are observed to break into two or more pieces. A much larger percentage show flares in brightness, an indirect evidence of breaking. The high altitude of the disappearance of the photographic Giacobinid meteors of October 9, 1946, as observed by P. M. Millman and analyzed by L. Jacchia and Z. Kopal,[8] suggests that those meteoric bodies may have been unusually fragile or porous. It is difficult to defend the hypothesis that, as a whole, the bodies producing photographic meteors possess great physical rigidity or strength.

A careful determination of the relative abundances of the primitive ices in the nucleus of a comet and their physical properties will require an exhaustive study of the theory of

[3] *Bull. astr.*, **28**, 168, 1911.

[4] *Mitt. Hamburger Sternw., Bergedorff*, Vol. **8**, No. 51, 1943.

[5] *Rev. Mod. Phys.*, **14**, 164–178, 1942.

[6] *Ann. d'ap.*, **11**, 124, 1948.

[7] See, e.g., P. M. Millman, *Harvard Ann.*, **82**, 113, 1932, and **82**, 149, 1935; F. G. Watson, *Between the Planets* (Philadelphia: Blakiston Co., 1941), p. 108.

[8] Private communication.

cometary spectra and related phenomena, including evolutionary hypotheses. Only a few comments will be made here. The observed gases CH, CH^+, CH_2, CO, NH, NH_2, OH, and OH^+ can be accounted for by four possible parent-molecules of great stability, viz., CH_4, CO_2, NH_3, and H_2O. Photodissociation appears capable of producing the various radicals from these parent-molecules, although Wurm prefers CO instead of CO_2. Only the very important observed C_2, N_2^+, and CN molecules are unaccounted for above. The choice of C_2N_2 as a parent-molecule does not seem desirable because the dissociation of C_2N_2 is exothermic; nevertheless, I shall include it in the present discussion for lack of a better substitute (C_2H_2, N_2, HCN?). Quite possibly some of the radicals can exist permanently at very low temperatures.

The metals *Na*, *Fe*, *Ni*, and *Cr*—all observed in meteor spectra—have been observed in comet spectra at small solar distances. They require the presence of metals or, more generally, meteoric materials in molecular or atomic forms within the comet nucleus.

Some physical data for five of the possible parent-gases are given in Table 1.

TABLE 1*

PROPERTIES OF CERTAIN MOLECULES

	Molecule				
	CH_4	CO_2	NH_3	C_2N_2	H_2O
Melting point (° K)	90	217	198	239	273
Heat of fusion (cal/gm)	50	45	108	. . . . .	80
Boiling point at 1 atm. (° K)	111	195	240	252	373
Heat of vaporization from solid (cal/gm)	188+	138+	435+	103++	670+
Vapor pressure at 191° K (atm.)	45.8	0.74	0.038	8.0×10^{-3}	3.7×10^{-9}

* Sources: *International Critical Tables of Numerical Data* (New York: McGraw-Hill Book Co., 1933) and the *Handbook of Chemistry and Physics* (Cleveland: Chemical Rubber Pub. Co., 1949).

As our model comet nucleus approaches perihelion, the solar radiation will vaporize the ices near the surface. Meteoric material below some limiting size will blow away (Part II, forthcoming) because of the low gravitational attraction of the nucleus and will begin the formation of a meteor stream. Some of the larger or denser particles may be removed by shocks (see below), but the largest particles or matrix will remain on the surface, to produce an insulating layer. After a short time (probably in the geologic past for all known comets) the loss of gas will be reduced materially by the insulation so provided.

A comet such as Encke's, if made of a nonvolatile solid, would come eventually to a temperature of approximately 140° K at aphelion.[9] Thus CH_4 would melt and vaporize quickly, while the other ices of Table 1 would vaporize more slowly. At perihelion temperatures, all the substances in Table 1 would be gaseous, even under high pressures. The quasi-equilibrium state arising from a slow external heating of the extremely cold ices can be visualized qualitatively as follows: at the base of the meteoric layer, only the ice with the lowest vapor pressure will still remain; hence this layer will consist only of "rotten" ice (H_2O) and meteoric material; the next layer will contain, in addition, C_2N_2 (if present), etc.

It is important to note that practically all heat reaching the ice (H_2O) at temperatures above about 180° K will be used in vaporization. The H_2O vapor that does not escape the comet will condense on the cooler layers beneath, producing evaporation of these materials.

[9] M. G. J. Minnaert, *Kon. Ned. Akad. Wet. Amsterdam*, **50**, 826, 1947.

The outer icy layers will arrive at a quasi-equilibrium state in the order of the vapor pressures of the ices at low temperatures. The thicknesses of the various layers will depend upon the temperature gradient, which, in turn, will depend upon the effective heat conductivities of the layers and the temperature of the outer layer. It will be shown below that the effective conductivities of such a conglomerate must be very low. The deep interior of the cometary nucleus will remain extremely cold, not only because of the low heat conductivity but also because the available heat will be used in vaporization, an extremely effective cooling mechanism in a vacuum. Hence the comparative rates of escape of the various primitive gases from the nucleus will depend primarily not upon their physical-chemical properties but upon their abundances. Some second-order effects may occur because of the variation of temperature gradient in the upper layers with the external heating; but such effects should not be manifest, for example, in correlations of cometary emission spectra with age except in the most extreme stages of disintegration.

The weakening of the upper layers of the icy core by selective vaporization of the ices may be expected to produce cometary activity of considerable intensity, especially near the sun. The surface gravities of cometary nuclei are certainly extremely low; hence surprisingly weak structures can persist over rather large areas of the nucleus. At irregular intervals collapses must occur. The heated meteoric material will then fall into the ices and produce rapid vaporization. The dust and smaller particles held in the upper layers will be shaken out and blown away, so that insulation produced by this material will be much reduced. Solar heat, consequently, will be much more effective in vaporizing the ices in the pit until equilibrium is again established. Such "cave-ins" might spread over appreciable areas. Other effects might occur if "pockets" of an ice with low melting points exist within an ice of higher melting point. Phenomena of mildly explosive, jet, or cracking types may occur, forcing out pieces of material much larger than those carried normally by the outgoing gas. Hence the type of nuclear activity that is observed for large comets with small perihelion distances would be expected from this type of comet model.

If the primitive ices constitute a large percentage of the total mass, the comet truly disintegrates with time. Its actual substance vaporizes; the surface gravity decreases; and, finally, all activity ceases as the last of its ice reservoir is exhausted. The observed sequence of phenomena in dying comets is entirely consistent with this picture. In the later stages, only a very small nucleus of the largest meteoric fragments remains (note the asteroid Hidalgo as a possible example).

The period of rotation of a comet with a single spheroidal nucleus would generally remain constant with age, so that the comet might dissipate slowly and uniformly. If, however, the nucleus were multiple or irregular in shape, the vaporization of ices could materially affect the rotation. Suppose, for example, a part of the surface were nearly in a plane passing through the center of gravity of the nucleus, while the remaining surface were generally smooth and approximately oval in shape. Meteoric material would fall from the vertical surface, exposing it to the full action of sunlight. Hence the excess of gas evolved from this surface would exert a force moment on the nucleus as a whole.

The effect of the resulting rotation, depending upon the initial circumstances, might easily produce rotational instability, permitting the sun's tidal action to complete the splitting of the nucleus. If the larger parts of the separated nucleus were unstable, the comet might disappear quickly. On the other hand, the pieces might be large enough to persist for a long period of time as individual comets. In fact, the phenomenon of splitting has occurred for several comets and has been followed by disappearance in some cases, but not in others. Either possibility may be expected on the basis of the present comet model, depending upon the mass, shape, and rotation of the nucleus.

It is clear that the answers to certain of the problems concerning the proposed comet model can best be determined in the laboratory rather than by theory. A pertinent experiment would involve the making of conglomerates of the various ices and meteoric

materials, submitting them to small pressures and then observing the vaporization when the conglomerates were exposed to radiation from one surface, the other surfaces remaining insulated or refrigerated. An exhaust pump could simulate the conditions of low gas pressure in space, while even the action on meteoric material might be studied by utilizing fine powders to compensate the model for the large terrestrial gravity.

Even without such experiments, however, the suggested model of a comet nucleus is subject to a number of tests, both by theory and by observation. Certain phases of the problem will be discussed in the following sections, and the conclusions will be applied to demonstrate possible mechanisms for the observed acceleration of the mean motion of Comet Encke (and similar phenomena for other comets) and to explain in more detail the ejection of meteoric material from comet nuclei.

B. THE PROBLEM OF HEAT TRANSFER

It is obvious that the total solar radiation falling upon our model comet nucleus would be sufficient, in a relatively short time, to melt and vaporize quite sizable masses. In 1 year at 1 A.U. from the sun, a layer of ice some 4 meters thick would be vaporized from the surface of a spherical body, if all the solar radiation were absorbed. A much thicker layer of the other ices in Table 1 would be lost. Hence a cometary nucleus, 1 km in diameter and made of such ices, would scarcely persist for a hundred perihelion passages within 1 A.U. Also Minnaert[10] has shown that the temperature rise within the solid nucleus of a periodic comet is relatively rapid if the material conducts heat like ordinary stone. The surface layers of meteoric material, however, will greatly reduce the rate of heat transfer as compared to that of a solid body, and vaporization will maintain a low internal temperature. Let us consider, therefore, the likely processes of heat transfer.

If the meteoric layer is a coarse aggregate, very poorly cemented, direct conduction of heat by solids will be very slow because of the small areas of contact between discrete particles on the surface of the nucleus. The coefficient of heat conduction for the compact solid may be reduced by the order of ten thousand times, making this form of heat transfer negligible except within the particles themselves.

Heinrich Hertz[11] demonstrated that, for a steel sphere pressed by its own weight under the earth's gravity against a rigid horizontal steel plane, the radius of the circle of pressure contact, β, is related to the radius of the sphere, s, approximately as follows: $\beta/s = 10^{-3} \times s^{1/3}$ (mm). Since the surface gravity of a cometary nucleus is several orders of magnitude less than that of the earth, since the meteoric layer will be relatively thin, and since irregular particles should have much the same area of contact as spheres and the same order of elasticity as steel, it can be seen easily that the areas of contact for the transmission of heat among the particles may be less than 10^{-4} the cross-section of the solid material.

Further confirmation of this argument is provided by laboratory measures of heat conductivity through powders at various air pressures. The work of M. Smoluchowski[12] on powders with grain sizes between 0.0003 and 0.03 cm, and of W. G. Kannuluik and L. H. Martin[13] on similar powders has been reviewed by A. F. Wesselink.[14] The conductivities in pressures as low as 0.05 mm of *Hg* are in the neighborhood of 3×10^{-6} cal cm^{-1} $sec^{-1}(^{\circ}C)^{-1}$, as compared to typical conductivities of 0.14 for iron and 0.005 for sandstone. Wesselink, whose problem of radiation from the lunar surface closely parallels the heat-conduction problems of this discussion, concludes that heat transfer by

[10] *Ibid.*

[11] "Contact of Elastic Solids," from *Misc. Papers*, trans. D. E. Jones and G. H. Schott (1896), p. 159.

[12] *Bull. Acad. Sci. Cracovie, A*, 1910, p. 129, and *A*, 1911, p. 548.

[13] *Proc. R. Soc. London, A*, **141**, 144, 1933.

[14] *B.A.N.*, **10**, 351, 1948.

radiation becomes important *in vacuo* for particles of the order of 0.05 cm and larger, at temperatures in the neighborhood of 300° K.

Conduction of heat by gases must be small for our cometary nucleus. Where the mean free path of molecules is greater than the dimensions of the interstices between the meteoric particles, the conduction will increase with the density of the gas, but the heat conducted will be negligible. Interplanetary space in the neighborhood of the earth's orbit contains less than 10^3 electrons per cubic centimeter[15] and therefore probably a comparable number of atoms, since all are presumably ionized. Mean free paths are large compared even to the cometary nucleus. The only gas capable of carrying appreciable heat would be that vaporized within the nucleus, again at a relatively low density. Hence, for the moment, we can neglect gas conduction of heat as also negligible; but the subject must be reinvestigated when accurate information is available as to the quantity of gas involved.

The scattering of sunlight among the meteoric particles will fall off exponentially with depth, and, for particles of low probable albedo, cannot contribute greatly to heat transfer.

We are left, therefore, with the radiative transfer of heat from layer to layer via the normal low-temperature radiation and absorption by the meteoric particles, as the most likely mechanism for the transfer of solar energy from the surface of the nucleus to the icy core.

To gain an idea as to the properties of such radiation transfer in a vacuum, let us visualize a situation that will represent crudely the equilibrium conditions.[16] Suppose we substitute for the meteoric layers ideal flat layers of gray-body material with zero thickness, complete opacity, zero heat capacity, a low-temperature albedo of A_1, and a solar-radiation albedo of A_0. Suppose also that these layers, $1, 2, \ldots, i, \ldots, n$, are infinite parallel planes, separated by unspecified but finite distances. Let the normal energy flux per unit area absorbed by both sides of the surfaces be represented by F_i and the corresponding radiation from each of the two sides be represented by E_i.

For boundary conditions we postulate that layer 1 absorbs the normal flux of solar radiation $(1 - A_0)F_0$ and that layer n, on the side away from the incoming radiation, is connected to a heat sink at constant temperature T_n, which absorbs excess energy at a rate Q per unit area and time, where

$$F_n - E_n = Q \,. \tag{1}$$

For all the other layers,

$$F_i = 2E_i \qquad (i \neq n) \,. \tag{2}$$

Layer 1 absorbs the flux $(1 - A_0)F_0$ from the sun, $E_2(1 - A_1)(1 + A_1^2 + A_1^4 + \ldots)$ after reflections from layer 2, and $E_1(1 - A_1)(A_1 + A_1^3 + A_1^5 + \ldots)$ by reflection of its own radiation from layer 2.

If we let A be the corrected albedo after multiple reflections, given by

$$1 - A = (1 - A_1)(1 + A_1^2 + A_1^4 + \ldots) \,, \tag{3}$$

then

$$A = (1 - A_1)(A_1 + A_1^3 + A_1^5 + \ldots) \,. \tag{4}$$

[15] F. L. Whipple and J. Gossner, *Ap. J.*, **109**, 380, 1949.

[16] This simplified solution, derived independently by the author, embodies the basic viewpoint given by Wesselink (*loc. cit.*).

Hence, from equations (2), (3), and (4) we derive the equilibrium equations for the layers 1, i, and n, noting that the ith layer receives its reflected radiation from two sides:

$$2E_1 = (1 - A_0) F_0 + AE_1 + (1 - A) E_2 , \tag{5}$$

$$2E_i = (1 - A) E_{i-1} + 2AE_i + (1 - A) E_{i+1} \qquad (i \neq 1, n) , \tag{6}$$

and

$$F_n = (1 - A) E_n - 1 + AE_n . \tag{7}$$

Since no heat is taken up by the system except at the nth layer, the quantity Q is given by

$$Q = (1 - A_0) F_0 - E_1 , \tag{8}$$

leading to the following relation, from equation (1):

$$F_n = Q + E_n = (1 - A_0) F_0 - E_1 + E_n . \tag{9}$$

From equations (2), (5), (6), (7), and (9) we can now write the n equations of equilibrium in the form:

$$\frac{2 - A}{1 - A} E_1 - E_2 = \frac{1 - A_0}{1 - A} F_0 , \tag{10_1}$$

$$E_1 - 2E_2 + E_3 = 0 , \tag{10_2}$$

. . . . . .

$$E_{i-1} - 2E_i + E_{i+1} = 0 , \tag{10_i}$$

. . . . . .

$$E_{n-2} - 2E_{n-1} + E_n = 0 , \tag{10_{n-1}}$$

$$\frac{1}{(1 - A)} E_1 + E_{n-1} - E_n = \frac{1 - A_0}{1 - A} F_0 . \tag{10_n}$$

Since we have established boundary conditions by F_0 and E_n, there are only $n - 1$ unknowns in these n equations. Hence the determinant must be zero; the sum of the last $n - 1$ equations of (10), is, indeed, identical with the first.

We can solve for E_1 from the sum of the $n - 1$ equations $(10_1) + (10_2) + \ldots (i - 2)(10_i) + \ldots (n - 2)(10_n)$, with the following results:

$$E_1 = \frac{n - 1}{n - A} (1 - A_0) F_0 + \frac{1 - A}{n - A} E_n ; \tag{11}$$

and, by equation (8),

$$Q = \frac{1 - A}{n - A} [(1 - A_0) F_0 - E_n] . \tag{12}$$

By substitution in the successive equations (10), we find

$$E_i = \frac{n - i}{n - A} (1 - A_0) F_0 + \frac{i - A}{n - A} E_n . \tag{13}$$

We see that Q, the flux transferred to the heat sink, approaches zero for large values of n, even though no heat is retained by the intermediate layers. It can be shown easily that this result holds even in the limiting case when $A = A_1 = 0$, a situation where the albedo is zero and the layers absorb all the radiation incident upon them.

For large values of n, we can differentiate equation (13) for the gradient of E_i with layer number i, obtaining,

$$\frac{dEi}{di} = \frac{-1}{n-A}\left[(1-A_0)F_0 - E_n\right]. \tag{13a}$$

Hence the gradient in emission is uniform with layer number. This shows that the emission falls uniformly from layer 1 (if $[1-A_0]F_0 > E_n$) to the heat sink and that the emission gradient is inversely proportional to the number of layers. The total heat transfer is thus proportional to the emission gradient. It can be shown that the temperature gradient is not linear with layer number.

The maximum value of the surface temperature of the nucleus of the comet is of considerable interest. Its value, obtained from equation (11) and Stefan's law, is given by

$$T_1^4 = \frac{(n-1)(1-A_0)}{(n-A)(1-A_1)}\frac{F_0}{\sigma} + \frac{1-A}{n-A}T_n^4. \tag{14}$$

We can derive a maximum value of T_1 by setting $n = \infty$ in equation (14). The result is

$$T_1\,(\text{max.}) = \left(\frac{1-A_0}{1-A_1}\frac{F_0}{\sigma}\right)^{1/4}. \tag{15}$$

If A_0 and A are small, approximately 0.1, and if we equate them, we can derive the well-known relation for the maximum temperature[17] of the comet model:

$$T_1\,(\text{max.}) = 390^\circ\, r^{-1/2}\,(\cos\theta)^{1/4}, \tag{16}$$

where r is the solar distance in astronomical units and θ is the zenith distance of the sun from a point on the sunlit side of the comet.

Equation (16), which agrees well with the measurements by E. Pettit[18] of the temperature (370° K) of the lunar surface at the subsolar point, leads to relatively high values of the temperature. The melting point of water (normal pressure), for example, is reached at the great solar distance, $r = 2$.

One notes that, in this idealized problem of heat transfer by radiation, the equilibrium condition is attained instantly. In the actual comet model, the heat capacity of the layers will introduce a time lag. Hence a solution for the accurate temperature distribution in the insulating layers with variable insolation becomes more complex.

Let us now investigate roughly the radiative conductivity between finite layers of matter. A differentiation of Stefan's radiation equation, connecting rate of energy transfer, E, and temperature, T, for a gray body gives

$$dE = 4\sigma(1-A_1)T^3dT. \tag{17}$$

For layers, each of thickness l, the effective conductivity, K_l, in calories per centimeter per second per 1° C is, for infinite conductivity of the material,

$$K_l = 4\sigma(1-A_1)T^3l, \tag{18}$$

where

$$\sigma = 1.36\times10^{-12}\ \text{cal cm}^{-2}\ \text{sec}^{-1}\ (^\circ\text{C})^{-4}.$$

At temperatures of 200°, 273°, and 500° K, the conductivity (if $1-A_1 = 0.9$) becomes $K_1 = 0.00004\,l$, $0.00010\,l$, and $0.00061\,l$, respectively. For comparison, the conductivity of ground cork in air at room temperature is 0.00012. Hence the radiative con-

[17] See, e.g., Minnaert, *loc. cit.*

[18] *Ap. J.*, 91, 408, 1940.

ductivity of layers of thickness 1 cm is like that of ground cork, a good heat insulator. Since the conductivity of the solid meteoric material is presumably much larger, it will not affect appreciably the radiative conductivity of the layers, so long as their individual thickness does not exceed a few centimeters.

Equation (18), for $l = 0.026$ cm and $T = 418°$ K, yields a conductivity of $K = 9 \times 10^{-6}$ cal cm^{-1} sec^{-1} (° C)$^{-1}$. The value is in rough agreement with Smoluchowski's measures, mentioned above, for the coarsest powders at $T = 45°$ C. It appears that the conductivity (or areas of contact) for very fine powders is greater than would be suggested by Hertz's theory.

With the value of K_l given by equation (18) we can now compute the thickness, L, of the material required to transmit a fraction, χ, of the incident solar radiation to the bottom of the layers, if the total temperature differential is ΔT. The incident energy flux is $F_0(1 - A_0)/r^2$, so that,

$$\chi F_0 (1 - A_0) = \frac{K_l \Delta T}{L}. \tag{19}$$

For $r = 1$ A.U. and $T_s = 200°$ (a generous value), we find

$$L = \frac{K_l}{\chi} \times 7 \times 10^3. \tag{20}$$

Hence, for the temperature range from 200° to 500° K, L/l varies from $0.3/\chi$ to $4/\chi$. If we accept a 1 per cent efficiency ($\chi = 0.01$) in solar heat transfer, the number of layers varies between 30 and 400. This result checks the general order of magnitude of equation (12), which would give $n = L/l$, or about $1/\chi$.

C. TIME LAGS IN HEAT TRANSFER

The question of time lags in heat transfer through the meteoric layers of a rotating cometary nucleus is of great importance in the discussion of the acceleration of Comet Encke. Since the classical theories of periodic heat flow are not applicable to the general case of a rotating cometary nucleus if heat transfer is primarily by radiation, this problem must be investigated by methods of numerical integration. Such an investigation is under way and will be presented in a later paper. Nevertheless, some fragmentary information can be obtained from classical heat theory if constant values of the conductivity and diffusivity are assumed.

The diffusivity, h^2, in units of square centimeters per second, is given by

$$h^2 = \frac{K_l}{C_l \rho_l}, \tag{21}$$

where C_l and ρ_l are, respectively, the effective specific heat and the density of the meteoric layers, including interstices. We may adopt $\rho_l = 2$ gm/cm^3 for an aggregate of stony-iron particles and a corresponding specific heat, $C_l = 0.15$ cal/gm.

It is apparent from equations (17) and (18) that the rate of transport of heat from the heated surface to the interior of a cold body will increase much more rapidly with temperature for a given temperature gradient if the transport is by radiation rather than by conduction through a solid. Hence, if we adopt a conductivity corresponding to the radiative value at the surface temperature, we shall overestimate the inward heat flux at the maximum of the cycle and underestimate the time lags within the cometary nucleus.

With these limitations in mind, let us adopt the value of K_l from equation (18) and the maximum surface temperature from equation (16) to derive the following expression for h^2:

$$h^2 = 9.67 \times 10^{-4} l \left(r_{\text{A.U.}}\right)^{-3/2}. \tag{22}$$

For meteoric layers of thickness $l = 1$ cm and a solar distance $r = 1$ A.U., the value of h^2 is 0.001 cm^2 sec^{-1}. As a comparison, an accepted typical value of the diffusivity of average soil is 0.005. It appears that we have adopted a rather large value for h^2 in view of the fact that the conglomerate meteoric material may itself conduct heat very poorly. The consequence of this large value of h^2 will be to reduce further the calculated amount of the lag in heat transfer to the icy core.

The classical theory for heat transfer through a "semi-infinite solid" with a periodic temperature variation at one surface and a heat sink of constant temperature at the other surface is complicated, involving a Fourier expansion.[19] Considering the general roughness of the present solution, we can better apply the "cold-wave" approximation as used by L. R. Ingersoll and O. J. Zobel.[20] Here the solution for the heat transfer in an infinite solid with a simple periodic temperature variation at a plane surface is applied to a solid not completely in equilibrium under the variation. The application appears rather satisfactory in the case of measured and calculated temperatures at moderate depths in the earth at the end of meteorological "cold waves" of a few days' duration.

For a periodic variation in surface temperature, of the form $T\,(\text{surface}) = \sin(2\pi/P)t$, where P is the period, the lag in temperature maximum[21] at a depth x from that at the surface is $x/2h\sqrt{P/\pi}$. The instant of maximum inflow of heat at any depth precedes the maximum temperature by one-eighth of a period.[22] Hence the lag in maximum heat flux at a depth $x = nl$ is given by the equation

$$\frac{\text{Flux lag}}{\text{Period}} = \frac{nl}{2h\sqrt{\pi P}} - \frac{1}{8}. \tag{23}$$

After the substitution of h from equation (22), the lag becomes

$$\frac{\text{Flux lag}}{\text{Period}} = 9.1n\,(r_{\text{A.U.}})^{3/4}\sqrt{\frac{l}{P}} - \frac{1}{8}, \tag{24}$$

where n is dimensionless, l is expressed in centimeters, and P in seconds.

The quantity n represents the depth, measured in layers of meteoric material, and, from equation (12), its inverse represents roughly the proportion of the heat flux at the surface transmitted to the nth layer. Hence equation (24) shows that the lag in the time of flux maximum from the time of maximum surface temperature attains the greatest fraction of the comet's period of rotation when (*a*) the number of meteoric layers is large, corresponding to a slow rate of evaporation of the ices; (*b*) the meteoric material is coarse; (*c*) the solar distance is great; and (*d*) the period of rotation is short.

Even though the constants and exponents in equation (24) will be changed by a more rigorous analysis, the writer believes that the qualitative conclusions in the preceding paragraph will still be valid for heat transfer by radiation. The lag measured from the instant of noon will be greater than the lag given by equation (24) because of a lag in the attainment of maximum surface temperature; but this effect probably will be considerably smaller than the one-eighth period correction.[23] For extremely small values of n the total lag in maximum rate of vaporization after the instant of noon will become negligible.

[19] See, e.g., H. S. Carslaw, *Mathematical Theory of the Conduction of Heat in Solids* (New York: Macmillan Co., 1921), p. 68.

[20] *An Introduction to the Mathematical Theory of Heat Conduction* (Boston: Ginn & Co., 1913), p. 40.

[21] See Ingersoll and Zobel, *loc. cit.*

[22] See, e.g., Wesselink, *loc. cit.*

[23] The corresponding lag in temperature for the moon during and after eclipse was only a few minutes (see Pettit, *loc. cit.*). The particle sizes, as shown by Wesselink, are less than 0.03 cm, however.

Numerical application in equation (24) shows that the lag in maximum rate of heat transfer after maximum surface temperature is zero for a cometary nucleus rotating in a period 6 days, at a depth of ten layers, for meteoric particles 1 cm thick at a solar distance of 1 A.U. Since the surface temperature is taken as 390° K and the temperature of the top of the ice layer must be in the neighborhood of 200° K, it is apparent that our adopted coefficient of conductivity is much too high and that an appreciable lag should occur under these circumstances if more accurate calculations were made. The actual conductivity near the ice layer would be appreciably less than is assumed in the derivation of equation (24). It should be noted also that equation (24) applies to the equatorial zone of a cometary nucleus of zero obliquity to the ecliptic. Other latitudes will be subject to more lag. If the obliquity were appreciable, further corrections would be needed.

Nevertheless, we now have some basis for estimating the general order of magnitude of time-lag effects to be expected in the vaporization of ices in the rotating model cometary nucleus.

D. THE LUMINOSITY LAW

With regard to the theory that all cometary gases result from desorption, a view brilliantly supported by Levin,[24] one effect might possibly provide a critical test between the hypothesis that the gases are replenished at great solar distances and the hypothesis that gases are stored in the nucleus. Carbon atoms captured from interplanetary space would have been subjected to the direct effects of cosmic radiation, hence should show an appreciable quantity of the isotope C_{14}. On the other hand, C_{14} atoms, if protected sufficiently well for long periods of time (much greater than 5700 years) by the outer layers of the cometary nucleus would disintegrate and not appear in cometary spectra. The isotope ratio C_{14}/C_{12} is normally so small, however, that measures of C_{14} from the spectra of comets would require impossibly long exposures at the high dispersion necessary.

The process of adsorption must, nevertheless, play a role in the processes of the proposed comet model. The side of the comet turning away from the sun will cool rapidly to extremely low temperatures. The gases vaporized by the in-moving heat wave will therefore tend both to be absorbed and even possibly to condense on the cold surfaces of the outer meteoric particles. Note that all comets must rotate to some extent with respect to the direction of the sun, if for no other reason than because of libration.

A quantity of extreme importance in Levin's theory is the exponent of r in the equation for the total luminosity of a comet. N. T. Bobrovnikoff,[25] from an extremely careful study of the luminosities of forty-five comets, derived a value of 3.32 ± 0.16 for the exponent, differing appreciably from the value 2, appropriate to a purely reflecting body of fixed dimension. He finds no indication of a phase-angle effect—evidence that direct reflection from solid particles may not play an important role in cometary luminescence.

The observed fluctuations in the exponent are enormous from comet to comet and even for a given comet during a single approach to the sun. Bobrovnikoff finds a maximum value of 11.4, not well determined, and a minimum value of -11 (for Comet Westfal, which disappeared as it approached perihelion). For comets with the exponent less than the mean, the median value is 2.4, and for those with the exponent greater than the mean, the median is 4.4.

If the light from our comet model is to arise essentially from re-emission by gases generated proportionally to insolation and if the lifetimes of the radiating gases are both short and independent of solar distance, then the predicted exponent would be 4.0. Various factors, however, complicate enormously this simple prediction. The contribution to the comet's luminosity from light directly reflected by the nucleus should vary as $1/r^2$, reducing the exponent somewhat, but not greatly, for comets with strong molecular spectra. The reduction of the gaseous output below proportionality with insola-

[24] *Russian A.J.*, **21**, 48, 1943.

[25] *Contr. Perkins Obs.*, Nos. 15 and 16, 1941–1942.

tion at great solar distances should increase the exponent, particularly in the zone between 1 and 2 A.U. Quite large values should be expected in this transition region between reflection and gaseous re-radiation.

Another very important factor in the luminosity exponent arises from the finite lifetimes of the radicals, particularly C_2 and CN conspicuous near the nucleus. Wurm[26] has calculated that these molecules have short lifetimes, proportional to r^2. Hence their contribution to the luminosity law should vary as $1/r^2$ if their production is assumed to be proportional to the insolation.

The problem of the exponent of r to be expected from a gas with a long lifetime and from the dust escaping the nucleus becomes rather difficult. The exponent depends upon the rate of escape of the gases and dust from the region of the nucleus and upon the precise method of measurement of the comet luminosity, as well as upon the value of the lifetime of the gas. Since all these factors may vary while the comet is under observation, the problem is nearly insoluble at the present phase of cometary theory.

If the lifetime of the gas is short compared with the period of observation of the comet, but long compared to the time of escape from the head, and if the period of escape depends upon a solar repulsive force proportional to r^{-2}, then time of escape should be proportional to r. The luminosity law would then vary as $1/r^3$. A somewhat similar argument applies to light reflected from escaping fine dust.

The law to be predicted from the present comet model depends upon these various factors properly weighted. Any estimate would have to be made for the particular circumstances of an individual comet. An average value of about 3 for the exponent appears reasonable, allowing some correction for the transition from reflection to gaseous re-emission. The exponent should be much larger in the transition region. The fact that the exponent should be in the general neighborhood of Bobrovnikoff's measured value may be taken as slightly encouraging to the present model.

Particularly is this true in view of the large variations in the exponent that are both observed and expected from this type of model. Vsessviatsky's[27] result of a mean exponent of 4.12 ± 0.24, obtained from observations of forty-six comets, is in poorer agreement with the model. There are reasons, however, to rely more on Bobrovnikoff's results because he applied carefully determined systematic corrections to the observations to reduce them to a uniform system of telescope aperture and observing conditions.

Twelve of the forty-five comets studied by Bobrovnikoff pass perihelion in the solar distance range from 1.0 to 1.5 A.U. The mean value (weighted as recommended by Bobrovnikoff) of the luminosity exponent for these twelve comets is 4.5, conspicuously greater than for comets of greater or smaller perihelion distances. The exponent is below 3.32 for only three of the twelve comets. We may conclude that the transition region must occur at a solar distance just below 1.5 A.U.; observations of cometary spectra are in rough agreement with this conclusion.

E. THE ACCELERATIONS OF COMET ENCKE AND OTHER COMETS

The systematic increase in mean motion and the decrease in the eccentricity of Encke's Comet, conspicuous during the first half of the nineteenth century and smaller but definite since then, has long been a subject of speculation. Theories of a resisting medium stumble upon the lack of other evidence for the medium, upon the variation in the rate of acceleration with time, and upon the lack of uniformity or nonoccurrence of such effects for other comets. We will first discuss some of the observations, both for Comet Encke and for other comets.

F. Tisserand[28] quotes V. Asten as having obtained for Encke's Comet a value of

[26] *Loc. cit.*

[27] *Russian A.J.*, 2, Part 3, 68, 1925.

[28] *Traité de mécanique céleste* (Paris: Gauthier-Villars, 1896), IV, 226.

$+0''.1044$ for $\Delta\mu$, the change per revolution in the mean daily motion. The corresponding change in the eccentricity was $\Delta\phi = -3''.68$. These values applied for the interval from 1819 to 1865, but the secular changes appeared to be inappreciable from 1865 to 1871. For the period 1871–1894, Backlund[29] used $\Delta\mu = +0''.0677$ and $\Delta\phi = -2''.39$. In the interval 1894–1904 he found that the values $\Delta\mu = +0''.0486$ and $\Delta\phi = -1''.69$ led to a good representation of the observations for five oppositions, but for the opposition of 1908 the values $\Delta\mu = +0''.0126$ and $\Delta\phi = -0''.42$ gave best results. For the interval from 1918 to 1934 Matkiewicz[30] found that the changes were quite dependent upon the details of analysis. He reports that Backlund had been able to fit the observations from 1901 to 1914 with $\Delta\mu = +0''.0375$. Matkiewicz gives, as one set of solutions for $\Delta\mu$, the values $+0''.046$ for 1918–1924, $+0''.020$ for 1921–1928, and $+0''.097$ for 1924–1931. For the period 1924–1934 he obtained $\Delta\mu = +0''.044$. At times he adopts the relation $\Delta\phi = -30\Delta\mu$, in rough agreement with Asten's results and Backlund's published values, but his least-squares solutions for the elements suggest that the value is numerically too high in the interval 1918–1931.

From these results we cannot escape the following conclusions: first, that the mean motion of Encke's Comet is generally accelerated with time and, second, that the acceleration is variable and does not certainly become negative at any time. The eccentricity appears to suffer a concomitant diminution, less well determined but generally giving $\Delta\phi = -30\Delta\mu$, or smaller, numerically. Averaged over longer intervals of time, the mean value of $\Delta\mu/\mu$ per revolution is about $+9.7 \times 10^{-5}$ for 1819–1865 and about $+4.2 \times 10^{-5}$ for both the intervals 1865–1901 and 1901–1934. The corresponding values of Δe are -9.4×10^{-6} and -4×10^{-6}, respectively. For comparison purposes an acceleration of 9.7×10^{-5} corresponds to 2.7 hours per period, an effect that is relatively large and cumulative over successive periods.

Tisserand found that Asten's measured relation between $\Delta\mu$ and $\Delta\phi$ is consistent with an acceleration of the comet produced by a resisting medium in which the resistance varies as some direct power of the velocity and an inverse power of the solar distance. He found that the ratio is not very sensitive to the actual powers, over the range from 1 to 5 in velocity and 2 to 4 in solar distance.

Bobrovnikoff[31] points out that Comet Encke is by no means the only comet to show peculiar changes in its motion. Period Comet Wolf I, for example, suffers a *decrease* in mean motion of $4''.2 \times 10^{-7}$ per day, according to the study by Kamienski[32] covering all the observations of the comet from 1884 to 1942. With the present (1942) value of $\mu = 428''.2$, corresponding to a period of 8.3 years and a perihelion distance of 2.4 A.U., the value of $\Delta\mu/\mu$ per revolution is then -3.0×10^{-6}. In 1884, before the recent close approach to Jupiter, when $\mu = 524''$, $P = 6.8$ years, and $q = 1.57$, the corresponding value of $\Delta\mu/\mu$ was -2.0×10^{-6}. The deceleration in the mean motion of Comet Wolf I is relatively less than a tenth that for Comet Encke. Kamienski apparently does not require a secular change in the eccentricity to fit the observations. It is difficult to assess the significance of the small deceleration in the motion of Comet Wolf I as derived by Kamienski, particularly as a very close approach to Jupiter is included in the interval of the solution. Most unfortunately, many of the calculations were destroyed during the recent war.

Comet Wolf I is of particular interest because of its large decrease in magnitude at recent solar approaches. Bobrovnikoff[31] concludes that the comet had faded 2–3 mag. in 1934 and 1942 in comparison to its fairly constant "absolute magnitude" of 11 from 1884 to 1925. He also finds that the apparent diameter of the comet is relatively much greater after perihelion than before at the same solar distances—less than 4 A.U.

[29] *Mem. Acad. St. Petersburg*, Ser. 8, Vol. **22**, No. 2, 1911.

[30] *Bull. Obs. Poulkovo*, Vol. **14**, No. 6, 1935.

[31] *Pop. Astr.*, **56**, 130, 1948.

[32] *M.N.*, **106**, 267, 1947.

Another comet that has shown evidence of a change in motion is periodic Comet D'Arrest. A. W. Recht,[33] from extensive calculations, has found systematic changes per revolution amounting to $+1.51 \times 10^{-4}$ in a and $+1.69 \times 10^{-5}$ in e, over the eight observed solar approaches from 1851 to 1923. Since the period is about 6.7 years (the perihelion distance is 1.32 A.U.), the change in mean motion per revolution is $\Delta\mu/\mu = -6.4 \times 10^{-5}$, of the same order of magnitude as for Comet Encke but of opposite sign. The secular change in e is also of the opposite sign to that for Comet Encke and somewhat greater. Recht concludes that the deceleration is unquestionably real.

There are other comets whose motions do not seem to have conformed well to simple Newtonian theory. Examples are periodic Comets Brooks, Kopff, and Brorsen-Metcalf, while others could undoubtedly be found. Even Halley's Comet arrived late at perihelion in 1910 by 2.7 days.[34] This tardiness after 76 years seems small, but the corresponding value of $\Delta\mu/\mu$ is equal to the older value for Comet Encke, though of the opposite sign.

Hence we see that there are at least two well-authenticated examples of systematic changes in the mean motions of comets, one showing an acceleration (Encke) and one a deceleration (D'Arrest). Also there is suspicion of such effects in the motions of other comets. In both the two best examples the eccentricity also changes systematically, $\Delta\phi$ bearing a fairly constant ratio to $\Delta\mu/\mu$ but being opposite in sign. Both comets are intrinsically faint.

The proposed comet model provides a possible mechanism for accelerating or decelerating the motion of a rotating comet. The gas escaping from the nucleus will leave with a velocity corresponding roughly to the mean speed of the gas molecules at the temperature of the surface layer of the meteoric blanket. The momentum of the escaping gas will exert a force on the nucleus. If there is an appreciable lag between the time of gas escape and the meridian passage of the sun with respect to the rotating nucleus, this force will possess a component perpendicular to the radius vector of the comet's orbit. The force may act in any direction, depending upon the direction of the axis and the sense of rotation of the nucleus.

Suppose that the cometary nucleus is spherical, of mass M, and that it loses mass at a rate dM/dt with an average speed $\bar{v}$. If γ represents the dimensionless component of the force $\bar{v}dM/dt$ perpendicular to the radius vector and in the orbit plane, positive with respect to the motion of the comet, the acceleration to the cometary nucleus, S_T, in the same sense as γ, will be given by

$$S_T = +\frac{1}{M}\frac{dM}{dt}\bar{v}\,. \tag{25}$$

If ζ represents the dimensionless component of the total force along the radius vector outward from the sun, the net outward acceleration, S_R, is, correspondingly,

$$S_R = +\zeta\frac{1}{M}\frac{dM}{dt}\bar{v}\,. \tag{26}$$

Let us assume that the acceleration perpendicular to the orbital plane is zero in the case of a cometary nucleus rotating with its pole perpendicular to the ecliptic.

The average speed of a gas of molecular weight m and temperature T_g is given by

$$\bar{v} = \left(\frac{8kT_g}{\pi m}\right)^{1/2}, \tag{27}$$

[33] *A.J.*, **48**, 65, 1939.

[34] P. H. Cowell and A. C. D. Crommelin, *M.N.*, **71**, 320, 1911.

where k is the Boltzmann constant. The temperature to be applied in equation (27) can be adopted from equation (16), as a slightly high value. The zenith angle of the sun, θ, will depend both upon the time lag of the escaping gas and upon the mean latitude. Since $\cos\theta$ will enter equation (27) only to the one-eighth power, let us simply assume a more reasonable temperature than that of equation (16), $T = 300\, r^{-1/2}(^\circ\,\mathrm{K})$. We may then define η by the following, derived from equation (27):

$$\bar{v} = \frac{\eta}{(r_{\text{A.U.}})^{1/4}} = \left(\frac{8 \times 300^\circ K}{\pi m}\right)^{1/2} \frac{1}{(r_{\text{A.U.}})^{1/4}}. \tag{28}$$

If we adopt $m = 20 \times 1.661 \times 10^{-24}$ gm as typical of the gases in Table 1, we find $\eta = 0.56 \times 10^{-5}$ cm/sec.

Now the average velocity $\bar{v}$ may be assumed to be random in direction as the gas leaves any small area of the cometary nucleus. Hence the average velocity component normal to the surface can be shown to be $2\bar{v}/3$. If, now, the gas vaporizing from a hemisphere is produced proportionately to the effective insolation centered at the subsolar point, the average velocity of the gas perpendicular to the plane of the hemisphere is $4\bar{v}/9$. This value of the average velocity applies to a nonrotating cometary nucleus vaporized by sunlight. The small correction arising from the dependence of $\bar{v}$ upon the temperature at various parts of the nucleus is sufficiently allowed for in the low value of T_φ adopted previously. The effect in a rotating nucleus would be almost the same as for a stationary nucleus if the direction of the velocity component were corrected by the appropriate angle of lag. A minor error will arise, however, from the greater lag in the regions at high latitudes. We may neglect this effect and adopt the approximation that the maximum numerical value of both γ and ζ separately is $4/9$. If the lag is zero, for example, $\gamma = 0$, and $\zeta = 4/9$.

The value of $(1/M)dM/dt$ for the comet must be found from observation. It will be nearly proportional to the solar flux at small and moderate solar distances. At great distances where the vapor pressure of ice (H_2O) becomes negligible (approximately 160° K) the effective conductivity of the meteoric layers will be reduced by the added insolation of the ice (H_2O) layer. It is not possible to generalize as to the solar distance at which this effect takes place. The upper limit is in the neighborhood of 4 A.U. (eq. [16]), but the meteoric layer may reduce the distance very appreciably. The amount of the effect will depend also upon the abundance of H_2O. Let us adopt $r_m = 3$ A.U. as the practical limit to the loss of mass for short-period comets. If we combine various factors involving the area and structure of the cometary nucleus and various radiation constants in a coefficient, ξ, we may write

$$\frac{1}{M}\frac{dM}{dt} = +\frac{\xi}{r^2}. \tag{29}$$

By the definitions of equations (25), (26), and (28) the accelerations become

$$S_T = \frac{\gamma}{\zeta} S_R = \frac{\xi \gamma \eta}{r^{9/4}} \tag{30}$$

Returning to perturbation theory and noting that the resistance and outward force are symmetrical with respect to perihelion, we write the standard equations[35] for the

[35] See, e.g., Moulton, *Introduction to Celestial Mechanics* (New York: Macmillan Co., 1923), p. 404.

perturbations in the elements a, e, and the longitude of perihelion, ϖ, in terms of the forces and true anomaly, v_1, noting that the terms in (sin v_1) times (powers of r) cancel out,

$$\frac{1}{a}\frac{da}{dt} = \frac{2\sqrt{1-e^2}}{\mu r} S_T , \tag{31$_1$}$$

$$\frac{de}{dt} = \frac{\sqrt{1-e^2}}{\mu a^2 e}\left[\frac{ap}{r} - r\right] S_T , \tag{31$_2$}$$

$$\frac{d\varpi}{dt} = -\frac{\sqrt{1-e^2}}{\mu a e}\cos v_1 S_R , \tag{31$_3$}$$

where p is the parameter of the orbit.

For a partial revolution of the comet from $-v_0$ to $+v_0$, the time integral, I, of any function, $f(v_1)$, becomes

$$I = \frac{2}{k\sqrt{p}}\int_0^{v_0} r^2 f(v_1)\, dv_1 , \tag{32}$$

where k^2 is the gravitational constant for motion about the sun.

Hence we find, for the perturbations in the elements and for the loss of mass during one revolution,

$$\frac{\Delta a}{a} = \frac{4\xi\gamma\eta}{k\mu a^{1/2}}\int_0^{v_0} r^{-5/4} dv_1 , \tag{33$_1$}$$

$$\Delta e = \frac{2\xi\gamma\eta}{k\mu a^{5/2} e}\int_0^{v_0} r^{-5/4}(ap - r^2)\, dv_1 , \tag{33$_2$}$$

$$\Delta\varpi = -\frac{2\xi\zeta\eta}{k\mu a^{3/2} e}\int_0^{v_0} r^{-1/4}\cos v_1 dv_1 \tag{33$_3$}$$

and

$$\frac{\Delta M}{M} = \frac{2\xi v_m}{kp^{1/2}} , \tag{33$_4$}$$

where $\Delta\varpi$ is the longitude of perihelion, v_m corresponds to $r = 3$ A.U., and v_0 represents the limits to which the force S_T is operative.

The limit in true anomaly, v_0, beyond which the force S_T becomes zero, can only be guessed on the basis of physical arguments. From equation (24), the lag in heat transfer should be greater at great solar distances, presumably enhancing the tangential acceleration if the lag were small near perihelion. On the other hand, secondary processes other than the reduction in the rate of vaporization will tend to reduce the tangential acceleration. In particular, adsorption of gases in the meteoric layer will increase as the gas output decreases and as the general temperature level falls. Hence the gas vaporized on the night hemisphere may be carried around to the morning limb before being released. Condensation of gases other than H_2O may also occur, adding to the effect.

The ratio of $\Delta e/(\Delta\mu/\mu)$ provides, fortunately, a measure of the general region beyond which tangential acceleration is small. In the case of Comet D'Arrest, Recht's measure of this ratio corresponds almost exactly to a constant value of the perihelion distance, q. Tangential acceleration very near to perihelion would produce such a result, while acceleration over a large range in v would greatly reduce the relative value of Δe. Since $q = 1.32$, the upper limit of v_0 at $r = 2$ A.U. appears reasonable. The same limit gives consistent results for Comet Encke.

Let us assume, then, that the nucleus of Comet Encke rotates in a retrograde direction with a fairly small obliquity of the ecliptic. Its period must exceed 3 hours, the approximate period of a surface satellite about a sphere of density 1.5 gm/cm, for the weak nucleus to remain intact. If the period is less than a week (or possibly considerably longer) and the very stringent conditions of equation (24) are fulfilled, the gas will escape predominantly on the forward face, and a resisting force will oppose the motion.

The orbital elements needed for the present calculations are $a = 2.217$ A.U., $e = 0.847$, and $\mu = 1070''$ per day or 6.0×10^{-8} radians per second. The integrals, I, in equations (33_1)–(33_3) to a limit of $v_0 = 145°$ ($r = 2$ A.U.) and $v_m = 169°$ ($r = 3$ A.U.) are, respectively, $I_e = 5.8 \times$ (A.U.)$^{-5/4}$, $I_a = 6.2 \times$ (A.U.)$^{3/4}$, and $I_m = 0.87$ (A.U.)$^{-1/4}$, while $v_m = 2.8$.

Since $\Delta a/a = -2\Delta\mu/(3\mu)$, the ratio of the secular changes in e and μ becomes

$$\Delta e = -\frac{\Delta\mu}{\mu}\frac{1}{3a^2e}\frac{I_e}{I_a}. \tag{34}$$

The calculated value of Δe derived from $\Delta\mu/\mu = 9.7 \times 10^{-5}$ is -8.3×10^{-6}, to be compared with Asten's value -9.4×10^{-6}. The agreement could be improved by reducing v_0, but Matkiewicz did not fully confirm the older ratio of $\Delta e/(\Delta\mu/\mu)$, obtaining a somewhat smaller numerical value. If v_0 is permitted to run to π, including the entire orbit, the relative value of Δe is reduced to about half the adopted value.

By eliminating ξ from equations (33_1) and (33_4), we can solve for $\Delta M/M$ per revolution in terms of the ratio $\Delta\mu/\mu$. The result is

$$\frac{\Delta M}{M} = \frac{\Delta\mu}{\mu}\frac{\mu}{3\eta\gamma\sqrt{1-e^2}}\frac{v_m}{I_a} \times (1 \text{ A.U.})^{5/4}. \tag{35$_1$}$$

After substituting numerical values, we find that, for Comet Encke, per revolution,

$$\frac{\Delta M}{M} = -\frac{\Delta\mu}{\mu}\frac{4.9}{\gamma}. \tag{35$_2$}$$

If we adopt for γ, the component of the emitted gas in the orbit plane perpendicular to the radius vector, the conservative value of -0.1 and adopt the older maximum value of $\Delta\mu/\mu = 9.7 \times 10^{-5}$, we find, for the relative loss of mass per revolution,

$$\frac{\Delta M}{M} = 0.0048. \tag{35$_3$}$$

In other words, the comet need lose no more than one-half of 1 per cent of its mass per revolution to be accelerated at the maximum observed rate. At the lower present-day acceleration of $\Delta\mu/\mu = 4 \times 10^{-5}$, the mass loss need not exceed one-fifth of 1 per cent per revolution. With a uniform loss of radius corresponding to the maximum rate above, the comet could persist for some six hundred revolutions, or more than a thousand years. The magnitude over the past century and a half since discovery need not have changed appreciably (about 0.1 mag.).

Vsessviatsky[36] came to the conclusion that Comet Encke has faded by 1 mag. in the last 100 years. The conclusion is subject to some question. I have not been able to correlate variations in the brightness of the comet at various apparitions with variations in $\Delta\mu/\mu$. It appears doubtful that the general decrease in $\Delta\mu/\mu$ is associated physically with the suspected secular diminution in brightness, although such a correlation is still possible.

With regard to the more remote history of Comet Encke, particularly its association

[36] *Russian A.J.*, **4**, 298, 1927.

with the Taurid meteors,[27] the present hypothesis opens up an area of investigation too large for elaboration here. Of particular interest is the question whether Comet Encke was "captured" into a short-period orbit by Jupiter. Such a capture requires the aphelion distance of Comet Encke to have been reduced from Jupiter's distance to its present value of 4.1 A.U. A second study of the intricate relationships between the Taurid meteors and Encke's Comet is planned for the future.

In applying the above theory to Comet D'Arrest, equations (33) may be integrated directly by removal of the $r^{-1/4}$ term from under the integrals. The variation in $r^{-1/4}$ from perihelion, 1.32–2 A.U., is small. Pertinent orbital elements are $a = 3.55$ A.U., $e = 0.627$, and $\mu = 532''$ per day. The integrals in equations (33_1)–(33_3) to a limit of $v_0 = 83°$ ($r = 2$ A.U.) and $v_m = 117°$ ($r = 3$ A.U.) are, respectively, $I_a = 0.86 \times (\text{A.U.})^{-3/4}$, $I_e = 4.58 \times (\text{A.U.})^{3/4}$, and $I_\varpi = 0.88$, while $v_m = 2.0$.

With the same assumptions for Comet D'Arrest as for Comet Encke, except that the rotation of the comet must be direct, we find that, for $\Delta\mu/\mu = -6.4 \times 10^{-5}$, $\Delta M/M = 0.005$ and $\Delta e = +1.5 \times 10^{-5}$. Hence the comet needs to lose only one-half of 1 per cent of its mass per revolution, while the calculated increase in e per revolution is near the observed value of 1.7×10^{-5}.

For Comet Wolf I, the results depend upon the assumed orbital elements, which were changed markedly by Jupiter during the period of observation. The elements for 1912, $a = 3.6$ A.U. and $q = 1.59$, if $\Delta\mu/\mu = -2 \times 10^{-6}$, lead to $\Delta M/M = 1.4 \times 10^{-4}$ and $e = +6 \times 10^{-7}$. The elements for 1925, $a = 4.1$ A.U. and $q = 2.44$, if $\Delta\mu/\mu = -3 \times 10^{-6}$ when the integrations are carried to $r_0 = 3$ A.U., lead to $\Delta M/M = 2.3 \times 10^{-4}$ and $e = 1.2 \times 10^{-6}$. The cometary rotation, of course, must be direct. The calculated loss of mass per revolution is very small, only one- or two-hundredths of 1 per cent, while the predicted secular change of eccentricity, about one part in a million, would be undetectable. The fact that Kamienski did not find a secular change in e is therefore consistent with the present theory.

The predicted secular change in the direction of perihelion, $\Delta\varpi$ per revolution, from equation (33_3) is a very small quantity (of the order of a second of arc). It becomes zero as the integration is carried to $v_m = \pi$. It is of interest that the above-calculated losses of mass per revolution to explain the secular accelerations of Comets Encke, D'Arrest, and Wolf I do not appear excessive.

F. EFFECTIVE SOLAR ATTRACTION FOR COMETS

If comets are losing material in the manner proposed in the preceding discussion, there is little question that the component of ejection will be greater statistically along the radius vector toward the sun than normal to it. Certainly, this will be true whenever the time lag in vaporization corresponds to less than an eighth period of cometary rotation, when the rotation is extremely slow or when irregular ejection occurs because of "cave-ins." In the case of extremely great time lags the H_2O ice may tend to freeze on the night hemisphere of the nucleus, while all gases will be adsorbed to a greater or lesser extent on the night hemisphere. Hence, statistically, the cometary nuclei will tend to emit material toward the sun. The phenomenon of the sunward ejection of material from cometary nuclei has long been recognized for the bright comets. Early drawings show the effect strikingly.

The sunward component of the ejection momentum will reduce the solar attraction for a cometary nucleus and affect its orbital motion. We may adopt the rough approximation that the quantity of gas ejected toward the sun by vaporization is proportional to the solar radiation flux and, therefore, inversely proportional to the solar distance. If we neglect the small variation with solar distance of the average speed of the ejected gas particles, the resultant force on the cometary nucleus varies according to the in-

[27] F. L. Whipple, *Proc. Amer. Phil. Soc.*, **83**, 711, 1940.

verse-square law of solar distance. The effective radial force is represented in equation (26), if $\bar{v}$ of equation (28) is taken as constant so that an inverse-square law results. As a consequence, the present comet model predicts an effective reduction in the gravitational constant for comets. The effect of the repulsive force should be observable statistically in cometary orbits observed at single apparitions.

The reality of such a predicted decrease in the Gaussian constant, k^2, can be investigated by means of published definitive orbits for comets. The final least-squares solution for corrections to the elements can be made to include a seventh unknown, Δk^2, with relatively little effort. The statistical mean value of Δk^2 for a number of comets should be significantly negative if the present comet model is essentially correct.

The solution for Δk^2 from a definitive comet orbit is relatively simple because, in the observational equations in right ascension and declination, the differential coefficient for Δk^2 is equal to that for ΔT_0 (T_0 = time of perihelion passage) multiplied by $(T_0 - t)/k^2$, where t is the reduced time of observation. Hence the tabulated values of the perihelion-passage coefficients in the observation equations for the normal positions can be used to derive the coefficients for Δk^2. The least-squares solution can be repeated with the seventh unknown to yield the most probable value of Δk^2.

Since few comets are observed at very great distances from perihelion, the neglect of the variation in $\bar{v}$ with solar distance and the neglect of possible variations of vaporization from linearity with insolation are of little consequence in practice.

The Harvard graduate students listed below are now analyzing the definitive orbits of the following comets to determine the respective values of Δk^2: 1862 III, S. Hamid; 1882 II, F. Kameny; 1886 II, H. J. Smith; 1905 III, A. Hoag; and 1911 II, D. Murcray. The results will be published elsewhere. Preliminary results indicate that the true value of Δk^2 is often masked by a relatively large value of its probable error. Small comets that might give larger values Δk^2 are usually faint and observed for only a short time, while the large comets are well observed but show a small effect. In almost all cases the residuals in the observational equations are markedly reduced by the solution for Δk^2.

No significantly positive values of Δk^2 have been obtained for any of the five comets under investigation. The most significant value of Δk^2 has been obtained from the definitive orbit of Comet 1905 III (Giacobini) by S. Szelegowski.[35] Mr. Hoag finds that $\Delta k^2 = -0''.31 \pm 0''.10$ (m.e.), or $\Delta k^2/k^2 = -9 \times 10^{-6}$, and that the mean error of a single normal position is reduced by a factor of 2. Pertinent orbital elements for Comet 1905 III are $a = 37$ A.U., $e = 0.970$, $q = 1.114$ A.U., and $i = 40°$.

To evaluate $\Delta k^2/k^2$ in terms of the relative loss of cometary mass per period $\Delta M/M$, we may integrate equation (29) with respect to time within $r_m = 3$ a.u., or $v_m = 1.86$, obtaining the following relation with the coefficient, ξ:

$$\frac{\Delta M}{M} = \frac{2\,\xi\,v_m}{k\sqrt{p}}. \tag{36}$$

A comparison of the radial force, S_R, in equation (30) with the gravitational acceleration of the sun, and the evaluation of ξ from equation (36), lead to the following expression for $\Delta M/M$:

$$\frac{\Delta M}{M} = \frac{\Delta k^2}{k^2}\,\frac{2\,r^{\frac{1}{4}}\,v_m}{\zeta\,\eta\,\sqrt{p}}\,\sqrt{\frac{GM_\odot}{1\text{ A.U.}}}, \tag{37}$$

where $M_\odot$ is the mass of the sun and c.g.s. units apply except for p and r (A.U.).

If we adopt $r = 1.5$ A.U., $v_m = 1.86$, $\Delta k^2/k^2 = -9 \times 10^{-6}$, ζ as 0.3 near its maximum of 4/9, and $p = 2.2$ A.U. for Comet 1905 III, we find that $\Delta M/M = 0.04$ per revolution.

[35] *Acta Astr.*, Ser. a, **3**, 57, 1934.

The mass loss so derived may possibly seem rather great. On the other hand, it might still persist for fifty or more apparitions. Perhaps the comet, a rather faint one, is actually dying, or perhaps the value of $\Delta k^2/k^2$ derived for a comet from a single apparition is too much affected by systematic errors in the observations. Such errors may well arise if the cometary emanations systematically displace the apparent center of the comet from the nucleus.

It is clear that values of $\Delta k^2/k^2$ should be derived from orbits of periodic comets at more than one apparition. Such a solution, coupled with a determination of the systematic changes in period eccentricity and direction of perihelion, will yield the ratio of the acceleration components along and normal to the radius vector in the orbit plane, ζ and γ, respectively. It will also provide a check on v_m. Such a result would establish the value of $\Delta M/M$ fairly satisfactorily, even though the acceleration component normal to the orbit plane probably cannot be detected from the observations. Its predicted effects on the inclination and node are very small and are compounded in a complex fashion with the direction of the axis of rotation when the axis is not normal to the orbit.

Near the completion of the present manuscript, the writer's attention was called to the research by A. D. Dubiago,[39] entitled "On the Secular Acceleration of Comets." Secular accelerations are studied for the five comets Encke, Biela, Brooks, Winnecke, and Wolf I. A critical summary of the conclusions is presented. Of especial value are Dubiago's determinations of the accelerations for Comets Brooks and Winnecke. He then calculates the quantity $\bar{v}\Delta M/M$ to account for the observed accelerations by ejection of matter from the comets near perihelion. He rejects gaseous emission (as an insufficient mechanism) and favors a force based on the expulsion of solid particles. It is interesting to note that, among the six comets discussed by Dubiago and the writer, three exhibit a positive value of $\Delta\mu/\mu$ and three a negative value. If the accelerations arise as a consequence of rotation, the sense of the rotation appears to be at random.

Dubiago bases his calculations of mass loss on the theory developed by Bessel.[40] It was of great interest to the writer to learn that Bessel proposed[41] and later defended strongly the proposition that the acceleration of Comet Encke need not arise from a resisting medium. He argued, particularly from his beautiful drawings of jets from the nucleus of Halley's Comet,[42] that material streams out from a comet; if so, the orbital motion of the comet must be affected. Only the amount of the changes can be in question.

In the forthcoming second part of this paper the results of this first part will be interpreted in terms of the physical characteristics of certain comets; some of the pertinent information from observations of meteor streams will be introduced to augment the picture.

[39] *A.J. Soviet Union*, **25**, No. 6, 361, 1948.

[40] *A.N.*, **13**, 345, 1836.

[41] *Ibid.*, p. 3.

[42] *Ibid.*, p. 185.

RADIAL OSCILLATIONS OF THE GENERALIZED ROCHE MODEL*

ZDENĚK KOPAL
Massachusetts Institute of Technology
Received October 31, 1949

ABSTRACT

The object of this paper was to investigate the necessary and sufficient conditions for which a generalized Roche model—consisting of a compressible homogeneous core, of finite dimensions, surrounded by an infinitesimally thin envelope in which the density falls off with inverse square of the distance from the center—is capable of performing small, adiabatic radial oscillations. It will be established that such oscillations are possible only for certain ratios of specific heats of the material constituting our composite configuration (which restricts the extent of the homogeneous core to certain fractional dimensions) and only if the amplitudes of oscillation of the core and of its envelope are such as to insure the continuity of motion across the interface.

When these conditions are met, the spectrum of the eigen-frequencies, in which our configuration as a whole may perform small radial oscillations, is discrete, and the respective eigen-amplitudes turn out to be expressible in terms of the Jacobi polynomials. Tables are given which summarize the characteristic ratios of specific heats, the permissible relative dimensions of the core, as well as the amplitude ratios appropriate for various modes of oscillation—all computed on the assumption that the chemical compositions of the core and the envelope are identical.

The generalized Roche model, consisting of a compressible homogeneous core, of finite dimensions, which is surrounded by an infinitesimally thin envelope, was introduced in astronomical considerations by Jeans,[1] and its significance and minimal properties were later pointed out by a number of writers.[2] Jeans's interest in the generalized Roche model centered around its stability under tidal pull or fast rotation, and he established that the core and its envelope will, under stress, break up in a distinctly different manner. The present investigation will be concerned with the properties of the generalized Roche model under less extreme conditions. Suppose that a configuration built up according to this model is disturbed from its state of equilibrium in such a way that a small, purely radial motion results. The radial oscillations of a special case of the Roche model consisting of a central mass-point surrounded by an atmosphere of infinitesimal weight, in which the density varies as the inverse square of the distance from the center, were investigated previously by Sterne,[3] who found that the envelope is characterized by a discrete set of free periods of oscillation.

The model considered by Sterne cannot, however, be properly regarded as a composite configuration. Radial oscillations of the generalized Roche model possessing a core of finite dimensions were studied subsequently by Sen.[4] The correctness of his investigation was, however, challenged by Cowling[5] on grounds of insufficient generality. In order to clarify the situation, we shall, therefore, resume the investigation of the problem *de novo*, with the aim of ascertaining the precise conditions for which a generalized Roche model can perform radial oscillations. In conformity with all previous investigators, we shall limit ourselves to small, adiabatic oscillations which are purely harmonic in time; squares and higher powers of their amplitudes will be consistently ignored. Cowling's contention that Sen's work involved unnecessary restrictions will be confirmed, and the necessary

* An investigation completed under Contract N5ori-07843 with the Office of Naval Research.

[1] *Principles of Cosmogony and Stellar Dynamics* (Cambridge: At the University Press, 1919), § 154.

[2] Cf., e.g., Sterne, *M.N.*, **99**, 670, 1939.

[3] *Ibid.*, **97**, 582, 1937 (Model 1).

[4] *Proc. Nat. Acad. India*, **13**, 44, 1943.

[5] *Math. Rev.*, **8**, 60, 1947.

and sufficient conditions will be formulated for which our configuration is capable of performing free radial oscillations. It will transpire that such oscillations are possible only for certain ratios of specific heats of the material constituting the core and the envelope of our composite configuration, which restrict the extent of the homogeneous core to certain fractional dimensions, and only if the amplitudes of oscillation of the core and its envelope are in proper ratios to insure the continuity of motion across their interface. The accompanying tables will summarize the characteristic ratios of specific heats, the permissible relative sizes of the core, as well as the amplitude ratios appropriate for various modes of oscillation, computed on the assumption that the chemical composition of the core and that of its envelope are identical.

EQUATIONS OF THE PROBLEM

Let R be the radius of the initially undisturbed configuration built up according to the generalized Roche model, and let a be the radius of its core. Within this core, the density ρ will be regarded as constant and equal to ρ_m; outside the core the density of the surrounding envelope will be supposed to vary as $\rho = k/r^2$, where r denotes the distance from the center and k is an arbitrary constant. Furthermore, let $\bar{\rho}$ stand for the mean density of the configuration as a whole. Inside the envelope ($a < r < R$), the mass $m(r)$ enclosed within any sphere of radius r will be

$$m(r) = 4\pi \int_0^r \rho r^2 dr = \tfrac{4}{3}\pi R^3 \bar{\rho} - 4\pi k (R - r); \tag{1}$$

the gravitational acceleration, g, at any point becomes

$$g = G\frac{m(r)}{r^2} = \tfrac{4}{3}\pi R^3 G\bar{\rho}\left\{1 - \frac{3k}{R^2\bar{\rho}}\right\}\left\{\frac{1}{r^2} + \frac{4\pi G k}{r}\right\}, \tag{2}$$

G being the gravitational constant, while the pressure P follows from the equation of hydrostatic equilibrium,

$$\frac{dP}{dr} = -g\rho, \tag{3}$$

as

$$P = \tfrac{4}{9}R^3 G\bar{\rho}k\left\{1 - \frac{3k}{R^2\bar{\rho}}\right\}\left\{\frac{1}{r^3} - \frac{1}{R^3}\right\} + 2\pi G k^2\left\{\frac{1}{r^2} - \frac{1}{R^2}\right\}, \tag{4}$$

where the constant of integration has been adjusted so as to make P vanish when $r = R$.

Let us suppose now, consistent with our definition of the generalized Roche model, that the mass of the envelope is to be infinitesimally small, which can be achieved by allowing k to approach zero. As $k \to 0$, the above value of the gravity tends to a definite limit, while ρ and P both approach zero, but in such a way that

$$\frac{\rho}{P} \to \frac{9r}{4\pi G\bar{\rho}(R^3 - r^3)}. \tag{5}$$

Inside the homogeneous core ($0 < r \leq a$), then, the mass varies as $(4/3)\pi\rho_m r^3$, while the undisturbed values of gravity and pressure are

$$g = \tfrac{4}{3}\pi G\rho_m r \tag{6}$$

and

$$P = \tfrac{2}{3}\pi G\rho_m^2(a^2 - r^2), \tag{7}$$

respectively.

Let us now suppose that our composite model is disturbed from its state of equilibrium by an instantaneous impulse in such a way that a small, purely radial motion results. If the changes in pressure and density invoked by a displacement δr of any mass particle in r are adiabatic and if δr is so small that its squares and higher powers can be ignored, Eddington[6] has shown that the Lagrangian hydrodynamical equations governing such oscillations can be reduced to the well-known second-order differential equation,

$$\frac{d^2\xi}{dr^2}+\frac{4-\mu}{r}\frac{d\xi}{dr}+\left\{\frac{\nu^2\rho}{\gamma P}-\frac{a\mu}{r^2}\right\}\xi=0\,, \tag{8}$$

where $\xi \equiv \delta r/r$,

$$\mu=\frac{g\rho r}{P}\,, \qquad \text{and} \qquad a=3-\frac{4}{\gamma}\,,$$

γ being the ratio of specific heats of the material; ν the appropriate frequency of oscillation; and g, ρ, and P denoting the equilibrium values of gravity, density, and pressure of our configuration.

The boundary conditions of our problem require that there be no displacement at the center and no variation of pressure at the boundary, the latter condition being tantamount to a requirement that the displacement at the boundary be finite. In order to ascertain free periods of radial oscillation of our generalized Roche model, of properties specified above, the solutions of equation (8), satisfying prescribed boundary conditions in the homogeneous core (of finite but arbitrary dimensions) as well as in the envelope, are evidently prerequisite. In what follows, such solutions will be given.

SOLUTION OF THE EQUATIONS

Let us consider, first, the homogeneous core, in which the equilibrium values of gravity and pressure are given by equations (6) and (7), respectively. Introducing a nondimensional independent variable $x = r/a$, we find that

$$\mu=\frac{2x^2}{1-x^2}\,, \qquad \frac{\rho}{P}=\frac{3}{2\pi G\rho_m a^2(1-x^2)}\,,$$

as a result of which Eddington's equation (8) takes the form

$$(1-x^2)\frac{d^2\xi}{dx^2}+\frac{4-6x^2}{x}\frac{d\xi}{dx}+J\xi=0\,, \tag{9}$$

where we have abbreviated

$$J=\frac{3\nu^2}{2\pi G\rho_m\gamma}-2a\,. \tag{10}$$

The writer has shown elsewhere[7] that a substitution $x^2 = y$ transforms equation (9) into a hypergeometric equation and that a requirement of regularity at the origin restricts its solution to be of the form

$$\xi(x)=AF\left\{\tfrac{5}{4}+\sqrt{\frac{25}{16}+\frac{J}{4}}\,,\quad \tfrac{5}{4}-\sqrt{\frac{25}{16}+\frac{J}{4}}\,,\quad \tfrac{5}{2};\quad x^2\right\}, \tag{11}$$

where A is an arbitrary constant and $F(a, b, c; x^2)$ denotes an ordinary hypergeometric series of the type ${}_2F_1$. The second part of our boundary conditions, requiring ξ to remain finite on the surface, presupposes that the hypergeometric series on the right-hand side of

[6] *M.N.*, **79**, 2, 1918; cf. also *The Internal Constitution of the Stars* (Cambridge: At the University Press, 1926), pp. 186 ff.

[7] *Proc. Nat. Acad. Sci.*, **34**, 377, 1948.

equation (11) must either converge for $x = 1$ or—if divergent—must be terminating. A glance at equation (11) discloses that, in the present case, the sum of the first two indices of our series equals the third, in which case a hypergeometric series of unit radius is known to diverge. Hence, if equation (11) is to represent an admissible solution, the series on its right-hand side must reduce to a polynomial; and this it will do if either of its first two indices is equal to zero or some negative integer. The admissible values of J are thereby restricted to

$$J = 2i(2i+5), \qquad i = 0, 1, 2, \ldots, \tag{12}$$

which, inserted in equation (11), reduces the eigen-functions of our problem to

$$\xi_i(x) = AG_i\left(\tfrac{5}{2}, \tfrac{5}{2}, x^2\right), \tag{11.1}$$

where G_i denotes the respective Jacobi polynomial.[8]

Equation (12) combined with equation (10) leads, furthermore, to

$$\nu^2 = \tfrac{4}{3}\pi G\rho_m\gamma\{i(2i+5) + a\} \tag{13}$$

as the permissible frequencies in which a homogeneous sphere, disturbed slightly from its state of equilibrium, may perform radial oscillations. These frequencies are real, provided that the ratio γ of specific heats of our material satisfies the inequality

$$\gamma > \frac{4}{3 + i(2i+5)};$$

it is seen that the limit of γ below which the instability sets in depends on the order of the excited mode.

Let us turn now to the envelope of infinitesimal mass, the density of which is supposed to fall off as the inverse square of the distance from the center. The equilibrium values of the gravity and pressure are now given by equations (2) and (4), respectively, in which $k = 0$, while the ratio ρ/P is given by equation (5). Introducing a nondimensional variable, $x = r/R$, we obtain

$$\mu = \frac{3}{1-x^3}, \qquad \frac{\rho}{P} = \frac{9x}{4\pi G\bar{\rho}R^2(1-x^3)},$$

by virtue of which, equation (8) takes the form

$$(1-x^3)\frac{d^2\xi}{dx^2} + \frac{1-4x^3}{x}\frac{d\xi}{dx} + \left(J'x - \frac{3a}{x^2}\right)\xi = 0, \tag{14}$$

where

$$J' = \frac{9\nu'^2}{4\pi G\bar{\rho}\gamma}. \tag{15}$$

In order to solve equation (14), change over to a new independent variable, $x^3 = y$, which transforms it into

$$y^2(1-y)\frac{d^2\xi}{dy^2} + y(1-2y)\frac{d\xi}{dy} + \tfrac{1}{9}(Jy - 3a)\xi = 0. \tag{14.1}$$

This is again an equation of the Riemann type, and its solution can therefore be expressed in terms of hypergeometric series of the form

$$B_1 \cdot {}_2x^{\pm q}F\left\{\tfrac{1}{2} \pm \frac{q}{3} \pm \sqrt{\frac{1}{4} + \frac{J'}{9}}, \quad \tfrac{1}{2} \pm \frac{q}{3} \mp \sqrt{\frac{1}{4} + \frac{J'}{9}}, \quad 1 \pm \tfrac{2}{3}q, \quad x^3\right\}, \tag{16}$$

[8] In the notations of Courant-Hilbert, *Methoden der mathematischen Physik* (Berlin: Julius Springer, 1931), 1, 77.

where $q = \sqrt{3\mathfrak{a}}$ and $B_{1,2}$ are arbitrary constants. Barring exceptional cases when $\mathfrak{a} = 3n^2/4$ ($n = 0, 1, 2, \ldots$),[9] these are the two independent solutions of equation (14), and their linear combination furnishes, therefore, the complete primitive. It should be stressed that, since, in the presence of a homogeneous core of finite radius a, the validity of equation (16) is not expected to extend up to the center but only within $a \leqslant x \leqslant R$, no physical reason is known which should compel us to discard the second particular solution corresponding to the negative value q.[10] The requirement that ξ be finite at the boundary continues to hold good, however, and, in order to meet it, the hypergeometric series on the right-hand side of equation (16)—clearly divergent for $x = 1$—must be terminated by putting

$$J' = (3j \pm q)(3j \pm q + 3), \qquad j = 0, 1, 2, \ldots, \tag{17}$$

which, inserted in equation (15), leads to the frequencies ν' of radial oscillations of the envelope given by

$$\nu'^2 = \tfrac{4}{9}\pi G\tilde{\rho}\gamma(3j \pm q)(3j \pm q + 3). \tag{18}$$

As in the case of the homogeneous core, the period of any particular mode is a diminishing function of γ; but, contrary to the homogeneous model, no oscillation in any mode is possible if $\gamma < 4/3$.

If the above condition (18) is fulfilled, the primitive of our fundamental equation (14) ultimately takes the form

$$\xi_j(x) = Bx^{\pm q} G_j\left(1 \pm \frac{2q}{3}, 1 \pm \frac{2q}{3}, x^3\right), \tag{16.1}$$

where G_j again denotes the respective Jacobi polynomial. It should be stressed that, since only one of the two series (16) can be made to terminate by an appropriate choice of J', the foregoing eigen-function $\xi_j(x)$ contains only one arbitrary constant, q being either positive or negative, depending on which one of the two infinite series (16) was reduced to a polynomial.

MODES OF OSCILLATION

Having obtained the solutions of equation (8) for the core and the envelope of our generalized Roche model separately, it remains for us to specify the conditions under which the model as a whole is susceptible of performing small radial oscillations. Our basic premise, which is consistent with our definition that the mass of the envelope is infinitesimal, will be the expectation that *free oscillations of the core are sensibly unaffected by the surrounding envelope*, and their frequencies will, therefore, continue to be given by equation (13). It is, furthermore, obvious that the periods of free oscillation of an envelope floating on the core must conform to those of the core if such oscillations are to be possible at all. Our problem thus reduces to an investigation of the conditions for which this may be the case. In the course of this investigation, three cases can be distinguished: (*a*) the core is incompressible; (*b*) the core is compressible but quiescent; (*c*) both the core and its envelope oscillate.

Case *a* is the simplest of the three. It is well known that an incompressible fluid sphere is incapable of exhibiting purely radial oscillations; consequently, the oscillations of the envelope alone remain to be investigated. The only boundary condition to be fulfilled asserts that the amplitude of radial oscillation should vanish at the interface; since the core

[9] Should this be the case, the primitive of our equation changes its character and will, in general, contain a logarithmic function. The most conspicuous case of this nature is the one of neutral equilibrium, for which $\gamma = 4/3$ and thus $\mathfrak{a} = 0$. For $\gamma < 4/3$, leading to negative values of $\mathfrak{a}$, the solution (16) becomes imaginary.

[10] It was one of the oversights in Sen's work to disregard the existence of this second solution, which led him, in effect, arbitrarily to put $B_2 = 0$.

is supposed to be incompressible, the pressure variation at the interface is clearly irrelevant. Now equation (16.1) discloses that, for $B \neq 0$, the oscillation will vanish if

$$G_j(1 \pm \tfrac{2}{3}q\ ,\ 1 \pm \tfrac{2}{3}q\ ,\ x^3) = 0\ , \tag{19}$$

i.e., if the extent a/R of the homogeneous core happens to be the root of the foregoing Jacobi polynomial.[11] The orthogonality of these polynomials permits us to assert that, in general, G_j will possess j roots between 0 and 1 which are real and distinct; these roots correspond to j possible values of a/R characterizing the dimensions of the incompressible core, with the surrounding envelope oscillating in the $(j-1)$st mode for the first of such roots (arranged in order of increasing magnitude) and in the fundamental mode for the jth root. A brief table of six-digit roots $a/R = x_j$ of equation (19) for $j = 1, 2, 3$, and $q = 0, \pm\sqrt{0.6}, \pm\sqrt{1.2}$, and $\pm\sqrt{1.8}$ corresponding to $a = 0, 0.2, 0.4$, and 0.6 is given (Table 1).

TABLE 1

a	q	$j=1$	$j=2$		$j=3$		
		x_1	x_1	x_2	x_1	x_2	x_3
0.6	$\sqrt{1.8}$	0.868236	0.943715	0.699505	0.968828	0.835192	0.587376
	$-\sqrt{1.8}$	.457074	.881932	.296329	.947596	.720798	.227972
0.4	$\sqrt{1.2}$	.858954	.940900	.685002	.967628	.828930	.572049
	$-\sqrt{1.2}$	.596661	.892876	.401709	.950690	.738228	.312652
0.2	$\sqrt{0.6}$	.844652	.936772	.663642	.965918	.819920	.549965
	$-\sqrt{0.6}$	.688215	.904360	.465499	.954208	.757614	.380449
0	0	0.793702	0.923017	0.595640	0.960926	0.793702	0.483033

Case *b*, consisting of a quiescent compressible core and oscillating envelope, can be restated as follows: Suppose that the envelope of a generalized Roche model has been excited to oscillate in the jth mode. Is it possible that it can continue to do so without disturbing the core? The answer would be in the affirmative, provided that a sphere of no displacement (nodal surface) could be found at which the pressure remains constant and that this sphere represents the extent of the homogeneous core. It is, however, easy to prove that (save, perhaps, for very special conditions) this requirement cannot be met. Let us recall[12] that the variation in pressure δP, accompanying the radial oscillations, is related to the displacement δr in radius by

$$\frac{d\,\delta P}{d\,r} = \left(\nu^2 + 4\,\frac{g}{r}\right)\rho\,\delta r\,. \tag{20}$$

The quantity factoring δr on the right-hand side of this equation is nonvanishing and positive through the interior of an oscillating configuration; hence the zeros of δr are seen

[11] Since the external attraction of a sphere is known to be equivalent to that of a central point of the same mass, the validity of eq. (16) has not been impaired by replacing a central mass-point of the preceding section by a spherical core of finite dimensions, irrespective of whether this core is at rest or performs radial oscillations.

[12] Cf. nn. 3 and 6.

to coincide with the zeros, not of δP, but of its derivative. But the consecutive zeros of $d\delta P/dr$ separate, by definition, the loops where $\delta P = 0$. Hence equation (20) alone makes it evident that surfaces of no displacement and no variation in pressure cannot coincide in the interior of an oscillating envelope. Such oscillations, with the pressure varying at the interface, are bound to excite synchronous oscillations in the compressible core as well, if the core is capable of such oscillations; otherwise they will get dissipated. This leads us to the third, most general, case, *c*, in which the entire configuration oscillates as a whole.

The first and obvious condition for the possibility of the coexistence of such a regime is a requirement that the respective free periods of radial oscillation of the core and its envelope be equal. Equating ν and ν' as given by equations (13) and (18), respectively, and eliminating the frequency between these two equations, we find that this will be true if, and only if, the mean densities of the core and its envelope are in the ratio of

$$\frac{\bar{\rho}}{\rho_m} = \frac{3\gamma\{i(2i+5)+\alpha\}}{\gamma'\{(3j\pm q)(3j\pm q+3)\}}, \tag{21}$$

where i and j are zero or any positive integer; γ and γ' denote the effective ratios of specific heats of material in the core or the envelope; and $\alpha = 3 - 4/\gamma$, while $q^2 = 9 - 12/\gamma'$. The ratios of specific heats in the core and its envelope need not necessarily be the same. In what follows we shall, however, for simplicity's sake, set $\gamma = \gamma'$, in which case $q^2 = 3\alpha$. Since, moreover, by definition

$$\frac{\bar{\rho}}{\rho_m} = \left(\frac{a}{R}\right)^3,$$

it follows that oscillations of the core and the envelope can coexist, provided that the fractional radius of the core is not arbitrary, but is given by

$$\frac{a}{R} = \left\{\frac{3i(2i+5)+q^2}{(3j\pm q)(3j\pm q+3)}\right\}^{1/3}. \tag{22}$$

This fact was first pointed out by Sen.[4] For the fundamental modes of oscillation ($i = j = 0$), equation (22) yields $a/R = (1 \pm \sqrt{3/\alpha})^{-1/3}$. Since, under conditions of physical interest, $0.1 < \alpha < 0.6$, the foregoing equation discloses that the square root must be taken positively, and the fractional radius of the core should then be between 53 and 68 per cent of that of the configuration as a whole, making its volume less than 31 per cent of that of the whole sphere. This does not mean that our composite configuration could not oscillate for an infinity of other sizes of the core; for almost any value of a/R can be obtained from equation (22) by making i and (or) j sufficiently large. But, if so, the order of the mode of the corresponding oscillation may be very high, and such oscillations may be difficult to maintain in the presence of any dissipative forces.

The condition $\nu = \nu'$ is necessary, but not sufficient, for a generalized Roche model to oscillate as a whole. The remaining two conditions which must be fulfilled are the continuity of motion ($\delta r/r$) and of pressure ($\delta P/P$) at the interface between the core and its envelope.[13] Equating $\delta r/r \equiv \xi$ as defined by equations (11.1) and (16.1), we find the continuity of motion requires that

$$AG_i\left(\tfrac{5}{2}, \tfrac{5}{2}, 1\right) = B\left(\frac{a}{R}\right)^{\pm q} G_j\left(1 \pm \tfrac{1}{2}q, 1 \pm \tfrac{1}{2}q, \frac{a^3}{R^3}\right), \tag{23}$$

where the permissible values of a/R are given by equation (22).

[13] A failure to recognize the continuity of $\delta P/P$ at the interface was the second cause that vitiated Sen's work.

Equation (23) contains two arbitrary constants or one arbitrary ratio. In order to determine them, recourse must be had to the continuity of $\delta P/P \equiv \eta$. Consistent with the solution developed earlier in this paper, both P and δP vanish separately at the boundary of the homogeneous core, but in such a way that their ratio η remains finite and equal to[14]

$$\eta\left(\frac{a}{R}\right) = -\left(4+\nu^2\frac{R}{g}\right)\xi_i(1) = -3\gamma A G_i\left(\tfrac{5}{2},\tfrac{3}{2},1\right) \tag{24}$$

by equations (6), (11.1), and (13). If the envelope is to oscillate freely in synchronism with the core, it is clear that $\delta P/P$ in the envelope must reduce to equation (24) at the interface. The solution for $\xi_j(x)$ in the envelope being given by equation (16.1), that for $\eta_j(x)$ can be obtained in terms of $\xi_j(x)$ either from equation (20) by integration or by a differentiation of the condition

$$\eta = -\gamma\left(3\xi + x\frac{d\xi}{dx}\right), \tag{25}$$

which insures that the oscillations are adiabatic.[15] The outcome discloses that if

$$\xi_j(x) = Bx^{\pm q}G_j(\pm q), \tag{16.1}$$

where

$$G_j(\pm q) \equiv {}_3F_1\left[\begin{matrix}1\pm\frac{2}{3}q+j, -j, \\ 1\pm\frac{2}{3}q\end{matrix}\; x^3\right],$$

then

$$\eta_j(x) = -\frac{12B}{3\mp q}x^{\pm q}H_j(\pm q), \tag{26}$$

where

$$H_j(\pm q) = {}_3F_2\left[\begin{matrix}2\pm\frac{1}{3}q,\ 1\pm\frac{2}{3}q+j, -j, \\ 1\pm\frac{1}{3}q,\ 1\pm\frac{2}{3}q\end{matrix}\; x^3\right]$$

is a (terminating) generalized hypergeometric series of the type ${}_3F_2$. Equating η at the interface between the core and the envelope by means of equations (24) and (26), we find the continuity of pressure at the interface to require that

$$AG_i\left(\tfrac{5}{2},\tfrac{3}{2},1\right) = B\left(1\pm\tfrac{1}{3}q\right)\left(\frac{a}{R}\right)^{\pm q}H_j(\pm q), \tag{27}$$

where a/R is given by equation (22). Equations (23) and (27), which must be fulfilled simultaneously, both contain the common ratio A/B. Eliminating it between them and taking advantage of the identity

$$3G_i\left(\tfrac{5}{2},\tfrac{3}{2},1\right) = (2i+3)(i+1)G_i\left(\tfrac{5}{2},\tfrac{5}{2},1\right),$$

we establish that the second (and last) necessary condition for the coexistence of simultaneous radial oscillations of the core and the envelope takes the explicit form

$$\frac{G_j(\pm q)}{H_j(\pm q)} = \frac{3\pm q}{(2i+3)(i+1)}. \tag{28}$$

[14] This is the boundary condition of our oscillation problem (cf. Sterne, *M.N.*, **97**, 582, eq. [1.9]).

[15] Cf. nn. 3 and 6. The reader may also observe that, while the continuity of motion requires that $\xi(x)$ be continuous at $x = a/R$, the continuity of pressure requires, in addition, the continuity of $d\xi/dx$ at the interface.

For given modes of oscillation of the core and the envelope (i.e., given the values of i and j) the foregoing equation contains q as the sole disposable parameter. It transpires, therefore, that *our composite configuration cannot, in general, oscillate as a whole in any mode unless the ratio of specific heats γ of its material satisfies equation (28)*. This condition is necessary, but it is also sufficient; for when it is met, the fractional radius of the solid core is specified uniquely by equation (22) and the continuity of motion can then always be secured from equation (23) or equation (27) by choosing A/B so as to satisfy these equations. One (or more) values of γ characteristic of each pair i and j and leading to the fractional radius of the homogeneous core such that $0 < a/R < 1$ can always be found, provided that $j > i > 0$. If $i = j$, the characteristic fractional radius of the core is unity; while if $i > j$, equation (28) cannot be solved for γ in terms of real numbers.

TABLE 2

j	i		
	1	2	3
1	1.35 (0.3333)	.....	.....
2	1.3455 (0.2854)	1.3333 (0)	.....
3	1.3394 (0.2012)	1.3626 (−0.4396)	1.3611 (−0.4286)

TABLE 3

j	i		
	1	2	3
1	1.0000 (2.0455)	.....	.....
2	0.7122 (0.6065)	1.0000 (7.0000)	.....
3	0.5723 (0.5327)	0.8326 (2.9424)	1.0000 (11.8486)

The numerical values of the characteristic γ's for $i, j = 1(1)3$ are given in Table 2; the number in parentheses which accompanies each entry indicates the underlying value of q. It is seen that all such γ's are practically between 1.33 and 1.36—i.e., very close to values appropriate for a polyatomic gas. In order that the composite oscillation may be possible for such characteristic values of γ, it is, furthermore, necessary that the fractional radius of the core be consistent with the adopted trio i, j, and γ in the light of equation (22). This makes it evident that, at best, *only one mode of oscillation of the core and the envelope can be excited at a time*. The fractional radii a/R corresponding to the lowest three modes of oscillation are given in Table 3, while the numbers in parentheses accompanying each entry give the appropriate values of A/B. Whether or not a generalized Roche model, possessing a core of arbitrary fractional dimensions and char-

acterized by an arbitrary value of γ is capable of oscillating as a whole in some definite frequency is a problem which is difficult to settle in full generality. The answer is probably in the affirmative, but the order of the respective modes may be very high.

In conclusion, the writer takes pleasure in expressing his sincere appreciation to Miss Jeannie R. B. Carmichael for carrying out all numerical computations involved in Tables 1, 2, and 3.

APPENDIX

In preceding sections we have investigated the radial oscillations of a composite model consisting of a homogeneous core, surrounded by an envelope in which the density falls off as the inverse square of the distance from the center. The differential equations governing small oscillations of both the core and the envelope turned out to be of the hypergeometric type, and the discrete character of the frequency spectra of their free oscillations was found to be a consequence of the necessity to terminate a divergent hypergeometric series of unit radius. Radial oscillations of fluid configurations which are wholly homogeneous or in which the envelope extends down to a mass-point core representing the total mass of the configuration were previously investigated by Sterne[3] (Models 1 and 3), who considered, in addition, the oscillations of another model, similar to 3, but in which the density varied continuously as the inverse square of the radius from the center to the surface (Model 2). Equation (8), governing such oscillations for Sterne's Model 2, took the form

$$(1-x^2)\frac{d^2\xi}{dx^2}+\frac{2-4x^2}{x}\frac{d\xi}{dx}+(J''x^2-2a)\frac{\xi}{x}=0\,, \tag{29}$$

where

$$J''=\frac{3\nu''^2}{2\pi G\bar{\rho}\gamma}\,. \tag{30}$$

We wish to point out that, like equations (9) and (14), equation (29) is also one of the Riemann type, and its solution can therefore be expressed in terms of appropriate hypergeometric series. The particular solution of equation (29) which remains finite at the origin readily takes the form

$$\xi = A\,x^q F\,(a,\ b,\ c;\ x^2)\,, \tag{31}$$

where

$$a=\frac{3+2q}{4}\pm\frac{\sqrt{9+4J''}}{4}\,,\qquad b=\frac{3+2q}{4}\mp\frac{\sqrt{9+4J''}}{4}\,,\qquad c=\frac{3+2q}{2}\,,$$

and

$$2q=\sqrt{1+8a}-1\,,$$

while A denotes an arbitrary constant. Since $a+b=c$, the hypergeometric series on the right-hand side of equation (31) diverges for $x=1$ and must therefore be reduced to a polynomial if ξ is to remain finite on the surface. This will be the case if either a or b is equal to zero or some negative integer—that is, if

$$J''=(2j+q)(2j+q+3)\,,\qquad j=0,\ 1,\ 2\ \ldots\,. \tag{32}$$

The eigen-functions (31) of our oscillation problem then become

$$\xi_j(x)=A\,x^q G_j\left(q+\tfrac{3}{2},\ q+\tfrac{3}{2},\ x^2\right), \tag{33}$$

while the eigen-frequencies are

$$\nu''^2=\tfrac{2}{3}\pi G\bar{\rho}\gamma\,(2j+q)(2j+q+3)\,. \tag{34}$$

Quite recently, Prasad[16] called attention to two other models for which the problem of small radial oscillations admits of an analytical solution. The first configuration considered by Prasad consisted of a central mass-point, surrounded by a homogeneous envelope. If the mass of the core and its envelope are in the ratio of 2 to 1, Prasad has shown that equation (8) reduces to

$$(1+x^2)\frac{d^2\xi}{dx^2}+\frac{3-6x^2}{x}\frac{d\xi}{dx}+(J'''x^2-a)\frac{\xi}{x^2}=0\,, \tag{35}$$

where

$$J'''=\frac{9\nu'''^2}{4\pi G\gamma\bar{\rho}}-2a\,. \tag{36}$$

This again is an equation of the hypergeometric type, and its particular solution which remains finite at the origin is again of the form (31), where

$$a=\frac{5+2q}{6}+\frac{\sqrt{25+4J'''}}{6}\,,\qquad b=\frac{5+2q}{6}-\frac{\sqrt{25+4J'''}}{6}\,,\qquad c=\frac{5+2q}{3}\,,$$

and

$$q=\sqrt{1+a}-1\,.$$

Since again $a+b=c$, the series on the right-hand side of equation (31) must be terminating if ξ is to remain finite at $x=1$, and this can be effected by setting

$$J'''=(3j+q)(3j+q+5)\,,\qquad j=0,\,1,\,2\,\ldots\,. \tag{37}$$

If so, the eigen-functions of Prasad's first model become

$$\xi_j(x)=Ax^qG_j(\tfrac{5}{3}+\tfrac{2}{3}q\,,\tfrac{5}{3}+\tfrac{2}{3}q\,,x^2) \tag{38}$$

with the eigen-frequencies

$$\nu'''^2=\tfrac{4}{9}\pi G\gamma\bar{\rho}\{2a+(3j+q)(3j+q+5)\}\,. \tag{39}$$

The second model, considered by Prasad in his latest paper (*M.N.*, **109**, 103, 1949), is characterized by a continuous density distribution $\rho=\rho_c(1-x^2)$ vanishing on the surface and without central singularity. In such a case, Eddington's equation (8) was shown to reduce to

$$(1-x^2)(1-\tfrac{1}{2}x^2)\frac{d^2\xi}{dx^2}+\frac{4-11x^2+5x^4}{x}\frac{d\xi}{dx}+(J^{\mathrm{IV}}+3ax^2)\xi=0\,, \tag{40}$$

where

$$J^{\mathrm{IV}}=\frac{3(\nu^{\mathrm{IV}})^2}{2\pi G\gamma\bar{\rho}}-5a\,. \tag{41}$$

This equation can no longer be reduced to the simple hypergeometric type; but, as will be shown, its solution can be expanded in terms of hypergeometric polynomials precisely of the form already encountered earlier in this paper.

Letting $x^2=y$, we may rewrite the preceding equation as

$$\alpha(y-1)(y-a)\frac{d^2\xi}{dy^2}+\{\bar{\gamma}(y-1)(y-a)+\bar{\delta}y(y-a)+\bar{\epsilon}y(y-1)\}\frac{d\xi}{dy}+\hat{\alpha}\bar{\beta}(y-h)\xi=0 \tag{42}$$

[16] *M.N.*, **108**, 414, 1948; **109**, 103, 1949.

where $a = 2$, $\bar{\gamma} = 2.5$, $\bar{\delta} = 2$, $\bar{\epsilon} = 1$, $h = -J^{IV}/3\mathfrak{a}$, and

$$\bar{\alpha} + \bar{\beta} = \tfrac{9}{2}, \qquad \bar{\alpha}\bar{\beta} = \tfrac{3}{2}a,$$

the value of $\bar{\alpha} + \bar{\beta}$ being chosen so as to satisfy Riemann's relation,

$$\bar{\alpha} + \bar{\beta} - \bar{\gamma} - \bar{\delta} - \bar{\epsilon} + 1 = 0.$$

Equation (42) then represents the standard form of the Fuchsian equation of second order with four singularities and one accessory parameter (the Heun equation).

The simplest way of representing the functions defined by the Heun equation is to do so in terms of power series which represent such functions in a circle with one singularity on the boundary, and another one at the center, of the domain of convergence. The former singularity can, however, be avoided by a suitable choice of h. This way was followed by Prasad (*ibid.*), who constructed a particular solution of his equation (40) in ascending powers of x^2, which could be made regular on the surface of the oscillating configuration by restricting the values of J^{IV} to the roots of a transcendent equation obtained by setting a certain infinite fraction equal to zero. The spectrum of the eigen-frequencies is thus again discrete, and the corresponding eigen-amplitudes are expressible in terms of certain infinite series. The leading terms of such series corresponding to the four lowest modes of oscillation were explicitly evaluated by Prasad for four different values of $\mathfrak{a}$.

Now a more powerful process of solution of the Heun equation was devised by Svartholm,[17] who pointed out that every solution of equation (42) which is regular for $y = 1$ admits of an expansion in terms of the hypergeometric polynomials. In our present case, this solution takes the form

$$\xi_j(y) = \sum_{i=0}^{\infty} c_i(J_j^{IV}, \mathfrak{a})\, {}_2F_1(i + \tfrac{5}{2}, -i, \tfrac{5}{2}, y), \tag{43}$$

where the coefficients $c_i(J_j^{IV}, \mathfrak{a})$ satisfy a certain three-term recursion formula, the explicit form of which was given by Svartholm (*op. cit.*, §5, eq. [25]). The regularity of $\xi_j(1)$ requires again that h (i.e., J_j) be the jth root of a transcendent equation obtained by equating to zero a certain infinite fraction. The explicit form of this equation was established later by Erdélyi.[18]

An inspection of Svartholm's recursion formula for the c_i's reveals that if $\mathfrak{a}$ is non-negative (as it is in our physical problem) the recursion formula and, therefore, the sum on the right-hand side of equation (43) will never terminate, $\xi_j(y)$ being a transcendent Heun function expressible by infinite series. The point we wish to make concerns, however, the particular form of the hypergeometric polynomials in which such functions can be developed. A glance at equation (43) discloses, namely, that ${}_2F_1(i + \frac{5}{2}, -i, \frac{5}{2}, y) = G_i(\frac{5}{2}, \frac{5}{2}, x^2)$, the latter being identical with the Jacobi polynomial on the right-hand side of equation (11.1) expressing the eigen-amplitudes of the homogeneous model. It transpires, therefore, that *the characteristic amplitudes of small radial oscillations of Prasad's second model can be expressed in terms of the characteristic amplitudes of a homogeneous compressible gas sphere.* The coefficients c_i factoring the partial amplitudes on the right-hand side of equation (43) will, in general, depend on $\mathfrak{a}$ as well as on J^{IV} and will there-

[17] *Math. Ann.*, **116**, 413, 1939. [18] *Duke Math. J.*, **9**, 48, 1942.

fore differ for each particular mode; but the resultant amplitude will always remain a linear combination of an infinite number of the $G_i(\frac{3}{4}, \frac{5}{4}, x^2)$'s.

Thus, it appears that, for all models whose oscillating properties have so far been investigated analytically, Eddington's equation (8) governing small radial oscillations of compressible gas spheres turns out to be one of the hypergeometric type, or its solution is expansible in terms of such functions. The fact that such models can oscillate only in certain frequencies follows from the divergence of the respective hypergeometric series of unit radius and from the necessity to terminate such series by putting one index of the hypergeometric series equal to zero or some negative integer. Thus, although the physical considerations at the basis of all these models were quite different, their mathematical character turns out to be very much the same. Any generalization of the oscillatory properties of all these models to fluid configurations of unrestricted specifications should, therefore, be approached with caution.

ETA CARINAE. I. THE NEBULOSITY

E. GAVIOLA
Córdoba Observatory, Córdoba, Argentina
Received May 25, 1949

ABSTRACT

A series of photographs taken with the Córdoba 61-inch reflector discloses the complex structure of the nebula surrounding η Car. Isophote-curves are drawn for a wide scale of exposure times. The blending of the star's nebula with the galactic nebulosity is shown. Identifiable parts of the nebula, measured previously as stellar components, are shown to be moving radially away from the nucleus at speeds compatible with the assumption that they were ejected from the star in 1843 or later.

INTRODUCTION

Two different clouds are called "the nebulosity surrounding Eta Carinae"; one is Herschel's "Key-Hole Nebula," NGC 3372, which covers many square degrees of one of the two brightest parts of the southern Milky Way; this I shall call the "galactic nebulosity." The other is the group of nubeculae measured repeatedly since 1914 as a multiple-star system by southern double-star observers; the latter covers a disk not larger than about 10″ in radius around the star;[1] this group I shall call the "star's nebulosity." There is no positive evidence of a physical or causal relation between the galactic nebulosity and the star η Car. In spite of the fact that the latter has changed in magnitude from -1 (1843) to about 8.4, the luminosity of the galactic nebulosity seems not to have decreased. B. A. Gould wrote[2] in 1871: "But such observations of the nebula around η Argus as I have been able to make, compared with Sir John Herschel's drawings, have tended strongly to impress me with the conviction that the alleged change is altogether imaginary." B. J. Bok[3] accepts "this verdict as final." There is, on the other hand, evidence that the star's own nebulosity undergoes relatively rapid changes, as we shall see in this paper.

OBSERVATIONAL RESULTS

The complex structure of the brighter part of the star's nebulosity—within 6″ of the center—was observed at Bosque Alegre with the 61-inch reflector the first time the star was put on the slit of the new spectrograph in the early morning of January 9, 1944. Under a power of 1200 diameters and star images not larger than 1″ a shape resembling a "homunculus," with its head pointing northwest, legs opposite and arms folded over a fat body, could be clearly seen.

Many attempts were made afterward to obtain on a plate the same clear detail observed visually. A special camera was built for the Cassegrain focal plane of the 61-inch reflector, with an equivalent focal distance of about 33 meters, mounted in such a way that it can be put into operation—whenever the star images seen on the slit jaws of the spectrograph are fine enough—by turning a plane mirror into the light beam. Fourteen months later, on March 7, 1945, two excellent plates were obtained. Each has nine

[1] A series of photographs appeared in the *Memoria* of the Córdoba Observatory for the years 1944 and 1945, published by *Revista astronomica*, Vol. **18**, No. 5, 1946; one reproduction was printed in *Nature*, **158**, 403, 1946; a composite sketch, based on photographs, and a description have been published by A. D. Thackeray in *Observatory*, **69**, 31, 1949.

[2] *M.N.*, **32**, 16, 1871.

[3] *A Study of the η Carinae Region* ("Harvard Reprints," No. 77 [Groningen: Hoitsema Bros., 1932]), p. 71.

images, the times starting with 1 second and doubling for each successive exposure. Stellar images were small—1″ or less—and steady. No guiding was necessary, and none was used. Figure 1 reproduces the images of one of these plates.

The original plate—Ilford HP2—was enlarged first on Kodak Lantern Slide Medium plates; these were enlarged on contrast paper. As the reproductions are negatives, west is at the left and north is at the top. The enlargements were carried out with the same exposure and developing times, so that the series of pictures can be used as an approximate photometric scale, since the original exposure times were rather short (less than 5 minutes). Details of the exposures are described below.

Figure 1a.—1-second exposure. The image is not stellar (compare with *F* in Fig. 1*f*) or round: it has a prominence pointing to the northeast. The two components observed by van den Bos[4] (195°, 0″.2) cannot be seen.

Figure 1b.—2-second exposure. The northeast prominence has grown; two others, one to the northwest and one to the south, appear. They are perhaps already present in the previous picture.

Figure 1c.—4 seconds. The northeast and northwest prominences are growing equally, but the first still keeps the lead. They correspond to the supposedly stellar components C and B measured by Innes, van den Bos, and others (*Southern Double Star Catalogue* [Johannesburg, 1927]). No separation from the nucleus can be seen on the enlargements or on the original plates. The two prominences appear rather as eruptions coming from the center.

Figure 1d.—8 seconds. The northwest eruption has taken the lead. The northeast one appears rotated toward the south, at a position angle of about 90°.

Figure 1e.—16 seconds. The last eruption has grown and rotates still farther, pointing toward 102°. The whole looks like an inverted conventional heart. The legs of the homunculus are appearing.

Figure 1f.—32 seconds. The eruption at 102° of the previous picture has rotated farther (to 112°, 3″.8) and extends to form the upper part of the right leg of the homunculus. Two other nubeculae appear that may be separated from the main body by a zone of lesser density: *b* (175°, 2″.6) and *c′* (147°, 3″.1). Their separation is not definitely proved by the photographs; they may still be prominences or eruptions growing out of the main body. This is made probable for *b* by the rotation of its center of density in the next picture to 187°, 2″.9, agreeing better with van den Bos's *b* (195°, 1″.9)—at least in position angle. The condensation *c* measured at Johannesburg shows a dispersion in distance of nearly 1″.5. The measurements refer, probably, to *c′* and to *c* (141°, 4″.7), which can be seen better in the next picture. The stars *E* and *F* show clearly. The diameter of *F* is less than 1″. The distances $\eta - F = 13''.5$ and $E - F = 5''$ furnish the scale of the enlargements. That they are stars and not parts of the complex nebulosity is indicated by their unchanging distance[5] and by their spectra (Part II of this paper).

Figure 1g.—64 seconds. Three nubeculae appear that seem to deserve the name of local condensations: *c*, *d*, and *g* (see Fig. 5). The first two complete the left and right legs of the homunculus; *g* forms the left shoulder. The position of *d* agrees fairly well with that of van den Bos. A new eruption appears at *i* (30°, 2″.8). The head is inclined toward the northwest.

Figure 1h.—128 seconds. The shape of the head is now revealed, showing a condensation, *h* (310°, 4″.9), well separated from the body by a zone of lesser photographic density. The symmetrical position of *h* in relation to (*c* + *d*) should be noted.

Figure 1i.—256 seconds. Nothing new is added; the close isophote-curves indicate a steep gradient in intensity. This gives the impression, by visual inspection, that the nebulosity ends here; photographs show that it extends farther. The star showing about

[4] *Union Obs. Circ.*, No. 100, p. 522, 1938; No. 106, p. 207, 1948.

[5] Mr. J. Bobone has measured the following values on a plate taken by Dartayet on February 18, 1945: $\eta - E(59''.5, 13''.62)$; $\eta - F$ (39″.7, 13″.85); $E - F$ ($d = 4''.72$).

3″ north of the head in Figure 1*h* and *i* does not belong there; it belongs to Figure 1*f* and *g*, respectively (successive images were displaced from south to north).

The "halo" of the homunculus is shown in Figures 2*a*, *b*, and *c* and 3*a*. They were taken with the Newtonian camera of the 61-inch reflector ($F = 748$ cm). Figures 2*a*, *b*, and *c* are 15-second, 1-minute, and 3-minute exposures on the same plate, Ilford HP2, taken on February 1, 1944.

The sensitivity of the plates seems to have been much greater than one year later, as a 15-second exposure appears several times denser than one exposed over 4 minutes at the Cassegrain focus (Fig. 1*i*). The ratio of light-concentration for extended objects is about 19. By equal seeing and plate sensitivity the density of the 15-second image (Fig. 2*a*) should be only slightly larger than that of Figure 1*i*. Comparison with other plates (not reproduced here) allows one to estimate the density ratio to be about 4.

Figure 2a.—15 seconds at Newtonian focus. Three new prominences appear faintly (curve *10′*). The first has a peculiar shape; starting from the main body at p.a. 248°, it spreads out at about 8″ from the center toward the southeast and mainly toward the northwest. This spreading has suggested to Thackeray[1] the presence of an elliptical shell. The pictures show no further evidence for it. Thackeray appears not to have noticed the cylindrical radial column.

The second prominence—seen by Thackeray as part of the elliptical shell—appears as a system of curved streamers coming from the central body between p.a. 160° and 185°. The third points a little to the north of star *F* (p.a. 28°). The star just east of η Car does not belong there.

Figure 2b.—1-minute exposure. The prominences have grown in outline without changing their general appearance. Some of the streamers due south curve to the east.

Figure 2c.—3 minutes. The two first prominences (*k* and *l*, Fig. 5) adopt the shape of hammerheads; the third appears conical. The diffraction due to the diagonal supports begins to show, particularly east. The peculiar arch formation at the north may be due in full or in part to diffraction. There may be a fourth prominence pointing east (*n* in Fig. 5).

Figure 3a.—This is an enlargement of a 20-minute exposure on an Ilford Ortho Process plate taken on June 21, 1944. The limits of the nebulosity are pushed to between 9″ and 10″ from the nucleus. The somewhat square shape is due to the diffraction-cross, in addition to prominences *k*, *l*, and perhaps *n*.

Figure 3b.—This is a 30-minute exposure on Ilford HP2 emulsion taken on March 18, 1944. New streamers in addition to the diffraction-cross appear. Some of them probably belong to the star's nebulosity, others to the galactic nebulosity. A discrimination is difficult because their densities are of the same order of magnitude. This is shown in Figure 3*c*, which is a smaller enlargement of the same plate used for Figure 3*b*. Herschel's "Key-Hole" shows on the left, also parts of the very bright nebulosity flanking it.

Figure 4.—This figure shows the brightest part of the galactic nebulosity. It is a 60-minute exposure on Eastman 103-O emulsion taken on April 25, 1944, at the Newtonian focus of the reflector. The rectangle indicates the extent of the previous figure. West is now at the right, since the reproduction is a positive.

ISOPHOTE-CURVES

Enlarging Figures 2*a*, *b*, and *c* and 3*a* to the same scale as the others and using a pantograph, I have obtained the series of isophote-curves reproduced in Figure 5. The numbers of the curves correspond to the figures as given in Table 1, with the exception of *10* and *10′*. These two were drawn from the same picture, *10′* following a line of weak and *10* one of larger density. The exposure times grow geometrically with a ratio of 2 from curve *1* to curve *9*. The density ratio between *10′* and *9* is estimated—as explained above—to be about 4. Further, $t\,(11)/t\,(10) = 4$ and $t\,(12)/t\,(11) = 3$. The density ratio between *13* and *12* cannot be given, as a different type of plate was used.

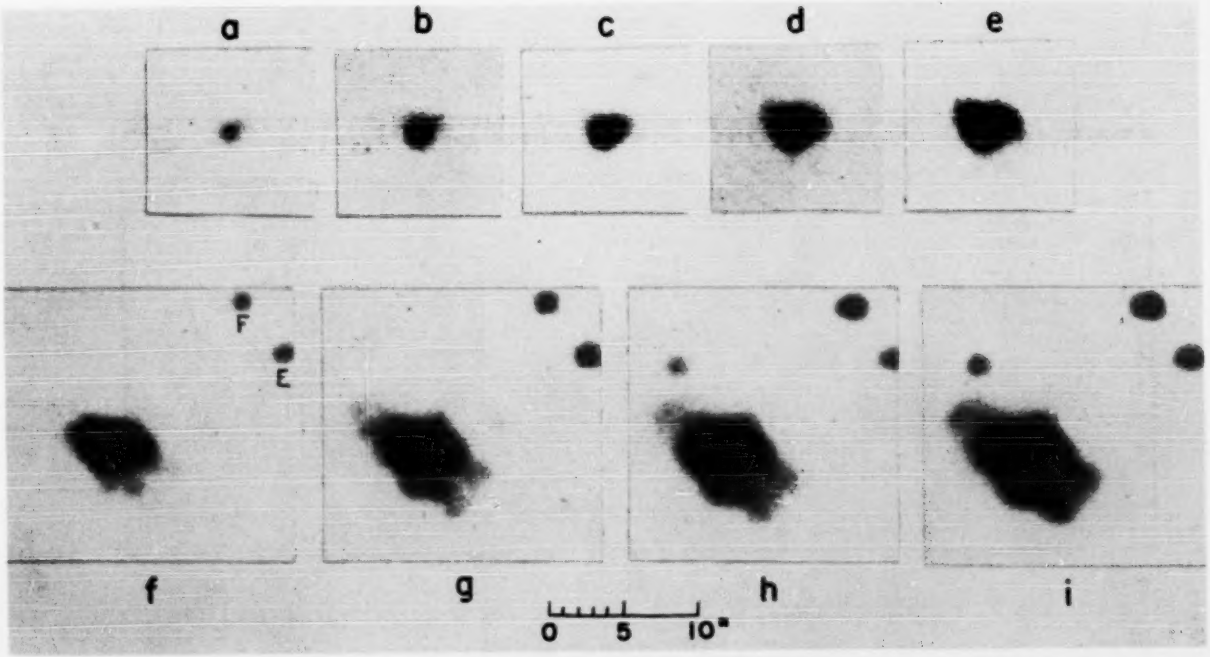

FIG. 1.—Series of photographs of η Car, taken on the same plate and night at the Cassegrain focus on Ilford HP2 emulsion, doubling the time on successive exposures—1–256 seconds. North is at the top; west at the left.

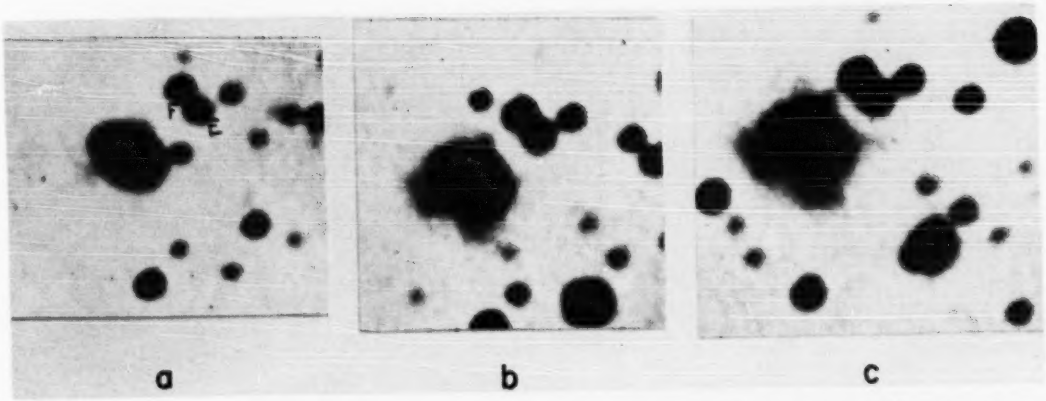

FIG. 2.—15 second, 1-minute, and 3-minute exposures on η Car on the same plate and night at the Newtonian focus on Ilford HP2 emulsion. A number of spurious images are present. Orientation is the same as in Fig. 1.

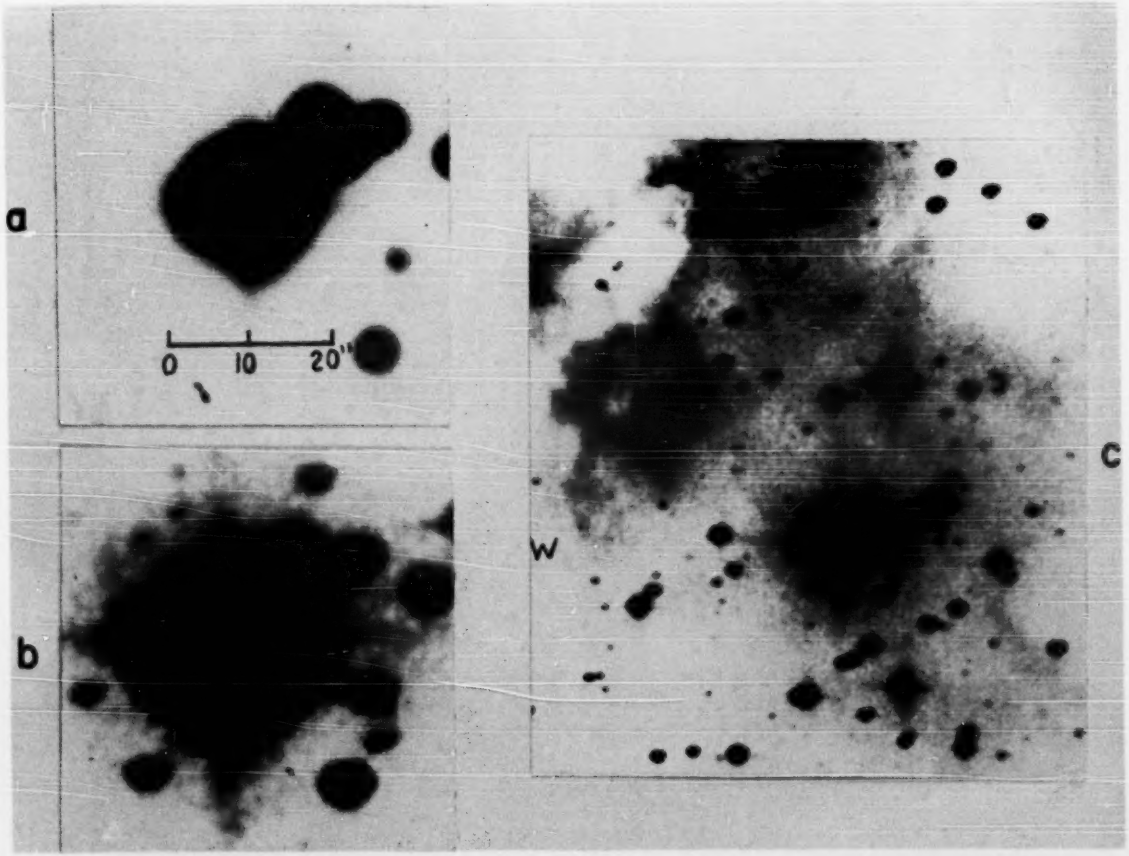

FIG. 3.—*a*, 20-minute exposure on Ilford Ortho Process plate at Newtonian focus; *b*, 30-minute exposure on Ilford HP2 emulsion, Newtonian focus; *c*, same as *b*, showing blending of the star's nebula with the galactic nebulosity.

FIG. 4.—The galactic nebulosity. Positive print indicating the extent of Fig. 3c. A 60-minute exposure on Eastman 103-O emulsion at the Newtonian focus.

The stars *F* and *E* are plotted for orientation. The letters designate eruptions, prominences, condensations, or nubeculae that have a certain individuality. I have kept, as far as possible, the letters used by van den Bos. Table 2 gives position angles and distances of the formations listed for the years 1945.2 and 1944.1.

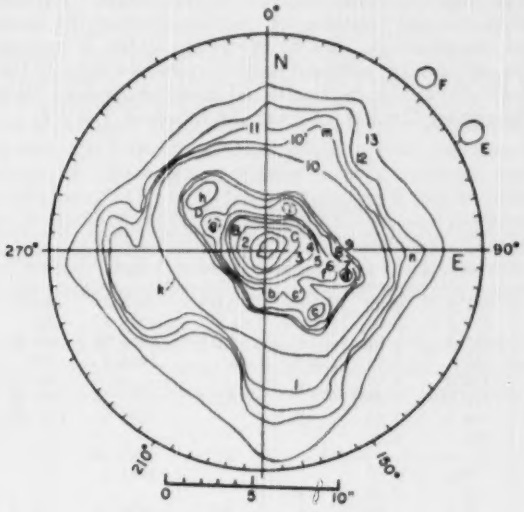

FIG. 5.—Isophote-curves

TABLE 1

Curve	Figure	Curve	Figure	Curve	Figure	Curve	Figure
2	1*b*	5	1*e*	8	1*h*	11	2*b*
3	1*c*	6	1*f*	9	1*i*	12	2*c*
4	1*d*	7	1*g*	10	2*a*	13	3*a*

TABLE 2

POSITION ANGLES AND DISTANCES FOR FORMATIONS

Date	Name	p.a.	*d*	Date	Name	p.a.	*d*
1945.2	B	312°	2".0	1945.2	*d*	108°	4".9
1945.2	C	65	1.9	1945.2	*f*	112	3.8
1945.2	*g*	296	3.4	1945.2	*i*	30	2.8
1945.2	*h*	310	4.9	1944.1	*k*	250	7.5
1945.2	*b*	188	2.9	1944.1	*l*	173	7.0
		175	2.6	1944.1	*m*	25	7.5
1945.2	*c'*	147	3.1	1944.1	*n*?	90	8.2
1945.2	*c*	141	4.7				

DISCUSSION OF RESULTS

Eta Car has been measured repeatedly as a multiple-star system since 1914; estimates date from John Herschel. Van den Bos expressed in 1938[4] his doubt about the stellar character of the components: ". . . nebular character of this unusual multiple system. . . . The companions may be nebular nuclei or involved stars." Thackeray considers the Radcliffe observations[1] as not "settling the question whether the components are truly stellar or nebulous condensation," but he favors the latter. A comparison of distances and position angles measured at different dates throws new light on the subject.

Table 3 contains the available data collected from the *Southern Double Star Catalogue* and the *Union Observatory Circulars*, adding the values of Table 2.

TABLE 3

MEASURES OF COMPONENTS

Name	Date	p.a.	*d*	Observer	Name	Date	p.a.	*d*	Observer
AB	1915.3	311°.8	0".87	Innes	AD*	1926.3	269°.9	2".04	B
	1915.3	319.4	0.82	Voute	*g*	1945.2	296	3.4	
	1917.1	312.5	0.98	I	AD†	1934.05	305.8	4.44	B
	1921.5	316	1.04	Bos	*h*	1945.2	310	4.9	
	1922.4	320.0	1.02	I					
	1926.3	216.6	1.40	I	Ab	1933.24	194.6	1.86	B
	1933.24	316.6	1.65	B		1945.2	175–188	2.6–2.9	
	1945.2	312	2.0						
					Ac	1933.24	141.3	3.98	B
AC	1914.4	74.4	1.07	I		1945.2	141	4.7	
	1914.4	75.3	0.80	V					
	1915.3	72.2	1.07	V	Ad	1934.79	103.3	4.45	B
	1915.3	74.2	1.06	I		1945.2	108	4.9	
	1916.4	72.1	0.98	I					
	1918.4	70.2	1.02	I					
	1921.5	70.0	1.08	B					
	1922.4	70.6	1.12	I					
	1926.3	69.0	1.12	I					
	1933.24	64.2	1.53	B					
	1945.2	65	1.9						

* Refers to *g*?
† Refers to *h*?

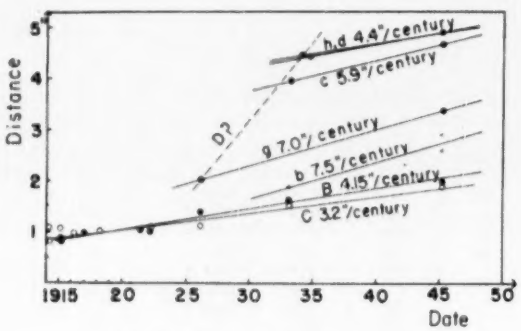

FIG. 6.—Motions of nubeculae

An inspection of the distances shows that they grow with time in a systematic way, while the position angles do not, or vary slowly. If we plot the distances of the components from the nucleus as a function of time, we obtain Figure 6.

The values given for *D* in the *Southern Double Star Catalogue* and in the *Union Observatory Circulars* are discordant in position angle and in distance. If we assume that the first measurement refers to our *g* and the last to our *h*, the changes fall in line with the others, although the position angles do not agree well in the first case. There is, therefore, evidence that the nubeculae forming the complex system move radially with speeds ranging from $3''.2$ to $7''.5$ per century. Not too much weight should be given to the individual values, as the objects measured are nebulous and not always easy to identify, but the order of magnitude is certainly significant: $5''$ per century or less could be taken as a weighted mean motion; the main eruption happened in 1843, just over a century before the last measurements, and the distances of the nubeculae concerned are about $5''$ or less.

Eta Car's own nebulosity as far as $5''$ from the nucleus is formed, therefore, by clouds ejected by the star around 1843 or later. The spectra—whose description will form Part II of this report—confirm this assertion. The radial velocities measured allow calculations of parallax. Objects *E* and *F* are stars, since their distances from η Car have not varied since Herschel estimated them in 1834, and their spectra are stellar.

It is a pleasure to thank Mr. Martin Dartayet for taking the plates at the Newtonian focus; Dr. Ricardo Platzeck for his constant help and for making possible the completion of this work; and M. Leon Fourvel Rigolleau for generously supporting part of it.

PHOTOELECTRIC STUDIES. III. COLOR-LUMINOSITY ARRAYS FOR THE COMA BERENICES AND URSA MAJOR CLUSTERS*

OLIN J. EGGEN
Lick Observatory, University of California
Received December 28, 1949

ABSTRACT

Magnitudes and colors of fifty-five stars in the Coma Berenices cluster and of nine nucleus stars of the Ursa Major cluster—a total of 275 observations—have been determined with a photomultiplier photometer attached to the Washburn 15-inch and the Lick 12-inch refractors.

With the exception of ten stars, consisting of eight known binaries, one possible nonmember of the cluster, and one shell star, those stars known from their radial velocities and proper motions to be certainly members of the Coma Berenices cluster populate the sequences described in Papers I and II of this series, as follows: dwarf (16), bright-dwarf (1), blue-dwarf (5), and bright blue-dwarf (4).

The nine nucleus stars of the Ursa Major cluster are distributed in the color-luminosity array as follows: dwarfs (4), bright-dwarfs (1), blue-dwarfs (1), and bright blue-dwarfs (3).

In Papers I and II[1] of this series, the color-luminosity arrays for the Hyades and the Pleiades stars were discussed. The present paper is the result of a similar investigation of the Coma Berenices cluster and of the "nucleus" stars of the Ursa Major group. The photometer and color systems have been described in Paper I.

COMA BERENICES CLUSTER

The most complete study of this cluster has been made by R. J. Trumpler,[2] who separated the cluster members from the field stars on the basis of proper motion and radial velocity. The present discussion is based upon 242 photometric observations of fifty-five cluster and field stars made with the Lick 12-inch and the Washburn 15-inch refractors. The results are given in Table 1, where the various columns contain the following information: column 1, the number given each star in Trumpler's catalogue; columns 2, 3, and 4, the photographic magnitude and color, on the International System, Pg_p and C_p, determined from the Lick photoelectric measures by means of conversion formulae given in Paper I (column 4 contains the number of nights, n, that each star was observed); columns 5, 6, and 7, same as columns 2, 3, and 4 for the observations made at Madison; columns 8 and 9, the mean values for Pg_p and C_p; columns 10 and 11, the absolute magnitudes derived in this paper and the spectral types given by Trumpler; columns 12 and 13, the probability, according to Trumpler,[2] that each star is a cluster member as judged by the proper motion, μ, and the radial velocity, ρ; column 14, the Flamsteed numbers of the stars, where available, and remarks concerning duplicity. The following explanation of the symbols, *, ×, ·, and o, for proper motion and radial velocity, is quoted from Trumpler's work:

Proper motion:

* $\Delta\mu \leqq 0''.010$, $\epsilon \leqq \pm 0''.003$. Such stars have accurately determined proper motions which agree closely with the group motion; they have a high probability of being physical members.

× $0''.010 < \Delta\mu \leqq 0''.015$, $\epsilon \leqq \pm 0''.003$; $\Delta\mu \leqq 0''.020$, $\epsilon > \pm 0''.003$.

The proper-motion limits are drawn wider so that most of the members not included in the first will be found among the stars of the second rating.

* *Contributions from the Lick Observatory*, Ser. II, No. 27.

[1] *Ap. J.*, **111**, 65, 81, 1950.

[2] *Lick Obs. Bull.*, **18**, No. 494, 167, 1938.

TABLE 1

COMA BERENICES CLUSTER

No. Trumpler	Lick			Madison			Mean		MP_{Cp}	Sp. Trumpler	μ	ρ	Remarks
	P_{Cp}	C_p	n	P_{Cp}	C_p	n	P_{Cp}	C_p					
(1)	(2)	(3)	(4)	(5)	(6)	(7)	(8)	(9)	(10)	(11)	(12)	(13)	(14)
8	10.95	+1.34	1				10.95	+1.34			o		
*10	6.01	+0.05	4	6.00	+0.05	5	6.00	+0.05	+1.50	A3n	•	·	Var. vel.
13	8.19	+0.73	2	8.20	+0.75	2	8.20	+0.74			o		
*19	8.30	+0.29	1	8.34	+0.29	4	8.32	+0.29	+3.82	dF4	×	×	
*36	8.30	+0.30	2	8.34	+0.28	3	8.32	+0.29	+3.82	dF2	•	•	
39	5.80	+0.85		5.82	+0.86		5.81	+0.855		gG8	·	o	7 Com
44	9.25	+0.94	1				9.25	+0.94			o		
*49	8.00	+0.25	2	8.04	+0.26	3	8.02	+0.26	+3.52	dF1s	•	×	
*53	9.05	+0.40	3	9.07	+0.39	2	9.06	+0.395	+4.55	dF9s	×	×	
54	10.85	+0.85	2				10.85	+0.85			·		
*58	9.13	+0.395	3	9.15	+0.40	2	9.14	+0.40	+4.64	dF9	•	×	
*60	6.49	+0.10	4	6.46	+0.10	2	6.48	+0.10	+1.98	A4n	•	×	
62	6.34	+0.09		6.30	+0.09	3	6.32	+0.09	+1.82	A5	•	•	8 Com
*65	9.42	+0.46	3	9.46	+0.48	2	9.44	+0.47	+4.94	dG1	•	×	Var. vel.
*68	6.79	+0.11	3	6.78	+0.10	4	6.78	+0.105	+2.28	A4n	×	•	
*76	9.47	+0.46	3	9.49	+0.44	2	9.48	+0.45	+4.98	dG0	•	×	
79	9.04	+0.06	2				9.04	+0.06		A3	·	o	
*82	7.50	+0.17	2	7.49	+0.16	3	7.50	+0.165	+3.00	A9	•	•	
*85	9.70	+0.47	2	9.74	+0.48	3	9.72	+0.475	+5.22	dG3	•	×	
*86	8.80	+0.355	2	8.84	+0.35	4	8.82	+0.35	+4.32	dF6s	•	•	
*90	8.83	+0.35	3	8.84	+0.34	2	8.84	+0.345	+4.34	dF7	×	×	
*91	5.15	+0.395	3	5.17	+0.39	3	5.16	+0.39	+0.66	gF4+A	•	•	S.B., 12 Com
*97	9.51	+0.44	2	9.53	+0.46	3	9.52	+0.45	+5.02	dG0	•	·	Var. vel.
*101	8.64	+0.33	2	8.64	+0.33	2	8.64	+0.33	+4.14	dF4s	•	×	
*102	9.70	+0.55	2				9.70	+0.55	+5.20	dG2	•	·	Var. vel.
*104	6.84	+0.14	3	6.80	+0.12	2	6.82	+0.13	+2.36	A6	•	•	
*107	5.10	+0.03	3	5.06	+0.03	2	5.08	+0.03	+0.58	A2s	•	•	13 Com
*109	6.58	+0.19	3	6.51	+0.17	2	6.55	+0.18	+2.05	A9n	•	×	Vis. dbl.
*111	8.46	+0.43	4	8.46	+0.43	2	8.46	+0.43	+3.96	dF8n	•	•	
*114	8.86	+0.36	2	8.88	+0.36	2	8.87	+0.36	+4.37	dF6	×	×	
116	8.71	+1.08	2	8.70	+1.08	2	8.70	+1.08			×		
*118	8.58	+0.34	1	8.62	+0.32	1	8.60	+0.33	+4.10	dF5s	•	×	
*125	5.06	+0.19	3	5.02	+0.19	2	5.04	+0.19	+0.54	A9	•	×	14 Com
129	5.38	+1.04	2	5.40	+1.04	2	5.39	+1.04			o		15 Com
*130	4.93	+0.04	3	4.90	+0.02	3	4.92	+0.03	+0.42	A3s	•	×	16 Com
*132	10.36	+0.60	2				10.36	+0.60	+5.86	dG6	•	×	
×135	10.94	+0.83	3				10.94	+0.83	+6.44		×		
*139	6.73	+0.08	3	6.70	+0.08	3	6.72	+0.08	+2.22	A3s	•	•	
*144	6.59	+0.10	3	6.55	+0.08	3	6.57	+0.09	+2.07	A3s	•	×	S.B.
*145	6.71	+0.10	3	6.68	+0.10	3	6.70	+0.10	+2.20	A2s	•	•	
*146	5.06	−0.08	3	5.03	−0.08	2	5.05	−0.08	+0.55	A0s	×	•	17 Com
147	8.95	+0.41	3				8.95	+0.41		dF5	·		
149	5.80	+0.33	1	5.78	+0.33	1	5.79	+0.33		gF5s	·	o	18 Com
*150	10.40	+0.71	4				10.40	+0.71	+5.90	dG9	×	×	Var. vel.
*160	5.38	−0.03	3				5.38	−0.03	+0.88	A2	•	•	21 Com
*162	8.82	+0.36	4				8.82	+0.36	+4.32		×	•	
175	10.74	+0.57	1				10.74	+0.57					
*183	6.26	0.00	2	6.30	0.00	2	6.28	0.00	+1.78	A3s	•	•	22 Com
192	9.34	+0.49	2				9.34	+0.49		[illegible]9	·		
193	10.09	+0.67	3				10.09	+0.67					
×A13	10.97	+0.60	2				10.97	+0.60	+6.47	K0			
×A14	10.60	+0.64	2				10.60	+0.64	+6.10	G5			
×A21	11.03	+0.70	2				11.03	+0.70	+6.53	G7			

o $\Delta\mu > 0''.020, \epsilon < \pm 0''.004$; $\Delta\mu > 5\epsilon, \epsilon > \pm 0''.004$.
Stars with such proper motions can be eliminated as nonmembers with practical certainty.

· This rating is given to the remaining stars; cluster members among these should be very rare.

Radial velocity:

* $\Delta\rho \leqq 2.0$ km/sec, $\epsilon \leqq \pm 1.5$ km/sec,

× $2.0 < \Delta\rho \leqq 5.0$ km/sec,

o $\Delta\rho > 4\epsilon$,

· The remaining stars, mostly with very uncertain mean velocities because of variability.

An asterisk preceding the number of the star in column 1 designates those stars considered by Trumpler to be very probably members of the cluster. The stars marked with a cross in the same column are possible members, but for them no radial velocities are available.

Figure 1 shows the result of a comparison of Pg_p with the photographic magnitudes derived by Trumpler,[2] $Pg(T)$. The differences, $Pg_p - Pg'(T)$, where $Pg'(T) = Pg(T) - 0^m.10$, are plotted against Pg_p. The correction of -0.10 mag. to Trumpler's magnitudes forces agreement of the two scales over the same range, 5.9–8.3 mag., as the Pg_p's were adjusted to Pg_{int} in Paper I. If the Pg_p's are adjusted to Pg_{int} at 6.0 mag. in

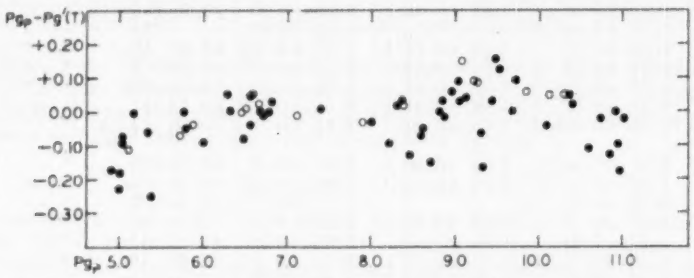

FIG. 1.—A plot of Pg_p against the photographic magnitudes given by Trumpler, $Pg'(T)$, where $Pg'(T) = Pg(T) - 0^m.10$. The open circles indicate $Pg_p - Pg_{int}$ for stars of the North Polar Sequence.

the North Polar Sequence, we must add 0.07 mag. to Pg_p, which leaves a zero-point difference, $Pg(T) - Pg_{int}$, of $+0.03$ mag. The open circles in Figure 1 represent the values of $Pg_p - Pg_{int}$ for stars in the North Polar Sequence as taken from Paper I.

The color-luminosity array for the cluster is shown in Figure 2. The solid portions of the curves are taken from the color-luminosity arrays given for the Hyades and the Pleiades stars in Papers I and II, respectively; the dashed portion is an extension indicated by stars in the Coma Berenices cluster. The adjustment of the color-magnitude array of the Coma Berenices cluster stars to the color-luminosity arrays derived in Papers I and II gave a modulus $m - M = 4.50$ mag. for the cluster; the corresponding parallax is $0''.0126$. The only available trigonometric parallaxes for cluster stars are apparently those for six stars observed at the Allegheny Observatory; the mean is $+0''.0125 \pm 0''.0025$. The stars in Figure 2 include thirty-six of the thirty-seven stars considered by Trumpler to be certainly cluster members. Since it is necessary to use a rather large diaphragm in the photometer, because of the color-curves of the 12-inch and 15-inch refractors, the remaining star, Trumpler No. 92, which lies near a bright star, was excluded because of possible influence on its light by the brighter companion. Of the nine stars in Figure 2 indicated by crosses, there are eight that deviate from the various sequences populated by the Hyades and the Pleiades stars. Seven of these eight stars are known binaries for which there is the following additional information.

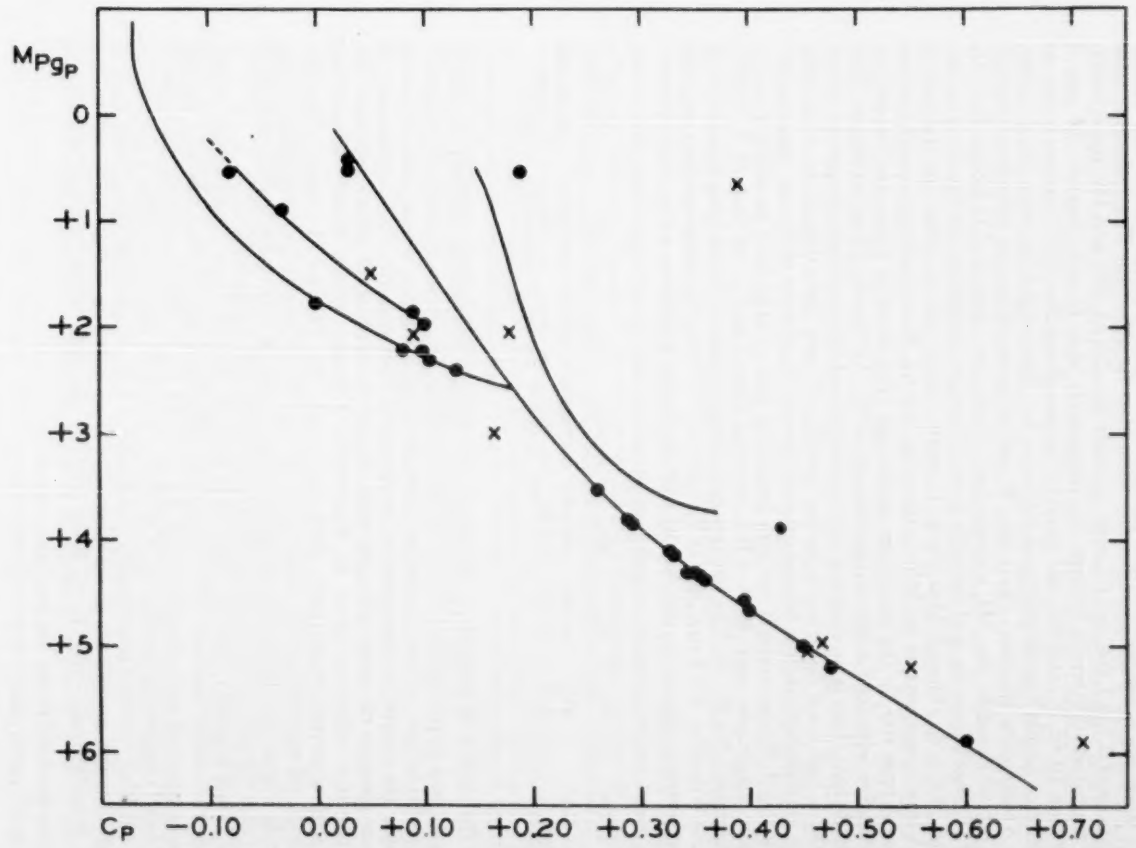

FIG. 2.—The color-luminosity array for the stars in the Coma Berenices cluster. The curves are taken from the color-luminosity array defined in Papers I and II by the stars in the Hyades and the Pleiades clusters. The crosses indicate eight known binaries and one possible nonmember of the cluster.

1. *Variable velocity.*—Stars Nos. 10, 65, 97, 102, and 150 show large variations in radial velocity, with ranges of 48, 24, 61, 54, and 41 km/sec, respectively, from five plates per star.[2] With one exception, star No. 97, these stars lie above the dwarf sequence with deviations of 0.2, 0.2, 0.4, and 0.7 mag. for stars Nos. 10, 65, 102, and 150, respectively. The magnitude differences between the components must be quite large in the case of stars Nos. 10, 65, 97, and 102, and small in the case of star No. 150. Trumpler makes no mention of double lines in spectra of the latter, but this star is faint, with $Pg_p = 10^m40$.

2. *Spectroscopic binaries.*—Stars Nos. 91 and 144 are spectroscopic binaries with available orbital elements. No. 144, a single-lined binary, has a period of 11.8 days. Star No. 91, 12 Comae Berenices, is of special interest. Trumpler states that the spectrum is composite, gF4 + A, although Miss Vinter Hansen[3] was not able to detect spectral lines of the A-type component on the Mills three-prism spectra. More recently, a search for lines of the A-type star, in the ultraviolet region, has been made by Cesco and Sahade[4] on plates taken with the Cassegrain spectrograph of the McDonald 82-inch reflector. They conclude that there is no evidence for the spectrum of the secondary component except for the K line, *Ca* II 3933, which gave a velocity differing from that of the other lines. From unpublished magnitudes and colors of stars in the vicinity of the sun, made in connection with this program, it has been found that giant F stars have an absolute photographic magnitude near $M = +2^m5$, whereas from Table 1 we find $M = +0^m66$, photographic, for No. 91. The spectroscopic absolute magnitude has been determined at Mount Wilson[5] as +2.4 mag., and at Victoria[6] as +3.1 mag. We might compare, as in the accompanying tabulation, star No. 91 with 31 Comae Berenices, a star which lies out-

Star	Pg_p	C_p	MPg_p	$\mu_\alpha \cos\delta$	μ_δ	$\pi(t)$	ρ(Km/Sec)$^{-1}$
91 (12 Com)	5^m16	+0.39	+0.66	−0″010	−0″018	+0″011±6	+0.48 orbit
31 Com	5.50	+0.53	+1.00	− .013	− .024	+ .010±7	−1.6±0.8
Cluster				−0.013	−0.017	+0.012±3	−0.4

side the cluster as defined by Trumpler, but which, nevertheless, satisfies the radial velocity and proper-motion criteria of membership. The values for the proper motion and radial velocity of the cluster are those given by Trumpler. We see that 31 Comae satisfies the criteria for membership as closely as does star No. 91. Furthermore, 31 Comae presents the same difficulty with respect to its absolute magnitude, since the spectroscopic values are given as +2.3 and +2.0 mag. by the Mount Wilson[5] and Victoria[6] observers, respectively. Both 12 Comae (No. 91) and 31 Comae, therefore, probably are members of the cluster; their relation to the color-luminosity array, as defined in Figure 2, will become clearer in a later paper of this series dealing with those stars near the sun which are associated with W. Baade's[7] population II.

3. *Visual binaries.*—Star No. 109, ADS 8539, is the only close visual binary known among the cluster members. The components differ by about 1.0 mag. visually. The observed magnitude and color of the pair, $Pg_p = 6^m55$, $C_p = +0.18$, could be produced by two dwarf components having $Pg_p = 6^m80$, $C_p = +0.16$, and $Pg_p = 7^m65$, $C_p = +0.25$. The resulting absolute magnitudes, +2.30 and +3.35, would then place these stars in Figure 2 as the only dwarfs in the interval of $M = +0^m5$ to $+3^m5$.

4. *Miscellaneous.*—Star No. 82 is the only one that falls below the dwarf sequence in

[3] *Lick Obs. Bull.*, **19**, No. 504, 101, 1940.

[4] *Ap. J.*, **99**, 317, 1944.

[5] Adams, Joy, Humason, and Brayton, *Ap. J.*, **81**, 187, 1935; *Mt. W. Contr.*, No. 511.

[6] Young and Harper, *Pub. Dom. Ap. Obs. Victoria*, **3**, 1, 1924.

[7] *Ap. J.*, **100**, 137, 1944; *Mt. W. Contr.*, No. 696.

Figure 2. If this star is a cluster member, it is anomalous. There is, however, the possibility that, out of the thirty-seven stars considered to be members on the basis of the proper-motion and radial-velocity criteria, at least one may be a background object. For the present we shall therefore consider star No. 82 as a nonmember of the cluster.

Star No. 125 is 14 Comae, and a discussion of the spectrum of this star has been published by W. W. Morgan,[8] who has called attention to the fact that it possesses both diffuse and sharp lines. A later discussion of spectra taken with the 82-inch reflector at the McDonald Observatory has been published by Struve and Swings,[9] who propose the existence of a gaseous shell to explain the anomalies pointed out by Morgan. Struve and Swings state that the underlying photosphere is that of a main-sequence A5 star—the latest spectral type known to possess a shell—and they also classify the shell spectrum as of somewhat later type: "Except for the effect of dilution, the spectrum of the shell superficially resembles that of a supergiant star of spectral type F. . . ."[9] We may recall from Paper II that a shell star in the Pleiades—Pleione—was reddened 0.03 mag. relative to the blue-dwarf sequence with which it probably is associated. If we attribute this reddening to the effect of the shell, we see that the same phenomenon would explain the displacement of star No. 125 from the bright-dwarf sequence. We should then expect the underlying star to be of spectral and luminosity class A5–A7 III and to possess a high rotational velocity. Struve and Swings state: "The line λ 4481 (*Mg* II) is present only in the reversing layer, as a very diffuse and shallow band whose rotational broadening corresponds to about 200 km/sec."[9]

The remaining twenty-eight stars, plotted in Figure 2 as filled circles, consist of seventeen dwarfs, one bright-dwarf, five blue-dwarfs, and five bright blue-dwarfs. Among the latter are two stars of particular interest: No. 146 (17 Comae) and No. 160 (21 Comae). Both stars are in the catalogue of spectrum variables compiled by A. Deutsch.[10] The spectra have been discussed by Morgan[11] as follows:

17 Comae.—This star also belongs to the "Chromium" group. *Cr* II 4558 varies from an intensity decidedly greater than λ 4549 to approximate equality with λ 4555. The line *Sr* II 4215 varies even more in intensity than does *Cr* II 4558. The star is considered peculiar in the *Henry Draper Catalogue* because of the strength of the *Si* II doublet λ 4128 and λ 4131. The doublet is very faint and the violet component seriously blended on Yerkes plates.

21 Comae.—The line *Sr* II 4215 is about equal in intensity at minimum to λ 4198 and λ 4481. At maximum intensity it is far greater than these lines and is much stronger than any other line in the spectrum with the exception of the Balmer series and the other member of the ultimate *Sr* II doublet at λ 4077. The last-named line is also probably variable, but the plates are weak in this region and it is not possible to decide with certainty.

Trumpler also noted the abnormal strength of the *Sr* II lines in star No. 160. Furthermore, Deutsch[10] states that star No. 145, which is 145″ from No. 146 (17 Comae), is a metallic-line star. Since the absolute magnitude and color of No. 145, $M = +2^{m}.20$, $C_p = +0.11$, are similar to the values for stars Nos. 68, 104, and 139, we might expect these stars also to be metallic-line objects. This expectation might also include the spectroscopic binary, No. 144, mentioned above.

There are five stars in Table 1 for which the proper-motion data indicate cluster membership but for which no radial velocities are available. The numbers given these stars in column 1 are preceded by a cross, and they are plotted in Figure 3 as crosses. The continuous curve in Figure 3 is taken from the Hyades color-luminosity array given in Paper I; the small dashed curve in the diagram indicates a portion of the subdwarf sequence defined by stars in the Hyades and in the vicinity of the sun.[12] We see that three of these stars—Nos. 132, A14, and A21—probably are cluster members. Also, if star No.

[8] *Ap. J.*, **76**, 144, 1932.

[9] *Ap. J.*, **94**, 305, 1941.

[10] *Ap. J.*, **105**, 283, 1947.

[11] *Ap. J.*, **76**, 275, 1932.

[12] Eggen, *Pub. A.S.P.*, **61**, 258, 1949.

A13 is a member of the cluster, it may be a subdwarf similar to star No. 7 in the Hyades (BD+19°641) and to μ Cassiopiae,[12] a high-velocity star in the solar region. Also plotted in Figure 3 are three stars for which cluster membership is all but ruled out by their proper motions. These three stars—Nos. 54, 147, and 192—are indicated by open circles, and, as expected, none appears to be a member of the cluster. Stars Nos. 175 and 193, for which neither radial velocity nor proper motion is available, are also indicated by open circles. If star No. 175 is a cluster member, it also may be a subdwarf. An inspection of Appendix A to Trumpler's catalogue[2] indicates the possibility that several stars, fainter than magnitude 11, which satisfy the proper-motion criterion, remain to be added as cluster stars; some of these may be subdwarfs.

URSA MAJOR CLUSTER

The recognition of the common proper motions of β, γ, δ, ϵ, and ζ Ursae Majoris extends back to the work of R. A. Proctor.[13] The common radial velocities of β, ϵ, and ζ Ursae Majoris were first discussed by H. Ludendorff.[14] E. Hertzsprung[15] later suggested

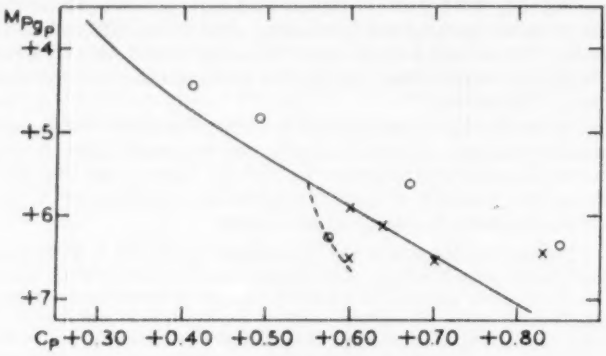

FIG. 3.—The crosses represent the five stars in Table 1 for which the proper-motion data indicate cluster membership but for which no radial velocities are available. The open circles represent three stars for which membership would not be expected from the proper-motion data, plus two stars for which neither radial velocities nor proper motions are available. The short broken curve indicates a portion of the subdwarf sequence.

that the group was much more extensive than previously supposed, and he added a few stars widely scattered over the sky, the most notable being Sirius. Subsequent researches have tended to increase the size of the group; for example, in a recent discussion, Miss Nancy Roman[16] considers a nucleus containing eleven stars within 9 parsecs of the nucleus and an additional twenty-one stars lying within 135 parsecs of this nucleus. In what follows we shall refer to the nucleus stars as the "nucleus cluster." A study of the concentration of the space velocities of the A and F stars around the Ursa Major group velocity, by J. Delhaye,[17] indicates the existence of a preferential motion in the same direction with a dispersion between 2 and 3 km/sec in each co-ordinate. We may recall that G. Strömberg[18] had suggested this possibility as early as 1926. If these stars form an extended cluster, the dispersion in space and in velocity is greater than that found in any known cluster. Delhaye appears to prefer an alternative hypothesis: "that of a

[12] *Proc. R. Astr. Soc., London*, **18**, 169, 1869.
[13] *A.N.*, **180**, 265, 1909.
[14] *Ap. J.*, **30**, 135, 1909.
[15] *A.J.*, **53**, 116, 1948.
[16] *B.A.N.*, **10**, 409, 1948.
[17] *Ap. J.*, **57**, 77, 1923.

preferential motion amongst the early-type stars in a direction near that of the velocity of the Ursa Major nucleus, the nucleus stars forming a small cluster, which follows that preferential motion."[18]

The present discussion is based upon magnitudes and colors of nine of the eleven nucleus stars; the two stars omitted are the close visual components of ζ Ursae Majoris, which are not resolvable with the 12-inch photometer. The extended group will be discussed in a subsequent paper of this series. The nine stars observed are listed in Table 2; all observations were made with the Lick 12-inch refractor.

We may apply three criteria to establish membership in a cluster: (1) proper motion, (2) radial velocity, and (3) the absolute magnitude or parallax deduced from the color-luminosity array.

TABLE 2

URSA MAJOR, NUCLEUS STARS

Star	α (1900)	δ (1900)	μ*	θ	Wt.	ρ* (Km/Sec)	Wt.	$P\varepsilon_p$	C_p	Sp.
37 UMa	10^{h}32^{m}0	+57° 20′	0".074	64°.5	2	− 9.8	5	5.33	+0.27	F1V
β UMa	10 58.8	+56 39	.087	71.7	3	−12.5	5	2.23	− .05	A0V
γ UMa	11 51.2	+53 58	.094	87.8	3	−13.6	2	2.31	− .06	A0V
δ UMa	12 18.0	+57 19	.106	88.6	3	−14.6	1	2.28	+ .05	A3V
ϵ UMa	12 51.8	+56 14	.114	95.5	3	− 8.0	2	1.62	− .11	A0p
78 UMa	12 58.6	+56 38	.115	97.9	2	− 8.7	3	5.08	+ .30	F0V
80 UMa	13 23.2	+55 15	.120	101.3	2	− 9.1	1	4.05	+ .13	A5V
HR 4867	12 46.5	+60 36	.107	92.8	1	−10.2	1	6.13	+ .36	F6V
HD 115043	13 11.6	+56 58	0.115	107.5	1	− 7.9	2	7.27	+0.53	G2V

* The proper motions and the radial velocities, with their respective weights, have been taken from Petrie's paper, *Pub. Dom. Ap. Obs. Victoria*, **8**, 117, 1949.

1. *Proper motion.*—To test for membership the nine stars of Table 2 by criterion 1, we consider two recent determinations of the convergent point of the cluster:

$$a) \quad A = 298°.0 \pm 5°.7, \qquad D = -31°.6 \pm 6°.2;$$

$$b) \quad A = 307.5 \pm 0.9 \qquad D = -39.3 \pm 0.5,$$

of which convergent a was derived by R. M. Petrie[19] from the nucleus stars alone, while b was obtained by W. M. Smart[20] from a consideration of the nucleus stars plus several "members" of the extended group. Petrie used the two conventional methods of finding the convergent from the proper motions, one following the solution of Charlier and the other that of Bohlin. Although the two solutions are merely different arrangements of a fundamental relation, Petrie found widely differing convergents. He concluded: "The explanation appears to be that, in solving [Charlier's and Bohlin's] equations, different quantities are minimized. The answers differ by a considerable amount because the proper motions, being nearly the same for all stars, produce a nearly indeterminate solution."[19] Since the criterion of the best convergent to be derived from the proper motions is that it should represent the position angles of those motions with a minimum of disagreement, Petrie derived the convergent a, above, by a differential method which corrected a preliminary value so as to minimize the sum of the weighted differences between the observed and computed position angles, θ, of the proper motions. The probable errors of A and D for convergent b are smaller than those for a, since b was derived from more stars, widely scattered. Table 3 contains the residuals, $\Delta\theta$, of the position angles, in the

[19] *Pub. Dom. Ap. Obs. Victoria*, **8**, 117, 1949. [20] *M.N.*, **99**, 441, 1939.

sense of observed *minus* computed, for the two convergents *a* and *b*. We should expect convergent *a* to give the better fit because of the manner in which it was derived.

2. *Radial velocity.*—From the observed radial velocities, given in Table 2, and the expression

$$\rho = V \cos \lambda ,$$

we find that the weighted mean value of the cluster velocity is $V = 15.8$ km/sec for convergent *a* and $V = 13.0$ km/sec for convergent *b*. The residuals, observed ρ *minus* computed ρ, are given as $\Delta\rho_1$ in Table 3. We find that convergent *a* and convergent *b* with these two values for the cluster velocity satisfy the observed proper motions and radial velocities about equally well.

3. *Color-luminosity array.*—In Figure 4 the principal sequences in the color-luminosity array of Figure 2 are shown with the stars in Table 2 plotted as open circles after their luminosities had been computed with an assumed mean parallax of 0".0470. This parallax, then, must be reasonably well duplicated by the mean of the values of

$$\pi = \frac{4.738\mu}{V \sin \lambda} .$$

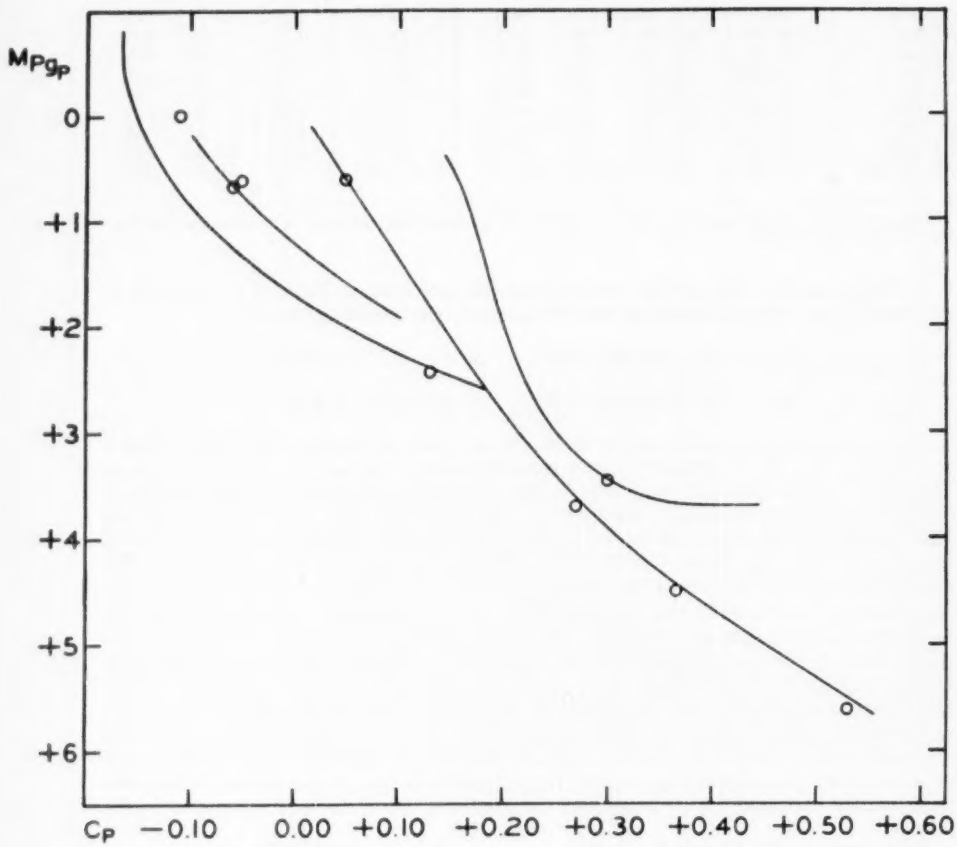

FIG. 4.—The color-luminosity array for the Ursa Major nucleus cluster with luminosities derived from a mean parallax of 0".0470.

determined from the convergent and space velocity of the cluster. We find from convergent *a*, with $V = 15.8$ km/sec, a mean parallax of 0".040 for the stars in Table 2; this value would cause all these stars to lie about 0.35 mag. below the color-luminosity array of Figure 4. Similarly, from convergent *b*, with $V = 13.0$ km/sec, we derive a mean parallax of 0".059; this value would place the stars of Table 2 about 0.45 mag. above the color-luminosity array of Figure 4.

If, instead of solving for the parallax, we use the relation in the form

$$V = \frac{4.738\mu}{\pi \sin \lambda}$$

to derive the cluster velocity necessary to give a mean parallax of 0".0470, that is to say, to satisfy the color-luminosity array, we find $V = 13.4$ km/sec for convergent *a* and $V = 16.0$ km/sec for convergent *b*. The residuals in ρ, derived with these values of V,

TABLE 3

RESIDUALS FROM CONVERGENTS *a* AND *b*

STAR	CONVERGENT *a*				CONVERGENT *b*			
	λ	$\Delta\theta$	$\Delta\rho_1$* (Km/Sec)	$\Delta\rho_2$* (Km/Sec)	λ	$\Delta\theta$	$\Delta\rho_1$† (Km/Sec)	$\Delta\rho_2$† (Km/Sec)
37 UMa	142°.5	+0°.5	+2.7	+0.8	153°.3	+2°.5	−1.9	+4.5
β UMa	139.4	−0.4	−0.5	−2.3	150.2	0.0	−1.2	+1.4
γ UMa	132.5	+0.6	−2.9	−4.6	143.4	+0.1	−3.1	−0.8
δ UMa	129.3	−0.3	−4.6	−6.1	140.2	+0.5	−4.5	−2.3
ϵ UMa	123.9	−1.9	+0.8	−0.5	134.8	−1.4	+1.3	+3.3
78 UMa	123.1	−0.5	−0.1	−1.4	134.0	+0.2	+0.5	+2.4
80 UMa	119.4	−2.7	−1.3	−2.5	130.3	−2.1	−0.4	+1.3
HR 4867	125.1	−0.6	−1.1	−2.5	135.9	+1.3	−0.7	+1.5
HD 115043	121.4	+6.7	+0.3	−0.9	132.3	+7.7	+1.0	+2.9

* $\Delta\rho_1$ assumes $V = 15.8$ km/sec; $\Delta\rho_2$ assumes $V = 13.4$ km/sec.
† $\Delta\rho_1$ assumes $V = 13.0$ km/sec; $\Delta\rho_2$ assumes $V = 16.0$ km/sec.

are given as $\Delta\rho_2$ in Table 3. We may recall that, in computing convergent *b*, Smart found that a cluster velocity of 19.1 km/sec, derived from the parallax and proper motion of Sirius—one of the stars of the extended group—gave the best fit to the observed radial velocities of the stars he used. Smart included several "members" of the extended group in his solution, and, as a result, his value of V left a preponderately large number of positive residuals for the nucleus stars.

To summarize, then, although convergents *a* and *b* satisfactorily represent the observed proper motions, the observed radial velocities place the cluster at a distance which is greater (convergent *a*) or smaller (convergent *b*) than that demanded by the color-luminosity array of Figure 4. In other words, the radial-velocity and parallax criteria cannot be satisfied simultaneously for either of the two convergents in question. It was therefore suspected that values for A and D intermediate between those of convergents *a* and *b* not only might maintain the fit to the proper motions but would also satisfy the other two criteria. To this end, the following convergent was assumed:

$$A = 302°, \qquad D = -35°,$$

which we shall refer to as "convergent *c*." From the λ's computed with convergent *c* and the observed velocities, we obtain $V = 14.3$ km/sec; the resulting mean parallax is 0".0471, which agrees with that required by the color-luminosity array. The individual parallaxes, computed from the proper motions, are listed in Table 4, together with their corresponding absolute magnitudes. The available trigonometric parallaxes are given

in the last three columns of Table 4 for comparison. The resulting fit to the color-luminosity array of these nine stars of the nucleus cluster is shown in Figure 5. One or two of the stars deviate from the array by as much as 0.1 mag., but an error of 0".005 in the proper motions, or ±0.01 mag. in color, could easily account for these departures. A better fit might be obtained from slightly different values for A and D, but convergent c is sufficiently accurate for the present purpose.

Since the above discussion of the nucleus cluster was written, the results of a comprehensive study of the Ursa Major group have been published by Miss Nancy Roman.[21] The spectral types listed in Table 2 are taken from her work. Miss Roman added to the nucleus cluster three stars that have not been observed on the present program. With the use of a method similar to that described by Petrie,[19] she derived the values $A = 306°.2$, $D = -37°.1$ for the convergent of the nucleus stars; these values are nearer to those for convergent b, derived by Smart, than to those for convergent a, given by Petrie. From the observed radial velocities of the nucleus stars and her convergent, Miss Roman determined

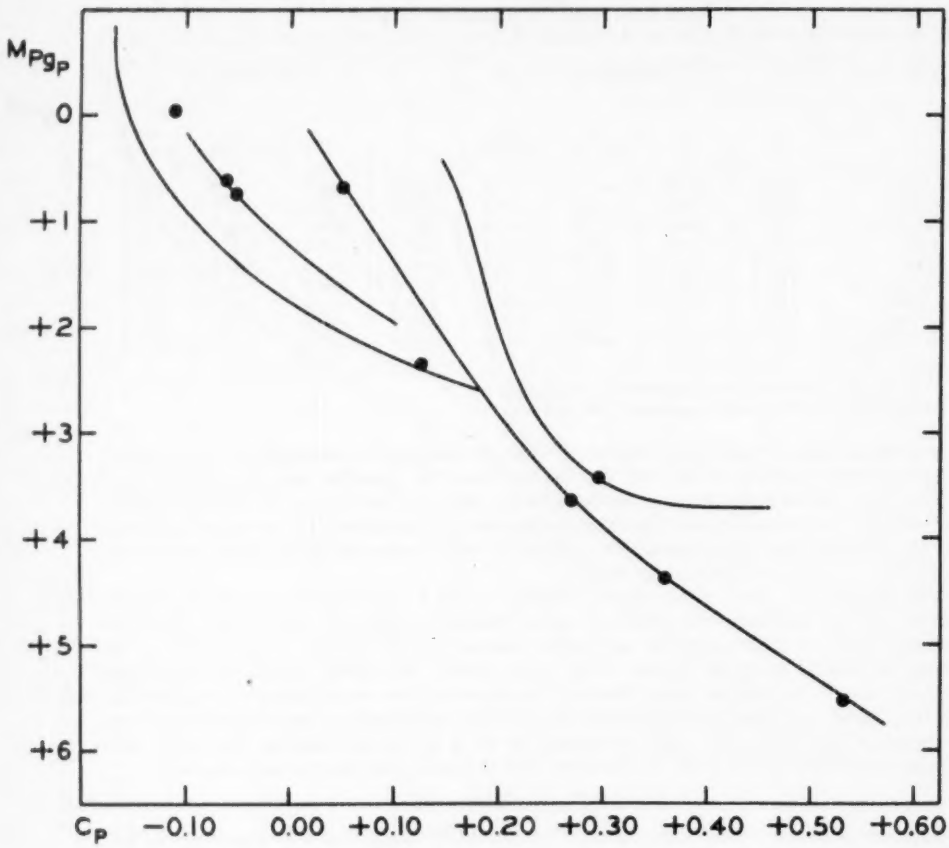

FIG. 5.—The final color-luminosity array for the Ursa Major nucleus cluster obtained from the convergent $A = 302°$, $D = -35°$, a mean cluster velocity of 14.3 km/sec, and individual proper motions.

[21] *Ap. J.*, 110, 205, 1949.

the speed of the cluster as 15.7 ± 0.8 km/sec. The deviations of the observed position angles of the proper motions and of the radial velocities from the computed values based on these constants are given in Table 5. Also, Table 5 lists the computed parallaxes for the stars in Table 2. The mean value of the computed parallax, 0".0465, is in excellent agreement with the value 0".0470 which we found above to be required by the color-luminosity array. The fact that all three criteria for cluster membership are satisfied about equally well by convergent c and by that derived by Miss Roman is consistent

TABLE 4

RESIDUALS, PARALLAXES, AND LUMINOSITIES COMPUTED FROM CONVERGENT c

STAR	λ	$\Delta\theta$	$\Delta\rho$ (Km/Sec)	CLUSTER PARALLAX	Mp_{gv}	TRIGONOMETRIC PARALLAX		
						Allegheny	McCormick	Mount Wilson
37 UMa	147°.2	+1°.7	+2.2	0".0453	3.58	0".033±11	.....	.....
β UMa	144.1	+0.2	−0.9	.0492	0.66	.047± 6	0".029±10	.....
γ UMa	137.3	+0.8	−3.1	.0459	0.59	.027± 7	.002± 9	.....
δ UMa	134.1	+0.4	−4.6	.0489	0.70	.050± 6	.068±14	.....
ϵ UMa	128.5	−1.9	+0.9	.0482	0.01	.....	.....	.....
78 UMa	127.6	−0.5	0.0	.0481	3.46	.030±10	.....	.....
80 UMa	124.2	−2.4	−1.1	.0480	2.45	.039± 9	0.033±11	.....
HR 4867	129.8	+0.2	−1.0	.0462	4.41	0.038±10	.....	0".041±11
HD 115043	126.2	+7.0	+0.5	0.0476	5.63	.....	.....	0.045± 9
Weighted means	.....	±1.4	±1.4	0".0471	.....	.....	.....	.....

TABLE 5

RESIDUALS AND PARALLAXES FOR THE NUCLEUS STARS, WITH THE CONVERGENT AT $A = 306°.2$, $D = -37°.1$, AND $V = 15.8$ KM/SEC

Star	$\Delta\theta$	$\Delta\rho$* (Km/Sec)	π_c	Star	$\Delta\theta$	$\Delta\rho$* (Km/Sec)	π_c
37 UMa	+ .5	+1.2	0".0462	80 UMa	−2.4	+0.5	0".0461
β UMa	−0.1	+1.9	.0503	HR 4867	+2.2	−2.9	.0447
γ UMa	−0.1	−1.2	.0455	HD 115043	+2.3	+1.6	0.0454
δ UMa	+0.5	−4.4	.0480				
ϵ UMa	−2.5	+3.7	.0465	Weighted means	±1.4	±1.5	0.0465
78 UMa	−0.8	−0.5	0.0462				

* These residuals are obtained from the radial velocities given by Miss Roman for the nucleus stars; these $\Delta\rho$'s differ slightly from those taken from Petrie's work and listed in Table 2.

with Petrie's statement, quoted above, that the convergent point of the motions of the nucleus stars is nearly indeterminate. Miss Roman has used the trigonometric parallaxes of the nucleus stars as a distance criterion to check the cluster velocity, with the result that a cluster speed of 18.4 km/sec is required to satisfy the observed parallaxes. She has adopted 17.0 km/sec as a mean value between the two values 15.7 and 18.4 km/sec. Since, however, the color-luminosity array probably is preferable to the trigonometric parallaxes as a distance criterion, we may assume that the cluster speed derived by Miss Roman from the observed radial velocities is the best determinable at the present time. Miss Roman's work will be considered more extensively in a future paper of this series concerned with the extended Ursa Major group.

THE MOVING CLUSTER IN PERSEUS

NANCY G. ROMAN AND W. W. MORGAN
Yerkes Observatory
Received December 21, 1949

ABSTRACT

The visual clustering around α Persei is examined. This supergiant and twenty-five other stars of types B3–A2 appear to be members of a cluster, about 180 parsecs from the sun, which is moving with a velocity of 16 km/sec toward $l = 215°$ and $b = +17°$. There is no evidence of an appreciable number of fainter cluster members. Five other stars within 35 parsecs of α Persei may also share the cluster motion, but the evidence is not conclusive.

From a study of the B-type stars contained in the PGC, Eddington,[1] Boss,[2] and Kapteyn[3] independently announced that many of the stars in and near Perseus appear to form a moving cluster or stream. Eddington listed sixteen members of this group, fourteen of which are within 60 square degrees. Backhouse[4] noted that nine of these stars form part of a prominent naked-eye cluster which Trumpler describes as "a moderately rich cluster of 50–100 members, composed of bright and faint stars, not well detached but passing gradually into the environs."[5] In 1921 Rasmuson extended the list of members of the group to include forty-five stars of all spectral types, scattered over 5 hours of right ascension.[6] These stars were chosen primarily on the basis of the direction of the proper motion.

In one of a series of papers on the reality of the various moving clusters, Smart and Ali studied this extended list of members.[7] Since the stars in Eddington's list were too concentrated in the sky to determine the convergent of their motion, Smart and Ali determined this position from the entire list of forty-eight stars. The resulting position agreed well with the directions of the individual motions. The radial velocities of the cluster members are small and poorly determined; thus the distance of the cluster must be obtained from spectroscopic parallaxes. Smart and Ali decided that the individual differences between the cluster parallaxes and the spectroscopic parallaxes were not large enough to invalidate the assumption of common space motion for the stars. Next they considered the radial velocities. The average residual from common motion was approximately 4 km/sec, from which Smart and Ali concluded that *all* the stars considered could not form a moving cluster. To test the possibility that some of the stars might form a cluster, they used the values of the space motion and the K term which they had determined from the forty-eight stars, a group which they had concluded had no physical significance. In this way they distinguished sixteen possible members of the cluster, but these showed no concentration in the sky, and only five had been included in Eddington's original list. Had Smart and Ali used the motion of α Persei as representative of the group or that of several of the B-type stars listed by Eddington which are within the visual cluster, they would have found good evidence for the reality of this smaller group.

Figure 1 is a small-scale photograph of the region near α Persei. A clustering is apparent. The center lies about 5° south of the galactic equator, near a region of moderately heavy absorption. The colors of the cluster stars indicate that the cluster may be behind

[1] *M.N.*, **71**, 43, 1910.
[2] *A.J.*, **26**, 163, 1910.
[3] *Trans. Internat. Solar Union*, **3**, 215, 1910.
[4] *M.N.*, **71**, 523, 1911.
[5] *Lick Obs. Bull.*, **14**, 154, 1930.
[6] *Lund Medd.*, Ser. II, No. 26, p. 28, 1921.
[7] *M.N.*, **100**, 560, 1940.

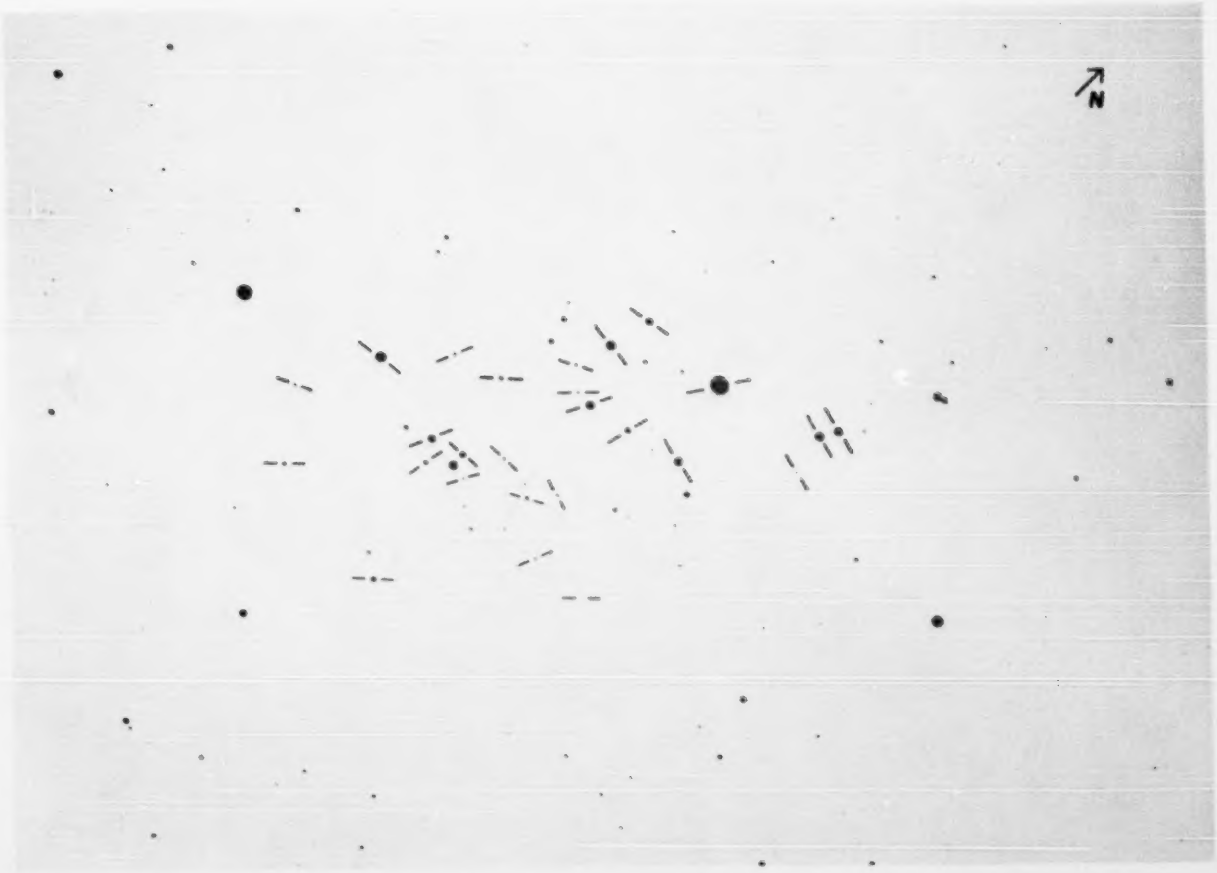

FIG. 1.—The region of α Persei, enlarged about 29× from a Leica negative. Cluster members are marked. The field illustrated is approximately 6° by 8° in size.

this absorption, but this is probably not the cause of the apparent clustering. Within the area covered by the cluster, 60 per cent of the GC stars share the proper motion of α Persei, while this percentage is only 12 per cent in the surrounding area. Moreover, among the HD stars in the clustering, there is a fairly good correlation between spectral type and apparent magnitude, while there is no such correlation in the surrounding area.

Figure 2 is a plot of the proper motions of all stars brighter than 6.5 mag. of types B5 and earlier between the right ascensions 2^h40^m and 4^h and between the declinations $+30°$ and $+60°$. The stars within the clustering are plotted as open circles. It is obvious that these stars are moving together. On the other hand, the motions of the remaining stars in the diagram show no concentration. A study of the motions of the B-type stars in the more extended region covered by Rasmuson leads to the same conclusion; there is no evidence of the concentration of these motions toward the motion of the Perseus or any other cluster.

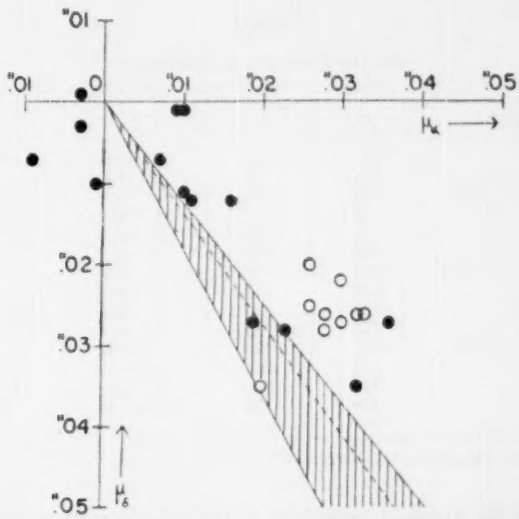

FIG. 2.—The proper motions of the O–B5 stars brighter than 6.5 mag. between the right ascensions 2^h40^m and 4^h and between the declinations $+30°$ and $+60°$. The stars within the visual clustering are indicated by open circles. The shaded area is the range of the direction of parallactic drift in the region covered by the diagram; the dashed line is the direction of parallactic drift near α Persei.

Proper motions were collected for as many as possible of the HD stars within the clustering. For those not included in the GC or the EBL II, motions were computed from the positions given in the *Geschichte des Fixsternhimmels* and the *Index der Sternörter*, corrected and weighted according to the GC system. All motions were then reduced to the corrected GC system.[8] Forty per cent of the proper motions available for stars within the concentration are consistent with cluster membership, although the uncertainty in these motions is large for many of the fainter stars.

The proper-motion data are probably complete to the eighth magnitude, but it is desirable to know whether there are many fainter cluster members. Plates of the field of α Persei taken in 1908 and 1913 with the 40-inch refractor were available, and Mr. Frank Edmonds kindly obtained an additional plate of this field. On each plate the magnitude

[8] Blaauw and Delhaye, *B.A.N.*, **10**, 473, 1949.

of α Persei had been reduced to that of a ninth-magnitude star by means of a rotating sector. The proper motions of thirteen stars within 15′ of α Persei and between 9 and 11 mag. were measured and are given in Table 1. These motions were measured with respect to the mean motion of seven stars of intermediate magnitude; the difference between the corrected GC motion of α Persei and its measured relative motion was then added to the motion of each star to reduce it to the corrected GC system. The mean error of the relative motions is approximately ±0″.002/year. It is seen that none of the stars measured share the proper motion of α Persei. While this does not exclude the existence of fainter cluster members outside the region covered by these plates, such stars are probably not numerous. This is consistent with the indication on the photograph that the clustering does not extend to stars fainter than 7.5 mag.

For the 29 stars selected on the basis of proper motion and space position, Table 2 gives the name, HR number or HD number, the observational data with their

TABLE 1

PROPER MOTIONS NEAR α PERSEI

BD+49°	X	Y	μ_X	μ_Y
	27	40	−0″.010	+0″.007
911	31	60	− .002	− .004
912	38	160	+ .011	+ .006
	69	124	+ .006	+ .005
913	73	116	+ .031	− .037
917*	100	109	+ .027	− .024
921	141	88	+ .019	− .028
922	147	75	+ .005	− .013
923	153	182	+ .008	+ .001
924	154	25	+ .019	− .002
926	167	148	.000	− .005
927	173	181	+ .054	− .036
	176	161	+ .014	− .007
	199	154	+0.060	−0.029

* α Persei. The corrected GC motion has been assumed for this star.

mean errors, and the absolute magnitude derived from cluster membership. The two-decimal magnitudes have been taken from the HD; the remainder are visual magnitudes estimated from a photograph of the cluster and the adjacent selected area, No. 23. The selected-area magnitudes used were those from the *Bergedorfer spektral Durchmusterung*, which contains more bright stars than the Harvard or the Mount Wilson sequences. Only A-type stars were used, and the magnitudes of these stars were first reduced to visual magnitudes by applying the appropriate color indices.

Although colors have been published by Stebbins, Huffer, and Whitford for nine of the brighter stars,[9] the color data are not as numerous as would be desirable. The range of 0.1 mag. in color excess across the cluster and particularly the large color excess for HR 1047 indicate that the absorption in front of the cluster is not uniform. However, the magnitudes of the stars for which no colors have been published have been corrected by 0.5 mag.

The radial velocities are in fair agreement. Many of the stars have poor lines, and the uncertainties in their velocities are large. HR 1029 may be an exception. The lines in this star are moderately good, and the discrepancy may be large enough to indicate that

[9] *Ap. J.*, **91**, 20, 1940.

this star is not a member of the cluster, although the remaining evidence opposes this conclusion. Allowing 1 km/sec as the relativity shift for the B-type stars and giving α Persei a weight equal to that of the other thirteen stars, we obtain −1.3 km/sec as the radial velocity of the cluster.

Figure 3 illustrates the HR diagram for the cluster. A distance modulus of 6.3 mag. fits the observations well. The three stars plotted as open circles are probably not cluster members, although the possibility of large absorption in front of HD 21942 is not excluded. For the remaining stars on the diagram, the spectroscopic evidence strongly

TABLE 2

OBSERVATIONAL DATA FOR THE CLUSTER STARS

Name	μ		θ	ρ	m	E_1	m_{cor}	Sp.	M
29 Per	0".042	±0".005	128°.3*	− 5.1±2.6 V	5.30	+0.07	4.8	B3 V	−1.5
HD 20391	.030	.033	120.0†		7.90		7.4	A1 V	+1.1
31 Per	.036	.004	133.9*	+ 3 6	5.08	.03	4.9	B5 V	−1.4
HD 20475	.02		117 ‡		8.7		8.2	F2 V	+1.9
HD 20701	.028	.033	132.2†		7.8		7.3	A1 V	+1.0
HR 1011	.033	.006	127.6*	+ 4.8 2.0	5.30	.05	5.0	B5 V	−1.3
α Per	.036	.001	131.6*	− 2.4 0.2	1.90		1.4	F5 Ib	−4.9
HD 20961	.041	.012	129.1§		7.60		7.1	A0 V	+0.8
HR 1029	.037	.008	126.3*	+ 9.0 1.5	5.91	.06	5.5	B6 V	−0.8
HD 21091	.039	.015	111.2§		7.55		7.1	A0 V	+0.8
HD 21181	.042	.035	125.2*		6.87		6.4	B9 V	+0.1
HR 1034	.040	.005	135.0*	+ 7.1 3.2 V	4.94	.13	4.0	B3 V	−2.3
HR 1037	.041	.006	129.1*	0 9 V	5.64	.09	5.0	B6 V	−1.3
HD 21375	.038	.003	148.0†		7.3		6.8	A1 V	+0.5
HD 21398	.023	.009	145.6§		7.40		6.9	B9 V	+0.6
34 Per	.040	.005	132.0*	− 0.8 4.5	4.67	.11	3.9	B3 IV	−2.4
HR 1047	.040	.014	150.5*	+ 0.1 2.1	6.20	.19	4.9	B5 V	−1.4
HD 21479	.052	.008	136.5§		7.4		6.9	A2 V	+0.6
HD 21480	.051	.005	141.3†		8.0		7.5	A7 V	+1.2
HD 21481	.035	.014	155.5*		7.5		7.0	A0 V	+0.7
HR 1051	.045	.006	129.6*	+10 6 V	6.04		5.5	B8 IV	−0.8
HD 21641	.048	.007	131.6*	+14 3.6	6.77		6.3	B9 V	0.0
HD 21672	.063	.044	151.4*‖		6.62		6.1	B8 V	−0.2
HR 1063	.033	.006	138.6*	+ 1.2 1.5	5.52		5.0	B8 III	−1.3
HD 21931	.033	.009	127.9§		7.25		6.7	B9 V	+0.4
HD 21942	.041	.023	102.7‡		8.9		8.4	A0 V	+2.1
HD 22136	.040	.029	117.2*	+10.7 3.6	6.76		6.3	B8 V	0.0
ψ Per	.038	.004	132.9*	+ 0.3 0.6	4.26	+0.06	3.9	B5 e	−2.4
HD 22401	0.029	±0.009	149.0§	− 1.9±4.2 V?	7.6		7.1	A0 V	+0.8

* GC. ‡ Bgd.
† Computed. § 2 Grw 25.
‖ The GC proper motion for this star is based on only two epochs. The motion in 2 Grw 25 is 0".048±0".012 toward $\theta = 121°.4$.

indicates the same distance. The absolute magnitude of α Persei is −4.9, a value in good agreement with the appearance of the spectrum.

The distance obtained from the HR diagram is 180 parsecs, corresponding to a parallax of 0".0055. The distance obtained from the upsilon-component of the proper motion is 120 parsecs, corresponding to a distance modulus of 5.4 mag., but this is incompatible with the appearance of the spectra. With the larger distance, the tangential motion of the cluster is 33 km/sec toward $\theta = 132°$, and the radial motion, corrected for galactic rotation, is +1.5 km/sec. The velocity corrected for solar motion is 16 km/sec toward galactic longitude 215° and galactic latitude +17°.

Table 3 lists five B-type stars brighter than 5.5 mag. whose proper motions indicate

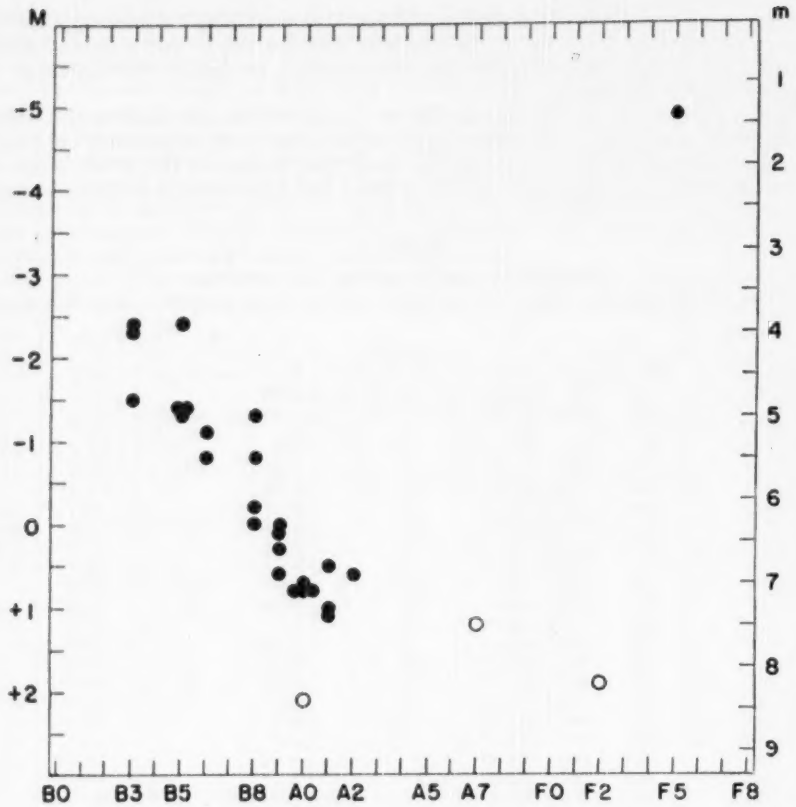

FIG. 3.—The HR diagram for the stars listed in Table 2. The three stars plotted as open circles are probably not members of the cluster.

TABLE 3

STARS NOT IN THE VISUAL CLUSTER WHICH SHARE THE CLUSTER PROPER MOTION

Name	$\alpha_{(1900)}$	$\delta_{(1900)}$	m	μ	θ	$\Delta\theta$	Dist. (Psc)	Sp.	E_1	M
HD 18537	2^h53^m7	+51° 57′	5.42	0".043	130°.2	+5°	165	B7 V	+0.02	−0.9
30 Per	3 11.0	+43 39	5.38	.047	128.1	−1	153	B8 V	+ .03	−0.7
δ Per	3 39.3	+47 38	3.10	.048	136.7	+3	150	B5 III	+ .05	−3.2
ε Per	3 51.1	+39 43	2.96	.036	140.5	+4	198	B0.5 V	+ .05	−3.9
48 Per	4 1.4	+47 27	4.03	0.039	138.1	0	183	B3 e	+0.05	−3.2

that they may have the same space motion as the cluster. The distances included in the table are derived on this assumption from the amount of the proper motion. In every case the radial velocity is also consistent with the cluster motion, although the uncertainty is large for most of the stars.

The star δ Persei lies near the edge of the arbitrarily drawn boundaries of the cluster, but the difference between the proper motion of this star and that of the stars within the boundaries is too large to attribute to observational errors. If this star is a member of the cluster, it lies about 30 parsecs in front of the nucleus. The stars HD 18537 and 30 Persei also lie in front of the cluster and are separated from the nucleus by more than 5° in the sky. The spectroscopic and cluster parallaxes are in good agreement. The hydrogen lines in the Be star, 48 Persei, are too strong for a normal star of absolute magnitude −3.2, but it may be that the high surface gravity at the pole of such a star simulates a star of lower luminosity. The star ε Persei lies still farther from the nucleus. The absolute magnitude derived from the cluster motion is in better agreement with the appearance of the spectrum than that indicated by the assumption that the observed proper motion results solely from solar reflex.

The spectroscopic evidence indicates that four, and possibly all, of the stars which move in the same direction as the cluster may also have the same space motion. If they do, they form a shell around the nucleus approximately 35 parsecs in radius. This may be the case, but it must be remembered that the direction of the cluster motion deviates little from that of parallactic drift.

NOTES

NOTE ON THE SPECTRUM OF THE AIRGLOW IN THE RED REGION*

The light emitted by the upper atmosphere other than the polar aurora has had a variety of names. In the earlier literature it was called the "permanent aurora" or the "nonpolar aurora" and, more recently, "the light of the night sky." The last designation is particularly objectionable, since the light from the night sky is composite in origin, consisting not only of the light emitted by the upper atmosphere but of the zodiacal light, the unresolved stars, galactic light, polar aurora, and extensive areas of diffuse nebulosity. In searching for a short descriptive name, I propose to adopt one suggested by Dr. Otto Struve, namely, "airglow." The term "airglow" is thus defined as the light emitted by the upper atmosphere other than that which is known as the "polar aurora."

TABLE 1

WAVE LENGTHS OF AIRGLOW LINES

Date (1949)	Exposure Time	Wave Lengths in Angstroms					
Aug. 21–22	8h00m	6249	6467	.....	6564	.....	6846
Aug. 22–23	7 40	6236	.....	6542	.....	.....	6839
Aug. 23–24	7 47	.....	.....	.....	6564	6705	6851
Aug. 25–26	8 00	.....	.....	.....	6566	.....	6855
Aug. 28–29	7 48	6243	.....	.....	.....	.....	6844
Sept. 16–17	4 12	6247	6466	.....	6563	.....	6849
Sept. 17–18	9 07	6238	6480	.....	6559	.....	6842
Mean	.....	6243	6471	6542	6563	6705	6847
H. W. Babcock	.....	6235 6258	6464	.....	6569	.....	.....

The spectrum of the airglow has been observed on many occasions, but the red region has been somewhat neglected. Observations in this region of the spectrum were made with a CI spectrograph manufactured by Huet in Paris. The spectrograph has glass optics and covers the spectrum from 4000 to 7000 A. The camera is an enlarged and modified microscope objective with a numerical aperture $f/0.7$. The focal length is 80 mm, and the resulting linear dispersion is 650 A/mm at 6000 A and 1050 A/mm at 7000 A. Although the dispersion is low, the definition of the spectrograms is very good and permits quite accurate wave-length measurements for faint sources, such as the airglow.

Seven good spectrograms of the airglow with the CI spectrograph were obtained at the McDonald Observatory, Fort Davis, Texas, during the period August 21–September 18, 1949. Eastman spectroscopic plates, type 103*a*-F, were used without hypersensitization. Most of the exposures were of about 8 hours' duration. All the spectrograms had a comparison spectrum, usually consisting of argon, helium, and mercury.

In addition to the green auroral line, 5577 A, the two red auroral lines, 6300 A and 6364 A, and the blended sodium D lines, 5893 A, the features listed in Table 1 were measured. The wave lengths measured by H. W. Babcock[1] are given for comparison.

* *Contributions from the McDonald Observatory, University of Texas*, No. 187.

[1] *Pub. A.S.P.*, 51, 47, 1939.

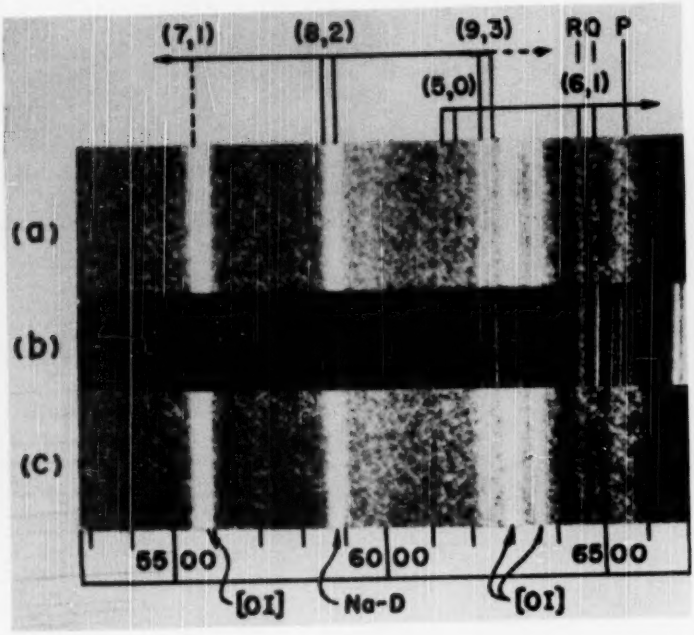

FIG. 1.—Comparison of the spectrum of the night sky in the visible region with the rotation-vibration bands of *OH*. Spectrum *b* is the 8347 A (6, 2) *OH* band reduced to the same wave-number scale as the night-sky spectrum by Babcock, spectra *a* and *c*.

The line at 6563 A is wide and nearly always present in the spectrum. On one occasion it was too faint to be measured, and a sharp line, 6542 A, was measured. The wide line, 6563 A, agrees well in wave length with $H\alpha$ and has the same characteristics as the hydrogen lines seen in diffuse aurorae and the upper parts of auroral rays.[2] Hence the above line is tentatively identified as hydrogen $H\alpha$. The line whose wave length measures 6847 A is a well-defined line and is always present. Its identity has not been established. The other lines of the table correspond to components of the first positive system of nitrogen and probably belong to that system.

Previous observations by Elvey and Farnsworth[3] with a spectrograph of low dispersion, about 2000 A/mm at 6500 A, indicated a line or band of uncertain origin at about 6560 A, which was enhanced in the spectrum of the twilight. Observations now made with the CI spectrograph do not confirm the existence of this line. The line measured, especially on spectrograms of twilight, was fictitious, being caused by the effect of the prismatic dispersion, spectral sensitivity of the emulsion, and atmospheric absorption bands. A spectrogram of twilight taken with spectrograph "B" of the McDonald Observatory, a grating instrument, showed no evidence of an emission in this region.

I wish to express my appreciation to Dr. Struve for the invitation to carry out this and other work at the McDonald Observatory and to the Office of Naval Research, which has supported this work under Project NR-082-045.

C. T. ELVEY

U.S. NAVAL ORDNANCE TEST STATION
CHINA LAKE, CALIFORNIA

November 7, 1949

IDENTIFICATION OF THE 6560 A EMISSION IN THE SPECTRUM OF THE NIGHT SKY

The spectrum of the night sky in the visible region, obtained by H. W. Babcock[1] at Lick Observatory in 1939, showed numerous radiations in the red region for which it has been difficult to obtain satisfactory identifications. This is particularly true of the broad emission near 6560 A. Swings[2] has associated it with the first positive system of N_2. From current studies of this emission, however, Elvey[3] has identified this broad emission as the $H\alpha$ Balmer line. The broad profile was interpreted as Doppler broadening, similar to the $H\alpha$ line that is observed in some auroral spectra. It is the opinion of the author that these identifications are incorrect.

The recent identification of the intense infrared emissions as due to the rotation-vibration bands of *OH* has made it possible to predict the positions of other *OH* bands.[4] The origin of the (6, 1) band is found to be at 6500 A. This position is shown in Figure 1. The spectrum of the night sky by Babcock (*a* and *c*) shows a sharp emission at 6502 A

[2] C. T. Elvey and Don Williams, observations of aurora made with the same spectrograph in Alaska (unpublished); C. W. Gartlein, *Phys. Rev.*, **74**, 1208, 1948; L. Vegard and G. Kvifte, *Geofys. Pub.*, Vol. 16, No. 7, 1946.

[3] *Ap. J.*, **96**, 451, 1942.

[1] *Pub. A.S.P.*, **51**, 47, 1939.

[2] Chap. v, in G. P. Kuiper, *Atmospheres of the Earth and Planets* (Chicago: University of Chicago Press, 1949).

[3] See current issue of the *Astrophysical Journal*.

[4] A. B. Meinel, *Ap. J.*, **111**, 207, 1950. The full analysis of the *OH* bands and their identification as rotation-vibration bands will appear in the May issue of the *Astrophysical Journal*.

that coincides with the *Q* branch of the (6, 1) band. Spectrum *b* is made by reducing photographically the (6, 2) band at 8347 A until the wave-number scale is the same as in spectra *a* and *c*. This figure shows clearly that the broad emission at 6560 A is merely the *unresolved P branch of the (6, 1) OH band and not Hα or due to* N_2. The maxima observed by Babcock and the computed centers of gravity of the (6, 1) 6500 A *OH* band are shown in Table 1.

In addition to the (6, 1) band, the (5, 0) 6172 A, (9, 3) 6258 A, and (8, 2) 5890 A transitions are present in Babcock's spectrum. The *R* and *Q* branches of the (9, 3) transition are clearly visible; however, the *P* branch is obscured by the intense red auroral lines at 6300 A and 6364 A. The *R* and *Q* branches of the (5, 0) transition are barely

TABLE 1

COMPUTED (6, 1) *OH* BAND POSITIONS

Babcock λ (Obs.) A	I	(6, 1) *OH* λ (Comp.) A	I	Branch
6464	2	6464.3	2	*R*
6502	2	6503.5	2	*Q*
6560	3bb	6563.2	3	*P*

detectable; while these branches of the (8, 2) band are obscured by the *Na* D lines. The *P* branch of the latter band, however, is observable at 5965 A.

In conclusion, it is felt that the presence of the new band system, in addition, renders all former identifications of emissions from the first positive system of N_2 very doubtful.

This investigation has been sponsored by the Office of Naval Research.

A. B. MEINEL

LICK OBSERVATORY AND YERKES OBSERVATORY
March 2, 1950

SPECTROSCOPIC DISTANCE MODULI FOR 224 O AND B STARS

The objects observed are included in Adams' list[1] of three hundred early-type stars showing interstellar calcium lines. The plates were obtained by W. W. Morgan and his associates at the Yerkes Observatory with the small spectrograph attached to the 40-inch refractor; the plates had been taken in connection with the general parallax program for B stars. The spectrograms were classified on the system of the *Atlas of Stellar Spectra*, by Morgan, Keenan, and Kellman. Most of the eighty-three standard stars chosen were cluster members with well-determined distances; the classification consisted in interpolating between these standards.

Cluster distance moduli were used for members of the Pleiades, Orion group, Scorpio-Centaurus, and the three clusters of B stars in Perseus (double cluster, Eddington's cluster, and the cluster near *o* Persei discussed by Blaauw[2]). Blaauw's data[3] for the Scorpio-Centaurus cluster members were used. The distance moduli have been corrected for interstellar absorption by means of the color measures of Stebbins, Huffer, and Whitford.[4]

The results are listed in Table 1. The columns give (1) the name of the star, (2) the apparent magnitude, (3) the apparent magnitude corrected for interstellar absorption (seven times the color excess), (4) the spectral type, and (5) the true distance modulus.

[1] *Ap. J.*, **109**, 354, 1949.
[2] *B.A.N.*, **10**, 29, 1944.
[3] *Pub. Kapteyn Astr. Lab. Groningen*, No. 52, 1946.
[4] *Ap. J.*, **91**, 20, 1940.

TABLE 1

SPECTRAL TYPES AND DISTANCE MODULI FOR 224 O AND B STARS

Name or HD No.	m	m_{corr}	Sp.	Mod.-corr	Name or HD No.	m	m_{corr}	Sp.	Mod.-corr
1337	6.12	5.6	O9	10.1	ψ Ori	4.66	4.5	B2	7.5
1976	5.36	4.9	B3	6.7	35921	6.71	5.0	O9.5	9.5
ξ Cas	4.85	4.4	B3	6.2	χ Aur	4.88	3.3	B3	8.8
4142	5.55	5.5	B5	6.5	δ Ori ft	6.9	.....	B2	7.5
o Cas	4.70	4.1	B3	7.1	δ Ori br	2.5	2.2	O9.5	7.5
ν And	4.42	4.3	B5	5.3	υ Ori	4.64	4.1	B0	7.5
6300	6.50	6.0	B3	7.8	120 Tau	5.50	4.6	B2	7.1
ξ Ari	5.53	5.4	B5	6.4	36591	5.30	5.0	B1	7.5
55 Ari	4.58	4.0	B3	5.8	VV Ori	5.37	5.1	B1	7.5
π Ari	5.30	5.0	B5	6.0	121 Tau	5.28	4.7	B2	7.2
30 Per	5.38	5.2	B8	5.9	ϕ^1 Ori	4.53	4.0	B0	7.6
29 Per	5.30	4.8	B3	6.3	36960	4.67	4.5	B0.5	7.5
31 Per	5.08	4.9	B5	6.3	37016	6.28	5.7	B3	7.5
τ Ari	5.17	4.8	B5	5.8	37017	6.54	5.8	B2	7.5
20809	5.30	5.0	B5	6.3	42 Ori	4.65	4.3	B2	7.5
21278	4.94	4.2	B5	6.3	θ^1 Ori	5.36	3.6	O6	7.5
34 Per	4.67	3.9	B3	6.3	Bond 619	6.8	.....	B2	7.5
21856	5.80	5.1	B2	7.1	Bond 640	6.7	.....	B1	7.5
ψ Per	4.26	3.8	B5	6.3	37040 br	6.29	5.7	B3	7.5
22780	5.57	5.0	B5	6.0	θ^2 Ori	5.17	4.4	O9.5	7.5
40 Per	5.04	4.0	B1	7.1	ι Ori	2.87	2.6	O9	7.5
o Per	3.94	2.8	B1	7.1	ϵ Ori	1.75	1.3	B0	7.5
16 Tau	5.43	5.3	B8	6.3	37150	6.45	6.0	B2	7.5
17 Tau	3.81	3.5	B6	6.3	125 Tau	5.00	4.8	B3	7.8
19 Tau	4.37	4.1	B6	6.3	σ Ori	3.78	3.0	O9.5	7.5
20 Tau	4.02	3.8	B7	6.3	ω Ori	4.54	4.0	B2	7.5
21 Tau	5.85	.....	B8	6.3	126 Tau	4.87	4.5	B3	6.5
23 Tau	4.25	3.8	B6	6.3	ζ Ori br	2.05	1.7	O9.5	7.5
23478	6.51	5.0	B3	7.1	κ Ori	2.20	1.5	B0.5	7.5
η Tau	2.96	2.9	B7	6.3	57 Ori	5.89	5.5	B2	7.5
23753	5.51	.....	B8	6.3	139 Tau	4.90	4.2	B0.5	8.7
30 Tau	5.03	4.7	B3	6.5	χ^2 Ori	4.71	3.2	B2	10.5
27 Tau	3.80	.....	B8	6.3	41335	5.12	4.7	B2	6.7
24131	5.73	4.5	B1	7.1	ν Ori	4.40	4.3	B3	6.1
ζ Per	2.91	1.4	B1	7.1	3 Gem	5.76	4.5	B3	10.5
X Per	6.3	4.2	B0p	7.1	69 Ori	4.92	5.1	B6	6.1
24640	5.48	4.6	B2	7.1	ξ Ori	4.35	4.1	B3	5.9
ϵ Per	2.96	2.5	B0.5	6.4	S Mon	4.68	4.5	O7	8.7
ξ Per	4.05	3.1	O7	7.1	48434	5.78	5.0	B0	9.6
λ Tau	4.2	3.8	B3	5.6	15 CMa	4.66	4.3	B1	7.8
25539	6.70	5.5	B3	7.1	ι CMa	4.4	.....	B3	8.9
40 Tau	5.33	4.8	B3	6.6	52382	6.36	5.0	B1	10.5
25799	6.87	5.8	B3	7.1	19 Mon	4.89	4.6	B2	7.1
25833	6.61	5.8	B5	7.1	o^2 CMa	3.1	.....	B3	9.6
48 Per	4.03	3.4	B3	6.3	55879	5.99	5.7	O9.5	10.3
μ Tau	4.32	3.7	B3	5.7	τ CMa	4.40	4.3	O9	9.0
53 Per	4.89	4.2	B3	6.0	58050	6.37	6.0	B2	10.1
ν Eri	4.12	4.0	B2	8.1	58343	5.20	4.5	B3	6.4
29309	7.1	.....	B3	9.1	η CMa	2.43	.....	B5	8.9
π^4 Ori	3.78	3.5	B2	7.5	o Pup	4.59	4.1	B0.5	7.1
π^5 Ori	3.87	3.7	B2	7.5	67880	5.54	5.0	B3	6.8
AE Aur	5.8	4.4	O9.5	8.5	87015	5.59	5.3	B3	7.1
ρ Aur	5.12	4.8	B5	5.8	89688	6.53	6.0	B3	8.0
λ Lep	4.29	4.0	B0.5	7.5	ρ Leo	3.85	3.5	B1	9.0
22 Ori	4.65	4.3	B2	7.5	104337	5.28	.....	B2	7.8
23 Ori	4.99	4.7	B2	7.5	1 Sco	4.8	.....	B3	6.2
35395	6.83	4.9	B0.5	8.9	λ Lib	5.1	.....	B3	6.2
η Ori	4.5	4.3	B1	7.5	142184	5.4	.....	B3	6.2
114 Tau	4.83	4.5	B2	7.6	δ Sco	2.54	2.2	B0	6.4

TABLE 1—*Continued*

Name or HD No.	m	m_{corr}	Sp.	Mod.-corr	Name or HD No.	m	m_{corr}	Sp.	Mod.-corr
β Sco br	3.4	3.0	B0.5	6.5	22 Cyg	4.87	4.7	B5	7.7
β Sco ft	5.06	4.4	B2	6.4	189066	6.04	5.9	B5	7.1
ω^1 Sco	4.13	3.6	B1	6.5	189178	5.43	5.2	B5	8.2
ν Sco	4.29	3.5	B2	6.4	25 Cyg	5.15	4.7	B3	6.5
σ Sco	3.08	2.0	B1	6.5	190066	6.55	5.2	B0.5	9.6
147888	6.56	5.1	B5	6.1	190603	5.69	3.0	B1	10.2
ρ Oph br	5.22	3.8	B2	6.3	190919	7.30	5.6	B1	10.6
χ Oph	4.85	3.3	B2p	5.8	28 Cyg	4.82	4.6	B3	6.4
ζ Oph	2.70	1.7	O9.5	5.7	191877	6.11	5.2	B1	9.2
149881	6.59	6.1	B0.5	10.1	192685	4.82	4.5	B3	6.3
154445	5.62	4.7	B2	7.8	193322	5.82	4.4	O9	8.9
U Oph	6.3	5.7	B6	7.0	193536	6.28	5.8	B2	8.3
u Her	4.8	4.5	B3p	6.3	194279	7.05	3.1	B2	10.4
163472	5.73	4.6	B2	7.6	194335	5.68	5.3	B2	9.7
67 Oph	3.92	3.4	B5	8.9	ω^1 Cyg	4.89	4.4	B2	6.9
165174	6.09	5.1	B0	9.1	195592	7.15	3.2	O9	9.7
102 Her	4.32	4.0	B2	7.3	28 Vul	5.04	5.0	B6	6.0
16 Sgr	6.02	5.1	O9	10.8	196775	5.92	5.6	B3	7.4
15 Sgr	5.42	4.5	B0	11.0	α Cyg	1.33	1.3	A2	8.5
167838	6.64	4.7	B5	11.7	51 Cyg	5.41	4.7	B2	7.3
168797	6.04	5.3	B3	8.3	λ Cyg	4.47	4.3	B6	6.9
170650	5.72	5.4	B5	8.9	55 Cyg	4.89	2.9	B3	9.4
170740	5.80	3.9	B2	6.4	198846	7.7	6.7	O9.5	10.7
171780	5.93	5.8	B5	8.3	57 Cyg	4.68	4.4	B5	5.6
174179	5.78	5.6	B3	8.6	199140	6.44	6.0	B2	10.0
8 Lyr	5.77	5.4	B2	7.5	199478	5.76	4.2	B8	11.4
174959	6.01	5.9	B6	7.9	201819	6.40	5.8	B0	10.3
δ^1 Lyr	5.51	5.3	B3	7.1	σ Cyg	4.28	3.7	B9	10.2
176162	5.36	4.8	B5	5.8	υ Cyg	4.42	4.0	B3	5.8
176818	6.86	5.6	B2	8.7	69 Cyg	5.84	5.4	B0	10.8
176819	6.55	5.3	B2	7.8	70 Cyg	5.20	4.8	B3	8.8
176871	5.50	5.2	B6	7.0	π^1 Cyg	4.78	4.3	B3	7.3
177109	6.22	5.8	B5	7.3	π^2 Cyg	4.26	3.8	B3	6.8
178175	5.41	4.6	B2	7.1	207563	6.16	5.7	B3	7.5
ι Lyr	5.13	5.1	B6	7.0	16 Peg	5.05	4.7	B3	6.5
20 Aql	5.37	3.9	B3	5.7	o Aqr	4.66	4.7	B8	5.5
1 Vul	4.60	4.3	B5	5.8	30 Peg	5.35	4.2	B5	5.7
2 Vul	5.40	4.4	B0.5	8.1	31 Peg	4.93	4.4	B2	7.5
181409	6.32	6.0	B2	8.9	2 Lac	4.66	4.3	B5	5.3
2 Cyg	4.86	4.4	B3	6.2	π Aqr	4.64	4.2	B1	6.6
183143	6.93	3.1	B6.5	10.3	212978	6.07	5.6	B2	8.1
183362	6.36	6.0	B3	7.8	6 Lac	4.54	3.9	B2	7.0
8 Cyg	4.85	4.5	B3	7.3	8 Lac ft	6.55	6.6	B2	9.1
κ Aql	5.04	4.2	B0.5	8.2	8 Lac br	5.83	5.1	B2	9.1
σ Aql	5.17	4.2	B2	6.7	10 Lac	4.91	4.6	O9	8.6
185859	6.44	4.3	B0.5	10.3	12 Lac	5.18	4.9	B2	8.9
185936	5.84	5.5	B5	7.0	215191	6.22	5.5	B2	9.6
187459	6.35	5.0	B0.5	10.0	14 Lac	5.84	4.7	B3	6.7
187879	5.62	4.8	B1	8.4	16 Lac	5.54	5.0	B2	8.8
188209	5.51	4.8	O9.5	11.3	217101	6.07	5.6	B2	8.3
188252	5.70	5.3	B2	9.3	217543	6.39	5.9	B3	7.9
57 Aql br	5.78	5.6	B6	6.6	219188	6.93	6.1	B0.5	10.1
188439	6.15	5.7	B0.5	9.7	223229	5.84	5.3	B3	7.1

I am indebted to Dr. Morgan and his associates for making the plates available and for unpublished distance moduli, as well as for their kind assistance.

JANE RAMSEY

YERKES OBSERVATORY
November 8, 1949

RADIAL VELOCITIES OF FIFTEEN STARS OF THE RR LYRAE TYPE

During January, 1948, and February, 1949, Miss W. Iwanowska, of Torun, Poland, and Mr. O. Struve obtained a series of thirty-three spectrograms of fifteen variables of the RR Lyrae type principally for the purpose of investigating the spectroscopic fea-

TABLE 1

RADIAL VELOCITIES

Name	Period	JD 24329+	Helioc. Phase (Days)	Spectral Class	V (Km/Sec)
TZ Aur	0.392	50.708	0.074	A2	+ 58
TT Cnc	.563	39.868	.192	.....	+111
		40.843	.040	F0	+ 40
		54.667	.341	F0	+ 56
RX Cet	.574	53.592	.565	A5	−143
		54.590	.415	F0	− 73
RZ Cet	.511	38.632	.408	F0	+ 9
RY Com	.469	39.990	.079	A5	− 36
		48.028	.145	A5	− 22
		53.990	.011	A5	− 37
SV Eri	.714	32.606	.626	.....	+ 20
		32.728	.034	A5	+ 1
BB Eri	.570	40.667	.071	A5	+216
		40.726	.130	.....	+259
		53.646	.511	A3	+260
		53.681	.546	A5	+229
UU Hya	.524	48.806	.359	A5	+339
TV Leo	.402	47.785	.287	A0	−128
		47.897	.339	A2	−109
UZ Leo	.524	36.933	.032	F0	+ 44
		37.000	.099	A3	+ 21
AR Per	.426	32.863	.397	.....	+ 5
		32.639	.343	F5	+ 15
		36.698	.402	A5	− 38
		36.736	.015	A5	− 43
XX Pup	.517	47.721	.504	A5	+398
		47.746	.012	A0	+375
BB Pup	.480	53.754	.427	F0	+220
		53.809	.003	.....	+290
AT Vir	.526	53.922	.079	A2	+339
AU Vir	0.343	48.854	.314	A0	+129
		50.899	.300	A0	+140
		53.878	0.190	A0	+129

tures of these stars. This part of the work is being undertaken by Miss Iwanowska. The spectrograms have now been measured for radial velocity, and the results are given in Table 1. All spectrograms were secured with the $f/2$ quartz spectrograph attached to the 82-inch reflector of the McDonald Observatory, on Eastman 103*a*-O film. The dispersion was 170 A/mm at $H\gamma$. On most of the plates only the hydrogen lines and *Ca* II K could be measured, but on a few plates several additional lines, up to a total of thirteen, could be used. The photometric elements in the table are those given in the *Catalogue of Variable Stars* by Kukarkin and Parenago in 1948. For the stars TZ Aurigae and RY Comae the variation in the period was taken into account.

A. COLACEVICH*

YERKES AND MCDONALD OBSERVATORIES
November 5, 1949

ON THE SPECTROSCOPIC BINARY τ^9 ERIDANI

The spectroscopic binary τ^9 Eridani[1] was discovered as such by Frost[2] from nine spectrograms taken at the Yerkes Observatory. Its spectrum is classified in the *Henry Draper Catalogue* as A0p; the peculiarity being that "the lines 4077.9, 4128.1 and 4131.1 are very strong."[3] Actually, τ^9 Eri is one of the peculiar A stars which belong to the so-called "silicon" group.

The determination of the period and the orbital elements was undertaken by Struve and Hujer[4] several years after Frost's announcement. Their investigation, based on fifty-three spectrograms taken mostly at Yerkes through 1907, 1908, 1924, 1925, and 1926, led to the following results: (*a*) that the period was variable, its mean value being 0.8544075 days; (*b*) that the *Mg* II line belonging to the secondary star could be measured on the best plates corresponding to the phases of maximum relative velocity; and (*c*) that some of the lines were suspected to vary in intensity.

With the addition of the results from spectrographic material secured at the Lick Observatory in 1909–1910 and at the Yerkes Observatory in 1928, Hujer,[5] at Struve's suggestion, re-examined the question of the period and found that two periods represented the observations quite satisfactorily, namely, 0.8542336 and 5.9542159 days, respectively. A third possible period, 1.19790 days, was rejected because it led to a plot with greater dispersion. Although there was "a slight advantage in the case of the five-day period," the question as to which of the two should be adopted could not be settled with observations at northern latitudes because of "the (small) range in hour angle during which the star is accessible." To decide this point, the star was observed at Bosque Alegre with the Wood-grating spectrograph attached to the 154-cm reflecting telescope, which gives a dispersion of about 42 A/mm.

There is a list of wave lengths for the spectral features of τ^9 Eri, in the interval λλ 3930–4862 in Struve and Hujer's paper and a more complete list in the wavelength interval 3982–4673 by Morgan.[6]

* Fellow of the Italian National Research Council.

[1] $\alpha = 3^h58^m2$; $\delta = -24°10'$ (1950.0). 36 Eridani = 161 G. Eridani = BS 1240 (4.69 mag.) = Boss 923 = CD − 24°2022 = HD 25267 (Sp. A0p).

[2] *A.N.*, **177**, 174, 1908.

[3] *Harvard Ann.*, **91**, 290, 1918.

[4] *Ap. J.*, **65**, 300, 1927.

[5] *Ap. J.*, **67**, 399, 1928.

[6] *Pub. Yerkes Obs.*, **7**, Part 3, 67, 1935.

TABLE 1

ADOPTED STELLAR WAVE LENGTH

H	*Si* II	*Mg* II	*Ca* II
3797.90	3853.66	4481.23	3933.66
3835.39	3856.02		
3889.05	3862.59		
3970.08	4128.05		
4101.74	4130.88		
4340.47			

TABLE 2

RADIAL VELOCITIES OF r^9 ERIDANI

Plate	Date	U.T.	Phase* (Period)	Radial Velocity (Km/Sec)
S 589	1947 July 28	10:08	0.009	+29.7
336	1946 Oct. 16	3:36	.093	+12.9
337	16	3:54	.095	+ 4.1
338	16	4:14	.098	+12.9
341	16	6:34	.114	+ 2.8
342	16	6:52	.116	− 1.1
346	16	8:38	.128	− 7.6
347	16	8:53	.130	− 6.3
314	11	5:38	.268	−23.1
315	11	6:04	.271	−19.9
350	17	5:10	.272	−22.0
316	11	6:28	.274	−12.5
317	11	6:44	.275	−16.5
351	17	5:46	.276	−17.5
318	11	7:02	.277	−19.8
319	11	7:27	.280	−15.4
322	11	8:58	.291	−23.7
630	1947 Aug. 11	10:12	.360	− 7.7
I 629	1949 Aug. 25	7:04	.472	+23.9
S 536	1947 July 7	9:00	.474	+15.4
537	7	9:40	.478	+20.6
558	25	9:44	.502	+31.9
559	25	10:03	.504	+31.1
637	Aug. 12	7:08	.507	+29.4
601	6	10:08	.520	+38.1
549	July 8	8:57	.641	+50.1
550	8	9:12	.643	+43.6
357	1946 Dec. 6	2:54	.655	+60.7
569	1947 July 26	9:55	.672	+58.8
570	26	10:09	.674	+57.0
503	3	10:00	.809	+62.6
504	3	10:16	.811	+67.0
363	1946 Dec. 7	3:20	.826	+58.5
613	1947 Aug. 8	10:06	.852	+52.6
326	1946 Oct. 15	5:40	.940	+50.2
327	15	5:56	.942	+42.7
329	15	7:07	.950	+49.6
513	1947 July 4	10:12	0.978	+37.9

* The origin was arbitrarily taken at JD 2417600.000.

The observations at Bosque Alegre were made in 1946 and 1947 on Eastman 103*a*-O emulsion, with the exception of plate S 537, which was taken on Eastman 103*a*-F emulsion. One additional spectrogram was secured in 1949 on Eastman II*a*-O emulsion. The equivalent slit-width was, in all cases, of the order of 0.8 A. On the 103*a*-O plates the exposure times were of the order of 12 minutes, in fair seeing.

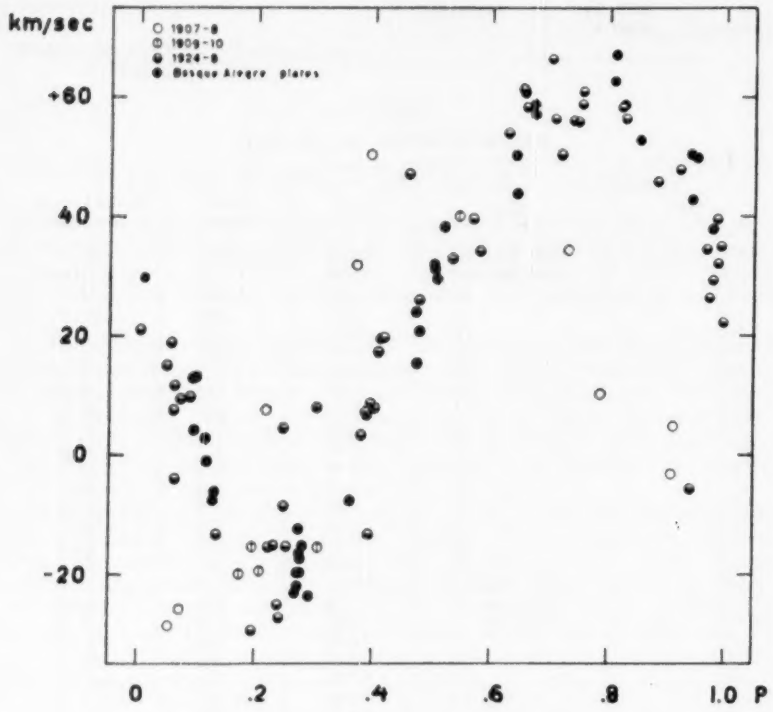

FIG. 1.—Revised velocity-curve for τ^9 Eridani

Table 1 lists the stellar wave lengths used for the determination of the radial velocities, and the numerical values of the latter are shown in Table 2 and are plotted in Figure 1.

Periods of about 1 day are ruled out by the results from our spectrograms obtained in October, 1946, and, therefore, our radial velocities were first plotted with $P = 5.9542159$ days. This plot showed a shift of the Bosque Alegre radial velocities from Hujer's velocity-curve, and, accordingly, the period was adjusted to the value 5.95367 days. This new

period represents the observations[7] from 1909 to 1949. For the plot in Figure 1 the origin was arbitrarily taken at JD 2417600.000, that is, quite close to the date of the earliest spectrogram of τ^9 Eri, taken at Yerkes on February 16.040, 1907 (U.T.). Only the earliest results, obtained from the Yerkes spectrograms of 1907 and 1908, fall quite outside the rest of the observations, a fact which the writer is unable to explain.[8]

Orbital elements were derived from all the available radial velocities (except those of 1907 and 1908) by applying the Wilsing-Russell method; they are listed in Table 3, together with those previously computed by Hujer. The agreement is good.

TABLE 3

ORBITAL ELEMENTS OF τ^9 ERIDANI

	Hujer's	Sahade's
P	5.9542159 days	5.95367 days
γ	+ 25.0 km/sec	+ 24.9 km/sec
e	0.115	0.100
K	37.5 km/sec	37.6 km/sec
ω	142°	151°
T	1.332 days*	0.161 P†
$a \sin i$	3.0×10^6 km	3.1×10^6 km
$f(m)$	$0.0324 \odot$	$0.032 \odot$

* Origin in October 15.000, 1926 [JD 2424803.500].

† Origin in JD 2417600.000.

The spectrograms of τ^9 Eri were examined for variations in line intensities and for the presence of double lines. The lines λλ 4201, 4233, and 4235 seem to be definitely variable, but on our plates the variability of λλ 4123, 4325, and 4472 is doubtful. Double lines were not detected even at the critical phases.

I am indebted to Mr. Julio Albarracín for checking the reduction of the plates.

JORGE SAHADE

OBSERVATORIO ASTRONÓMICO DE CÓRDOBA
CÓRDOBA, ARGENTINA
November 2, 1949

[7] The results, previous to the Bosque Alegre ones, are listed in the papers by Struve and Hujer and by Hujer.

[8] *Note added in proof:* The reason for the discrepancy of the earliest radial velocities has become clear after recent correspondence with Dr. O. Struve. The dates, published in *Ap. J.*, **65**, 300, 1927, for the spectrograms taken in 1907 and 1908 and for the ones whose times of mid-exposure are indicated as being 1924, December 1.242, and 1925, January 10.090; January 31.08, and February 5.070, should be corrected by the addition of one day. When this is done, it is found that the new period represents very well all the radial velocities.

SPECTROGRAPHIC OBSERVATIONS OF THE STAR η_1 HYDRI

The star η_1 Hydri[1] was observed in 1946, 1947, and 1948 by Sahade with the Wood grating spectrograph attached to the 154-cm reflecting telescope at Bosque Alegre. The dispersion was about 42 A/mm, and the equivalent slit width was 1.2 or 1.5 A. Prior to October, 1946, the spectrograms were taken on Eastman 103-O or 103-F emulsion and, thereafter, on Eastman 103*a*-O emulsion. The star η_1 Hyi shows a spectrum of about type A0; the only features which can be seen are the broad and shallow *H* lines; but on some of the plates one can barely notice *Ca* II, *Mg* II, and perhaps *He* I. Thirty-one spectrograms were measured for radial velocity, almost all of them by Albarracín. The spectrograms were rather difficult to measure.

The star is included in Schneller's *Katalog* for 1939 with the indication that a variation in brightness in the range 6.7–9.2 mag. had been detected, and the remark "Unveränderlich?" The bibliography to 1936 and the relevant data are found in Prager's *Geschichte und Literatur des Lichtwechsels der veränderlichen Sterne*. Both Prager and Schneller mention the magnitude 9.2 as the faintest ever observed. This value was obtained by Kapteyn from one plate taken on November 24, 1885, which was "rejected."[2] Two reliable observations by Kapteyn on June 7, 1889, gave values of 6.6 and 6.5 mag.

The star η_1 Hyi had been suspected of variability by Gould,[3] who reported a range of 6.6–7.5 mag.; the suggestion was made that the star is probably a long-period variable. Previously, Lacaille had indicated in his zones that the object was of the fifth magnitude and in his catalogue that it was of the sixth.

Innes[4] also detected a variation in brightness with a range from 6.3 (February 18, 1896) to 7.0 mag. (January 23, 1896). Further photometric observations were reported later by R. Müller[5] and by C. Payne-Gaposchkin.[6] The former made twenty-eight observations in the interval August 17–November 14, 1928, and did not detect any variation in magnitude. Then Mrs. Gaposchkin stated that "this bright A0 star has been examined on only 81 plates. It is too bright for satisfactory study, but no evidence of variability was found from these measures."

The available photometric data of η_1 Hyi indicate that only Gould and Innes have actually detected a variation in brightness and that the observed range was of nearly 1 mag. Since Gould and Innes were very reliable observers and since no law for the variation was found, it may be that the star shows only sporadic light-fluctuations. If this is the case, photometric and spectrographic observations should be carried on simultaneously.

The dispersion of our radial-velocity determinations is probably not significant, and the results indicate that there has been no appreciable variation in velocity, if any at all, during the times at which our observations were made.

The mean value from all our plates is $+15 \pm 1.8$(m.e.) km/sec.

JORGE SAHADE
JULIO ALBARRACÍN

OBSERVATORIO ASTRONÓMICO
CÓRDOBA, ARGENTINA
September 20, 1949

[1] $\alpha = 1^h51^m2$; $\delta = -68°11'$ (1950.0). 19 G. Hydri (var.) = CD−68°87 (7.0 mag.) = CPD−68°96 (6.6 mag.) = HD 11733 (Sp. A0).

[2] *Cape Obs. Ann.*, **9**, Part II, 7, 1903.

[3] *Uranometria argentina*, pp. 133, 241, 1879.

[4] *J. British Astr. Assoc.*, **6**, 489, 1896.

[5] *A.N.*, **243**, 410, 1931.

[6] *Harvard Ann.*, **115**, 116, 1947.

A NOTE ON THE SPECTRUM OF SIGMA ORIONIS

The star σ Orionis has five visual components, of which all but one have distances greater than 10″ from the primary component. Aitken's new *General Catalogue* lists the magnitudes of A and B as 4.0 and 6.0. Frost and Adams[1] suspected σ Orionis of being a spectroscopic binary; Henroteau[2] listed it among the β Canis Majoris stars; but Heard[3] concluded from thirty-six radial velocities that there are no variations greater than can be attributed to errors of measurement.

On a plate taken March 2.91, 1948, U.T., at the Heidelberg Observatory with a dispersion of 51 A/mm at $H\gamma$, the spectrum is O9.5 on the system of the Yerkes atlas. The star is a member of the main sequence, luminosity class V, and has diffuse lines. The Balmer lines can be traced in absorption to $H17$.

Three spectrograms taken in February, 1949, show a greatly changed appearance: the lines of *H* and *He* I are double, the lines *He* II 4686, *Si* IV 4119, and the blend at λ 4650 are broadened. The total absorptions of the components of the double lines are much smaller than those observed during the single-line stage.

These features cannot be due to component B, since the latter does not contribute appreciably to the total light. The separation of the components of the double lines on February 20.76, 1949, was about 280 km/sec. On two plates taken on October 28, 1949, the spectrum had returned to the single-line stage. In connection with this change in the spectrum of σ Orionis, it may be of interest to quote a remark by Frost and Adams: "There appear on one or two plates to be evidences of complexity in the spectrum, but these are scarcely sufficient to justify conclusions on the subject."[1]

G. R. Miczaika

Heidelberg Observatory
November 4, 1949

ON A GENERALIZATION OF THE VARIATIONAL METHOD FOR PROBLEMS OF RADIATIVE TRANSFER

In a recent paper[1] D. H. Menzel and H. K. Sen have published a new solution of Milne's problem of radiative transfer for the gray case. Their method is presented as an operational one, i.e., based on the utilization of the operator $D = \partial/\partial\tau$, which is well known to be equivalent to the use of the Laplace transform. They use the development first used by the author,[2] namely,

$$B = a + b\tau + \sum_{j=0}^{m} A_j K_{j+2}(\tau), \tag{1}$$

and show that the parameters a and A_j are determined by a set of linear equations of the form

$$\sum_{j=0}^{m} C_{nj} A_j = \frac{a}{n+1} - \frac{1}{n+2} \qquad [n = 1, 2, \ldots, (m+2)], \tag{2}$$

where the coefficients C_{nj} are given by rather simple formulae.

[1] *Ap. J.*, **19**, 151, 1904.

[2] *Pub. Dom. Obs., Ottawa*, **5**, 333, 1922.

[3] *Ap. J.*, **109**, 185, 1949.

[1] *Ap. J.*, **110**, 1, 1949.

[2] V. Kourganoff, *C.R.*, **227**, 1020, 1948.

A careful study of Menzel-Sen's method discloses, however, the fact that if their method gives interesting results, it is not due to the virtues of the "operational technique" but rather to the merits of an averaging process which they introduce as a secondary[3] algebraic trick. However, we shall show that equation (2) can be derived in a straightforward manner, from a very general principle, using only certain well-known facts, such as Milne's integral equations.

In the alternative treatment we propose here, the averaging process of Menzel-Sen's method acquires a simple mathematical and physical meaning and clarifies the difficulties and the possibilities of the method.

Consider the derivative of the flux

$$\eta(\tau) = \frac{\partial \mathfrak{F}(\tau)}{\partial \tau} = \frac{\partial \Phi\{B\}}{\partial \tau} = 4\{\Lambda_\tau\{B\} - B\}, \tag{3}$$

where Λ_τ is the operator well known in this theory. The constancy of the flux demands that $\eta(\tau)$ should be identically zero in the whole field ($0 \leqslant \tau < \infty$). This leads to Milne's equation,

$$\Lambda_\tau\{B\} = B. \tag{4}$$

Now multiply $\eta(\tau)$ by an arbitrary "weight function" $f(\tau)$ and form the functional,[4]

$$\Re\{\eta, f\} = \int_0^\infty \eta(\tau) f(\tau) d\tau; \tag{5}$$

we may call this the "arbitrary mean residual."

We now formulate the following principle: *For a given family of approximate solutions the best ones are those which give to $\Re\{\eta,f\}$ the value zero for the widest variety of weighting functions $f(\tau)$, or, better still, for all possible $f(\tau)$.*

Expanding $f(\tau)$ in a generalized Fourier series,

$$f(\tau) = \sum_{n=0}^{\infty} D_n F_n(\tau), \tag{6}$$

we observe that the principle is equivalent to the following statement:

$$\int_0^\infty \eta(\tau) F_n(\tau) d\tau = 0 \qquad (n = 0, 1, 2, \dots). \tag{7}$$

Here $F_n(\tau)$ represents any system of n functions. But if we restrict ourselves to arbitrary functions $f(\tau)$ which can be expanded in a power (Taylor) series or, even more particularly, to arbitrary polynomials of degree p, we will obtain the following system of equations:

$$\int_0^\infty \eta(\tau) \tau^n d\tau = 0 \qquad (n = 0, 1, \dots, p). \tag{8}$$

Now if we substitute equation (1) in equation (3) and explicitly calculate equation (8), we find, after some elementary reductions, a system of equations of the form (2) with

[3] We quote their statement about it: Finding an equation containing factors $e^{-\tau/\mu}$, they say: "The exponential factor in $Q(n)$ is troublesome, but we can turn the difficulty by adopting a set of weighted mean values through the layers. Multiply $Q(n)$ by $\tau^k d\tau$ and integrate from 0 to ∞." No other comment about it is made!

[4] We operate on $\eta(\tau)$ in order to find Milne's first integral equation $\Lambda_\tau\{B\} = B$, which is implicitly used by Menzel and Sen. But the method can be applied to the flux itself by introducing $\eta_1(\tau) = \mathfrak{F}(\tau) - F$, in which case we shall have Milne's second integral equation $\Phi_\tau\{B\} = F$.

the same coefficients C_{nj} as given by Menzel and Sen. The foregoing treatment enables us to explain the "mysterious" tendency to indeterminacy of the system (2) for increasing n, which was noted by Menzel and Sen: For the bigger n is, the less is the difference between equation (8) for n and $(n+1)$, and in the limit $n \to \infty$ they tend to become identical; the determinant, therefore, tends to contain two identical lines, and this is the origin of the indeterminacy. It is now apparent that this result is due only to the very particular choice of F_n as τ^n and not to the properties of the expansion (1) as suggested by Menzel and Sen.

It is also clear that the method can be easily extended to the nongray case, the fundamental equations in this case being

$$\int_0^\infty d\nu \left\{ \int_0^\infty \kappa_\nu \left[\Lambda_{\tau_\nu} \{B_\nu\} - B_\nu \right] \tau_\nu^n d\tau_\nu \right\} = 0 \qquad (n = 0, 1, 2, \ldots, p). \tag{9}$$

The reason for the relative simplicity of the C_{nj}'s is that the integrals involved are much simpler than in the variational methods which involve

$$\int_0^\infty \Lambda\{u_n\}\Lambda\{u_j\}\, d\tau \qquad \text{and} \qquad \int_0^\infty u_n \Lambda\{u_j\}\, d\tau\,, \tag{10}$$

while, according to formula (8), we have only to deal with

$$\int_0^\infty \tau^n \Lambda\{u_j\}\, d\tau = \int_0^\infty u_j \Lambda\{\tau^n\}\, d\tau\,. \tag{11}$$

Since we can have more equations than unknowns by letting $m < p$, we can give more weight to the vicinity of the surface or to great depths as we choose. Menzel and Sen always take values of n between 1 and $(m+2)$, thus favoring the origin. This explains why they find excellent values of $q(0)$ and bad ones of $q(\infty)$, for which they borrow the value given by other methods; but, by taking values of n from $n+q$ to $n+q+m+1$, the situation would be reversed. This is illustrated by the linear approximation; then $A_j \equiv 0$, and the only unknown, a, is given by

$$a_n = \frac{n+1}{n+2} \qquad (n = 1, 2, \ldots), \tag{12}$$

according to the power of τ employed as weight function; a_n then takes all values between $\frac{2}{3}$ and 1, just as in classical methods, which give:

0.577 .. (Wick-Chandrasekhar, which is best near $\tau = 0$)
0.66(6) (Milne-Eddington, which is best near $\tau = 0.4$)
0.7191. Kourganoff (variational method, which is best near $\tau \to \infty$)

Finally, we may note that if, instead of entirely arbitrary functions $F(\tau)$, we restrict ourselves to those functions which appear as coefficients of a and A_j in the expansion of $\eta(\tau)$, the corresponding equations (7) will be identical with those obtained variationally by taking the minimum of

$$\sigma' = \int_0^\infty \eta^2 d\tau\,. \tag{13}$$

Thus our new principle can be considered as an extension and a simplification of our variational method.

V. KOURGANOFF

INSTITUT D'ASTROPHYSIQUE, PARIS
December 31, 1949

NOTE ON THE CHEMICAL COMPOSITION OF THE SUN

In a previous paper[1] the chemical composition of the sun has been determined on the assumption that the opacity of the sun is due entirely to photoelectric absorption. This assumption is not strictly true, since at high temperatures there is another physical process which becomes of importance. This process is scattering by free electrons. In order to determine the effect on the chemical composition of the sun of the inclusion of electron scattering, we have computed a stellar model in which the heavy elements are represented by a combination of 75 per cent Russell mixture and 25 per cent oxygen.

If photoelectric absorption were the only source of stellar opacity, then the Rosseland mean coefficient, κ_i, would be given by

$$\kappa_i = \frac{\kappa_0 \rho}{\tau_i T^{3.5}}. \tag{1}$$

On the other hand, if electron scattering were the only source of stellar opacity, then the Rosseland mean coefficient κ_e would be given by

$$\kappa_e = 0.19(1+X). \tag{2}$$

When both are important, we must form the Rosseland mean of the combined absorption coefficient κ_{e+i}. This was done by combining the appropriate section of Table 1 of the previous paper with equation (1) and using the empirical formula given by Strömgren.[2] As a first approximation we used the values of X, Y, ρ, and T as computed for the 100 per cent Russell mixture model. A second approximation was not necessary.

The notation and method were the same as that used previously. For this model we have, outside:

$$\tau_{e+i} = 1.2948\rho^{-0.0404}, \qquad \log \rho \leqslant -0.1931, \tag{3}$$

$$Q = \frac{3\kappa_0 L}{16\pi a c} \frac{\rho_0^{2.0404}}{1.2948 T_0^{7.5} R}; \tag{4}$$

and inside:

$$\tau_{e+i} = 1.5686\rho^{+0.5075}, \qquad \log \rho \geqslant -0.1931, \tag{5}$$

$$Q_0 = \frac{3\kappa_0 L}{16\pi a c} \frac{\rho_0^{1.4955} a^{2.0135}}{1.5686 T_0^{7.5} R}. \tag{6}$$

From the integrations we find, the same as before,

$$\log Q = -4.9968, \qquad \log Q_0 = -4.7081;$$

$$\rho_c = 163.1 \frac{M}{R^3}, \qquad T_c = 27.73 \times 10^6 \mu \frac{M}{R}, \tag{7}$$

where M and R are expressed in solar units.

If the eigen-value Q found by the integration is introduced into equation (4), we obtain the mass-luminosity relation. Expressing L, M, and R in solar units, we have

$$[2X + \tfrac{3}{4}Y + \tfrac{1}{2}(1-X-Y)]^{7.5}(1+X)(1-X-Y) = \frac{1.84 M^{5.4596}}{L R^{0.3788}}. \tag{8}$$

[1] *Ap. J.*, **108**, 310, 1948.

[2] Cf. S. Chandrasekhar, *An Introduction to the Study of Stellar Structure* (Chicago: University of Chicago Press, 1939), p. 272.

Several corrections[3] have been made in the energy-output equation. For the nitrogen reaction at a temperature of 18×10^6 degrees the exponent of T is now 19, the mean life of the carbon cycle is 1.3×10^6 years, and $C + N = 0.25(1 - X - Y)$. The integration over the core then gives

$$\frac{L}{M} = \frac{\epsilon_0 \rho_c T_c^{19}}{53}. \tag{9}$$

The energy-output equation can then be written in the form

$$\frac{[2X + \frac{3}{4}Y + \frac{1}{2}(1 - X - Y)]^{19}}{(1 - X - Y)X} = 3533 \times 10^2 \frac{M^{21}}{LR^{22}}. \tag{10}$$

The main features of this model are

$$\rho_c = 163.1\,, \quad T_c = 17.31 \times 10^6\,, \quad \mu = 0.624\,;$$

$$X = 0.69\,, \quad Y = 0.28\,, \quad 1 - X - Y = 0.03\,.$$

In conclusion we might add that, if the above corrections are made in the energy-output equation for the model which does not include electron scattering, we find that we get the same results as those given above. Thus we conclude that the addition of electron scattering does not appreciably alter the computed chemical composition of the sun.

I wish to record my indebtedness to Dr. S. Chandrasekhar of the Yerkes Observatory for his constant guidance.

MARJORIE HALL HARRISON

VAN NUYS, CALIFORNIA
November 22, 1949

NOTE ON THE EFFECT OF UNEQUAL MOLECULAR WEIGHTS ON THE INTERNAL TEMPERATURE-DENSITY DISTRIBUTION OF A STAR

During the course of certain investigations in 1941 into the internal temperature-density distribution of main-sequence stars, we performed one calculation on Sirius A assuming a larger average molecular weight in the stellar atmosphere (defined as the region with a temperature below 1,000,000°) than in the remainder of the star. It seems worth while—even at this late date—to report the results of this calculation, as it bears on an old hypothesis of Eddington that the central temperature and density of a star are influenced only to a minor extent by the conditions in the stellar atmosphere.[1] In order to maximize the effect, we assumed that ionization was completely absent in the atmosphere of Sirius A, and, in order to make the comparison as close as possible, we chose a combination of hydrogen and Russell mixture—35 per cent hydrogen and the

[3] G. P. Kuiper, *The Atmospheres of the Earth and Planets* (Chicago: University of Chicago Press, 1949), p. 309.

[1] A. S. Eddington, *The Internal Constitution of the Stars* (Cambridge: At the University Press, 1926), p. 127.

remainder Russell mixture—which had been used in a previous calculation.[2] With this choice of hydrogen content, the average molecular weight in the atmosphere is 2.625 and in the remainder of the star 0.96339.

A procedure identical to the one used in Paper I was followed, taking account, as before, of the variation of guillotine factor throughout the star. Assuming $\mu = 2.625$, Strömgren's method led to initial values of t, T, ρ, and u, namely, $t = 1.055$, $T = 1.02995 \cdot 10^6$, $\rho = 0.001549$, and $u = 0.999800$. We then assumed continuity of temperature and density in crossing over into the region of $\mu = 0.96339$.[3] With these initial values it was a straightforward matter to integrate the equations of stellar equilibrium (6)–(8) in Paper I. The integration was carried along as usual until $n \equiv (d \log \rho / d \log T) = 1.5$ (onset of convective equilibrium) at which point $t = 9.463$, $T = 26.074 \cdot 10^6$, $\rho = 36.346$, and $\mu = 0.1184$.

With the above values, the two associated Emden functions U and V of polytropic index 1.5 become equal, respectively, to 0.874 and 1.259. This leads to corresponding values of ξ, namely, $\xi(U) = 1.01$ and $\xi(V) = 1.212$ and therefore to $\xi_{av} = 1.111$ and $\Delta\xi = -0.203$. The value for ξ_{av} yields $T_c = 32.2 \cdot 10^6$ and $\rho_c = 49.7$. These are not the correct values for T_c and ρ_c, but the value for $\Delta\xi$ enables us, with the help of the two integrations in Paper I for constant molecular weight, to arrive at approximately correct values of the central temperature and density for the present case. It will be recalled that, for the first integration in Paper I ($X_H = 0.35$), we obtained $\xi_{av} = 1.225$ and $\Delta\xi = 0.068$; using $\xi_{av} = 1.225$, we found $T_c = 29.5_5 \cdot 10^6$ and $\rho_c = 36.9$. For the second integration ($X_H = 0.40$) we obtained $\xi_{av} = 1.001$, $\Delta\xi = -0.113$, $T_c = 32.5_5 \cdot 10^6$, and $\rho_c = 52.5$. Thus a total $\Delta\xi$ of -0.181 leads to a ΔT_c of $-3.00 \cdot 10^6$ and a $\Delta\rho_c$ of -15.6. If we use linear interpolation (which seems reasonable, cf. n. 11 in Paper I), we must add $-3.00 \times 0.203/0.181 = -3.36$ million degrees to the value $32.2 \cdot 10^6$ obtained above from $\xi_{av} = 1.111$, thereby arriving at $28.84 \cdot 10^6$ for Sirius A on the assumption of unequal molecular weights; in a similar fashion we find $\rho_c = 32.2$ and $X_H = 0.296$. These numbers are to be compared with the numbers obtained on the assumption of constant molecular weight, namely, $T_c = 30.7 \cdot 10^6$, $\rho_c = 42.8$, and $X_H = 0.369$. The differences which are thus made manifest are to be regarded as an upper limit on the effect of incomplete ionization in the atmosphere of Sirius A on its internal temperature-density distribution.

We are indebted to Miss M. Ramsey and Mr. W. Waller for assistance with the numerical calculations.

R. E. Marshak
and
G. M. Wing

University of Rochester
and
University of California at Los Angeles
November 14, 1949

[2] R. E. Marshak and G. Blanch, *Ap. J.*, **104**, 82, 1946; this paper will be referred to hereafter as "Paper I."

[3] These assumptions are not so physical as the assumptions of the continuity of temperature and pressure (cf. M. Schönberg and S. Chandrasekhar, *Ap. J.*, **96**, 161, 1942) and would lead to dynamical instability. They should be thought of as equivalent to a mathematical alteration of atmospheric initial conditions in order to test the effect on the internal temperature-density distribution.

Astronomical

LANTERN SLIDES

Since 1905, the Yerkes Observatory of the University of Chicago has been reproducing in lantern slides, transparencies, and prints the original astronomical photographs made at Williams Bay.

The lantern slides are uniformly 4×3½ inches in size. The frequent call for small sets of slides for school and lecture purposes has led to the preparation of a list of 100 representative slides, a catalogue of which may be obtained upon request to the University of Chicago Press, 5750 Ellis Avenue, Chicago.

Prints as well as slides can be furnished, and for many subjects window transparencies are also supplied.

For catalogue and further information write

The University of Chicago Press
5750 Ellis Avenue, Chicago, Ill.

POPULAR ASTRONOMY

A magazine now in its fifty-eighth year, devoted to the elementary aspects of Astronomy and allied sciences.

Published monthly, except July and September.

Yearly subscription rates: Domestic $4.00; Canadian $4.25; Foreign $4.50 (U.S. dollars).

Address

POPULAR ASTRONOMY
CARLETON COLLEGE
NORTHFIELD, MINNESOTA, U.S.A.

PRINCIPLES OF STELLAR DYNAMICS

By S. CHANDRASEKHAR, Yerkes Observatory

A concise and authoritative account of current investigations by the author and others on the dynamics of the galaxy, spiral nebulae, and star clusters.

$5.00

In the *Astrophysical Monographs Series*

UNIVERSITY OF CHICAGO PRESS

". . . . a well-rounded book which should for many years to come be 'must' reading for every prospective student of galactic structure and dynamics."—BART J. BOK, *Science*.

". . . . to a specialist in the field this brilliant work should prove invaluable."—LYMAN SPITZER, JR., *Popular Astronomy*.

"The book fills an obvious gap in astronomical literature, and it should give a valuable stimulus to research."—A. S. EDDINGTON, *Nature* (England).

THE OBSERVATORY

FOUNDED 1877

* * *

A Magazine presenting current developments in Astronomy by means of Articles, Correspondence, Notes on discoveries and Reviews of important astronomical books. The papers read at the Meetings (Astronomical & Geophysical) of the Royal Astronomical Society and the discussions which follow are also fully reported.

* * *

Annual subscription for 6 issues, post free, 15/- should be sent to

The Editors, **ROYAL OBSERVATORY**
Greenwich, London S.E., 10

THE ATMOSPHERES OF THE EARTH AND PLANETS

Papers presented at the Fiftieth Anniversary Symposium of the Yerkes Observatory—September, 1947

Edited by GERARD P. KUIPER

CONTRIBUTORS: A. Adel, H. Brown, R. T. Chamberlin, H. E. Clearman, T. Dunham, E. Durand, J. Franck, J. L. Greenstein, G. Herzberg, L. Jacchia, Z. Kopal, G. P. Kuiper, M. V. Migeotte, C.-G. Rossby, L. Spitzer, P. Swings, H. C. van de Hulst, F. L. Whipple

366 pages | 6½×9¼ | Illustrated | $7.50

THE UNIVERSITY OF CHICAGO PRESS